

**Characterization of the fusogenic properties of COPI vesicles:  
a role for PI(4,5)P<sub>2</sub>**

**Frédéric Laporte  
McGill University, Montréal**

**January, 2009**

**A thesis submitted to McGill University in partial fulfilment of the  
requirements of the degree of Ph.D.**

**©Frédéric Laporte, 2009**

## **Preface**

Erudition .....	i
Dedication .....	ii
Acknowledgements .....	iii-iv
Contributions of authors .....	v
Materials and Methods.....	vi-xi
Abbreviations .....	xii-xiv
List of figures and tables.....	xv-xviii
Table of contents .....	xix-xxi
Appendix outline.....	xxii

### **Erudition**

“Do not worry about your difficulty in mathematics, mine are still greater.”

– Albert Einstein

À ma femme, Karen. Les mots sont pauvres pour faire le constat de tous tes attributs.

À ma famille. Vous êtes le roc sur lequel nous bâtissons notre avenir.

To the memory of our friend and collaborator, Dr. Dennis Shields.

## **Acknowledgements**

First my apologies. As you know, I am always kind of late, so this will be short. Nevertheless, I want to let you know that I truly appreciate the contributions from the people here, even if my words are not so eloquent.

First, to my wife, Karen, who is the source of my inspiration and the greatest little woman I have ever met. You amaze me every day. With your kindness, generosity and compassion, you are a model to everyone else. An o a lay.

À mon père et à Mo, auquel le support, l'aide et parfois l'omniprésence sont tout de même très appréciés.

À ma mère, qui a toujours su prendre soin de nous.

À mes frères, qui m'ont toujours offert une source de compétition et de motivation soutenue. À mon filleul, Alexandre : il n'existe de limites que celles que tu observes. À Julie; prends soin de Sébastien et prends soin de ta petite famille.

À tous, mille fois merci

I would first like to also thank my supervisor, John and also Tommy, who supervised all of my work for their help and support. It has been great to know you.

In chronological order from 2001 to 2007, I would like to thank the following:

Ali and Alex who helped and guided me at the beginning.

Joachim, for the expertise which made this project possible.

Dr. John Presley and Dr. David Thomas for your contribution to my committee which was very appreciated. John also, and Archana, for the use of your cell culture.

Dr. Barry Posner and Victor Dumas, for their help to set up the viral culture. This project would not have been possible without your help.



Jacqui and Fred, whose support was always welcome, especially when I was homesick. To Fred also for his help in this project. It was truly appreciated. You all are truly great individuals.

À Markus, qui aurait tellement apprécié que nous passâmes plus de nuits sur la paille. Dieu sait qu'on aurait du prendre plus de bières ensemble. Et merci pour la correction également.

To Johan, Julia, Lennart and Marlies, for their help in these experiments, as well as for your support and friendship. To Maria... hmm, I hope I did a better 2<sup>nd</sup> impression than the 1<sup>st</sup> time we met....

Dr. McPherson, Dr. Shields as well as Anirban and Christian, whose help and advice is greatly appreciated.

Dr. Lépine and Dr. Boismenu, for their help in planning and accomplishing the MS experiments.

Fiona, who's help was quite handy.

Hisao and Hitochi, who made me appreciate Japanese culture.

Dr. Wada and his wife who hosted us so well.

Cat, Ryan, Carey and Annalyn, who were my companions through all of this.

Thanks!

## **Contribution of authors**

### **Thesis:**

The following persons contributed to the thesis:

- Fredrik Kartberg, Johan Hiding and Joel Lanoix purified COPI vesicles that were used throughout the thesis.
- Fredrik Kartberg did the western in figure 1f and figure 2c of the thesis and helped plan these experiments.
- Fredrik Kartberg also contributed to purify the 5'kinase.
- François Lépine let me use his mass spectrometer and helped process the samples.
- Joachim Ostermann is responsible for most of chapter 6 and some of chapter 2. I repeated/expanded his experiments.
- Anirban Siddhanta and Dennis Shields, taught me how to do thin layer chromatography.
- Markus Grabenbauer contributed one EM picture.
- Experimental planning: experiments were designed in concert by Frédéric Laporte, Tommy Nilsson, John Bergeron and Joachim Ostermann.
- Julia Fernandez-Rodriguez helped with immunofluorescence in chapter 8.
- Marlies Otter-Nilsson and Lennart Asp helped with the Cell culture in chapter 8.

### **Other Contributions:**

I have joined two more publications:

- In Lee et al., I helped plan the experiments and provided technical advice and expertise.
- In Kartberg et al. I performed the lipid analysis of treated Golgi with mass spectrometry and thin layer chromatography.
- Dr. Lee as well as Dr. Elsner and Fredrik Kartberg provided editorial help.

## **Materials and methods**

### **Reagents**

All reagents were of analytical grade or higher. Unless mentioned otherwise, all chemicals were purchased from Sigma Chemical Co. (St-Louis, MO). Reagents for the COPI vesicle budding assay were obtained as described previously <sup>1, 2</sup>. Tritiated uridine bisphosphate n-Acetyl-D-Glucosamine was obtained from PerkinElmer (Wellesley, MA). PD-10 desalting columns, protein G sepharose beads and P<sup>32</sup> labeled ATP were obtained from Amersham Biosciences (Piscataway, NJ). Phospholipids standards, (PI(4,5)P<sub>2</sub>, PA, PS and PI(4)P) was obtained from Avanti Lipids (Alabaster AL). GTP, PMSF, N-Ethylmaleimide, PBS-Tween (0,05%) and Kodak Biomax<sup>TM</sup> X-Omat XAR or MR films were from Sigma-Aldrich (Stockholm, Sweden). ATP, creatine phosphate, and creatine kinase were from Roche AB (Stockholm, Sweden). ECL detection kit was from GE Healthcare Bio-Sciences AB (Uppsala, Sweden). 30% (wt/vol) acrylamide/0.8% (wt/vol) bis-acrylamide solution was from Bio-Rad (Sundbyberg, Sweden). Protran nitrocellulose membranes (0.45 µm) were from Schleicher and Schuell (Dassel, Germany).

Mouse GST-PI4P5K type Iβ, a generous gift of Y. Kanaho <sup>3</sup>, was cloned, sequenced and introduced to pGEX-2T (Amersham, Piscataway, NJ) to generate a GST-PI4P5K type Iβ fusion protein which was expressed and purified from *E. coli* BL21 cells.

The PI(4,5)P<sub>2</sub> 5'phosphatase domain (residues 592-900) of yeast Synaptojanin-like 2 (Inp52p) was a generous gift of P. De Camilli (Yale University, CT). Clones were sequenced and found to have two sequence alterations, one silent (G<sub>705</sub>), the other replacing Q<sub>799</sub> with R. This alteration did not have any effect on the phosphatase specificity. The construct was cloned in pET-28A (Novagen, San Diego, CA) and transformed in BL21 cells. Phosphatase activity was measured with a malachite green colorimetric assay <sup>4</sup>.

Recombinant His 6-tagged NSF, α-SNAP<sup>wt</sup> and α-SNAP<sup>mut</sup> were purified on Ni-NTA-agarose as described <sup>5</sup>. Recombinant proteins were desalted using a PD-10 column pre-

equilibrated in 20 mM Hepes, pH 7.2, 150 mM NaCl, 1 mM MgCl<sub>2</sub>, 5% glycerol, 1 mM GSH and in the case of NSF, 5 mM ATP. Recombinant His6tagged  $\alpha$ -SNAP<sup>mut</sup> was aliquoted and snap-frozen.

Recombinant VSV-G(TS045)-KDELr-Myc was a kind gift of Dr. Nelson B. Cole.

### **Mass spectrometry**

ESI-MS was performed in negative ion mode using a Micromass Quattro II triple quadrupole mass spectrometer (Waters, Canada) equipped with a Z-spray interface. PI(4,5)P<sub>2</sub> from standards or extracted from purified rat liver Golgi employing the chloroform/methanol/1N HCl (1:1:1) method of Siddhanta et al. <sup>6</sup>, dried under a stream of N<sub>2</sub> and then resuspended in acetonitrile/water/triethylamine (70%/30%/30mM) was used for ESI-MS analysis. Analysis was accomplished by direct infusion using a Harvard model 11 infusion pump at 5  $\mu$ L/min. MassLynx 3.5 software was employed for data accumulation in multiple-channel analysis mode and for data analysis. Nitrogen was used as drying gas (150 l/h) and nebulising gas (20 l/h). The ESI-MS analyses were performed with the electrospray capillary set at 4.7 kV, the cone voltage of 45 V, a scan rate of 400 Da/s and an interscan delay of 0.1 s. For tandem MS experiments, Argon at a partial pressure of  $2 \times 10^{-3}$  mbar was employed as collision gas, with collision energies of 35 V for tandem MS and 100 V for precursor ions scans.

### **Fusion assay**

The fusion assay was performed as described previously <sup>7</sup>. Briefly, purified COPI-derived vesicles were generated in the budding assay and incubated in the presence of 20% Lec1 cytosol, 10% VSV-infected Lec1 Golgi membranes, an ATP Regenerating system (final 50uM ATP, 250uM UTP, 5mM creatine phosphate, 8U/ml creatine kinase), 10X hepes buffer (final 25mM Hepes/KOH pH 7.2, 2.5mM MgOAc<sub>2</sub>), 1.5  $\mu$ Ci of previously evaporated tritiated N-acetyl-Glucosamine and final sucrose and KCl concentration adjusted to 0.25 M and 30-60mM, respectively.

Pre-Incubation of the COPI-derived vesicles in the presence of the mouse GST-PI(4)P5Kinase type I $\beta$  or the 5'phosphatase domain of Inp52p was performed in 0.25 M sucrose, 150mM KCl, 25mM Hepes/KOH pH 7.4, 1mM EGTA, 2.5mM MgCl<sub>2</sub>. 250 $\mu$ M ATP was added for pre-incubation with GST-PI(4)P5KI $\beta$ . The vesicles were then added to the fusion assay and the sucrose and salt concentration was adjusted to meet the requirements mentioned above. For protease K, vesicles were incubated in the same buffer as above in the presence of PK for 30 min at 4°C. 1 mM PMSF final dissolved in ETOH was added to the reaction after incubation. Vesicles were then introduced to the fusion assay.

After 2 hours incubation at 37°C, reactions were stopped at 4°C. Samples were added to the antibody complex (purified mouse anti-VSV-G and goat anti-mouse, optimized for sensitivity) in lysis buffer (50mM Tris pH 7.4, 250mM NaCl, 5mM EDTA, 1% Triton X-100), mixed and incubated for one hour at RT. Samples were then filtered on blocked glass fiber prefilters (Sigma GF/C or Millipore APFC02500), washed 5 times with lysis buffer, dried and counted.

#### **Cell culture, cytosol and membranes purification.**

CHO Lec1 cells <sup>8</sup> were obtained from the ATCC. For cytosol purification, cells were pelleted and washed once with PBS, once with 200mM sucrose/10mM tris pH 7.4 (ST) buffer and resuspended in identical buffer. They were then homogenized using a ball-bearing homogenizer (Boehring Ingelheim, Mannheim, Germany) and centrifuged at 14000 rpm for 3x10 min. until no pellet was visible. Cytosol was then desalted in PD10 column, aliquoted, snap-frozen and kept at -80°C.

For Lec1 Golgi membrane preparations, cells were pelleted and resuspended in 50 ml VSV infection media containing VSV, alpha-MEM, 25mM Hepes/KOH pH 7.2, 0.5 mg actinomycin D) for 45 min. at 37°C. After the infection, 200ml of 10% FBS alpha-MEM medium was added to the volume and incubated for 2h15 min at 37°C. In order to concentrate the VSV-G in the CGN, the cells were incubated or 3h15min at 15°C. Cells were washed and homogenized as described above. To purify Golgi membranes, the

homogenate was mixed 1:1 with 62% sucrose, 10mM Tris pH 7.4, 1mM EDTA. The fraction was then introduced to the bottom of SW 40 Ultraclear tubes (Beckman, Fullerton, CA). Sucrose fractions of 35% and 29% were applied at the top of the tubes, centrifuged for 90 min. at 40 000rpm. Golgi membranes were collected at the 29-35% sucrose interface, aliquoted, snap-frozen and stored at  $-80^{\circ}\text{C}$ . The budding assay was performed as described previously <sup>2</sup>.

### **Thin layer chromatography**

All TLC were performed as described previously <sup>6</sup>. Briefly, samples were incubated in kinase/phosphatase buffer (final 0.25M Sucrose, 25mM Hepes/KOH pH 7.4, 150mM KCL, 1mM EGTA, 2.5mM  $\text{MgCl}_2$  and 250 $\mu\text{M}$  ATP) for 60min. at  $37^{\circ}\text{C}$  in the presence of radiolabeled  $^{32}\text{P}$ -ATP. The phospholipids were extracted with MeOH/Chloroform/1N HCL, (1:1:1) dried, resuspended in chloroform:MeOH:9N HCL (200:100:1.33) and resolved by TLC. Phospholipids were identified by co-migration with known standards <sup>6</sup>.

### **Antibodies and electron microscopy**

Mouse monoclonal antibodies to VSV-G, a kind gift from P. Melancon (University of Alberta, Edmonton) were purified from hybridomas. The degree of antibody complex formation was assayed by mixing varying quantities of mAB to VSV-G and Anti-Mouse Goat AB (ICN, Montreal, Canada) until the optimal ratio was obtained in the fusion assay. Mouse monoclonal IgG<sub>2b</sub> antibody to phosphatidylinositol 4,5-bisphosphate was obtained from Assay Designs Inc. (Ann Arbor, MI). Mouse monoclonal antibody against Golgin-84, p115 and GM130 were obtained from BD Biosciences. Rabbit polyclonal antibodies against PI(4)P5'kinase type 1 $\alpha$  and 1 $\beta$  were kind gifts of Dr. Dennis Shields. Antibodies to  $\beta$ -cop were a kind gift from Drs. Rothman and Kreis. HRP labeled AB for western were obtained from Dianova (Hamburg, Germany). All other antibodies were kind gifts of Dr. Tommy Nilsson.

For electron microscopy, vesicles were prepared, immuno-labeled with an antibody directed towards the cytoplasmic domain of p24 $\beta_1$ , (a small transmembrane protein enriched in COPI vesicles <sup>9,10</sup>) and analyzed by negative stain as described previously <sup>11</sup>.

## Graphs and curvefitting

All curvefitting was done with the help of Maccurvefit 1,5 (Kavin Raner Software ([www.krs.com.au](http://www.krs.com.au))). In regards to the fusion assay, a non-saturation amount of vesicles refers to an amount of vesicles that would normally generate a signal that is a fraction of the maximum signal, generally a 1:1 ratio of vesicles to Golgi cisternae<sup>7</sup>. While experiments done under these conditions provide accurate and reliable data, the precise extent of how the fusion assay is affected can only be ascertained by comparing the apparent concentration of vesicles. All error bars refer to one standard deviation in both directions, calculated with EXCEL (Microsoft, Seattle, WA).

## Immunofluorescence

Transfections were performed according to manufacturer instructions (Invitrogen, Carlsbad, California). For immunofluorescence, cells were washed with PBS, fixed with 4% paraformaldehyde and further permeabilized with 0.2% saponin. Alexa Antibodies of wavelengths 488 nm and 594 nm were obtained from invitrogen (Carlsbad, California) and were excited with a 488 nm Argon laser and a HeNe laser to excite at 594 nm. Cells were visualized with Axiovert 200/LSM 510 META system microscope (Carl Zeiss) with a 40x objective.

## References-Materials and Methods

1. Fredrik Kartberg, J.H., Tommy Nilsson *Purification of COPI vesicles*. (Elsevier Academic Press, 2006).
2. Kartberg, F., Elsner, M., Froderberg, L., Asp, L. & Nilsson, T. Commuting between Golgi cisternae--mind the GAP! *Biochim Biophys Acta* 1744, 351-363 (2005).
3. Yamazaki, M. *et al.* Phosphatidylinositol 4-phosphate 5-kinase is essential for ROCK-mediated neurite remodeling. *J Biol Chem* 277, 17226-17230 (2002).
4. Martin, B., Pallen, C.J., Wang, J.H. & Graves, D.J. Use of fluorinated tyrosine phosphates to probe the substrate specificity of the low molecular weight phosphatase activity of calcineurin. *J Biol Chem* 260, 14932-14937 (1985).
5. Barnard, R.J., Morgan, A. & Burgoyne, R.D. Stimulation of NSF ATPase activity by alpha-SNAP is required for SNARE complex disassembly and exocytosis. *J Cell Biol* 139, 875-883 (1997).
6. Siddhanta, A., Backer, J.M. & Shields, D. Inhibition of phosphatidic acid synthesis alters the structure of the Golgi apparatus and inhibits secretion in endocrine cells. *J Biol Chem* 275, 12023-12031 (2000).
7. Ostermann, J. Stoichiometry and kinetics of transport vesicle fusion with Golgi membranes. *EMBO Rep* 2, 324-329 (2001).
8. Stanley, P., Caillibot, V. & Siminovitch, L. Selection and characterization of eight phenotypically distinct lines of lectin-resistant Chinese hamster ovary cell. *Cell* 6, 121-128 (1975).

9. Sohn, K. *et al.* A major transmembrane protein of Golgi-derived COPI-coated vesicles involved in coatamer binding. *J Cell Biol* 135, 1239-1248 (1996).
10. Lanoix, J. *et al.* Sorting of Golgi resident proteins into different subpopulations of COPI vesicles: a role for ArfGAP1. *J Cell Biol* 155, 1199-1212 (2001).
11. Lanoix, J. *et al.* GTP hydrolysis by arf-1 mediates sorting and concentration of Golgi resident enzymes into functional COP I vesicles. *Embo J* 18, 4935-4948 (1999).



## Abbreviations

<b>5'Phosphatase:</b>	5-phosphatase domain of Inp52p
<b>5'Kinase:</b>	Mouse GST-PI(4)P 5-Kinase type I $\beta$
<b>AA:</b>	Amino acid
<b>ARF1 (Arf1):</b>	ADP-rybosylation factor 1
<b>ARFGAP1:</b>	ARF GTPase activating protein 1
<b>ADP:</b>	Adenosine diphosphate
<b>ATP:</b>	Adenosine triphosphate
<b>BIG:</b>	Brefeldin A inhibited GEF
<b>CID:</b>	Collision induce dissociation
<b>CGN:</b>	Cis-Golgi-Network
<b>CHO:</b>	Chinese Hamster Ovary
<b>COG:</b>	Conserved oligomeric Golgi complex
<b>COPI:</b>	Coatomer protein I
<b>COPII:</b>	Coatomer protein II
<b>C<sub>v</sub><sup>app</sup>:</b>	Concentration of vesicles which is apparent
<b>CPM:</b>	Counts per minute
<b>DAG:</b>	Diacylglycerol
<b>DCV:</b>	Dense core vesicles
<b>DPM:</b>	Disintegrations per minute
<b>EM:</b>	Electron microscopy
<b>ER:</b>	Endoplasmic Reticulum
<b>GAP:</b>	GTPase activating protein
<b>GBF1:</b>	Golgi specific brefeldin A resistance factor
<b>GEF:</b>	Guanosine Exchange Factor
<b>GFP:</b>	Green Fluorescent Protein
<b>GlcNacT1:</b>	N-acetyl-Glucosamine Transferase 1
<b>GLP:</b>	Glycerophospholipids
<b>GST:</b>	Gluthathione S-Transferase
<b>GTP:</b>	Guanosine triphosphate

<b>HI:</b>	Heat Inactivated
<b>HPLC:</b>	High Pressure Liquid Chromatography
<b>HOPS:</b>	Homotypic fusion and vacuole protein sorting
<b>IF:</b>	Immunofluorescence
<b>IFRAP:</b>	Inverse fluorescence recovery after photobleaching
<b>IgG:</b>	Immunoglobulin of type G
<b>INPP5B:</b>	Type II inositol polyphosphate 5-phosphatase
<b>Inp52p:</b>	Yeast Synaptojanin-like 2/yeast inositol polyphosphate 5-phosphatase
<b>KB:</b>	Kinase buffer
<b>KCL:</b>	Potassium Chloride
<b>Man:</b>	Mannose
<b>Mg<sup>2+</sup>:</b>	Ionic Magnesium
<b>MS:</b>	Mass spectrometry
<b>NEM:</b>	N-Ethylmaleimide
<b>NSF:</b>	NEM Sensitive factor
<b>OCRL1:</b>	Oculocerebralrenal syndrome of Lowe (protein 1)
<b>PA:</b>	Phosphatidic Acid
<b>PH:</b>	Pleckstrin Homology
<b>PI:</b>	Phosphatidylinositol
<b>PIkinase:</b>	Phosphatidylinositol kinase
<b>PI(4)P:</b>	Phosphatidylinositol 4-phosphate
<b>PI(3,4)P<sub>2</sub>:</b>	Phosphatidylinositol 3,4-bisphosphate
<b>PI(4,5)P<sub>2</sub>:</b>	Phosphatidylinositol 4,5-bisphosphate
<b>PI(3,4,5)P<sub>3</sub>:</b>	Phosphatidylinositol 3,4,5 triphosphate
<b>PI-PLC:</b>	Phosphoinositol specific Phospholipase C
<b>PLC:</b>	Phospholipase C
<b>PLCA1:</b>	Phospholipase C delta1
<b>PLD:</b>	Phospholipase D
<b>PK:</b>	Proteinase K
<b>PM:</b>	Plasma Membrane

<b>PS:</b>	Phosphatidylserine
<b>SL:</b>	Sphingolipids
<b>SNAP:</b>	Soluble N-Ethylmaleimide-sensitive attachment protein
<b>SNARE:</b>	SNAP receptor
<b>STD:</b>	Standard Deviation
<b>TGN:</b>	Trans-Golgi-Network
<b>TLC:</b>	Thin Layer Chromatography
<b>VSV:</b>	Vesicular Stomatitis Virus
<b>VSV-G:</b>	Vesicular Stomatitis Virus Glycoprotein
<b>VTC:</b>	Vesiculo-Tubular Cluster

## **List of Tables and figures**

### **Literature Review**

Figure A. The Golgi apparatus.....	8
Figure B. The vesicular transport model.....	10
Figure C. The cisternal maturation model .....	12
Figure D. The percolating Golgi .....	14
Figure E. The two speeds/heavy workload model .....	15
Figure F. The Golgi Lipid gradient.....	22
Figure G. The Rapid Partitioning within a Two-Phase Membrane System .....	23
Figure H. Two models for the role of the ARFGAP1 in COPI vesicle formation.....	29
Figure I. Localisation of Mammalian and Yeasts SNAREs. ....	33
Figure J. The SNARE fusion machinery. ....	34
Figure K. PI(4,5)P2 and other phospholipids .....	39
Figure L. Synthesis of phosphoinositides. ....	40

### **Chapter 1.**

Figure 1a. Purification of COPI vesicles in the budding assay.....	49
Figure 1b. Schematic representation of the fusion assay .....	52
Table 1. CHO Lec1 Golgi were infected by VSV to produce VSV-G .....	53
Figure 1c. Diagrammatic representation of <i>N</i> -acetylglucosamine addition.....	54
Figure 1d. Representation of a fusion assay .....	56
Table 2. Fusogenicity of vesicles can be evaluated reproducibly by their $C_v^{app}$ .....	57
Figure 1e. The fusion assay monitors the fusion of COPI vesicles .....	59

### **Chapter 2.**

Figure 2a. Inactivation of COPI vesicles .....	63
Figure 2b. Digestion of COPI vesicles .....	64
Figure 2c. Golgi and COPI vesicles possessed similar PK sensitivity .....	65
Figure 2d. COPI Vesicles remained active after proteolysis .....	66
Figure 2e. Vesicles treated with PK still became inactivated over time.....	67

Figure 2f. Target Golgi was sensitive to PK treatment.....	68
Figure 2g. PI(4,5)P <sub>2</sub> .....	69
Figure 2h. Schematic representation of the aminoglycoside neomycin.....	70
Figure 2i. Neomycin has an inhibitory effect on the fusion assay .....	71
Figure 2j. Monoclonal IgG against PI(4,5)P <sub>2</sub> inhibits the fusion of COPI vesicles .....	72
Figure 2k. Wortmannin inhibited fusion of vesicles.....	73

### Chapter 3.

Figure 3a. Mass spectrometry scan .....	77
Figure 3b. Fragmentation of the m/z 522 peak .....	78
Figure 3c. Precursor ion scan.....	79
Figure 3d. ESI-MS analysis of Golgi extract in chloroform/methanol/HCl .....	81
Figure 3e. Generation of PI(4,5)P <sub>2</sub> by treatment of purified rat liver Golgi with rat brain cytosol in the presence of ATP. ....	82
Figure 3f. PI(4)P 5'kinase type 1 $\beta$ synthesized PI(4,5)P <sub>2</sub> on the surface of Golgi apparatus .....	84
Figure 3g. Alteration of the phospholipids composition by the mouse GST-PI(4)P 5'kinase type I $\beta$ .....	85
Figure 3h. 5'Kinase rescued inactivated COPI vesicles .....	86
Figure 3i. Determination of C <sub>v</sub> <sup>app</sup> .....	87

### Chapter 4.

Figure 4a. Purification of the 5'phosphatase .....	90
Figure 4b. 5'phosphatase domain protein removed the 5' phosphate of PI(4,5)P <sub>2</sub> .....	91
Figure 4c. Removal of the 5'phosphate from PI(4,5)P <sub>2</sub> on the surface of COPI vesicles by 5'phosphatase.....	93
Figure 4d. 5'phosphatase inhibited the fusion of COPI vesicles .....	94
Figure 4e. An incubation with 5'phosphatase resulted in significant changes in C <sub>v</sub> <sup>app</sup> ....	95

### Chapter 5.

Figure 5a. Sequential manipulation of PI(4,5)P <sub>2</sub> on COPI vesicles.....	98
Figure 5b. 5'kinase mediated rescue of COPI vesicle inactivation was reversed by treatment with 5'phosphatase .....	99
Figure 5c. Determination of $C_v^{app}$ after treating the inactivated COPI vesicles with 5'kinase followed by 5'phosphatase .....	100
Figure 5d. Modification of the PI(4,5)P <sub>2</sub> synthesis on target Golgi membranes .....	101
Figure 5E. Study of the fusogenicity by modifications of PI(4,5)P <sub>2</sub> levels in the target Golgi .....	102

## Chapter 6.

Figure 6a. Fate of the COPI vesicles.....	106
Figure 6b. Dilution experiment.....	108
Figure 6c. Dilution and PK experiment .....	109
Figure 6d. The [binding/(binding+inactivation)] ratio dropped following PK treatment	110
Figure 6e. The effects of PK on fusion kinetics.....	111
Figure 6f. The fusion assay was sensitive to NSF depletion .....	113
Figure 6g. PK treated vesicles were also sensitive to NSF depletion .....	114
Figure 6h. $\alpha$ -SNAP <sup>mut</sup> inhibited the fusion of COPI vesicles treated with PK .....	115
Figure 6i. Pre-incubation of vesicles and target Golgi membranes with $\alpha$ -SNAP <sup>mut</sup> .....	117

## Chapter 7.

Figure 7a. Golgin-84 and its antibody .....	120
Figure 7b. Abundance and enrichment of proteins from COPI vesicles to Golgi .....	121
Figure 7c. Golgin-84 is resistant to PK degradation.....	122
Figure 7d. Golgin-84 PK resistant core is only present on fusogenic COPI vesicles.....	124
Figure 7e. Vesicles without protease resistant Golgin-84 have lower fusogenicity .....	126
Figure 7f. The protease resistant core of Golgin-84 is not affected by removal of PI(4,5)P <sub>2</sub> .....	127

## Chapter 8.

Figure 8a. VSV-G(TS045)KDEL-MYC.....	131
--------------------------------------	-----

Figure 8b. PI(4)P5'kinase type 1 $\beta$ .....	132
Figure 8c. PI(4)P5'kinase type 1 $\beta$ localization in BSC1, Hela cells .....	133
Figure 8d. PI(4)P5'kinase type 1 $\alpha$ localization in Hela cells cells. ....	134
Figure 8e. The pSuper.Retro vector. ....	135

## **Table of Contents**

<b>Abstract.....</b>	<b>1</b>
<b>Abrégé .....</b>	<b>2</b>
<b>Thesis introduction .....</b>	<b>4</b>
<b>Literature review.....</b>	<b>6</b>
Section 1: The secretory pathway. ....	6
Section 1.1: The Golgi apparatus and Golgi transport models. ....	7
Section 1.2: The static vesicular transport model. ....	9
Section 1.3: The cisternal maturation model.....	10
Section 1.4: Improvement on cisternal maturation: the percolating model . ....	13
Section 1.5: Improvement on cisternal maturation: the heavy workload model....	14
Section 1.6: Improvement on cisternal maturation: Rapid partitioning with a two phase membrane system.....	18
Section 2: COPI vesicles. ....	26
Section 2.1: Anterograde versus retrograde.....	26
Section 2.2: Budding of COPI vesicles.....	27
Section 2.3: COPI vesicles fusion. ....	32
Section 3: PI(4,5)P <sub>2</sub> .....	39
Section 3.1: Metabolism of PI(4,5)P <sub>2</sub> .....	40
Section 3.2: Roles of PI(4,5)P <sub>2</sub> . ....	41
PI(4,5)P <sub>2</sub> in vacuoles. ....	42
PI(4,5)P <sub>2</sub> at the plasma membrane.....	43
PI(4,5)P <sub>2</sub> in the Golgi.....	45
<b>Results .....</b>	<b>47</b>
Chapter 1: Establishment of the biochemical investigation process.....	47
Introduction. ....	47
Results. ....	48
Discussion .....	60
Chapter 2 : Determining the potential involvement of lipids in the fusion process. ....	62



Introduction .....	62
Results .....	62
Discussion .....	74
Chapter 3: Identification and manipulation of PI(4,5)P <sub>2</sub> on the surface of the COPI vesicles .....	75
Introduction .....	75
Results .....	75
Discussion .....	87
Chapter 4: Removal of PI(4,5)P <sub>2</sub> accelerated the inactivation of COPI vesicles . ....	89
Introduction .....	89
Results .....	89
Discussion .....	95
Chapter 5: Specific modification of the levels of PI(4,5)P <sub>2</sub> on COPI vesicles , but not the target Golgi, modulated the fusion process. ....	97
Introduction .....	97
Results .....	97
Discussion .....	103
Chapter 6: Investigation of PI(4,5)P <sub>2</sub> associated factors: removal of the proteins on the cytoplasmic surface of the COPI vesicles affected the first step of the fusion. ....	104
Introduction .....	104
Results .....	104
Discussion .....	118
Chapter 7: A PK resistant core of the tethering factor Golgin-84 is present on the surface of COPI vesicles. ....	119
Introduction .....	119
Results .....	119
Discussion .....	127
Chapter 8: PI(4,5) <sub>2</sub> <i>in vivo</i> : methodology and ongoing work. ....	130
Introduction .....	130
Results .....	130
Discussion .....	136

<b>Thesis discussion .....</b>	<b>137</b>
Analysis.....	140
Future outlook .....	141
<b>List of original contributions .....</b>	<b>144</b>
<b>References .....</b>	<b>145</b>

# **Thesis**

## **Abstract**

Coatomer proteins 1 (COPI) are recruited to Golgi membranes in an ADP ribosylation factor 1 (ARF1)-dependent manner that couples protein sorting to vesicle formation. Using a modified intra-Golgi transport assay with highly purified COPI vesicles, we demonstrate that fusion of retrograde-directed vesicles with Golgi membranes requires phosphatidylinositol 4,5-bisphosphate (PI(4,5)P<sub>2</sub>). The dependency on PI(4,5)P<sub>2</sub> appears to be COPI vesicle associated since pre-treatment of the vesicles with either a specific 5'phosphatase or a 5'kinase resulted in inhibition or gain of fusion, respectively. In contrast, corresponding pre-treatment of Lec1 Golgi target membranes had no effect on the efficiency or extent of COPI vesicle fusion with the Lec1 Golgi membranes.

We continued our investigation in order to determine the identity of the protein(s) recruited by PI(4,5)P<sub>2</sub> which enable the fusion process. Using Protease K (PK) treatment of both vesicles and target Lec1 Golgi to investigate the cytoplasmic protein requirements, we detected a marked asymmetry between the target Golgi and COPI vesicles, as PK treated vesicles were still able to fuse with limited cytoplasmic proteins while target Golgi rapidly lost all fusogenicity. Kinetic evaluation of vesicles treated as such observed a decrease in the binding constant, however we observe little or no effect on the actual fusion constant. Furthermore, we were able to identify a Protease K resistant core of Golgin-84 whose location was limited to fusogenic COPI vesicles. Investigation of a potential link between Golgin-84 and PI(4,5)P<sub>2</sub> was unsuccessful. We were also able to determine that while the Golgin-84 resistant core was necessary for fusion to occur, it was not sufficient.

Fusion of COPI vesicles to Golgi membranes involves a heterotypic event supporting the notion that COPI vesicles are both biochemically and functionally distinct from Golgi cisternae. We propose that, simultaneously to the budding of the COPI vesicles, ARF1 recruits the kinase responsible for PI(4,5)P<sub>2</sub> synthesis and, in a still unidentified mechanism, alters the conformation of Golgin-84. ARF1 can therefore effectively prime COPI vesicles for fusion already at the onset of vesicle formation.

## Abrégé

Les protéines de coatomer de type 1 (COPI) sont recrutées par l'appareil de Golgi sous l'action de l'activité de la protéine ADP-Ribolysation factor 1 (ARF1), ce qui permet d'associer la formation de vésicules et l'incorporation spécifique des protéines et lipides qui forment ces vésicules. Avec l'aide d'un protocole expérimental mesurant le transport intra-Golgien, nous avons démontré que la fusion de vésicules COPI rétrograde est dépendante de la présence de phosphatidylinositol 4,5-bisphosphates (PI(4,5)P<sub>2</sub>). Cette dépendance apparaît associée aux vésicules COPI étant donné que leur prétraitement en présence de 5'kinase ou 5'phosphatase spécifique résulte en une activation ou inhibition respective. De façon contrastante, le même prétraitement des membranes de Golgi cibles issues de cellules CHO Lec1 n'affecte pas la fusion entre les vésicules et les membranes de Golgi.

Nous avons continué notre investigation pour déterminer l'identité des protéines recrutées par PI(4,5)P<sub>2</sub> qui permettent la fusion. Avec l'aide de l'enzyme protéase K (PK), nous avons détecté une asymétrie entre les vésicules COPI ainsi que les membranes de l'appareil de Golgi : tandis que les vésicules étaient en grande partie résistantes au traitement avec PK, les membranes de Golgi se montraient très susceptibles et perdaient toute fusogenicité. Une évaluation cinétique des vésicules soumis à ce traitement a permis de détecter une diminution du rythme d'association des vésicules mais aucun ou très peu de changement significatif du rythme de fusion ne fut détecté. De plus, nous avons identifié un noyau de la protéine Golgin-84 résistant au traitement avec PK présent sur la surface des vésicules COPI. Une recherche plus poussée ne nous a pas permis cependant d'identifier un lien entre Golgin-84 et PI(4,5)P<sub>2</sub>. Nous avons également pu déterminer que même si Golgin-84 est nécessaire à la fusion des vésicules COPI, sa présence seule n'est pas suffisante.

La fusion des vésicules COPI au Golgi implique un mécanisme hétérogène, ce qui supporte la notion que les vésicules COPI sont des organelles biochimiquement et fonctionnellement différentes de l'appareil de Golgi. Nous proposons que, simultanément

à la formation de vésicules COPI, ARF1 recrute la kinase responsable pour la synthèse de  $\text{PI}(4,5)\text{P}_2$  et, avec un mécanisme non-identifié, altère la conformation de Golgin-84. ARF1 peut dans ce cas primer la vésicule pour fusionner au moment même où elle contribue à la formation de la vésicule.

## **Thesis introduction**

The goals of the investigations presented here is to further the understanding of the Golgi apparatus, the central organelle of the early secretory pathway. Located along the secretory pathway, the Golgi apparatus process proteins and lipids transported from the endoplasmic reticulum. Within the Golgi, resident enzymes are responsible for extensive post-translation modifications; most importantly extensive N- and O- linked glycosylation and proteolytic processing. Both the regulation of the enzymatic reactions and the mechanisms of transport to, from and within the Golgi have been the subject of decades of intensive research.

Our investigation concentrated on studying the properties of COPI vesicles, a controversial transport intermediate of the Golgi apparatus essential for the maintenance of Golgi homeostasis. It does so by transporting proteins and lipids between Golgi cisternae and from the Golgi apparatus to the endoplasmic reticulum. However, the mechanisms of budding from and fusion with the Golgi cisternae are largely unknown and are at the core of the previously mentioned debate about the Golgi.

This thesis will first review the current literature. We will start by providing an overview of the different models for Golgi transport. These models try to explain the experimental observations that have been collected by a large number of researchers and are the subject of intensive debate. We will then continue by summarizing the current knowledge about the budding and fusion of COPI vesicles. Emphasis will be on the potential versatility of COPI vesicles in mediating multiple transport events within the Golgi apparatus.

Within this scope, our investigations specifically tried to further the understanding of the fusion mechanisms of COPI vesicles. For this, we developed a cell-free assay using purified COPI vesicles and Golgi membranes. We were able to show that efficient fusion requires the presence of glycerophospholipid, PI(4,5)P<sub>2</sub>. Therefore, with these premises, the last part of our literature review will examine the roles of PI(4,5)P<sub>2</sub> within the cell and the links between PI(4,5)P<sub>2</sub> and membrane fusion

Finally, our result section will explain that after the positive identification of PI(4,5)P<sub>2</sub> as a promoter of vesicles fusion, our research attempted to identify the protein(s) mediating the PI(4,5)P<sub>2</sub> requirement. While our attempts were successful in discovering another requirement for the fusion of COPI vesicles in the identification of Golgin-84, we were unsuccessful in demonstrating a link between PI(4,5)P<sub>2</sub> and Golgin-84 in the fusion process of COPI vesicles.



## **Literature Review**

### **Section 1: The secretory pathway**

Every cell possesses mechanisms that allow it to replenish its proteins constituents and keep it in homeostasis. Parts of these homeostasis mechanisms are mediated by secreting proteins in the interstitial space or by synthesizing the correct receptor on the surface of the cell. The pathway that is responsible for regulating most of these interactions between the cell and its environment is termed the secretory pathway<sup>24-26</sup>.

Production of new proteins starts in the nucleus with the transcription of mRNA from DNA. The mRNA sequence is then exported to the cytosol, where it attaches to ribosomes for translation. After translation, the newly synthesized peptide chain can be targeted to certain organelles, such as mitochondria, peroxisomes or chloroplasts. In the case of secretory proteins, a signal sequence incorporated in their peptide chain targets them to the endoplasmic reticulum (ER) for processing<sup>25, 27-29</sup>.

Upon entering the ER, the newly synthesized proteins are glycosylated and folded into the appropriate conformation. Protein folding is accomplished by chaperone mediated quality control mechanisms that allow for the sensing of protein conformation<sup>30-32</sup>. Unfolded or misfolded proteins are retained in the ER until they become properly folded or are targeted for proteolysis if a stable conformation cannot be attained<sup>for review 33</sup>.

Upon reaching appropriate conformation, newly synthesized proteins destined for latter part of the secretory pathway are gathered at ER exit sites where they are incorporated into COPII vesicles<sup>34</sup> which mediate exit of secretory cargo proteins from the ER<sup>for review see 35</sup>. After exiting from the ER, the COPII vesicles can fuse to form vesiculo-tubular clusters (VTC) which are then transported along microtubules to the Golgi apparatus<sup>36</sup>.

Upon arrival to the *cis* face of the Golgi apparatus, the VTCs coalesce and form the *cis*-Golgi-network (CGN). Cargo proteins are then transported to the *cis* face of the Golgi

apparatus (see section 1.1), where they are sequentially glycosylated. During this process, they move through the Golgi until they reach the *trans*-Golgi-Network (TGN) where they are sorted according to their destination and packaged into vesicles <sup>37-40</sup>. After exiting from the Golgi apparatus, cargo proteins that follow the default pathway are then secreted (for luminal proteins) or are incorporated into the plasma membrane (for proteins with transmembrane domains or membranes anchors). Alternatively, at the exit from the Golgi apparatus, proteins can also be directed to endosomes, lysosomes (through endosomes) or secretory vesicles <sup>for review see 25, 41-44</sup>.

In the direction opposite to the flow of COPII vesicles, another type of vesicles termed COPI mediates the transport of lipids and proteins from the Golgi apparatus back to the ER <sup>45-48 for review see 18, 49</sup>. ER proteins that are transported to the Golgi by COPII vesicles and proteins that are required for the generation of COPII vesicles are retrieved from the Golgi apparatus through motifs present on the cytoplasmic tails of their transmembrane domains <sup>50-54</sup>. This mechanism provides a pathway where the budding machinery as well as the lipids from the ER that have been incorporated within the COPII can be recycled and reused. This distillation process is also used within the Golgi apparatus, where Golgi resident enzymes are segregated and recycled from cargo proteins by COPI vesicles <sup>11, 55</sup> (see section 1.1). The methods involved in the recycling of Golgi resident enzymes are the main interest of this thesis.

### **Section 1.1: The Golgi apparatus and Golgi transport models**

The Golgi apparatus is composed of a series of flattened and elongated membranous cisternae stacked in parallel (fig. A). In animal cells, it is located in the juxtanuclear region and is composed of an average of 5 to 7 cisternae <sup>18, 22</sup>. However the amount of cisternae can vary greatly from one cell to another, depending on the secretion workload of the cell <sup>e.g. 56</sup>. The Golgi apparatus is also polarized: it has a *cis* face, where VTCs carry newly formed proteins from the ER, and a *trans* face, where cargo is exported from the ER to post-Golgi compartments.

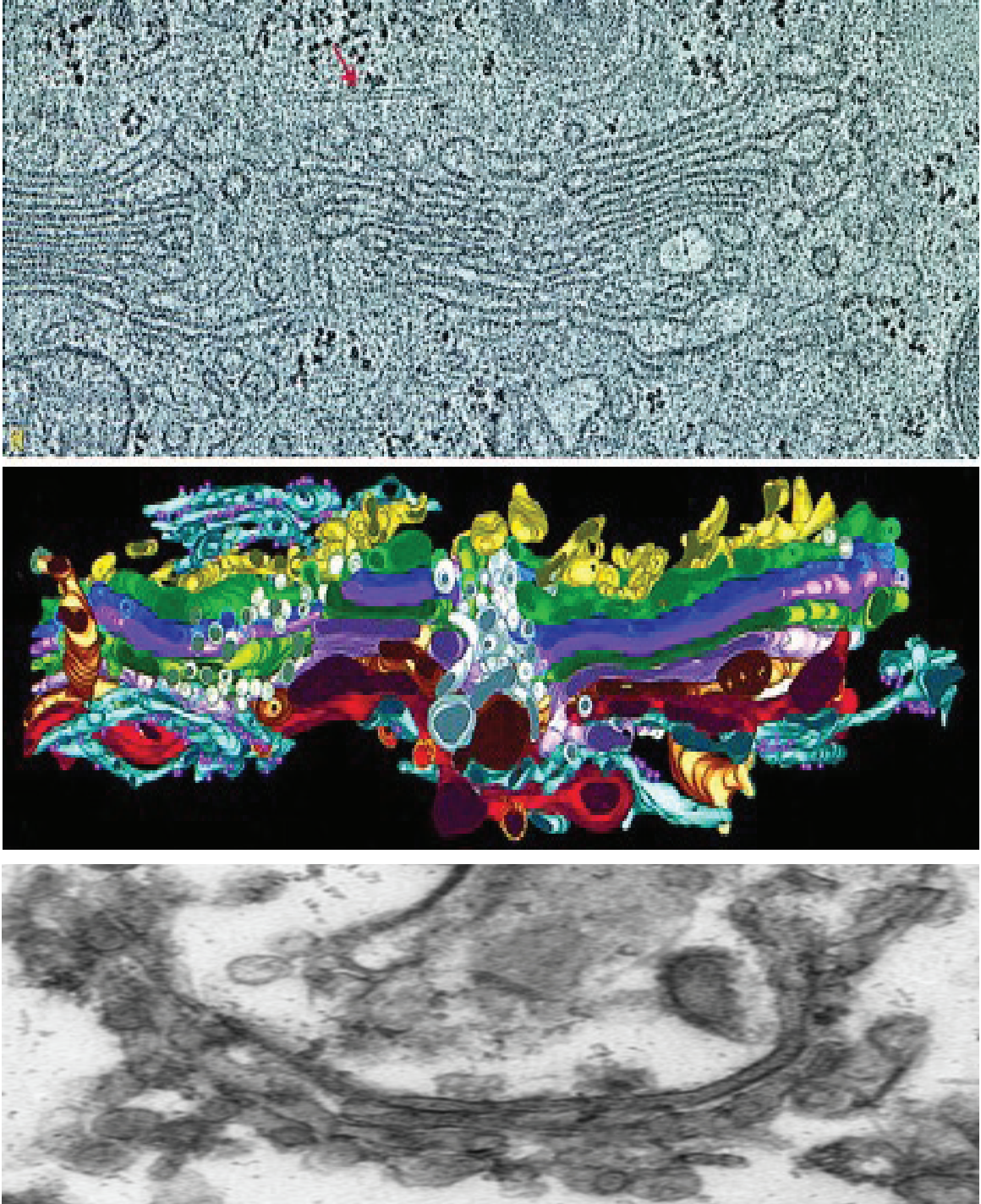


**Figure A. The Golgi apparatus.** Electron microscopy (EM) representation of the Golgi within a cell (**up**), after 3d tomography analysis (**middle**) or as it appear after sucrose gradient purification (**bottom**) as in <sup>17</sup>. \*Figures (up and middle) are from <sup>22</sup>. Note: a microtubule is identified for comparison (red arrow).

The elucidation of the mechanisms underlying the transport of cargo proteins within the Golgi apparatus is currently the subject of great debate <sup>14, 18, 19, 57</sup>. Several models have been proposed over the course of the years. These models tried to explain how an organelle could sequentially and efficiently glycosylate cargo molecules and at the same time segregate the glycosylation enzymes from the cargo protein flow in order to maintain the Golgi apparatus distinctive molecular and morphological identity.

## **Section 1.2: The Static Vesicular Transport Model**

In a classical experiment, Jamieson and Palade, were able to inhibit protein synthesis and discovered that it had little effect on the shape of the Golgi apparatus at the level of electron microscopy <sup>58</sup>. It appeared to be static. Subsequent electron microscopy studies of the Golgi apparatus also determined that small, spherical membranous structures were located in proximity to the flattened cisternae <sup>59, 60</sup>. Furthermore, EM studies revealed that each cisterna of the Golgi apparatus had different proportions of glycosylation enzymes, organized *cis* to *trans* to sequentially glycosylate cargo proteins <sup>61-64</sup>. In order to accommodate a model to the investigative results presented in these experiments, i.e. static Golgi, abundant vesicles and enzymatic gradient, a novel working model that would explain these findings was suggested.

In the vesicular transport model <sup>60</sup>, cisternae are distinct from each other and possess their characteristic ratios of glycosylation enzymes. Movement of cargo from one cisterna to another is the consequence of anterograde vesicular transport: vesicles sequentially bud from one cisterna and fuse with the next cisterna located in the *trans* direction, forming a cycle that is repeated until the cargo proteins have visited every cisterna. Newly formed cargo proteins would therefore be sequentially glycosylated as they move from one cisterna to the next (fig. B). Therefore, cargo proteins would encounter each of the glycosylation enzymes in sequence. At the same time, Golgi resident enzymes are envisaged to be excluded from the vesicles and remain into their cisternae, thus keeping the ratio of glycosylation enzymes intact.

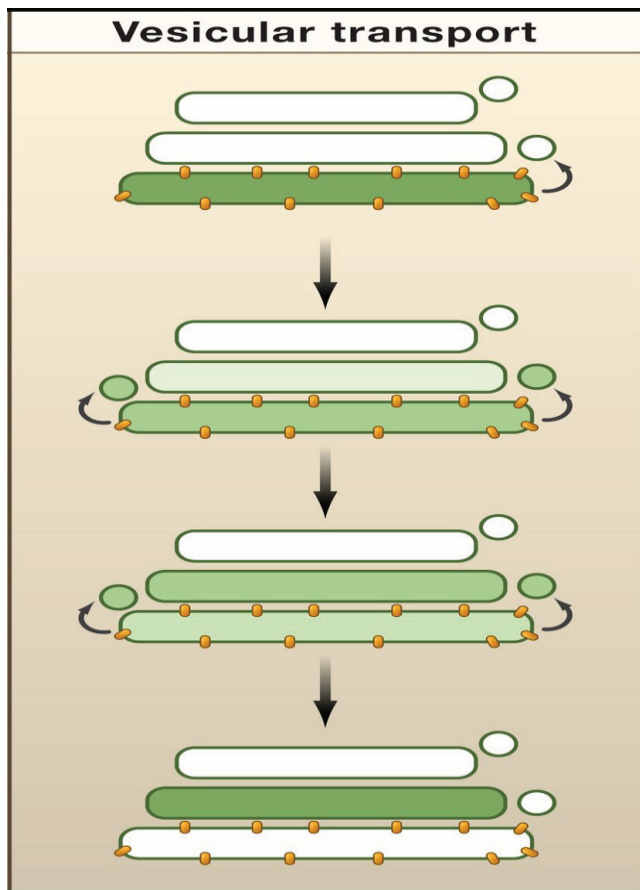


**Figure B. The vesicular transport model.** In this model, glycosylation enzymes are in gold, while cargo is represented in green. The cis face is at the bottom and the trans face is at the top<sup>from 19</sup>. Cargo is seen moving from one cisternae to the next, while Golgi resident enzymes are static.

This model was able to explain the finding of the vesicles under EM as well as the structured glycosylation enzymes distribution of the Golgi apparatus. It was also supported by investigations that demonstrated that transport could occur between purified cisternae from different cells and that these transport events were mediated by cargo contained within vesicles<sup>65, 66</sup>. At the same time, it was demonstrated that vesicle formation was dependent on coatamer proteins I (COPI proteins)<sup>59, 66-69</sup>.

### Section 1.3: The Cisternal Maturation model

However, contradictory evidence surfaced that jeopardized the vesicular transport model. First and foremost, the vesicular transport model would never be able to explain the transport of proteins larger than the 50 to 100 nm size of vesicles seen under electron

micrograph<sup>70-74</sup>. How could large proteins, in these cases<sup>70-74</sup> fish scales and procollagen, be secreted in such a model?

Second, new evidence pointing to COPI vesicles mediating retrograde transport was uncovered<sup>45, 46</sup>. COPI vesicles were discovered to possess Golgi resident enzymes and P24s proteins but only a small quantity of cargo proteins<sup>7, 8, 11, 12, 55, 75-78</sup>. It was also discovered that the CGN and the ER were the target of COPI derived vesicles<sup>45, 46, 55, 76</sup>, and that cargo could migrate through the Golgi without leaving the lumen of the cisternae<sup>79</sup>. Therefore, it appeared that the transport observed previously in the Rothman transport assay was not the result of cargo VSV-G being transported from one cisterna to the other, but rather the results of the transport of Golgi enzymes.

Furthermore, if the Golgi apparatus was by definition a static organ, one would expect to have a mechanism of inheritance similar to that of other organelles, such as mitochondria. However, studies of the Golgi apparatus during mitosis revealed that rather than separating equally, the Golgi apparatus actually disassembles and is dispersed stochastically throughout the cell and within the ER<sup>80-82</sup>.

Lastly, while the static vesicular transport model can explain the flux of proteins between the organelles of the secretory pathway, it failed to explain the flux of lipids. In effect, such a system would result in a very large flux of lipids from the ER to the Golgi and eventually from the Golgi to post-Golgi organelles. The next model would have to accommodate the lipid flux as well and present a way to recycle them.

In the wake of these observations, a second model, the cisternal maturation/progression model was developed. This model actually predated the vesicular transport model but had been abandoned in the wake of the success of the vesicular transport model<sup>83</sup>. In this model, transport is achieved through the Golgi by each cisterna slowly maturing from the *cis* to the *trans* face of the Golgi apparatus. This system allowed for large proteins that were unable to be incorporated within vesicles to be sequentially glycosylated<sup>72</sup>.

In this model, when cisternae are moving from *cis* to *trans*, they are acquiring Golgi resident enzymes from previous cisternae. These enzymes move in a retrograde direction, from *trans* to *cis*. This movement of Golgi resident enzymes is mediated by COPI vesicles. Therefore, as the cisterna progress along the Golgi apparatus, it matures by obtaining a new set of glycosylation enzymes.

Therefore when new VTC's arrive from the ER, they would slowly become a cisterna by fusing with COPI vesicles that would bud off from the Golgi apparatus. This process would be repeated over and over from cisternae to cisternae where the *trans* most cisternae would continuously send retrograde vesicles to *cis* located cisternae. In the process, cargo proteins would be sequentially glycosylated. Eventually, the cisternae evolve into the TGN where their membrane is vesicularised and the cargo is sent to post-Golgi targets (fig. C) <sup>for review 18, 57, 84-88</sup>. Overall, retrograde oriented COPI vesicles can account for the continuous recycling occurring along the Golgi apparatus, as well as from the Golgi apparatus to the ER. It also allows the Golgi apparatus to remain in a lipidic steady state, where the amount of lipids going to the Golgi is equivalent to those exiting from the Golgi.

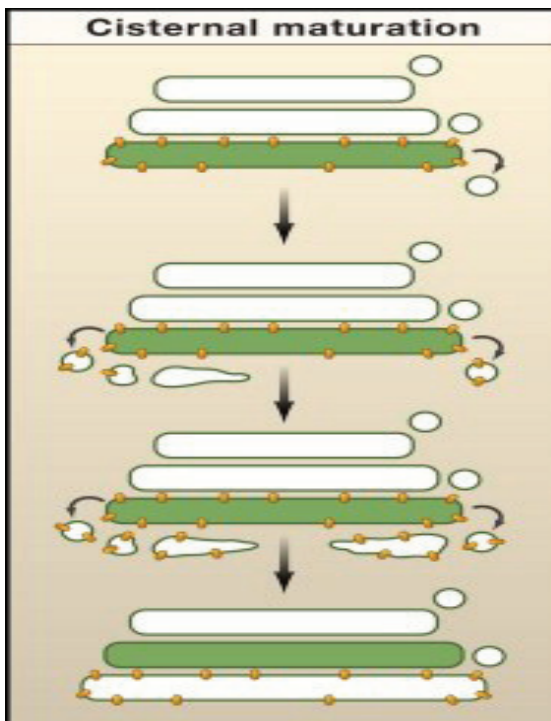


**Figure C. The cisternal maturation model.** A Golgi resident enzyme is represented as gold circles, while cargo proteins are green <sup>from 19</sup>. Here, it is the Golgi resident enzymes which are incorporated into vesicles.



#### **Section 1.4: Improvements on Cisternal Maturation: The percolating model <sup>14</sup>**

Following the development of the cisternal maturation model, it was noticed that while it can account for the data about the processing of large macromolecules, it appeared at first (see <sup>79</sup> for conflicting results) that the rate at which macromolecules were being processed was much slower than the transition time of smaller molecules <sup>14, 72</sup>. When the Golgi apparatus was modified to allow large fusion proteins to enter vesicles, the rate at which the large proteins were processed was greatly increased, implying that the vesicles could move in an anterograde direction <sup>89</sup>. Furthermore, while the presence of retrograde transport carriers had been widely accepted, two publications from the Orci and Rothman group <sup>90, 91</sup> demonstrated that COPI vesicles around the Golgi apparatus were depleted of Golgi resident enzymes and contained cargo instead. It was suggested that there could be more than one type of COPI vesicles <sup>90</sup>. A model was put forth that explained these results: large macromolecule would move along the Golgi apparatus by cisternal maturation, while smaller molecules would bud and fuse back and forth between cisternae in the anterograde direction, alike what had been proposed in the vesicular transport model. At the same time, concurrent COPI vesicles would recycle ER and Golgi resident enzymes in a retrograde direction (fig. D).

Since this model has been proposed, several subtypes of COPI vesicles have been identified. Lanoix et al. <sup>11</sup> was able to purify two subtypes, one enriched in p24 and one enriched in Golgi resident enzymes. This work was followed by Malsam et al. <sup>55</sup> which were able to purify two different types of COPI vesicles using tether pairs as purification tools: one with Golgi resident enzymes and one with p24 and cargo proteins. This was further investigated by Béthune et al. <sup>49</sup> who demonstrated that COPI can discriminate between ER enzymes and p24 proteins. The ability of COPI vesicles to sense specific cargo proteins and differentiate between them could point to a mechanism that would make COPI vesicles very polyvalent in terms of the cargo they transport.



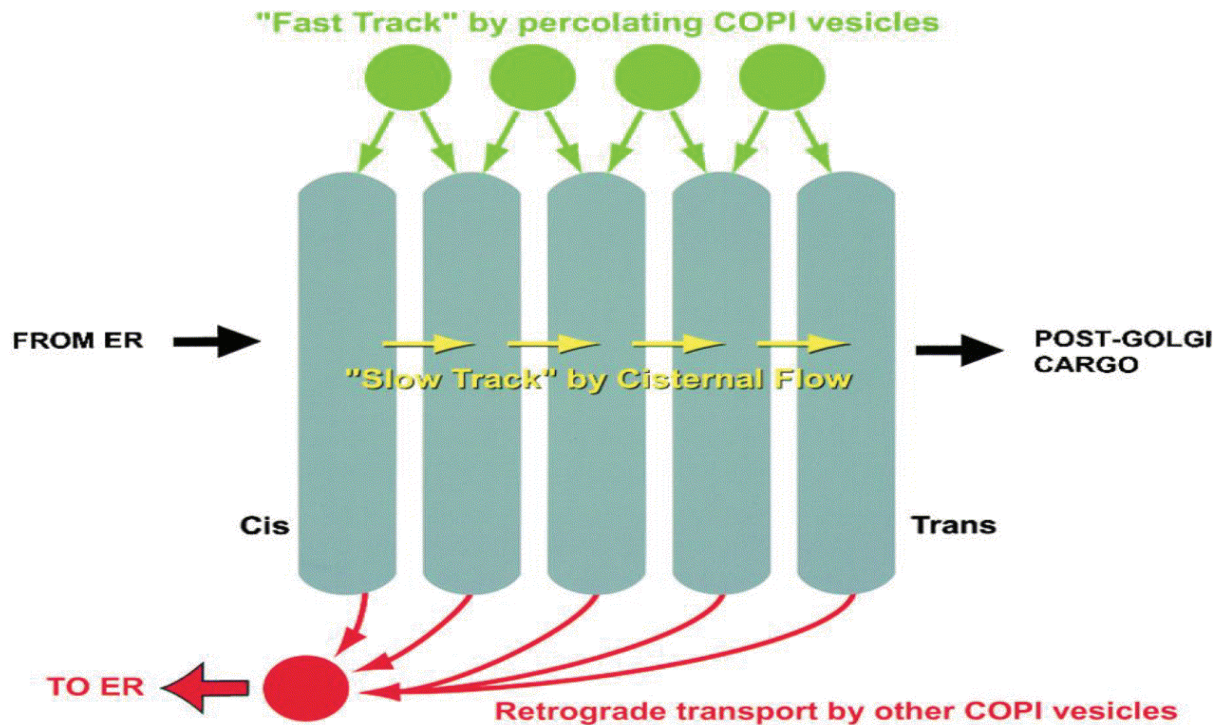


**Figure D. The percolating Golgi.** In this model, COPI vesicles percolate, both with anterograde cargo (green) and with ER and Golgi resident enzymes (red \*note: the percolation here is not shown<sup>see 14</sup>), the red arrows indicate the overall direction of flow in a retrograde direction. At the same time, large proteins and molecules move by slow cisternal maturation<sup>from 14</sup>.

### Section 1.5: Improvement on Cisternal Maturation: The heavy workload model<sup>18</sup>

Another version of the cisternal maturation model was proposed recently to account for the observed formation of membranous bridges, which were later termed "tubules", within the Golgi apparatus that connect different cisternae<sup>23, 40, 56, 92-95</sup>. To explain the presence of these tubules, it was demonstrated that these tubules often did not occur within cells with a normal secretory load, but rather when the cells were submitted to a temperature block resulting in the accumulation of cargo<sup>23, 92</sup>, in heavy secretory cells<sup>56</sup> or when it was submitted to secretory stimulus<sup>93</sup>. Simultaneously, other groups examining the structure of the Golgi failed to observe any tubules<sup>22, 77, 79, 96-99</sup> for review see<sup>100</sup>. Therefore, a new variant of the cisternal maturation model was established: at normal Golgi secretory activity, COPI vesicles would move back and forth from one cisterna to the other, in both retrograde and anterograde directions, while the cisternae would mature

from *cis* to *trans*. Under stress to augment secretory output, tubules would start to appear simultaneously to the transport by COPI vesicles (as seen in 23, 93) in order to give cargo proteins faster access to glycosylation enzymes (fig. E) <sup>18</sup>.

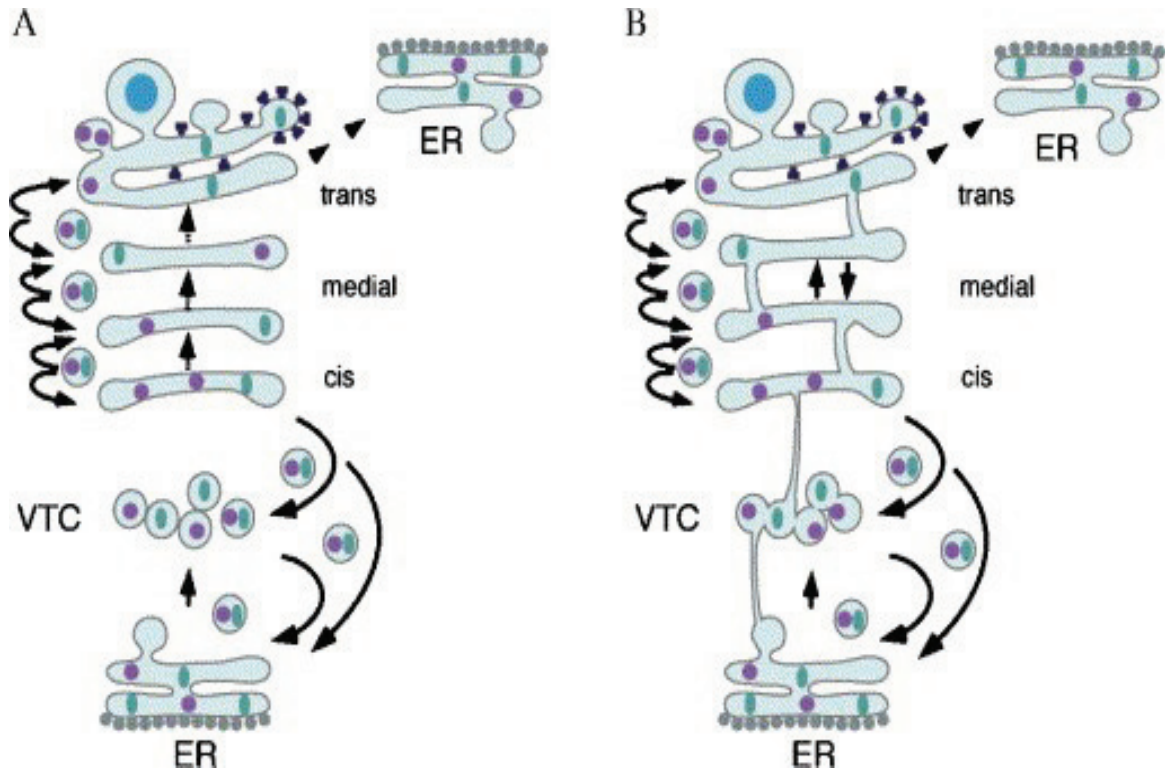


**Figure E. The two speeds/heavy workload model.** At normal secretory workload (**left**), cisternae maturation is supplemented with transport via anterograde and retrograde vesicles. When the Golgi experience superior secretory workload, tubules start to appear (**right, membranous connections between cisternae**) that mediate a faster glycosylation of proteins. Furthermore, this model also accounted for the COPI-independent recycling pathway from the Golgi to the ER, which is thought to be a way for the Golgi to recycle membranes <sup>from 18</sup>.

Furthermore, this new model also tried to give an explanation for two ongoing discoveries in connection with the Golgi apparatus. First the discovery of a COPI-independent transport pathway between the Golgi and the ER <sup>101-103</sup> and the fact that the ER and the Golgi appear to be closely associated at the TGN <sup>22, 96</sup> was interpreted as a way for the Golgi apparatus to get rid of excess membranes that could accompany the cisternal maturation model <sup>18</sup>.

Lastly, Kartberg et al.<sup>18</sup> tried to explain the mechanisms that could be involved in the gradient distribution of Golgi resident enzymes. The model implies that this is accomplished by COPI mediated transport<sup>7, 11, 55, 75, 77</sup> and that sorting within the COPI vesicles is dependent on ARFGAP1 through its action on ARF1<sup>11, 12, 104-106</sup>. However, the association between ARF1 and ARFGAP1 sorting and the actual selection of the proteins incorporated within the vesicles is open to debate. While it has been shown that some Golgi resident enzymes possess known cytoplasmic tail that interact with coatamer proteins, most Golgi resident enzymes do not have this characteristic<sup>18</sup>. Therefore, two possibilities have been put forward as to the mechanism that drives Golgi resident enzymes to establish a gradient along the cisternae of the Golgi apparatus.

The first one links the localization of proteins within the Golgi to the composition of their transmembrane domains<sup>107-109</sup>. It has been previously published that the concentration of cholesterol and sphingomyelin in the Golgi membranes increases from *cis* to *trans*, which in turn leads to an increase membrane thickness<sup>110</sup>. Considering that Golgi resident enzymes possess unusually short transmembrane domains with low hydrophobicity compared to PM proteins<sup>111-113</sup>, it was suggested that the size of the lipid bilayer would dictate in which Golgi cisternae the Golgi resident enzymes would locate<sup>18</sup>. In such a model, Golgi resident enzymes which are located in *trans* of their preferred cisternae would segregate to local regions of lower sphingomyelin and cholesterol content within the cisternae. It was shown that COPI vesicles form preferentially in regions with such lipid characteristics<sup>114, 115</sup>.

However, other studies have shown that often, the size of the transmembrane domain was not sufficient for Golgi localization<sup>116-120</sup>. Therefore, another model was proposed: in the "kin" recognition model, the gradient distribution of Golgi resident enzymes is due to the formation of complexes (homo- or hetero-dimers) between Golgi resident enzymes. An enzyme would thus be retained within cisternae depending on its ability to form complexes<sup>121-123</sup>. Furthermore, it was also hypothesized that the pH might play an important role in the sorting of Golgi resident enzymes, since pH seems to be a critical factor in the formation of complexes and that pH loses one log value between the ER and

*trans* cisternae<sup>118</sup>. Therefore, different proteins would form complexes at certain pH's. In this scenario, an enzyme's ability to form complexes would determine its rate of incorporation within COPI vesicles and its localization within the Golgi apparatus<sup>18, 118, 124-126</sup>.

## Analysis

A recent publication<sup>127</sup> proposed another mechanism that would explain the retention of glycosyltransferases into COPI vesicles. They discovered, using yeast genetics, that the protein Vps74p served as a linker that binds multiple Golgi resident proteins as well as COPI proteins. They were able to demonstrate that deletion of the Vps74 gene resulted in mislocalization of Golgi resident enzymes. They were also able to pinpoint a conserved amino acid sequence present on the cytoplasmic tail of the Golgi resident enzyme necessary for their binding to Vps74p and proper localization. Therefore, it is possible that a third factor would come into play; the localization of the Golgi resident enzymes might depend on their affinity for adaptor proteins that would mediate their recruitment into COPI vesicles. A similar system is seen in clathrin coated vesicles with AP-1 and its homologues<sup>128, 129</sup>.

With regards to the last two models that include anterograde directed COPI vesicles transport, a criticism can arise from the fact that while intra-Golgi anterogradely-directed vesicles have been identified on EM<sup>90, 91, 130</sup>, they have yet to be isolated biochemically. Recent studies, as well as our own development of the fusion assay have not demonstrated the presence of these vesicles<sup>7, 8, 10, 55</sup>, even when the cells displayed high level of secretory activity<sup>77, 79, 131</sup>. Furthermore, the findings of peri-Golgi vesicles depleted of Golgi resident enzymes<sup>132</sup> have been under severe criticisms, as it has been argued that the techniques used to make these discoveries were not optimal<sup>133</sup>.

Kartberg et al.<sup>18</sup> acknowledges this problem, and stipulates that, since some anterograde COPI vesicles have been found and are probably active between VTCs and the CGN or in the cis-most part of the Golgi<sup>55</sup>, anterograde vesicles could exist in other parts of the

Golgi apparatus<sup>18</sup>. In contrast, Rabouille and Klumperman<sup>133</sup> dismiss this<sup>55</sup> evidence for anterograde vesicles. They observe that while the “anterograde” vesicles described in Malsam et al.<sup>55</sup> were shown to have more cargo protein than the “retrograde” vesicle, it was not shown to be more concentrated than in the cisternae<sup>55</sup>. In this<sup>55</sup> as well as in previous publications<sup>90, 91, 130</sup>, it is possible that the cargo proteins found in peri-Golgi vesicles are due to insufficient sorting from the COPI machinery resulting in the leaking of cargo in COPI vesicles. This concept has been demonstrated in a recent proteomics study, where cargo was present but not enriched in COPI vesicles<sup>7</sup>. It is to be noted that the absence of evidence is not evidence itself as there might be a mechanism that would allow an anterograde subtype of COPI vesicles to be formed: ARF1 sorting abilities allows for the selection of various cargoes<sup>11, 55, 78, 134</sup> which in combination with the recent discovery of new coatomer sub-units allows the possibility for multiple coatomer polymerization pathways that could influence the selection of cargo proteins<sup>135</sup>. Furthermore, since Malsam et al.<sup>55</sup> demonstrate a link between subtypes of COPI vesicles and their tethers, it could be possible that the tethers are involved in the cargo selection process themselves<sup>133</sup>.

Lastly, the last two models do not take into account that VSV-G and pro-collagen 1, a 300 nm protein, were demonstrated to be transported through the Golgi apparatus at the same rate, without leaving the lumen of the cisternae and in the absence of observable tubules<sup>79</sup>.

## **Section 1.6: Improvement on Cisternal Maturation: Rapid Partitioning within a Two-Phase Membrane System model<sup>19</sup>**

While the cisternal maturation model can account for most experimental findings concerning the regulation of Golgi transport, it does not explain all findings. Publications from the Lippincott-Schwartz laboratory and others using proteins tagged with GFP suggested that rather than consisting of separate static cisternae, the Golgi apparatus was able to communicate quite easily between the different cisternae, either through tubules, or through vesicles<sup>14, 36, 136</sup>. Their group first proposed a model of the Golgi which would

be more dynamic and in which tubules are the norm, not the exception as in Kartberg et al.<sup>18</sup>. This view was further supported by the demonstration that tubules, not vesicles, were responsible for the transport of proteins across the Golgi Stack<sup>132</sup> and that peripheral Golgi vesicles were depleted of Golgi resident enzymes, which would be expected in the typical cisternal maturation model<sup>91, 132</sup>. Furthermore, the Mironov and Luini groups also proposed that not only cargo, but also Golgi resident enzymes could travel from one cisterna to another via these tubules<sup>23, 132</sup>.

In contradiction to what would be expected from the dynamic model, Trucco et al.<sup>23</sup> also demonstrated that, when cargo proteins were incorporated into the Golgi apparatus, they did not readily redistribute to all cisternae, but rather advanced smoothly over time from the *cis* face of the Golgi apparatus to the *trans* face, similar to what would be expected of the cisternal maturation model.

In this context of controversy, Patterson et al.<sup>19</sup> studied the exit and entry rates from the Golgi apparatus of secretory cargo proteins. They first infected cells with three different types of secretory cargoes. Using an inverse fluorescence recovery after photobleaching methodology (iFRAP), they then bleached the whole cell except of the Golgi apparatus and studied the transfer of signal from the Golgi apparatus to the remainder of the cell. Using a large luminal, a small luminal and a transmembrane cargo protein, they were able to determine that the different cargoes would exit the Golgi apparatus in a decreasing exponential curve, in which the exit rate from the Golgi apparatus was proportional to the amount of cargo present. This result seems to indicate that all Golgi cisternae behave as one common organelle.

They continued this investigation with a short pulse experiment in order to determine if cargo proteins, once they have entered the Golgi, could exit rapidly, in accordance with their model. They infected cells with a variant of the VSV which stably express VSV-G(TS045)-GFP. However, in this experiment, they first started by bleaching the Golgi apparatus, which was followed by a 5 minute pulse allowing the VSV-G(TS045)-GFP to repopulate the Golgi apparatus. Following the pulse, they bleached the whole cell and



recorded the loss of signal from the Golgi apparatus as proteins were being exported. Again the loss of signal had the characteristics of an exponential curve. In order to make sure that no new signal would come from the ER, they performed these sets of experiment at the non-permissive temperature (40°C) in order to avoid newly produced VSV-G(TS045)-GFP from forming<sup>137</sup>. Furthermore, the incubation time had been chosen to be much less than what was previously demonstrated to be needed for the cisternal maturation model<sup>23, 79</sup>.

Their experimental data suggest that any cargo molecule, when it is present in any cisterna of the Golgi apparatus, has an equal chance of being exported from the Golgi, independently of when they arrived in the Golgi. This leads to a first order kinetic curve where the quantity of protein that is being exported is directly proportional to the amount of protein that is present in the Golgi apparatus, and not proportional to the amount of cargo protein present in the TGN, as would be predicted by the cisternal maturation model. Furthermore, their model proposes that not only the TGN, but also that every cisterna has export sites. Such a system could explain the discoveries of peri-Golgi vesicles that were enriched in cargo and not Golgi resident enzymes<sup>90, 91, 132</sup> and also the discovery of novel proteins thought to be potentially involved in transport from Golgi/TGN to the PM<sup>138, 139</sup>.

With the use of Berkeley-Madonna, a software used to design biological models<sup>e.g. 8</sup>, they examined the ability of the current cisternal maturation model, with progressive movement of cargo along the Golgi apparatus and continuous recycling of Golgi resident enzymes, to fit the experimental data. They controlled two variables; the rate of cisternal maturation and the rate of enzyme recycling. They were able to obtain a model that would explain these rates, but only when they substantially increased the rate of cisternal maturation to much higher values than previously observed and after they had reached a level of recycling of 30%. However, such a recycling rate was unable to sustain a cargo wave like the one seen in Trucco et al.<sup>23</sup>, as the wave would rapidly lose its cargo content to extensive recycling.

Previous work had demonstrated that the Golgi apparatus possess specialized exit domains, which export cargo from the Golgi apparatus and could probably not be from the TGN <sup>140</sup>. Patterson et al. studied the partition of newly formed cargo compared to these export domains and were able to demonstrate that upon entering the Golgi, cargo proteins readily distribute themselves in regions where processing enzymes were present as well as regions where exit domains were located. They also demonstrated that cargo proteins were able to exchange between these domains, therefore always keeping the exit domain supplied with cargo to export.

While their model could fit and explain the behavior of cargo within their experimental setup, a hypothesis had to be put forth in order to explain the behavior of Golgi resident enzymes, more precisely their gradient distribution across the Golgi stack <sup>61-64</sup>. Patterson et al. stipulated that the Golgi apparatus consisted of a lipid gradient across the stack, with various compositions of lipids. According to their theory and alike what was mentioned before, the *cis* face of the Golgi had a more ER-like lipid composition as its main lipid component was glycopospholipids, while the *trans* most cisternae resembled the PM, which is composed predominantly of sphingolipids. The cisternae in between gradually change their lipid composition *cis* to *trans* <sup>62, 141-143</sup>. The resulting changes in lipid composition modify the size of the lipid bilayer. Golgi resident enzymes then migrate to the layer that is the most energetically favorable for them, resulting in the formation of the observed gradient <sup>111, 144</sup>. It is also to be noted that in order for the lipid gradient to remain stable, the rate of exchange of lipids from one cisterna to the other during vesiculo-tubular cargo transport must remain below a certain value; if not, the lipid gradient would not be stable and the Golgi apparatus would become mixed and undifferentiated *cis* to *trans*.

Patterson et al. then used their model to explain the results seen in Trucco et al. <sup>23</sup>. According to their model, the 40°C to 15 °C temperature shift needed to concentrate the VSV-G in the CGN also results in a shift of the lipid composition of the CGN, resulting in an increased presence of sphingolipids in the CGN (see fig. F) and the destruction of the normal Golgi lipid gradient. When the cells are allowed back at the permissive



temperature, each cisterna slowly recuperates its steady state gradient. Since VSV-G also possess a preferential GPI/SL in *cis* cisternae<sup>19</sup>, it would migrate from one cisterna to the other as their lipid composition changes to a GPL/SL ratio that corresponds more to CGN values which is preferential for the localization of VSV-G, reproducing what could be seen as a wave of cargo inside one cisterna<sup>23</sup> which is maturing from *cis* to *trans*.

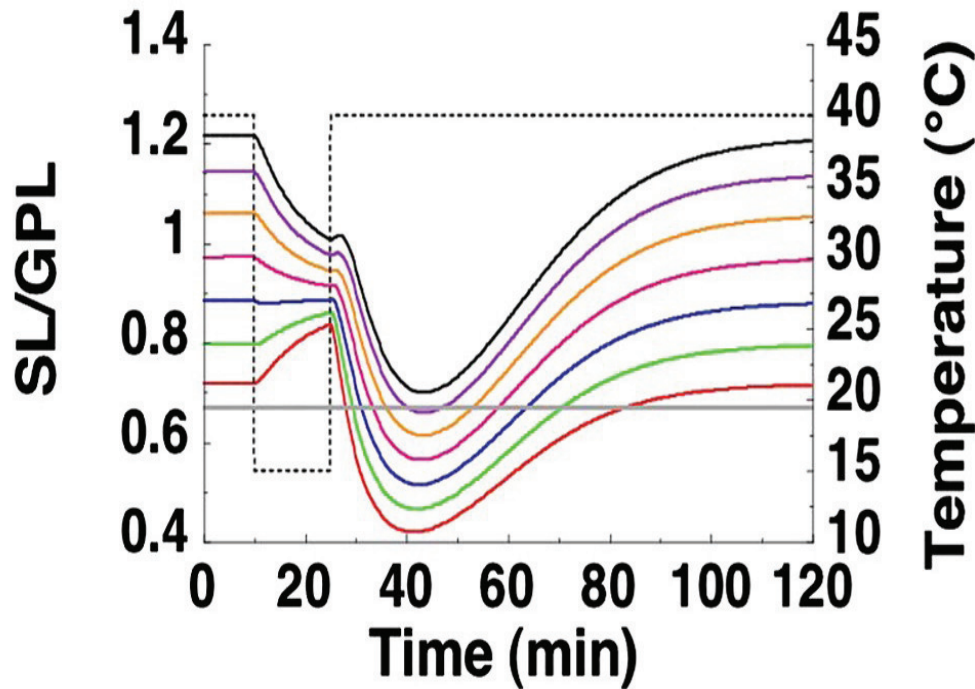


**Figure F. The Golgi Lipid gradient** from <sup>19</sup>. SL/GPL ratios (left axis) in the Golgi exit domains are shown for cisternae 1 (red line) through 7 (black line). The temperature is indicated by the dashed black line (right axis) and indicates the 40°C-15°C-40°C shifts, while the horizontal gray line indicates the SL/GPL ratio hypothesized to be optimal for VSV-G partitioning. verify if the vsv-g is more stable in *trans* how come, the grey line is so low?. The course of the Horizontal grey line indicates that VSV-G would rapidly migrate from *cis* to *trans* and then equilibrate between cisternae, as seen in <sup>23</sup> (Text was adapted from <sup>19</sup>).

Overall, the resulting model is determined by concepts that are derived from the observed kinetics of cargo export and from previously published data (fig. G):

- 1) There is a lipid gradient between ER-lipids (glycerophospholipids) and PM-lipids (sphingolipids).
- 2) The Golgi resident enzymes preferentially settle in certain ratios of ER-like vs PM-like lipids.

- 3) There is a constant kinetic for vesiculo-tubular traffic (the publication is not more precise to determine if the transport is vesicular or tubular) that shuttles cargo back and forth between the Golgi cisternae.
- 4) Cargo exit is allowed from all cisternae, and cargo can shuttle from cargo exit sites to processing sites.
- 5) There is constant retrograde and anterograde transport between the Golgi and ER and between the PM and the Golgi.

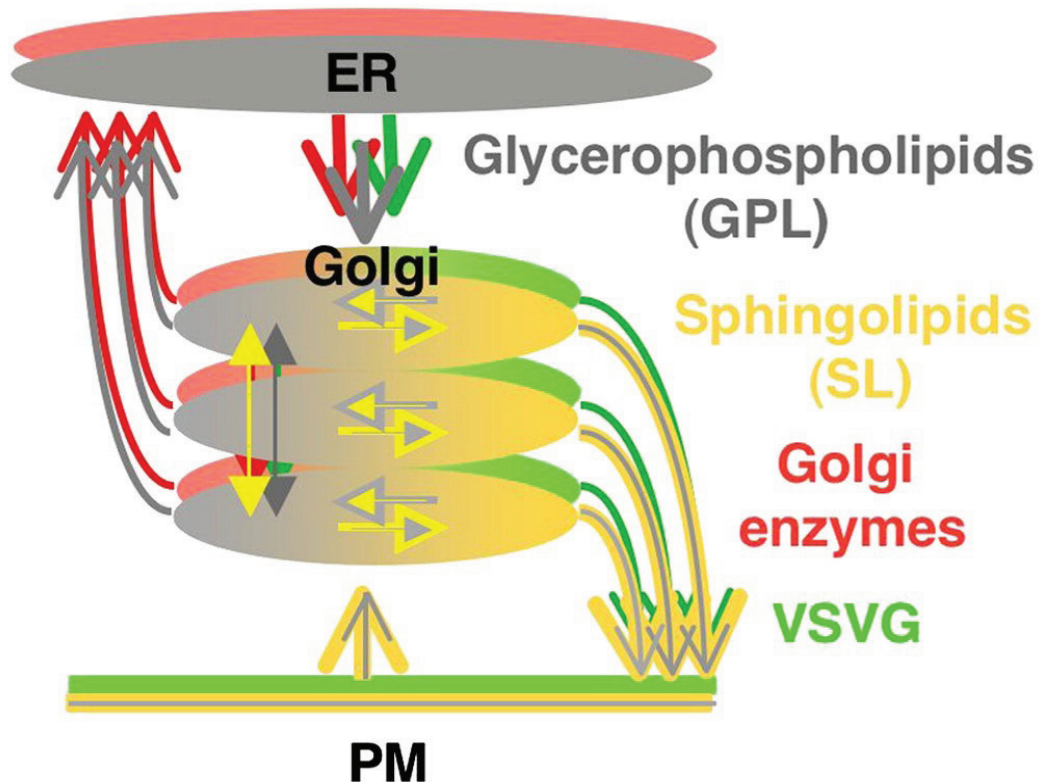


**Figure G. The Rapid Partitioning within a Two-Phase Membrane System** <sup>From 19</sup>. The Golgi is composed of rapidly transported cargo between cisternae (**vertical arrows**). Transport of Golgi resident enzymes (**red**) and cargo (**green**) is due to their stability in GPL (**grey**) versus SL (**yellow**) lipids, the gradient of which increase from *cis* to *trans*. Furthermore, VSV-G can exchange from regions enriched in Golgi resident enzymes to regions with exit sites (**horizontal arrows**). The Golgi is in constant flux between the ER and PM (**curved arrows**).

## Analysis

Patterson et al., seems able to explain much of the contradictory information emerging from the study of the Golgi apparatus. They present a new model that consistently

summarizes their previous findings and can explain the contradictory finding of Trucco et al.. However, we should point out the following items:

1) One problem is that it oversimplifies the interaction between the proteins and the lipids that surround these proteins. While the thickness of the bilayer leaflet affects the entropy of a protein in a given system, its interactions are not limited to size. The lipid charge and the resulting ionic interactions as well as the identity of the lipid head group allows for numerous non-covalent interactions (example see 128, 145-149). However, this criticism is partly addressed in a recent publication that demonstrated that the inhibition of non-vesicular lipid flow from the ER to the Golgi leads to inhibition of post Golgi transport as the VSV-G has a decrease ability to leave the Golgi apparatus <sup>150</sup>. Furthermore, the increasing evidence that COPI mediates localization (see previous section) points to the possibility that cytoplasmic tails as well as adaptor proteins plays a role in the localization of Golgi resident enzymes <sup>127</sup>.

2) While its first data for the export kinetics uses a trio of reporter proteins, most of the data is generated with a VSV-G(TS045). It would be interesting to know if endogenous cargo proteins behave in the same fashion.

3) The model requires the equilibration of anterograde cargo proteins over the Golgi stack. This is said to be done with a “vesiculo-tubular” character, similar to what had been predicted <sup>14</sup>. While the presence of tubules had been demonstrated, they have been so only in very specific conditions that might or might not reflect the Golgi apparatus at steady state. Furthermore, the publication acknowledges that there would be a possibility, in the presence of the formation of constant and numerous tubules, that the lipid gradient would be lost due to the mixing of lipids between the cisternae. Therefore, the rate of tubule formation should be high enough to allow migration of cargo through the cisternae and low enough so that the lipid gradient is maintained. The same reasoning applies to models that would use vesicles instead of tubules <sup>14, 18</sup>, as they also carry lipids.

4) It is a possibility that other models would also fit the experimental data. The description of the recycling mechanism of the Golgi apparatus is not optimal, as it has been shown that several subtypes of COPI vesicles exist which do not recycle proteins in the same manner and have different targets<sup>11, 75, 78</sup>. The description of recycling is that COPI vesicles can fuse with any *cis* cisterna. It has been shown that vesicles have distinct targets, one of them being the CGN<sup>55, 76</sup>. While it has been demonstrated that these vesicles are not concentrated in cargo proteins, they do contain some cargo proteins<sup>7, 55, 75, 76</sup> and the result of sending cargo in *cis* to the Golgi apparatus would definitively flatten the last portion of the curve. One would be curious to know if the cisternal maturation with continuous recycling model, with these modifications and taking into account that all cisternae can have exit sites, would also fit the data.

5) While exit from the Golgi is demonstrated to be the quasi-monopole of the TGN<sup>review 37</sup>, White et al.<sup>140</sup> do show potential evidence of TGN independent post-Golgi transport. However, even the authors were reluctant to classify this as such. One can also wonder if their model requires the presence of such exit sites: if there is rapid and discrete connections between stacks of the Golgi and between Golgi and the TGN, would that not imply that theoretically, all cargoes have access to the TGN and therefore are equally susceptible of being exported?

6) Finally, it also seems this model could explain previous contradictory findings in regards to COPI vesicles. Preceding publications<sup>90, 91, 132</sup> had demonstrated the presence of round spherical structures in the vicinity of Golgi apparatus which seemed deprived of Golgi resident enzymes and enriched in cargo proteins. These spherical structures were thought to be COPI derived vesicles and therefore a controversy arose about the nature of COPI vesicles, *i.e.* if they contained cargo or Golgi resident enzymes. With the discovery of exit sites present in every cisterna of the Golgi apparatus and in the context of Patterson *et al.* practical demonstration of this model<sup>19, 140</sup>, it would be possible that the vesicles identified previously are not retrograde COPI vesicles (as described in<sup>7, 11, 55</sup>) but rather another type of vesicles of yet undetermined nature that would bud from the Golgi exit sites.

## Section 2: COPI vesicles

### Section 2.1 : Anterograde vs retrograde

Fries et al.<sup>151</sup> and Balch et al.<sup>65</sup> first demonstrated that transport was possible between two Golgi cisternae isolated from different cells by studying the glycosylation of VSV-G. Using the glycoprotein as a reporter within a cell line that did not have an active N-acetyl-Glucosamine transferase (GlcNac-T1) and therefore was unable to correctly glycosylate VSV-G, they were able to complement the glycosylation of VSV-G by incubating purified mutated Golgi membranes *in vitro* with purified Golgi membranes from non-mutated cells. The question was asked: how did the VSV-G travel from one cisterna to the other?

COPI vesicles were first discovered in EM as round profiles devoid of clathrin markers in the peri-Golgi region<sup>59</sup> which were later associated with coatamer proteins<sup>68, 152</sup>. As a follow-up on its previous transport experiments, the Rothman group then demonstrated that the transport assay was dependent on the presence of coatamer generated vesicles<sup>66</sup>. They therefore assumed that these vesicles were transporting VSV-G glycoproteins from one cisterna to the other. Within the vesicular transport model, these vesicles were thus thought to transport cargo proteins in an anterograde direction, from a *cis* cisterna to one located in *trans*<sup>14</sup>.

However, the discovery of dilysine retrieval sequences on the cytoplasmic tail of ER proteins which were able to bind coatamer proteins provided first evidence of a retrograde transport mechanism<sup>45, 46</sup>. In the cell, ER proteins with these motifs that had escaped to the CGN or the Golgi are recycled back to the ER in a COPI dependent mechanism.

Following this discovery, sucrose gradient analysis of Golgi membranes revealed that VSV-G co-migrates with Golgi cisternae, and not within the same sucrose gradient as vesicles<sup>75</sup>. This observation was followed by the reproduction of GlcNac-T1 transport

from the Golgi to the CGN *in vitro*, which was later identified to be mediated by COPI vesicles that were enriched in glycosyltransferases and depleted of cargo <sup>12, 76</sup>. Measurements of the fusion kinetics of COPI vesicles as well as proteomic evaluation of protein content of purified COPI vesicles further demonstrated a potential role in retrograde transport <sup>7, 8</sup>. Finally, EM demonstrating the presence of peri-Golgi COPI vesicle enriched in Golgi resident enzymes seem to validate once more that COPI vesicles mediate retrograde transport <sup>77</sup>.

However, recent discoveries of up to three different types of COPI vesicles <sup>11, 55</sup> as well as contradicting evidence demonstrating the presence of peri-Golgi COPI vesicles depleted in Golgi resident enzymes <sup>90, 91, 132</sup> tend to demonstrate that a role for anterograde mediated COPI transport should not be excluded. This review, by the analysis of budding and fusion mechanisms, will try to identify levels of selectivity that could lead to the formation of COPI vesicle subtypes <sup>for review 18, 133</sup>.

## Section 2.2: Budding of COPI vesicles

The successful formation of COPI vesicles is the result of a sequential chain of events. First, the GDP bound form of ARF1 is recruited to Golgi <sup>153</sup> which leads to the recruitment and subsequent polymerization of coatamer proteins <sup>154-156</sup>. Upon binding to the membrane, ARF1 dimerizes and, with coatamer, modifies the curvature of the membrane which results in the formation of a bulge <sup>157, 158</sup>. Simultaneously, ARFGAP1 mediation of ARF1's GTPase activity mediates the sorting of proteins into vesicles. This is accomplished with the help of ARFGAP1, which also activates the subsequent uncoating of vesicles by releasing ARF1 into the cytosol <sup>for review 18 and figure H. \*</sup> To be noted, while the thesis was being published, a novel publication proposed a new mechanism for the recruitment of ARF1 to the membranes, see 153.

While coatamer complex continuously shuffles from the Golgi apparatus to the cytoplasm <sup>159, 160</sup>, its polymerization is dependent on the recognition of discrete motifs present in the cytoplasmic tails of integral membrane proteins <sup>45, 46</sup>. These motifs often, but not always,

contain a dilysine residue <sup>127, 161</sup>. This association is necessary for the successful polymerization of the coatomer complex required for vesicle formation.

Coatomer complexes themselves are composed of 7 subunits ( $\alpha$ ,  $\beta$ ,  $\gamma$ ,  $\delta$ ,  $\epsilon$ ,  $\zeta$ ,  $\beta'$ ), and are required for the successful budding of COPI vesicles. In this process, some level of diversification has been demonstrated which could explain in part the formation of several subtypes of vesicles <sup>55</sup>. First, it has been demonstrated with the discovery of two novel coat subunits,  $\gamma^2$  and  $\zeta^2$ , that the composition of the COPI coat can vary <sup>135</sup>. With the help of immunofluorescence, these two new subtypes did not colocalize with their isoforms  $\gamma$  and  $\zeta$  <sup>135</sup>, but rather seem active in different regions of the Golgi apparatus. It has also been suggested that the recruitment and assembly of proteins incorporated into COPI vesicles might be helped by adaptor proteins or lipids which would mediate the interaction of the cytoplasmic tails of membrane proteins with the coatomer <sup>127, 149, 162</sup>, thus referring another potential level of selectivity.

Since coatomer polymerization is dependent on the continuous association of ARF1<sup>GTP</sup> to the membrane, regulation of ARF1 is of critical importance. Similar to coatomer but with seemingly different kinetics, ARF1 shuttles back and forth between the cytosol and Golgi membranes <sup>159, 160</sup>. Its binding to Golgi membranes is tightly regulated by guanine exchange factors (GEFs) as well as GTPase activating proteins (GAPs) <sup>for review 18</sup>.

The importance of GEFs can be asserted by their sensitivity to brefeldin A, a fungal metabolite: incorporation of brefeldin A inhibits the exchange of ARF<sup>GDP</sup> to ARF<sup>GTP</sup> by blocking the GEFs and results in the dissociation of the Golgi apparatus and its redistribution to the ER <sup>163</sup>. One GEF, Golgi specific brefeldin A resistance factor (GBF1), seems to be particularly important in the Golgi apparatus <sup>6, 164-167</sup>. First, GBF1 was linked to the accumulation of coatomer on the Golgi apparatus in vivo <sup>168, 169</sup>. It was also demonstrated to be required for the reassembly of the Golgi apparatus after BFA treatment and for Golgi integrity, as knockdown of GBF1 resulted in the redistribution of the Golgi apparatus towards the CGN and the ER <sup>169</sup>. Surprisingly, knockdown of GBF1 also resulted in inhibition of secretion of transmembrane proteins, but not of luminal



proteins<sup>169</sup>. Furthermore, it seems that various GEFs might be involved in the regulation of ARF activity within the Golgi, as KO of other GEFs known as brefeldin A inhibited GEFs (BIG1 and BIG2) as well as depletion of GBF1 also impaired TGN activity<sup>170, 171</sup>. Considering that these GEFs and their family have been shown to modulate the different activities of several ARF family members<sup>172</sup> it would be interesting to investigate how GEFs contribute to COPI vesicle distinctiveness<sup>153, 173</sup>.

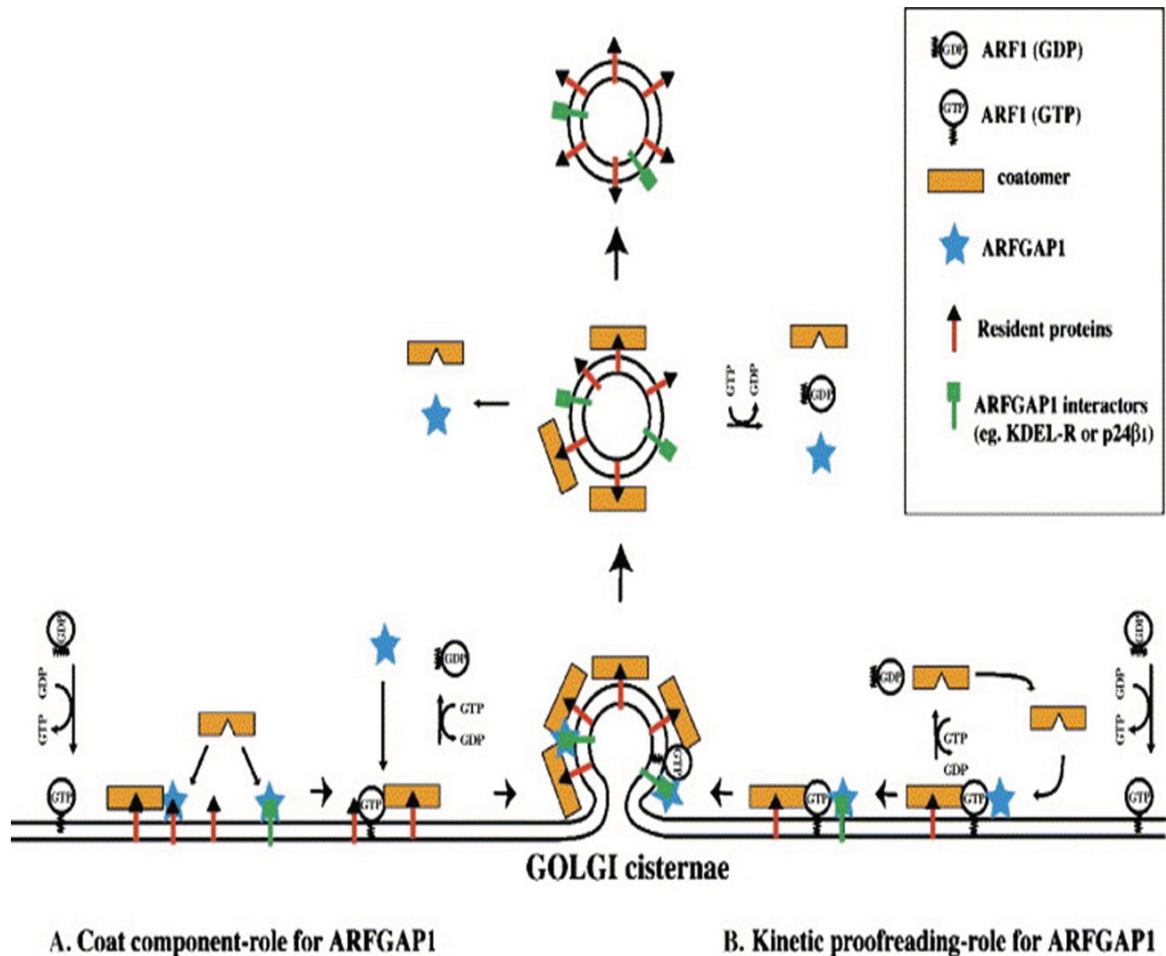


**Figure H. Two models for the role of the ARFGAP1 in COPI vesicle formation.** (A) In the coat component model, ARFGAP1 can recruit coatmer onto the cytoplasmic domains of cargo proteins. ARFGAP1 can also be recruited to pre-budding complexes consisting of ARF1/COPI when added to Golgi membranes. The GTP hydrolysis by ARF1, stimulated by ARFGAP1, then promotes budding of vesicles. Nascent-coated vesicles contain COPI and ARFGAP1 in stoichiometric amounts but appear to be relatively depleted of ARF1. This lack of ARF1 leaves the coat in an instable state that leads to subsequent uncoating. (B) Kinetic proofreading envisions a functional cycling of ARF1 on the membrane for sorting of cargo molecules. A cargo-dependent sequestering of ARFGAP1 inhibits GTP hydrolysis by ARF1. This results in a longer residence time of ARF1/COPI on the membrane allowing for coat polymerization, membrane deformation and vesicle budding. The sharp increase in ARFGAP1 activity as a result of membrane deformation may then overcome this inhibition enabling the vesicle to uncoat.

Text and figure from 18



The association of ARF1 with the Golgi membrane is also tightly controlled by GAPs, which regulate the hydrolysis of ARF1<sup>GTP</sup> to ARF1<sup>GDP</sup>. In the Golgi, ARFGAP1, which colocalizes with coatamer proteins to the juxtanuclear region of cells<sup>174, 175</sup>, has been shown to greatly enhance the GTPase activity of ARF1<sup>175</sup>. Overexpression of ARFGAP1 led to the redistribution of coatamer and ARF1 to the cytosol as well as redistribution of the Golgi resident proteins into the ER<sup>176</sup>. Furthermore, while coatamer and ARF1 are sufficient to create budding vesicles<sup>55, 177</sup>, the complementary action of ARFGAP1 is necessary for the sorting, uncoating and fission of COPI vesicles<sup>11, 104, 106, 178-180</sup>.

First, the recruitment of ARFGAP1 to the Golgi membranes is dependent on its interaction with the cytoplasmic tails of transmembrane proteins which also stabilize its activity<sup>11, 181</sup> and see figure H and probably through its interactions with ARF1<sup>182</sup>. After binding, ARFGAP1 has been shown to be involved in the sorting of Golgi resident enzymes into COPI vesicles<sup>11, 78, 106</sup>, as incubation of Golgi membranes with a non-hydrolysable form of GTP, GTP- $\gamma$ -S, leads to a continuously active ARF1 and to inefficient sorting of COPI vesicles<sup>7, 11</sup>.

ARFGAP1 has also been shown to stabilize the polymerization of coatamer by increasing the rate of binding between coatamer and the cytoplasmic tails of resident proteins<sup>181</sup>. Following the formation of the vesicles, ARFGAP1 mediates the hydrolysis of ARF1<sup>GTP</sup> to ARF1<sup>GDP</sup> which results in its dissociation from budded COPI vesicles<sup>175</sup>. The release of ARF1<sup>GDP</sup> then triggers the release of coatamer from the vesicles<sup>178</sup>.

In order to understand the process behind the uncoating of the vesicles, it became important to determine what factors could influence the activity of ARFGAP1. Bigay et al.<sup>183</sup> demonstrated that ARFGAP1 activity increased in areas with high positive membrane curvature. It does so by the action of two amphipathic regions of its non-catalytic domain that senses the curvature of the membrane as well as the presence of negatively charged lipids<sup>184, 185</sup>. Therefore, it was suggested that simultaneously to the

bulging and budding of the membrane, the activity of ARFGAP1 would increase, leading to the sequential uncoating of the vesicles <sup>186</sup>.

Finally, the actual membrane bulging and final vesicle fission also seem to be tightly regulated by ARF1 and ARFGAP1, respectively. The creation of vesicles requires the deformation of the membrane bilayer where a central region of positive curvature is surrounded by regions of negative curvature <sup>see 187 for details</sup>. ARF1, through its modulation of phospholipase D (PLD), increases the local concentration of phosphatidic acid (PA) <sup>188, 189</sup>. PA in return is degraded to diacylglycerol (DAG), an inverse-cone shaped lipid that further promotes the formation of negatively curved membranes <sup>190</sup>. Simultaneously, PA recruits the protein BARS-50 which <sup>191</sup>, with the help of ARFGAP1 <sup>192</sup>, finalizes the fission of COPI vesicles from the Golgi membranes <sup>180, 193</sup>.

The modulation of ARF1 GTPase activity by ARFGAP1 is primordial for the formation of COPI vesicles. However, recent studies have demonstrated that ARFGAP1 is not the only ARFGAP involved in the formation of COPI vesicles, as ARFGAP2 and ARFGAP3 are also implicated <sup>194</sup>. Complementing what had been previously done in yeast <sup>for review 18</sup>, they were able to knockout the synthesis of ARFGAP2 which affected the retrograde transport of COPI vesicles. Furthermore, they demonstrated a functional overlap between ARFGAP1 and ARFGAP2/3 as any of them was able to rescue the cell from lethality when all of them were knocked down.

Overall, the versatility and variability of coatomer, GEFs and ARFGAPs could potentially explain the formation of COPI vesicle subtypes. It is possible that unique combinations of these three elements could be responsible for the formation of subtypes of COPI vesicles.

### Section 2.3: COPI vesicles fusion

With the use of the *in vitro*-based transport assay<sup>65</sup> where the glycosylation status of VSV-G protein is monitored, Rothman and co-workers could identify, confirm or in other ways characterize most of the important intra-Golgi transport components that we use today. The identification of NSF (N-Ethylmaleimide sensitive factor) and  $\alpha$ -SNAP (soluble NSF attachment protein) as being required for fusion of vesicles led to the insight that the membrane constituents of synaptic vesicles, VAMP and Syntaxin, were in fact receptors for NSF and SNAP<sup>195</sup>. Henceforth, these receptors were termed SNAREs (soluble NSF attachment receptors) and today form a large family of receptors that consists of 36 members in humans and is used in different complexes throughout the secretory pathway<sup>for a recent review, see 20</sup> (fig. I).

On a structural basis, SNAREs can be separated into R- and Q-SNAREs which form stable complexes consisting of 3Q and 1R SNARE (Q and R refers to amino acids glutamine and arginine, respectively, that are found in the central position of the SNARE motif, which is responsible for mediating fusion<sup>196</sup>). The 3Q:1R ratio is important for SNARE function *in vivo*<sup>197, 198</sup>. Currently, the most likely mechanism seems to be that 3Q SNAREs on the membrane (e.g. target Golgi) interact through their coiled-coil domains with 1R SNARE on the opposite membrane (e.g. COPI vesicles) and form parallel bundles, resulting in a *trans* SNARE complex (fig. J). According to the SNARE-pin hypothesis for membrane fusion<sup>199</sup>, the formation of a *trans* complex of SNAREs bridging both membranes is suggested to pull the membranes to within 4 nm of each other<sup>200</sup>. Indeed, Weber et al.<sup>199</sup> could fuse artificial liposomes containing SNAREs and this, together with the finding that such fusion depends on how the SNAREs are anchored to the membranes<sup>201</sup>, provide evidence for a SNARE-pin scenario which, albeit slowly, can drive fusion *in vitro*. These stable receptor complexes persist after fusion and such *cis* SNARE complexes then need to be dissociated in order for SNARE proteins to be reused in further fusion cycles<sup>202, 203</sup>. This dissociation is mediated by the NSF complex, which is recruited through the binding of  $\alpha$ -SNAP molecules to the SNARE complex<sup>195, 204-206</sup>.

After NSF mediated unwinding, the 3Q SNAREs are ready for another round of fusion while the 1R SNARE can be recycled (fig. J).

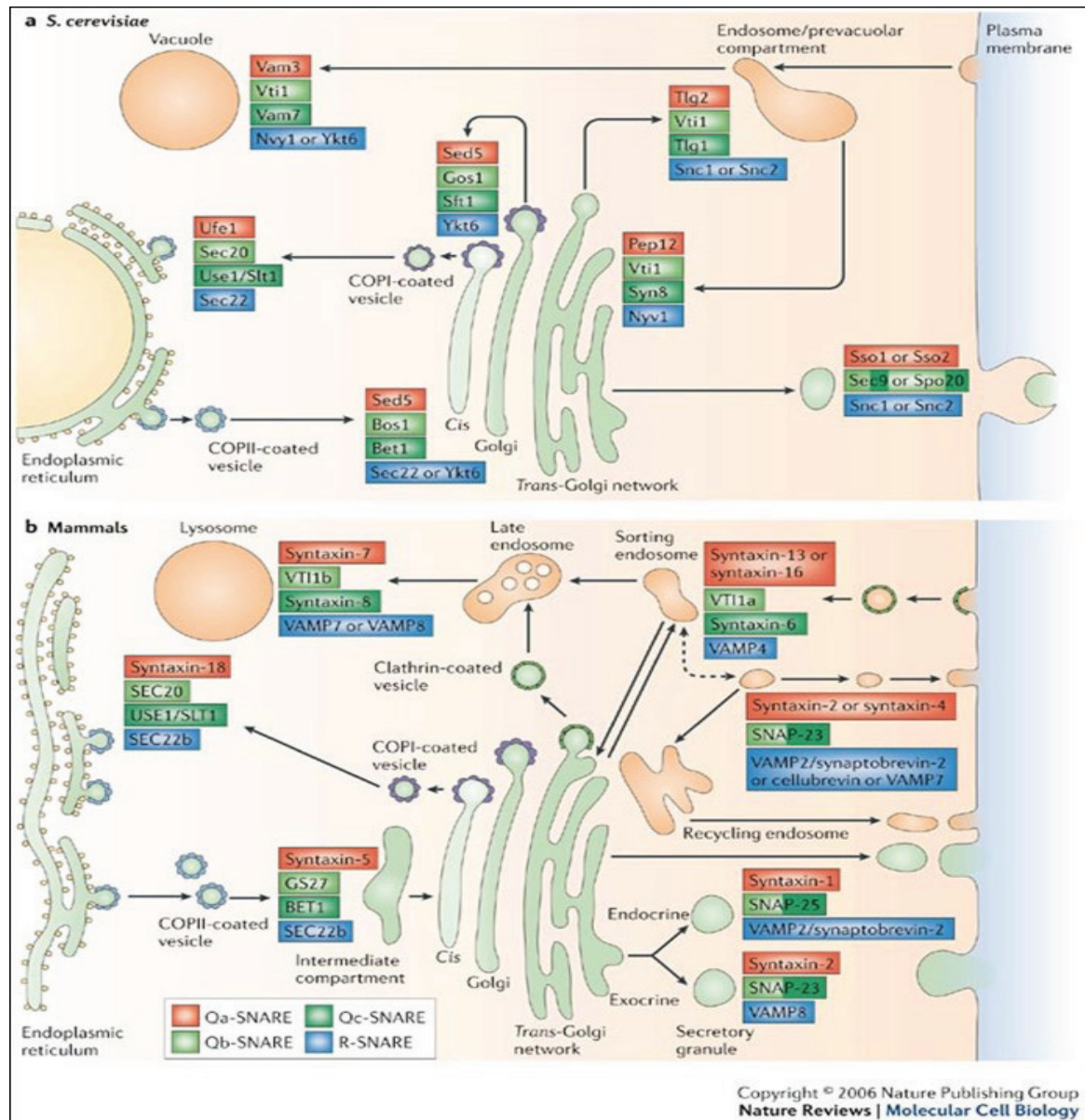
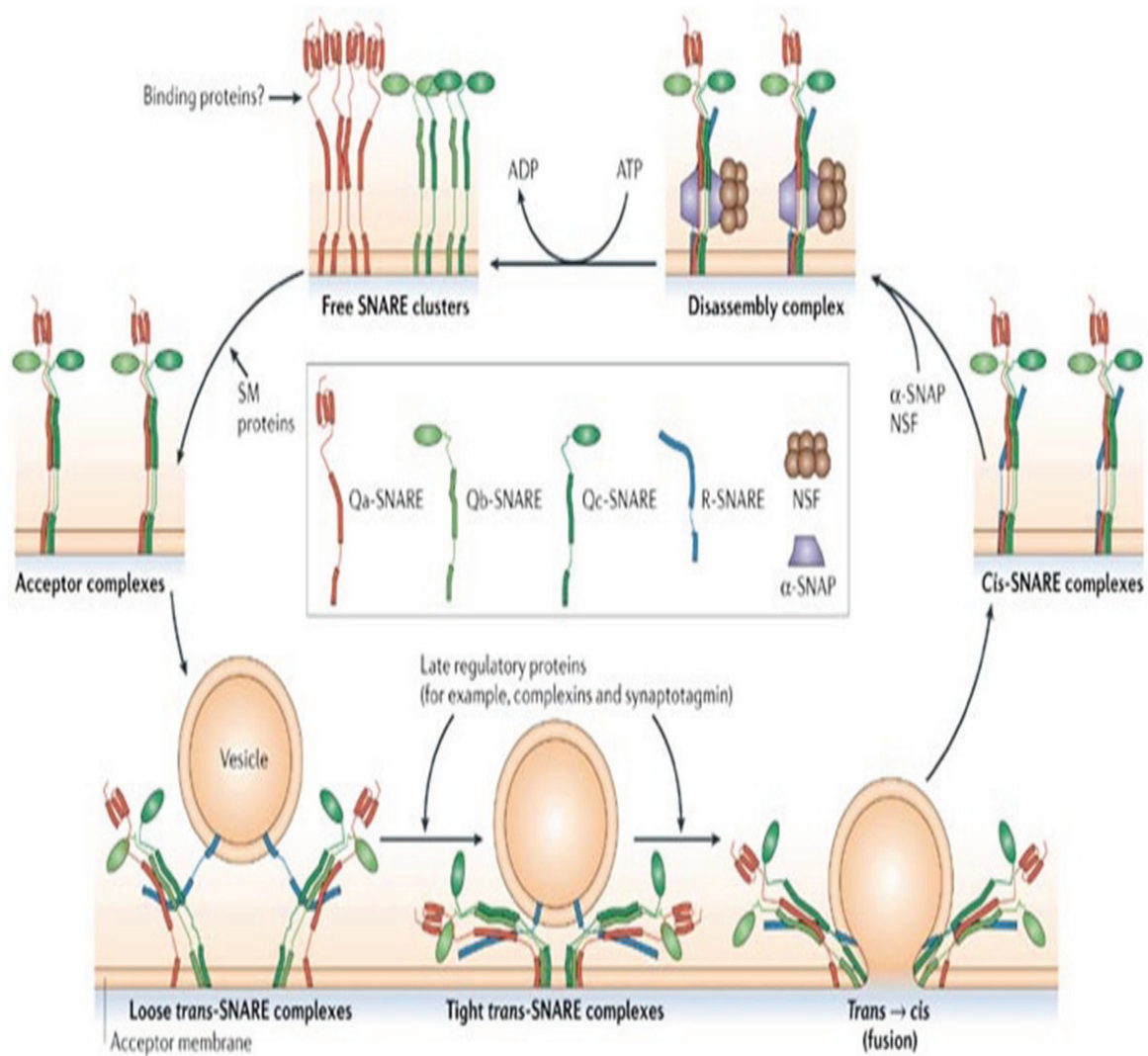


**Figure I. Localisation of Mammalian and Yeast SNAREs.** For many of the fusion reactions, SNAREs have not yet been unambiguously identified. Also shown are the specialized storage organelles for regulated exocytosis. The dashed double-headed arrow indicates homotypic fusion between two sorting endosomes. **Legend:** COPI, coatamer protein complex-I; Gos1, Golgi SNARE protein-1; GS27, Golgi SNARE of 27 kDa; SNAP-23, 23-kDa synaptosome-associated protein; SNAP-25, 25-kDa synaptosome-associated protein; SNARE, soluble N-Ethylmaleimide-sensitive factor attachment protein receptor; Spo20, sporulation-specific protein-20; Syn8, syntaxin-8; Tlg, t-SNARE affecting a late Golgi compartment; Use1/USE1, unconventional SNARE in the ER protein-1; Vam, vacuole membrane; VAMP, vesicle-associated membrane protein; Vti1/VTI1, Vps ten interacting-1. <sup>Figure and text adapted from 20.</sup>  
**Note:** while investigating the literature, we found divergent views of the SNAREs that would be involved in the fusion process of COPI vesicles <sup>see 21.</sup>



Copyright © 2006 Nature Publishing Group  
Nature Reviews | Molecular Cell Biology

**Figure J. The SNARE fusion machinery.** As an example, we consider three Q-SNAREs on a Golgi cisternae and an R-SNARE on a COPI vesicle. Q-SNAREs, which are organized in clusters (top left), assemble into acceptor complexes, and this assembly process might require SM (Sec1/Munc18-related) proteins. Acceptor complexes interact with the vesicular R-SNAREs through the N-terminal end of the SNARE motifs, and this nucleates the formation of a four-helical trans-complex. Trans-complexes proceed from a loose state (in which only the N-terminal portion of the SNARE motifs are 'zipped up') to a tight state (in which the zippering process is mostly completed), and this is followed by the opening of the fusion pore. In regulated exocytosis, these transition states are controlled by late regulatory proteins that include complexins (small proteins that bind to the surface of SNARE complexes) and synaptotagmin (which is activated by an influx of calcium). During fusion, the strained trans-complex relaxes into a cis-configuration. Cis-complexes are disassembled by the AAA<sup>+</sup> (ATPases associated with various cellular activities) protein NSF (N-Ethylmaleimide-sensitive factor) together with SNAPs (soluble NSF attachment proteins) that function as cofactors. The R- and Q-SNAREs are then separated by sorting, details of which is still unknown <sup>Figure and text from 20</sup>.



Is this from another paper, did I miss a reference? However, doubts were raised to determine if SNAREs were sufficient *in vivo* to drive the fusion of membranes. Recent biochemical data suggest that the initial fusion pore of vacuoles is not lipidic (as is the case in the Weber et al.<sup>199</sup> model) but rather a proteinaceous channel formed by two opposing V0 hexamers of vacuolar H<sup>+</sup>-ATPases, binding head-to-head in a process that requires Ypt7-GTP and calmodulin. Upon signalling by calcium-bound calmodulin, the V0 hexamers segregate whereby lipids are thought to invade the space to form an aqueous fusion pore<sup>207</sup>. Fusion of vacuolar membranes requires the action of protein phosphatase 1 (PP1) which is in a complex with calmodulin. This step is thought to be the final step triggering the actual fusion event and placed downstream of the action of SNARE proteins<sup>208</sup>. Therefore, much data exist to suggest that the current model for how SNARE proteins drive fusion is too simplistic and that other steps and components are likely to be required.

One of the problems is a question of specificity. What are the mechanisms that allow the fusion of two different lipid bilayers, while at the same time inhibiting the fusion with other bilayers than the intended target? One of the postulates of the original SNARE hypothesis formulated by Rothman and coworkers in the early 90's was that SNARE proteins specifically target transport vesicles to the right membrane with which they are to fuse. In other words, each "cognate" SNARE proteins form stable complexes in only one particular trafficking step. This was later supported by findings showing that cognate SNAREs result in better fusion than non-cognate ones using artificial liposomes<sup>209, 210</sup>. However, Scheller and coworkers<sup>210</sup> showed that the plasma membrane R-SNAREs synaptobrevin-2/VAMP-2 binds to different syntaxins. The yeast SNAREs Sed5p and Vti1p, also seem to function in more than one transport step suggesting extensive promiscuity among SNARE proteins<sup>211</sup>. *In vitro*, complexes formed by four different SNAREs further shows that one of the Q-SNAREs has to belong to the syntaxin subfamily and the two others to subfamilies homologous to the first and the second SNARE motif of SNAP-25, respectively. Substitution of particular SNAREs within these defined subfamilies can occur without influencing complex formation<sup>212</sup>. This results in

the manipulation of SNAREs to perform fusion events that does not occur physiologically<sup>213</sup>. Therefore, it seems that the Q-SNARE complex do not recognize one R-SNARE per se, but will recognize one subfamily of R-SNAREs.

One level of control provided by the SNARE machinery to identify target membranes from non-target membranes is provided by inhibitory SNAREs. In the target membrane, the acceptor complex is composed of 3Q-SNAREs. In the presence of an additional inhibitory SNARE, the acceptor complex can no longer form, which inhibits the fusion of vesicles to the membrane<sup>214</sup>. This mechanism confers another level of specificity, as certain combinations of SNAREs seem to be inhibitory, therefore fine tuning the targeting of vesicles<sup>214</sup>. According to this model, a vesicle can only fuse if its R-SNARE matches the 3Q-SNARE on the target membrane and if no inhibitory SNARE is present. Furthermore, it seems the SNARE fusion machinery is also dependent on the recognition of associated fusion factors, like MUNC-18, SEC1, Complexin-I and Synaptotagmin-I at the PM, which promote the fusion process by greatly enhancing its rate. These interactions of SNAREs by specific local chaperones might enhance their specificity<sup>215-218</sup>.

In COPI vesicles, the specific identity of the R-SNARE has yet to be determined beyond reasonable doubt. Recent publications from the Rothman group<sup>21, 219</sup> as well as from the Jahn group<sup>20</sup> attribute GS15 (as well as rBET1) and Sec22 as the R-SNAREs involved in the fusion of the vesicles, respectively. The situation is complicated by the fact that rBET1 and GS15 are not identified as R-SNAREs<sup>7, 220</sup>. In order to further clarify the situation, we were able to show in a proteomic study<sup>7</sup> that all three are present on the surface of the vesicles, albeit in very different quantities. While a large quantity of Sec22 and a homolog of Sec22 were identified in COPI vesicles, GS15 or rBET1 were only present in small quantities. In contrast, it should also be considered that a different R-SNARE could be+ required for every subtypes of COPI vesicles and that our study is thought to contain mostly one subtype as it is enriched in sugar transferases and depleted in p24 proteins.

In addition to SNAREs, another level of specificity is thought to involve the presence of tethering factors <sup>221, 222</sup> for review <sup>223</sup>. The function of these tethers is proposed to be the recognition of the intended target membrane as well as bringing the target membrane in sufficient proximity for the SNAREs to continue the fusion process. There are at least two types of tethers present in the Golgi apparatus: the cytosolic tethering complexes and the long coiled-coil tethers with a transmembrane domain. Three tethering complexes have been shown to be involved in the transport of COPI vesicles. First, depletion of one of the subunits of the conserved oligomeric Golgi complex (COG) results in the accumulation of peri-Golgi vesicles in HeLa cells <sup>224</sup>. COG has also been shown to bind to Golgi SNAREs as well as protein coat subunits <sup>224, 225</sup>. However, it is not sure if COG is involved in COPI mediated transport: while the authors demonstrates that the Shiga toxin is unable to move in a retrograde direction to the ER and concluded that it interfere with COPI mediated transport, they did not consider that Shiga toxin has been demonstrated to migrate to the ER in a COPI-independent retrograde transport from the Golgi <sup>101, 102</sup>. Two other tethering complexes, TRAPPII and DslIp, have also been shown to be involved at the Golgi complex <sup>226</sup>, as they associate with coat proteins <sup>227-229</sup>. DslIp depletion was shown to inhibit the retrieval of Sec22 from the Golgi to the ER <sup>227</sup>, confirming a potential role in SNARE mediated transport.

The coiled-coil domains of the tethers are thought to mediate the binding of COPI vesicles through the interaction of their coiled-coil domain with a specific matching tether pair present on their target Golgi. The coiled-coil tethers have been directly linked to the fusion as well as the identification of COPI vesicles subtypes <sup>55</sup>: two tethers were identified that led to the characterization of two subtypes of vesicles. First the Golgin-84 vesicle tether was associated with the tether CASP in the Golgi apparatus, which was shown to be involved in the retrograde transport of COPI vesicles enriched in glycosyltransferases. The second vesicles subtype was characterized by the tether Giantin, which is known to associate itself to tethers GM130 as well as p115 <sup>230, 231</sup>. The vesicles possessing this tether were remarkably different from the Golgin-84 tethers, as they were shown to be enriched in p24 and possess greater concentration of anterograde cargo <sup>55</sup>. Inhibition of Golgin-84 function *in vivo* resulted in inhibition of COPI mediated



retrograde transport <sup>55</sup>. Furthermore, the formation of two *trans* SNARE complexes, GS15–Ykt6–GOS-28–Syntaxin-5 complex and the Membrin–Bet1–Sec22–Syntaxin-5 complex, have been previously linked to be dependent on the tether p115 <sup>232</sup>. Taken together, this information seems to confirm the previously established hypothesis that identified tethers as the bridge between specificity and the start of the fusion process <sup>232</sup>.

Another level of specificity can also be demonstrated by the regulation of the docking step by small GTPases termed Rabs <sup>233</sup>. In the Golgi, additional regulation is provided by Rab1/Ypt1p as it has been shown to mediate COPI retrograde transport in yeast and also to help recruit coatomer during the COPI budding process <sup>233, 234</sup>. Furthermore, Rab1 interacts with the tethers p115, GM130, Golgin-84, and COG as well as being critical for the integrity for the Golgi apparatus <sup>225, 233, 235-238</sup>. It has been proposed that Rab1 acts as a “leash” of sorts that keep the vesicles in close proximity to the Golgi apparatus while at the same time helping the vesicles find their target. Hydrolysis of Rab1<sup>GTP</sup> to Rab1<sup>GDP</sup> leads to its dissociation, which allows the fusion to proceed <sup>18, 22</sup>. However, it should be kept in mind that the actual functions of Rabs within the Golgi apparatus are still under investigation <sup>for other views see 223, 239</sup>.

### Section 3: PI(4,5)P<sub>2</sub>

Phosphatidylinositol 4,5-bisphosphate (PI(4,5)P<sub>2</sub>) is a phospholipid whose main characteristic is its two negatively charged phosphate groups mounted on an inositol ring (fig K.). This large negative charge on its headgroup is rare among phospholipids and confers an attraction focus in an otherwise positively charged or neutral lipid bilayer (see fig. K for example). PI(4,5)P<sub>2</sub>, which compose up to 1% of all phospholipids in the cell, contains two variable acyl chains, one glycerol-phosphate linker group followed by the inositol ring and the two phosphate groups at the 4' and 5' position <sup>for complete review 5, 240</sup>.

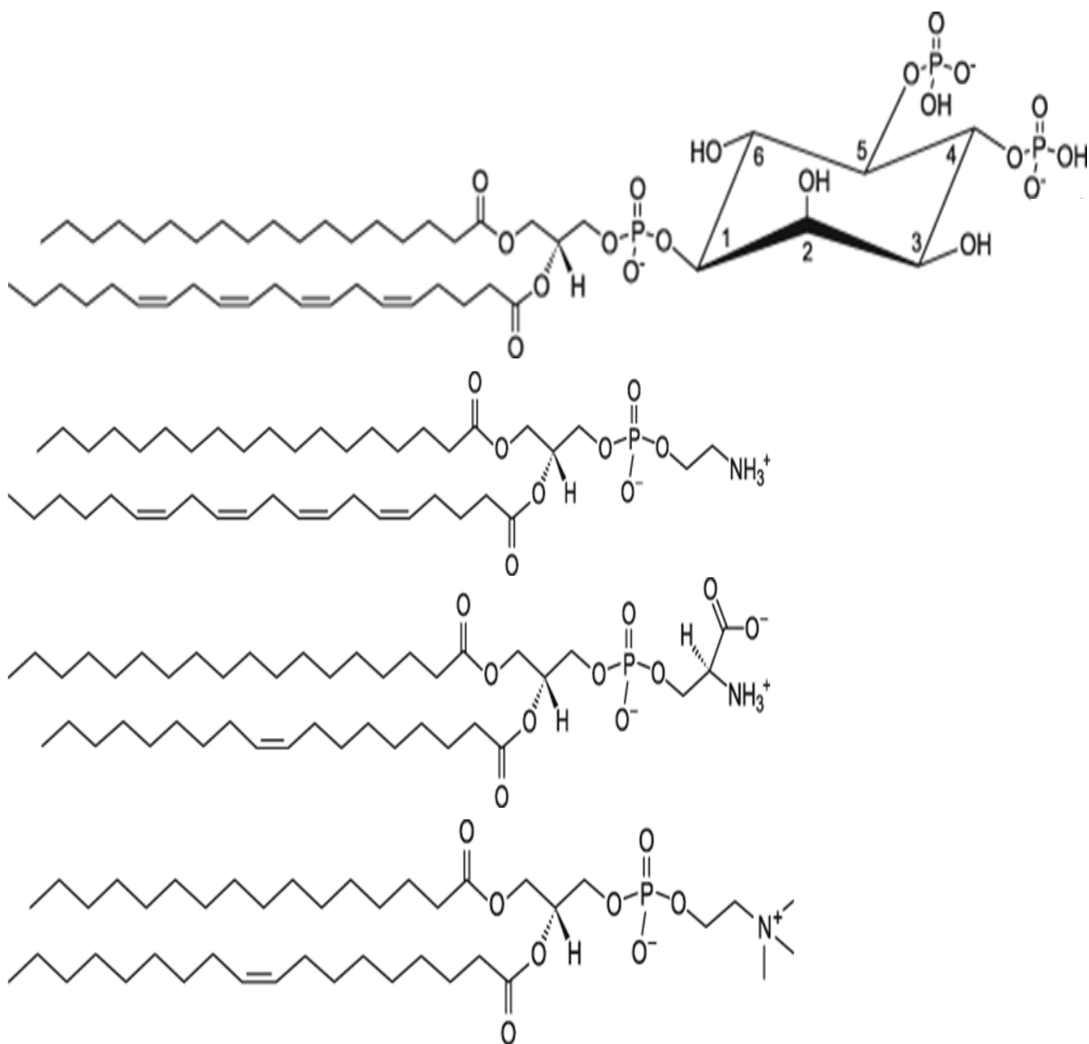


**Figure K. PI(4,5)P<sub>2</sub> and other phospholipids.** Visualization of PI(4,5)P<sub>2</sub> compared to other common phospholipids present on the surface of the membrane bilayer. **Top;** PI(4,5)P<sub>2</sub>, **second from top;** phosphatidylethanolamine, **second from bottom;** phosphatidylserine, **bottom:** phosphatidylcholine. These phospholipids are represented with 18:0, 20:4; 18:0, 18:1 and 16:0, 18:1 acyl chain conformation.  
© Avanti-Lipids

### Section 3.1: Metabolism of PI(4,5)P<sub>2</sub>

Synthesis of PI(4,5)P<sub>2</sub> is mediated by a series of kinases that use phosphatidylinositol (PI) as a substrate and sequentially add phosphate groups to the 4' and 5' positions (fig. L). The mechanism by which it does so depends on the intermediate substrate, as PI(4,5)P<sub>2</sub> can be generated from both phosphatidylinositol 4-phosphate (PI(4)P) and phosphatidylinositol 5-phosphate (PI(5)P). However, it is much more common within the cell to use PI(4)P as a substrate and these proteins are referred to as type I PI(4)P kinases (fig. L). The PI(4)P kinase type 1 family consists of three proteins which are currently known to produce PI(4,5)P<sub>2</sub> from PI(4)P:  $\alpha$ ,  $\beta$  and  $\gamma$  (which contains 3 isoforms) <sup>review 16,</sup>

240.

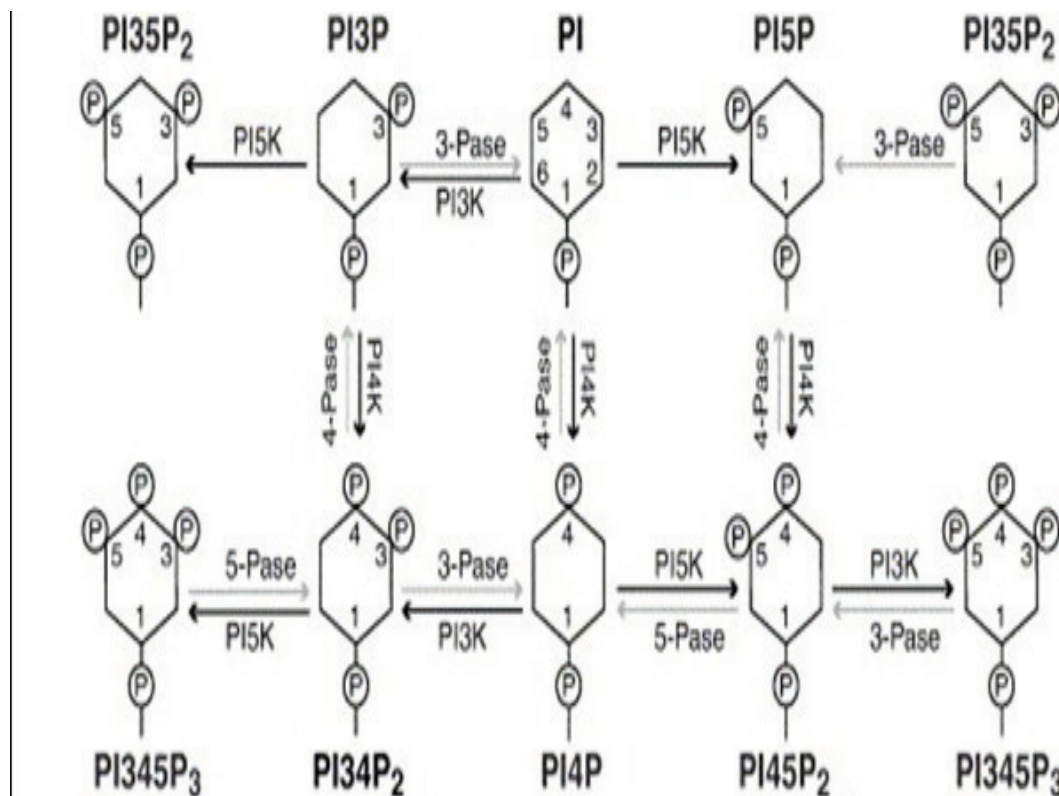


**Figure L. Synthesis of phosphoinositides.** Legend: PI(X)K; refers to phosphatidylinositol kinase at the x position. X-Pase; phosphatase that remove the phosphate at the X position. From <sup>16</sup>

Other phosphoinositides, which includes a family of 8 distinct PI derivatives, also serve in different functions throughout the cell: e.g. PI(4)P is implicated in the formation of clathrin coated vesicles at the TGN while PI(3)P is involved in endosome metabolism and also plays a role in the fusion of yeast vacuoles<sup>128, 148, 241</sup>.

The removal of phosphate groups from PI(4,5)P<sub>2</sub> is accomplished in two ways: first, with the help of a phosphatase, PI(4,5)P<sub>2</sub> can be degraded to revert back to PI(4)P or PI. Second, it can also be degraded by phospholipase C (PLC), which revert PI(4,5)P<sub>2</sub> back to diacylglycerol (DAG) and inositol 1,4,5-trisphosphate (INP<sub>3</sub>). Binding of these proteins as well as other proteins affecting PI(4,5)P<sub>2</sub> mechanism is dependent on a series of domains. Some of them can be grouped into categories, alike pleckstrin homology (PH) domains, which mediate the association of PI(4,5)P<sub>2</sub> with PLCs, and epsin N-terminal homology (ENTH) domains, which mediate the association of AP-2 and other adaptors during clathrin coat formation. However, many other proteins have domains that can bind PI(4,5)P<sub>2</sub> and the only common characteristic is that they are comprised of a cluster of basic/aromatic residues. Since the conformation is dependent on the final three-dimensional structure of the protein, it is challenging to predict PI(4,5)P<sub>2</sub> binding domains from an amino-acid sequence as they occur without any discernable pattern. These domains do not have many common characteristics besides the fact that their three-dimensional structure allows them to bind large negative charges with high affinity<sup>240</sup>.

### **Section 3.2: Roles of PI(4,5)P<sub>2</sub>**

The functions of PI(4,5)P<sub>2</sub> within the cell are numerous and widespread. It is used at the plasma membrane to mediate signaling, endocytosis, exocytosis as well as membrane shuffling, activation of enzymes and actin polymerization. It is a very versatile lipid. As an example, one of the best known pathways of PI(4,5)P<sub>2</sub> is the PLC mediated generation of the secondary messengers DAG and IP<sub>3</sub> in response to certain cell signaling events. In

return, DAG activates protein kinase C (PKC) and IP<sub>3</sub> releases intracellular calcium stores<sup>for complete review 240</sup>.

### **PI(4,5)P<sub>2</sub> in vacuoles**

Vacuoles are a unique feature of yeast as well as other lower eukaryotes. They are involved in the regulation of cell homeostasis through multiple pathways such as protein degradation, autophagy and storage of molecules<sup>for review, see 242</sup>. When undergoing mitosis, or cell fusion, these vacuoles have been shown to fuse with each other<sup>243-245</sup>. In order to understand the fusion process, a study model using purified vacuoles was developed, *in vitro*<sup>243</sup>. This model was first used to determine that the vacuoles fusion process was divided into 4 steps: priming, tethering, docking and fusion, the first 3 steps require the function of the NSF and  $\alpha$ -SNAP yeast homologues Sec18p and Sec17p<sup>202, 246, 247</sup>.

Mayer et al.<sup>248</sup> were able to demonstrate the involvement of PI(4,5)P<sub>2</sub> in two steps of the homotypic fusion process of vacuoles. First, they were able to demonstrate that PI(4,5)P<sub>2</sub> is involved in Sec18p mediated priming of the SNAREs, which are ultimately responsible for the fusion to occur<sup>in addition see 203, 249</sup>. Furthermore, the publication demonstrated that PI(4,5)P<sub>2</sub> was also involved in a second pre-fusion step just prior to the BAPTA(a Ca<sup>2+</sup> chelator) sensitive step, which inhibits the final influx of Ca<sup>2+</sup>, the last step before fusion.

Recent advances in the understanding of the role of PI(4,5)P<sub>2</sub> in the fusion of vacuoles have been accomplished by the discovery of a novel tethering complex, HOPS, as a binding partner for PI(4,5)P<sub>2</sub><sup>250</sup>. Upon binding to PI(4,5)P<sub>2</sub>, HOPS has been shown to mediate the function of SNAREs and to promote fusion<sup>251</sup>. Furthermore, experiments using proteoliposomes with the basic fusion machinery of vacuoles (SNAREs, tethers, specific lipids, Sec18p and Sec17p) have shown that removal of PI(4,5)P<sub>2</sub> leads to severe inhibition of proteoliposome fusion<sup>148</sup>. The function of HOPS has been shown to involve the promotion of fusion through interaction with *trans* SNAREs complex<sup>251-253</sup>. It appears also that in this system, the quantity of PI(4,5)P<sub>2</sub> is tightly regulated as over-production of PI(4,5)P<sub>2</sub> leads to inhibition of fusion between vacuoles<sup>254</sup>.

## **PI(4,5)P<sub>2</sub> at the plasma membrane**

The plasma membrane contains one of the largest pools of PI(4,5)P<sub>2</sub> present in the cell<sup>255</sup>. Within the organelle, PI(4,5)P<sub>2</sub> is generated mostly by PI(4)P5'kinase type 1  $\gamma$  and has been demonstrated to be regulated by ARF6, another member of the ARF family<sup>256-259</sup>. PI(4,5)P<sub>2</sub> is required for many trafficking purposes, most notably for the fusion of dense core vesicles (DCV) as well as for the endocytic and exocytic pathways of synaptic vesicles<sup>260-265</sup>. It was shown that PI(4,5)P<sub>2</sub> mediates exocytosis by recruiting the cytosolic CAPS-1/2 proteins in order to promote Ca<sup>2+</sup>-triggered fusion of docked DCV's with the plasmalemma<sup>262, 266-269</sup>

Furthermore, a recent publication<sup>145</sup> demonstrated a potential link between PI(4,5)P<sub>2</sub> and SNAREs in the fusion of DCV. In this publication, the authors sought to understand the mechanisms involved in PI(4,5)P<sub>2</sub> mediated DCV exocytosis. Using purified PM extracts obtained from PC12 cell, they probed the inside of the plasma membrane with a PH domain tagged with GFP which was shown to bind to PI(4,5)P<sub>2</sub>. They first were able to show that PI(4,5)P<sub>2</sub> concentrates on micro-domains on the PM and that it co-localizes with DCV's and CAPS. Furthermore, they were able to show that Ca<sup>2+</sup> introduction to the system resulted in the fusion of the DCV with the PM, but preferentially in areas that contained both PI(4,5)P<sub>2</sub> and CAPS. This confirmed previous experiments demonstrating the PI(4,5)P<sub>2</sub>-CAPS-DCV relationship.

They continued their experiments using liposomes which had been optimized by integrating physiological quantities of SNAREs to mimic DCV fusion<sup>199</sup>, but without any cytosol or cytosolic proteins. With this system, they were able to demonstrate that PI(4,5)P<sub>2</sub> introduction in this assay inhibited liposome fusion, in contradiction to previous publications. It also seemed that the inhibitory effect was not limited to PI(4,5)P<sub>2</sub> but rather that it was also mediated by other phosphoinositides like PI(4)P and PI(3,4)P<sub>2</sub>. While the main cause of this inhibition remain unknown, it was suggested that it might be

due to the fact that PI(4,5)P<sub>2</sub> is an inverse cone lipid, which would be very unfavorable to the hemi-fusion transition state that occurs during the fusion of two membranes<sup>270</sup>.

Analysis of the interaction of the SNAREs SNAP-25/Syntaxin-1 with PI(4,5)P<sub>2</sub> revealed an association between the juxtamembranous basic residues of the protein and PI(4,5)P<sub>2</sub>. Mutation studies were performed to determine whether deletion of these amino acid residues would increase the fusogenicity of liposomes. Surprisingly, the mutant inhibited the fusion of liposomes. In light of these results, it was suggested that Syntaxin-1, by sequestration of PI(4,5)P<sub>2</sub> through its juxtamembranous basic residues, facilitates the fusion process. This provided a first account that PI(4,5)P<sub>2</sub>-SNARE interaction actually facilitates the fusion process at the PM.

Further investigation of the liposome fusion assay revealed that insertion of CAPS into the assay dramatically increased the fusogenicity of the liposome, but only if PI(4,5)P<sub>2</sub> and SNAREs were present in the liposomes. CAPS is ineffective in rescuing the fusogenicity of liposomes that did not contain any SNAREs, or with SNAREs that had been cleaved by protease botulinum neurotoxin B. The study also found that the CAPS-PI(4,5)P<sub>2</sub> activation of liposome fusion was asymmetrical; it only worked when the PI(4,5)P<sub>2</sub> was located with the proteoliposomes containing PM SNAREs SNAP-25/Syntaxin-1, *in sync* with previously published work that demonstrate a requirement of PI(4,5)P<sub>2</sub> at the surface of the PM<sup>17, 23</sup>.

The presence of inhibitory and activating phosphoinositides raises the question if such a system could also be present in the Golgi apparatus. PI(4)P, which has been shown to be present in large quantities within the Golgi apparatus<sup>128, 271</sup>, could inhibit the fusion between cisternae similar to the mechanism seen above. The synthesis of PI(4,5)P<sub>2</sub> from PI(4)P would have the added benefit of transforming an inhibitor of fusogenicity to an activator.

## PI(4,5)P<sub>2</sub> in the Golgi apparatus

While only small amounts of PI(4,5)P<sub>2</sub> can be detected at steady-state<sup>255</sup>, synthesis of PI(4,5)P<sub>2</sub> is enhanced by incubation of ARF1 with the Golgi apparatus<sup>271-273</sup>. Similar to the action of ARF6 at the PM<sup>258, 274</sup>, PI(4,5)P<sub>2</sub> synthesis within the Golgi is tightly regulated by ARF1, which mediates its levels by activating two different pathways. Firstly, ARF1 directly stimulates the activity of PI4'Kinase type IIIβ and a PI(4)P 5'kinase type I<sup>271, 272, 275</sup>. Secondly, ARF1 activates the formation of phosphatidic acid (PA) through its interaction with phospholipase D (PLD). PA in turn increases the rate of formation of PI(4,5)P<sub>2</sub> through the same kinases<sup>189, 276-280</sup>. This creates a positive feedback loop as PI(4,5)P<sub>2</sub> has also been shown to activate PLD<sup>281</sup>. The overall result is a 10-fold increase in the quantity of PI(4,5)P<sub>2</sub> when purified Golgi membranes are incubated with ARF1 and cytosol<sup>271</sup>.

It was also discovered that the Golgi apparatus has a high intrinsic PI(4,5)P<sub>2</sub> 5'phosphatase activity<sup>282</sup>, which could explain the low levels of PI(4,5)P<sub>2</sub> *in vivo*<sup>255</sup>. This discovery was followed by the identification of two PI(4,5)P<sub>2</sub> 5'phosphatases, OCRL1 and INPP5B, which localize to the Golgi apparatus<sup>283-285</sup>. One of those, INPP5B, has recently been shown to be implicated in the retrograde transport from the ERGIC to the ER<sup>283</sup>.

It was also demonstrated that the integrity of the Golgi apparatus was dependent on both the activity of PI4Kinase type IIIβ<sup>271</sup> as well as the formation of PI(4,5)P<sub>2</sub><sup>282, 286</sup>. Inhibition of PI(4,5)P<sub>2</sub> formation resulted in the fragmentation and vesicularisation of the Golgi apparatus. This suggests a possible requirement of PI(4,5)P<sub>2</sub> for the maintenance of the Golgi apparatus at the level of membrane fusion. Furthermore, the overall PI(4,5)P<sub>2</sub> level has also been shown to be increased when ARF1 is incubated in the presence of GTP-γ-S, which renders it continuously active and also inhibits the uncoating and fusion of COPI vesicles and results in its accumulation<sup>12, 271</sup>.



Lastly, Luna et al.<sup>287</sup> demonstrated a potential link between the presence of PI(4,5)P<sub>2</sub> in the Golgi apparatus and the successful polymerization of actin on its surface. Inhibition of CDC42, which polymerizes actin on the surface of the Golgi, and N-WASP, which anchors actin to the surface of membrane bilayers by binding to PI(4,5)P<sub>2</sub>, were shown to severely inhibit both COPI dependent and COPI independent Golgi to ER transport. Furthermore, it was later demonstrated that ARF1 can regulate actin polymerization at the surface of PI(4,5)P<sub>2</sub> containing liposomes<sup>288</sup> and that PI(4,5)P<sub>2</sub>-enriched lipid rafts can successfully be utilized by N-WASP and actin for the migration of vesicles<sup>288, 289</sup>. Therefore, it is a possibility that PI(4,5)P<sub>2</sub> could serve as an anchor on the surface of the vesicles for actin polymerization and that this process would lead to the successful migration of COPI vesicles. However, since CDC42 depletion inhibits both modes of Golgi to ER transport and is not COPI specific, it might also be a possibility that the inhibition of retrograde transport is the result of destabilization of the Golgi apparatus resulting from loss of contact to the cytoskeleton as could also be suggested in<sup>282</sup>.

Overall, ARF1, through its multiple roles within the Golgi apparatus, could simultaneously stimulate the budding process as well as to prime vesicles for fusion by introducing PI(4,5)P<sub>2</sub>. A possible mechanism would stipulate that upon formation of the vesicles, PI(4,5)P<sub>2</sub> recruits the fusion machinery to the surface of the vesicles. After fusion, PI(4,5)P<sub>2</sub> would be metabolized in order to avoid other fusion events, which could explain the high 5'phosphatase in the Golgi apparatus<sup>282, 286</sup>.

## Chapter 1: Establishment of the biochemical investigation process.

---

### Introduction

Previous work (for review, see <sup>18</sup>) has demonstrated a two-step mechanism in the COPI mediated intra-Golgi transport involving both COPI vesicles budding and fusion. During the vesicles budding, coatamer proteins are recruited to the Golgi cisternae concurrently with positive segregation of Golgi resident enzymes as well as depletion of secretory cargo proteins <sup>8, 11, 12, 55, 75, 77, 78, 106</sup>. This assembly process, mediated by ARF1 <sup>156, 155</sup>, leads to the formation of COPI protein complexes on the surface of the Golgi cisternae. This latter triggers the bulging of the membrane <sup>11, 13, 159, 160, 186</sup> and the subsequent formation of spherical buds that pinch off the Golgi surface <sup>290</sup> as functional COPI vesicles <sup>66, 178, 290</sup>. At the end of this process, ARFGAP1 hydrolyzes ARF1<sup>GTP</sup> to ARF1<sup>GDP</sup> <sup>178</sup> in order to induce the dissociation and release of the coatamer coat from the budding vesicles <sup>11</sup>. The final spherical COPI derived vesicles are approximately 45-60 nm in diameter <sup>7, 159, 160</sup> (fig. H).

Further biochemical studies and the recent use of proteomics have confirmed that COPI vesicles are highly enriched in Golgi resident enzymes <sup>7, 55</sup>. In addition, there was evidence that the Golgi apparatus produces in fact at least three subtypes types of COPI vesicles <sup>11, 55</sup>. The first one is enriched in p24 proteins and is thought to mediate the retrograde transport between the CGN and the ER, while the second one is enriched in p24's as well as cargo proteins. The last known subtype is mostly enriched in sugar transferases and mediates the transport within the Golgi apparatus as well as from the cis cisternae to the CGN <sup>11, 55</sup>. While some of the characteristics of the fusion machinery have been investigated, especially in regards to the tethering factors involved <sup>55, 232</sup>, little is known about the underlying mechanisms. Hence, the goal of this thesis was to elucidate the targeting, tethering and fusion of these COPI vesicles.

A significant challenge in such investigation was to experimentally separate the budding and fusion process of COPI vesicles. For this purpose, we have developed two highly

specific cell-free *in vitro* assays, termed the budding and fusion assay respectively. The budding assay was performed to generate large quantities of purified COPI vesicles. The concentrated vesicles were subsequently used in the fusion assay, which studied the fusion of vesicles by monitoring their consumption by target Golgi cisternae. As described in the following chapters, the development of these two assays has been proven to be essential in the discovery of potential factors involved in intra-Golgi transport.

## **Results**

### **The Budding assay**

For our experiments, the main purpose of setting up a budding assay was to produce highly purified COPI vesicles that were generated from donor Golgi membranes *in vitro*. Briefly, the procedure was as follows (details described in Materials and Methods and in <sup>291</sup>): enriched preparations of Golgi membranes <sup>6</sup> were incubated with salt buffers, sucrose and cytosol, which reproduced a milieu in which ARF1, ARFGAP1 and coatamer proteins initiate the budding reaction. An ATP-regenerating system composed of ATP, GTP, creatine kinase and creatine phosphate was also added to supply the energy necessary for this process <sup>291</sup>.

A critical step in the assay was to prevent the fusion of the formed vesicles back to the Golgi cisternae, i.e. to trap them in a budded and uncoated yet unfused state <sup>11</sup>. To do so, a mutant form of  $\alpha$ -SNAP, which is normally responsible for the proper alignment of SNAREs in the fusion process <sup>203</sup>, was strategically introduced to the budding assay to act as a competitive inhibitor of the endogenous wild type proteins. This approach has allowed us to harvest a higher quantity of unfused COPI vesicles as revealed by the Golgi resident enzyme marker, Golgi mannosidase II. In a typical budding assay, up to 20% of the total Golgi mannosidase II pool could be found incorporated into budded COPI vesicles <sup>11</sup> (fig. 1a, ii).

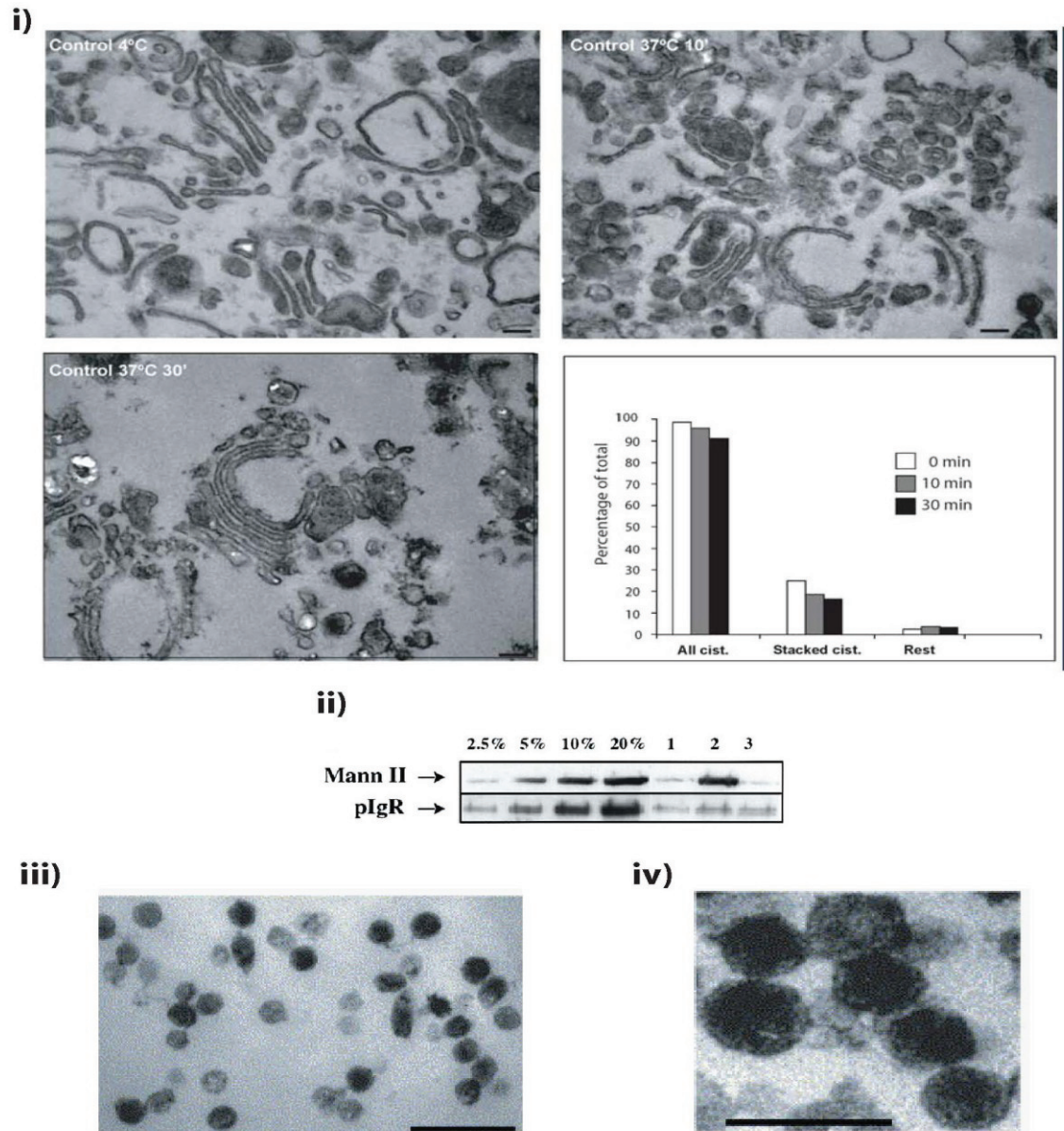


**Figure 1a. Purification of COPI vesicles in the budding assay.** **i)** In order to demonstrate that the COPI derived vesicles generated in the budding assay was not the product of fragmented Golgi, we removed the budded vesicles and collected the Golgi membranes by sedimentation at the beginning (up, left), after 10 minutes (up, right) and 30 minutes (bottom, left) of incubation under the budding conditions. We submitted them to epon embedding and examined them by EM to compare the quantity and quality of cisternae (bottom, right): first series of columns show the amount of cisternae compared to control, the second, the amount of stacked cisternae and the third, the amount of membrane remnants (bar 100  $\mu$ m) <sup>from 7</sup>. **ii)** COPI vesicles are enriched in Golgi resident enzymes. By western blots, the protein content was compared between COPI vesicle fractions generated under normal conditions at 37°C (lane 2), under inhibitory temperature of 4°C (lane 1) or in the absence of an ATP regenerating system (lane 3). These fractions were also compared with Golgi membranes (2.5%, 5%, 10%, 20% of starting material, left) for their levels in MannII and pIgR <sup>from 11</sup>. **iii-iv)** Ultrathin sections of the COPI vesicles preparation were stained with tannic acid. They were randomly selected for examination by electron microscopy (bar: 250 nm and 100 nm) <sup>from 7, 12, 13</sup>

The purification of the COPI vesicles involved a series of centrifugation steps that separated the denser Golgi membranes from the COPI vesicles. First, vesicles were detached from surrounding membranes with a highly concentrated KCl solution. The majority of the Golgi membranes were then pelleted. To further remove the contaminants, the resulting supernatant was applied to a sucrose cushion composed of one 30% (w/w) and one 50% (w/w) sucrose layers. Following an ultracentrifugation for 45 min at 126,000  $g_{max}$  and 4°C (3 hours at 407,000  $g_{max}$  and 4°C for large scale preparation<sup>291</sup>), the COPI vesicles migrated to the 30-50% interface, where they were collected and snap frozen in liquid nitrogen to preserve their fusogenicity<sup>291</sup>. In figure 1a, we demonstrate the quality and purity of the preparation by using EM. While the starting material was composed of stacked Golgi cisternae, the collected end product was almost devoid of them and contained a high concentration of COPI vesicles<sup>7, 11, 12</sup>.

Our budding assay generated both types of vesicles described in the introduction,<sup>11</sup> as shown by their enrichment in MannII and p24 proteins characterized in our previous studies<sup>7, 11</sup>. However, only MannII enriched vesicles that contain the GlcNacT1 enzyme can be detected in the fusion assay<sup>8, 10</sup>.

### **The Fusion Assay**

In the fusion assay, we added the purified COPI vesicles, now as donor compartments, to intact acceptor purified Golgi membranes in a reconstituted medium (containing buffering salt, sucrose, an ATP-regenerating system and cytosol) and allowed them to fuse with each other. In order to monitor this fusion process, we specifically used Golgi cisternae isolated from a spinner culture of CHO Lec1 cells, which have a mutation that makes them unable to synthesize a functional GlcNacT1<sup>292</sup>. GlcNacT1 is a key enzyme involved in glycosylation of cellular proteins as well as viral products such as VSV-G. In order to introduce a reporter protein to the system, the spinner CHO Lec1 cells were infected with VSV and were incubated to produce large quantities of VSV-G. As a consequence, when the CHO Lec1 cells were synthesizing VSV-G, they were improperly glycosylated (fig.

1b). Furthermore, previous investigations had revealed the fusion assay to be optimal when the CHO Lec1 cells had been preincubated at 15°C which concentrated the VSV-G within the CGN. The CGN had been shown to be the most fusogenic compartment within the Golgi apparatus. Therefore, the CHO Lec1 cells were infected, grown at 37°C to allow synthesis of sufficiently large quantities of VSV-G which was then concentrated in the CGN by incubating the cells at 15°C. Golgi enzymes were then purified and snap frozen before being use in the fusion assay<sup>75</sup>. The glycosylation of VSV-G in GlcNAcT1<sup>-/-</sup> CGN becomes possible only when wild type copies of GlcNAcT1 are transferred to the Golgi cisternae from the COPI vesicles upon their fusion. In other words, the fusion assay was based on the monitoring of the transfer of GlcNAcT1 and the extents of the VSV-G glycosylation, reflected by the incorporation of tritiated UDP-*N*-acetylglucosamine, which is included in the medium of the assay, to VSV-G(fig. 1b).

# The Golgi cell-free fusion assay

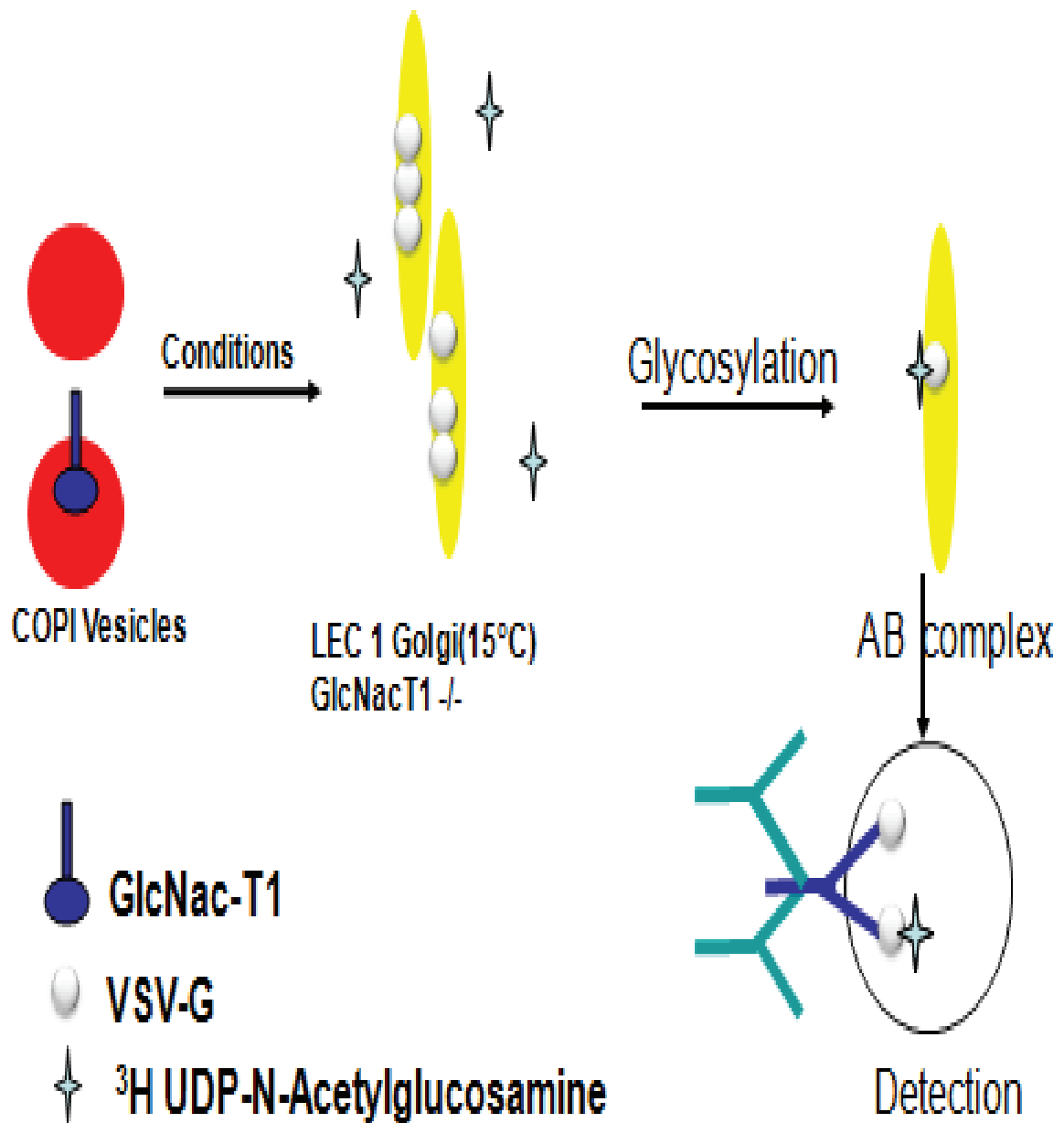


**Figure 1b. Schematic representation of the fusion assay.** GlcNacT1-positive COPI vesicles (left), were incubated with Golgi membranes purified from GlcNacT1-negative CHO Lec1 cells infected with VSV-G. The fusion of COPI vesicles rescued the enzyme deficiency and allowed the glycosylation of the VSV-G within the Golgi cisternae (right). The assay was performed in the presence of tritiated UDP-N-acetylglucosamine. The lysate from the reaction product was incubated with antibodies against the VSV-G. The immune complexes were then collected on glass fiber filters that were directly counted (bottom right).



<b><u>Golgi prep</u></b>	<b><u>(n)</u></b>	<b><u>Westerns</u></b>
30/06/2002	9	Lane 1
09/10/2002	9	n/a
24/03/2003	25	Lane 2
27/03/2003	15	Lane 3
28/08/2005	28	Lane 4

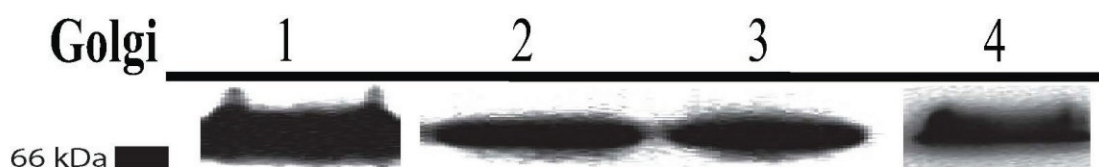


**Table 1. CHO Lec1 Golgi were infected by VSV to produce VSV-G. Top,** List of CHO Lec 1 Golgi preparations that were used for different fusion assays during the course of the thesis ((n) represents the number of detailed cell free transport experiments using multiple concentrations of COPI vesicles performed with these preparations, see table 2). **Bottom,** multiple western blots of VSV-G (a 67 kDa protein) of the above Golgi preparations (its expression was not probed in the preparation made in 09/10/2002, also it is to be noted that these are not controlled to be compared to each other, but rather that the infection process was successful, as it represents multiple different westerns).

In table 1, control for the infection of VSV infection in different batches of CHO Lec1 cells is shown by demonstrating the expression levels of the viral proteins in their Golgi membrane fractions<sup>10, 65, 75, 76, 151, 293</sup> (table 1).

Following the mixing of the COPI vesicles and the Golgi membranes, they were incubated at 37°C for 2 hours to ensure that all fusion events led to complete glycosylation of the VSV-G present in the cisternae<sup>8</sup>. Membranes were then lysed with triton X-100 and the VSV-G was precipitated with primary mouse anti-VSV-G followed by secondary goat anti-mouse IgG. The resulting complexes were filtered and washed to remove any excess free radiolabeled UDP-*N*-acetylglucosamine. The amount of



radioactivity detected on the filters corresponded to the amount of glycosylation events, which in turn represented the number of fusion events that had happened (fig. 1b)<sup>8, 10</sup>.

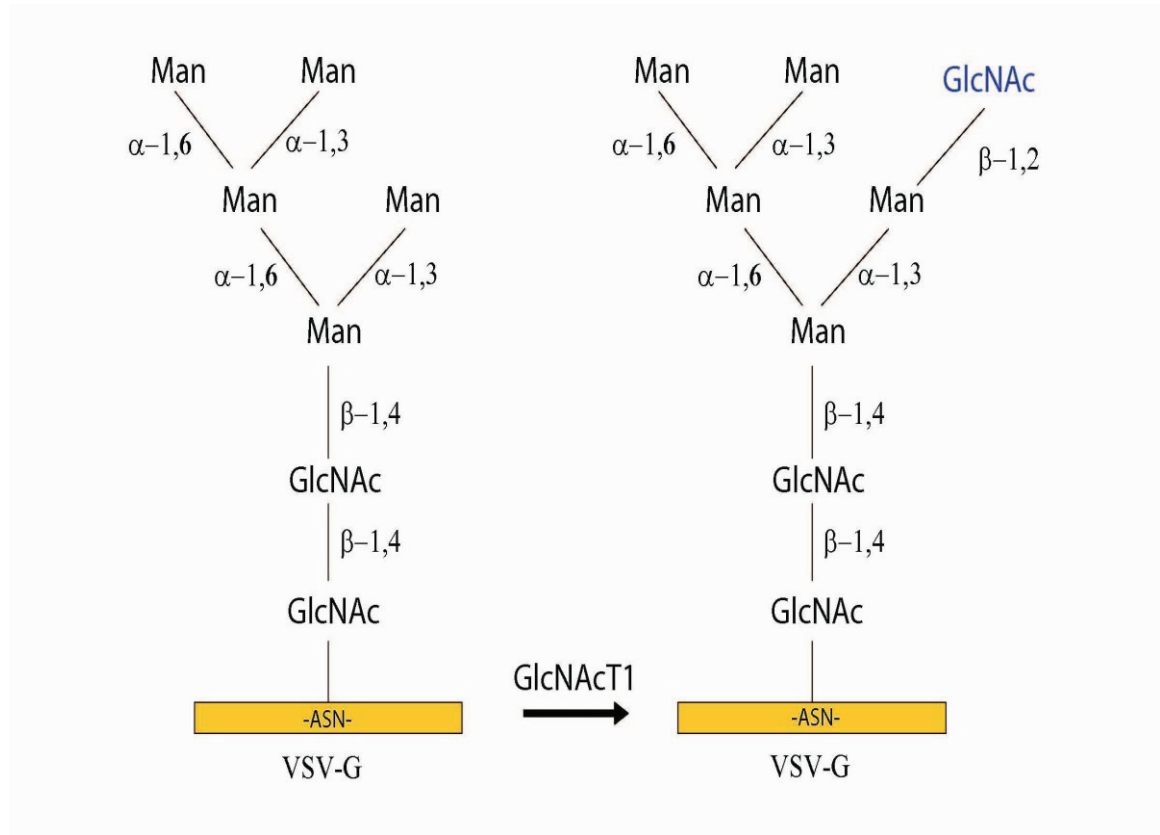


**Figure 1c. Diagrammatic representation of *N*-acetylglucosamine addition.** CHO Lec1 cells are deficient in GlcNAcT1 enzyme. In these cells, the VSV-G glycosylation is incomplete (left). Upon fusion with the COPI vesicles, GlcNAcT1 is transferred to the Golgi cisternae allowing the incorporation of tritiated *N*-acetylglucosamine in the carbohydrate tree of VSV-G.

In order to more precisely evaluate the fusogenicity of COPI vesicles, we have developed a simple method by which the vesicles were serially titrated while the concentration of acceptor membranes were kept constant. The resulting curve, plotting the detected fusogenic signal versus the amount of vesicles being added, was used to determine the ability of the vesicle preparation to fuse (fig. 1d). This relationship could be mathematically defined by the equation  $a + c(1 - e^{(-bx)})$ <sup>8</sup>, where the parameters “a”, “b” and “c” correspond to the minimal signal, the slope of the curve and the maximum signal respectively. In practice, the variable “a” was directly related to the amount of radioactivity that was counted when no vesicles were added to the fusion reaction, serving

to calculate the overall background of the assay. The variable “c”, the maximum amount of counted radioactivity after the subtraction from “a”, measured the total amount of glycosylated VSV-G present in the system that in turn proportionally reflected the quantity of Golgi membranes.

Importantly, this maximum amount of glycosylated VSV-G or “c” should not be misinterpreted as the equivalent of vesicle fusogenicity. In fact, the maximum signal of the assay will be the same independent of their fusogenicity: given a limited quantity of “target” Golgi at which the fusion can occur, an increase of fusogenic vesicles will not necessarily result in an increase of signal, as vesicles will likely fuse to Golgi membranes that have already been fused with one or more COPI vesicles <sup>8</sup>. In this case, the signal is said to have become saturated. Furthermore, this variable “c” could be influenced by the ratio of endogenous non-radiolabeled versus radiolabeled *N*-acetylglucosamine substrates in the assay; glycosylation of VSV-G with the former will not yield any signal. The source of non-radiolabeled *N*-acetylglucosamine might be from the cytosol as well as the Golgi membranes themselves <sup>8</sup>. Therefore, the variable of interest in this assay was “b”, which represented the relationship between the concentration of vesicles and the slope of the curve at which the maximum signal was obtained.

The slope at which the fusion proceeded depended on two factors. First, the amount of vesicles which are present in the solution and second, the ability of these vesicles to fuse. The assay only detected fusogenic vesicles. To put these factors into consideration, the slope variable “b” was re-termed “ $C_v^{app}$ ” <sup>8,10</sup> a.k.a. the *concentration of vesicles that is apparent*, thus capable of generating a signal. For example, a non-saturating population of vesicles with a higher  $C_v^{app}$  will generate a stronger signal than the one with a greater vesicle concentration but with an overall lesser  $C_v^{app}$ . With this value, it is possible to compare the fusogenicity of different preparations of vesicles (table 2).

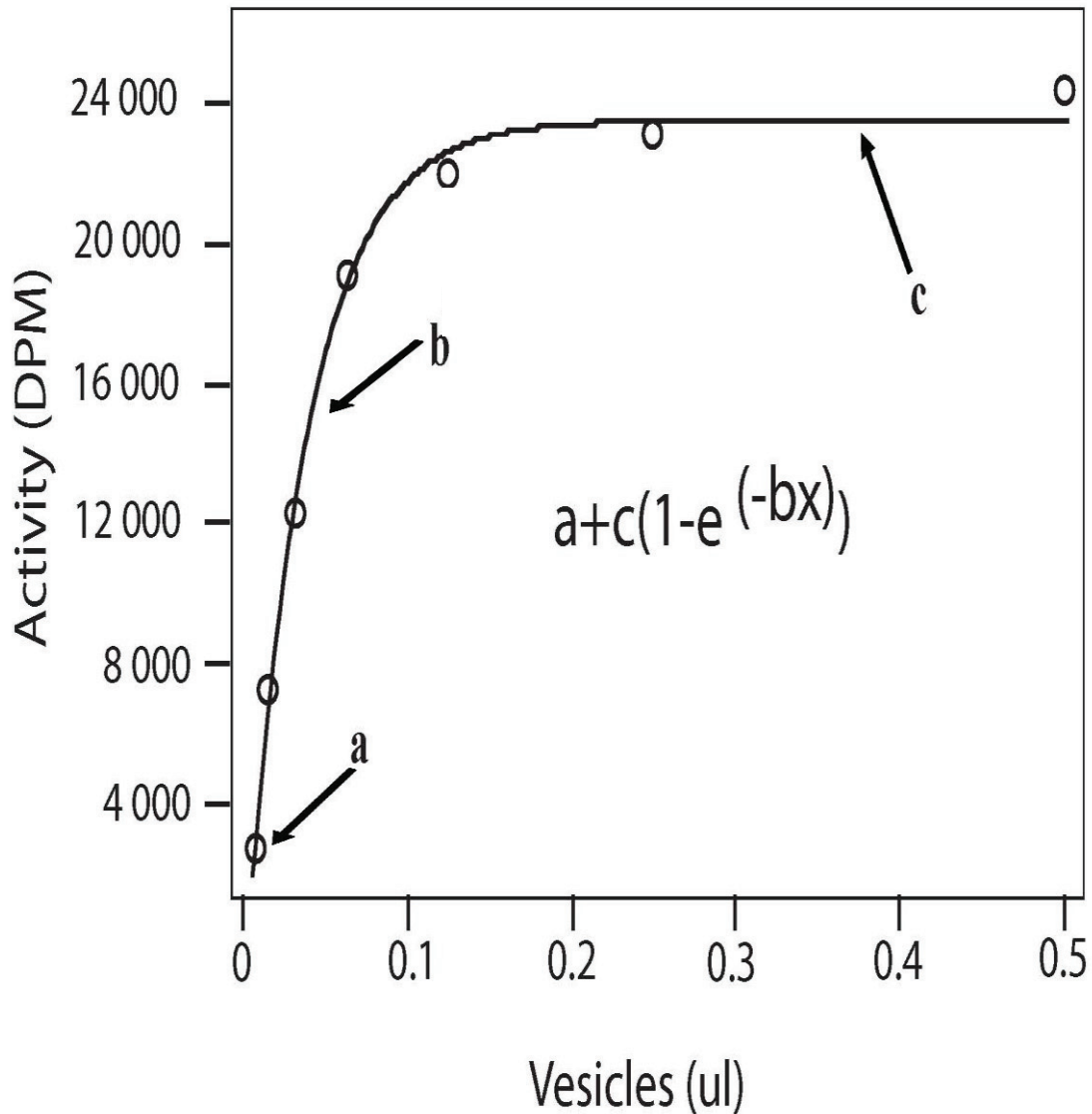


**Figure 1d. Representation of a fusion assay.** In this experiment, an increasing amount of vesicles was added to a fixed amount of acceptor Golgi. The reaction was allowed to proceed until all VSV-G from a Golgi cisternae that had fused with a COPI vesicles was glycosylated. The resulting radioactivity was counted and plotted on the graph above. The ordinate, expressed in disintegration per minute (DPM but sometimes expressed as counts per minutes, CPM), represents the counts that were detected on the filters. The abscissa represents the amount of vesicles in micro liters ( $\mu$ l) that were introduced to the fusion assay. The fusion assay success is determined by establishing the signal generated in relation of the amount of vesicles added. The curve corresponds to the equation  $a + c(1 - \exp^{-bx})$ . We display here 'a', the minimum signal, 'c', the maximum signal, and the critical portion of the curve between 'a' and 'c' where the slope of the curve, 'b', was estimated to be the slope of the fusion reaction from which it goes from 'a' to 'c'.

<b><u>Vesicles</u></b>	<b><u>C<sub>v</sub><sup>app</sup></u></b>	<b><u>STDEV</u></b>	<b><u>(n)</u></b>
Sep-02	53.2	14.7	10
Jan-03	21.5	4.16	8
Apr-03	22.8	5.34	22
Apr-03*	10.4	1.84	12
Jan-05	13.3	3.25	3
Oct-05	5.17	1.66	8
Apr-06	4.08	1.38	5
Oct-06	4.55	0.97	3

**Table 2. Fusogenicity of vesicles can be evaluated reproducibly by their C<sub>v</sub><sup>app</sup>.** Although different preparations of vesicles can have variable C<sub>v</sub><sup>app</sup>, depending on the quality of the Golgi membranes and cytosol extracts as well as their production scale, the same preparation always gave a constant C<sub>v</sub><sup>app</sup>. (\*) Experiment with an additional pre-incubation for 1 hour at 37°C.

The developed fusion assay has been proven a reliable tool for the investigation of intra-Golgi transport based on at least 3 important observations: First, it was strictly dependent on the presence of cytosolic components, most probably  $\alpha$ -SNAP and NSF that are known to be crucial for the fusion to occur<sup>8, 9, 195, 294</sup>. Second, while still in spinner culture, the target Golgi must be pre-incubated at 15°C in order to concentrate the VSV-G in the CGN, which is the most fusogenic sub-compartment of the Golgi apparatus. Purification of the acceptor Golgi cisternae at higher temperatures resulted in VSV-G that migrated instead to the medial and *trans* parts of the Golgi, which do not support the fusion of COPI vesicles<sup>76</sup>. Third, we provided evidence that the fusion was specifically mediated by COPI vesicles but not by any other donors. While GlcNacT1 is shown to be mostly enriched in COPI vesicles, it could also be found in COPII vesicles generated from ER contaminants in the Golgi fraction or in clathrin-coated vesicles derived from the TGN. Even though the level of GlcNacT1 activity present in the aforementioned organelles is very low, it may be sufficient to produce a signal when these organelles actually fuse with the target Golgi in the assay. To control for this possibility, we

modified the budding assay by removing  $\beta$ -cop from the cytosol such that the formation of COPI vesicles was inhibited (fig. 1e) <sup>10</sup>. This was achieved by pre-incubating the cytosol with anti- $\beta$ -cop antibodies coupled to gelatin beads. Lanoix *et al.* <sup>12</sup> had previously shown that this technique prevents the formation of COPI coats and allows complete removal of all coatomer subunits. They also demonstrated that the inhibition is reversible by addition of purified coatomer proteins alone. Figure 1e (i) compares the levels of remaining  $\beta$ -cop between control, mock and depleted cytosol preparations. These cytosol preparations were then collected and incorporated into separate budding assays. The budded vesicles were introduced to fusion assays and their fusogenicity was monitored (fig. 1e(ii)), which revealed that compared to control, the fraction that was generated with depleted coatomer proteins was 25 times less fusogenic than control. Significantly, there was a clear correlation between the amount of  $\beta$ -cop present in the budding assay and the fusogenicity of the collected vesicle fraction. Thus, we were convinced that the fusogenic products collected in budding fraction and participating in the fusion were indeed COPI vesicles <sup>10</sup>.

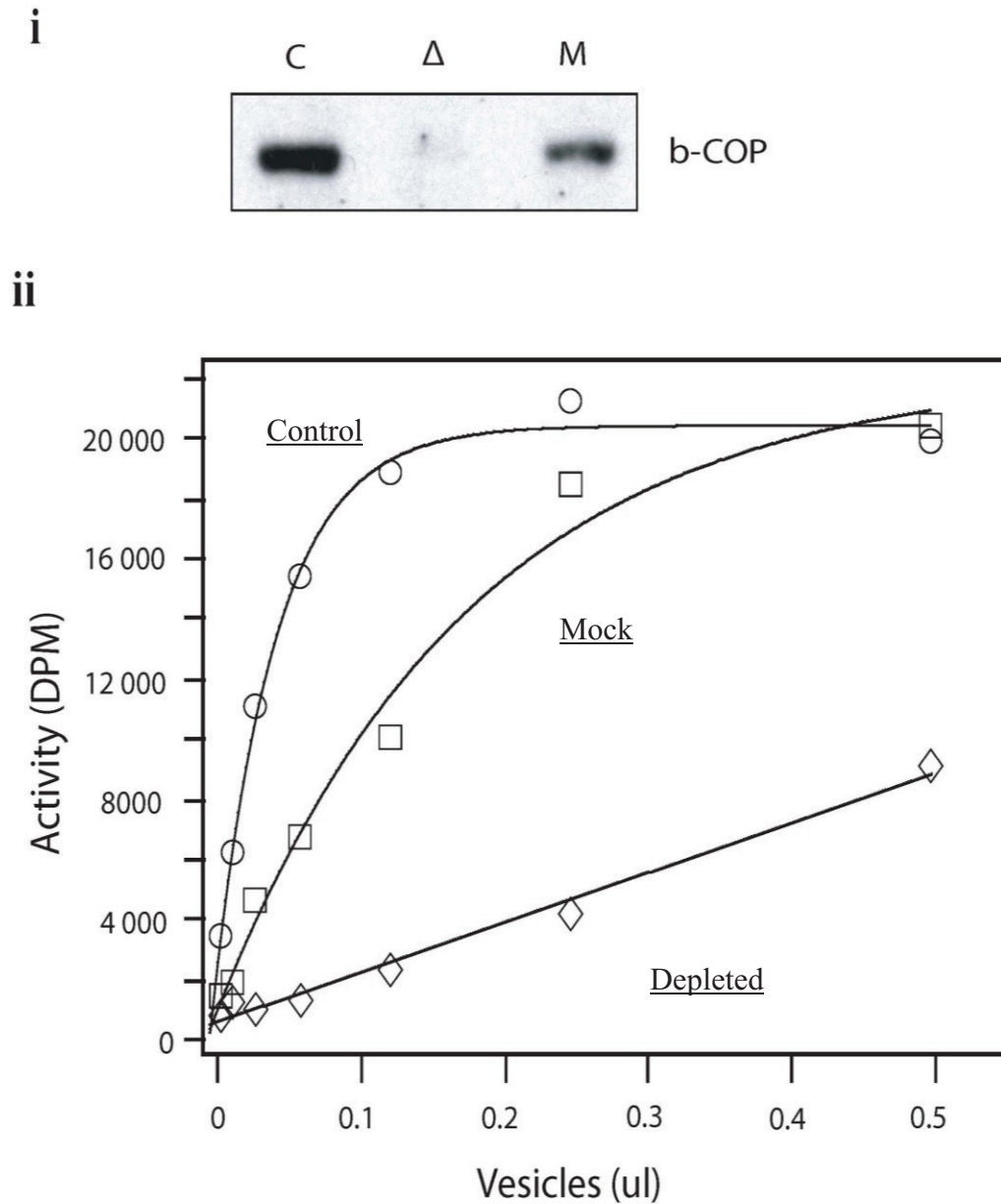


**Figure 1e. The fusion assay monitors the fusion of COPI vesicles.** **i)** COPI vesicles were generated with normal (C), mock-depleted (M) or  $\beta$ -cop proteins-depleted cytosol ( $\Delta$ ). Their  $\beta$ -cop levels were examined by immunoblotting. **ii)** Vesicle fractions generated by using the above different cytosol preparations were titrated as in standard fusion assays. The experiments with mock-depletion ( $\square$ ) and  $\beta$ -cop depletion ( $\diamond$ ) had a  $C_v^{app}$  that was  $0.45 \pm 0.28$  and  $0.04 \pm 0.01$  of control ( $\circ$ ) respectively <sup>10</sup>. (Here, like in following experiments, the presented figure is a representation of a typical experiment. The data was expressed as MEAN  $\pm$  STD obtained from at least three independently repeated experiments)

## **Discussion**

This chapter described in depth the setup of the budding and fusion assays that enabled us to reliably reproduce *in vitro* the molecular events in intra-Golgi transport. We used the budding assays to purify COPI vesicles. Our method, however, differs from the methodology previously described by Malsam *et al.* <sup>55</sup>. While our technique used snap-frozen purified cytosol to generate the vesicles in the budding assay, their method supplied only purified ARF1 and coatomer. Another key player, ARFGAP1, known to be involved extensively in the budding of COPI vesicles <sup>18</sup>, was missing. Consequently, their final vesicles appeared to remain coated under EM and were 75 nm wide, significantly larger than our vesicle preparation. They explained that the coating of the vesicles was preserved to inhibit the fusion and to facilitate their purification; a function similar to that of  $\alpha$ -SNAP<sup>mut</sup> in our protocol. However, we favored the use of  $\alpha$ -SNAP<sup>mut</sup> because it did not affect the composition of the vesicles. Indeed, their vesicles have been shown to be more heterogeneous and contaminated with other organelles. They were biochemically distinct from vesicles produced with hydrolysable GTP and working ARFGAP1. In addition, how the lack of other factors normally found in the cytosol has affected the vesicle formation *in vitro* remained to be speculated. For instance, diacylglycerol (DAG), phosphoinositides as well as BARS-50 are known to play a role in COPI vesicle budding <sup>10, 190, 192, 193</sup>. Altogether, the final uncoating step mediated by ARFGAP1 is crucial in determining the composition of COPI vesicles (for review see <sup>18</sup>). Without this enzyme, vesicles produced by the method of Malsam *et al.* were likely to resemble more to those generated with GTP- $\gamma$ -S <sup>7</sup>, which is an inhibitor of ARFGAP1 activity.

Another significant difference found in their technique was that they incorporated a second step that precipitated the COPI vesicles by beads coated with CASP, a Golgin tethering factor that was shown *in vivo* to play a role in the Golgi-to-ER transport <sup>55</sup>. This pull-down offered the advantage of allowing different pools of COPI vesicles to be sorted out and selected. Unlike the vesicles observed in average prior to the precipitation, the subpopulation recognized by CASP (constituting only 10% of the total) was smaller and uncoated, probably biochemically closer to our preparation <sup>7</sup>. It is possible that they were

generated with the aid of residual ARFGAP1 found in the Golgi membranes used during the budding procedure.

With the purified COPI vesicles, we next sought to examine the consumption of COPI vesicles by Golgi cisternae by developing the fusion assay. We provided supporting evidence that our fusion assay reproduces *in vitro* the retrograde transport of Golgi resident enzymes in COPI derived vesicles and can be used as a standardized and reproducible tool to monitor the vesicle fusogenicity. Furthermore, we demonstrated that the fusogenic content present within the fraction was indeed derived from COPI vesicles. By depleting  $\beta$ -COP from the budding assay, no fusogenic vesicles were collected (see fig. 1e).

We herein defined the fusogenicity of COPI vesicles as the ability at which they fuse with the target Golgi membrane. This attribute can be measured by the slope of the fusion curve or be mathematically represented by “b” in an important equation that we introduced:  $a+c(1-e^{-bx})$ . Since only the fraction of vesicles that are fusogenic can be detected, this variable was termed “ $C_v^{app}$ ”, a.k.a. the concentration of vesicles that are apparent. Emphasis was made on the fact that “ $C_v^{app}$ ” should not to be used as an absolute indicator of the vesicle fusogenicity, but rather as a relative value within the same preparation of vesicles. For example, one can modify certain parameters or experimental conditions of the fusion assay and determine if the modifications can lead to a change in “ $C_v^{app}$ ”, i.e. the fusogenicity. This tool was the foundation of our subsequent endeavor in the investigation of the fusion process.



## **Chapter 2: Determining the potential involvement of lipids in the fusion process.**

---

### **Introduction**

The fusion of COPI vesicles had been previously suggested to involve SNAREs<sup>14, 21, 215, 295-297</sup> as well as tethering factors<sup>55, 298</sup>. However, the precise underlying mechanism that allows COPI vesicles to fuse with Golgi cisternae remains largely unknown. There were many reports using purified organelles to characterize the stepwise fusion process in other organelles (see the work of Wickner, W., Martin, T.F., and associates<sup>145, 248, 262, 299</sup>). In a similar manner, we aimed to further elucidate vesicle transport within the Golgi apparatus using the fusion assay described in the previous chapter.

### **Results**

Our first interesting observation was that even in the presence of all required fusogenic factors, COPI vesicles eventually lost their ability to fuse with time when incubated at 37°C<sup>8</sup>. We began by verifying if this loss of fusogenicity was intrinsic to the COPI vesicles or extrinsic and due to a factor from the cytosol. For this prospect, COPI vesicles were pre-incubated only in vesicles buffer without any cytosol before submitting them to the fusion assay. The experiment demonstrated that vesicles still lost their fusion activity. Therefore, we concluded that an intrinsic mechanism present in the vesicles explains their own inactivation (fig. 2a)<sup>10</sup>.

Under normal conditions, the proteins responsible for the formation of the COPI vesicles, namely ARF1, coatamer and ARFGAP1 (referred as the “trinity” in 300), prime the vesicles to fuse simultaneously to the budding process. This priming could be achieved by changing the conformation of certain proteins such as SNAREs<sup>212, 301, 302</sup>. We hypothesized that the loss of fusogenicity over time could be caused by a slow reversal of the conformation of SNARE proteins from fusogenic to non-fusogenic. Alternatively, the fusion may depend

on the reversible modification of a protein or a lipid on the surface of the vesicles (e.g. phosphorylation), which slowly returns to the original state over an extended period of time.

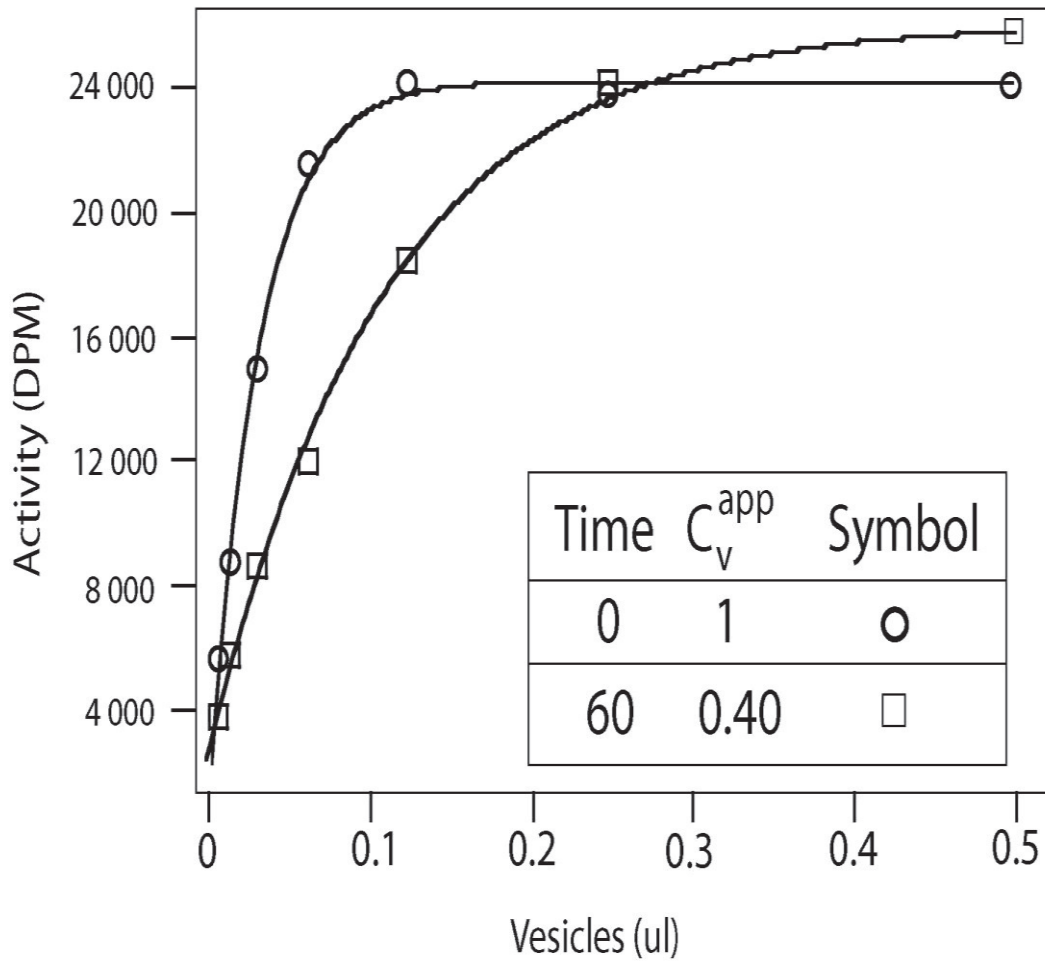


**Figure 2a. Inactivation of COPI vesicles.** Vesicles were pre- incubated for 0 or 60 min at 37°C in the presence of buffer (25 mM hepes pH 7.4, 150 mM KCl, 2.5mM MgCl<sub>2</sub>, 1mM EGTA, 0.25 mM ATP) prior to the cell-free assay. The fusogenicity of vesicles incubated for 60 minutes at 37°C (□) was only  $0.40 \pm 0.06$  times that of vesicles without any pre-incubation. (○).

In order to determine if cytoplasmic oriented proteins on the COPI vesicles were modified after the budding process as well as during the course of their inactivation, we treated the vesicles with proteinase K (PK) (fig. 2b), a serine protease that exhibits a broad cleavage specificity<sup>303</sup>. It has been shown that certain SNAREs become resistant to

PK degradation upon conformational change, and that this conformation change is mediated by ARFGAP1<sup>301</sup>.

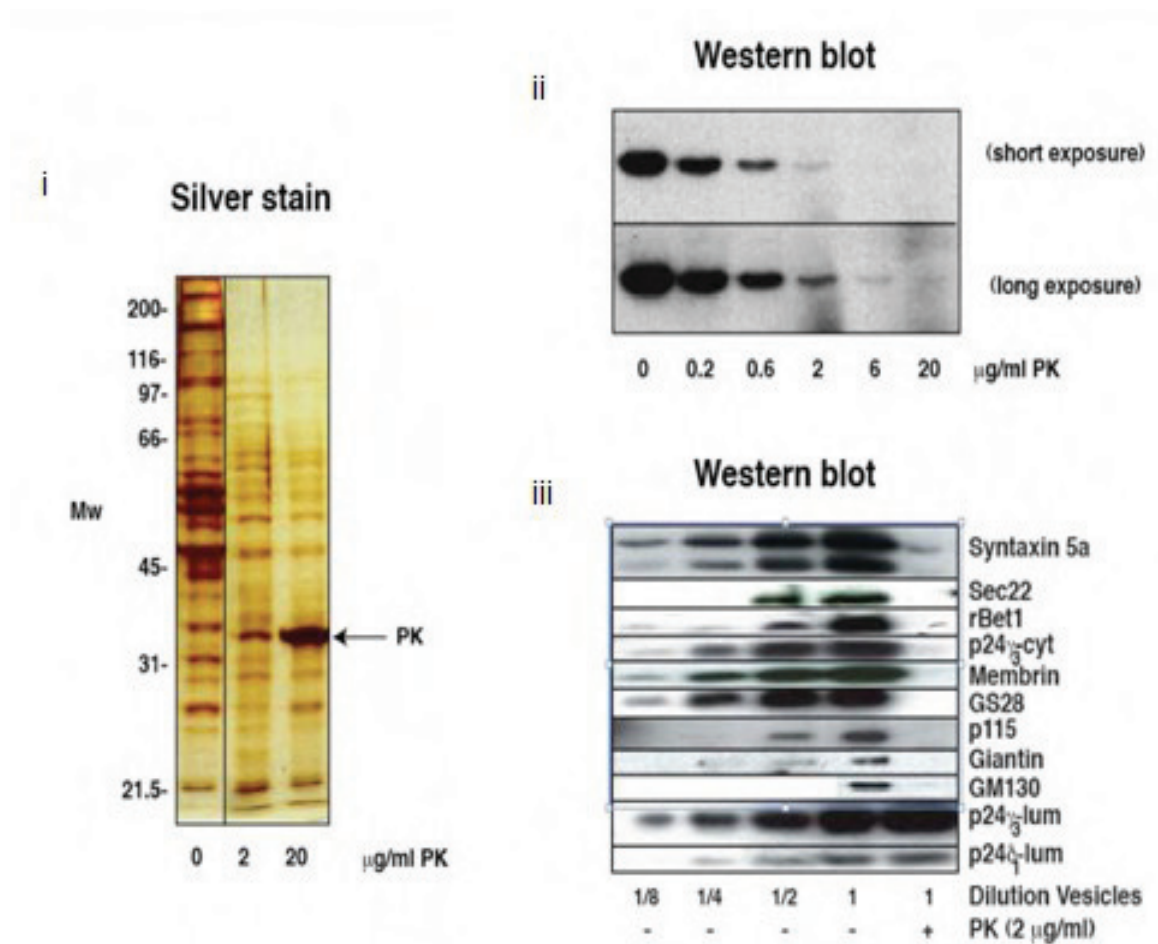


**Figure 2b. Digestion of COPI vesicles.** **i)** COPI vesicle preparations were incubated in the presence or absence of proteinase K (PK) on ice at the indicated concentrations for 30 minutes. After the incubation, 1mM PMSF was added to inactivate the PK. Vesicles were then precipitated with 10% TCA and studied by SDS-PAGE. Proteins were detected by silver staining. PK band is indicated by the arrow. **ii,** Western blot of GS28, with two different exposures. PK was added in increasing amounts to a constant concentration of vesicles. **iii,** In order to determine if there were any PK resistant SNAREs, we performed a series of western blots of proteins known to be present on the surface of vesicles. Increasing quantities of vesicles were used (1/8X – 1X concentration). The largest concentration of vesicles was subject to PK treatment (1+) in comparison to without treatment. Samples of the largest concentration (1- and 1+) were also probed for luminal proteins as control. In the current experiment, we were unable to detect any PK resistant proteins (see chapter 7).

Using SNARE protein GS28 as a marker, we found that the COPI vesicles were sensitive to PK protease similar to Golgi membranes (fig. 2c). We further examined other SNAREs and tethering factors indigenous to the Golgi apparatus as well as COPI vesicles.

However, we were unable to find – at least at the beginning (see chapter 7) - any PK-resistant cytoplasmic proteins by western analysis (fig. 2b,iii). Intriguingly, COPI vesicles could still fuse with the target Golgi even after being treated with up to 20  $\mu\text{g/ml}$  of PK (fig. 2d). In contrast, the same PK treatment had a very rapid and drastic effect on the target Golgi; fusion was totally abolished at 0.05  $\mu\text{g/ml}$  of PK (fig. 2f). Furthermore, we found that PK treated (2  $\mu\text{g/ml}$ ) vesicles also became inactivated (fig. 2e), suggesting that the observed loss of fusogenic function was most likely not a consequence of protein modification. Altogether, these findings lead us to believe that a non-peptide factor might be involved in the fusion of COPI vesicles instead.

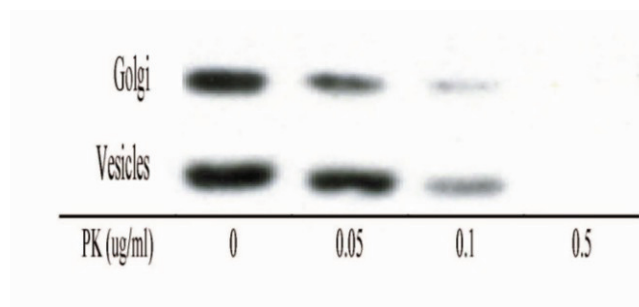


**Figure 2c. Golgi and COPI vesicles possessed similar PK sensitivity.** Golgi and COPI vesicles were incubated in the presence of different concentrations of PK for 30 min. at 4°C. Digestion was stopped by adding 1mM PMSF to the reaction. Equal quantity of GS28 was then loaded on a denaturing gel and the susceptibility to PK was analyzed by western analysis against GS28. The western was unable to demonstrate a change in PK sensitivity between COPI vesicles and Golgi membranes.

### Preliminary lipid experiments

In consideration to the findings above, it was postulated that something else other than protein, such as a lipid incorporated within the COPI vesicles, might be responsible for their fusion. A subsequent literature review was performed to search for a lipid that met the following requirements: 1) this potential target lipid has been identified as a mediator of fusion by multiple publications; 2) it has been shown to be present in the Golgi apparatus.

Phosphatidylinositol 4,5-bisphosphate (PI(4,5)P<sub>2</sub>) (fig. 2g), a divalent negatively charge phospholipid, has been associated with the Golgi apparatus as well as a mediator of vacuolar and synaptic fusion (see literature review). Interestingly, a dependence of

PI(4,5)P<sub>2</sub> synthesis on ARF1 activity within the Golgi apparatus has been documented<sup>271</sup>,<sup>272</sup>. ARF1 has also been shown to couple the COPI vesicle budding to its fusion process<sup>69</sup>. Therefore, we investigated if PI(4,5)P<sub>2</sub> was responsible for mediating the fusion of COPI vesicles to the Golgi cisternae.

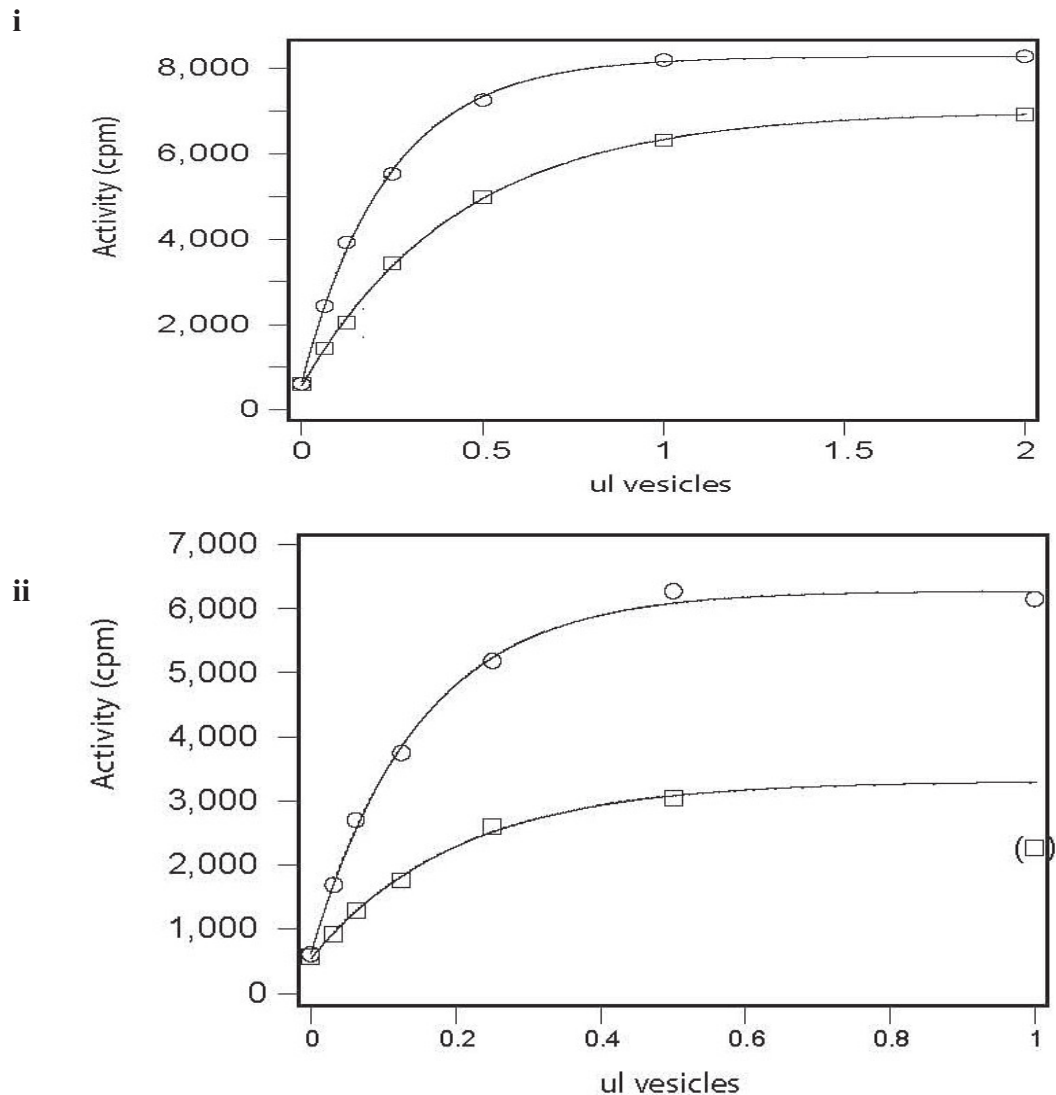
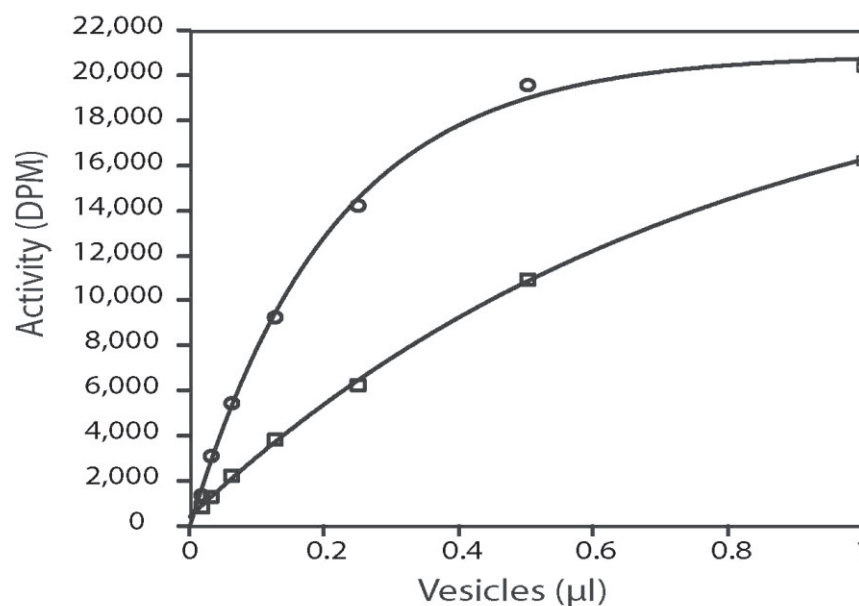


**Figure 2d. COPI Vesicles remained active after proteolysis.** COPI vesicles were incubated in the presence of 2 µg/mg (i) PK for 30 min. at 4°C (□) and their fusogenicity was  $0.624 \pm 7.8$  of control (○). Vesicles also remained active after treatment with 20 µg/ml PK (ii) and yielded similar fusogenicity (ii). To note, while the slope “b” of the curve did not significantly differ from each other, the maximum signal “c” was decreased by the higher dose of PK. Since only a small quantity of PK was needed to have a drastic effect on the target Golgi membrane (fig. 2f), we presume that a reduction in “c” was a result of incomplete PK inactivation by PMSF with residual enzymatic activity in the fusion assay. ( ) denotes an outlier not taken into consideration during the calculation of the curve.

i



ii

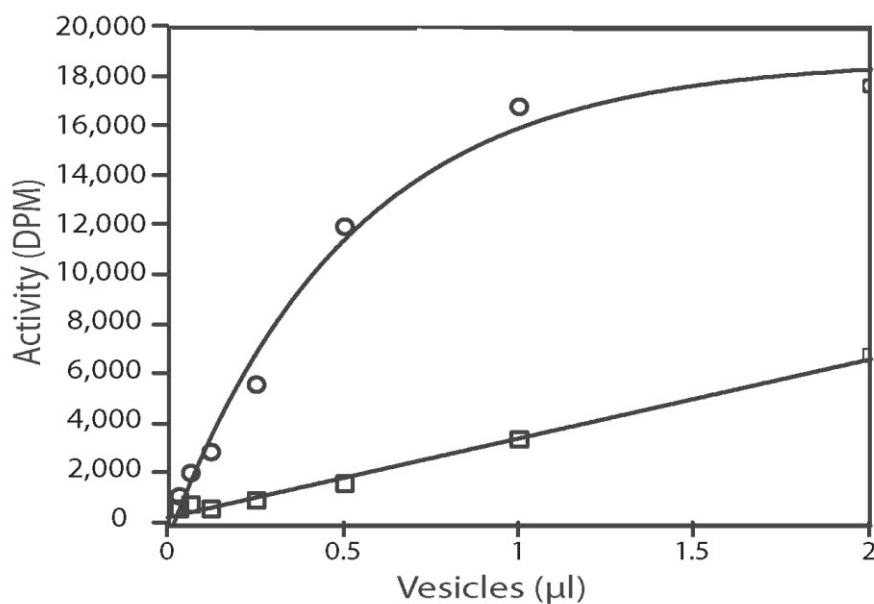


**Figure 2e. Vesicles treated with PK still became inactivated over time.** Untreated vesicles (i) or vesicles treated with 2  $\mu\text{g/ml}$  of PK (ii) were incubated for 30 min at 37°C (□) or kept on ice (○). Following the incubation, vesicles were introduced to the fusion assay and their  $C_v^{\text{app}}$  was measured. Vesicles with or without PK treatment retained  $0.138 \pm 0.026$  and  $0.256 \pm 59$  of their original fusogenic activity, respectively. This data indicated that not only PK treated vesicles still became inactivated when incubated at 37°C like their untreated counterpart, but also they appeared to do so in a more rapid manner. A possible explanation is that, like mentioned in chapter 6, this change in rate was due to modifications in their binding abilities.

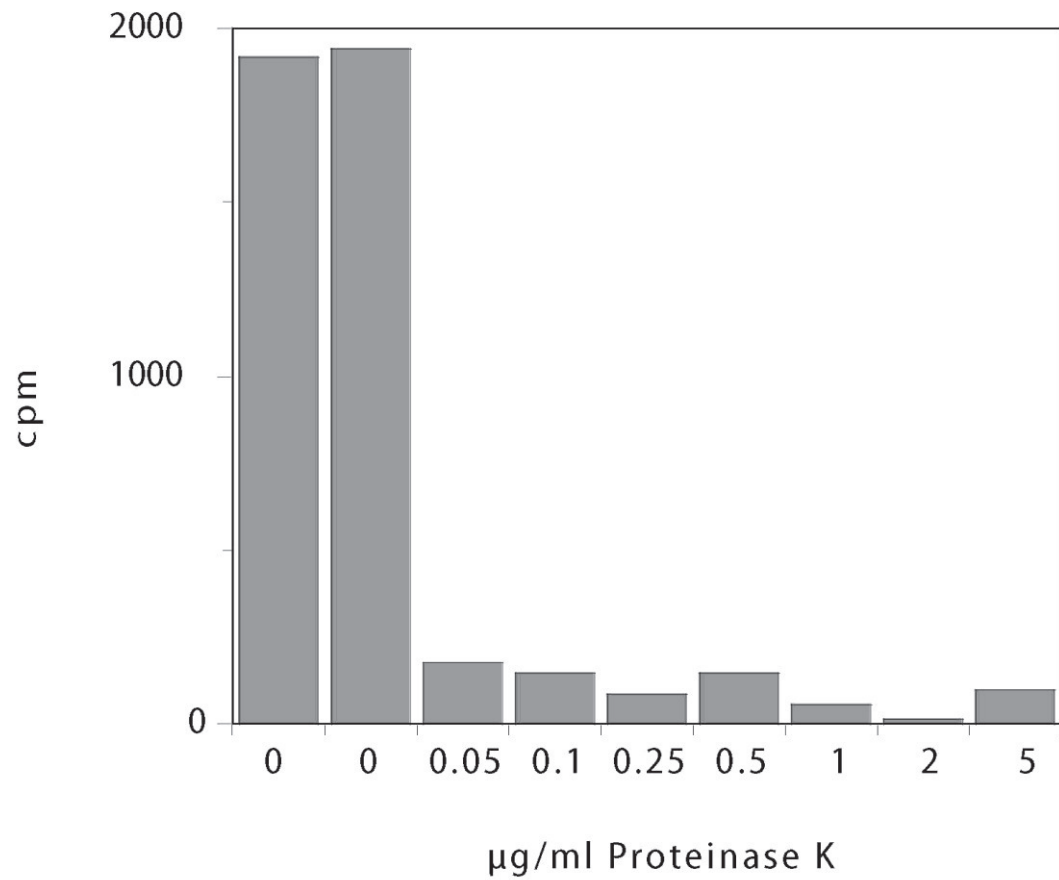


**Figure 2f. Target Golgi was sensitive to PK treatment.** Lec1 "target" Golgi membranes were incubated with the indicated concentrations of PK for 30 min on ice. The protease activity was terminated by 1 mM PMSF. The membranes were then introduced to the fusion assay and incubated for 2 hours in the presence of fusogenic COPI vesicles. As control (second lane from left), 1 mM PMSF was added to the fusion assay in order to exclude the possibility of an experimental artifact by this reagent.



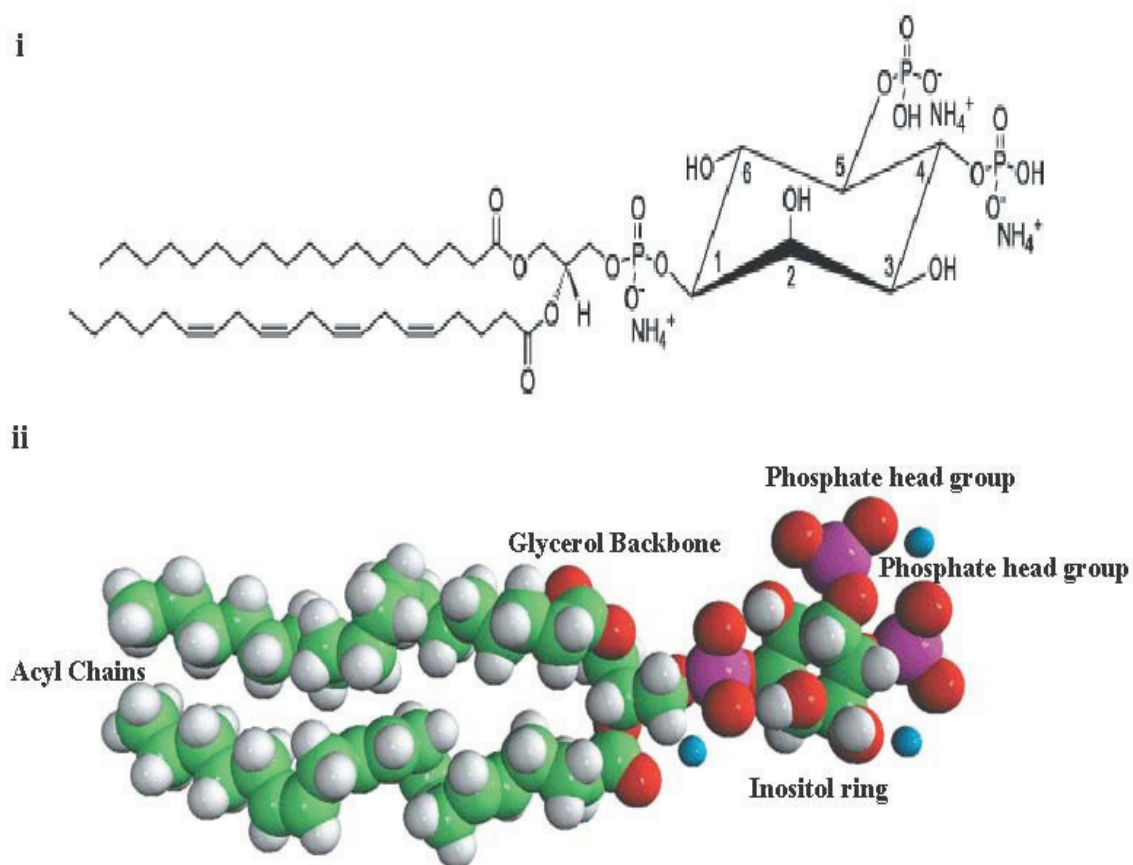


**Figure 2g. PI(4,5)P<sub>2</sub>.** Schematic representation of the PI(4,5)P<sub>2</sub> phospholipid in stick (i) as well as space filling model (ii). The molecule is constituted by two acyl chains, a glycerol backbone and a phosphoester linkage to an inositol ring with two phosphate groups that confer the lipid its prominent negative charge. There exist many PI(4,5)P<sub>2</sub> species with variable acyl chains <sup>5</sup>. In (i), the model is made of 20:4 and 18:0 acyl chains. Three ammonium ions are also represented (© Avanti lipids).

The first experiment involved the testing of neomycin, a divalent cationic antibiotic (fig. 2h) most commonly used for its antibacterial properties but also known for its ability to bind to phosphoinositides <sup>304, 305</sup>. In order to study its effects on COPI vesicles, a series of fusion assays were performed at various concentrations of neomycin. Increasing amount of neomycin in the fusion assay resulted in a loss of  $C_v^{app}$ : at 0.125 mM neomycin, the fusion activity decreased to  $48 \pm 9\%$  of control; at 0.5 mM neomycin, only  $14 \pm 3\%$  remained. Neomycin clearly inhibited the fusion of COPI vesicles (fig. 2i, i). However, this inhibition could be a false positive caused by a PI(4,5)P<sub>2</sub> independent interaction with



substrates in the fusion assay. For example, neomycin might simply have precipitated the coatamer proteins at the concentrations tested above, which could have inhibitory activity as this could also trigger the precipitation of other proteins necessary for fusion or, for that matter, precipitate COPI vesicles themselves <sup>306</sup>.

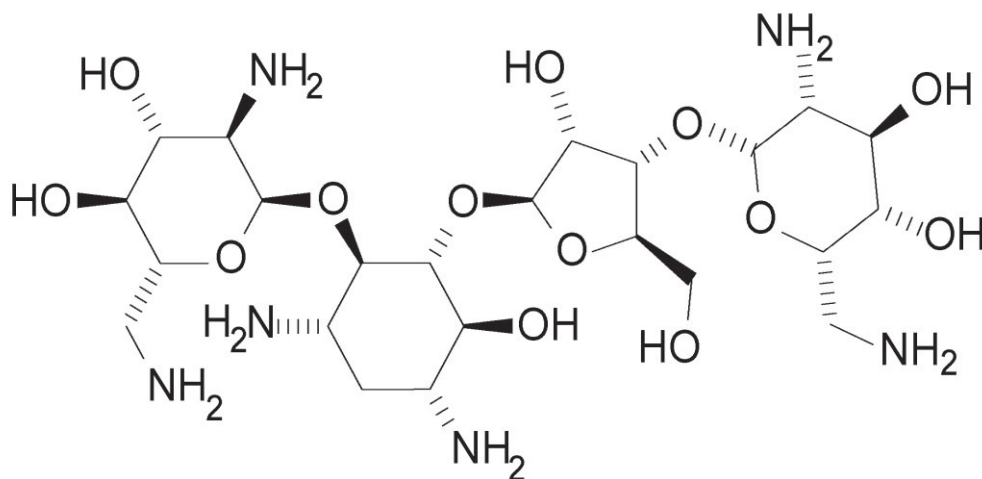


**Figure 2h. Schematic representation of the aminoglycoside neomycin.**

In order to eliminate this possibility, we titrated the amount of neomycin in the presence of a fixed concentration of vesicles. The neomycin was first introduced either to the vesicles or to the rest of the fusion assay consisting of cytosol, target Golgi and buffering solution. Such titration series involving variable amount of the factor in question is another way to determine the fusogenicity of COPI vesicles and similar experiment has previously been done by Mayer *et al.* <sup>248</sup>. It is important to emphasize that, in this type of fusion assay, a non-saturating amount of vesicles should be used generating, for instance, a fusion signal equal to about 2/3 of “c”. It would have been impossible to monitor the effects on the vesicles should a saturated signal were already achieved. A reduction by half of the fusogenicity at saturation would have no significant impact on the overall observed fusion activity (fig. 1d).

As shown in fig. 2i, ii, the inhibition on fusion by neomycin was stronger when the reagent was first introduced to the vesicles, demonstrating that the inhibitory effect was

due to its binding to the vesicles rather than unspecific precipitation of some fusogenic proteins in the cytosol. The difference between adding the neomycin to vesicles and to the cytosolic fraction first could also be explained by a reduced availability of neomycin to the vesicles once the reagent became already bound in the cytosol. Both explanations support the notion that the effects of neomycin was on the COPI vesicles.

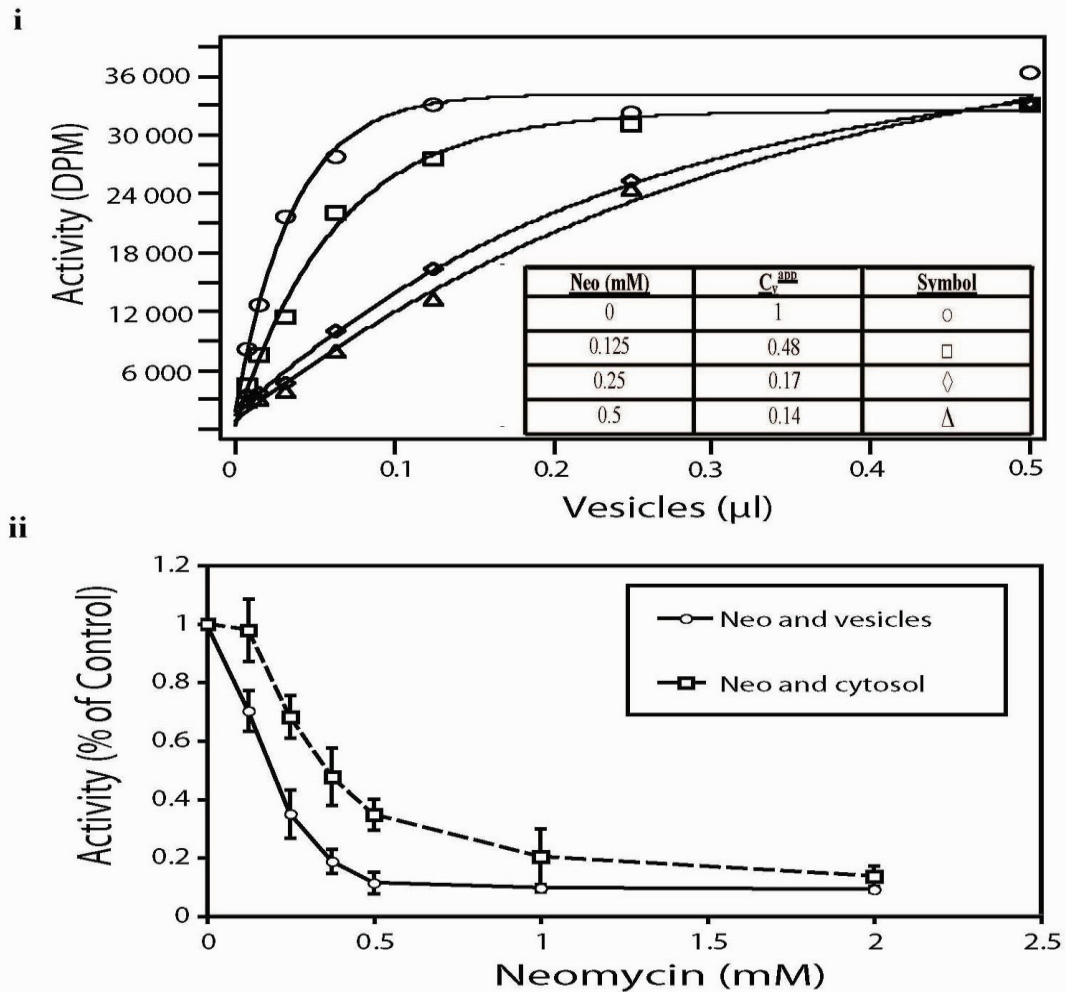


**Figure 2i. Neomycin has an inhibitory effect on the fusion assay. i)** A net decreased in  $C_v^{app}$  was observed when increasing amount of neomycin (0 (○), 0.125 (□), 0.250 (◇) or 0.500 (△) mM) was included in the fusion assay. The fusogenicity of COPI vesicles were only  $0.48 \pm 0.09$  (0.125 mM),  $0.17 \pm 0.11$  (0.25 mM) and  $0.14 \pm 0.03$  (0.5 mM) of control. **ii)** Titration of neomycin in presence of a constant amount of vesicles. The vesicle (○) and Golgi/cytosol (□) fractions were kept separately on ice and increasing amount of neomycin was added to either fraction. They were incubated on ice for 15 minutes before combining them for the fusion assay. (In this case and in the following titration experiments (e.g. fig. 2j), the data points and the error bars are the graphical representation of the MEAN  $\pm$  STDEV of 3 separate experiments from a single source of vesicles.)

We continued our investigation on PI(4,5)P<sub>2</sub> by examining the effects of an IgG antibody against PI(4,5)P<sub>2</sub> (from Assay Designs inc.). Similar to the previous titration experiments, we performed a series of fusion assays using various concentrations of anti-PI(4,5)P<sub>2</sub> in the presence of a non-saturating amount of vesicles. We found a drastic inhibitory effect of the antibody on the fusogenicity (Fig. 2j).

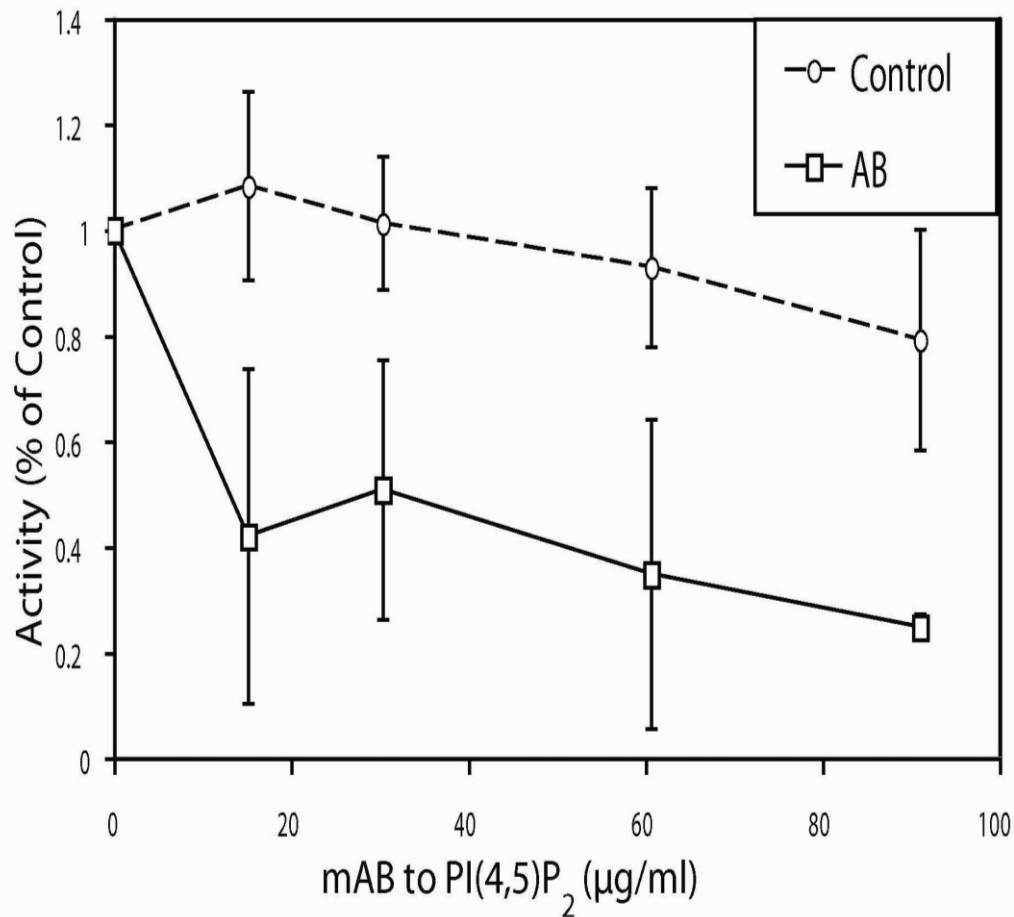


**Figure 2j. Monoclonal IgG against PI(4,5)P<sub>2</sub> inhibits the fusion of COPI vesicles.** Increasing concentration of purified monoclonal IgG antibody against PI(4,5)P<sub>2</sub> (□) was introduced to the fusion assay in the presence of a non-saturating amount of vesicles. Experimental control (○) was composed of either heat inactivated (HI, 95°C for 15 min) antibody or buffer alone (10% fetal calf serum, 0.1% sodium azide). No difference was found between the two controls (data not shown).

We next sought to determine if we could reproduce the inhibition on COPI vesicles by interfering with the PI(4,5)P<sub>2</sub> synthesis. For this purpose, we incubated the vesicles with increasing concentration of wortmannin, a PI3K inhibitor<sup>307</sup> also known to inhibit the formation of PI(4,5)P<sub>2</sub> stimulated by ARF1 within the Golgi apparatus<sup>271</sup>. Similar to neomycin and anti-PI(4,5)P<sub>2</sub>, wortmannin revealed itself to be inhibitory to the fusion of COPI vesicles (fig. 2l).

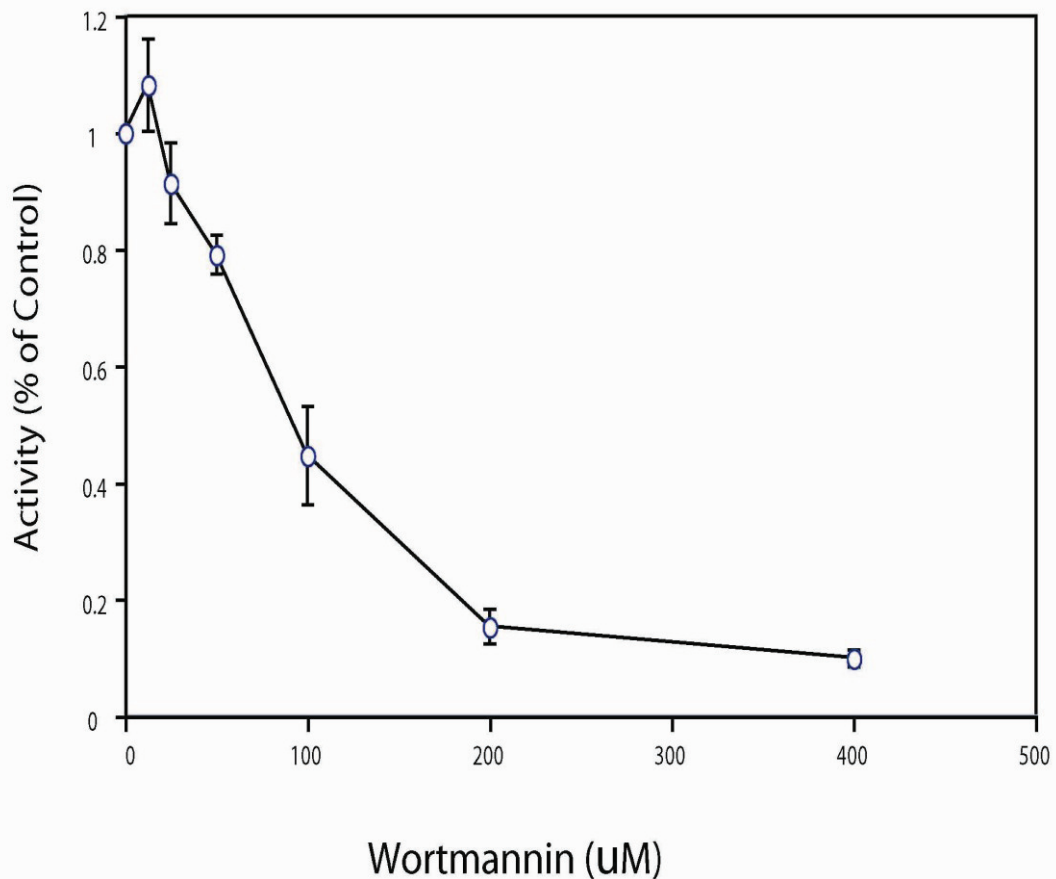


**Figure 2k. Wortmannin inhibited fusion of vesicles.** Increasing concentration of wortmannin (dissolved in DMSO) was introduced to the fusion assay in the presence of a non-saturating amount of vesicles. As control, DMSO was used and no change in the fusogenicity of vesicles was observed (Wortmannin, 0μM, an equal volume of DMSO was used in all solutions) .

## **Discussion**

In this chapter, we provided preliminary evidence that PI(4,5)P<sub>2</sub> mediates the fusion of COPI vesicles. Some concerns were raised, however, regarding to the mode of action and side effects of the reagents being used. For example, it was argued that neomycin might possibly have performed as a precipitating agent exerting an indirect effect on the vesicles<sup>306</sup>. It could also cause steric hindrance on the vesicles and thus prevent the fusion process. The experiments using wortmannin as a PI(4,5)P<sub>2</sub> inhibitor were likewise criticized because this reagent is also an inhibitor for the formation of other phosphoinositides, whose role in the fusion remains elusive. Furthermore, wortmannin is known to affect many pathways in the cell other than the one involving phosphoinositides<sup>307-310</sup>. While the monoclonal IgG against PI(4,5)P<sub>2</sub> appeared specific in its binding to the vesicles, it was still impossible to rule out the possibility that the inhibition was caused by sterically hindering other factors required for the fusion. Finally, although the synthesis of PI(4,5)P<sub>2</sub> within the Golgi apparatus has been shown to be stimulated by ARF1, a key player also responsible for the formation of COPI vesicles, none of the reagents present could unambiguously determine if the PI(4,5)P<sub>2</sub> was required on the surface of the COPI vesicles or on the surface of the target Golgi.

In an experiment that we have performed but was not presented in this thesis, we inserted PI(4,5)P<sub>2</sub> micelles into COPI vesicles and these modified vesicles were monitored for their fusion ability, like what had previously been accomplished in vacuoles<sup>248</sup>. When this experiment was attempted, the micelles demonstrated a very strong soap effect, probably due to the difference in size between COPI vesicles and vacuoles. Undoubtedly, more critical experiments were required to address the concerns above. In the next chapter, we described a novel reagent that exhibits a high level of specificity to PI(4,5)P<sub>2</sub> on either COPI vesicles or target Golgi, allowing us to corroborate the presence and involvement of PI(4,5)P<sub>2</sub> in the fusion process.

## Chapter 3: Identification and manipulation of PI(4,5)P<sub>2</sub> on the surface of the COPI vesicles.

---

### Introduction

The previous studies have suggested the involvement of PI(4,5)P<sub>2</sub> in the fusion process. The next objective of the investigation was to validate this preliminary result by determining if PI(4,5)P<sub>2</sub> is indeed found on COPI vesicles. While PI(4,5)P<sub>2</sub> has been identified in the Golgi apparatus both *in vitro*<sup>271, 282, 286</sup> and *in vivo*<sup>255</sup>, its detection remains a challenge in both conditions due to its instability within the Golgi apparatus and its high turnover rate<sup>282</sup>. Furthermore, PI(4,5)P<sub>2</sub> is not an easy target to manipulate as it contains both a hydrophilic and hydrophobic portion which, we will see later, makes it difficult to isolate and differentiate from other phospholipids. It is also a challenge to find reagents that affects the lipid specifically.

In this chapter, we described the setup of thin-layer chromatography (TLC) and electrospray ionization mass spectrometry (ESI-MS) to analyze the PI(4,5)P<sub>2</sub> content of COPI vesicles. We followed this investigation by developing reagents that were successful in modifying PI(4,5)P<sub>2</sub> which provided insight into the potential role for this lipid in the intra-Golgi transport.

### Results

The methods for studying PI(4,5)P<sub>2</sub> include TLC, high-pressure liquid chromatography (HPLC) and ESI-MS<sup>5, 248, 311, 312</sup>. Among them, TLC is the simplest and most widely used technique.

Unlike other kinds of phospholipids, PI(4,5)P<sub>2</sub> are particularly difficult to extract with the Folch extraction using a chloroform/methanol interface, as it is soluble in both organic and aqueous solvents. This physical property is due to its large hydrophilic head group

that confers its hydrophilic nature. To correct this problem, a modified Folch extraction method was used in which HCl was added to the extraction mixture. The acid served to directly neutralize the negatively charged head group, thus making PI(4,5)P<sub>2</sub> only soluble in the chloroform phase of the Folch extraction<sup>313, 314</sup>.

In TLC, lipids from the samples were first radiolabeled with <sup>32</sup>P before being extracted by the aforementioned modified Folch reagents. The organic extract was then washed to remove cell debris and proteins, dried and resuspended. Spots of these concentrated lipids as well as the lipid standards were applied on the bottom of a TLC plate, which was composed of a silicon based matrix. The plate was then introduced vertically to a TLC tank that contained a thin layer of solvent mixture consisting of chloroform/methanol/water/ammonia. The solvent was allowed to migrate up to the top of the plate by capillary action. The separated spots were subsequently revealed by <sup>32</sup>P autoradiography and identified with the aid of the co-migrating standards previously calibrated by HPLC<sup>312</sup>. The high sensitivity of radiolabeling allowed us to easily detect any minimal changes in the PI(4,5)P<sub>2</sub> levels after an experimental manipulation. While TLC is technically the simplest and most efficient way to identify lipids, its disadvantage is that it cannot differentiate species of PI(4,5)P<sub>2</sub> with variable acyl chains. In addition, isomeric forms of PIP<sub>2</sub> (i.e. PI(3,5)P<sub>2</sub>) will appear identical on TLC.

Because of these technical limitations, we sought to determine if we could also perform the same lipid analysis of COPI vesicles using MS<sup>5</sup>. Following the Folch extraction, the lipid fraction was dried under N<sub>2</sub>, resuspended in acetonitrile/water/triethylamine (70%, 30%, 30 mM) and directly injected into the MS. For our experiments, we used a Micromass Quattro II triple quadrupole equipped with a z-spray interface running in negative ion mode. Briefly, the lipid molecules were first ionized in solution. Then, applied voltage and N<sub>2</sub> stream in the nebulization cone led to their vaporization. The resulting vaporized molecules were introduced to a quadrupole where they were separated based on their mass to charge ratio (m/z). A typical MS graph displays the relative abundance as a function of the m/z ratio (see figure 3a).

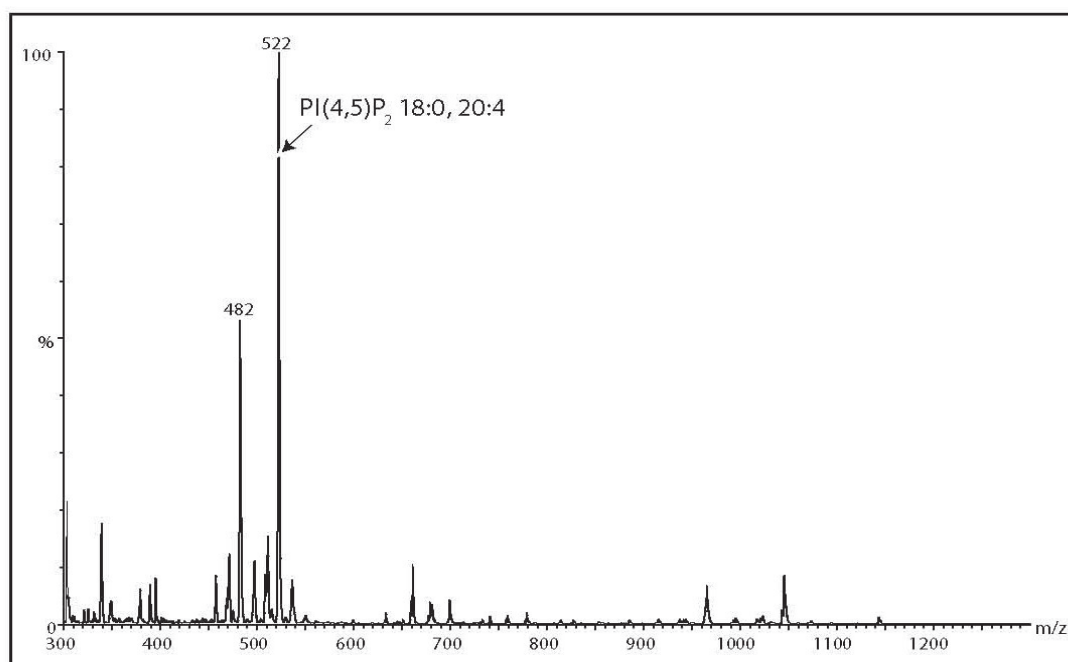


**Figure 3a. Mass spectrometry scan.** We show here a sample MS scan of purified PI(4,5)P<sub>2</sub>. In these types of graphs, the abscissa indicate the detected mass to charge ratio (m/z) of the ions while the ordinates mediate the relative intensity of the peaks compared to the main peak, in this case 522 m/z.

Before we tried to detect phosphoinositides in the Golgi membranes, we first established the fragmentation pattern of a commercially available PI(4,5)P<sub>2</sub> standard mix (from Avanti Lipids). Under the optimized experimental conditions, the major peak detected had a m/z ratio of 522, which corresponds to a molecule with a mass of 1045 and a charge  $Z = 2$ . This major constituent with double negative charge was identified as PI(4,5)P<sub>2</sub> with 18:0 and 20:4 acyl chains minus a hydrogen atom (fig 3a). Some decomposition of the standard could be seen in the form of PIP at an m/z of 482 ( $522 - (79(\text{PO}_4)/2)$ ). The fragmentation of this m/z 522 peak yielded 2 daughter ions with m/z of 303 and 283 confirming the identity of the 18:0 and 20:4 acyl chain groups. Other inositol related ions were also detected (fig. 3b). We further verified the presence of phosphate in this molecule as well as in the other minor species of PI(4,5)P<sub>2</sub> with different m/z by doing a precursor ion scan at m/z of 79 (PO<sub>4</sub>). With this technique, we were able to detect PI(4,5)P<sub>2</sub> at a concentration as low as 10 ng/ml (fig. 3c).



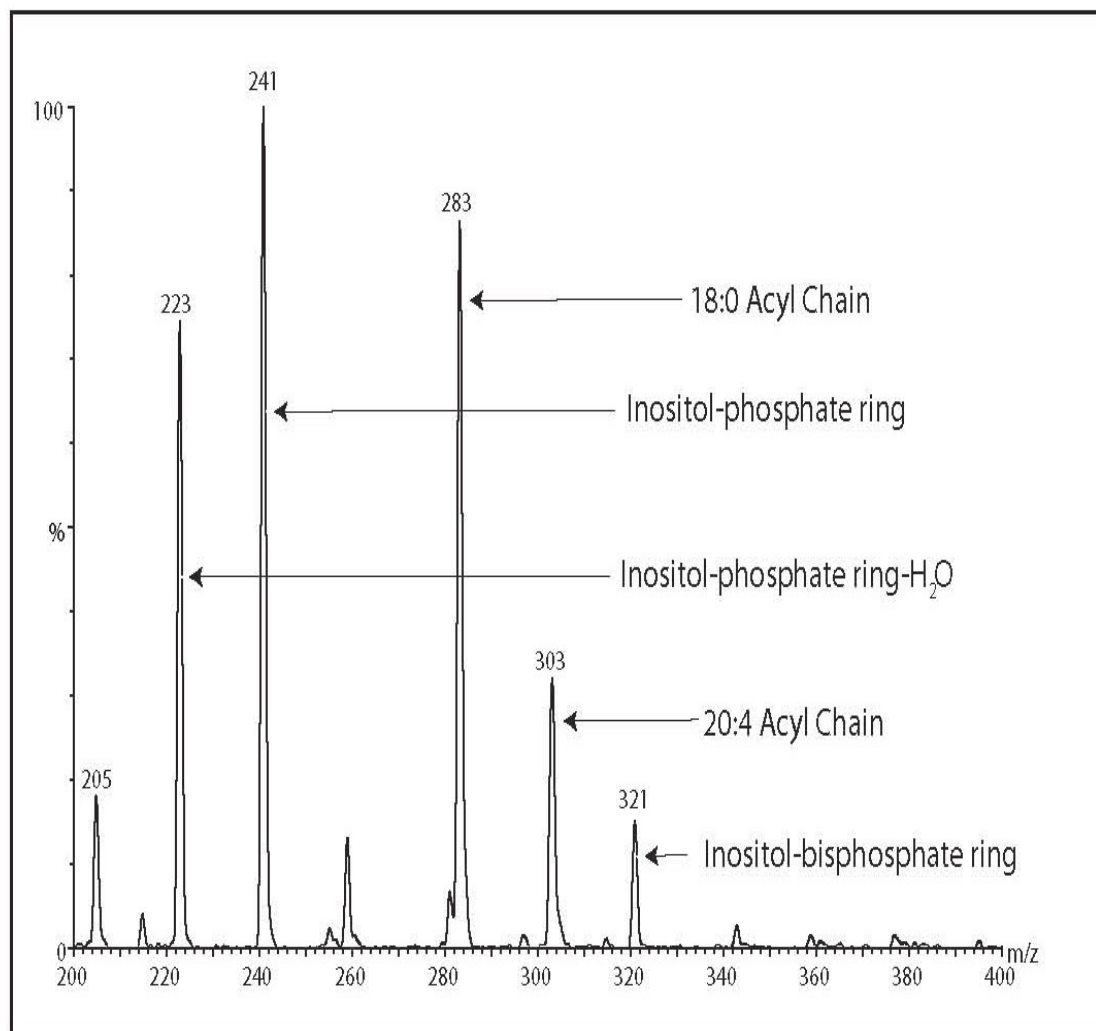


**Figure 3b. Fragmentation of the  $m/z$  522 peak.** The peaks corresponding to  $PI(4,5)P_2$  were selected and fragmented in the second quadrupole. The collision induced dissociation (CID) revealed fragments at  $m/z$  223, 241, 283, 303 and 321, which correspond to inositol with a phosphate minus a water molecule, inositol with a phosphate, the 18:0 acyl chain, the 20:4 acyl chain and inositol with two phosphates, respectively.

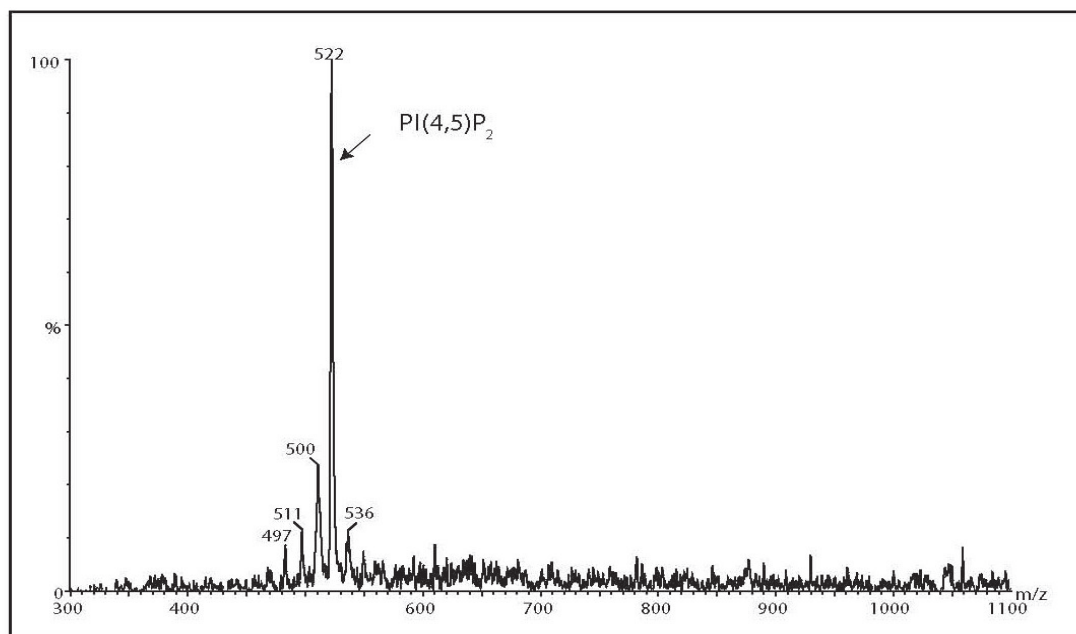


**Figure 3c. Precursor ion scan.** To increase the detection sensitivity, we pre-determined the detection range of PI(4,5)P<sub>2</sub> in the precursor ion mode. In this setup, the first quadrupole continuously selected ions of different m/z to be sent to the collision chamber but only those whose CID corresponded to a pre-selected daughter ion (in this case, phosphate PO<sub>4</sub>, m/z of 79) were recorded. This served to eliminate the background noise created by molecules that do not have any phosphate groups.

Once the setup of MS was established, we analyzed the phosphoinositides content in purified Golgi membranes. Our study found no detectable PI(4,5)P<sub>2</sub> but a very large amount of PI as well as a small quantity of PIP in these samples (fig. 3d, however the fragmentation pattern of the PI and PIP peaks is not shown). There was also a contaminating peak at m/z of 524. Since it had been previously described that the Golgi apparatus possess an intrinsic 5' phosphatase activity, we were not surprised that no PI(4,5)P<sub>2</sub> could be detected<sup>282, 286</sup>. Because the purification of Golgi membranes is a time consuming process, dephosphorylation of PI(4,5)P<sub>2</sub> might have occurred during the long preparation rendering it to below detectable levels. Furthermore, the formation of complex phosphoinositides is an energy dependent process, yet no ATP regenerating system was added when purifying the Golgi membranes. The fact that only a very small quantity of PIP could be detected as well seems to support this premise, as it was shown to be very important for clathrin mediated vesicle budding at the TGN<sup>128</sup>. Therefore, to mimic physiological conditions, we added cytosol and ATP to the Golgi membranes and

incubated them at 37°C. Under these conditions, we were able to detect the formation of PI(4,5)P<sub>2</sub> on the Golgi apparatus (fig. 3e).

Although we could obtain a signal for PI(4,5)P<sub>2</sub> in the MS, its strength and purity were suboptimal. We had extracted lipids from 100 µg of purified Golgi membranes, yet the resulting peak in the scans was barely more intense than the peaks representing the background noises. Furthermore, the presence of a heavily contaminating peak at m/z 524 made the reading and the interpretation of the MS scans even more difficult. Last and not least, because of its unique hydrophilic and hydrophobic qualities, PI(4,5)P<sub>2</sub> appeared to bind with affinity to walls within the MS machine. Different methods of purification, solubilization and nebulization failed to completely eliminate the contamination by residual PI(4,5)P<sub>2</sub> from the previously injected samples.

Given the potential false negative and false positive, it seemed doubtful that a reliable qualitative measurement of PI(4,5)P<sub>2</sub> with MS could be performed. Even with these concerns put aside, the need of several standardized large scale preparations to obtain 100 µg of COPI vesicles made this PI(4,5)P<sub>2</sub> analysis method technically infeasible. Therefore, we proceeded to employ TLC as our method of choice to examine the PI(4,5)P<sub>2</sub> content in COPI vesicles in all subsequent experiments.

By <sup>32</sup>P radiolabeling and TLC, we were able to demonstrate that PI(4,5)P<sub>2</sub> was produced in the vesicle fractions. To note, while the presence of this lipid was confirmed, this method could only detect lipids that were synthesized after <sup>32</sup>P labels were introduced to the system at the end of the budding prior to the fusion assay. Thus, we were not able to detect any PI(4,5)P<sub>2</sub> that was made during the budding reaction. It was assumed that there was no physiological difference between PI(4,5)P<sub>2</sub> produced before and after the budding of the vesicles and that the levels of radioactive PI(4,5)P<sub>2</sub> represented the entire PI(4,5)P<sub>2</sub> pool. Furthermore, it was presumed that signals derived from the labeling of possible contaminants in the COPI vesicles fractions were minimal.

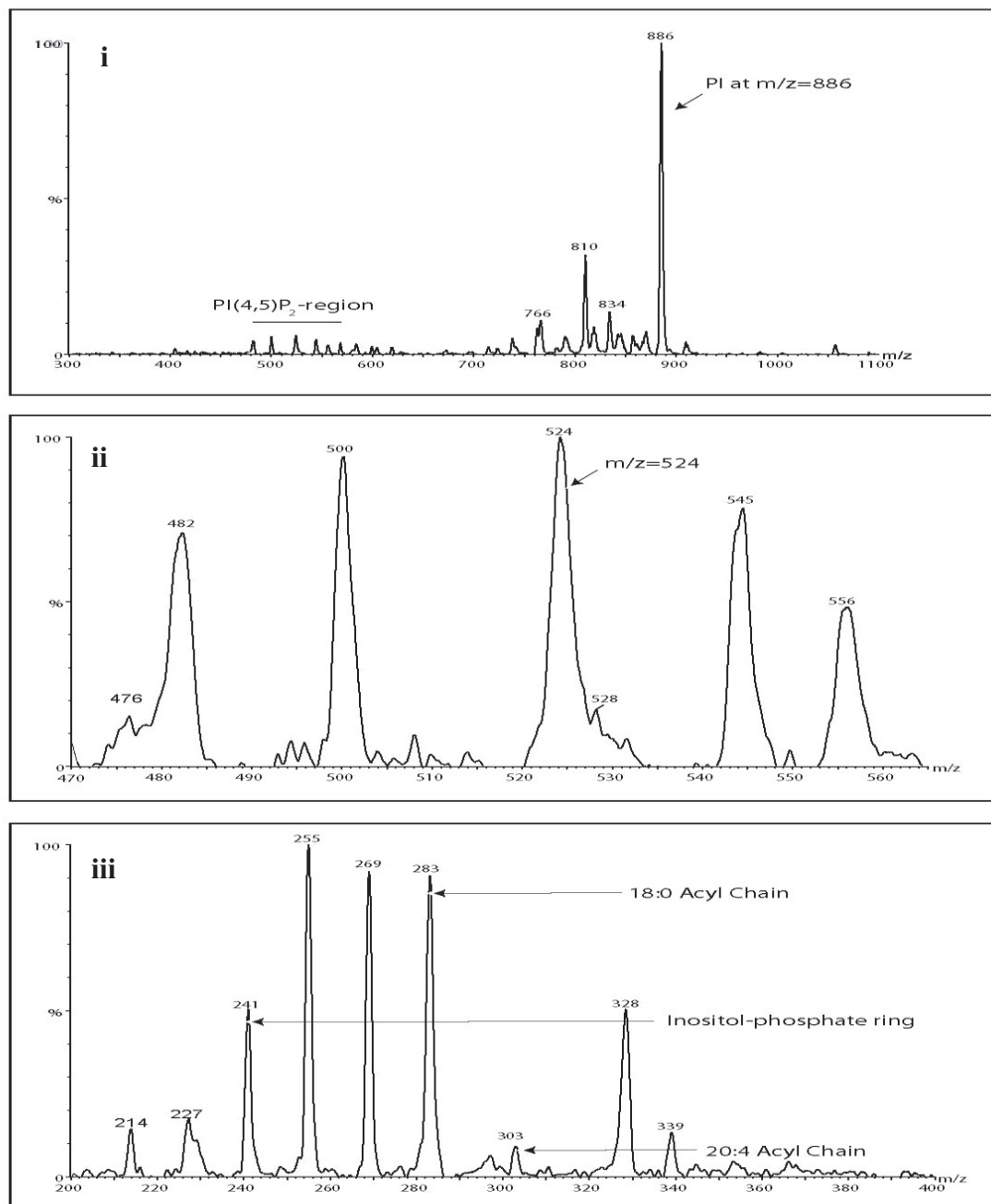


**Figure 3d. ESI-MS analysis of Golgi extract in chloroform/methanol/HCl.** **i)** Purified rat liver Golgi (100µg) was extracted and analyzed by precursor ion scan (m/z 79). **ii)** The region of the scan comprising the PI(4)P (m/z 482) and PI(4,5)P<sub>2</sub> (m/z 522) was enlarged. **iii)** CID of m/z 524 peak displaying the product ion profile. Note the differences in the overall signature between this and the previous figure despite a similar fractionation pattern. The identity of the fragments indicated was suggested only based on their m/z values.

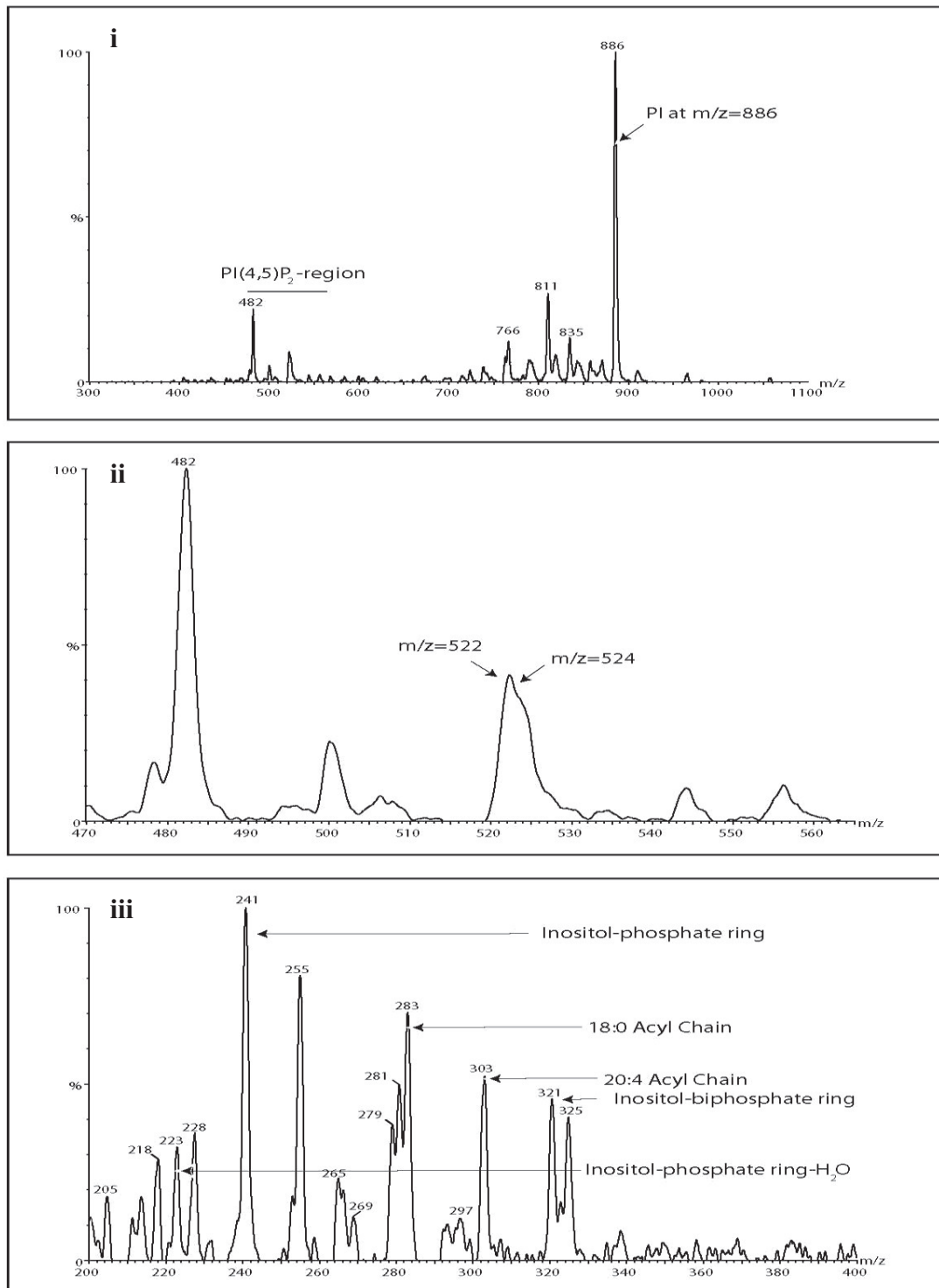


**Figure 3e. Generation of PI(4,5)P<sub>2</sub> by treatment of purified rat liver Golgi with rat brain cytosol in the presence of ATP.** Unlike in figure 3d, Golgi was pre-treated with rat brain cytosol (final concentration of 5mg/ml) in the presence of ATP (0.5 mM) prior to the phospholipid extraction. **i)** Precursor ion scan m/z 79 and **ii)** enlargement of its PI(4)P (m/z 482) and PI(4,5)P<sub>2</sub> (m/z 522) region. **iii),** CID of the m/z 522/524 ion displaying the product ion profile.

Once the presence of PI(4,5)P<sub>2</sub> in the COPI vesicles was corroborated, we investigated the effects of increasing the PI(4,5)P<sub>2</sub> levels on the fusion process. To do so, we catalyzed the reaction of PI(4,5)P<sub>2</sub> from PI(4)P by using purified GST-tagged mouse PI(4)P 5'kinase type 1 $\beta$ , which has been shown to be very specific and does not alter the status of other phosphoinositides<sup>315, 316</sup>. In order to verify if the purified enzyme maintained its enzymatic activity, we incubated the 5'kinase with the Golgi membranes and submitted the reaction products for MS analysis. In figure 3f, one can clearly see PI(4,5)P<sub>2</sub> being formed when the 5'kinase was added. The activity of the 5'kinase was further verified by TLC, which revealed a shift of PI(4)P to PI(4,5)P<sub>2</sub> when the enzyme was added to the vesicles (fig 3g).

Interestingly, while increasing the PI(4,5)P<sub>2</sub> levels by 5'kinase did not have any drastic effect on the fusogenicity of active COPI vesicles, this manipulation could rescue the inactivated vesicles (pre-incubated at 37°C, chapter 2) allowing them to fuse with Golgi cisternae (fig. 3h). The studies of C<sub>v</sub><sup>app</sup> quantitatively illustrated this effect: for example, vesicles that have been inactivated for 60 min at 37°C were able to recover 101%  $\pm$  16% of the original fusion activity when the inactivation occurred in the presence of 1.67  $\mu$ g/ml of 5'kinase (fig. 3i).

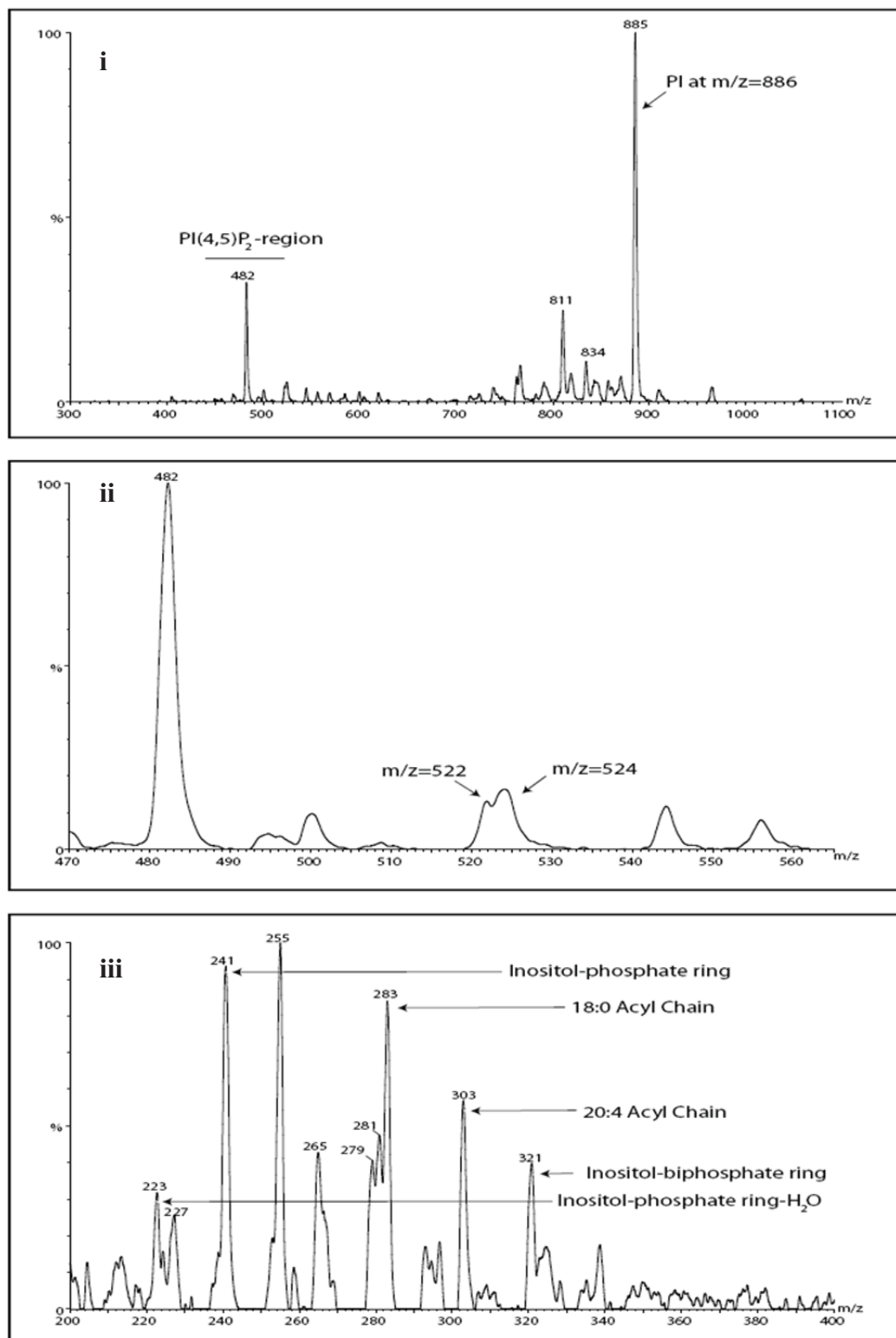


**Figure 3f. PI(4)P 5'-kinase type 1 $\beta$  synthesized PI(4,5)P<sub>2</sub> on the surface of Golgi apparatus.** The Golgi membranes (100  $\mu$ g) were incubated with purified kinase (3.125  $\mu$ g/ml) and ATP (0.5 mM) prior to the phospholipid extraction. **i**, Precursor ion scan of  $m/z$  of 79. **ii**, Enlargement of the PI(4)P and PI(4,5)P<sub>2</sub> region. **iii**, CID of the  $m/z$  522/524 ion displaying the product ion profile.

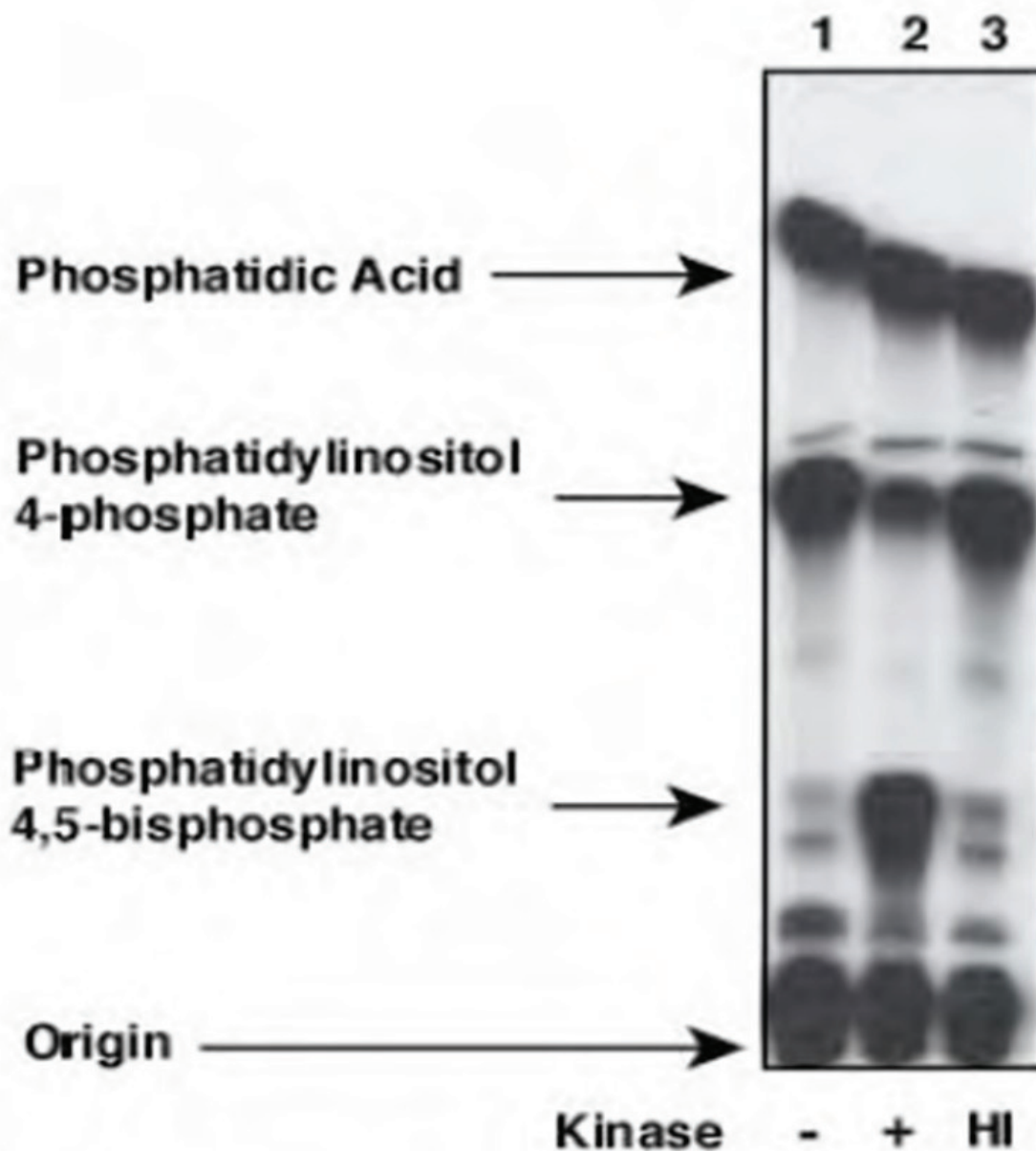


**Figure 3g. Alteration of the phospholipids composition by the mouse GST-PI(4)P 5'kinase type I  $\beta$ .** Purified COPI vesicles (1.25 $\mu$ g) were incubated in kinase buffer (see Materials & Methods) supplemented with  $^{32}$ P-ATP for 60 minutes at 37°C (lane 1 “-”) and 1.67 $\mu$ g/ml of purified mouse GST-PI(4)P 5'kinase type I  $\beta$  (lane 2 “+”) or heat inactivated (15 minutes at 95°C) enzyme (lane 3 “HI”). Note the conversion of PI(4)P to PI(4,5)P<sub>2</sub> in lane 2 compared to both controls.



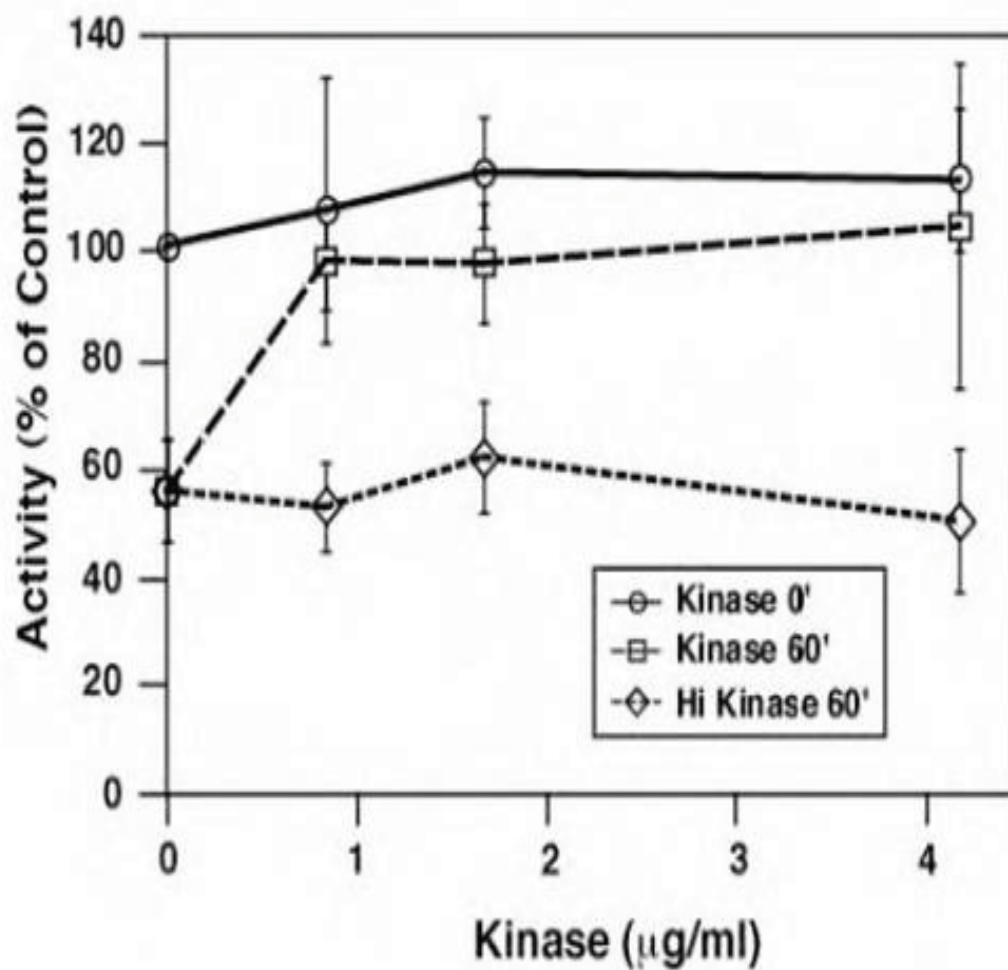


**Figure 3h. 5'Kinase rescued inactivated COPI vesicles.** A non-saturating amount of vesicles were treated with 5'kinase (□) or heat inactivated (HI) 5'kinase (◇) during the 60 min pre-incubation at 37°C before the fusion assay. In the presence of functional 5'kinase, the fusogenicity of COPI vesicles was restored (□) to the control levels (○).

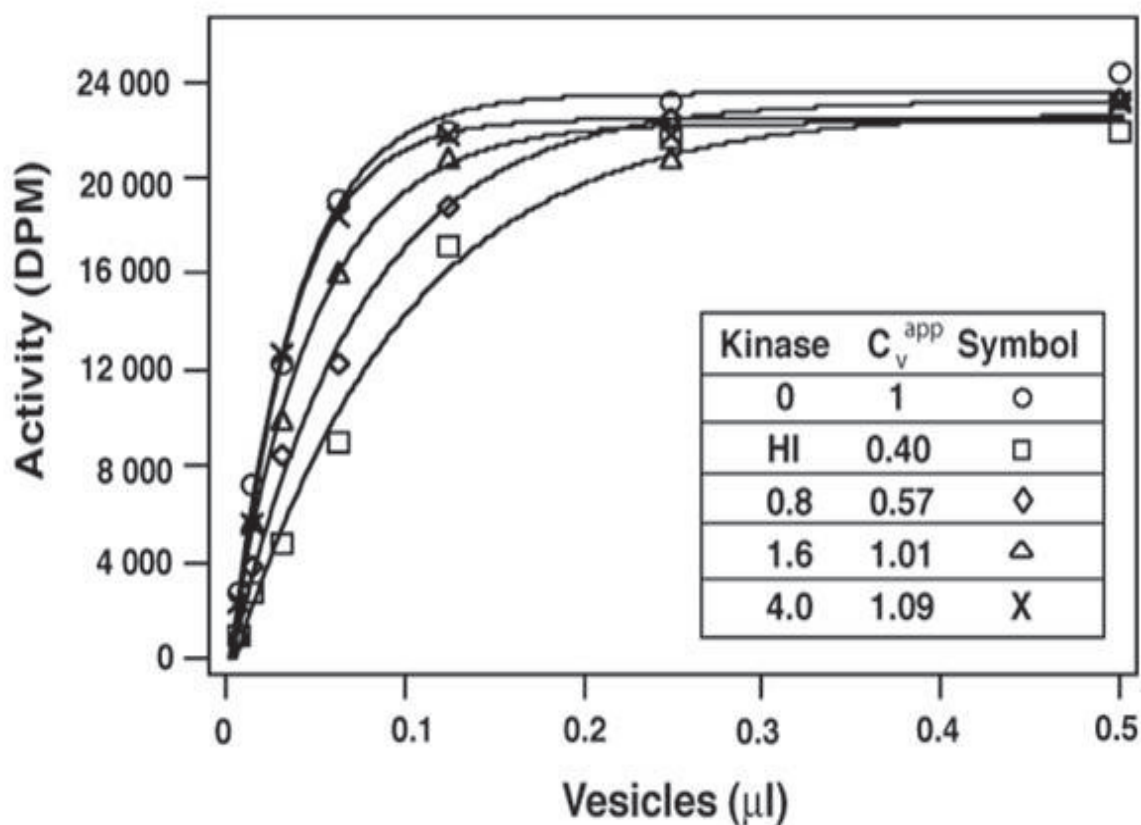


**Figure 3i. Determination of  $C_v^{app}$ .** Vesicles were incubated for 60 min at 37°C with 0 (□), 0.83 (◇), 1.67 (△) or 4.16 (X) μg/ml of kinase and were compared to the control that had not been pre-incubated (○). In the presence of heat inactivated kinase, vesicles were inactivated and their fusogenicity was only  $0.40 \pm 0.06$  of control. In the presence of kinase,  $C_v^{app}$  was restored to  $0.57 \pm 0.14$  (0.83 μg/ml kinase),  $1.01 \pm 0.16$  (1.67 μg/ml kinase) and  $1.09 \pm 0.30$  (4.16 μg/ml kinase) of control. This graph is a good example to illustrate the importance of a dose response curve: while the effect of the kinase is evident below 0.15 μl of vesicles, it was difficult to detect a difference when the vesicles become saturating.

## Discussion

At the end of the last chapter, we were left with the task to determine if PI(4,5)P<sub>2</sub> was present on the surface of the COPI vesicles and if a change in its levels could influence their fusogenicity. Previous investigation using electron microscopy have established the presence of PI(4,5)P<sub>2</sub>, albeit modest, within the Golgi apparatus<sup>255</sup>. Subsequent studies using TLC demonstrated the ability of Golgi to form PI(4,5)P<sub>2</sub> in a ARF1 dependent

manner<sup>271, 282</sup>. In this chapter, we confirmed that the COPI vesicles indeed contained PI(4,5)P<sub>2</sub> with TLC. The most significant finding in this chapter was that we unveiled that an increase in PI(4,5)P<sub>2</sub> synthesis could re-activate fusogenically incompetent COPI vesicles, therefore rescuing their fusogenic ability. However, in order to further provide supportive evidence for the association between PI(4,5)P<sub>2</sub> in the COPI vesicles and the fusion process, it would be necessary to repeat the data by additional experiments using another reagent that could alter the PI(4,5)P<sub>2</sub> levels.

## **Chapter 4: Removal of PI(4,5)P<sub>2</sub> accelerates the inactivation of COPI vesicles.**

---

### **Introduction**

In the last chapter, we demonstrated that a rise in the levels of PI(4,5)P<sub>2</sub> present on the surface of the COPI vesicles resulted in an increase in their fusogenicity. In the same line of thoughts, we sought to specifically remove PI(4,5)P<sub>2</sub> from the COPI vesicles and to determine if this modification has any effect in the fusion assay. If PI(4,5)P<sub>2</sub> is truly involved in the fusion process, their removal should lead to a proportional decrease in the observed fusogenicity.

The difficulty of such an experiment does not reside in removing PI(4,5)P<sub>2</sub>, but rather of removing only PI(4,5)P<sub>2</sub> from the COPI vesicles. Indeed, most phosphatidylinositol phosphatases as well as phospholipases do remove PI(4,5)P<sub>2</sub>, but they also remove other phosphoinositides. Some phosphatases affect only PI(4,5)P<sub>2</sub>, but removes more than one phosphate, therefore making it impossible to determine if an observed effect would be due to depletion of PI(4,5)P<sub>2</sub> or because of a subsequent enzymatic activity<sup>240, 317</sup>.

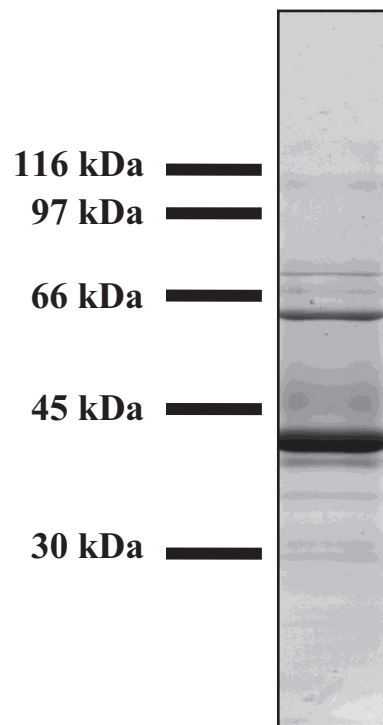
### **Results**

As previously mentioned, the main challenge in the suggested experiment was not to eliminate PI(4,5)P<sub>2</sub> but rather to specifically remove PI(4,5)P<sub>2</sub> from the external phospholipid layer of the COPI vesicles while leaving the other phospholipids intact. Preliminary attempts using phospholipase C (PLC) and phosphoinositol specific PLC (PI-PLC) showed an inhibitory effect on the vesicle fusion (data not shown). However, even though they had been used in the past for PI(4,5)P<sub>2</sub> related research<sup>248</sup>, none of these reagents were considered to be specific: PLC removes every phospholipids headgroups and transforms them to DAG while PI-PLC, slightly more selective, removes the headgroups of phosphoinositides only. Therefore, there was a need to purify a

phosphatase that would only act on PI(4,5)P<sub>2</sub> but not others including PI(4)P. The difficulty resided in the fact that while PI(4,5)P<sub>2</sub> phosphatases are common (Synaptojanins, SAC-1, among others), a PI(4,5)P<sub>2</sub> phosphatase that only targets the 5'phosphate group is exceedingly rare. Many phosphatases have polyphosphatase domains that remove all covalently bound phosphates. The different activities within these domains can be modulated *in vivo* by cofactors and associated proteins, yet this tuning does not exist *in vitro*.

In order to specifically remove the 5'phosphate headgroup in PI(4,5)P<sub>2</sub>, we acquired from Dr. Pietro di Camilli a construct for the 5'phosphatase domain (amino acids 592-900) of yeast Synaptojanin-like 2, (Inp52p), which has been shown to remove only the 5'phosphate of PI(4,5)P<sub>2</sub> and, to a lesser extent, PI(3,4,5)P<sub>3</sub> to form PI(4)P<sup>317, 318</sup>. We inserted the construct in a polyhistidine plasmid and we were able to express and purify the proteins (fig. 4a). The activity and specificity of the purified 5'phosphatase were tested with phosphatidylserine/PI(4,5)P<sub>2</sub> (1:1) liposomes (fig. 4b).

**Figure 4a. Purification of the 5'phosphatase.** A six-histidine tag was added to the 5'phosphatase domain (amino-acids 592-900) of yeast Synaptojanin-like 2 (also known as Inp52p) and the overall construct was cloned in pET-28a vectors and expressed in *E. coli* BL21 cells. The protein was purified with Talon™ beads. The final preparation was subjected to gel electrophoresis and stained with coomassie blue (right).



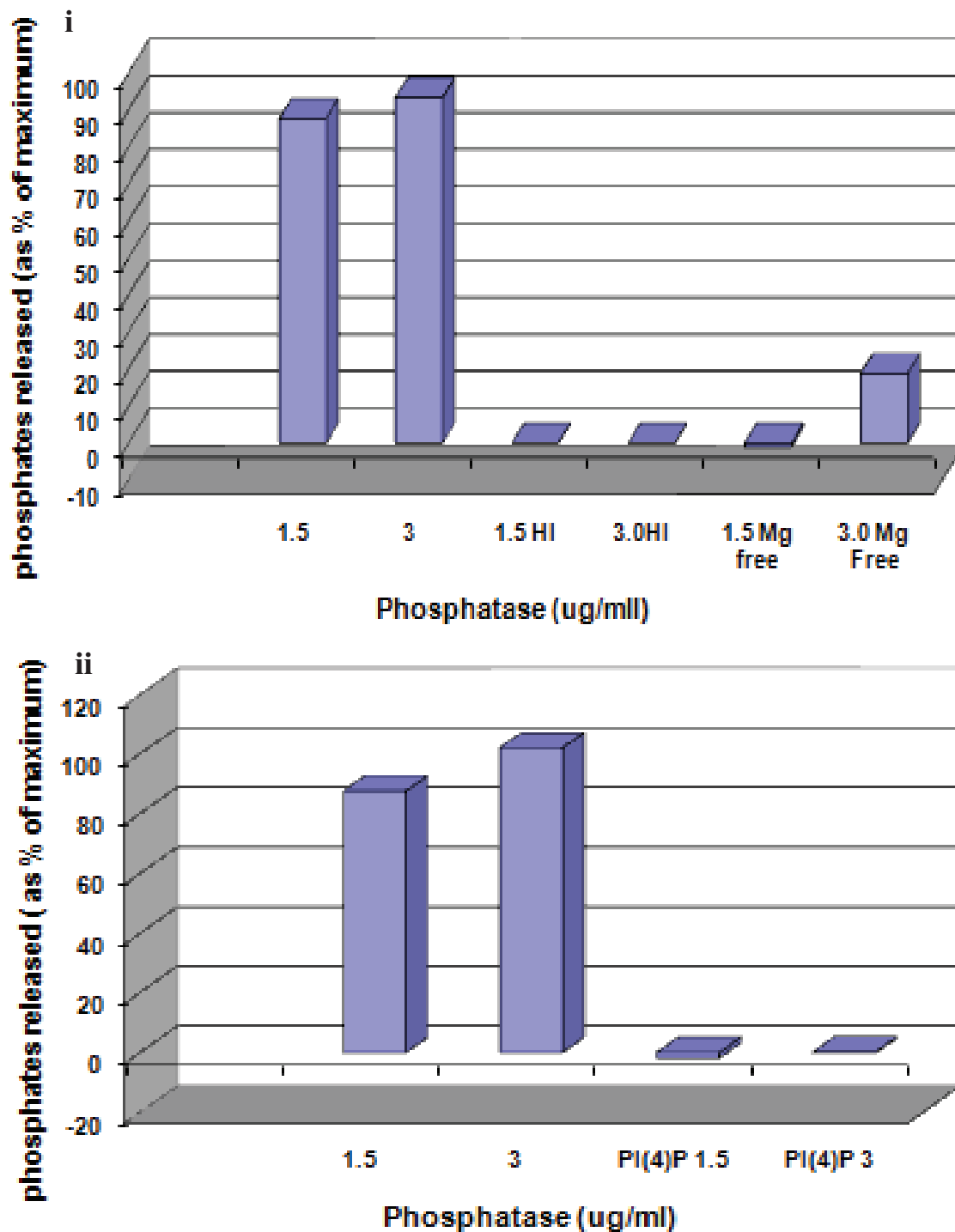


**Figure 4b. 5'phosphatase domain protein removed the 5' phosphate of PI(4,5)P<sub>2</sub>.** Using a phosphate release assay (from Biomol <sup>15</sup>), we detected the release of phosphates from the PS/PI(4,5)P<sub>2</sub> micelles. **i**, The micelles were incubated for 60 minutes at 37°C in the presence of 5'phosphatase, heat inactivated (HI) 5'phosphatase or 5'phosphatase in a buffer lacking Mg<sup>2+</sup> which is essential for the function of the enzyme. **ii**, 5'phosphatase was incubated with micelles constituted with PS/PI(4,5)P<sub>2</sub> or PS/PI(4)P. Similar results were obtained with phosphatidic acid.

We next determined if the 5'phosphatase protein could remove the 5'phosphate headgroup of PI(4,5)P<sub>2</sub> on the surface of COPI vesicles. We incubated the radiolabeled vesicles with the enzyme, extracted the lipids and analyzed them in TLC (figure 4c). We were able to demonstrate the successful removal of the 5'phosphate from PI(4,5)P<sub>2</sub> in the COPI vesicles by the purified 5'phosphatase.

To test the effects of the purified 5'phosphatase in the fusion assay, we pre-incubated a fixed, non-saturating quantity of vesicles with increasing amount of 5'phosphatase at 37°C for 60 minutes. An heat inactivated 5'phosphatase was used as negative control. We found a significant drop in the fusogenic activity when the vesicles were incubated with the 5'phosphatase (figure 4d). To note, this inhibition happened in addition to the inactivation of the vesicles. Therefore, it seems that the removal of the 5'phosphate accelerates the inactivation process. We further confirmed these observations by determining the changes in  $C_v^{app}$  (figure 4e).

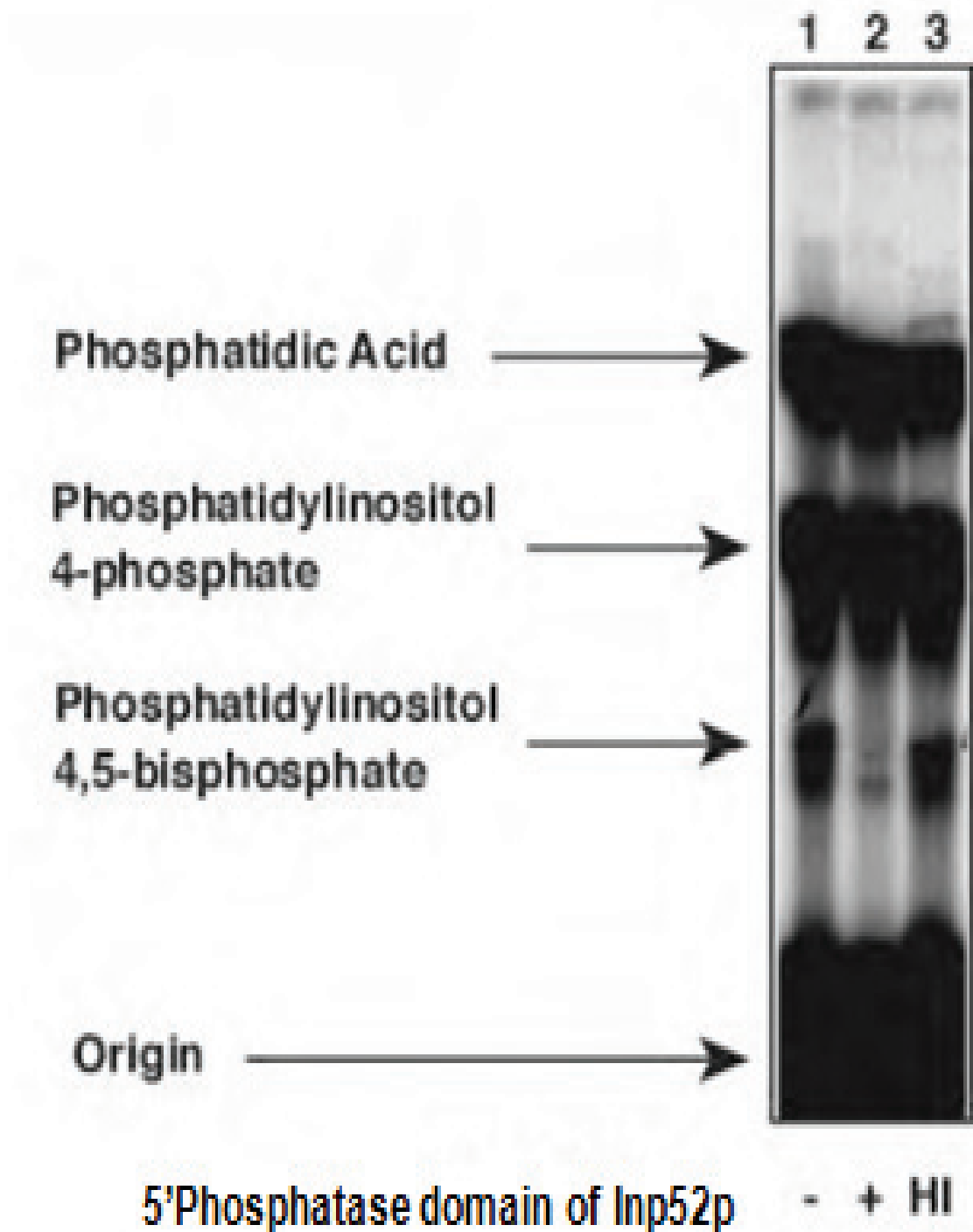


**Figure 4c. Removal of the 5'phosphate from PI(4,5)P<sub>2</sub> on the surface of COPI vesicles by 5'phosphatase.** COPI vesicles (1.25 µg) in kinase buffer supplemented with <sup>32</sup>P-γ-ATP were incubated alone (lane 1) or in the presence of 15 µg/ml 5'phosphatase (lane 2) or heat inactivated 5'phosphatase (HI) (lane 3) for 60 min at 37°C. The end product of the reaction was analyzed by TLC to detect changes in the phosphorylation status of the phospholipids. The film was exposed for 4 days in order to demonstrate the full effect.



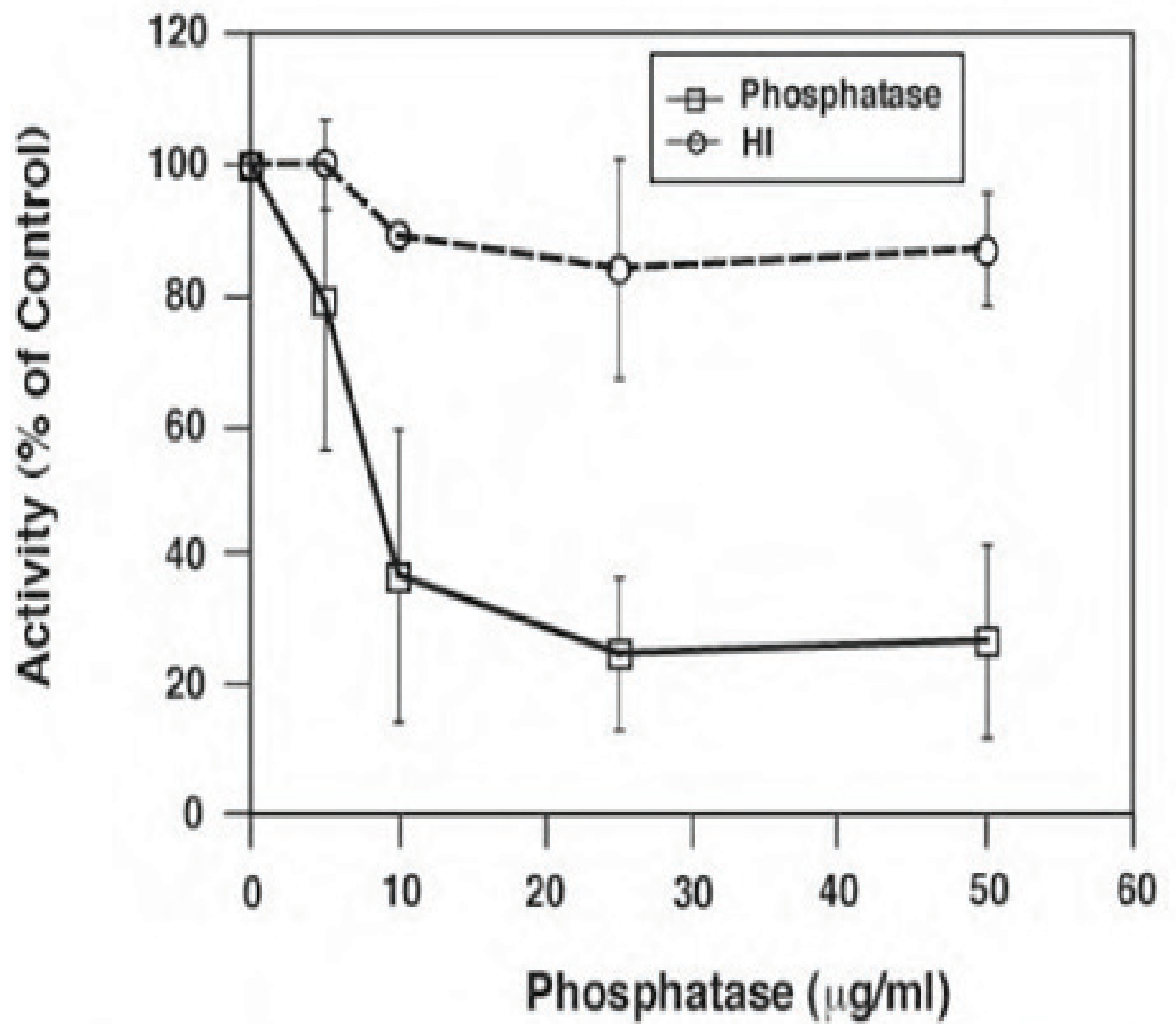


**Figure 4d. 5'phosphatase inhibited the fusion of COPI vesicles.** A non-saturating amount of vesicles was added to Lec1 membranes after pre-incubation for 60 min at 37°C with increasing amounts of 5'phosphatase ( $\square$ ) or heat inactivated (HI) 5'phosphatase ( $\circ$ ).

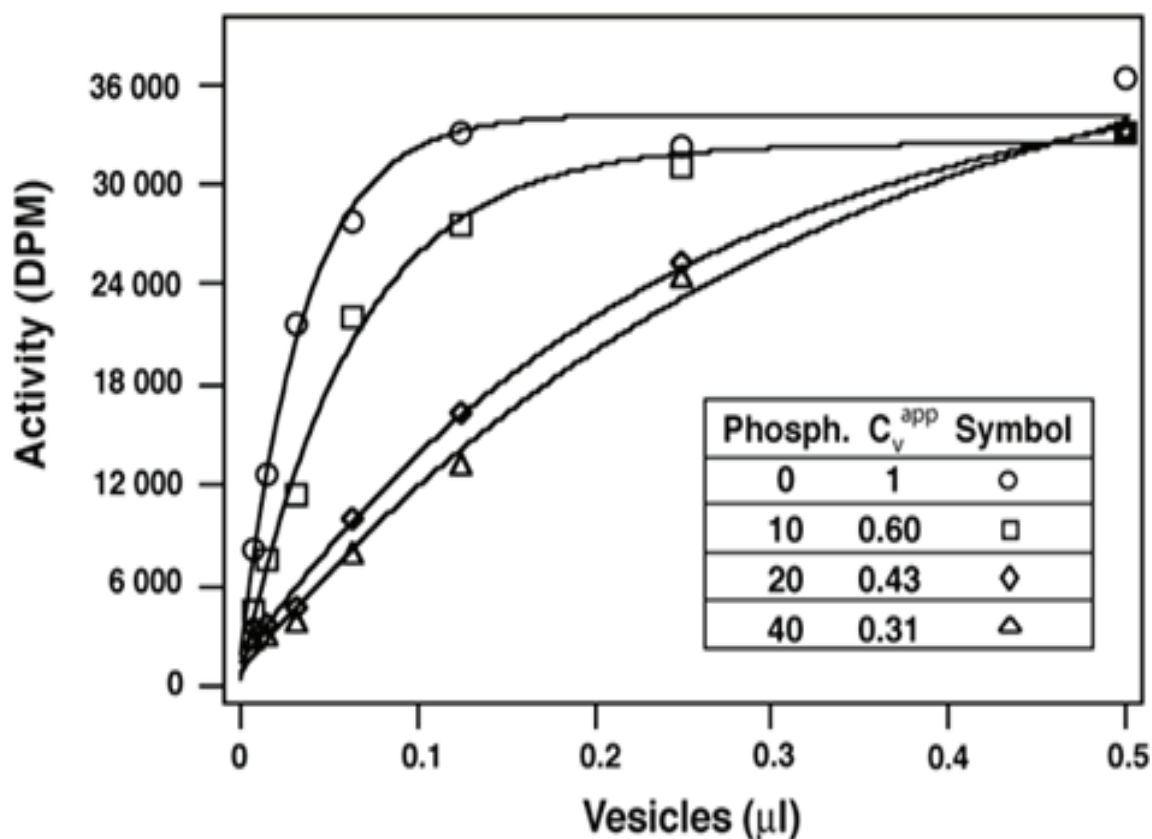


**Figure 4e.** An incubation with 5'phosphatase resulted in significant changes in  $C_v^{app}$ . The COPI vesicles were pre-incubated with 0 (○), 10 (□), 20 (◇) or 40 (△)  $\mu\text{g/ml}$  of the purified 5'phosphatase for 60 min at 37°C and their fusogenicity was determined. Their ability to fuse was found to be reduced to  $0.60 \pm 0.05$  (10  $\mu\text{g/ml}$ ),  $0.43 \pm 0.05$  (20  $\mu\text{g/ml}$ ) and  $0.31 \pm 0.02$  (40  $\mu\text{g/ml}$ ) when compared to control (HI 5'phosphatase).

## Discussion

When we investigated the possibility of obtaining a specific 5'phosphatase, it was nearly impossible to find one that had our requirements for specificity, as most had multiple enzymatic activities. We finally settled on the 5'phosphatase domain of Inp52p. While its major action is on  $\text{PI}(4,5)\text{P}_2$ , and more precisely the 5'phosphate, the main drawback of the phosphatase experiments was that the enzyme was not totally specific for  $\text{PI}(4,5)\text{P}_2$ , as it had a minor enzymatic activity for  $\text{PI}(3,4,5)\text{P}_3$ . It is possible that the observed inhibition was due to its activity on  $\text{PI}(3,4,5)\text{P}_3$ , whose presence in the COPI vesicles and role in the fusion remained unknown. Similar concern was raised regarding the use of wortmannin in

chapter 2, a known PI(3)kinase inhibitor, that can also act on PI(3,4,5)P<sub>3</sub>. However, since it was demonstrated in the previous chapter that the 5'kinase was a type 1 kinase, which uses only PI(4)P as a substrate and no other phosphoinositides, the involvement of PI(3,4,5)P<sub>3</sub> instead of PI(4,5)P<sub>2</sub> appeared less probable.

On the other hand, the data from the phosphatase experiments helped support some of the previous findings. For instance, one cannot exclude the possibility that the production of PI(4,5)P<sub>2</sub> by 5'kinase reported in chapter 3 led to an increase in the fusogenicity by creating a *de novo* fusogenic pathway, one which would not happen physiologically and is independent of the NEM sensitive factor (NSF), a known modulator of vesicle fusion within the Golgi apparatus. However, the fact that the 5'phosphatase promoted the inactivation of COPI vesicles without an addition of PI(4,5)P<sub>2</sub> by the 5'kinase beforehand suggested that this was not a novel mechanism.

In summary, we were able to specifically modify the levels of PI(4,5)P<sub>2</sub> in COPI vesicles demonstrating the corresponding changes in their fusion abilities. We rescued the inactivated vesicles by adding PI(4,5)P<sub>2</sub> on their surface with 5'kinase. Conversely, we accelerated their inactivation by removing the 5'phosphate of PI(4,5)P<sub>2</sub> with 5'phosphatase.

## **Chapter 5. Specific modification of the levels of PI(4,5)P<sub>2</sub> on COPI vesicles , but not the target Golgi, modulated the fusion process.**

---

### **Introduction**

The last chapters provided evidence for the requirement of PI(4,5)P<sub>2</sub> for the fusion of COPI vesicles. This was accomplished by augmenting or decreasing the level of PI(4,5)P<sub>2</sub> on their surface. An improved experimental design would be to modulate the COPI vesicles sequentially with 5'kinase and 5'phosphatase in the same experiment. Such manipulation allowed a direct reversal of the effects caused by each other. In addition, it was not clear at this time if PI(4,5)P<sub>2</sub> was also required on the surface of the target Golgi. Thus, we needed to repeat the 5'kinase and 5'phosphatase experiments on the target Golgi.

### **Results**

In order to further support the effects on the fusion caused by the 5'kinase and 5'phosphatase, which have opposite enzymatic functions, we investigated if they could be reversed when one treatment was followed by the other. One set of COPI vesicles were pre-incubated alone at 37°C for 60 minutes. In parallel, another set was performed similarly but in the presence of 5'kinase that rescued the fusogenic activity of the inactivated vesicles (fig. 5a). Then, we added 5'phosphatase to this reaction and incubated it for another 60 minutes before submitting the vesicles to the fusion assay. To note, it was decided to add the 5'kinase first and phosphatase second because the 5'kinase is dependent on the presence of ATP to function while the phosphatase is not. At the end of the first incubation with 5'kinase, it was presumed that the enzymatic reaction stopped with the depletion of ATP. If the sequence was selected otherwise, the newly synthesized PI(4,5)P<sub>2</sub> by 5'kinase would directly become the substrates of the 5'phosphatase remaining in the system, nullifying the intended purpose.

As we have hypothesized, the 5'phosphatase was able to inhibit the fusion of COPI vesicles that had previously been rescued with the 5'kinase. To confirm the results of the above experiment, we ran a series of  $C_v^{app}$  experiments employing the 5'kinase and 5'phosphatase (fig. 5b). By manipulating the levels of PI(4,5)P<sub>2</sub> on the vesicles, 5'kinase and 5'phosphatase led to a proportional change in the vesicle fusogenicity.

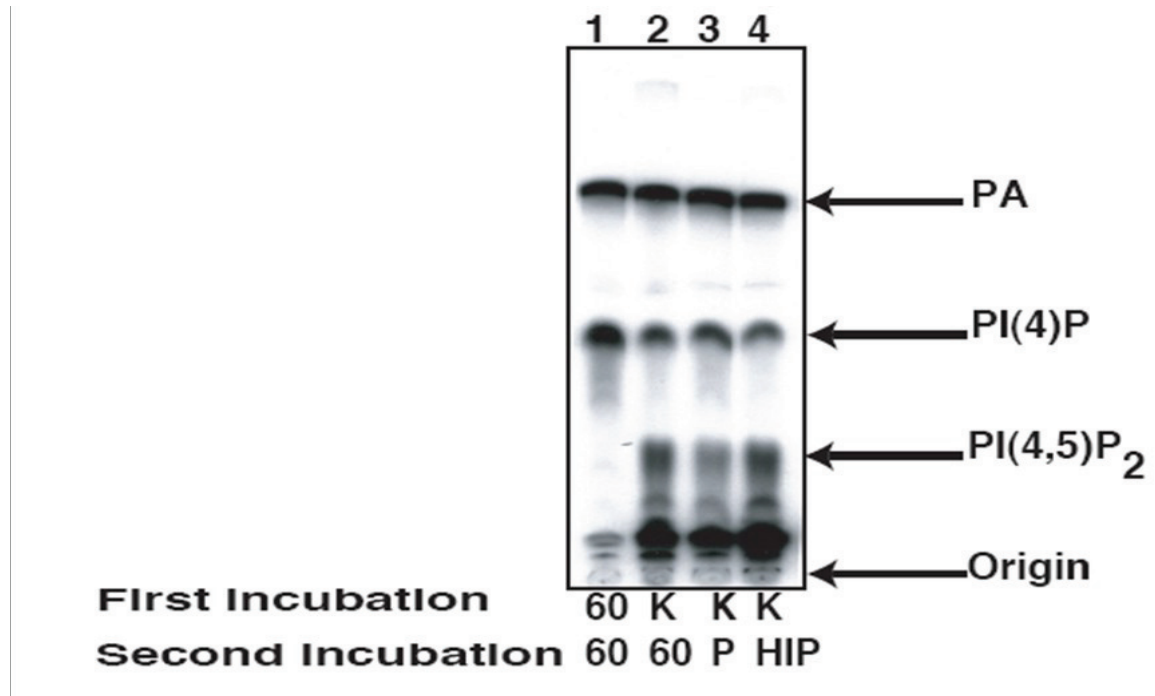


**Figure 5a. Sequential manipulation of PI(4,5)P<sub>2</sub> on COPI vesicles.** 1.25  $\mu$ g of COPI vesicles was incubated for 2 x 60 min in the presence of <sup>32</sup>P-ATP and either 5'phosphatase (10  $\mu$ g/ml), 5'kinase (1.67 $\mu$ g/ml) or heat inactivated of the 5'kinase (HIK). The lipids were extracted and submitted to TLC.

Our next objective was to determine if the modification of PI(4,5)P<sub>2</sub> levels on the surface of the target Golgi would also result in a change in the fusogenicity. To achieve this, the target Golgi was incubated with 5'phosphatase or the 5'kinase prior to a series of fusion assays. In figure 5d, changes in the PI(4,5)P<sub>2</sub> levels in the target Golgi were demonstrated by TLC. We also revealed that the target Golgi produced much more PI(4,5)P<sub>2</sub> than COPI vesicles (figure 5d) or liver Golgi preparations (data not shown). In spite of this observation, neither 5'phosphatase nor the 5'kinase had a significant effect on the  $C_v^{app}$  of the fusion assay (figure 5e).

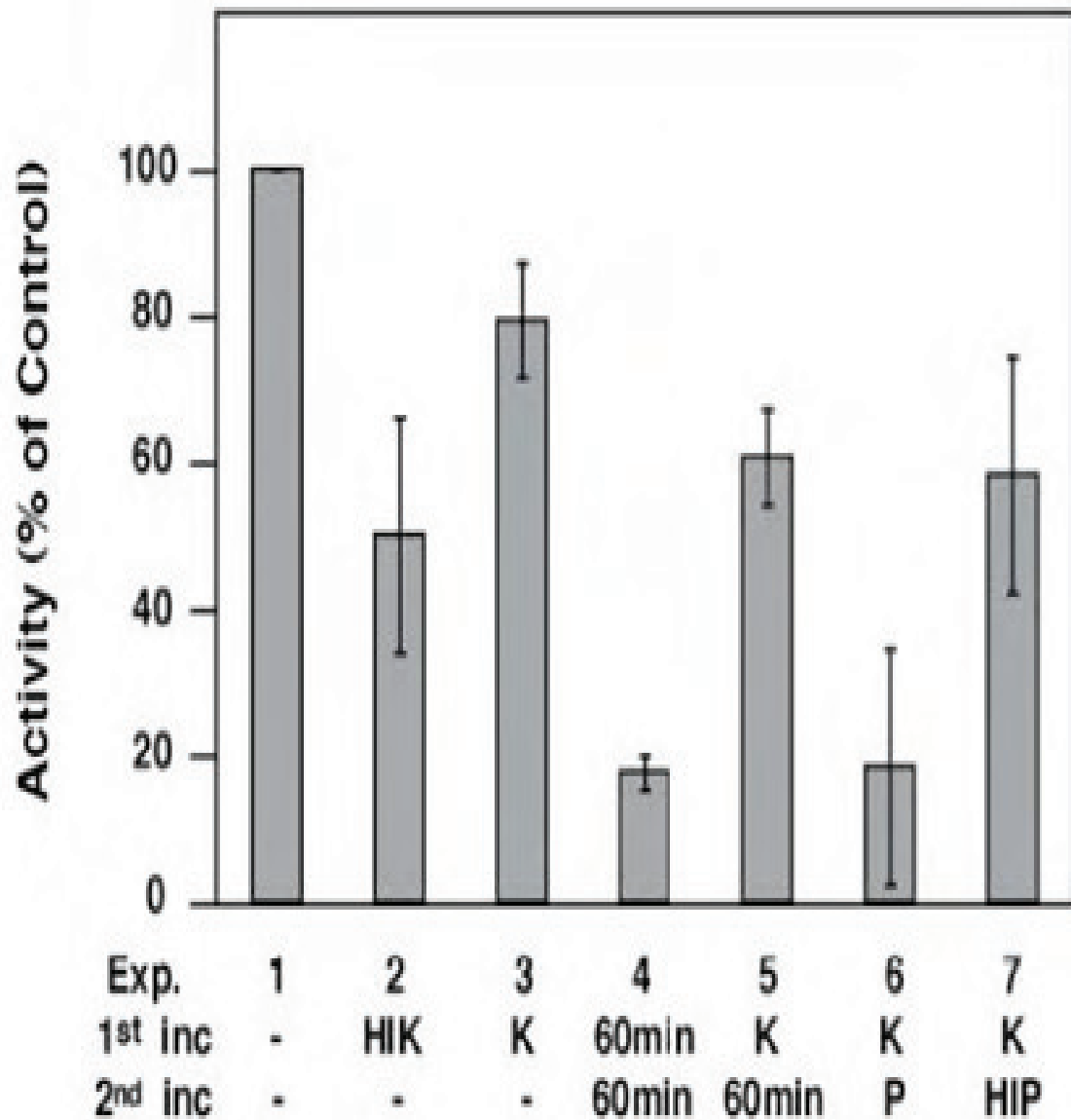


**Figure 5b. 5'kinase mediated rescue of COPI vesicle inactivation was reversed by treatment with 5'phosphatase.** A non-saturating amount of vesicles was incubated at 37°C for 60 min in presence of 1.67 µg/ml of 5'kinase (K, lanes 3,5,6,7) or heat inactivated 5'kinase (HIK, lane 2). Following the first incubation with 5'kinase, the vesicles were incubated again at 37°C for 60 min alone (60, lane 5) or in the presence of 10 µg/ml of 5'phosphatase (P, lane 6) or heat inactivated 5'phosphatase (HIP, lane 7). The control consisted of vesicles without pre-incubation (-, experiment 1) or with 2 incubations of 60min. (lane 4).

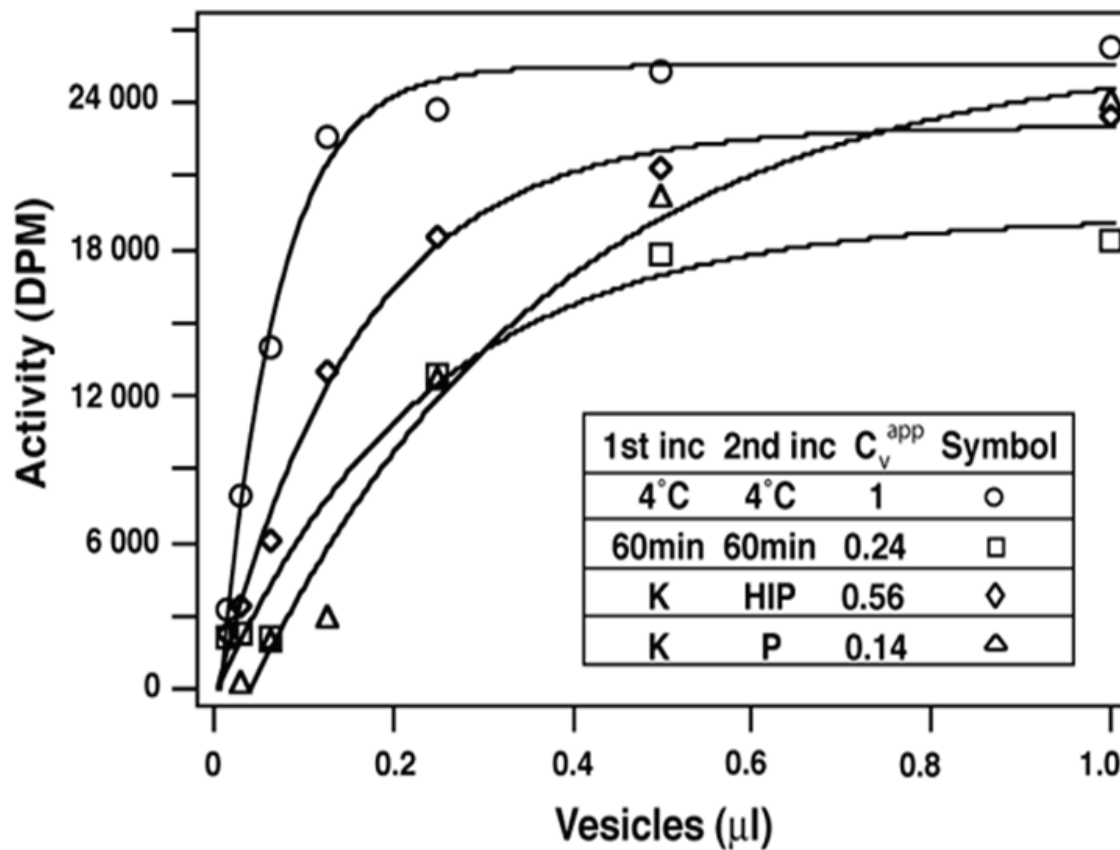


**Figure 5c. Determination of  $C_v^{app}$  after treating the inactivated COPI vesicles with 5'kinase followed by 5'phosphatase.** Increasing amounts of vesicles were incubated at 37°C alone for 2 x 60 min (□,  $0.24 \pm 0.03$ ), with 1.67  $\mu\text{g/ml}$  of 5'kinase during the first 60 min. and 10  $\mu\text{g/ml}$  5'phosphatase (△,  $0.14 \pm 0.04$ ) or heat inactivated 5'phosphatase (◇,  $0.56 \pm 0.16$ ) during the second 60 min. Controls were continuously kept on ice (○). The  $C_v^{app}$  curves above correspond to experimental data from lanes 1, 4, 6 and 7 from figure 5a.

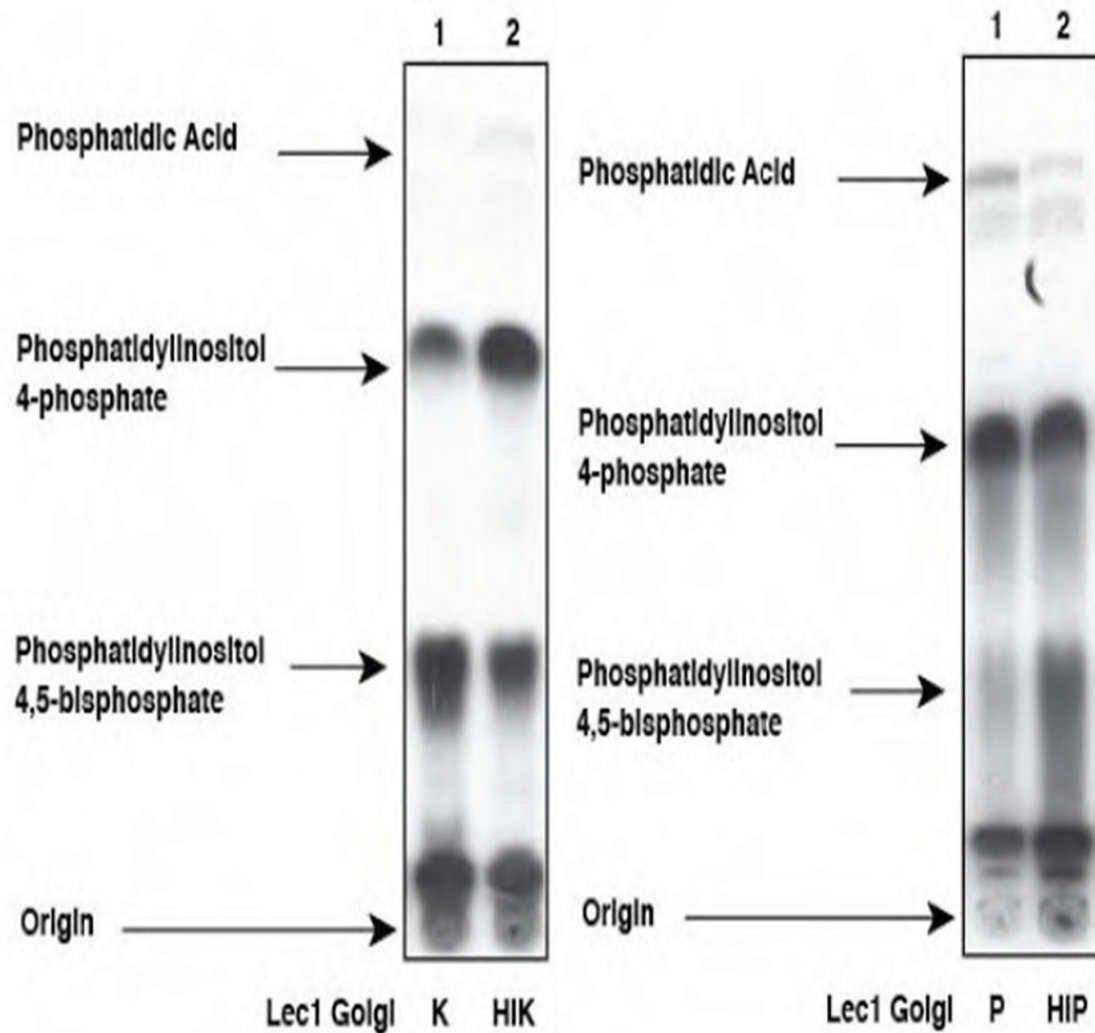


**Figure 5d. Modification of the PI(4,5)P<sub>2</sub> synthesis on target Golgi membranes.** Lec1 Golgi (2.7 µg) in kinase buffer were incubated with 20 µg/ml of active (P) or heat-inactivated (HIP) 5'phosphatase, or 4.16 µg/ml of active (K) or heat-inactivated (HIK) 5'kinase for 60 min at 37°C in the presence of <sup>32</sup>P-γ-ATP. After the incubation, lipids in the samples were extracted and analyzed by TLC. The film was exposed for 2 hours.



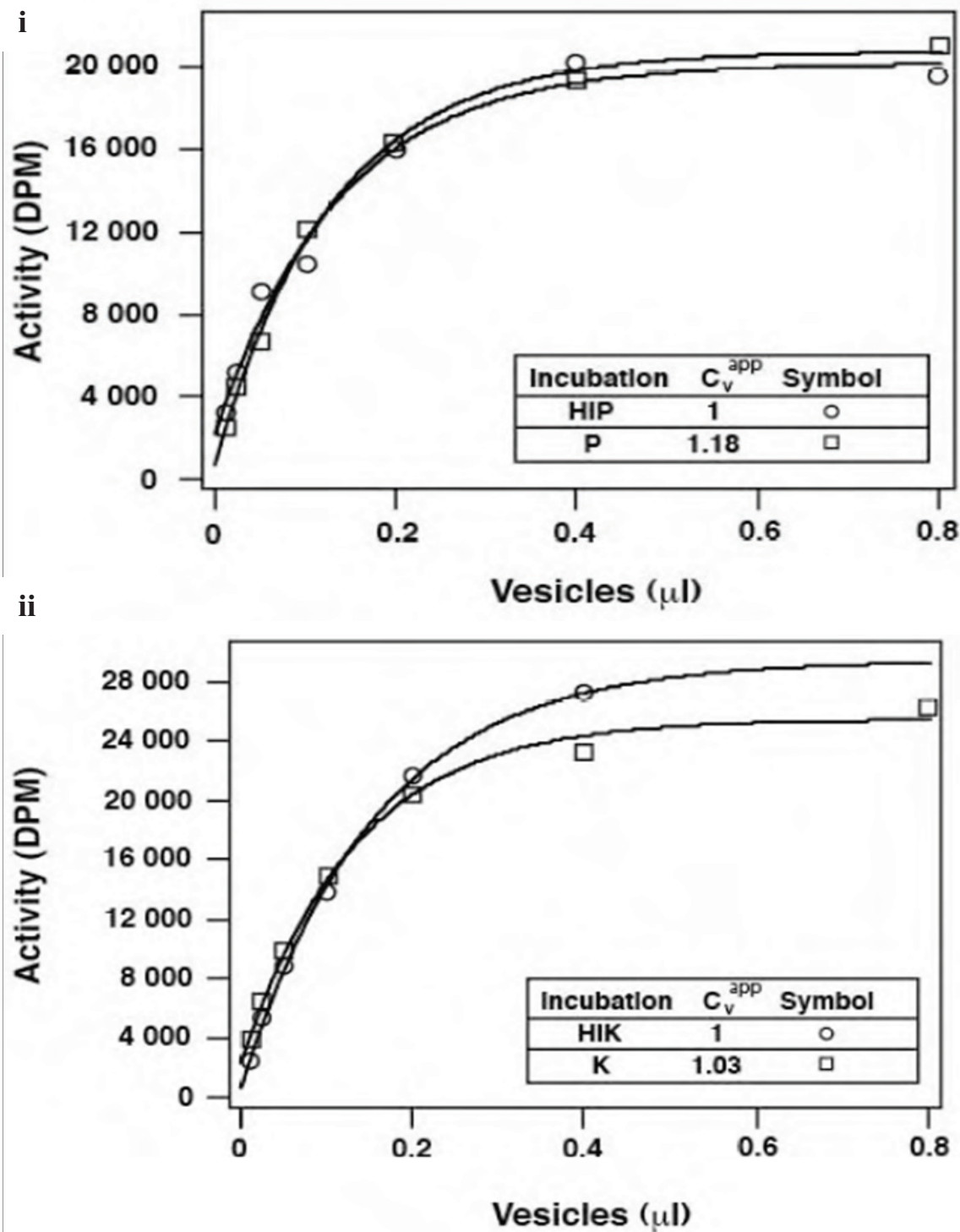


**Figure 5E. Study of the fusogenicity by modifications of PI(4,5)P<sub>2</sub> levels in the target Golgi.** i, Lec1 Golgi membranes pre-treated with 5'phosphatase (□) or heat-inactivated 5'phosphatase (○). The  $C_v^{app}$  measured after the treatment with 5'phosphatase was  $1.18 \pm 0.30$  compared to the incubation with heat-inactivated phosphatase. ii, Lec1 Golgi membranes pre-treated with 5'kinase (□) or heat-inactivated 5'kinase (○). The  $C_v^{app}$  after the treatment with 5'kinase was  $1.03 \pm 0.18$  compared to the incubation with heat-inactivated kinase.

## **Discussion**

In the previous chapters, we described the use of purified 5'kinase and 5' phosphatase to modulate the PI(4,5)P<sub>2</sub> levels in COPI vesicles. A pitfall in these experiments was that the enzymes could never be 100% pure (see fig. 4a): the resulting changes in the fusogenicity upon addition of these enzyme preparations might be due a contaminating substance. It might also be due to an unspecific activity from the phosphatase on PI(3,4,5)P<sub>3</sub> instead of PI(4,5)P<sub>2</sub> itself. In order to control for these possibilities, we used heat inactivated HI 5'kinase and 5' phosphatase for comparison purpose. However, heat inactivation was not a faultless control because this procedure could also inactivate the potential contaminant.

In this chapter, we designed another control experiment that consisted of a sequential treatment with 5'kinase and 5'phosphatase possessing opposite functions. By modulating in succession the fusogenicity of the vesicles with these reagents, we significantly reduced the possibility that the observed effects on the fusion process resulted from contaminants or a secondary enzymatic activity. Furthermore, the unspecific activity of the 5'phosphatase towards PI(3,4,5)P<sub>3</sub> became less relevant because the 5'kinase added a phosphate to PI(4)P only at the 5' and not 3' position.

We next sought to determine if the requirement of PI(4,5)P<sub>2</sub> was also applicable for the target Golgi, the complementary surface of COPI vesicles in the fusion process. Interestingly, large quantities of PI(4,5)P<sub>2</sub> were detected in the Golgi fraction by TLC. However, despite its abundance, we failed to find any effects on the fusion when we alter its levels by 5'kinase and the 5'phosphatase. The cause of this difference in PI(4,5)P<sub>2</sub> dependence is currently unknown. In chapter 2, we demonstrated that the PK treatment of the target Golgi had a drastic effect on the fusion process. Perhaps a protein rather than a lipid plays a more important role on that side of the fusion process.

Finally, it is often difficult, when comparing PI(4,5)P<sub>2</sub> bands on TLC, to clearly determine the absolute amount of PI(4,5)P<sub>2</sub> on the surface of the vesicle. This would explain the results seen in figure 5a, where a small pool of PI(4,5)P<sub>2</sub> is present in the third

lane without the vesicles being fusogenic. If one is to theorize the presence of two pools of PI(4,5)P<sub>2</sub>, one radioactive and one who isn't, they could propose that the de facto setting has only a small non-radioactive pool of PI(4,5)P<sub>2</sub> and the addition of 5'kinase increases the size of the radioactive pool of PI(4,5)P<sub>2</sub>, it most probably also increases disproportionally the overall size of the PI(4,5)P<sub>2</sub> pool present on the surface of the COPI vesicles, so that a large majority of the PI(4,5)P<sub>2</sub> is radioactive. When the 5'phosphatase is incorporated in the assay, it removes a large fraction of the PI(4,5)P<sub>2</sub> present on the COPI vesicles indifferently of its radioactivity. While all PI(4,5)P<sub>2</sub> are not totally removed, this new pool of PI(4,5)P<sub>2</sub> has a higher proportion of hot PI(4,5)P<sub>2</sub> and thus generated a higher signal than the original fraction, thus seemingly creating a paradox. This explanation also demonstrates that the 5'kinase and the 5'phosphatase should be used to monitor an absolute amount of PI(4,5)P<sub>2</sub>, but rather only in relation to a previous sample.

## **Chapter 6. Investigation of PI(4,5)P<sub>2</sub> associated factors: removal of the proteins on the cytoplasmic surface of the COPI vesicles affected the first step of the fusion.**

---

### **Introduction**

Following the discovery of PI(4,5)P<sub>2</sub> as a required factor for the fusion of COPI vesicles, we hypothesized that, alike in other fusion systems (e.g. <sup>145,248</sup>), PI(4,5)P<sub>2</sub> does not by itself participate in the membrane fusion. Rather, it served as a beacon that recruits the fusion machinery. Undoubtedly, the identification of these downstream effectors associated with PI(4,5)P<sub>2</sub> would shed light into the mechanism underlying the fusion process.

There are 3 putative sources of proteins available for the recruitment to the COPI vesicles: those located in the cytosol, on the surface of Golgi membranes or on the surface of the vesicles themselves. While the lipid binding domains known for PI(4,5)P<sub>2</sub> vary significantly from one protein to another <sup>240</sup>, they all share the high affinity for the high negative charges of PI(4,5)P<sub>2</sub>. We have previously shown that the fusion was partially resistant to PK treatment on the COPI vesicles (chapter 2). What is the function of their surface proteins and how do they acquire the PK resistance? And how could the dependence on PI(4,5)P<sub>2</sub> be linked in these events? In this chapter, we answered to the first question by showing that the some proteins on the cytoplasmic surface of the COPI vesicles mediate the tethering step in the fusion process.

### **Results:**

We started by investigating in greater details how the fusion process was affected when the COPI vesicles were treated with PK . Previous publications <sup>for example see 8, 9, 248</sup> had described the fusion as a two-step process, the initial binding/docking and the actual fusion. Since the proteolysis removed the cytoplasmically oriented proteins on the

surface of the vesicles, it is speculated that the limited reduction in vesicle fusogenicity by the PK treatment was due to a decreased ability of the vesicles to bind to the target Golgi but not a change in their ability to fuse per se.

It has been shown by us (chapter 2 and <sup>8</sup>) that the COPI vesicles became inactivated over time. Here, we proposed a model in which the kinetics of vesicle binding/docking are determined by two constants: the rate at which the COPI vesicles bind and fuse ( $K_b$ ) and the rate at which they are inactivated ( $K_i$ ).

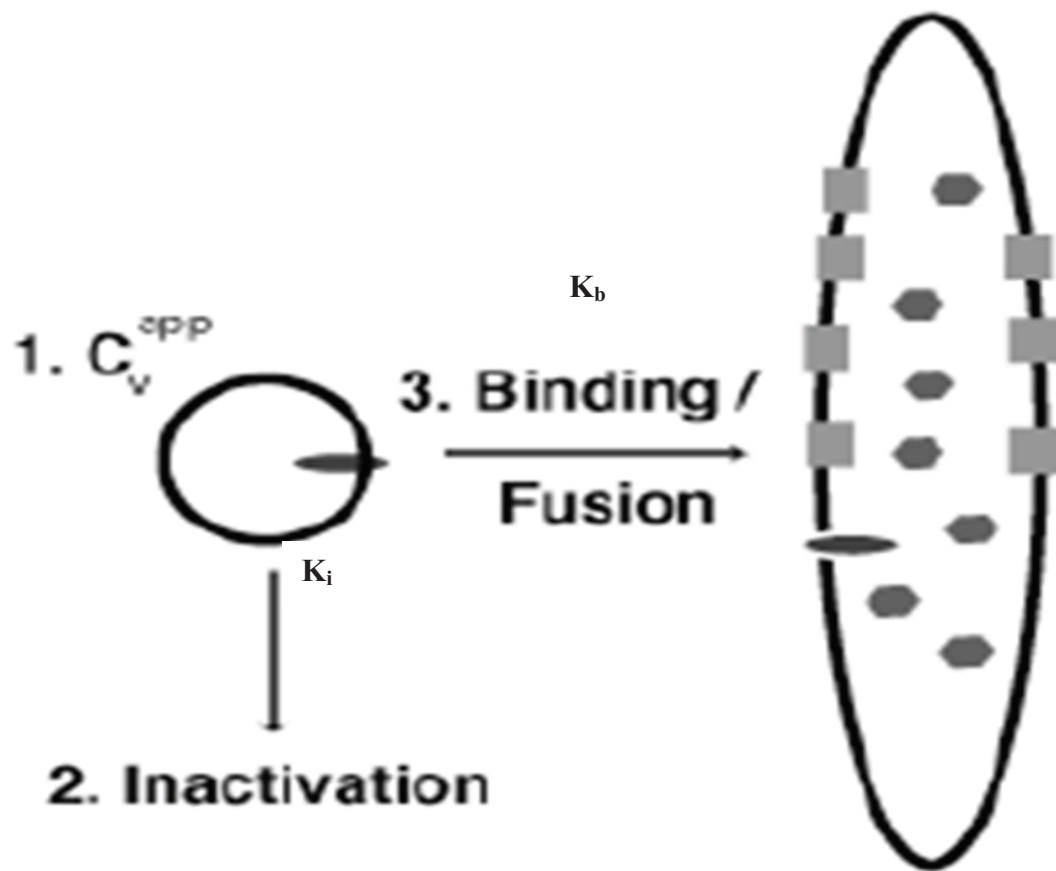


**Figure 6a. Fate of the COPI vesicles.** The fate of COPI vesicles is governed by two constants: the rate of inactivation ( $K_i$ ) and the rate of binding/fusion ( $K_b$ ). It is the ratio between these two competing rates that determines if a vesicle will fuse or become inactivated.

The inactivation of the vesicles could become evident when its rate matches that of binding and fusion. In order to determine these rates, we performed a dilution experiment whose experimental concept was the following: a normal  $C_v^{app}$  curve was first measured for a preparation of vesicles. A second series of fusion experiments was performed in a reaction volume that was doubled while both the amounts of COPI vesicles and target Golgi were kept constant, *de facto* reducing the probability of a COPI vesicle encountering its partnering target Golgi cisterna. This dilution resulted in a greater delay in the vesicle tethering. During this delay period, a portion of the vesicles were subject to inactivation, resulting in a loss of the overall fusogenicity that could be illustrated by measuring the new  $C_v^{app}$  (fig. 6b).

With the dilution experiments, we re-examined the overall effect of the PK treatment. If the PK induced loss of fusogenicity was due to a decreased ability for the vesicles to fuse after they have docked, the dilution should have no impact on the final  $C_v^{app}$ . If an increase in the vesicle inactivation constant was the cause, there would be a drastic decrease in the  $C_v^{app}$  as a result of the additive inhibitory effects. On the contrary, if the effect of PK treatment was on the fusion of the vesicle after they bind to the target Golgi, then the effect of dilution between PK treated vesicles and control vesicles would be the same. On the other hand, if the binding/docking step was affected, the  $C_v^{app}$  would also decrease, yet to a lesser extent, because the PK treated vesicles will stay unbound in solution for a longer period of time and become more prone to inactivation. Our results supported the latter hypothesis on vesicle tethering (fig. 6c). Furthermore, when we compared the  $C_v^{app}$  from the PK experiment and that calculated by removing the dilution effects in the PK/dilution combined experiment, we found a comparable loss in the binding ability of the COPI vesicles: (PK treatment:  $62.4\% \pm 7.8\%$ , see chapter 2; [(PK treatment + dilution)/dilution alone]:  $42.3\% \pm 3.7 / 64.3\% \pm 1.7\% = 65.7\% \pm 5.8\%$ ). This agreement confirmed our hypothesis that PK treatment exerted its inhibitory effects on the COPI vesicles by reducing their binding constant. To note, this experiment was feasible only if  $K_d$  and  $K_i$  were similar: if the inactivation constant were a log factor slower than the binding constant, the dilution would have no effects on the overriding binding and fusion steps. Conversely, if the inactivation constant was much faster than

the binding constant, only a very small fraction of the vesicles would fuse regardless of the concentration of the substrates in the reaction. Any reduction in the fusogenicity as a result of the dilution would be below the detection limit of the assay.

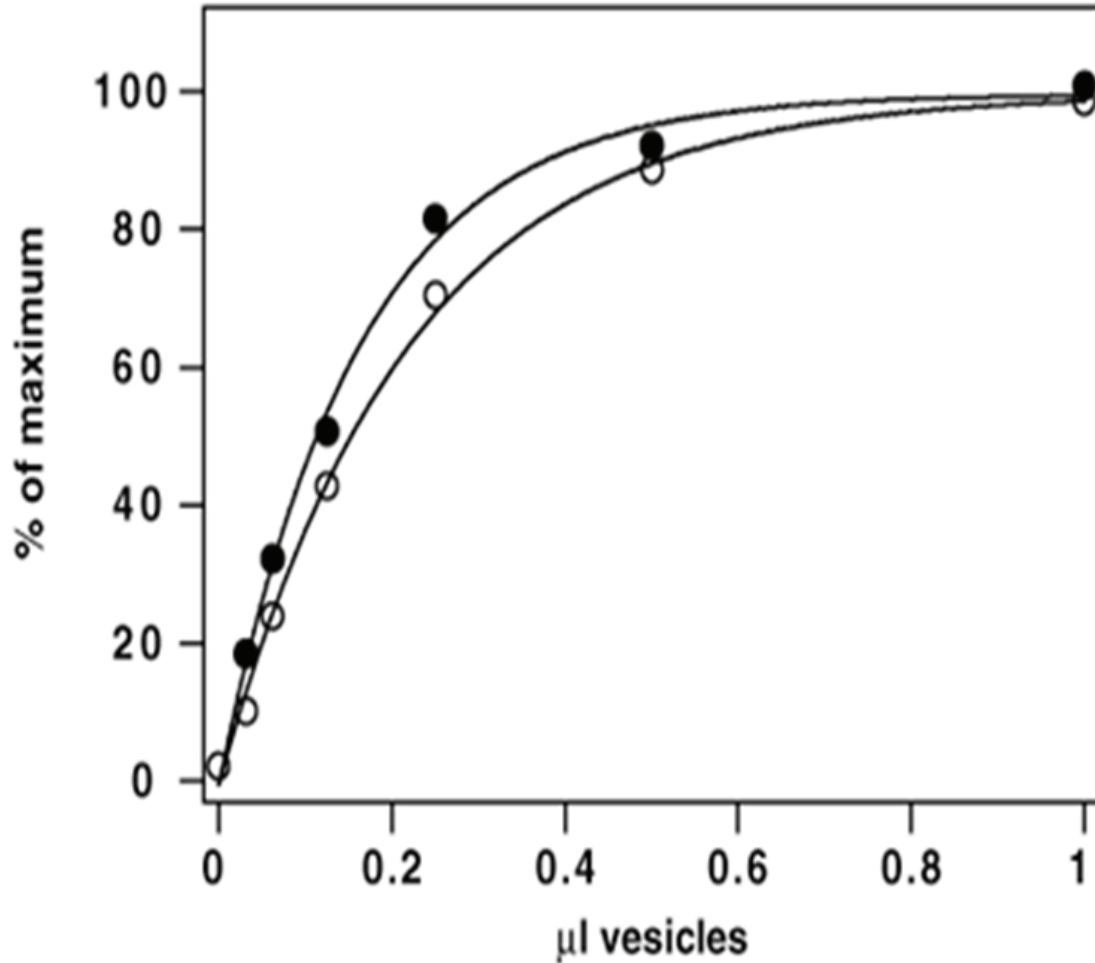


**Figure 6b. Dilution experiment.** The fusion assay was performed without (●) or with (○) a 2-fold dilution of the vesicles. The fate of the vesicles was determined by the ratio between the rate of binding over the rate of binding + inactivation  $[b/(b+i)]$ . For example., if the rate at which the vesicles were inactivated was the same as the rate of their binding and fusion to the target Golgi, half the vesicles will fuse and half of them will become inactivated (mathematically represented by  $[1/(1+1)] = 1/2$ ). On the other hand, if the vesicles were then diluted two-fold, their rate of binding was reduced two-fold as a consequence. According to the formula  $[0.5/(1+0.5)=1/3]$ , 1/3 of the vesicles bound and 2/3 of them were inactivated. Ostermann *et al.*<sup>8</sup> has established a simple formula that allowed a precise calculation of the binding and fusion kinetics (fb):  $fb = 2 - r$ , where  $r = C_v^{app} \text{ undiluted} / C_v^{app} \text{ diluted}$ . In this figure,  $C_v^{app} \text{ diluted} = 0.736 \pm 0.001$  of  $C_v^{app} \text{ undiluted}$ . Therefore,  $fb = 2 - 1/0.736 = 0.643 \pm 0.017$  of the vesicles bound while the remainder became inactivated. See<sup>8,9</sup> for references.

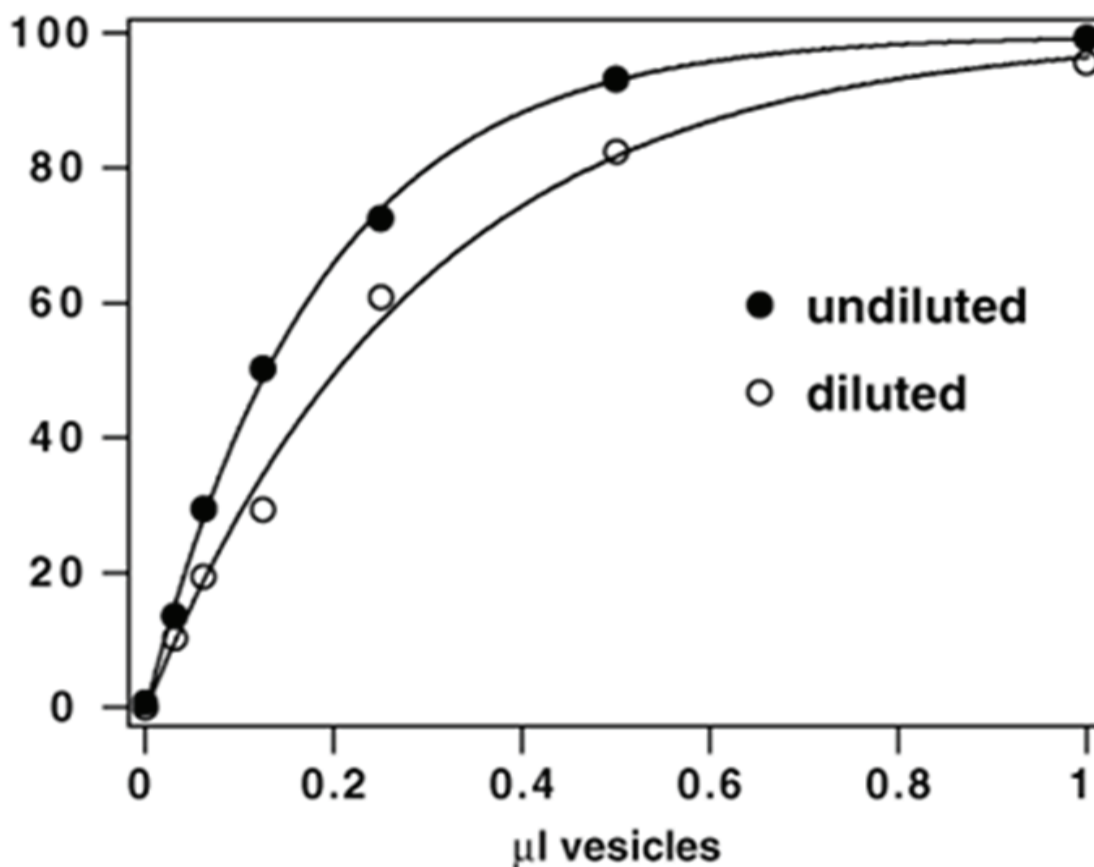


**Figure 6c. Dilution and PK experiment.** The COPI vesicles were treated with 2 µg/ml PK for 30 minutes at 4°C. The PK activity was terminated with 1mM PMSF before introducing the vesicles into the fusion assay with (○) or without (●) a twofold dilution. The  $C_v^{app}$  in the PK experiment with dilution was  $63.4 \pm 1.5\%$  of the PK experiment without dilution. Therefore, only  $42.3 \pm 3.7\%$  of the vesicles in the PK experiment with dilution actually bound and fused to the target Golgi. See <sup>8,9</sup>.

The overall effects of the PK treatment could alternatively be visualized as a function of [binding/(binding+inactivation)] ratio <sup>8</sup> (Fig. 6d). The PK experiment with dilution was repeated with increasing amounts of PK. As observed in figure 6c, as a result of the PK treatment there was a significant drop in this ratio representing the % of COPI vesicles successfully bound to the target Golgi. Intriguingly, however, the inhibitory effects of the PK treatment quickly reached a plateau. The reason why PK could not further decrease the binding of the vesicles was unknown. We will try to provide an explanation for this finding in the next chapter.



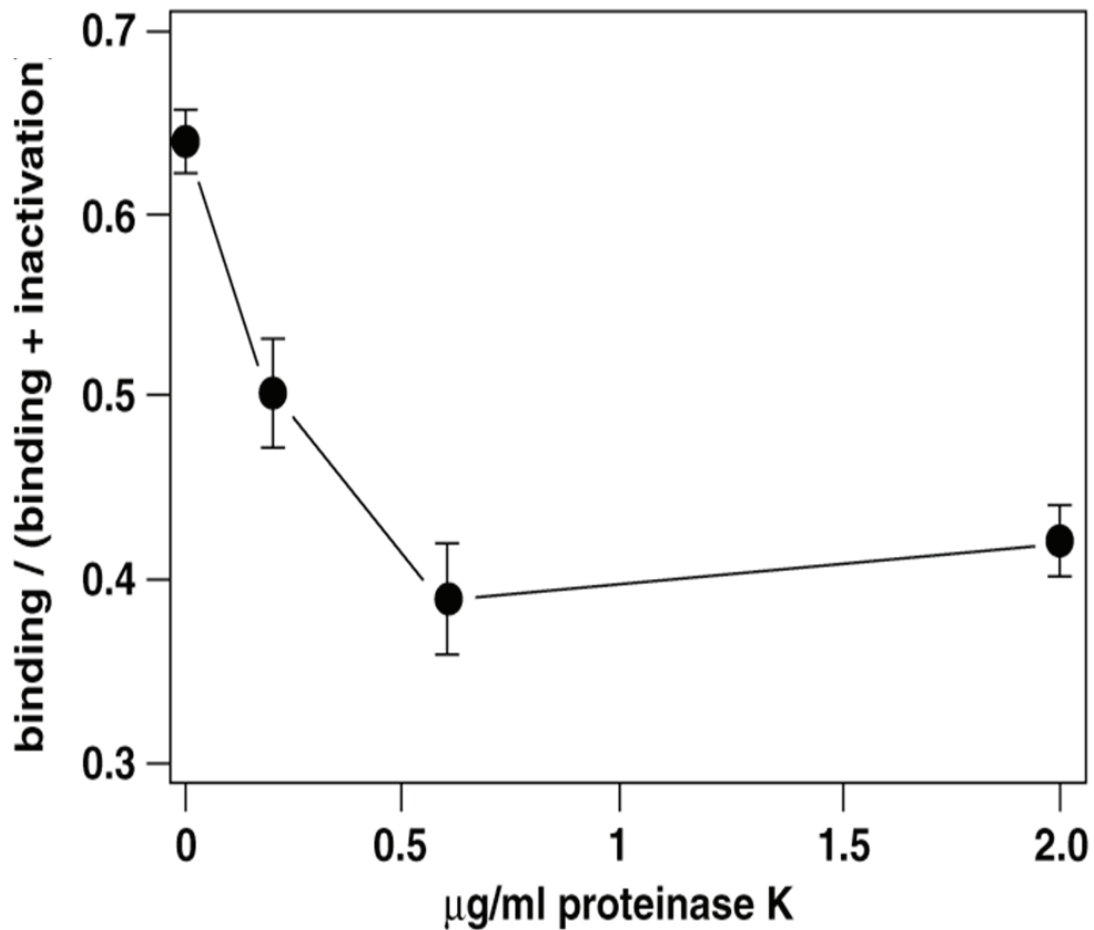


**Figure 6d. The [binding/(binding+inactivation)] ratio dropped following PK treatment.** We repeated the preceding dilution experiment with COPI vesicles treated with an increasing amount of PK. The inhibitory effects of the PK treatment quickly reached a plateau, after which it did not affect the binding of the vesicles anymore.

To further investigate the effect of the PK treatment on the fusion kinetics, BAPTA, a  $\text{Ca}^{2+}$  chelator, was used in the PK experiment to stop the fusion at different times<sup>8</sup>. Thus, we obtained a curve that monitored the progression of the fusion process using untreated or PK treated COPI vesicles (fig. 6e). With the help of the software Berkeley-Madonna, it established a model that could fit the experimental curves with a two constant model with similar kinetics. With the same software, the analysis of the curve revealed a disparity between these 2 conditions only in the initial kinetics ( $K_1$ ). No difference was found in the kinetics ( $K_2$ ) later on in the fusion process. The data was interpreted as a delay in the binding of the vesicles to the target Golgi membrane at the beginning that, once bound,

was followed by identical fusion kinetics. This model, in concordance with our dilution experiments can clearly demonstrate that PK treatment of the vesicles specifically affected only the binding step of the fusion process<sup>for further analysis see Laporte, F. Ostermann, J. in appendix</sup>.

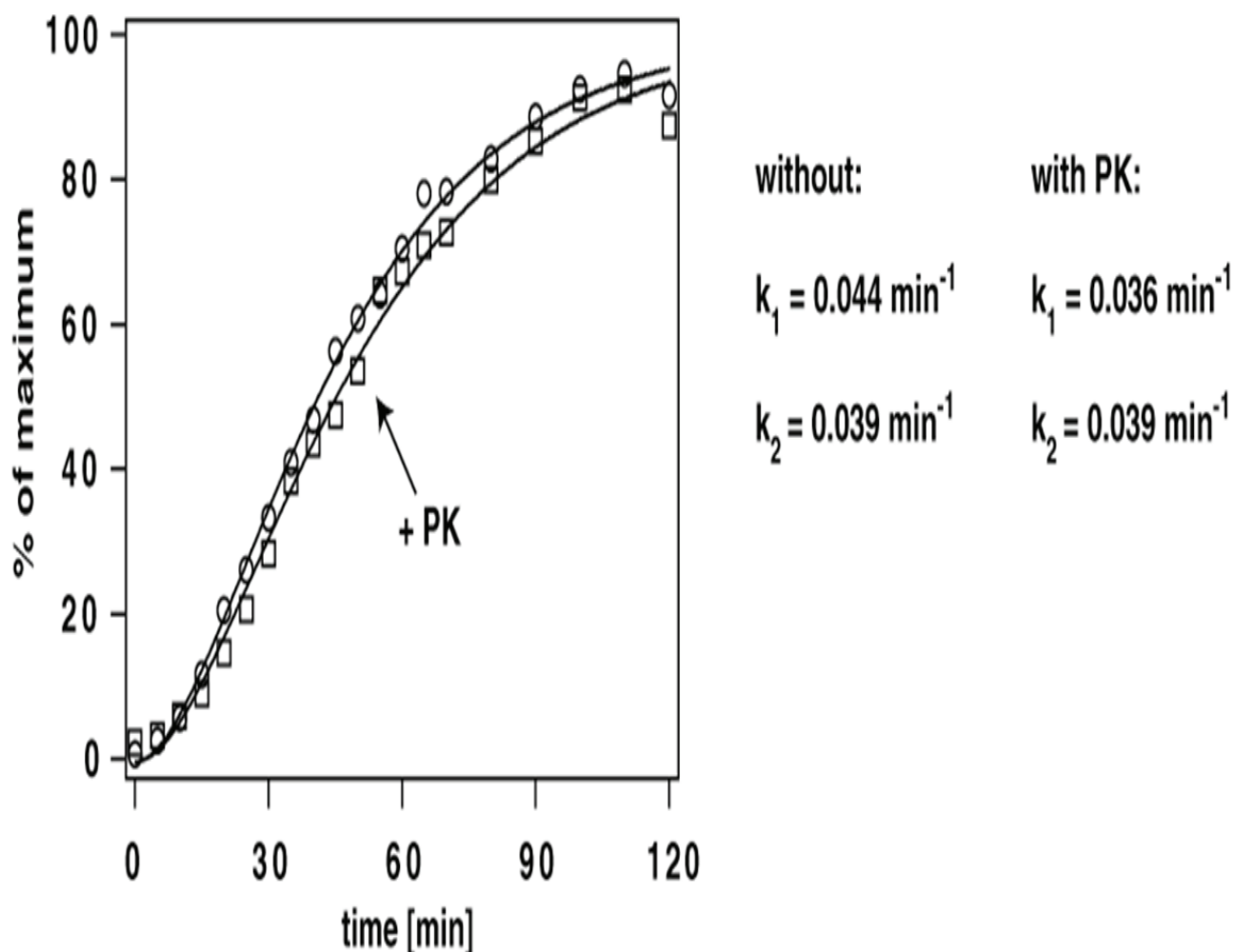


**Figure 6e. The effects of PK on fusion kinetics.** A non-saturating amount of vesicles were incubated with ( $\square$ ) or without ( $\circ$ ) PK for 30 min at 4°C. The activity of PK was terminated with 1mM PMSF before introducing the vesicles into the fusion assay. The fusion was stopped at the indicating times by the addition of BAPTA. The incubation of the assay was continued to allow the completion of the VSV-G glycosylation as a result of the fusion that has taken place. Each of the resulting curves was analyzed as being composed by 2 parts with distinct constants:  $K_1$  and  $K_2$ , corresponding to the binding and fusion steps. The differences between the 2 curves were explained by a drop in the  $K_1$  but not  $K_2$ . See<sup>9</sup> for reference.

In summary, we unveiled two essential findings that provided insights into the mechanism of the fusion process: the presence of PI(4,5)P<sub>2</sub> on the surface of COPI vesicles and the requirement of some cytoplasmically oriented proteins for an efficient binding to the target Golgi. To note, the identity and the nature of these proteins remained obscure as they appeared partially PK resistant, such that the PK treatment of the vesicles reduced but did not fully abolish the fusogenicity.

A possible explanation for this latest finding was that our assay had developed a novel fusion mechanism, one that was not physiologically relevant, and that our results were an artifact of a short circuit of the normal fusion process. The PK treatment could have created a non-physiological pathway for the fusion, as was stipulated previously for PI(4,5)P<sub>2</sub>. Since the cytoplasmically oriented proteins such as SNAREs are well known to be involved in the fusion process, there was a need to better control and take them into consideration in our fusion assays in order to eliminate this possibility.

To indisputably demonstrate that our assay was SNARE dependent, we examined our fusion system in the absence of NSF, a protein required for the proper function of the SNARE mechanism<sup>320</sup>. The NSF present in the membranes was inactivated by the addition of NEM while cytosolic NSF was heat-inactivated at 37°C. We showed that the depletion of NSF was totally inhibitory to the fusogenic activity. Furthermore, when purified NSF was re-introduced to the fusion assay, the COPI vesicles recovered their ability to fuse with the target Golgi (fig. 6f).

Simultaneously, we determined if the COPI vesicles after the PK treatment were still sensitive to NSF. Consistently to the above finding, the depletion of NSF rendered PK treated vesicles inactive confirming the involvement SNAREs in the fusion process (fig. 6g). Interestingly, while this inactivation was also reversible by the re-introduction of NSF, the recovery of the PK treated vesicles occurred at a slower rhythm (fig. 6g).

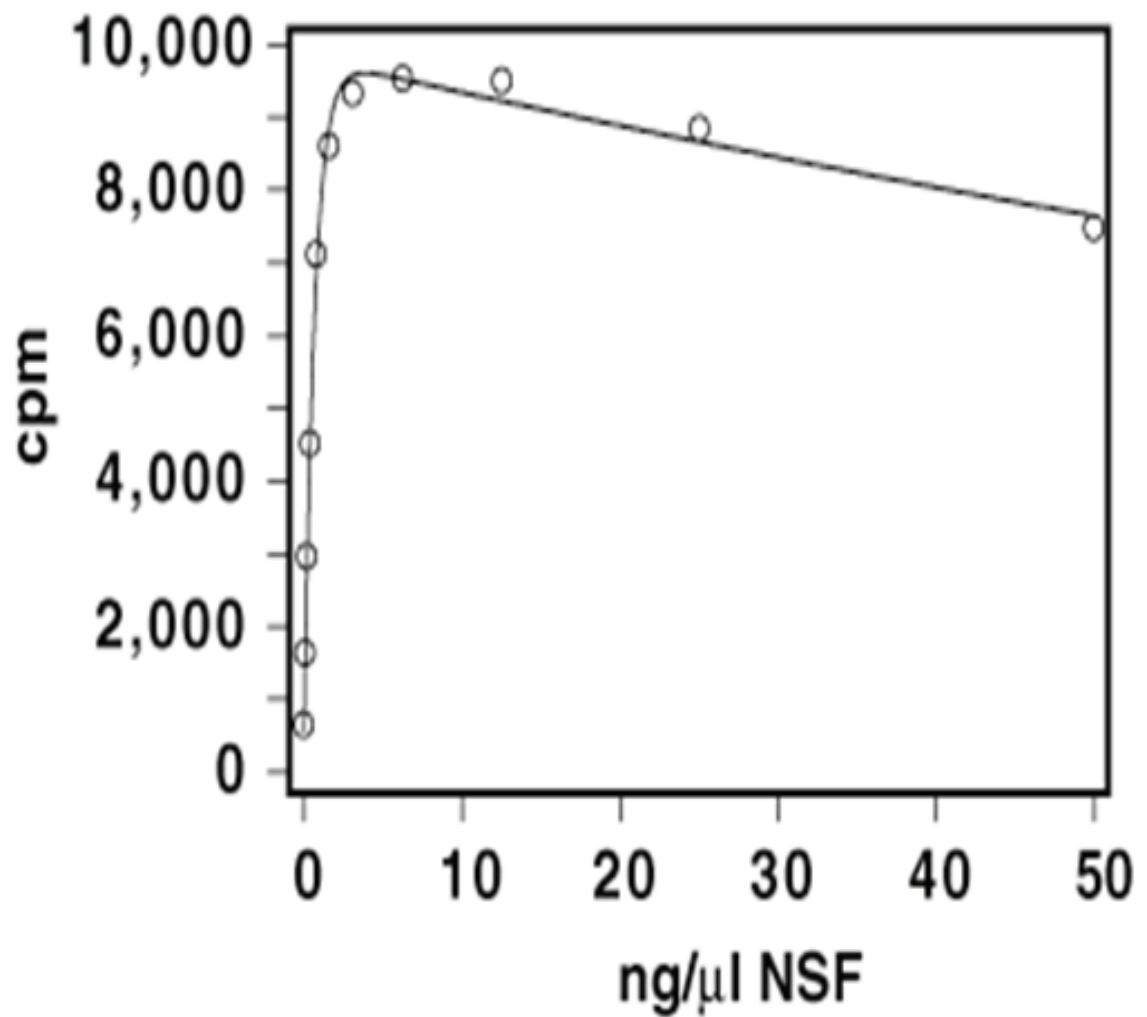


**Figure 6f. The fusion assay was sensitive to NSF depletion.** A non-saturating amount of PK treated (2 $\mu$ g/ml, inactivated with 1 mM PMSF) COPI vesicles were incubated in the absence of active NSF ( $\circ$ , at 0 ng/ $\mu$ l) or when NSF was re-introduced to a depleted fusion assay ( $\circ$ ). The removal or inactivation of NSF led to a drastic loss in the fusogenicity, which was recovered by rescuing the assay with NSF.

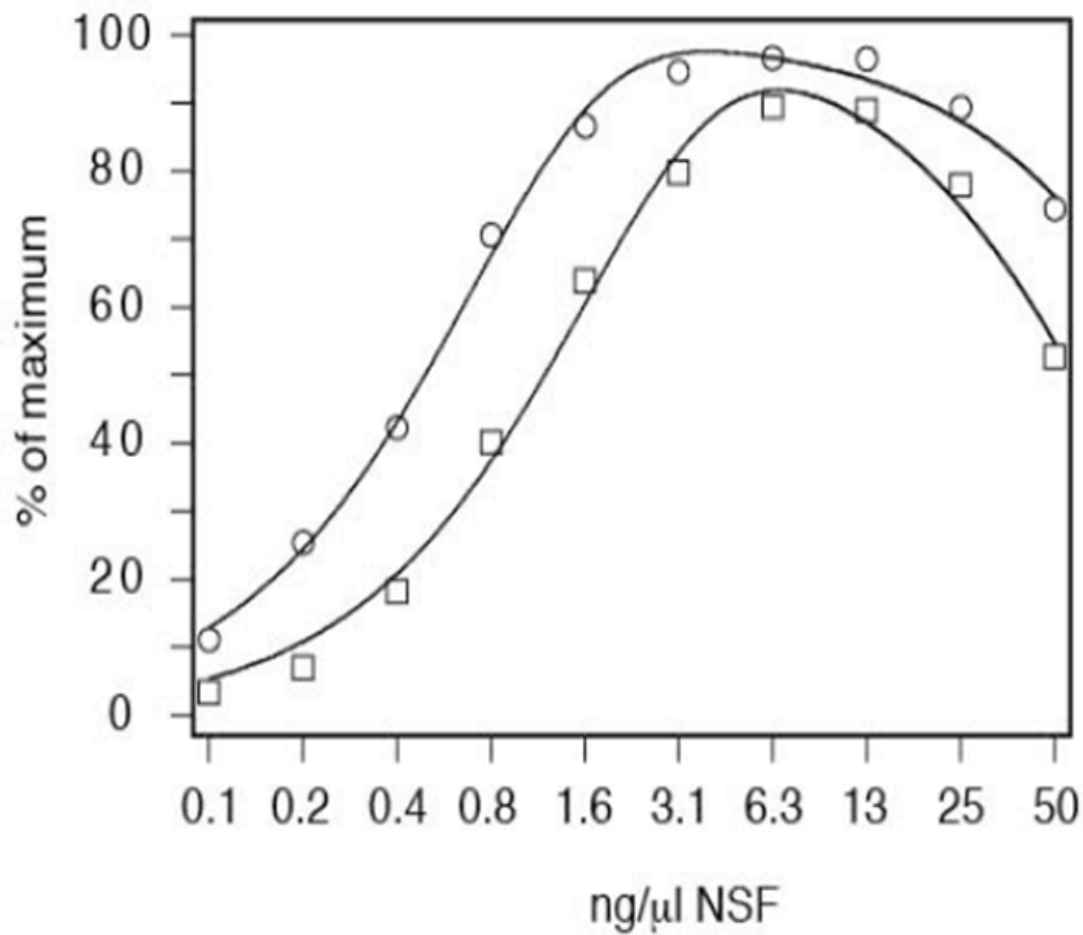


**Figure 6g. PK treated vesicles were also sensitive to NSF depletion.** This figure illustrates the % of maximal fusogenicity of COPI vesicles as a function of logarithmic changes in the concentration of NSF. Vesicles with (□) or without (○) PK treatment (2μg/ml, 30 min at 4°C) were compared. While PK treated vesicles were similarly sensitive to NSF depletion, their ability to recuperate their fusogenicity when NSF was reintroduced to the assay was only  $40.2 \pm 2.3\%$  of untreated vesicles. More than double the amount of NSF was necessary to obtain the same recovery.

To further confirm the above results on NSF, we used  $\alpha$ -SNAP<sup>mut</sup> as an alternative approach.  $\alpha$ -SNAP is another key player in the regulation of SNAREs mediated fusion, which has been shown to bind and unwind the SNAREs with the help of NSF<sup>203, 321-323</sup>. A mutant form of this protein,  $\alpha$ -SNAP<sup>mut</sup>, inhibits NSF, interrupting therefore the recycling of the SNARE machinery. This is the same mutant that was utilized to concentrate COPI vesicles during the budding assay (see chapter 1) by interfering with the binding of SNAREs with NSF. As shown in figure 6h, the fusion of both untreated and PK-treated vesicles were inhibited by  $\alpha$ -SNAP<sup>mut</sup>. However, the PK treatment significantly abolished

the residual levels of fusogenicity normally preserved under control conditions (fig. 6h). We speculated that the remaining fusogenicity was due to the endogenous  $\alpha$ -SNAP that was already associated to the membranes, and that the loss of this endogenous  $\alpha$ -SNAP by PK treatment was responsible for the more drastic effects of  $\alpha$ -SNAP<sup>mut</sup> on the COPI vesicles. Another possibility was that the PK treatment somehow diminished the ability of the vesicles to interact with  $\alpha$ -SNAP.

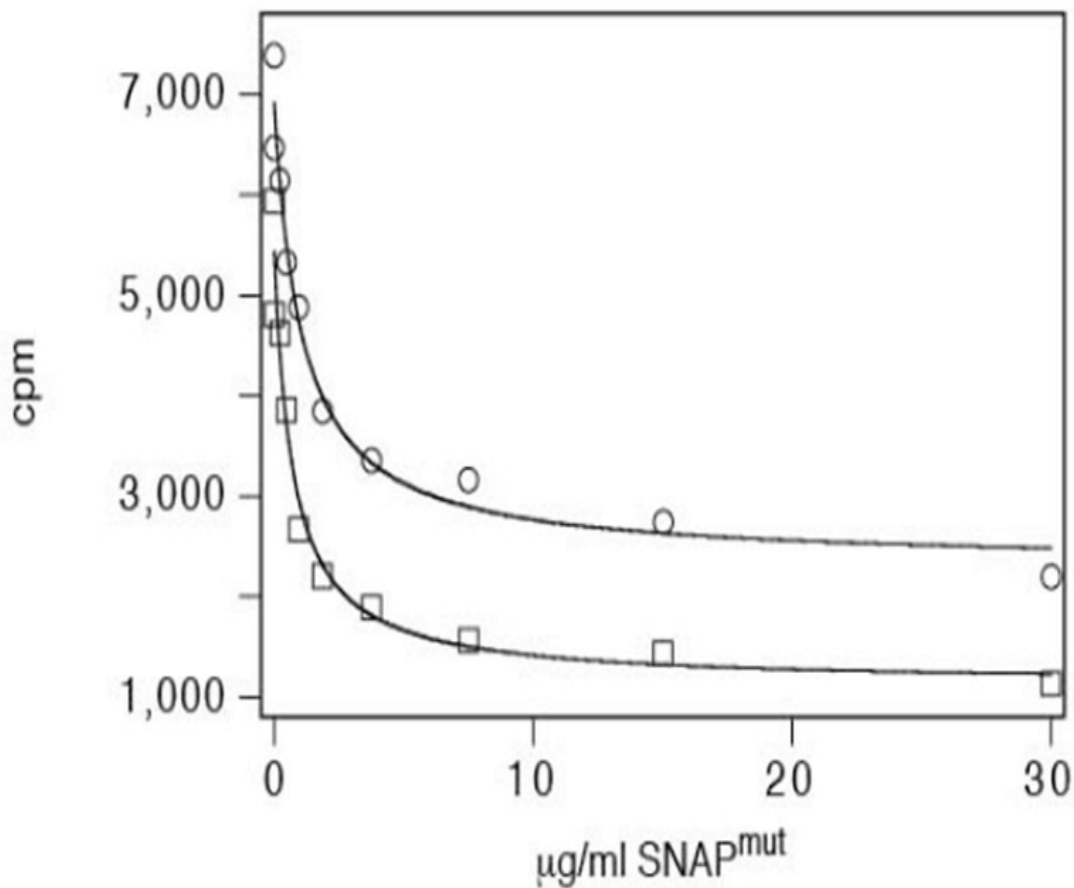


**Figure 6h.  $\alpha$ -SNAP<sup>mut</sup> inhibited the fusion of COPI vesicles treated with PK.** Fusion assays were performed in the presence of increasing amount of  $\alpha$ -SNAP<sup>mut</sup>. Two series of vesicles were compared, one treated with 2  $\mu\text{g/ml}$  of PK for 30 min at 4°C (□) and the untreated control (○).

It was demonstrated by Barnard et al.<sup>203</sup> that NSF contributes to the unwinding of the SNAREs after a fusion event. Therefore, a fusion assay where NSF is not able to function cannot proceed due to the target SNAREs still in the unwound conformation. However, recent evidence revealed other important functions of NSF and  $\alpha$ -SNAP within a cell (for review, see <sup>324</sup>).

To test the possibility that PK treated COPI vesicles lost their ability to interact with  $\alpha$ -SNAP, the vesicles were pre-incubated with  $\alpha$ -SNAP<sup>mut</sup> after the PK treatment but before the fusion assay during which a second  $\alpha$ -SNAP<sup>mut</sup> incubation occurred. The resulting fusogenicity was compared with that in the control experiment without any  $\alpha$ -SNAP<sup>mut</sup> preincubation. Because it was presumed that during the pre-incubation the endogenous proteins present on the membranes interchanged with the mutants, we predicted that a higher susceptibility to  $\alpha$ -SNAP<sup>mut</sup> and a further reduction in the residual fusion activity (fig. 6i).

These experiments were also compared with an experiment that included a preincubation with wild type  $\alpha$ -SNAP in both vesicles and Golgi membranes prior to the incubation with  $\alpha$ -SNAP<sup>mut</sup>. As shown in figure 6i, the residual fusogenicity went up for both untreated and PK treated vesicles up to 40% of control. This effect could be explained by the fact that the membranes were “saturated” beforehand with working  $\alpha$ -SNAP, out competing the mutant forms in the binding with SNAREs. In contrast, a pre-incubation of the untreated vesicles with  $\alpha$ -SNAP<sup>mut</sup> caused a reduction in the fusogenicity (2<sup>nd</sup> set of columns compared to 3<sup>rd</sup> set, black bars). Importantly, we could not detect any significant decrease when this pre-incubation with  $\alpha$ -SNAP<sup>mut</sup> acted on the PK treated vesicles (2<sup>nd</sup> set of columns compared to 3<sup>rd</sup> set, gray bars). This indifference to  $\alpha$ -SNAP<sup>mut</sup> demonstrated that the COPI vesicles lost their ability to interact with  $\alpha$ -SNAP as a consequence of the PK treatment. The observed increase in the fusogenicity compared to the control (1<sup>st</sup> set of columns) was mainly due to the effects of  $\alpha$ -SNAP on the target Golgi. Indeed, the largest change in the fusogenic signal was obtained when the target Golgi, not the COPI vesicles was pre-incubated with the  $\alpha$ -SNAP<sup>mut</sup> (4<sup>th</sup> and 5<sup>th</sup> sets of columns, fig. 6i). Therefore, it seems that the residual fusogenic activity detected in figure

6h was mostly due to the endogenous  $\alpha$ -SNAP present on the target membranes. This data also refuted the concept that the PK treatment inhibited the fusion by simply removing endogenous  $\alpha$ -SNAP on the COPI vesicles. Nonetheless, the ability of the vesicles to interact with  $\alpha$ -SNAP remained an important prerequisite in the fusion process, as its loss as a result of the PK treatment led to a greater sensitivity to  $\alpha$ -SNAP<sup>mut</sup> inhibition (fig 6h) and a lesser residual fusogenicity. The importance of this interaction could also explain why the reintroduction of NSF could not efficiently rescue the NSF-depleted fusion when vesicles were treated with PK (fig. 6g).

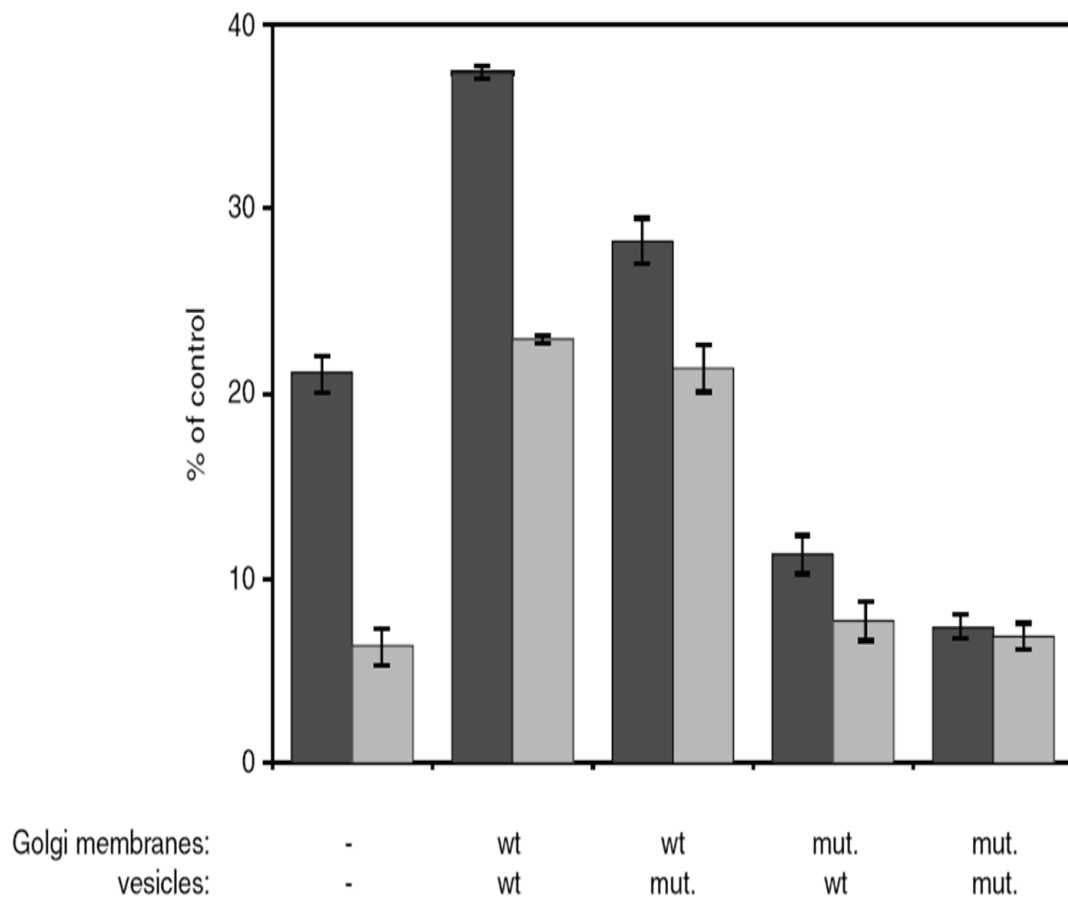


**Figure 6i. Pre-incubation of vesicles and target Golgi membranes with  $\alpha$ -SNAP<sup>mut</sup>.** Untreated vesicles (black bars) or vesicles treated with 2  $\mu$ g/ml PK for 30 min at 4°C (gray bars) were pre-incubated in the cytosol containing wild type  $\alpha$ -SNAP or  $\alpha$ -SNAP<sup>mut</sup> for 15 min before the fusion assay during which a second  $\alpha$ -SNAP<sup>mut</sup> incubation occurred. The same pre-incubation was given to the target Golgi membranes. The resulting fusogenicity were compared to the value (set as 100%) obtained in the experiment performed without  $\alpha$ -SNAP<sup>mut</sup> in the fusion assay. See <sup>9</sup>.



## **Discussion**

Following the discovery that both PI(4,5)P<sub>2</sub> and proteins were required for the fusion of COPI vesicles, we sought to expand our understanding of the relationship between the involvement of lipid and proteins in the fusion process. We have previously suggested that the partial resistance to the PK treatment was conferred by a conformational change in the surface proteins on the fusogenic COPI vesicles linked to the presence of PI(4,5)P<sub>2</sub> (chapter 2). In this chapter, we examined the mechanistic nature and the extents of this PK effect. Our ultimate goal would be to identify the proteins that act downstream of the PI(4,5)P<sub>2</sub>.

One of the chief findings was that the PK treatment hindered in fact the ability of the vesicle to bind and dock to, but not to fuse with, the target Golgi. Further controls of our fusion assay confirmed that the vesicles were still dependent on NSF/ $\alpha$ -SNAP to fuse, even after being treated with PK. However, the NSF/ $\alpha$ -SNAP largely acted on the target Golgi as previously described in the literature <sup>203</sup>. There was a minor but significant interaction between the COPI vesicles and  $\alpha$ -SNAP that contributed to the overall fusion, this interaction was clearly revealed by a decrease in the fusogenicity upon its loss when the vesicles were pre-incubated with PK.

Altogether, the fact that the COPI vesicles retained the ability to fuse after removal of the surface proteins by PK remained an intriguing dilemma. One hypothetical explanation was that the necessary components of the fusion machinery were all recruited from the cytosol. However, this would mean that none of integral proteins on the vesicles including v-SNAREs were required, an observation once reported yet to be further examined <sup>294</sup>. Another possible explanation would be that the fusion process was dependent on one or multiple protein(s) that were susceptible to some, but not all, aspects of the PK treatment and that there is what could be termed a protease resistant core of fusion proteins, whose members are still unidentified. This theory, if proven by the identification of any of these proteins, would advance our understanding on the mechanism underlying the COPI vesicle fusion.

## **Chapter 7: A PK resistant core of the tethering factor Golgin-84 is present on the surface of COPI vesicles.**

---

### **Introduction**

It was previously demonstrated that some SNARE proteins can change their conformation upon stimulation by ARFGAP1, rendering them resistant to PK<sup>301</sup>. While our attempt in chapter 2 to identify them in our fusion assays was unsuccessful, we reckoned that our investigation may have been incomplete, since we only tested for very limited numbers of proteins known for their potential implication in the vesicle fusion. A more thorough hunt was necessary as it was the only mean to shed light into the key twist in the mystery that would allow us to link the involvement of PI(4,5)P<sub>2</sub>, the role of protein(s) and the PK resistance of the COPI vesicles in the fusion process.

Therefore, we searched more in depth in the literature for any potential targets participating in or related to the fusion of COPI vesicles. One interesting candidate, Golgin-84, was shown by Malsam *et al.*<sup>55</sup> to mediate the transport of COPI vesicles inside the cell. As mentioned in chapter 1, the pool of vesicles that they collected with the aid of glass beads resemble our preparation. They also demonstrated that the uncoating of the vesicles was followed by the binding of Golgin-84 to its target Golgi tether, CASP. Furthermore, they provided evidence that the retrograde traffic from the Golgi to the ER was dependent on the unhindered activity of the Golgin-84-CASP tether. Remarkably, Golgin-84 was discovered as a binding partner of OCRL1, a PI(4,5)P<sub>2</sub> 5'phosphatase localized within the TGN<sup>1, 55, 285</sup>. The OCRL1 family relative, INPP5B, has also been shown to be involved in the traffic of the early secretory pathway<sup>283</sup>. Based on these findings, we proceeded to investigate the role of Golgin-84 in our fusion essay.

### **Results**

Golgin-84 is a 84 kDa protein with a single transmembrane domain located near the carboxyl-terminal. Most of the characterization of this protein has been done with an

antibody generated from rabbits against its amino acids 499-687<sup>1</sup>. In addition, it has been shown by its sensitivity to PK that most of its structure is oriented to the cytoplasm (fig. 7a).

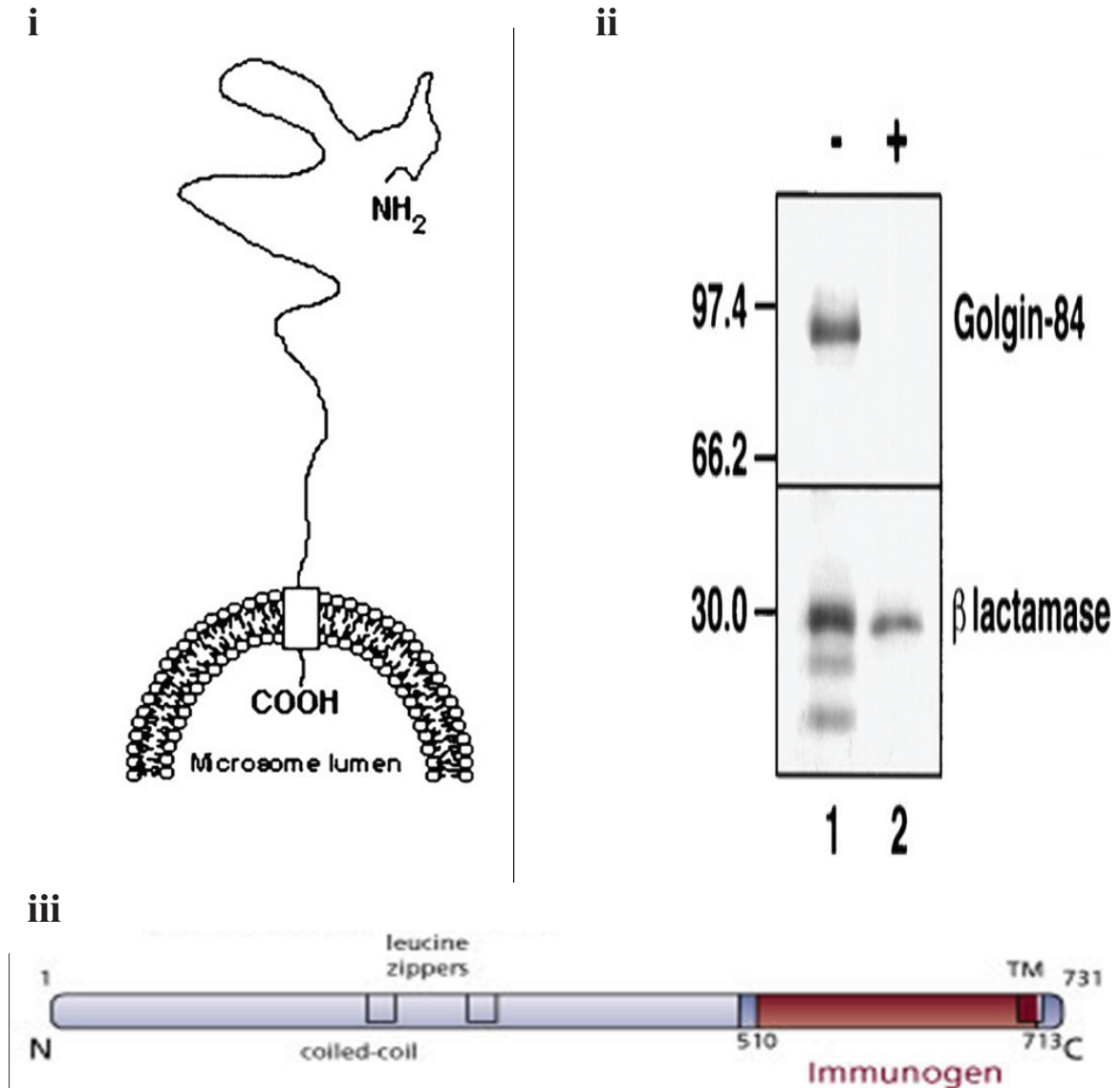


**Figure 7a. Golgin 84 and its antibody.** i) Golgin-84, as described in<sup>1</sup>. ii) The cytoplasmic orientation of Golgin-84 in microsomes was determined by its sensitivity to PK treatment (lane 2) compared to control (lane 1). The  $\beta$ -lactamase, a protein found in the lumen of the vesicles, was used as a negative control (from<sup>1</sup>). iii) The antibody used in these experiments was generated from rabbits against its amino acids 499-687. In this chapter, we used instead a commercially available antibody whose variable sequences recognizes the epitopes from amino acids 510-713 (BD Transduction Laboratories).

Our proteomics team has recently identified a whole spectrum of proteins present in both purified Golgi membranes and COPI vesicles, including those studied in chapter 2, Golgi-

84 and CASP <sup>7</sup>. Using peptide counting with MS, we were also able to determine the abundance of these proteins present in the preparation as well as the level of enrichment in the COPI vesicles relative to the Golgi membranes. In figure 7b, we listed a selection of proteins that are potentially involved in the fusion process. Among them, CASP, Golgin-84 and SEC22 homolog were found to be the most enriched in the COPI vesicles. While SEC22 is a SNARE known to promote the fusion, the exact function of SEC22 homolog is undetermined. To note, Golgin-84 was also one of the most abundant proteins, constituting over 2% of all peptides in the vesicles.

<b>Protein</b>	<b>Type</b>	<b>AVG %Total peptide COPI</b>	<b>AVG %Total peptide Golgi</b>	<b>Enrichment COPI Vesicles /Golgi</b>
GIANTIN	Tether	0.910	0.446	2.04
<b>GOLGIN-84</b>	Tether	<b>2.145</b>	0.313	<b>6.85</b>
SYNTAXIN 5	SNARE, Qa	0.063	0.145	0.43
MEMBRIN	SNARE, Qb	0.082	0.032	2.58
RBET1	SNARE Qc	0.046	0.023	1.99
SEC 22b	SNARE, R	0.497	0.294	1.69
P115	Tether	0.090	0.276	0.33
P24	P24 protein	0.132	0.218	0.61
GS28	SNARE, Qb	0.415	0.335	1.24
M-CASP	Tether	0.661	0.064	10.36
Sec22 Homolog	undetermined	0.251	0.036	6.94

**Figure 7b. Abundance and enrichment of proteins from COPI vesicles to Golgi.** Equal quantities of purified organelles were introduced to a 1D-electrophoresis gel. After the protein separation, the gel was cut and the proteins extracted. The embedded proteins were then subject to proteolysis and the resulting peptides were identified using MS. With the help of bioinformatics, the identities of the parent proteins were deduced from the peptide fragments <sup>6, 7</sup>. The total amount of peptides derived from each protein was calculated (3<sup>rd</sup> and 4<sup>th</sup> column) and expressed as a % of the total peptides. These quantities were then compared as a ratio of enrichment in COPI vesicles versus Golgi membranes (5<sup>th</sup> column). Golgin-84 constituted 2.145% of all peptides detected in the COPI vesicles fraction and was 6.85X enriched compared to the purified Golgi.

Given the highly suggestive pivotal role and its abundance and relative enrichment in COPI vesicles, the PK sensitivity experiment similar to those in chapter 2 was performed

on Golgin-84 and revealed by immunoblotting. We discovered a PK resistant protein, i.e. Golgin-84, on the surface of the vesicle (fig. 7c).

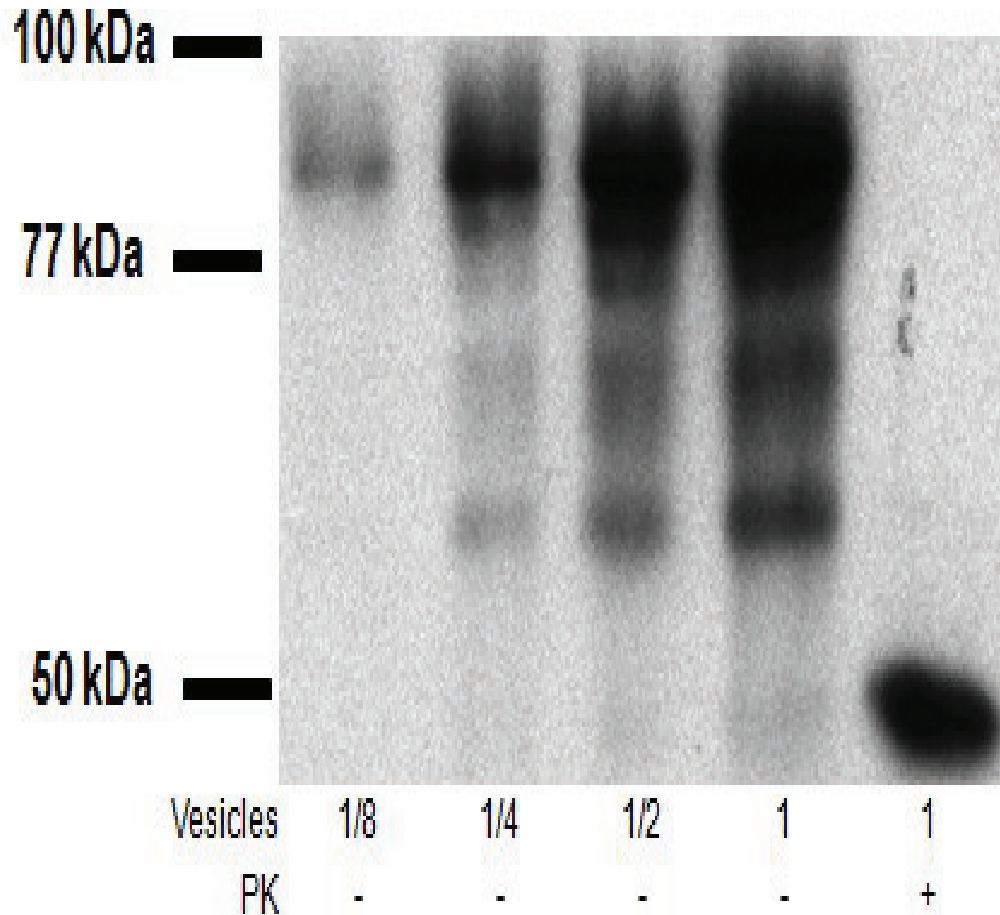


**Figure 7c. Golgin-84 is resistant to PK degradation.** Increasing amounts of COPI vesicles (up to 5  $\mu$ l) were loaded onto a denaturing gel and submitted to western analysis. On the last lane on the right, the same vesicles were treated with 2  $\mu$ g/ml of PK for 30 min at 4°C. PMSF (1 mM) was added to the reaction to terminate the PK activity as well as to all other samples. Upon the treatment with PK, a distinct band appeared at about 50 kDa, representing a protease resistant core of Golgin-84.

The presence of a PK resistant core had never been found by Bascom et al. <sup>1</sup>. Could the discrepancy regarding the PK sensitivity be due to the use of two different antibodies? While the protein sequences that they bound to only differed in 20 amino acids, both spanning the epitope region close to the carboxyl-terminus of Golgin-84 on the

cytoplasmic surface of the vesicles (fig. 7a), our antibody actually recognized in addition the protein transmembrane domain. It is possible that the observed PK resistant core consisted of a protein sequence embedded inside or laid in proximity to the lipid bilayer, hence being protected from the PK proteolysis. However, two arguments against this explanation seemed to favor the notion of protein conformational change as a cause of the PK resistance. First, the transmembrane region of Golgin-84 is very small. If the PK resistance were solely mediated by the protective shielding from the lipid, one would predict a PK resistance core much smaller than 50 kDa. Second, the presence of this core was observed only in the fusogenic vesicles and not in any other settings (See experiment below), hinting a change in the physical property under specific situations. Interestingly, Bascom *et al.* has shown that Golgin-84 could in fact dimerize. Using bioinformatics analysis, they predicted that the dimerization was induced by its a coiled coil domain (amino acids 217-632) that contained two leucine zippers at amino acids 227-248 and 301-322. Protein dimerization represents a plausible mechanism by which the COPI vesicles acquired its resistance to PK. The region that was resistant to PK and the precise location of the cleavage site(s) on the Golgin-84 that generated the 50 kDa band has not been determined. Further analysis by MS and biochemical studies will be necessary to confirm our hypotheses.

The presence of this unexplained PK resistant protein sequence propelled us to first investigate if it was present on COPI vesicles alone or if it could also be found in the in Golgi membranes. Because we had preliminary data showing that only preparations of vesicles with strong fusogenicity possessed the 50 kDa Golgin-84 band after the PK treatment (data not shown), we were interested in testing as well COPI vesicles generated with GTP- $\gamma$ -S. The resulting loss of fusogenicity was demonstrated separately in figure 7e. As revealed by Western blots, neither Golgin-84 in Golgi membranes nor that in non functional COPI vesicles was resistant to the PK proteolysis (fig. 7d).

The need of a conformational change of Golgin-84 into an active form has been suggested by Malsam *et al.* <sup>55</sup>. They showed that the active Golgin-84 promoted the fusion of COPI vesicles moving in a retrograde fashion while the inactive form trafficked from the ER-

Golgi intermediate compartment (ERGIC) and ER back to the CGN, where it was re-incorporated in the COPI vesicles. Furthermore, this finding could explain why only a small fraction of their vesicles was able to bind to CASP coated beads

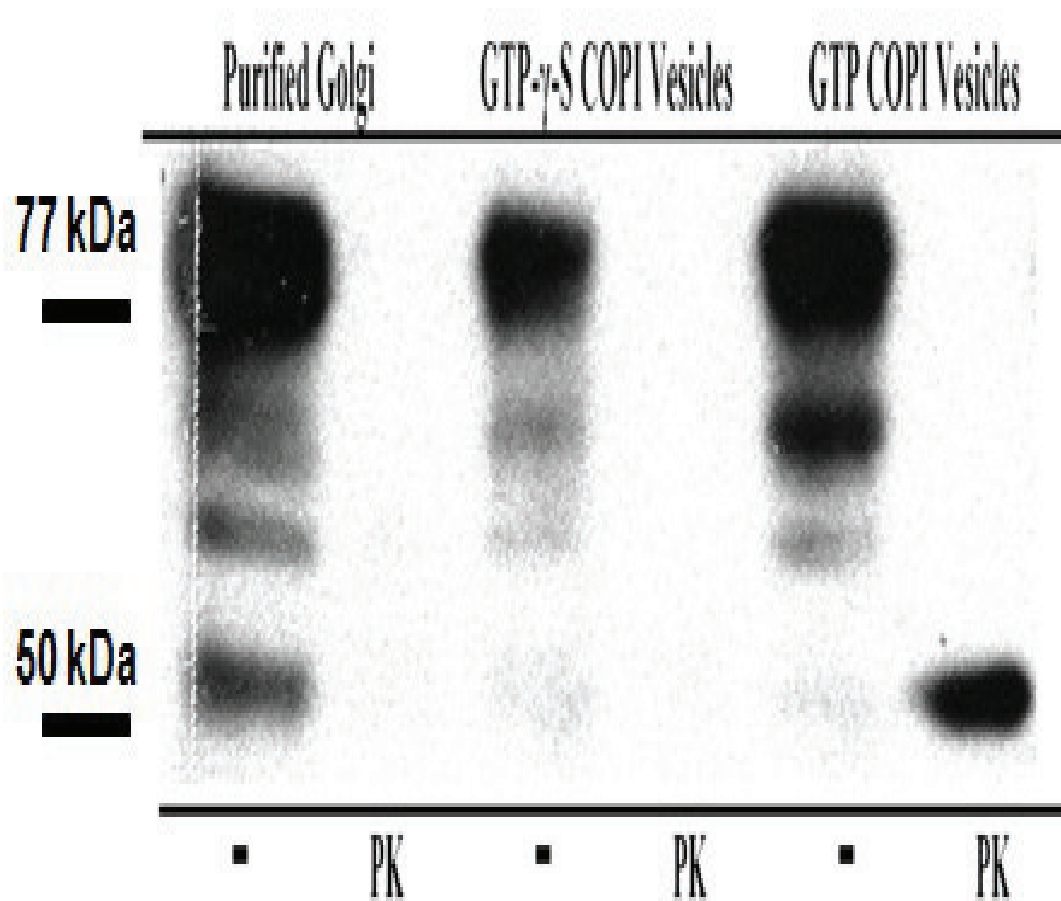


**Figure 7d. Golgin-84 PK resistant core is only present on fusogenic COPI vesicles.** An equal amount of Golgin-84 from the Golgi membranes, GTP- $\gamma$ -S or GTP (control) treated COPI vesicles was introduced on a denaturing gel with (PK) or without (-) prior PK treatment (2  $\mu$ g/ml, 30 min, 4°C). The 50 KDa band was only present on fusogenic (GTP-treated control) COPI vesicles. Note: Similar results were obtained when the film was overexposed (data not shown).

Two arguments could point to a possible relationship between PI(4,5)P<sub>2</sub> and Golgin-84. First, it was previously established that a relationship exists between ARF1 and PI(4,5)P<sub>2</sub> and that stimulation of ARF1, which are also responsible for the formation of the COPI vesicles, leads to increase PI(4,5)P<sub>2</sub> within the Golgi apparatus<sup>271, 272</sup>. This, in correlation with the susceptibility for GTP-γ-S for the PK resistant conformation of Golgin-84, points to these changes happening rather simultaneously during the synthesis of COPI vesicles, since GTP-γ-S hinders the action of ARFGAP1. Furthermore, the fact that Golgin-84 was cloned in the first place because of its association with OCRL1, a PI(4,5)P<sub>2</sub> 5'phosphatase, also points to a potential association between the two.

To test if there is a relationship between the change in conformation of Golgin-84 when introduced to COPI vesicles and the status of PI(4,5)P<sub>2</sub> on these vesicles, we submitted the vesicles to two incubations (fig. 7f). First, vesicles are incubated at 37°C in the presence of 5'phosphatase (0.125 mg/ml) for increasing periods of time, which is followed by PK treatment. The state of the protease resistant core is then ascertained by western. This protocol could not discover any link between the PI(4,5)P<sub>2</sub> status and the protease resistant core of Golgin-84.



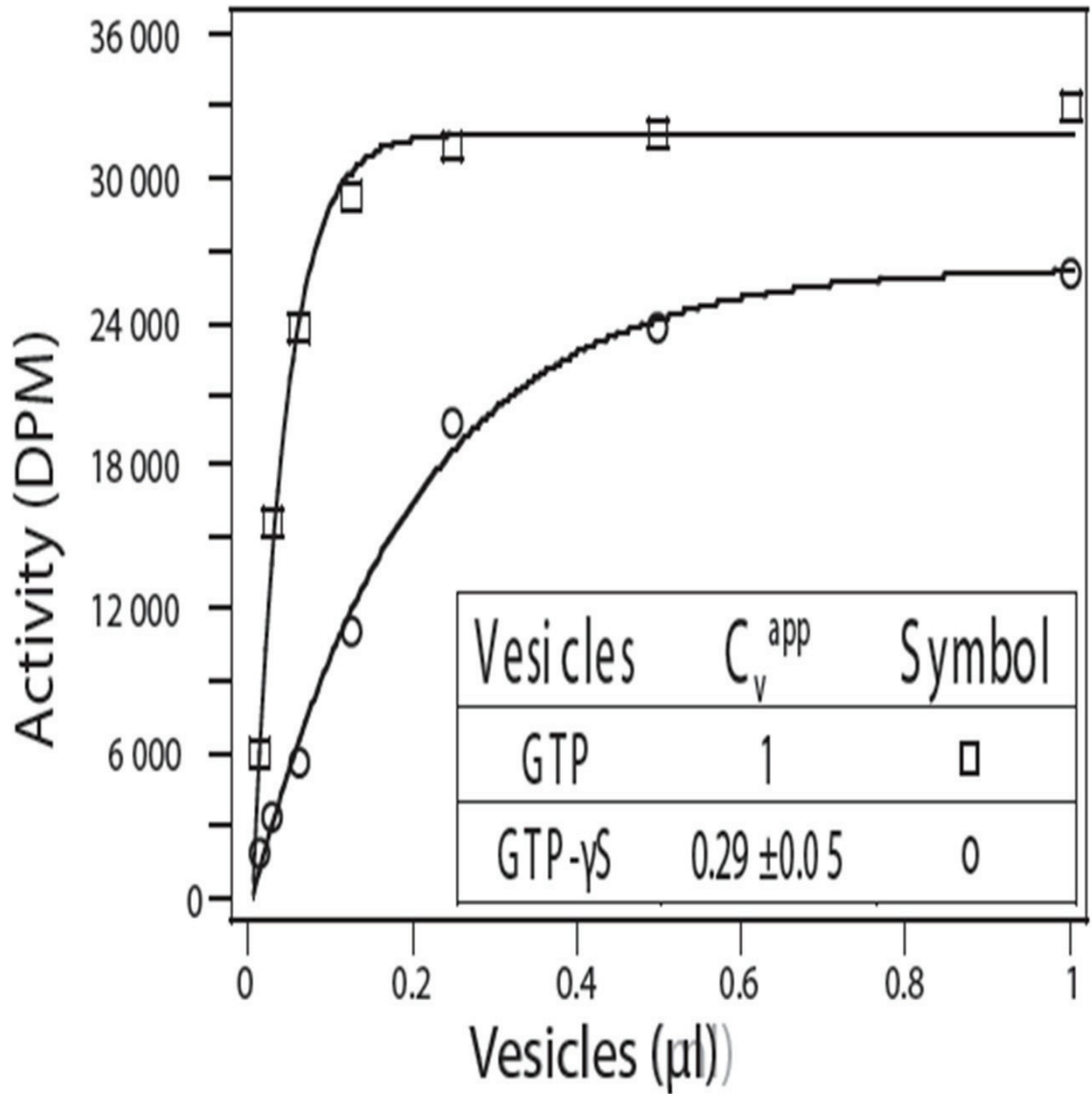


**Figure 7e. Vesicles without protease resistant Golgin-84 have lower fusogenicity.** Two preparations of vesicles were prepared simultaneously with the budding assay. During the budding assay, the first preparation was incubated with GTP (□) while the second was incubated with GTP-γ-S (○). These vesicles were then introduced to the fusion assay and their  $C_v^{app}$  calculated and compared. The ratio obtained was corrected for the protein concentration of each preparation. After this correction, it was determined that vesicles prepared with GTP-γ-S were only  $0.29 \pm 0.05$  as fusogenic as vesicles prepared with GTP. Figure represents a typical fusion assay before correction. Data was collected out of n=3 experiments with different preparations of GTP and GTP-γ-S vesicles and is expressed in the formula MEAN  $\pm$  STDEV.

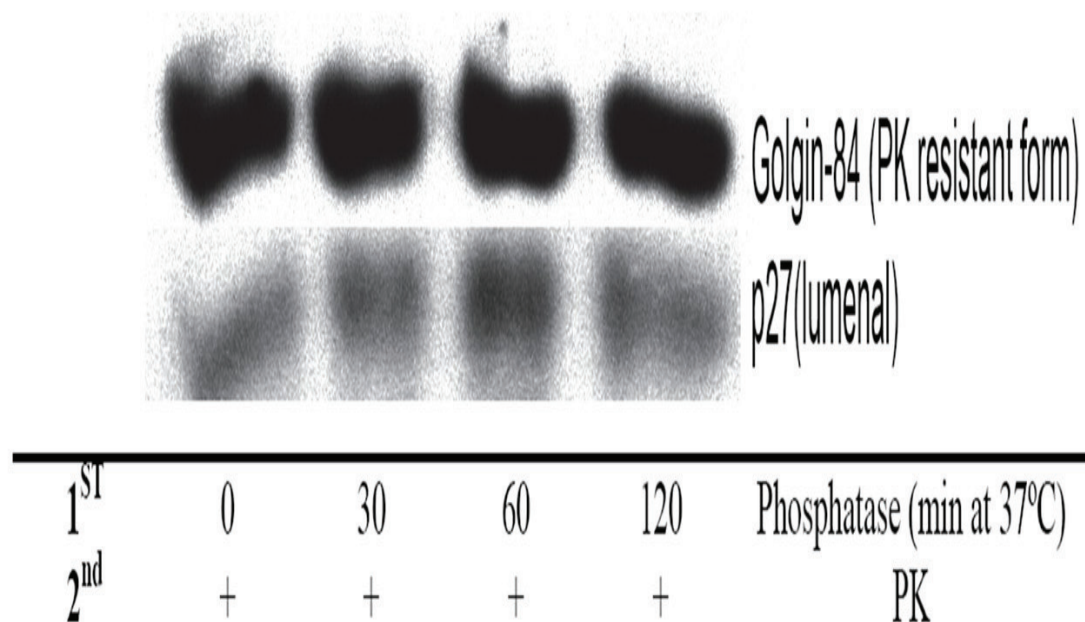


**Figure 7f. The protease resistant core of Golgin-84 is not affected by removal of PI(4,5)P<sub>2</sub>.** Vesicles were first incubated for increasing period of times in the presence of 0.125mg/ml of purified 5'phosphatase before being submitted to PK incubation (2ug/ml 30 min, 4°C, neutralized with 1mM PMSF). Second incubation was followed by western. The luminal domain of p27 was used to test for the integrity of the vesicles.

## Discussion

The discovery of a PK resistant tether conveys a potential explanation for the results observed in chapter 2 and chapter 6 of this thesis, where it was discovered that PK treated vesicles are still able to fuse to a certain degree. It was then shown that the binding of the vesicles was affected primarily, while the fusion of the vesicles after the binding did not differ between control vesicles and vesicles that had been treated with PK. It could be postulated from these and information in this chapter that the full form of Golgin-84 is necessary for optimal fusion, and that its protease resistant core is sufficient to allow binding to proceed.

The fact that this core was not discovered earlier is most probably due to the fact that PK treatment had not been tested on purified COPI vesicles. This discovery raises the question if such a protease resistant core exists with other proteins, and if so would we be able to identify them. While protease resistant cores had been shown in other potential docking proteins in certain conditions, such as SNAREs<sup>301, 302, 325-328</sup>, theoretically, their presence could remain a probability even in the absence of significant evidence on westerns, as the removal of the epitope which is not present within the protease resistant core could explain the loss of signal from the antibody on the western. A study using non-denaturing electrophoresis gels followed by MS should be able to determine if this conformation change in Golgi-84 has associated proteins.

This chapter also demonstrated that the presence of the protease resistant core was not dependent on the level of PI(4,5)P<sub>2</sub> on the vesicles. However, it is also a possibility that PI(4,5)P<sub>2</sub> could be required for this function at a certain point during the budding of the vesicle, when the conformation of Golgi-84 protease core is formed, and is not required after the budding of the vesicle. We could perform a budding reaction, alike the one done in figure 1e, where we depleted the PI(4)P 5'-kinase from the budding cytosol and observe if the vesicles produced are fusogenic and if they possess the Golgi-84 protease resistant core.

Another information that can be gathered from the last figure of this chapter is that after 120 minutes incubation in 0.125 mg/ml phosphatase, the vesicles are no longer fusogenic (see chapter 2 and 4), but the Golgi-84 resistant core is still present. From this, we can deduce that while Golgi-84 is required for the fusion of the vesicles (<sup>55</sup> and fig.7e), it is not sufficient for fusion.

It could also be argued that figure 7e is not optimal. In fact, the vesicles are different in terms of their protein content, as well as to the fact that GTP- $\gamma$ -S vesicles are thought to remain coated after budding<sup>7</sup>, which would affect their fusion ability regardless of their Golgi-84 status. While it is hypothesized that the ARFGAP1 as well as the GTP present in the fusion assay allows the vesicles to eventually uncoat, more experiments could be

developed to demonstrate this point further. Alike what was done with PI(4,5)P<sub>2</sub>, a better experiment would be able to modify only the protease resistant core, something that has not been attempted at this point.

Future work should try to pinpoint the involvement of Golgin-84 with the help of cytosol competitors to the tethers, alike to what was done *in vivo* in Malsam et al. One could also determine the relative affinities of CASP for the different conformation of Golgin-84, in order to confirm the hypothesis presented previously in this discussion.

Furthermore, the fact that the tethering factor involved in the fusion process is still present in part on the surface of the vesicles could explain the small diminished binding constant (kb) demonstrated in chapter 6. At the same time, it could provide a good hypothesis to explain why the vesicles are affected, but still can fuse in the end.

## Chapter 8: PI(4,5)<sub>2</sub> *in vivo*: methodology and ongoing work.

---

### Introduction

The ability to determine the traffic properties of the early secretory pathway has been revolutionized in the recent years by the ability to monitor organelles of the cells with the help of GFP and other chromatophores (e.g.<sup>36, 329, 330</sup>). While the precise monitoring of PI(4,5)P<sub>2</sub> is beyond the resolution of light microscope<sup>255</sup>, to be able to prove that it is involved in COPI transport *in vivo* would be of great scientific value.

### Results

In order to reproduce the cycling of COPI vesicles *in vivo*, the chimerical construct of a protein was obtained: VSV-G(TS045)-KDELr-Myc (from Nelson B. Cole<sup>137</sup>). This protein is specific in the following ways; first it is temperature sensitive: the protein will localize to the Golgi apparatus when incubated at 32°C. Since it contains the KDEL receptor protein in its sequence, a small part of the protein pool is always cycling between the ER and the Golgi<sup>137, 331, 332</sup> in a COPI dependent manner<sup>90</sup>.

Second, when the cells temperature is shifted from 32°C to 40°C, the VSV-G construct loses its conformation, becoming unfolded. Upon being transported to the ER, the proteins are unable to traffic back to the Golgi, as they are being sequestered by chaperones in the ER responsible for the proper folding of proteins<sup>137</sup>, for recent reviews<sup>333, 334</sup>.

Therefore, the planned experiment would monitor COPI dependent traffic by monitoring the speed of exchange between the Golgi and ER when the cells are shifted from 32 to 40°C. Inhibition of proper COPI fusion would lead to a pattern where the construct buds from the Golgi but is unable to fuse to the ER, severely altering the distribution pattern of the construct. This monitoring is done by IF against the myc epitope, which is not produced endogenously (fig. 8a).

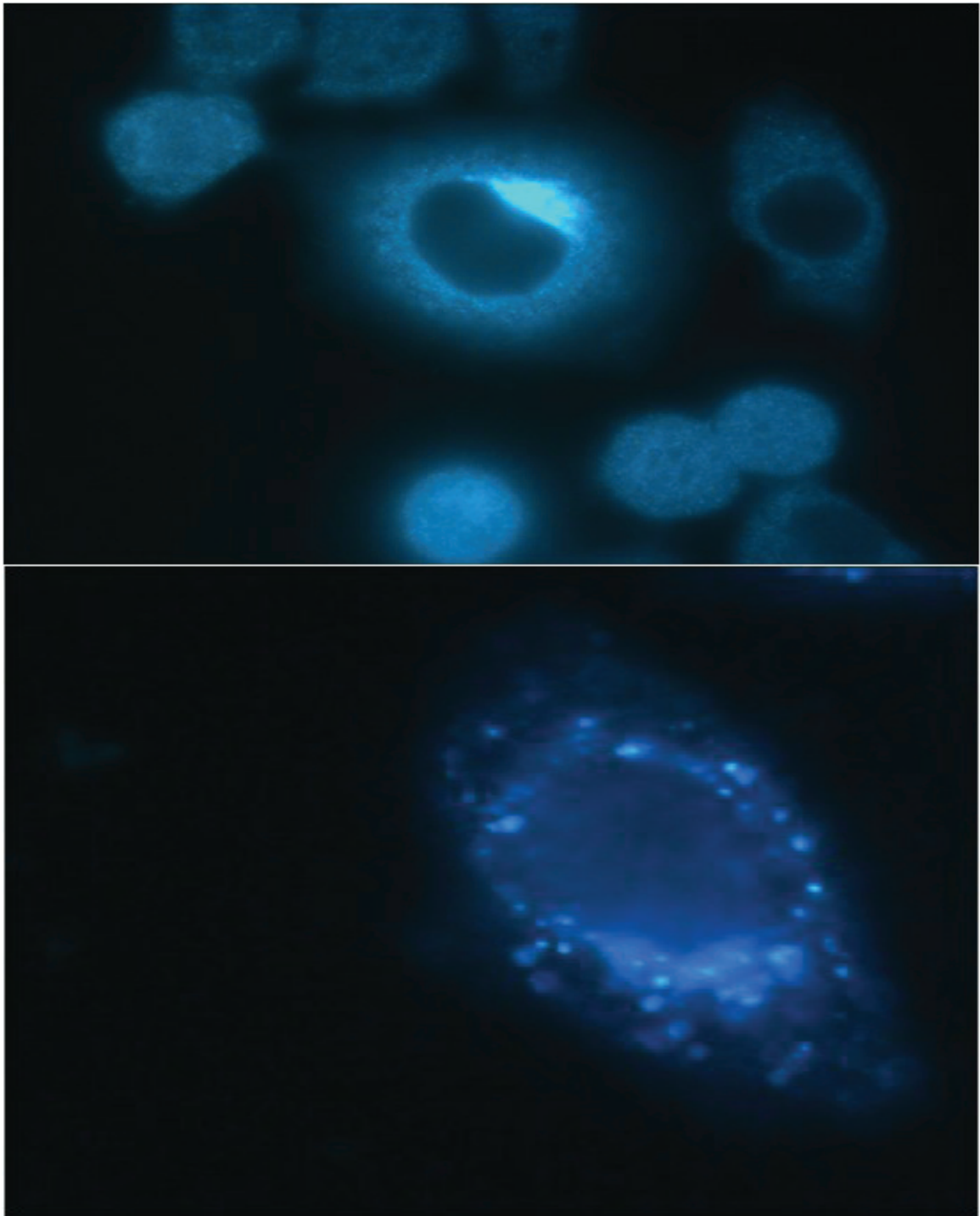


**Figure 8a.** VSV-G(TS045)KDEL-Myc. Upon transfection in HeLa cells, the construct is kept in the Golgi apparatus by incubating the cells at 32°C (up). After a short incubation at 40°C, the construct starts migrating to the ER (bottom).



PI(4,5)P<sub>2</sub> is produced within the cell from PI(4)P by three 5'kinase isoforms, PI(4)P5'kinase type 1  $\alpha$ ,  $\beta$  and  $\gamma$ . While the  $\gamma$  isoform is mostly located at the plasma membrane<sup>258, 315, 335</sup>, the  $\alpha$  and  $\beta$  isoform have been known to possess a cytoplasmic pool and a Golgi pool, in vitro<sup>271, 272, 316</sup>. We therefore investigated the possibility that these isoforms would colocalize with the Golgi apparatus with IF (fig. 8b,c,d)<sup>for review 336</sup>.

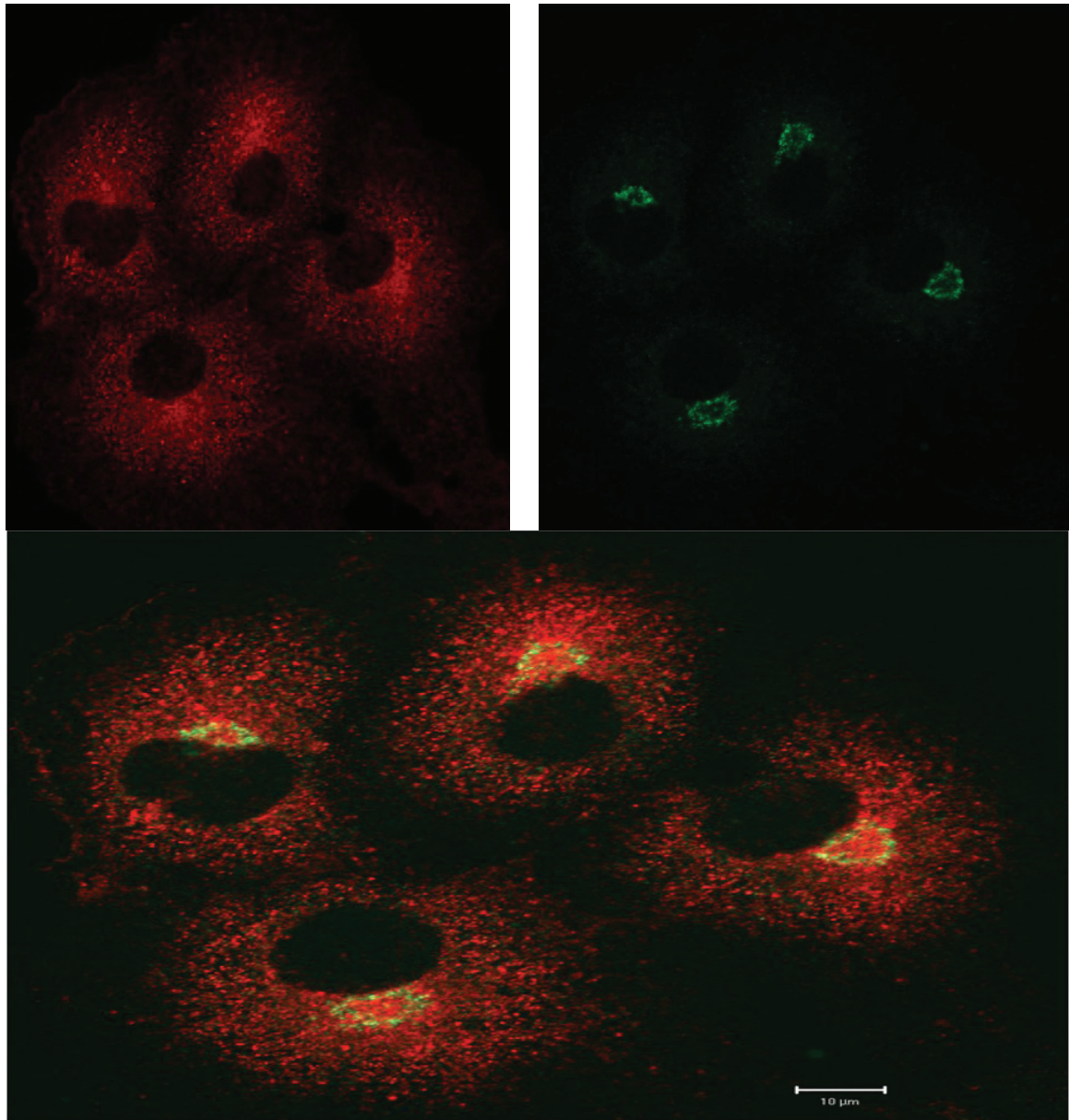


**Figure 8b. PI(4)P5'kinase type 1  $\beta$  localization in COS cells.** COS cells were probed against the protein PI(4)P5'kinase type 1  $\beta$  (up, left) or against gm130 (up, right). Merging reveals a mostly cytoplasmic localization. Bar, 10  $\mu$ M.

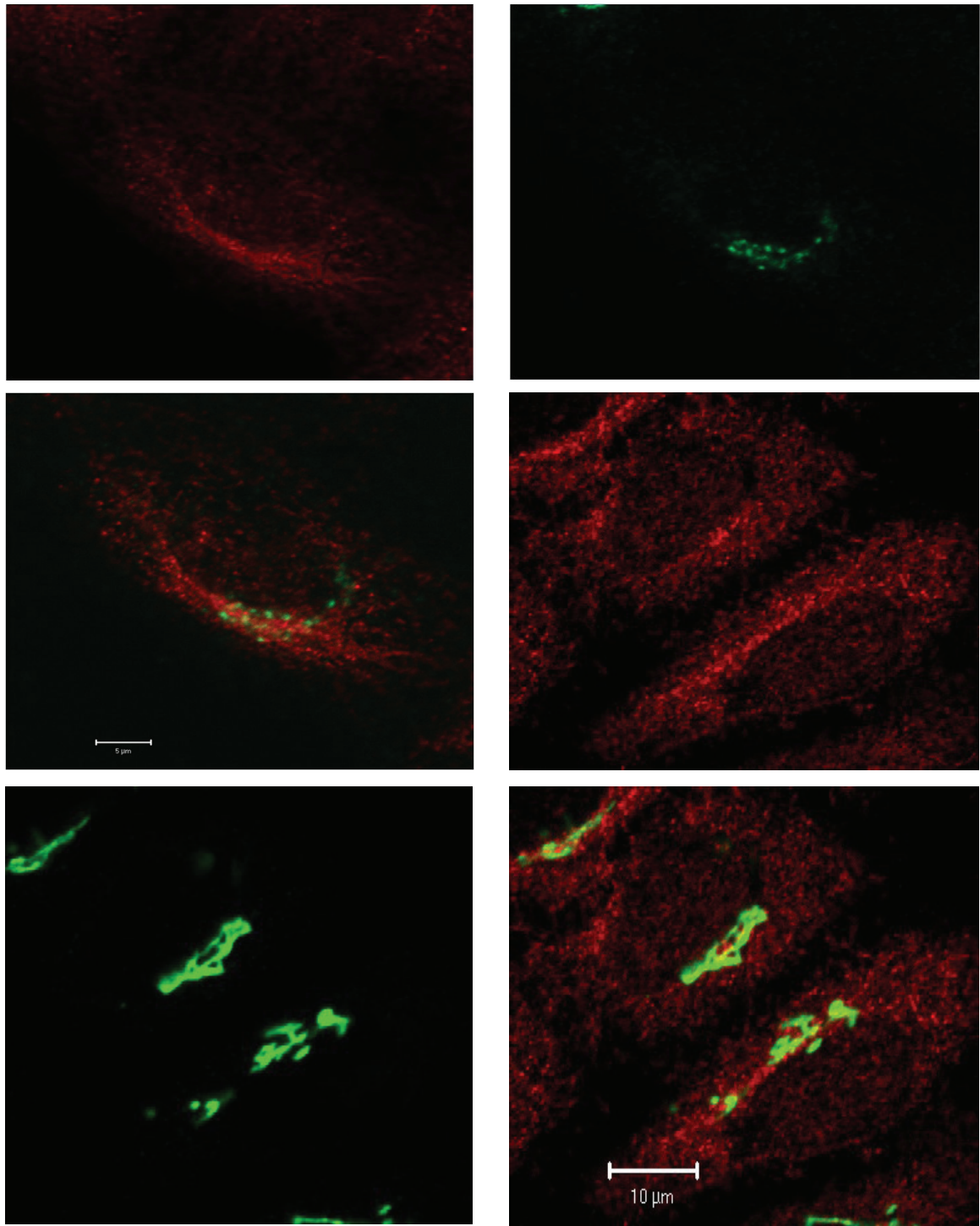


**Figure 8c. PI(4)P5'kinase type 1  $\beta$  localization in BSC1, HeLa cells.** Cells were probed against the protein PI(4)P5'kinase type 1  $\beta$  (BSC1 up left, HeLa middle right) or against gm130 (BSC1 up right, HeLa bottom left). Merging reveals a mostly cytoplasmic localization, described previously in <sup>4</sup> (BSC1 middle left, HeLa bottom right). \*Bar, 5  $\mu$ m (middle left) and 10  $\mu$ m (bottom right).



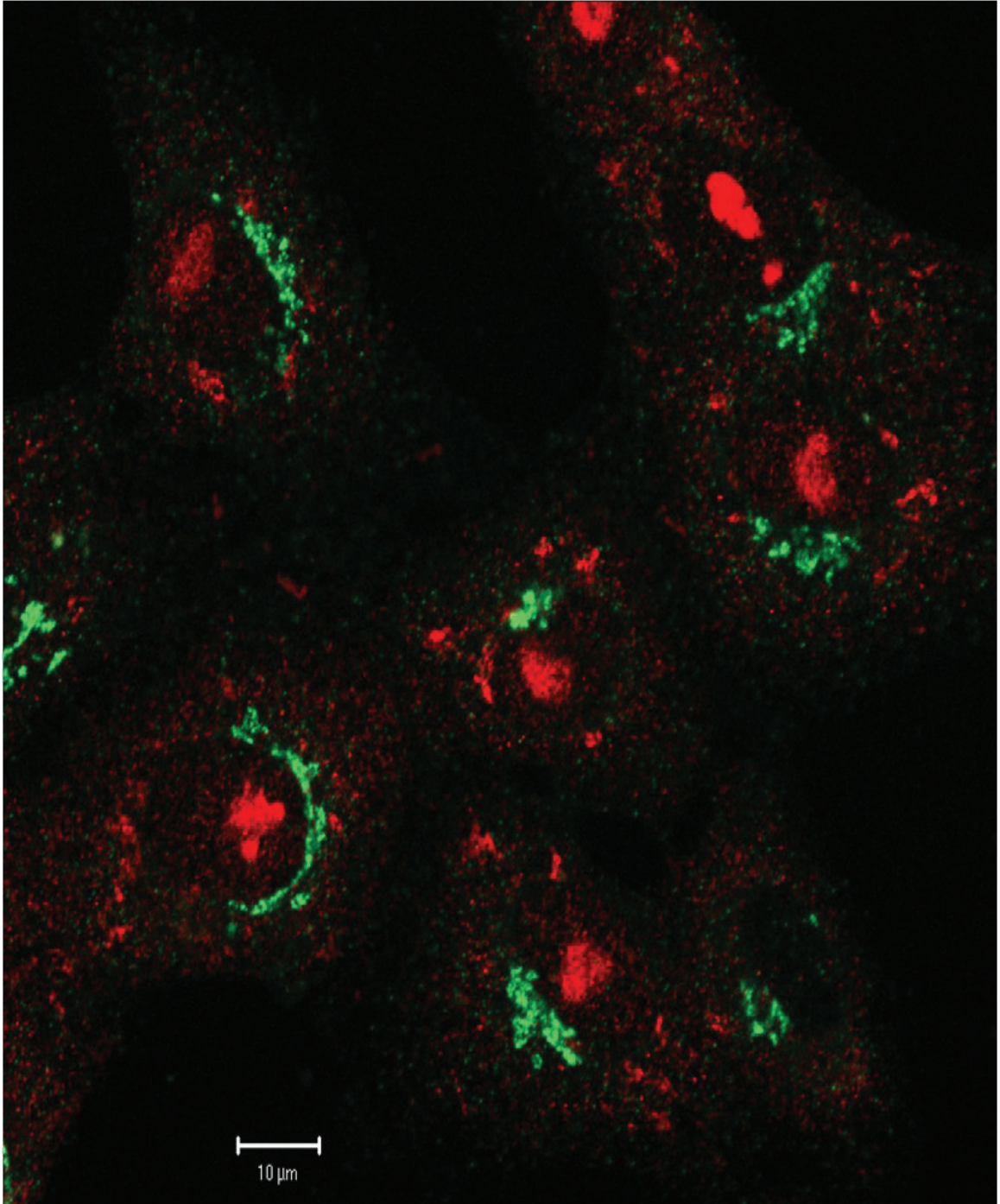


**Figure 8d. PI(4)P5'kinase type 1  $\alpha$  localization in HeLa cells.** Cells were probed against the protein GM130 (green), a Golgi marker and PI(4)P5'kinase type 1 $\alpha$  (red), which reveals a cytosolic as well as a nuclear speckle localization for the protein, alike what was seen in <sup>2,3</sup>. \*Bar 10  $\mu$ m.

Immunofluorescence studies demonstrated, at least in part, the cytoplasmic localization of both proteins, but with different pattern. While the  $\beta$  isoform was localized to the cytoplasm and more concentrated to the juxtannuclear region, the  $\alpha$  isoform is diffuse in the cytoplasm and strongly stains distinct locations of the nucleus. While none of them are clear Golgi markers, both of them could possibly be recruited to the Golgi apparatus. In any case, one of the isoform is recruited to the Golgi apparatus *in vitro* to produce PI(4,5)P<sub>2</sub> (see chapter 3).

The envisioned experimental protocol would have required, after transfection of the VSVG(TS045)-KDELr-Myc construct, the KO of the 5' kinases to inhibit the formation of PI(4,5)P<sub>2</sub> within the Golgi apparatus. This would have been accomplished with pSuperRetro vectors (see figure 8e) or RNAi that we obtained (from Dr. Shields and Dr. Pepperkok, respectively).

However, our experiments never got to the point where the KO were tested, the reason for this being that our TF protocol for VSVG(TS045)-KDELR-Myc failed to produce a long term viable cell line. The construct was extremely toxic to cells. While it was possible to obtain about 1% of successful transfect at the 48 hours stage, none of the cells were able to survive long enough to make an attempt at the KO possible.

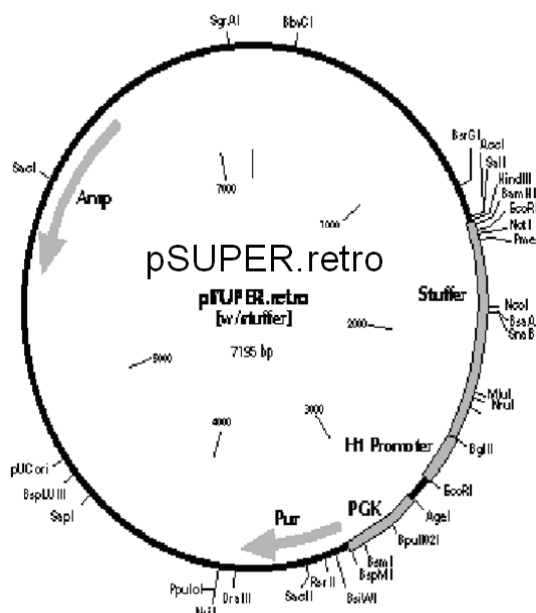


**Figure 8e. The pSuper.Retro vector.** When transfected into a cell, the vector produce an RNAi sequence that disables the target protein.

## **Discussion**

To specifically remove PI(4,5)P<sub>2</sub> *in vivo* has been attempted before. Among the difficulties experienced by the investigator was the fact that the 5'kinase isoforms tend to complement each other, and the activity of one or two isoforms can increase when another isoform is downregulated<sup>337</sup>. Therefore, this protocol most likely will require the KO of the isoforms  $\alpha$  and  $\beta$  simultaneously in order to completely abolish PI(4,5)P<sub>2</sub> within the Golgi.

Another problematic of this protocol is the fact that, in the event of a knockdown, it is not totally certain that an effect would be seen, or that too many effects would occur at the same time. PI(4,5)P<sub>2</sub> is required throughout the cell (see literature review) and a knockdown would affect many systems that could potentially interfere with our assay. Furthermore, this thesis demonstrate that PI(4,5)P<sub>2</sub> is required for the fusion of COPI vesicles to the 15°C compartment, also identified as the ERGIC. It is therefore not certain for sure that such a PI(4,5)P<sub>2</sub> requirement is needed for the fusion of COPI vesicles to the ER. A PI(4,5)P<sub>2</sub> knockdown could affect only a subpopulation of COPI vesicles and our *in vivo* model would not be able to detect it.

Other possibilities resides in the use of and inducible VSV-G(TS045) whose toxicity could be controlled and limited, or the use of Sar1<sup>dn</sup>, which can also be used to monitor Golgi to ER COPI vesicles traffic<sup>55</sup>. In any case, besides the potential pitfalls, it is of primordial importance to continue these experiments.

## **Thesis discussion**

In our literature review, we introduced the potential factors involved in the fusion of COPI vesicles: SNAREs, tethers, Rabs and other proteins that are involved in COPI mediated transport. However, while the function of these proteins are known in general, most of the details concerning the fusion of COPI vesicles remain a mystery. Questions like the identities of the SNAREs involved, the role of the tethers, Rabs or lipids still mostly remained unanswered. Furthermore, the process by which COPI vesicles could suddenly become fusogenic after budding from a non-fusogenic cisterna was of great interest: what was the process that allowed such a drastic change in membrane behavior?

The study of the fusogenic properties of membranes have been greatly helped in the past with the use of *in vitro* biochemical systems that were easy to manipulate and could therefore be used to answer hypotheses rapidly. In vacuoles, in the plasma membrane as well as originally with the Rothman fusion assay within the Golgi apparatus, these assays were used to determine the proteins and lipids involved in the fusion of organelles.

Lately, a strong emphasis has been made on the use of liposomes based assays<sup>for example 214, 297</sup>. These assays have the advantages of limiting the factors that can be inserted into one system, therefore reducing greatly the variables to be studied. Using these assays, information concerning the fusogenic abilities of SNAREs, for example, was obtained. However, emphasis should be directed on the fact that these assays have the risk of being too simplistic and that information obtained from them should be considered as such. This thesis is a good example that factors like lipid composition of the membranes as well as changes in conformation of integral membrane proteins should not be dismissed and are in fact critical. Therefore, simple liposomes assays are limited. Another category of liposomes assays, alike those developed with vacuoles or at the PM by the Wickner or Martin group<sup>145, 253</sup>, account for lipids and cytosolic proteins, which are closer to the environment of the cell. Still, these assays cannot account for all physiological events. Therefore, we sought to upgrade our experimental analysis and opted for purified

organelles. We were able to reproduce *in vitro* the fusion of COPI vesicles with Golgi cisternae.

First, while the literature review demonstrates the potential of ARF1, ARFGAP1, coatomer as well as tethers and potentially SNAREs at having a certain level of flexibility that could theoretically result in the formation of many subtypes of COPI vesicles, our assay only monitors the transfer of one enzyme, GlcNac-T1, in a retrograde direction from the Golgi apparatus to the CGN. Therefore, while it is presumed that we are investigating the fusion properties of all COPI vesicles, our discoveries applies only to this COPI vesicles subtype.

In the thesis, we were able to demonstrate that our assay indeed monitors the fusion of physiologically relevant COPI vesicles. We determined this by two experiments. First, in chapter 1, we demonstrated that fusion of the vesicles could only occur when they were budded in the presence of coatomer. Second, by removing NSF or incubating the vesicles in the presence of  $\alpha$ -SNAP<sup>mut</sup>, we were able to demonstrate that our assay was able to reproduce physiological requirements.

Following the characterization of the assay, we were able to determine, by observing the behavior of the vesicles, that the vesicles ability to fuse was dependent on an intrinsic factor present on their surface. We wondered, like it had been potentially suggested in Rein et al.<sup>301</sup>, if this could be due to a change in conformation of fusion proteins from fusogenic to non-fusogenic. In Rein et al., the Spang group was able to demonstrate that a change of conformation of SNAREs which rendered them PK resistant was dependent on ARFGAP1. As a mimic to their experiments, we used protease treatment to test for changes of conformation of known SNAREs and tethers, and were unsuccessful, at first, to discover a PK resistant protein. Furthermore, the discovery that vesicles that were treated as such were still fusogenic, pointed us to investigate if a lipidic component could be involved. These findings, cumulated by the discovery that protease treated target Golgi was very sensitive to PK treatment and rapidly became unable to support the fusion assay, informed us that something was different between the COPI vesicles and the target Golgi.

Since COPI vesicles are budded from Golgi membranes, the process that renders the vesicles fusogenic has to be linked to the budding process, as Golgi cisternae do not readily fuse by themselves.

ARF1 had been shown to trigger the formation of COPI vesicles and also of PI(4,5)P<sub>2</sub><sup>18, 139, 272</sup>, a lipid involved in the fusion process of other organelles<sup>145, 251</sup>. Therefore, we developed experiments that were able to manipulate PI(4,5)P<sub>2</sub> with great specificity. On COPI vesicles, changes in PI(4,5)P<sub>2</sub> levels resulted in proportional changes in fusogenicity of the vesicles. We were also able to demonstrate that PI(4,5)P<sub>2</sub> requirement is only on the surface of the vesicles.

We next sought to identify the proteins that would associate themselves with PI(4,5)P<sub>2</sub> and mediate the fusion process. Given the fact that PI(4,5)P<sub>2</sub> binding domains can vary quite extensively<sup>240</sup>, we opted for a wide approach and tried to determine if there was a link between PI(4,5)P<sub>2</sub> and the observed ability of vesicles to still fuse after PK treatment. We discovered that PK treatment, not surprisingly, affected the vesicles ability to bind to the target Golgi, but that once they were bound, their fusion proceeded normally. Furthermore, we determined that PK treated vesicles were still sensitive to  $\alpha$ -SNAP<sup>mut</sup> and NSF. This meant that the fusion process still proceeded in a target (Q)-SNARE dependent manner. We also determined that PK treatment abolished the ability of COPI vesicles to bind to  $\alpha$ -SNAP.

Concurrently, Malsam et al.<sup>55</sup> identified Golgin-84 to be involved in the fusogenic process of COPI vesicles. Therefore, we probed PK treated vesicles to determine the status of Golgin-84 and found a PK resistant core. We further demonstrated that this core was only present on the surface of COPI vesicles, that it was absent from Golgi membranes or from COPI vesicles that had been budded with GTP- $\gamma$ -S. We then tested the fusion ability of vesicles which did and vesicles which didn't have this novel confirmation of Golgin-84 and found a correlation between its presence and the fusogenicity of vesicles. However, further investigation of this PK resistant core determined that it is most probably not linked to PI(4,5)P<sub>2</sub> status. Furthermore, while the



core seems to be required for the fusion assay, we determined that it was not sufficient for the fusion process to occur.

## Analysis

One main criticism is that all of the data collected was done in an *in vitro* setting and therefore would be greatly enhanced by the same results being demonstrated *in vivo*. In contrast, one could argue that the experiment performed by Siddhanta et al.<sup>282</sup> where they inhibited the formation of PI(4,5)P<sub>2</sub> inside the Golgi and demonstrated a resulting vesicularization of Golgi membranes within cells is a demonstration of the requirement of PI(4,5)P<sub>2</sub>, *in vivo*. However, our hypothesis implies a role for PI(4,5)P<sub>2</sub> specifically in COPI vesicles, not the Golgi apparatus. We therefore sought to reproduce with IF the movement of COPI vesicles *in vivo* but technical delays made those results impossible to include in the thesis.

Furthermore, one could also pinpoint that protease treatment of vesicles is not a precise investigation tool as it cleaves proteins in a unspecific manner. Detection of a PK resistant core also point outs that there could be other resistant proteins on the surface of the vesicles. It would thus be presumptuous to conclude that Golgin-84 and PI(4,5)P<sub>2</sub> are the only vesicular requirement for COPI mediated fusion.

Another point presented to us was that if vesicles inactivate also *in vivo*, then the peri-Golgi region would become rapidly saturated with unfused COPI vesicles. Therefore, does inactivation occur within the cell or is it an artifact of the *in vitro* assay? We argued that, while our assay reproduce the physiological fusion process, there are differences between an *in vitro* and *in vivo* setting, one of which is that we are unable to reproduce correctly the molecular crowding present in a cell. While the fusion of COPI vesicle in a cell is a very rapid process and the vesicles travels only for distances in nm or  $\mu\text{m}$ , the fusion assay that we monitor *in vitro* is much slower and covers greater distances. We concluded that inactivation of vesicles probably happens *in vivo* too, but that the time frame is log factors faster so that few vesicles actually inactivate. Furthermore, it is also

possible that the micro-environment of the Golgi apparatus is able to rescue the few vesicles which do inactivate.

Lastly, Another issue that could be left to interpretation is the link between the inactivation of vesicles and PI(4,5)P<sub>2</sub>. We were able to demonstrate that addition and removal of PI(4,5)P<sub>2</sub> caused the rescue and the acceleration of the inactivation of vesicles, respectively. However, is the inactivation caused by a loss of PI(4,5)P<sub>2</sub> or is due to another requirement? One could argue that the inactivation of vesicles is the result of the intrinsic 5'phosphatase activity of the Golgi apparatus demonstrated in <sup>282</sup>. However, this inactivation mechanism would most probably not have survived PK treatment. Still it remains a possibility that either part of the 5'phosphatase remained active after PK or that the loss of PI(4,5)P<sub>2</sub> was accomplished by spontaneous dephosphorylation, alike what was seen in our MS samples. Finally, while the Shields group demonstrated the 5'phosphatase activity of the Golgi apparatus, the intrinsic 5'phosphatase activity of COPI vesicles is unknown.

By modifying the level of PI(4,5)P<sub>2</sub>, is it possible that we are compensating the fusion assay rather than an actual rescue of the inactivation? In retrospect, one way to determine this without a doubt would have been to make a dilution series of experiments with the 5'phosphatase and then compared it with a C<sub>v</sub><sup>app</sup> experiment, alike what was done in chapter 6 with PK. This would have told us if the inactivation constant of the vesicles was increased with 5'phosphatase, or if the observed loss of fusion was due to a loss of binding or fusion kinetics. Alternatively, the purified 5'kinase could also be utilized to rescue the inactivation in a dilution experiment.

## **Future outlook**

We demonstrated, in this thesis, a requirement for PI(4,5)P<sub>2</sub>. Such a requirement fits quite well into previously published data and explains quite a few past investigations from the literature. First, Elazar et al. <sup>69</sup> had previously demonstrated that the budding of the vesicles is coupled to their fusion process. Therefore, considering that two cisternae do



not readily fused but that a COPI vesicles is able to fuse with the same cisternae, an event must have occurred during the budding process that suddenly made the membrane fusogenic. Coincidentally, at the PM, PI(4,5)P<sub>2</sub> pool is dependent on the activation of ARF6 and also mediates exocytosis<sup>258</sup>. Similarly, the PI(4,5)P<sub>2</sub> pool at the Golgi apparatus is dependent on ARF1<sup>271, 272</sup>, which is the major enzyme responsible for the budding of the vesicles. Furthermore, the PI(4,5)P<sub>2</sub> pool seems also to be tightly regulated by a still unknown 5'phosphatase and the Golgi seems to possess very little PI(4,5)P<sub>2</sub> at steady state<sup>255, 282</sup>. Therefore, if one pieces this information together, they could possibly explain these results with the following mechanism: ARF1, simultaneously to the formation of the vesicle, promotes the production of PI(4,5)P<sub>2</sub> in the membrane bilayer and renders the vesicles fusogenic. Furthermore PI(4,5)P<sub>2</sub> activates the formation of PA, which helps pinch off the vesicle by creating negative membrane curvature. After uncoating, PI(4,5)P<sub>2</sub> recruits (or has already recruited) an unknown protein from the cytosol which is necessary for fusion to occur. Once fusion has proceeded or during the fusion process, PI(4,5)P<sub>2</sub> is cleaved back to PI(4)P by a 5'phosphatase, possibly INPP5B or OCRL1. In such a system the turnover of vesicles are quite rapid, which keep the overall concentration of PI(4,5)P<sub>2</sub> very low and explains the results seen in Watt et al.<sup>255</sup> Basically, the vesicle is ready to fuse as soon as it is made and is removed once the fusion is accomplish to inhibit the possibility of another round of fusion. This creates a regulated micro-environment, both spatial and temporal, that allows transport to proceed between two cisternae which are otherwise inhibitory to fusion. PI(4,5)P<sub>2</sub> is a marker used to control the extent of this fusion. One can also wonder if such a system could explain the formation of tubular connections within the Golgi apparatus, since technically, the vesicles could start uncoating and fusing before the budding has been completed.

The role of Golgin-84 in the fusion process of COPI vesicles has already been demonstrated<sup>55</sup>. Here, removal of 30 kDa of the n-terminal tail of Golgin-84 results in the loss of 20% of the initial binding constant of COPI vesicles, but does not change the fusion constant of COPI vesicles after the binding process. Furthermore, we successfully demonstrated a change in conformation of Golgin-84 simultaneously to the budding process. Therefore, it seems that once more, vesicles are primed for fusion during the

budding process, so that they are able to fuse as soon as the vesicles are uncoated. This shuffle between inactive and active forms had previously been predicted <sup>55</sup> and could explain why Golgin-84 only promotes the fusion of vesicles after the budding process and not in other occasions. Furthermore, it would seem that these results confirm that the fusogenic properties of Golgin-84, as predicted, are dependent on its coiled-coil domain. However, to be more certain of this, we should perform experiments similar to those in <sup>55</sup> but this time using only fragments of the protein.

A role between Golgin-84 and PI(4,5)P<sub>2</sub> had been previously considered, since the assay that was performed to identify Golgin-84 used OCRL-1, a 5'phosphatase, as bait <sup>1</sup>. However, we were unable to find any links experimentally between the two. It would be interesting to perform the budding of vesicles in an environment that does not allow the formation of PI(4,5)P<sub>2</sub> by depleting the PI(kinases type 1 from the cytosol and determining if it results in changes in the conformation of Golgin-84 on the collected vesicles (or if the vesicles are able to fuse or bud for that matter).

Lastly, recent publications linking the activity of ARF1 and PI(4,5)P<sub>2</sub> to the motility of membranes <sup>288</sup> and the fact that N-WASP and spectrin seems to be linked to PI(4,5)P<sub>2</sub> <sup>282, 287</sup> could point to a dual role of PI(4,5)P<sub>2</sub> within the Golgi apparatus; one for the fusion of the vesicles and one for the attachment of the Golgi apparatus to the cytoskeleton. This results would be in correlation with Watt et al. <sup>255</sup>, which were able to identify two distinct pool of PI(4,5)P<sub>2</sub> within the Golgi apparatus, one colocalized to vesicles and the other to the cisternae. While the role of PI(4,5)P<sub>2</sub> in concert with actin has been shown to inhibit COPI retrograde transport (and COPI-independent) <sup>287</sup>, it would be surprising if our fusion assay still contained an active cytoskeleton, as it was depolymerised during the purification of the Golgi apparatus.

### **List of original Contributions**

1. Developed and tested an in vitro COPI fusion assay using defined components in a cell-free system that is dependent on the presence of COPI coatomer during the budding process and on NSF and  $\alpha$ -SNAP during the fusion process therefore reproducing a physiological event.
2. Demonstrated a requirement for PI(4,5)P<sub>2</sub> for the fusion process.
3. Demonstrated that this requirement is present only on COPI vesicles, not on target Golgi membranes
4. Demonstrated, with protease K treatment of vesicles, that the cell free membrane fusion assay consists of a heterotypic fusion event, as COPI vesicles are partially resistant to protease treatment while the target Golgi membrane is not.
5. Demonstrated, that along with PI(4,5)P<sub>2</sub>, that this heterogeneity is also due to a proteinase K resistant core of Golgin-84 that is present only on fusogenic COPI vesicles generated from parent Golgi membranes with GTP.
6. Demonstrated that, while Golgin-84 protease resistant core is necessary for the fusion process, it is not sufficient to promote the fusion of COPI vesicles.
7. An ARF1/ARFGAP dependent process was defined to prime the vesicles during their formation from parent Golgi membranes.

## References

1. Bascom, R.A., Srinivasan, S. & Nussbaum, R.L. Identification and characterization of golgin-84, a novel Golgi integral membrane protein with a cytoplasmic coiled-coil domain. *J Biol Chem* **274**, 2953-2962 (1999).
2. Boronenkov, I.V., Loijens, J.C., Umeda, M. & Anderson, R.A. Phosphoinositide signaling pathways in nuclei are associated with nuclear speckles containing pre-mRNA processing factors. *Mol Biol Cell* **9**, 3547-3560 (1998).
3. York, J.D., Odom, A.R., Murphy, R., Ives, E.B. & Wente, S.R. A phospholipase C-dependent inositol polyphosphate kinase pathway required for efficient messenger RNA export. *Science* **285**, 96-100 (1999).
4. Doughman, R.L., Firestone, A.J., Wojtasiak, M.L., Bunce, M.W. & Anderson, R.A. Membrane ruffling requires coordination between type I  $\alpha$  phosphatidylinositol phosphate kinase and Rac signaling. *J Biol Chem* **278**, 23036-23045 (2003).
5. Wenk, M.R. *et al.* Phosphoinositide profiling in complex lipid mixtures using electrospray ionization mass spectrometry. *Nat Biotechnol* **21**, 813-817 (2003).
6. Bell, A.W. *et al.* Proteomics characterization of abundant Golgi membrane proteins. *J Biol Chem* **276**, 5152-5165 (2001).
7. Gilchrist, A. *et al.* Quantitative proteomics analysis of the secretory pathway. *Cell* **127**, 1265-1281 (2006).
8. Ostermann, J. Stoichiometry and kinetics of transport vesicle fusion with Golgi membranes. *EMBO Rep* **2**, 324-329 (2001).
9. Laporte, F., Ostermann J, Nillson T, Bergeron JJ in Manuscript(2007).
10. Laporte, F.e.a. in ManuscriptMontreal 2007).
11. Lanoix, J. *et al.* Sorting of Golgi resident proteins into different subpopulations of COPI vesicles: a role for ArfGAP1. *J Cell Biol* **155**, 1199-1212 (2001).
12. Lanoix, J. *et al.* GTP hydrolysis by arf-1 mediates sorting and concentration of Golgi resident enzymes into functional COP I vesicles. *Embo J* **18**, 4935-4948 (1999).
13. Stamnes, M., Schiavo, G., Stenbeck, G., Sollner, T.H. & Rothman, J.E. ADP-ribosylation factor and phosphatidic acid levels in Golgi membranes during budding of coatamer-coated vesicles. *Proc Natl Acad Sci U S A* **95**, 13676-13680 (1998).
14. Pelham, H.R. & Rothman, J.E. The debate about transport in the Golgi--two sides of the same coin? *Cell* **102**, 713-719 (2000).
15. Kessen, U., Schaloske, R., Aichem, A. & Mutzel, R. Ca(2+)/calmodulin-independent activation of calcineurin from Dictyostelium by unsaturated long chain fatty acids. *J Biol Chem* **274**, 37821-37826 (1999).
16. De Matteis, M.A., Di Campli, A. & Godi, A. The role of the phosphoinositides at the Golgi complex. *Biochim Biophys Acta* **1744**, 396-405 (2005).
17. Dominguez, M. *et al.* Fusogenic domains of golgi membranes are sequestered into specialized regions of the stack that can be released by mechanical fragmentation. *J Cell Biol* **145**, 673-688 (1999).
18. Kartberg, F., Elsner, M., Froderberg, L., Asp, L. & Nilsson, T. Commuting between Golgi cisternae--mind the GAP! *Biochim Biophys Acta* **1744**, 351-363 (2005).
19. Patterson, G.H. *et al.* Transport through the Golgi apparatus by rapid partitioning within a two-phase membrane system. *Cell* **133**, 1055-1067 (2008).
20. Jahn, R. & Scheller, R.H. SNAREs--engines for membrane fusion. *Nat Rev Mol Cell Biol* **7**, 631-643 (2006).
21. Volchuk, A. *et al.* Countercurrent distribution of two distinct SNARE complexes mediating transport within the Golgi stack. *Mol Biol Cell* **15**, 1506-1518 (2004).
22. Ladinsky, M.S., Mastronarde, D.N., McIntosh, J.R., Howell, K.E. & Staehelin, L.A. Golgi structure in three dimensions: functional insights from the normal rat kidney cell. *J Cell Biol* **144**, 1135-1149 (1999).

23. Trucco, A. *et al.* Secretory traffic triggers the formation of tubular continuities across Golgi sub-compartments. *Nat Cell Biol* **6**, 1071-1081 (2004).
24. Jamieson, J.D. & Palade, G.E. Role of the Golgi complex in the intracellular transport of secretory proteins. *Proc Natl Acad Sci U S A* **55**, 424-431 (1966).
25. Alberts, B. *Molecular biology of the cell*, Edn. 3rd. (Garland Pub., New York; 1994).
26. Caro, L.G. & Palade, G.E. Protein Synthesis, Storage, and Discharge in the Pancreatic Exocrine Cell. An Autoradiographic Study. *J Cell Biol* **20**, 473-495 (1964).
27. Blobel, G. & Potter, V.R. Studies on free and membrane-bound ribosomes in rat liver. II. Interaction of ribosomes and membranes. *J Mol Biol* **26**, 293-301 (1967).
28. Blobel, G. & Dobberstein, B. Transfer of proteins across membranes. I. Presence of proteolytically processed and unprocessed nascent immunoglobulin light chains on membrane-bound ribosomes of murine myeloma. *J Cell Biol* **67**, 835-851 (1975).
29. Blobel, G. & Dobberstein, B. Transfer of proteins across membranes. II. Reconstitution of functional rough microsomes from heterologous components. *J Cell Biol* **67**, 852-862 (1975).
30. Porter, A.C.M.D., and Ernest F. Fullam A STUDY OF TISSUE CULTURE CELLS BY ELECTRON MICROSCOPY. *The Journal of Experimental Medicine* **81**, 233-246 (1945).
31. Ni, M. & Lee, A.S. ER chaperones in mammalian development and human diseases. *FEBS Lett* **581**, 3641-3651 (2007).
32. Caramelo, J.J. & Parodi, A.J. Getting in and out from calnexin/calreticulin cycles. *J Biol Chem* **283**, 10221-10225 (2008).
33. Malhotra, J.D. & Kaufman, R.J. The endoplasmic reticulum and the unfolded protein response. *Semin Cell Dev Biol* **18**, 716-731 (2007).
34. Barlowe, C. *et al.* COPII: a membrane coat formed by Sec proteins that drive vesicle budding from the endoplasmic reticulum. *Cell* **77**, 895-907 (1994).
35. Tang, B.L., Wang, Y., Ong, Y.S. & Hong, W. COPII and exit from the endoplasmic reticulum. *Biochim Biophys Acta* **1744**, 293-303 (2005).
36. Presley, J.F. *et al.* ER-to-Golgi transport visualized in living cells. *Nature* **389**, 81-85 (1997).
37. De Matteis, M.A. & Luini, A. Exiting the Golgi complex. *Nat Rev Mol Cell Biol* **9**, 273-284 (2008).
38. Hirschberg, C.B. & Snider, M.D. Topography of glycosylation in the rough endoplasmic reticulum and Golgi apparatus. *Annu Rev Biochem* **56**, 63-87 (1987).
39. Ruoslahti, E. Structure and biology of proteoglycans. *Annu Rev Cell Biol* **4**, 229-255 (1988).
40. Kepes, F., Rambourg, A. & Satiat-Jeunemaitre, B. Morphodynamics of the secretory pathway. *Int Rev Cytol* **242**, 55-120 (2005).
41. Rodriguez-Boulan, E. & Musch, A. Protein sorting in the Golgi complex: shifting paradigms. *Biochim Biophys Acta* **1744**, 455-464 (2005).
42. Bard, F. & Malhotra, V. The formation of TGN-to-plasma-membrane transport carriers. *Annu Rev Cell Dev Biol* **22**, 439-455 (2006).
43. Nakayama, K. & Wakatsuki, S. The structure and function of GGAs, the traffic controllers at the TGN sorting crossroads. *Cell Struct Funct* **28**, 431-442 (2003).
44. van Meel, E. & Klumperman, J. Imaging and imagination: understanding the endo-lysosomal system. *Histochem Cell Biol* **129**, 253-266 (2008).
45. Cosson, P. & Letourneur, F. Coatamer interaction with di-lysine endoplasmic reticulum retention motifs. *Science* **263**, 1629-1631 (1994).
46. Letourneur, F. *et al.* Coatamer is essential for retrieval of dilysine-tagged proteins to the endoplasmic reticulum. *Cell* **79**, 1199-1207 (1994).
47. Majoul, I., Straub, M., Hell, S.W., Duden, R. & Soling, H.D. KDEL-cargo regulates interactions between proteins involved in COPI vesicle traffic: measurements in living cells using FRET. *Dev Cell* **1**, 139-153 (2001).
48. Dominguez, M. *et al.* gp25L/emp24/p24 protein family members of the cis-Golgi network bind both COP I and II coatamer. *J Cell Biol* **140**, 751-765 (1998).
49. Bethune, J. *et al.* Coatamer, the coat protein of COPI transport vesicles, discriminates endoplasmic reticulum residents from p24 proteins. *Mol Cell Biol* **26**, 8011-8021 (2006).
50. Nilsson, T., Jackson, M. & Peterson, P.A. Short cytoplasmic sequences serve as retention signals for transmembrane proteins in the endoplasmic reticulum. *Cell* **58**, 707-718 (1989).

51. Hui, N. *et al.* An isoform of the Golgi t-SNARE, syntaxin 5, with an endoplasmic reticulum retrieval signal. *Mol Biol Cell* **8**, 1777-1787 (1997).
52. Townsley, F.M. & Pelham, H.R. The KKXX signal mediates retrieval of membrane proteins from the Golgi to the ER in yeast. *Eur J Cell Biol* **64**, 211-216 (1994).
53. Sohn, K. *et al.* A major transmembrane protein of Golgi-derived COPI-coated vesicles involved in coatamer binding. *J Cell Biol* **135**, 1239-1248 (1996).
54. Pelham, H.R. Evidence that luminal ER proteins are sorted from secreted proteins in a post-ER compartment. *EMBO J* **7**, 913-918 (1988).
55. Malsam, J., Satoh, A., Pelletier, L. & Warren, G. Golgin tethers define subpopulations of COPI vesicles. *Science* **307**, 1095-1098 (2005).
56. Clermont, Y., Rambourg, A. & Hermo, L. Connections between the various elements of the cis- and mid-compartments of the Golgi apparatus of early rat spermatids. *Anat Rec* **240**, 469-480 (1994).
57. Elsner, M., Hashimoto, H. & Nilsson, T. Cisternal maturation and vesicle transport: join the band wagon! (Review). *Mol Membr Biol* **20**, 221-229 (2003).
58. Jamieson, J.D. & Palade, G.E. Intracellular transport of secretory proteins in the pancreatic exocrine cell. 3. Dissociation of intracellular transport from protein synthesis. *J Cell Biol* **39**, 580-588 (1968).
59. Orci, L., Glick, B.S. & Rothman, J.E. A new type of coated vesicular carrier that appears not to contain clathrin: its possible role in protein transport within the Golgi stack. *Cell* **46**, 171-184 (1986).
60. Jamieson, J.D. & Palade, G.E. Intracellular transport of secretory proteins in the pancreatic exocrine cell. I. Role of the peripheral elements of the Golgi complex. *J Cell Biol* **34**, 577-596 (1967).
61. Rabouille, C. *et al.* Mapping the distribution of Golgi enzymes involved in the construction of complex oligosaccharides. *J Cell Sci* **108** ( Pt 4), 1617-1627 (1995).
62. Holthuis, J.C., Pomorski, T., Raggars, R.J., Sprong, H. & Van Meer, G. The organizing potential of sphingolipids in intracellular membrane transport. *Physiol Rev* **81**, 1689-1723 (2001).
63. Roth, J. *et al.* Differential subcompartmentation of terminal glycosylation in the Golgi apparatus of intestinal absorptive and goblet cells. *J Biol Chem* **261**, 14307-14312 (1986).
64. Orci, L. *et al.* Heterogeneous distribution of filipin--cholesterol complexes across the cisternae of the Golgi apparatus. *Proc Natl Acad Sci USA* **78**, 293-297 (1981).
65. Balch, W.E., Dunphy, W.G., Braell, W.A. & Rothman, J.E. Reconstitution of the transport of protein between successive compartments of the Golgi measured by the coupled incorporation of N-acetylglucosamine. *Cell* **39**, 405-416 (1984).
66. Ostermann, J. *et al.* Stepwise assembly of functionally active transport vesicles. *Cell* **75**, 1015-1025 (1993).
67. Rothman, J.E. & Wieland, F.T. Protein sorting by transport vesicles. *Science* **272**, 227-234 (1996).
68. Waters, M.G., Serafini, T. & Rothman, J.E. 'Coatamer': a cytosolic protein complex containing subunits of non-clathrin-coated Golgi transport vesicles. *Nature* **349**, 248-251 (1991).
69. Elazar, Z. *et al.* ADP-ribosylation factor and coatamer couple fusion to vesicle budding. *J Cell Biol* **124**, 415-424 (1994).
70. Brown, R.M., Jr. Observations on the relationship of the golgi apparatus to wall formation in the marine chrysophycean alga *Pleurochrysis scherffellii* Pringsheim. *J Cell Biol* **41**, 109-123 (1969).
71. Marchi, F. & Leblond, C.P. Radioautographic characterization of successive compartments along the rough endoplasmic reticulum-Golgi pathway of collagen precursors in foot pad fibroblasts of [<sup>3</sup>H]proline-injected rats. *J Cell Biol* **98**, 1705-1709 (1984).
72. Bonfanti, L. *et al.* Procollagen traverses the Golgi stack without leaving the lumen of cisternae: evidence for cisternal maturation. *Cell* **95**, 993-1003 (1998).
73. Melkonian, M., Becker, B. & Becker, D. Scale formation in algae. *J Electron Microsc Tech* **17**, 165-178 (1991).
74. Karim, A., Cournil, I. & Leblond, C.P. Immunohistochemical localization of procollagens. II. Electron microscopic distribution of procollagen I antigenicity in the odontoblasts and predentin of rat incisor teeth by a direct method using peroxidase linked antibodies. *J Histochem Cytochem* **27**, 1070-1083 (1979).



75. Love, H.D., Lin, C.C., Short, C.S. & Ostermann, J. Isolation of functional Golgi-derived vesicles with a possible role in retrograde transport. *J Cell Biol* **140**, 541-551 (1998).
76. Lin, C.C., Love, H.D., Gushue, J.N., Bergeron, J.J. & Ostermann, J. ER/Golgi intermediates acquire Golgi enzymes by brefeldin A-sensitive retrograde transport in vitro. *J Cell Biol* **147**, 1457-1472 (1999).
77. Martinez-Menarguez, J.A. *et al.* Peri-Golgi vesicles contain retrograde but not anterograde proteins consistent with the cisternal progression model of intra-Golgi transport. *J Cell Biol* **155**, 1213-1224 (2001).
78. Malsam, J., Gommel, D., Wieland, F.T. & Nickel, W. A role for ADP ribosylation factor in the control of cargo uptake during COPI-coated vesicle biogenesis. *FEBS Lett* **462**, 267-272 (1999).
79. Mironov, A.A. *et al.* Small cargo proteins and large aggregates can traverse the Golgi by a common mechanism without leaving the lumen of cisternae. *J Cell Biol* **155**, 1225-1238 (2001).
80. Zaal, K.J. *et al.* Golgi membranes are absorbed into and reemerge from the ER during mitosis. *Cell* **99**, 589-601 (1999).
81. Altan-Bonnet, N. *et al.* Golgi inheritance in mammalian cells is mediated through endoplasmic reticulum export activities. *Mol Biol Cell* **17**, 990-1005 (2006).
82. Tang, D., Mar, K., Warren, G. & Wang, Y. Molecular mechanism of mitotic Golgi disassembly and reassembly revealed by a defined reconstitution assay. *J Biol Chem* **283**, 6085-6094 (2008).
83. Grasse, P.P. [Ultrastructure, polarity and reproduction of Golgi apparatus.]. *C R Hebd Seances Acad Sci* **245**, 1278-1281 (1957).
84. Glick, B.S., Elston, T. & Oster, G. A cisternal maturation mechanism can explain the asymmetry of the Golgi stack. *FEBS Lett* **414**, 177-181 (1997).
85. Glick, B.S. & Malhotra, V. The curious status of the Golgi apparatus. *Cell* **95**, 883-889 (1998).
86. Pelham, H.R. Getting through the Golgi complex. *Trends Cell Biol* **8**, 45-49 (1998).
87. Allan, B.B. & Balch, W.E. Protein sorting by directed maturation of Golgi compartments. *Science* **285**, 63-66 (1999).
88. Mironov, A.A., Weidman, P. & Luini, A. Variations on the intracellular transport theme: maturing cisternae and trafficking tubules. *J Cell Biol* **138**, 481-484 (1997).
89. Volchuk, A. *et al.* Megavesicles implicated in the rapid transport of intracisternal aggregates across the Golgi stack. *Cell* **102**, 335-348 (2000).
90. Orci, L. *et al.* Bidirectional transport by distinct populations of COPI-coated vesicles. *Cell* **90**, 335-349 (1997).
91. Orci, L., Amherdt, M., Ravazzola, M., Perrelet, A. & Rothman, J.E. Exclusion of golgi residents from transport vesicles budding from Golgi cisternae in intact cells. *J Cell Biol* **150**, 1263-1270 (2000).
92. Martinez-Alonso, E., Egea, G., Ballesta, J. & Martinez-Menarguez, J.A. Structure and dynamics of the Golgi complex at 15 degrees C: low temperature induces the formation of Golgi-derived tubules. *Traffic* **6**, 32-44 (2005).
93. Marsh, B.J., Volkmann, N., McIntosh, J.R. & Howell, K.E. Direct continuities between cisternae at different levels of the Golgi complex in glucose-stimulated mouse islet beta cells. *Proc Natl Acad Sci U S A* **101**, 5565-5570 (2004).
94. Tanaka, K., Mitsushima, A., Fukudome, H. & Kashima, Y. Three-dimensional architecture of the Golgi complex observed by high resolution scanning electron microscopy. *J Submicrosc Cytol* **18**, 1-9 (1986).
95. Tanaka, K. & Fukudome, H. Three-dimensional organization of the Golgi complex observed by scanning electron microscopy. *J Electron Microscop Tech* **17**, 15-23 (1991).
96. Marsh, B.J., Mastronarde, D.N., Buttle, K.F., Howell, K.E. & McIntosh, J.R. Organellar relationships in the Golgi region of the pancreatic beta cell line, HIT-T15, visualized by high resolution electron tomography. *Proc Natl Acad Sci U S A* **98**, 2399-2406 (2001).
97. Mollenhauer, H.H. & Whaley, W.G. An observation on the functioning of the Golgi apparatus. *J Cell Biol* **17**, 222-225 (1963).
98. Mogelsvang, S., Gomez-Ospina, N., Soderholm, J., Glick, B.S. & Staehelin, L.A. Tomographic evidence for continuous turnover of Golgi cisternae in *Pichia pastoris*. *Mol Biol Cell* **14**, 2277-2291 (2003).

99. Thorne-Tjomsland, G., Dumontier, M. & Jamieson, J.C. 3D topography of noncompact zone Golgi tubules in rat spermatids: a computer-assisted serial section reconstruction study. *Anat Rec* **250**, 381-396 (1998).
100. Marsh, B.J. Lessons from tomographic studies of the mammalian Golgi. *Biochim Biophys Acta* **1744**, 273-292 (2005).
101. Girod, A. *et al.* Evidence for a COP-I-independent transport route from the Golgi complex to the endoplasmic reticulum. *Nat Cell Biol* **1**, 423-430 (1999).
102. Storrie, B., Pepperkok, R. & Nilsson, T. Breaking the COPI monopoly on Golgi recycling. *Trends Cell Biol* **10**, 385-391 (2000).
103. Storrie, B. *et al.* Recycling of golgi-resident glycosyltransferases through the ER reveals a novel pathway and provides an explanation for nocodazole-induced Golgi scattering. *J Cell Biol* **143**, 1505-1521 (1998).
104. Lee, S.Y., Yang, J.S., Hong, W., Premont, R.T. & Hsu, V.W. ARFGAP1 plays a central role in coupling COPI cargo sorting with vesicle formation. *J Cell Biol* **168**, 281-290 (2005).
105. Weiss, M. & Nilsson, T. A kinetic proof-reading mechanism for protein sorting. *Traffic* **4**, 65-73 (2003).
106. Pepperkok, R., Whitney, J.A., Gomez, M. & Kreis, T.E. COPI vesicles accumulating in the presence of a GTP restricted arf1 mutant are depleted of anterograde and retrograde cargo. *J Cell Sci* **113 ( Pt 1)**, 135-144 (2000).
107. Nilsson, T., Lucocq, J.M., Mackay, D. & Warren, G. The membrane spanning domain of beta-1,4-galactosyltransferase specifies trans Golgi localization. *EMBO J* **10**, 3567-3575 (1991).
108. Munro, S. Sequences within and adjacent to the transmembrane segment of alpha-2,6-sialyltransferase specify Golgi retention. *EMBO J* **10**, 3577-3588 (1991).
109. Swift, A.M. & Machamer, C.E. A Golgi retention signal in a membrane-spanning domain of coronavirus E1 protein. *J Cell Biol* **115**, 19-30 (1991).
110. Nezil, F.A. & Bloom, M. Combined influence of cholesterol and synthetic amphiphilic peptides upon bilayer thickness in model membranes. *Biophys J* **61**, 1176-1183 (1992).
111. Bretscher, M.S. & Munro, S. Cholesterol and the Golgi apparatus. *Science* **261**, 1280-1281 (1993).
112. Masibay, A.S., Balaji, P.V., Boeggeman, E.E. & Qasba, P.K. Mutational analysis of the Golgi retention signal of bovine beta-1,4-galactosyltransferase. *J Biol Chem* **268**, 9908-9916 (1993).
113. Yuan, Z. & Teasdale, R.D. Prediction of Golgi Type II membrane proteins based on their transmembrane domains. *Bioinformatics* **18**, 1109-1115 (2002).
114. Brugger, B. *et al.* Evidence for segregation of sphingomyelin and cholesterol during formation of COPI-coated vesicles. *J Cell Biol* **151**, 507-518 (2000).
115. Orci, L., Schekman, R. & Perrelet, A. Interleaflet clear space is reduced in the membrane of COP I and COP II-coated buds/vesicles. *Proc Natl Acad Sci U S A* **93**, 8968-8970 (1996).
116. Burke, J., Pettitt, J.M., Schachter, H., Sarkar, M. & Gleeson, P.A. The transmembrane and flanking sequences of beta 1,2-N-acetylglucosaminyltransferase I specify medial-Golgi localization. *J Biol Chem* **267**, 24433-24440 (1992).
117. Graham, T.R. & Krasnov, V.A. Sorting of yeast alpha 1,3 mannosyltransferase is mediated by a luminal domain interaction, and a transmembrane domain signal that can confer clathrin-dependent Golgi localization to a secreted protein. *Mol Biol Cell* **6**, 809-824 (1995).
118. Chen, C., Ma, J., Lazic, A., Backovic, M. & Colley, K.J. Formation of insoluble oligomers correlates with ST6Gal I stable localization in the golgi. *J Biol Chem* **275**, 13819-13826 (2000).
119. Ma, J., Qian, R., Rausa, F.M., 3rd & Colley, K.J. Two naturally occurring alpha2,6-sialyltransferase forms with a single amino acid change in the catalytic domain differ in their catalytic activity and proteolytic processing. *J Biol Chem* **272**, 672-679 (1997).
120. Milland, J., Taylor, S.G., Dodson, H.C., McKenzie, I.F. & Sandrin, M.S. The cytoplasmic tail of alpha 1,2-fucosyltransferase contains a sequence for golgi localization. *J Biol Chem* **276**, 12012-12018 (2001).
121. Nilsson, T., Slusarewicz, P., Hoe, M.H. & Warren, G. Kin recognition. A model for the retention of Golgi enzymes. *FEBS Lett* **330**, 1-4 (1993).
122. Young, W.W., Jr. Organization of Golgi glycosyltransferases in membranes: complexity via complexes. *J Membr Biol* **198**, 1-13 (2004).
123. de Graffenried, C.L. & Bertozzi, C.R. The roles of enzyme localisation and complex formation in glycan assembly within the Golgi apparatus. *Curr Opin Cell Biol* **16**, 356-363 (2004).



124. Weisz, O.A., Swift, A.M. & Machamer, C.E. Oligomerization of a membrane protein correlates with its retention in the Golgi complex. *J Cell Biol* **122**, 1185-1196 (1993).
125. Yamaguchi, N. & Fukuda, M.N. Golgi retention mechanism of beta-1,4-galactosyltransferase. Membrane-spanning domain-dependent homodimerization and association with alpha- and beta-tubulins. *J Biol Chem* **270**, 12170-12176 (1995).
126. Sasai, K. *et al.* The critical role of the stem region as a functional domain responsible for the oligomerization and Golgi localization of N-acetylglucosaminyltransferase V. The involvement of a domain homophilic interaction. *J Biol Chem* **276**, 759-765 (2001).
127. Tu, L., Tai, W.C., Chen, L. & Banfield, D.K. Signal-mediated dynamic retention of glycosyltransferases in the Golgi. *Science* **321**, 404-407 (2008).
128. Wang, Y.J. *et al.* Phosphatidylinositol 4 phosphate regulates targeting of clathrin adaptor AP-1 complexes to the Golgi. *Cell* **114**, 299-310 (2003).
129. Robinson, M.S. Adaptable adaptors for coated vesicles. *Trends Cell Biol* **14**, 167-174 (2004).
130. Cosson, P., Amherdt, M., Rothman, J.E. & Orci, L. A resident Golgi protein is excluded from peri-Golgi vesicles in NRK cells. *Proc Natl Acad Sci U S A* **99**, 12831-12834 (2002).
131. Dahan, S., Ahluwalia, J.P., Wong, L., Posner, B.I. & Bergeron, J.J. Concentration of intracellular hepatic apolipoprotein E in Golgi apparatus saccular distensions and endosomes. *J Cell Biol* **127**, 1859-1869 (1994).
132. Kweon, H.S. *et al.* Golgi enzymes are enriched in perforated zones of golgi cisternae but are depleted in COPI vesicles. *Mol Biol Cell* **15**, 4710-4724 (2004).
133. Rabouille, C. & Klumperman, J. Opinion: The maturing role of COPI vesicles in intra-Golgi transport. *Nat Rev Mol Cell Biol* **6**, 812-817 (2005).
134. Goldberg, J. Decoding of sorting signals by coatomer through a GTPase switch in the COPI coat complex. *Cell* **100**, 671-679 (2000).
135. Wegmann, D., Hess, P., Baier, C., Wieland, F.T. & Reinhard, C. Novel isotypic gamma/zeta subunits reveal three coatomer complexes in mammals. *Mol Cell Biol* **24**, 1070-1080 (2004).
136. Cole, N.B. *et al.* Diffusional mobility of Golgi proteins in membranes of living cells. *Science* **273**, 797-801 (1996).
137. Cole, N.B., Ellenberg, J., Song, J., DiEuliis, D. & Lippincott-Schwartz, J. Retrograde transport of Golgi-localized proteins to the ER. *J Cell Biol* **140**, 1-15 (1998).
138. Wang, C.W., Hamamoto, S., Orci, L. & Schekman, R. Exomer: A coat complex for transport of select membrane proteins from the trans-Golgi network to the plasma membrane in yeast. *J Cell Biol* **174**, 973-983 (2006).
139. Godi, A. *et al.* FAPPs control Golgi-to-cell-surface membrane traffic by binding to ARF and PtdIns(4)P. *Nat Cell Biol* **6**, 393-404 (2004).
140. White, J., Keller, P. & Stelzer, E.H. Spatial partitioning of secretory cargo from Golgi resident proteins in live cells. *BMC Cell Biol* **2**, 19 (2001).
141. Moreau, P. & Cassagne, C. Phospholipid trafficking and membrane biogenesis. *Biochim Biophys Acta* **1197**, 257-290 (1994).
142. van Meer, G. & Sprong, H. Membrane lipids and vesicular traffic. *Curr Opin Cell Biol* **16**, 373-378 (2004).
143. Gkantiragas, I. *et al.* Sphingomyelin-enriched microdomains at the Golgi complex. *Mol Biol Cell* **12**, 1819-1833 (2001).
144. Lundbaek, J.A., Andersen, O.S., Werge, T. & Nielsen, C. Cholesterol-induced protein sorting: an analysis of energetic feasibility. *Biophys J* **84**, 2080-2089 (2003).
145. James, D.J., Khodthong, C., Kowalchyk, J.A. & Martin, T.F. Phosphatidylinositol 4,5-bisphosphate regulates SNARE-dependent membrane fusion. *J Cell Biol* (2008).
146. Haberkant, P. *et al.* Protein-sphingolipid interactions within cellular membranes. *J Lipid Res* **49**, 251-262 (2008).
147. Gong, H., Hocky, G. & Freed, K.F. Influence of nonlinear electrostatics on transfer energies between liquid phases: Charge burial is far less expensive than Born model. *Proc Natl Acad Sci U S A* (2008).
148. Mima, J., Hickey, C.M., Xu, H., Jun, Y. & Wickner, W. Reconstituted membrane fusion requires regulatory lipids, SNAREs and synergistic SNARE chaperones. *EMBO J* (2008).
149. Rohde, H.M. *et al.* The human phosphatidylinositol phosphatase SAC1 interacts with the coatomer I complex. *J Biol Chem* **278**, 52689-52699 (2003).

150. Peretti, D., Dahan, N., Shimoni, E., Hirschberg, K. & Lev, S. Coordinated Lipid Transfer between the Endoplasmic Reticulum and the Golgi Complex Requires the VAP Proteins and Is Essential for Golgi-mediated Transport. *Mol Biol Cell* (2008).
151. Fries, E. & Rothman, J.E. Transport of vesicular stomatitis virus glycoprotein in a cell-free extract. *Proc Natl Acad Sci U S A* **77**, 3870-3874 (1980).
152. Duden, R., Griffiths, G., Frank, R., Argos, P. & Kreis, T.E. Beta-COP, a 110 kd protein associated with non-clathrin-coated vesicles and the Golgi complex, shows homology to beta-adaptin. *Cell* **64**, 649-665 (1991).
153. Chun, J., Shapovalova, Z., Dejgaard, S.Y., Presley, J.F. & Melancon, P. Characterization of Class I and II ADP-Ribosylation Factors (Arfs) in Live Cells: GDP-bound Class II Arfs Associate with the ER-Golgi Intermediate Compartment Independently of GBF1. *Mol Biol Cell* **19**, 3488-3500 (2008).
154. Teal, S.B., Hsu, V.W., Peters, P.J., Klausner, R.D. & Donaldson, J.G. An activating mutation in ARF1 stabilizes coatamer binding to Golgi membranes. *J Biol Chem* **269**, 3135-3138 (1994).
155. Donaldson, J.G., Cassel, D., Kahn, R.A. & Klausner, R.D. ADP-ribosylation factor, a small GTP-binding protein, is required for binding of the coatamer protein beta-COP to Golgi membranes. *Proc Natl Acad Sci U S A* **89**, 6408-6412 (1992).
156. Palmer, D.J., Helms, J.B., Beckers, C.J., Orci, L. & Rothman, J.E. Binding of coatamer to Golgi membranes requires ADP-ribosylation factor. *J Biol Chem* **268**, 12083-12089 (1993).
157. Beck, R. *et al.* Membrane curvature induced by Arf1-GTP is essential for vesicle formation. *Proc Natl Acad Sci U S A* **105**, 11731-11736 (2008).
158. Krauss, M. *et al.* Arf1-GTP-induced tubule formation suggests a function of Arf family proteins in curvature acquisition at sites of vesicle budding. *J Biol Chem* (2008).
159. Elsner, M. *et al.* Spatiotemporal dynamics of the COPI vesicle machinery. *EMBO Rep* **4**, 1000-1004 (2003).
160. Presley, J.F. *et al.* Dissection of COPI and Arf1 dynamics in vivo and role in Golgi membrane transport. *Nature* **417**, 187-193 (2002).
161. Cosson, P., Lefkir, Y., Demolliere, C. & Letourneur, F. New COP1-binding motifs involved in ER retrieval. *EMBO J* **17**, 6863-6870 (1998).
162. Watson, P.J., Frigerio, G., Collins, B.M., Duden, R. & Owen, D.J. Gamma-COP appendage domain - structure and function. *Traffic* **5**, 79-88 (2004).
163. Sciaky, N. *et al.* Golgi tubule traffic and the effects of brefeldin A visualized in living cells. *J Cell Biol* **139**, 1137-1155 (1997).
164. Niu, T.K., Pfeifer, A.C., Lippincott-Schwartz, J. & Jackson, C.L. Dynamics of GBF1, a Brefeldin A-sensitive Arf1 exchange factor at the Golgi. *Mol Biol Cell* **16**, 1213-1222 (2005).
165. Garcia-Mata, R. & Sztul, E. The membrane-tethering protein p115 interacts with GBF1, an ARF guanine-nucleotide-exchange factor. *EMBO Rep* **4**, 320-325 (2003).
166. Zhao, X., Lasell, T.K. & Melancon, P. Localization of large ADP-ribosylation factor-guanine nucleotide exchange factors to different Golgi compartments: evidence for distinct functions in protein traffic. *Mol Biol Cell* **13**, 119-133 (2002).
167. Kawamoto, K. *et al.* GBF1, a guanine nucleotide exchange factor for ADP-ribosylation factors, is localized to the cis-Golgi and involved in membrane association of the COPI coat. *Traffic* **3**, 483-495 (2002).
168. Zhao, X. *et al.* GBF1, a cis-Golgi and VTCs-localized ARF-GEF, is implicated in ER-to-Golgi protein traffic. *J Cell Sci* **119**, 3743-3753 (2006).
169. Szul, T. *et al.* Dissecting the role of the ARF guanine nucleotide exchange factor GBF1 in Golgi biogenesis and protein trafficking. *J Cell Sci* **120**, 3929-3940 (2007).
170. Manolea, F., Claude, A., Chun, J., Rosas, J. & Melancon, P. Distinct Functions for Arf Guanine Nucleotide Exchange Factors at the Golgi Complex: GBF1 and BIGs Are Required for Assembly and Maintenance of the Golgi Stack and trans-Golgi Network, Respectively. *Mol Biol Cell* **19**, 523-535 (2008).
171. Lefrancois, S. & McCormick, P.J. The Arf GEF GBF1 is required for GGA recruitment to Golgi membranes. *Traffic* **8**, 1440-1451 (2007).
172. Richter, S. *et al.* Functional diversification of closely related ARF-GEFs in protein secretion and recycling. *Nature* **448**, 488-492 (2007).

173. Chantalat, S. *et al.* A novel Golgi membrane protein is a partner of the ARF exchange factors Gea1p and Gea2p. *Mol Biol Cell* **14**, 2357-2371 (2003).
174. Liu, W., Duden, R., Phair, R.D. & Lippincott-Schwartz, J. ArfGAP1 dynamics and its role in COPI coat assembly on Golgi membranes of living cells. *J Cell Biol* **168**, 1053-1063 (2005).
175. Cukierman, E., Huber, I., Rotman, M. & Cassel, D. The ARF1 GTPase-activating protein: zinc finger motif and Golgi complex localization. *Science* **270**, 1999-2002 (1995).
176. Aoe, T. *et al.* The KDEL receptor, ERD2, regulates intracellular traffic by recruiting a GTPase-activating protein for ARF1. *EMBO J* **16**, 7305-7316 (1997).
177. Spang, A. ARF1 regulatory factors and COPI vesicle formation. *Curr Opin Cell Biol* **14**, 423-427 (2002).
178. Tanigawa, G. *et al.* Hydrolysis of bound GTP by ARF protein triggers uncoating of Golgi-derived COP-coated vesicles. *J Cell Biol* **123**, 1365-1371 (1993).
179. Reinhard, C., Schweikert, M., Wieland, F.T. & Nickel, W. Functional reconstitution of COPI coat assembly and disassembly using chemically defined components. *Proc Natl Acad Sci U S A* **100**, 8253-8257 (2003).
180. Yang, J.S. *et al.* A role for BARS at the fission step of COPI vesicle formation from Golgi membrane. *EMBO J* **24**, 4133-4143 (2005).
181. Yang, J.S. *et al.* ARFGAP1 promotes the formation of COPI vesicles, suggesting function as a component of the coat. *J Cell Biol* **159**, 69-78 (2002).
182. Goldberg, J. Structural and functional analysis of the ARF1-ARFGAP complex reveals a role for coatamer in GTP hydrolysis. *Cell* **96**, 893-902 (1999).
183. Bigay, J., Gounon, P., Robineau, S. & Antonny, B. Lipid packing sensed by ArfGAP1 couples COPI coat disassembly to membrane bilayer curvature. *Nature* **426**, 563-566 (2003).
184. Bigay, J., Casella, J.F., Drin, G., Mesmin, B. & Antonny, B. ArfGAP1 responds to membrane curvature through the folding of a lipid packing sensor motif. *EMBO J* **24**, 2244-2253 (2005).
185. Levi, S., Rawet, M., Kliouchnikov, L., Parnis, A. & Cassel, D. Topology of amphipathic motifs mediating Golgi localization in ArfGAP1 and its splice isoforms. *J Biol Chem* **283**, 8564-8572 (2008).
186. Antonny, B. *et al.* Membrane curvature and the control of GTP hydrolysis in Arf1 during COPI vesicle formation. *Biochem Soc Trans* **33**, 619-622 (2005).
187. Shemesh, T., Luini, A., Malhotra, V., Burger, K.N. & Kozlov, M.M. Prefission constriction of Golgi tubular carriers driven by local lipid metabolism: a theoretical model. *Biophys J* **85**, 3813-3827 (2003).
188. Cockcroft, S. *et al.* Phospholipase D: a downstream effector of ARF in granulocytes. *Science* **263**, 523-526 (1994).
189. Brown, H.A., Gutowski, S., Kahn, R.A. & Sternweis, P.C. Partial purification and characterization of Arf-sensitive phospholipase D from porcine brain. *J Biol Chem* **270**, 14935-14943 (1995).
190. Lennart Asp, F.K., Tommy Nilsson *et al.* in submitted (2008).
191. Gallop, J.L., Butler, P.J. & McMahon, H.T. Endophilin and CtBP/BARS are not acyl transferases in endocytosis or Golgi fission. *Nature* **438**, 675-678 (2005).
192. Fernandez-Ulibarri, I. *et al.* Diacylglycerol is required for the formation of COPI vesicles in the Golgi-to-ER transport pathway. *Mol Biol Cell* **18**, 3250-3263 (2007).
193. Bonazzi, M. *et al.* CtBP3/BARS drives membrane fission in dynamin-independent transport pathways. *Nat Cell Biol* **7**, 570-580 (2005).
194. Frigerio, G., Grimsey, N., Dale, M., Majoul, I. & Duden, R. Two human ARFGAPs associated with COP-I-coated vesicles. *Traffic* **8**, 1644-1655 (2007).
195. Sollner, T. *et al.* SNAP receptors implicated in vesicle targeting and fusion. *Nature* **362**, 318-324 (1993).
196. Paumet, F., Rahimian, V. & Rothman, J.E. The specificity of SNARE-dependent fusion is encoded in the SNARE motif. *Proc Natl Acad Sci U S A* **101**, 3376-3380 (2004).
197. Katz, L. & Brennwald, P. Testing the 3Q:1R "rule": mutational analysis of the ionic "zero" layer in the yeast exocytic SNARE complex reveals no requirement for arginine. *Mol Biol Cell* **11**, 3849-3858 (2000).
198. Ossig, R. *et al.* Exocytosis requires asymmetry in the central layer of the SNARE complex. *EMBO J* **19**, 6000-6010 (2000).
199. Weber, T. *et al.* SNAREpins: minimal machinery for membrane fusion. *Cell* **92**, 759-772 (1998).

200. Jahn, R. & Sudhof, T.C. Membrane fusion and exocytosis. *Annu Rev Biochem* **68**, 863-911 (1999).
201. McNew, J.A. *et al.* Close is not enough: SNARE-dependent membrane fusion requires an active mechanism that transduces force to membrane anchors. *J Cell Biol* **150**, 105-117 (2000).
202. Mayer, A., Wickner, W. & Haas, A. Sec18p (NSF)-driven release of Sec17p (alpha-SNAP) can precede docking and fusion of yeast vacuoles. *Cell* **85**, 83-94 (1996).
203. Barnard, R.J., Morgan, A. & Burgoyne, R.D. Stimulation of NSF ATPase activity by alpha-SNAP is required for SNARE complex disassembly and exocytosis. *J Cell Biol* **139**, 875-883 (1997).
204. Hanson, P.I., Roth, R., Morisaki, H., Jahn, R. & Heuser, J.E. Structure and conformational changes in NSF and its membrane receptor complexes visualized by quick-freeze/deep-etch electron microscopy. *Cell* **90**, 523-535 (1997).
205. Lenzen, C.U., Steinmann, D., Whiteheart, S.W. & Weis, W.I. Crystal structure of the hexamerization domain of N-ethylmaleimide-sensitive fusion protein. *Cell* **94**, 525-536 (1998).
206. Yu, R.C., Hanson, P.I., Jahn, R. & Brunger, A.T. Structure of the ATP-dependent oligomerization domain of N-ethylmaleimide sensitive factor complexed with ATP. *Nat Struct Biol* **5**, 803-811 (1998).
207. Peters, C. *et al.* Trans-complex formation by proteolipid channels in the terminal phase of membrane fusion. *Nature* **409**, 581-588 (2001).
208. Peters, C. *et al.* Control of the terminal step of intracellular membrane fusion by protein phosphatase 1. *Science* **285**, 1084-1087 (1999).
209. McNew, J.A. *et al.* Compartmental specificity of cellular membrane fusion encoded in SNARE proteins. *Nature* **407**, 153-159 (2000).
210. Calakos, N., Bennett, M.K., Peterson, K.E. & Scheller, R.H. Protein-protein interactions contributing to the specificity of intracellular vesicular trafficking. *Science* **263**, 1146-1149 (1994).
211. Tsui, M.M. & Banfield, D.K. Yeast Golgi SNARE interactions are promiscuous. *J Cell Sci* **113** ( Pt 1), 145-152 (2000).
212. Fasshauer, D., Antonin, W., Margittai, M., Pabst, S. & Jahn, R. Mixed and non-cognate SNARE complexes. Characterization of assembly and biophysical properties. *J Biol Chem* **274**, 15440-15446 (1999).
213. Brandhorst, D. *et al.* Homotypic fusion of early endosomes: SNAREs do not determine fusion specificity. *Proc Natl Acad Sci U S A* **103**, 2701-2706 (2006).
214. Varlamov, O. *et al.* i-SNAREs: inhibitory SNAREs that fine-tune the specificity of membrane fusion. *J Cell Biol* **164**, 79-88 (2004).
215. Giraudo, C.G. *et al.* SNAREs can promote complete fusion and hemifusion as alternative outcomes. *The Journal of cell biology* **170**, 249-260 (2005).
216. Shen, J., Tareste, D.C., Paumet, F., Rothman, J.E. & Melia, T.J. Selective activation of cognate SNAREpins by Sec1/Munc18 proteins. *Cell* **128**, 183-195 (2007).
217. Tareste, D., Shen, J., Melia, T.J. & Rothman, J.E. SNAREpin/Munc18 promotes adhesion and fusion of large vesicles to giant membranes. *Proc Natl Acad Sci U S A* **105**, 2380-2385 (2008).
218. Bhalla, A., Chicka, M.C., Tucker, W.C. & Chapman, E.R. Ca(2+)-synaptotagmin directly regulates t-SNARE function during reconstituted membrane fusion. *Nat Struct Mol Biol* **13**, 323-330 (2006).
219. Cosson, P. *et al.* Dynamic transport of SNARE proteins in the Golgi apparatus. *Proc Natl Acad Sci U S A* **102**, 14647-14652 (2005).
220. Hay, J.C. SNARE complex structure and function. *Exp Cell Res* **271**, 10-21 (2001).
221. Broadie, K. *et al.* Syntaxin and synaptobrevin function downstream of vesicle docking in *Drosophila*. *Neuron* **15**, 663-673 (1995).
222. Hunt, J.M. *et al.* A post-docking role for synaptobrevin in synaptic vesicle fusion. *Neuron* **12**, 1269-1279 (1994).
223. Cai, H., Reinisch, K. & Ferro-Novick, S. Coats, tethers, Rabs, and SNAREs work together to mediate the intracellular destination of a transport vesicle. *Dev Cell* **12**, 671-682 (2007).
224. Zolov, S.N. & Lupashin, V.V. Cog3p depletion blocks vesicle-mediated Golgi retrograde trafficking in HeLa cells. *J Cell Biol* **168**, 747-759 (2005).
225. Suvorova, E.S., Duden, R. & Lupashin, V.V. The Sec34/Sec35p complex, a Ypt1p effector required for retrograde intra-Golgi trafficking, interacts with Golgi SNAREs and COPI vesicle coat proteins. *J Cell Biol* **157**, 631-643 (2002).



226. Sacher, M. *et al.* TRAPP, a highly conserved novel complex on the cis-Golgi that mediates vesicle docking and fusion. *EMBO J* **17**, 2494-2503 (1998).
227. Andag, U., Neumann, T. & Schmitt, H.D. The coatomer-interacting protein Dsl1p is required for Golgi-to-endoplasmic reticulum retrieval in yeast. *J Biol Chem* **276**, 39150-39160 (2001).
228. Andag, U. & Schmitt, H.D. Dsl1p, an essential component of the Golgi-endoplasmic reticulum retrieval system in yeast, uses the same sequence motif to interact with different subunits of the COPI vesicle coat. *J Biol Chem* **278**, 51722-51734 (2003).
229. Cai, H., Zhang, Y., Pypaert, M., Walker, L. & Ferro-Novick, S. Mutants in trs120 disrupt traffic from the early endosome to the late Golgi. *J Cell Biol* **171**, 823-833 (2005).
230. Sonnichsen, B. *et al.* A role for giantin in docking COPI vesicles to Golgi membranes. *J Cell Biol* **140**, 1013-1021 (1998).
231. Lesa, G.M., Seemann, J., Shorter, J., Vandekerckhove, J. & Warren, G. The amino-terminal domain of the golgi protein giantin interacts directly with the vesicle-tethering protein p115. *J Biol Chem* **275**, 2831-2836 (2000).
232. Shorter, J., Beard, M.B., Seemann, J., Dirac-Svejstrup, A.B. & Warren, G. Sequential tethering of Golgins and catalysis of SNAREpin assembly by the vesicle-tethering protein p115. *J Cell Biol* **157**, 45-62 (2002).
233. Kamena, F., Diefenbacher, M., Kilchert, C., Schwarz, H. & Spang, A. Ypt1p is essential for retrograde Golgi-ER transport and for Golgi maintenance in *S. cerevisiae*. *J Cell Sci* **121**, 1293-1302 (2008).
234. Alvarez, C., Garcia-Mata, R., Brandon, E. & Sztul, E. COPI recruitment is modulated by a Rab1b-dependent mechanism. *Mol Biol Cell* **14**, 2116-2127 (2003).
235. Satoh, A., Wang, Y., Malsam, J., Beard, M.B. & Warren, G. Golgin-84 is a rab1 binding partner involved in Golgi structure. *Traffic* **4**, 153-161 (2003).
236. Wang, W., Sacher, M. & Ferro-Novick, S. TRAPP stimulates guanine nucleotide exchange on Ypt1p. *J Cell Biol* **151**, 289-296 (2000).
237. Allan, B.B., Moyer, B.D. & Balch, W.E. Rab1 recruitment of p115 into a cis-SNARE complex: programming budding COPII vesicles for fusion. *Science* **289**, 444-448 (2000).
238. Moyer, B.D., Allan, B.B. & Balch, W.E. Rab1 interaction with a GM130 effector complex regulates COPII vesicle cis--Golgi tethering. *Traffic* **2**, 268-276 (2001).
239. Cai, H. *et al.* TRAPP1 tethers COPII vesicles by binding the coat subunit Sec23. *Nature* **445**, 941-944 (2007).
240. McLaughlin, S., Wang, J., Gambhir, A. & Murray, D. PIP(2) and proteins: interactions, organization, and information flow. *Annu Rev Biophys Biomol Struct* **31**, 151-175 (2002).
241. Corvera, S. Phosphatidylinositol 3-kinase and the control of endosome dynamics: new players defined by structural motifs. *Traffic* **2**, 859-866 (2001).
242. Frigerio, L., Hinz, G. & Robinson, D.G. Multiple Vacuoles in Plant Cells: Rule or Exception? *Traffic* (2008).
243. Conradt, B., Shaw, J., Vida, T., Emr, S. & Wickner, W. In vitro reactions of vacuole inheritance in *Saccharomyces cerevisiae*. *J Cell Biol* **119**, 1469-1479 (1992).
244. Wiemken, A., Matile, P. & Moor, H. Vacuolar dynamics in synchronously budding yeast. *Arch Mikrobiol* **70**, 89-103 (1970).
245. Weisman, L.S. & Wickner, W. Intervacuole exchange in the yeast zygote: a new pathway in organelle communication. *Science* **241**, 589-591 (1988).
246. Conradt, B., Haas, A. & Wickner, W. Determination of four biochemically distinct, sequential stages during vacuole inheritance in vitro. *J Cell Biol* **126**, 99-110 (1994).
247. Ungermann, C., Sato, K. & Wickner, W. Defining the functions of trans-SNARE pairs. *Nature* **396**, 543-548 (1998).
248. Mayer, A. *et al.* Phosphatidylinositol 4,5-bisphosphate regulates two steps of homotypic vacuole fusion. *Mol Biol Cell* **11**, 807-817 (2000).
249. Sollner, T., Bennett, M.K., Whiteheart, S.W., Scheller, R.H. & Rothman, J.E. A protein assembly-disassembly pathway in vitro that may correspond to sequential steps of synaptic vesicle docking, activation, and fusion. *Cell* **75**, 409-418 (1993).
250. Stroupe, C., Collins, K.M., Fratti, R.A. & Wickner, W. Purification of active HOPS complex reveals its affinities for phosphoinositides and the SNARE Vam7p. *EMBO J* **25**, 1579-1589 (2006).

251. Starai, V.J., Hickey, C.M. & Wickner, W. HOPS Proofreads the trans-SNARE Complex for Yeast Vacuole Fusion. *Mol Biol Cell* **19**, 2500-2508 (2008).
252. Collins, K.M., Thorngren, N.L., Fratti, R.A. & Wickner, W.T. Sec17p and HOPS, in distinct SNARE complexes, mediate SNARE complex disruption or assembly for fusion. *EMBO J* **24**, 1775-1786 (2005).
253. Collins, K.M. & Wickner, W.T. Trans-SNARE complex assembly and yeast vacuole membrane fusion. *Proc Natl Acad Sci U S A* **104**, 8755-8760 (2007).
254. Wiradjaja, F. *et al.* Inactivation of the phosphoinositide phosphatases Sac1p and Inp54p leads to accumulation of phosphatidylinositol 4,5-bisphosphate on vacuole membranes and vacuolar fusion defects. *J Biol Chem* **282**, 16295-16307 (2007).
255. Watt, S.A., Kular, G., Fleming, I.N., Downes, C.P. & Lucocq, J.M. Subcellular localization of phosphatidylinositol 4,5-bisphosphate using the pleckstrin homology domain of phospholipase C delta1. *Biochem J* **363**, 657-666 (2002).
256. Aikawa, Y. & Martin, T.F. ARF6 regulates a plasma membrane pool of phosphatidylinositol(4,5)bisphosphate required for regulated exocytosis. *J Cell Biol* **162**, 647-659 (2003).
257. Gong, L.W. *et al.* Phosphatidylinositol phosphate kinase type I gamma regulates dynamics of large dense-core vesicle fusion. *Proc Natl Acad Sci U S A* **102**, 5204-5209 (2005).
258. Brown, F.D., Rozelle, A.L., Yin, H.L., Balla, T. & Donaldson, J.G. Phosphatidylinositol 4,5-bisphosphate and Arf6-regulated membrane traffic. *J Cell Biol* **154**, 1007-1017 (2001).
259. Wenk, M.R. *et al.* PIP kinase Igamma is the major PI(4,5)P(2) synthesizing enzyme at the synapse. *Neuron* **32**, 79-88 (2001).
260. Cremona, O. & De Camilli, P. Phosphoinositides in membrane traffic at the synapse. *J Cell Sci* **114**, 1041-1052 (2001).
261. Di Paolo, G. *et al.* Impaired PtdIns(4,5)P2 synthesis in nerve terminals produces defects in synaptic vesicle trafficking. *Nature* **431**, 415-422 (2004).
262. Grishanin, R.N. *et al.* CAPS acts at a prefusion step in dense-core vesicle exocytosis as a PIP2 binding protein. *Neuron* **43**, 551-562 (2004).
263. Loyet, K.M. *et al.* Specific binding of phosphatidylinositol 4,5-bisphosphate to calcium-dependent activator protein for secretion (CAPS), a potential phosphoinositide effector protein for regulated exocytosis. *J Biol Chem* **273**, 8337-8343 (1998).
264. Ungewickell, E.J. & Hinrichsen, L. Endocytosis: clathrin-mediated membrane budding. *Curr Opin Cell Biol* **19**, 417-425 (2007).
265. Waselle, L. *et al.* Role of phosphoinositide signaling in the control of insulin exocytosis. *Mol Endocrinol* **19**, 3097-3106 (2005).
266. Sadakata, T. *et al.* The secretory granule-associated protein CAPS2 regulates neurotrophin release and cell survival. *J Neurosci* **24**, 43-52 (2004).
267. Murthy, V.N. & De Camilli, P. Cell biology of the presynaptic terminal. *Annu Rev Neurosci* **26**, 701-728 (2003).
268. Stojilkovic, S.S. Ca<sup>2+</sup>-regulated exocytosis and SNARE function. *Trends Endocrinol Metab* **16**, 81-83 (2005).
269. Wenk, M.R. & De Camilli, P. Protein-lipid interactions and phosphoinositide metabolism in membrane traffic: insights from vesicle recycling in nerve terminals. *Proc Natl Acad Sci U S A* **101**, 8262-8269 (2004).
270. Chernomordik, L., Chanturiya, A., Green, J. & Zimmerberg, J. The hemifusion intermediate and its conversion to complete fusion: regulation by membrane composition. *Biophys J* **69**, 922-929 (1995).
271. Godi, A. *et al.* ARF mediates recruitment of PtdIns-4-OH kinase-beta and stimulates synthesis of PtdIns(4,5)P2 on the Golgi complex. *Nat Cell Biol* **1**, 280-287 (1999).
272. Jones, D.H. *et al.* Type I phosphatidylinositol 4-phosphate 5-kinase directly interacts with ADP-ribosylation factor 1 and is responsible for phosphatidylinositol 4,5-bisphosphate synthesis in the golgi compartment. *J Biol Chem* **275**, 13962-13966 (2000).
273. Skippen, A., Jones, D.H., Morgan, C.P., Li, M. & Cockcroft, S. Mechanism of ADP ribosylation factor-stimulated phosphatidylinositol 4,5-bisphosphate synthesis in HL60 cells. *J Biol Chem* **277**, 5823-5831 (2002).

274. Honda, A. *et al.* Phosphatidylinositol 4-phosphate 5-kinase alpha is a downstream effector of the small G protein ARF6 in membrane ruffle formation. *Cell* **99**, 521-532 (1999).
275. Haynes, L.P., Thomas, G.M. & Burgoyne, R.D. Interaction of neuronal calcium sensor-1 and ADP-ribosylation factor 1 allows bidirectional control of phosphatidylinositol 4-kinase beta and trans-Golgi network-plasma membrane traffic. *J Biol Chem* **280**, 6047-6054 (2005).
276. Houle, M.G., Kahn, R.A., Naccache, P.H. & Bourgoin, S. ADP-ribosylation factor translocation correlates with potentiation of GTP gamma S-stimulated phospholipase D activity in membrane fractions of HL-60 cells. *J Biol Chem* **270**, 22795-22800 (1995).
277. Ktistakis, N.T., Brown, H.A., Waters, M.G., Sternweis, P.C. & Roth, M.G. Evidence that phospholipase D mediates ADP ribosylation factor-dependent formation of Golgi coated vesicles. *J Cell Biol* **134**, 295-306 (1996).
278. Jenkins, G.H., Fiset, P.L. & Anderson, R.A. Type I phosphatidylinositol 4-phosphate 5-kinase isoforms are specifically stimulated by phosphatidic acid. *J Biol Chem* **269**, 11547-11554 (1994).
279. Ktistakis, N.T., Brown, H.A., Sternweis, P.C. & Roth, M.G. Phospholipase D is present on Golgi-enriched membranes and its activation by ADP ribosylation factor is sensitive to brefeldin A. *Proc Natl Acad Sci U S A* **92**, 4952-4956 (1995).
280. Moritz, A., De Graan, P.N., Gispén, W.H. & Wirtz, K.W. Phosphatidic acid is a specific activator of phosphatidylinositol-4-phosphate kinase. *J Biol Chem* **267**, 7207-7210 (1992).
281. Liscovitch, M., Chalifa, V., Pertile, P., Chen, C.S. & Cantley, L.C. Novel function of phosphatidylinositol 4,5-bisphosphate as a cofactor for brain membrane phospholipase D. *J Biol Chem* **269**, 21403-21406 (1994).
282. Siddhanta, A., Radulescu, A., Stankewich, M.C., Morrow, J.S. & Shields, D. Fragmentation of the Golgi apparatus. A role for beta III spectrin and synthesis of phosphatidylinositol 4,5-bisphosphate. *J Biol Chem* **278**, 1957-1965 (2003).
283. Williams, C., Choudhury, R., McKenzie, E. & Lowe, M. Targeting of the type II inositol polyphosphate 5-phosphatase INPP5B to the early secretory pathway. *J Cell Sci* **120**, 3941-3951 (2007).
284. Janne, P.A. *et al.* Functional overlap between murine Inpp5b and Ocr1l may explain why deficiency of the murine ortholog for OCRL1 does not cause Lowe syndrome in mice. *J Clin Invest* **101**, 2042-2053 (1998).
285. Dressman, M.A., Olivos-Glander, I.M., Nussbaum, R.L. & Suchy, S.F. Ocr1l, a PtdIns(4,5)P(2) 5-phosphatase, is localized to the trans-Golgi network of fibroblasts and epithelial cells. *J Histochem Cytochem* **48**, 179-190 (2000).
286. Sweeney, D.A., Siddhanta, A. & Shields, D. Fragmentation and re-assembly of the Golgi apparatus in vitro. A requirement for phosphatidic acid and phosphatidylinositol 4,5-bisphosphate synthesis. *J Biol Chem* **277**, 3030-3039 (2002).
287. Luna, A. *et al.* Regulation of protein transport from the Golgi complex to the endoplasmic reticulum by CDC42 and N-WASP. *Mol Biol Cell* **13**, 866-879 (2002).
288. Heuveling, J., Franco, M., Chavrier, P. & Sykes, C. ARF1-mediated actin polymerization produces movement of artificial vesicles. *Proc Natl Acad Sci U S A* **104**, 16928-16933 (2007).
289. Rozelle, A.L. *et al.* Phosphatidylinositol 4,5-bisphosphate induces actin-based movement of raft-enriched vesicles through WASP-Arp2/3. *Curr Biol* **10**, 311-320 (2000).
290. Orci, L., Palmer, D.J., Amherdt, M. & Rothman, J.E. Coated vesicle assembly in the Golgi requires only coatamer and ARF proteins from the cytosol. *Nature* **364**, 732-734 (1993).
291. Fredrik Karlberg, J.H., Tommy Nilsson *Purification of COPI vesicles*. (Elsevier Academic Press, 2006).
292. Stanley, P., Caillibot, V. & Siminovich, L. Selection and characterization of eight phenotypically distinct lines of lectin-resistant Chinese hamster ovary cell. *Cell* **6**, 121-128 (1975).
293. Braell, W.A., Balch, W.E., Dobberty, D.C. & Rothman, J.E. The glycoprotein that is transported between successive compartments of the Golgi in a cell-free system resides in stacks of cisternae. *Cell* **39**, 511-524 (1984).
294. Otter-Nilsson, M., Hendriks, R., Pecheur-Huet, E.I., Hoekstra, D. & Nilsson, T. Cytosolic ATPases, p97 and NSF, are sufficient to mediate rapid membrane fusion. *Embo J* **18**, 2074-2083 (1999).
295. Rothman, J.E. & Warren, G. Implications of the SNARE hypothesis for intracellular membrane topology and dynamics. *Curr Biol* **4**, 220-233 (1994).

296. Hong, W. SNAREs and traffic. *Biochim Biophys Acta* **1744**, 493-517 (2005).
297. Burri, L. *et al.* A SNARE required for retrograde transport to the endoplasmic reticulum. *Proc Natl Acad Sci U S A* **100**, 9873-9877 (2003).
298. Gillingham, A.K. & Munro, S. Long coiled-coil proteins and membrane traffic. *Biochim Biophys Acta* **1641**, 71-85 (2003).
299. Speese, S. *et al.* UNC-31 (CAPS) is required for dense-core vesicle but not synaptic vesicle exocytosis in *Caenorhabditis elegans*. *J Neurosci* **27**, 6150-6162 (2007).
300. Fredrik Kartberg\*, L.A., Maria Smedh, Julia Fernandez-Rodriguez, Markus & Elsner, F.L., Rainer Duden2, John Bergeron1, Tommy Nilsson in Manuscript Göteborg; 2007).
301. Rein, U., Andag, U., Duden, R., Schmitt, H.D. & Spang, A. ARF-GAP-mediated interaction between the ER-Golgi v-SNAREs and the COPI coat. *J Cell Biol* **157**, 395-404 (2002).
302. Parlati, F. *et al.* Rapid and efficient fusion of phospholipid vesicles by the alpha-helical core of a SNARE complex in the absence of an N-terminal regulatory domain. *Proc Natl Acad Sci U S A* **96**, 12565-12570 (1999).
303. Ebeling, W. *et al.* Proteinase K from *Tritirachium album* Limber. *Eur J Biochem* **47**, 91-97 (1974).
304. Lodhi, S., Weiner, N.D. & Schacht, J. Interactions of neomycin with monomolecular films of polyphosphoinositides and other lipids. *Biochim Biophys Acta* **557**, 1-8 (1979).
305. Schacht, J. Purification of polyphosphoinositides by chromatography on immobilized neomycin. *J Lipid Res* **19**, 1063-1067 (1978).
306. Hudson, R.T. & Draper, R.K. Interaction of coatamer with aminoglycoside antibiotics: evidence that coatamer has at least two dilysine binding sites. *Mol Biol Cell* **8**, 1901-1910 (1997).
307. Powis, G. *et al.* Wortmannin, a potent and selective inhibitor of phosphatidylinositol-3-kinase. *Cancer Res* **54**, 2419-2423 (1994).
308. Ferby, I.M., Waga, I., Hoshino, M., Kume, K. & Shimizu, T. Wortmannin inhibits mitogen-activated protein kinase activation by platelet-activating factor through a mechanism independent of p85/p110-type phosphatidylinositol 3-kinase. *J Biol Chem* **271**, 11684-11688 (1996).
309. Vanhaesebroeck, B. *et al.* Synthesis and function of 3-phosphorylated inositol lipids. *Annu Rev Biochem* **70**, 535-602 (2001).
310. Liu, Y., Jiang, N., Wu, J., Dai, W. & Rosenblum, J.S. Polo-like kinases inhibited by wortmannin. Labeling site and downstream effects. *J Biol Chem* **282**, 2505-2511 (2007).
311. Hsu, F.F. & Turk, J. Characterization of phosphatidylinositol, phosphatidylinositol-4-phosphate, and phosphatidylinositol-4,5-bisphosphate by electrospray ionization tandem mass spectrometry: a mechanistic study. *J Am Soc Mass Spectrom* **11**, 986-999 (2000).
312. Siddhanta, A., Backer, J.M. & Shields, D. Inhibition of phosphatidic acid synthesis alters the structure of the Golgi apparatus and inhibits secretion in endocrine cells. *J Biol Chem* **275**, 12023-12031 (2000).
313. Lebaron, F.N. & Folch, J. The effect of pH and salt concentration on aqueous extraction of brain proteins and lipoproteins. *J Neurochem* **4**, 1-8 (1959).
314. Dawson, R.M. & Eichberg, J. Diphosphoinositide and triphosphoinositide in animal tissues. Extraction, estimation and changes post mortem. *Biochem J* **96**, 634-643 (1965).
315. Ishihara, H. *et al.* Type I phosphatidylinositol-4-phosphate 5-kinases. Cloning of the third isoform and deletion/substitution analysis of members of this novel lipid kinase family. *J Biol Chem* **273**, 8741-8748 (1998).
316. Ishihara, H. *et al.* Cloning of cDNAs encoding two isoforms of 68-kDa type I phosphatidylinositol-4-phosphate 5-kinase. *J Biol Chem* **271**, 23611-23614 (1996).
317. Guo, S., Stolz, L.E., Lemrow, S.M. & York, J.D. SAC1-like domains of yeast SAC1, INP52, and INP53 and of human synaptojanin encode polyphosphoinositide phosphatases. *J Biol Chem* **274**, 12990-12995 (1999).
318. Stolz, L.E., Huynh, C.V., Thorner, J. & York, J.D. Identification and characterization of an essential family of inositol polyphosphate 5-phosphatases (INP51, INP52 and INP53 gene products) in the yeast *Saccharomyces cerevisiae*. *Genetics* **148**, 1715-1729 (1998).
319. Frederic Laporte, J.O., Fredrik Kartberg, Joel Lanoix, John JM Bergeron and Tommy Nilsson in Manuscript 2008).
320. Block, M.R. & Rothman, J.E. Purification of N-ethylmaleimide-sensitive fusion protein. *Methods Enzymol* **219**, 300-309 (1992).



321. Clary, D.O., Griff, I.C. & Rothman, J.E. SNAPs, a family of NSF attachment proteins involved in intracellular membrane fusion in animals and yeast. *Cell* **61**, 709-721 (1990).
322. Weidman, P.J., Melancon, P., Block, M.R. & Rothman, J.E. Binding of an N-ethylmaleimide-sensitive fusion protein to Golgi membranes requires both a soluble protein(s) and an integral membrane receptor. *J Cell Biol* **108**, 1589-1596 (1989).
323. Wattenberg, B.W., Raub, T.J., Hiebsch, R.R. & Weidman, P.J. The activity of Golgi transport vesicles depends on the presence of the N-ethylmaleimide-sensitive factor (NSF) and a soluble NSF attachment protein (alpha SNAP) during vesicle formation. *J Cell Biol* **118**, 1321-1332 (1992).
324. Zhao, C., Slevin, J.T. & Whiteheart, S.W. Cellular functions of NSF: not just SNAPs and SNAREs. *FEBS Lett* **581**, 2140-2149 (2007).
325. Schiavo, G., Shone, C.C., Bennett, M.K., Scheller, R.H. & Montecucco, C. Botulinum neurotoxin type C cleaves a single Lys-Ala bond within the carboxyl-terminal region of syntaxins. *J Biol Chem* **270**, 10566-10570 (1995).
326. Lawrence, G.W. & Dolly, J.O. Ca<sup>2+</sup>-induced changes in SNAREs and synaptotagmin I correlate with triggered exocytosis from chromaffin cells: insights gleaned into the signal transduction using trypsin and botulinum toxins. *J Cell Sci* **115**, 2791-2800 (2002).
327. Lawrence, G.W. & Dolly, J.O. Multiple forms of SNARE complexes in exocytosis from chromaffin cells: effects of Ca<sup>2+</sup>, MgATP and botulinum toxin type A. *J Cell Sci* **115**, 667-673 (2002).
328. Fasshauer, D., Eliason, W.K., Brunger, A.T. & Jahn, R. Identification of a minimal core of the synaptic SNARE complex sufficient for reversible assembly and disassembly. *Biochemistry* **37**, 10354-10362 (1998).
329. Prasher, D.C., Eckenrode, V.K., Ward, W.W., Prendergast, F.G. & Cormier, M.J. Primary structure of the *Aequorea victoria* green-fluorescent protein. *Gene* **111**, 229-233 (1992).
330. Chalfie, M., Tu, Y., Euskirchen, G., Ward, W.W. & Prasher, D.C. Green fluorescent protein as a marker for gene expression. *Science* **263**, 802-805 (1994).
331. Pelham, H.R. The retention signal for soluble proteins of the endoplasmic reticulum. *Trends Biochem Sci* **15**, 483-486 (1990).
332. Lewis, M.J. & Pelham, H.R. Ligand-induced redistribution of a human KDEL receptor from the Golgi complex to the endoplasmic reticulum. *Cell* **68**, 353-364 (1992).
333. Nakatsukasa, K. & Brodsky, J.L. The recognition and retrotranslocation of misfolded proteins from the endoplasmic reticulum. *Traffic* **9**, 861-870 (2008).
334. Anelli, T. & Sitia, R. Protein quality control in the early secretory pathway. *EMBO J* **27**, 315-327 (2008).
335. Ling, K., Doughman, R.L., Firestone, A.J., Bunce, M.W. & Anderson, R.A. Type I gamma phosphatidylinositol phosphate kinase targets and regulates focal adhesions. *Nature* **420**, 89-93 (2002).
336. Doughman, R.L., Firestone, A.J. & Anderson, R.A. Phosphatidylinositol phosphate kinases put PI4,5P(2) in its place. *J Membr Biol* **194**, 77-89 (2003).
337. Padron, D., Wang, Y.J., Yamamoto, M., Yin, H. & Roth, M.G. Phosphatidylinositol phosphate 5-kinase Ibeta recruits AP-2 to the plasma membrane and regulates rates of constitutive endocytosis. *J Cell Biol* **162**, 693-701 (2003).

# **Appendix**

## **Appendix outline**

The outline includes three manuscripts and one publication.

-The first manuscript, Laporte et al. explains the PI(4,5)P<sub>2</sub> investigation. It is ready for submission. However, we might be waiting for *in vivo data*, depending on the decision of Dr. Bergeron and Dr. Nilsson.

-The second manuscript, Laporte et al. explains the protease K experiments. It is not ready for submission as the Golgin-84 angle has not been included at this point and will be done so after the thesis is submitted.

-The third manuscript, Asp et al. has been submitted and is due for final submission on 29/08/08. It has been published in time for the defense:

Early Stages of Golgi-Vesicle and -Tubule Formation Require Diacylglycerol. Asp L, Kartberg F, Fernandez-Rodriguez J, Smedh M, Elsner M, Laporte F, Bárcena M, Jansen KA, Valentijn JA, Koster AJ, Bergeron JJ, Nilsson T.

Mol Biol Cell. 2008 Nov 26.

-The fourth item is collaborative work with Ching Yin Lee.

These are followed by copyright licences as well as animal and radioactive permits. (not in e-thesis).

# **PI(4,5)P<sub>2</sub> is Required for the Fusion of COPI-Derived Vesicles with Golgi Cisternae**

Frédéric Laporte<sup>1</sup>, Johan Hiding, Fredrik Kartberg, François Lépine<sup>4</sup>, Markus Grabenbauer<sup>2</sup>, Anirban Siddhanta<sup>3</sup>, Dennis Shields<sup>3</sup>, Joachim Ostermann<sup>1</sup>, John J.M. Bergeron<sup>1\*</sup> and Tommy Nilsson\*.

Department of Medical Biochemistry, Göteborg University, 413 90 Göteborg Sweden. Tel: (+46) 31 773 3606 and <sup>1</sup>Department of Anatomy and Cell Biology, McGill University, Montreal, Québec, Canada, H3A2B2. Tel: (+1) 514 398 6352 Fax: 514 398 5047

<sup>2</sup>Structural and Computational Biology, EMBL, Meyerhofstr. 1, D-69117 Heidelberg, Germany

<sup>3</sup>Department of Developmental and Molecular Biology, Albert Einstein College of Medicine of Yeshiva University, 1300 Morris Park Avenue, Bronx, New York 10461

<sup>4</sup>INRS, Institut Armand-Frappier. 531 Boulevard Des Prairies, Laval, Québec, Canada, H7V 1B7

**Keywords:** Golgi Apparatus, Phosphoinositides, Fusion, COPI, ARF1

**Abbreviations used:** GEF, Guanine nucleotide exchange factor; (L)DCV, (Large) dense core vesicle; Inp52p, 5-phosphatase domain of yeast synaptojanin-like 2; PI, Phosphatidylinositol; PI(4)P, Phosphatidylinositol-4-phosphate; PI(4,5)P<sub>2</sub>, Phosphatidylinositol-4,5-biphosphate; TLC, thin layer chromatography.

\*Both corresponding authors contributed equally to this study

[john.bergeron@mcgill.ca](mailto:john.bergeron@mcgill.ca) and [tommy.nilsson@medkem.gu.se](mailto:tommy.nilsson@medkem.gu.se)

## **Abstract**

**Coatomer is recruited to Golgi membranes in an ARF1-dependent manner that couples protein sorting to vesicle formation. Using a modified intra-Golgi transport assay with highly purified COPI vesicles, we demonstrate that fusion of retrograde-directed vesicles with Golgi membranes requires phosphatidylinositol-(4,5)-bisphosphate (PI(4,5)P<sub>2</sub>). The dependency on PI(4,5)P<sub>2</sub> appears to be COPI vesicle-associated since pre-treatment of the vesicles with either a specific 5-phosphatase or a 5-kinase, resulted in inhibition or gain of fusion, respectively. In contrast, corresponding pre-treatment of Lec1 Golgi target membranes had no effect on the efficiency or extent of COPI vesicle fusion with the Lec1 Golgi membranes. As ARF1 recruits the kinase responsible for PI(4,5)P<sub>2</sub> synthesis in a GTP-dependent manner to Golgi membranes, ARF1 can effectively prime COPI vesicles for fusion already at the onset of vesicle formation.**

## Introduction

In the secretory pathway, cargo transport between organelles depends on different vesicular coat machineries. At ER cargo exit sites, small vesicular structures containing newly folded and quality- assured biosynthetic cargo bud via the COPII-coat machinery. Upon uncoating, COPII-derived vesicles either coalesce or fuse with pre-existing membrane structures. In mammalian cells, part of the COPII machinery link directly to microtubules via the dynein/dynactin complex<sup>1</sup>. This ensures subsequent transport of the nascent membrane carriers (also termed vesicular tubular clusters or pre-Golgi intermediates) towards the microtubule organizing centre and the juxta-posed Golgi apparatus<sup>2, 3</sup>. Another type of vesicle, termed COPI, transports cargo between Golgi cisternae and recycles resident proteins between cisternae and from the Golgi to the ER (e.g. SNARE proteins and other machinery proteins) so that these can be used for further rounds of ER to Golgi transport (see Kartberg et al<sup>4</sup> for a review).

The main roles of the COPII- and COPI- coats can be summarised as ensuring that cargo molecules and machinery proteins required for vesicle targeting - fusion are co-packaged efficiently. Though the two coats differ in composition, they show features similar to those of adaptor proteins involved in linking clathrin to cargo proteins. Indeed, both COPII and COPI components are able to bind cargo, in particular SNARE proteins to ensure their incorporation into budding vesicles<sup>5-9</sup>. As COPI vesicles also recycle SNARE proteins that, for example, are needed for anterograde COPII-derived transport, a mechanism must exist which distinguishes recycling SNARE proteins from those required for the actual fusion of recycling vesicles. Otherwise, SNARE proteins could not provide and maintain asymmetry between different transport compartments as postulated previously<sup>10</sup>. Some evidence exists for

a fusion-specific conformational state of SNARE proteins as reflected in their resistance to protease digestion though how this state is maintained is unknown<sup>11, 12</sup>.

Sorting of cargo molecules and machinery proteins is followed by coat assembly and vesicle-bud formation. This process is regulated by small GTPases termed Sar1 for COPII and ARF1 for COPI. Both require specific guanine nucleotide exchange factors (GEFs) that exchange GDP for GTP as well guanine activator proteins (GAPs) that catalyze GTP hydrolysis. The role of ARF1 in COPI coat assembly is highlighted by its ability to recruit coatamer to the membrane when in its GTP-state. A subsequent uncoating of budded vesicles occurs upon GTP hydrolysis. In addition, ARF1 GTP hydrolysis has been shown to influence cargo incorporation into budding COPI vesicles both *in vitro*<sup>13, 14</sup> and *in vivo*<sup>15</sup>. While it is well established that ARF1 can recruit the main component of the COPI coat, coatamer, to Golgi membranes<sup>16</sup>, the actual mechanism for coat recruitment and coat assembly/disassembly is still the subject of investigation. For example, studies comparing the spatial dynamics of different COPI coat components reveal differential binding/unbinding kinetics<sup>17-20</sup>. ARF1 displays a more rapid binding/unbinding rate than does coatamer implying a partial uncoupling between ARF1 and coatamer. In fact, ARF1 has additional roles in the Golgi apparatus. It is known that ARF1 stimulates the production of phosphatidic acid (PA) in the presence of the nonhydrolysable GTP analogue, GTP $\gamma$ S<sup>21, 22</sup> through activation of phospholipase D<sup>23-25</sup>. This results in increased vesicle production<sup>26-28</sup>. In turn, PA stimulates the conversion of phosphatidylinositol-(4)-phosphate (PI(4)P) into phosphatidylinositol-(4,5)-bisphosphate (PI(4,5)P<sub>2</sub>)<sup>32</sup>. These and other phosphoinositides play important regulatory roles in membrane fusion, formation of clathrin-coated buds and in the interaction between cytoskeleton and membranes.



They exert their effects mainly by recruiting signalling factors and regulatory proteins to membrane domains but can also affect the conformational states of proteins embedded or attached to the membrane. Phosphoinositides are also used to produce ubiquitous second messengers that act downstream of many G protein-coupled receptors and tyrosine kinases (for a recent review, see Oude Weernink et al.<sup>33</sup>).

In several membrane systems, formation of PI(4,5)P<sub>2</sub> is required for fusion or the regulation of fusion. How this is achieved is envisaged in at least three ways; First, priming of SNAREs as evidenced by studies in yeast showing a requirement for PI(4,5)P<sub>2</sub> in a SEC18p(NSF)-dependent priming of SNAREs as well as in the post docking/fusion event<sup>34</sup>. Second, in the regulation of the actin cytoskeleton and associated motility events<sup>35</sup> that for example, helps to remodel the cortical actin to allow for endocytosis and/or promotes fission through a dynamin-specific process to release endocytic vesicles<sup>36</sup>. Third, recruitment of cytosolic factors that are required for docking and/or regulation of fusion. For the fusion of (large) dense core vesicles ((L)DCVs), the plasmalemmal PI(4,5)P<sub>2</sub> pool is regulated by an ARF6-dependent recruitment of type I $\gamma$  PIP 5-kinase to the plasmalemma in PC12 cells<sup>37, 38</sup>. This PI(4,5)P<sub>2</sub> pool recruits CAPS-1/2 in order to promote Ca<sup>2+</sup>-triggered fusion of docked (L)DCV's with the plasmalemma<sup>39, 40</sup> (see also Murthy and DeCamilli<sup>41</sup> as well as Stojilkovic<sup>42</sup> for reviews). An additional specificity is likely mediated by the association of synaptotagmins on (L)DCVs with PI(4,5)P<sub>2</sub> and t-SNARE on the target plasmalemma<sup>43</sup>. Indeed, such microdomains formed by PI(4,5)P<sub>2</sub> at docked sites of (L)DCV's with the plasmalemma have been observed in PC12 cells<sup>44</sup>. The plasmalemmal PI(4,5)P<sub>2</sub> level also appears to regulate the releasable vesicle pool size

in chromaffin cells<sup>45, 46</sup>. In these cells, type I $\gamma$  PIP 5-kinase regulates PI(4,5)P<sub>2</sub> pool important for the fusion of (L)DCV's with the chromaffin cell plasmalemma.

In the Golgi apparatus, PI(4,5)P<sub>2</sub> may serve a similar role. Inhibition of PI(4,5)P<sub>2</sub> formation results in the fragmentation and vesicularisation of the Golgi apparatus<sup>47, 48</sup>. This suggests a possible requirement of PI(4,5)P<sub>2</sub> in the maintenance of the Golgi apparatus via membrane fusion. The level of PI(4,5)P<sub>2</sub> in the Golgi apparatus appears tightly regulated. Only small amounts of PI(4,5)P<sub>2</sub> can be detected at steady state<sup>49-52</sup> whereas upon ARF1 stimulation, a 10-fold increase is observed<sup>50</sup>. In fact, ARF1 directly controls the synthesis of PI(4)P and PI(4,5)P<sub>2</sub> through a nucleotide-specific recruitment and binding of corresponding kinases<sup>53, 54</sup>. As such, ARF1 is posed to control the flow from PC to PA as well as from PI to PI(4)P and PI(4,5)P<sub>2</sub> through direct and nucleotide-specific regulation. As ARF1 also recruits coatamer in a nucleotide-specific manner, it implies a coupling between phosphoinositides synthesis and COPI vesicle formation<sup>47, 48, 50</sup>.

In this study, we have investigated the role of PI(4,5)P<sub>2</sub> in COPI vesicle fusion, *in vitro*. Using a well characterized intra Golgi transport assay which monitors the fusion of Golgi derived COPI vesicles with the early Golgi membranes<sup>14, 55</sup>, we find a strict requirement for the presence of PI(4,5)P<sub>2</sub> on COPI vesicle membranes. As evidenced from the previous work of Elazar et al.<sup>56</sup>, a coupling likely exists between vesicle formation and fusion. The findings presented here supports a coupled event through ARF1-stimulated PI(4,5)P<sub>2</sub> production on the budding vesicle.

## Results and Discussion

The *in vitro* complementation assay to study intra Golgi transport<sup>57</sup> registers the complementation of GlcNacT-1 enzyme activity<sup>55</sup>. Cells of the GlcNacT-1-deficient CHO cell line, Lec1, are first infected with vesicular stomatitis virus (VSV) to express the N-linked glycosylated and temperature-sensitive protein G. Upon synthesis, VSV-G protein is retained in the *cis*-Golgi network<sup>58</sup> by transferring cells to 15°C (see Materials and Methods). Cells are homogenised and Golgi membranes containing the VSV-G protein are then purified and mixed with cytosol and corresponding Golgi membranes from wild type CHO cells devoid of the VSV-G protein but competent in GlcNacT-1 enzyme activity. Upon COPI-mediated vesicle transport, the assay then registers the transfer of <sup>3</sup>H-GlcNac onto the N-linked oligosaccharides of VSV-G<sup>57</sup>. By substituting the wild type Golgi membranes with that of purified COPI vesicles formed *in vitro* and enriched with glycosylation enzymes (including GlcNacT-1), we showed that COPI vesicles fuse in an NSF dependent manner with Golgi membranes derived from VSV-infected Lec1 cells validating the approach<sup>14</sup>. Using the same modified assay, Ostermann later identified four parameters<sup>59</sup> that essentially describe the kinetic aspects of this vesicle-based assay (fig 1a). The first parameter describes the concentration of COPI vesicles that are available for fusion (termed apparent vesicle concentration or  $C_v^{app}$ ). The second parameter describes a time-dependent decrease of the  $C_v^{app}$ . The third parameter describes the binding and fusion of COPI vesicles with the Lec1 membranes and the fourth parameter, the transfer of GlcNac onto VSV-G. This final parameter is not rate limiting as Ostermann showed that the content of one COPI vesicle sufficed to glycosylate the entire VSV-G content of one Lec1 Golgi cisternal acceptor compartment<sup>59</sup>.

COPI vesicles were purified<sup>60</sup> (fig. 1b) from rat liver Golgi membranes following a budding reaction and added to purified Lec1 membranes containing the VSV-G protein. A typical response curve of the complementation reaction is shown in figure 1c and is described by the equation  $a+c(1-e^{-bx})$ , where “b” is termed  $C_v^{app}$ , or the concentration of vesicles which is apparent. This influences the slope of the curve. The minimal and maximum signal corresponds to “a” and “c”, respectively (fig. 1c). The strict dependence on COPI to generate the signal is shown in figure 1d and e. Depletion of coatamer, the main component of the COPI coat machinery, from the rat liver cytosol used in the budding reaction results in an abolition of vesicle formation as shown previously<sup>14, 61</sup>. That this results in a corresponding loss of signal in the fusion assay is demonstrated in figure 1e. Depletion of coatamer from the cytosol as monitored by Western blot (fig. 1d) resulted in more than a 10-fold decrease in  $C_v^{app}$  compared to vesicle formed using mock-depleted cytosol. This shows that the main transfer of GlcNAc-T1 activity as monitored in the transport assay is via a COPI-dependent process. Note that the depletion procedure itself results in a lower amount of coatamer due to non-specific loss during the depletion experiment (compare Control (C) with Mock (M) depleted in fig. 1d and e). Consequently,  $C_v^{app}$  drops about two-fold compared to untreated cytosol.

Upon pre-incubation of the vesicles at 37°C in the absence of cytosol, fusion activity of vesicles decreases over time. As shown in figure 2a,  $C_v^{app}$  decreases from 1 to 0.4 ( $\pm 0.06$ ) after 60 min. incubation. To assess if this might correspond to changes in phosphoinositides, neomycin or Wortmannin were added to the fusion assay, both known PI(4,5)P<sub>2</sub> effectors. Both showed inhibitory effects supporting a role for phosphoinositides in fusion (data not shown). To test more specifically, we added a

monoclonal antibody specific for PI(4,5)P<sub>2</sub>. Increasing amounts of antibody revealed an antibody-specific inhibition at a concentration of less than 20µg/ml antibody (fig. 2b) suggesting that phosphoinositides such as PI(4,5)P<sub>2</sub> are required for the fusion process of COPI vesicles. Heat-inactivated antibodies added as control were ineffective in the assay. We then determined if the cytosol-independent, time-dependent inactivation shown in figure 2a could be rescued by PI(4,5)P<sub>2</sub> synthesis. A mouse PI4P5-kinase type 1β was expressed as a GST fusion protein, purified and tested for its ability to generate PI(4,5)P<sub>2</sub>. Lipids were extracted from purified COPI vesicles incubated in the presence of the kinase and P<sup>32</sup>-ATP and subsequently examined by thin layer chromatography (TLC). As can be seen in figure 3a, radio-labeled phospholipids separated by TLC showed a marked increase of PI(4,5)P<sub>2</sub> synthesis upon addition of the kinase (lane 2) whereas heat inactivated (HI) enzyme (lane 3) was similar to the control (lane 1). Note also the decrease of radio-labeled lipids in the spot co-migrating with PI(4)P (compare lane 2 with 1 and 3) in the presence of the kinase consistent with the conversion of PI(4)P to PI(4,5)P<sub>2</sub>. That PI(4,5)P<sub>2</sub> was indeed formed under these conditions was confirmed by mass spectrometry. As can be seen in supplementary figure 4, the spectrum shows new ions appearing at the m/z 522 upon incubation of Golgi membranes in the presence of the kinase. The m/z 522 ion is consistent with the formation of PI(4,5)P<sub>2</sub> and this was verified by collision-induced dissociation which resulted in peaks consistent with PI(4,5)P<sub>2</sub>. When introduced directly into the fusion assay, the kinase had only a mild stimulatory effect (fig. 3b-Kinase 0') presumably because of the presence of existing PI(4,5)P<sub>2</sub>. However, if allowed to compete with the cytosol-independent and time-dependent inactivation, the kinase rescued vesicle fusion (fig. 3b-Kinase 60'): in contrast, addition of heat-inactivated kinase had little effect (fig. 3b-HI Kinase 60').

This was further demonstrated quantitatively (fig. 3c). Taken together, these data suggest a role for PI(4,5)P<sub>2</sub> in the fusion of COPI vesicles.

If the above idea were correct, then treatment of COPI vesicles with a PI(4,5)P<sub>2</sub> phosphatase should abolish fusion. The phosphatase domain from yeast-synaptojanin like-2 (Sjl2p) (or Inp52p) previously shown to remove the 5-phosphate of PI(4,5)P<sub>2</sub><sup>62</sup> was exploited. The specificity of this enzyme was assayed on purified COPI vesicles (fig. 4a). Upon incubation with the phosphatase (lane 2), radio-labeled phospholipids separated by TLC showed less label in the spot co-migrating with PI(4,5)P<sub>2</sub> compared to samples treated with heat inactivated (HI) phosphatase (lane 3) or to the control (lane 1). When added to the transport assay directly, the phosphatase showed no significant effect (data not shown). In contrast, pre-incubation of vesicles with the phosphatase before addition to the to Lec1 membranes resulted in an inhibitory effect at approximately 10 µg/ml (fig. 4b). Heat inactivated (HI) phosphatase showed no such effect. Further studies to determine  $C_v^{app}$  confirmed this finding (fig. 4c). The phosphatase did not display any inhibitory effect in the absence of MgCl<sub>2</sub> (data not shown) highlighting the specificity of the reaction<sup>62</sup>. From this we can conclude that conversion of PI(4,5)P<sub>2</sub> into PI(4)P by the specific removal of the 5-phosphate results in a decreased fusion ability of COPI vesicles.

To investigate the influence of PI(4,5)P<sub>2</sub> on the fusion ability of COPI vesicles further, we subjected COPI vesicles to a two step incubation. Vesicles were first incubated in the absence of active kinase (fig. 5a, lane 2). In the presence of the kinase, most of the fusion activity (80%) remained (fig. 5a, lane 3). Subjecting vesicles to two consecutive incubations decreased their fusion activity even further

(fig. 5a, lane 4), to less than 20%. In the presence of the kinase, 60% of the fusion activity remained (fig. 5a, lane 5). Adding the kinase to the first incubation and the phosphatase to the second resulted in only 20% of the original fusion activity (fig. 5a, lane 6) whereas addition of heat-inactivated phosphatase (HI) to the second incubation led to the return of 60% of the fusion activity (fig. 5a, lane 7) which was comparable to the result seen in lane 5. The quantitative estimate of active vesicles ( $C_v^{app}$ ) was determined with 3 different incubation conditions compared to the control (fig. 5b) with the strongest inhibitory effect on fusion in the presence of the PI(4,5)P<sub>2</sub> phosphatase.

As pre-incubation of vesicles either alone, in the presence of phosphatase or in the presence of kinase affects  $C_v^{app}$ , we conclude that PI(4,5)P<sub>2</sub> is required on the COPI vesicle for fusion. A role for PI(4,5)P<sub>2</sub> could also exist on the VSV-G-containing Lec1 Golgi membrane. Although incubation of Lec1 membranes in the presence of 5-phosphatase revealed a loss PI(4,5)P<sub>2</sub> (fig. 6a-lane 1) compared to the control (heat-inactivated enzyme, fig. 6a-lane 2), no effect on fusion was detected (fig. 6c). Conversely, incubation of Lec1 membranes in the presence of 5-kinase increased the synthesis of PI(4,5)P<sub>2</sub> (fig. 6b-lane 1) compared to control (heat-inactivated enzyme, fig. 6b-lane 2). As with the phosphatase, no effect on the fusion was observed (fig. 6d).

In summary, we have found a requirement for the presence of PI(4,5)P<sub>2</sub> in the fusion of COPI vesicles with Golgi membranes, *in vitro*. Though the formation of PI(4,5)P<sub>2</sub> is important for Golgi function<sup>47, 48, 50, 63</sup>, the involvement of PI(4,5)P<sub>2</sub> in Golgi transport is considered controversial with a lack of agreement as to the location and

extent of enzymes producing PI(4,5)P<sub>2</sub> as well as to their significance. A conclusive role for PI(4,5)P<sub>2</sub> in membrane fusion has been previously demonstrated for the fusion of (L)DCVs with the plasmalemma via the recruitment of CAPS and the engagement of the SNARE machinery<sup>39, 43</sup>. Here, the paradigm may be extended to COPI-mediated vesicle transport. The identity of predicted CAPS-related protein as well as the relevant COPI PI(4,5)P<sub>2</sub> phosphatase is unknown but the cell-free assay used here may enable us to screen for these proteins. Although Golgi membranes contain very low levels of PI(4,5)P<sub>2</sub>, at steady state<sup>49-52</sup>, our results suggest that ARF1, the small GTPase required for COPI coat assembly, may also bind the two kinases required for PI(4)P and PI(4,5)P<sub>2</sub> synthesis in a GTP specific manner<sup>53, 54</sup>. By doing so, ARF1 would prime budding COPI vesicles for fusion. Evidence for a COPI-dependent coupling between budding and fusion has been reported previously<sup>56</sup>. The findings here provide a likely mechanistic explanation for the Elazar et al. study.

Finally, it has not escaped our attention that a regulated PI(4,5)P<sub>2</sub> phosphatase could lead to the breakdown of the Golgi via the inhibition of COPI vesicle fusion as shown here and may be relevant to the mechanism of Golgi partitioning during mitosis. In a broader context, PI(4,5)P<sub>2</sub> is clearly linked to membrane fission in endocytosis. Our studies do not rule out a PI(4,5)P<sub>2</sub>-mediated balance between vesicle fusion and fission events in the Golgi.



## Reagents

All reagents were of analytical grade or higher. Unless mentioned otherwise, all chemicals were purchased from Sigma Chemical Co. (St-Louis, MO). Reagents for the COPI vesicle budding assay were obtained as described previously<sup>60</sup>. Tritiated uridine bisphosphate n-Acetyl-D-Glucosamine was obtained from PerkinElmer (Wellesley, MA). PD-10 desalting columns, protein G sepharose beads and P<sup>32</sup> labeled ATP were obtained from Amersham Biosciences (Piscataway, NJ). Phospholipids standards, PI(4,5)P<sub>2</sub>, PA, PS and PI(4)P was obtained from Avanti (Alabaster AL).

Mouse GST-PI4P5K type I $\beta$ , a generous gift of Y. Kanaho<sup>64</sup>, was cloned, sequenced and introduced to pGEX-2T (Amersham, Piscataway, NJ) to generate a GST-PI4P5K type I $\beta$  fusion protein which was expressed and purified from *E. coli* BL21 cells.

The PI(4,5)P<sub>2</sub> 5-phosphatase domain (residues 592-900) of yeast Synaptojanin-like 2 (Inp52p) was a generous gift of P. De Camilli (Yale University, CT). Clones were sequenced and found to have two sequence alterations, one silent (G<sub>705</sub>), the other replacing Q<sub>799</sub> with R. This alteration did not have any effect on the phosphatase specificity. The construct was cloned in pET-28A (Novagen, San Diego, CA) and transformed into *E. coli* BL21 cells. Phosphatase activity was measured with a malachite green colorimetric assay<sup>65</sup>.

## Mass spectrometry

ESI-MS was performed in negative ion mode using a Micromass Quattro II triple quadrupole mass spectrometer (Waters, Canada) equipped with a Z-spray interface. PI(4,5)P<sub>2</sub> from standards or extracted from purified rat liver Golgi employing the

chloroform/methanol/1N HCl (1:1:1) method of Siddhanta et al. (2000), dried under a stream of N<sub>2</sub> and then resuspended in acetonitrile/water/triethylamine (70%/30%/30mM) was used for ESI-MS analysis. Analysis was accomplished by direct infusion using a Harvard model 11 infusion pump at 5µL/min. MassLynx 3.5 software was employed for data accumulation in multiple-channel analysis mode and for data analysis. Nitrogen was used as drying gas (150 l/h) and nebulizing gas (20 l/h). The ESI-MS analyses were performed with the electrospray capillary set at 4.7 kV, the cone voltage of 45 V, a scan rate of 400 Da/s and an interscan delay of 0.1 s. For tandem MS experiments, Argon at a partial pressure of  $2 \times 10^{-3}$  mbar was employed as collision gas, with collision energies of 35 V for tandem MS and 100 V for precursor ions scans.

### **Fusion assay**

The fusion assay was performed as described previously<sup>59</sup>. Briefly, purified COPI-derived vesicles were generated in the budding assay and incubated in the presence of 20% Lec1 cytosol, 10% VSV-infected Lec1 Golgi membranes, an ATP Regenerating system (final 50uM ATP, 250uM UTP, 5mM creatine phosphate, 8U/ml creatine kinase), 10X hepes buffer (final 25mM Hepes/KOH pH 7.2, 2.5mM MgOAc<sub>2</sub>), 1.5 µCi of previously evaporated tritiated N-acetyl-Glucosamine and final sucrose and KCl concentration adjusted to 0.25 M and 30-60mM, respectively.

Pre-Incubation of the COPI-derived vesicles in the presence of the mouse GST-PI(4)P5KIβ or the 5-phosphatase domain of Inp52p was performed in 0.25 M sucrose, 150mM KCl, 25mM Hepes/KOH pH 7.4, 1mM EGTA, 2.5mM MgCl<sub>2</sub>, 250µM ATP was added for pre-incubation with GST-PI(4)P5KIβ. The vesicles were then added to

the fusion assay and the sucrose and salt concentration was adjusted to meet the requirements mentioned above.

After 2 hours incubation at 37°C, reactions were stopped at 4°C. Samples were added to antibody complex in lysis buffer (50mM Tris pH 7.4, 250mM NaCl, 5mM EDTA, 1% Triton X-100), mixed and incubated for one hour at RT. Samples were then filtered on blocked glass fiber prefilters (Sigma GF/C or Millipore APFC02500), washed 5 times with lysis buffer, dried and counted.

#### **Cell culture, Cytosol and Membranes purification.**

CHO Lec1 cells<sup>66</sup> were obtained from the ATCC. For cytosol purification, cells were pelleted and washed once with PBS, once with 200mM sucrose/10mM tris pH 7.4 (ST)Buffer and finally resuspended in ST Buffer. They then homogenized using a ball-bearing homogenizer (Boehring Ingelheim, Mannheim, Germany) and centrifuged at 14000 rpm for 3x10 min. until no pellet was visible. Cytosol was then desalted in PD10 column, aliquoted, snap-frozen and kept at -80°C.

For Lec1 Golgi membrane preparations, cells were pelleted and resuspended in 50 ml VSV infection media containing VSV, alpha-MEM, 25mM Hepes/KOH pH 7.2, 0.5 mg actinomycin D) for 45 min. at 37°C. After the infection, 200ml of 10% FBS alpha-MEM medium was added to the volume and incubated for 2h15 min at 37°C. In order to concentrate the VSV-G in the CGN, the cells were incubated or 3h15min at 15°C. Cells were washed and homogenized as described above. To purify Golgi membranes, the homogenate was mixed 1:1 with 62% sucrose, 10mM Tris pH 7.4, 1mM EDTA. The fraction was then introduced to the bottom of SW 40 Ultraclear

tubes (Beckman, Fullerton, CA). Sucrose fractions of 35% and 29% were applied at the top of the tubes, centrifuged for 90 min. at 40 000rpm. Golgi membranes were collected at the 29-35% sucrose interface, aliquoted, snap-frozen and stored at  $-80^{\circ}\text{C}$ . The budding assay was performed as described previously<sup>60</sup>.

## **TLC**

All TLC were performed as described previously<sup>67</sup>. Briefly, samples were incubated in kinase/phosphatase buffer (final 0.25M Sucrose, 25mM Hepes/KOH pH 7.4, 150mM KCL, 1mM EGTA, 2.5mM  $\text{MgCl}_2$  and 250 $\mu\text{M}$  ATP) for 60min. at  $37^{\circ}\text{C}$  in the presence of radiolabeled  $\text{P}^{32}$ -ATP. The phospholipids were extracted with MeOH/Chloroform/1N HCL, (1:1:1) dried, resuspended in chloroform:MeOH:9N HCL (200:100:1.33) and resolved by TLC. Phospholipids were identified by co-migration with known standards<sup>67</sup>.

## **Antibodies and electron microscopy**

Mouse monoclonal antibodies to VSV-G, a kind gift from P. Melancon (University of Alberta, Edmonton) were purified from hybridomas. The degree of antibody complex formation was assayed by mixing varying quantities of mAB to VSV-G and Anti-Mouse Goat AB (ICN, Montreal, Canada) until the optimal ratio was obtained in the fusion assay.

Mouse monoclonal  $\text{IgG}_{2b}$  antibody to  $\text{PI}(4,5)\text{P}_2$  was obtained from Assay Designs Inc. (Ann Arbor, MI).

Vesicles were prepared, immuno-labeled with an antibody directed towards the cytoplasmic domain of  $\text{p}24\beta_1$ , a small transmembrane protein enriched in COPI vesicles<sup>61, 68</sup> and analyzed by negative stain as described previously<sup>14</sup>.

## **Graphs and Curvefitting**

All curvefitting was done with the help of Maccurvefit 1,5 (Kavin Raner Software ([www.krs.com.au](http://www.krs.com.au))). In regards to the fusion assay, a non-saturation amount of vesicles refers to an amount of vesicles that would normally generate a signal that is a fraction of the maximum signal, generally a 2:1 ratio of vesicles vs Golgi cisternae<sup>59</sup>. While experiments done under these conditions provide accurate and reliable data, the precise extent of how the fusion assay is affected can only be ascertained by comparing the apparent concentration of vesicles. All error bars refer to one standard deviation in both directions, calculated with EXCEL (Microsoft, Seattle, WA).

## **Acknowledgements**

We would like to thank Dr. Paul Melancon (U. of Alberta, Edmonton, Alberta) for the kind gift of all VSV-related material; Dr. Pietro De Camilli for the kind gift of the phosphatase construct and Dr. Yasu Kanaho for the 5-kinase and Dr. Alexander Bell (McGill) for critical and helpful advice on mass spectrometry. We would also like to thank colleagues at Göteborg University and McGill for helpful suggestions and help and Dr. Peggy Weidman (St-Louis University, MS) for sharing unpublished results. This work was supported by a Swedish Research Council grant to TN, a CIHR operating grant to JB and an NIH grant (DK21860) to DS.

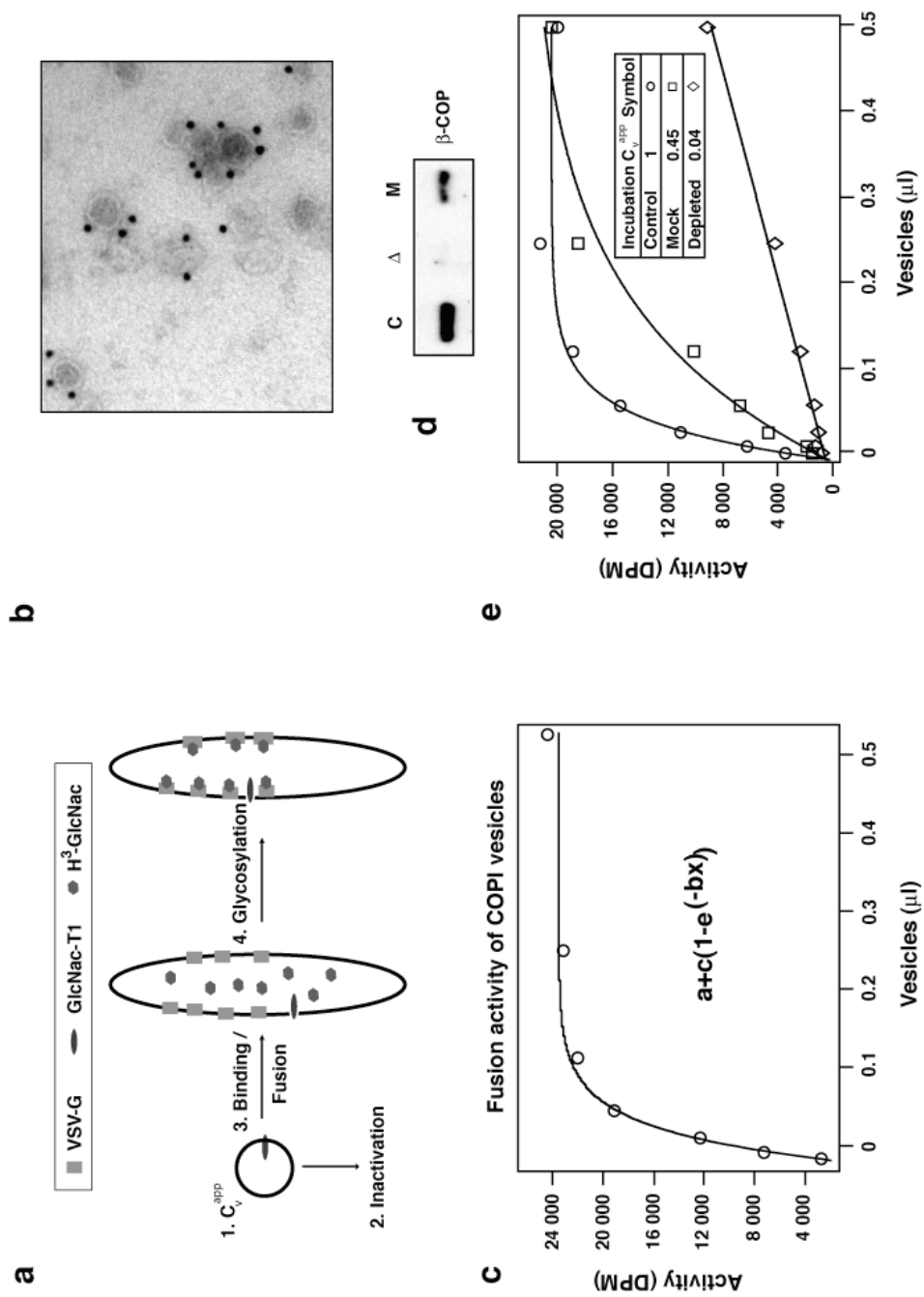
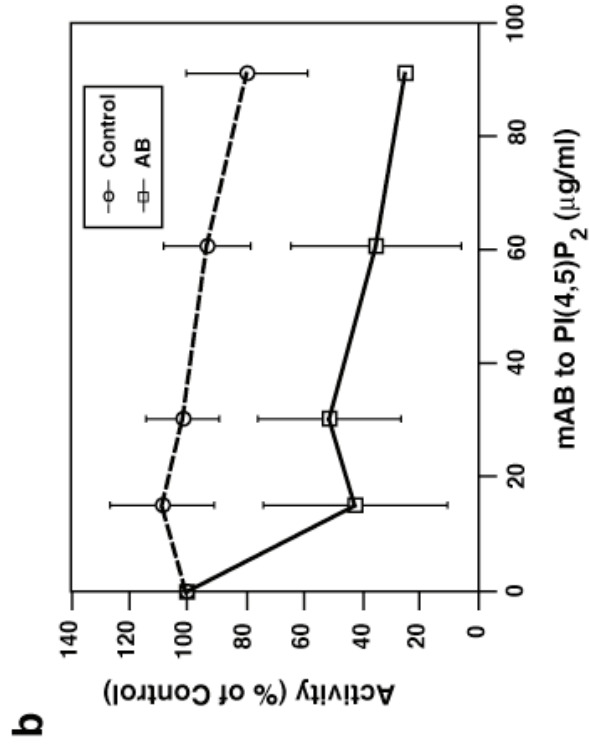
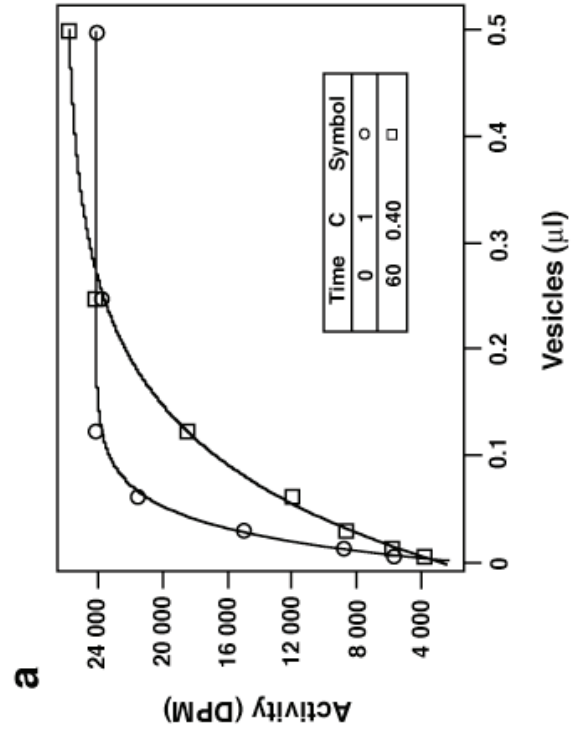


Figure 1, Laporte et al.



**Figure 2, Laporte et al.**



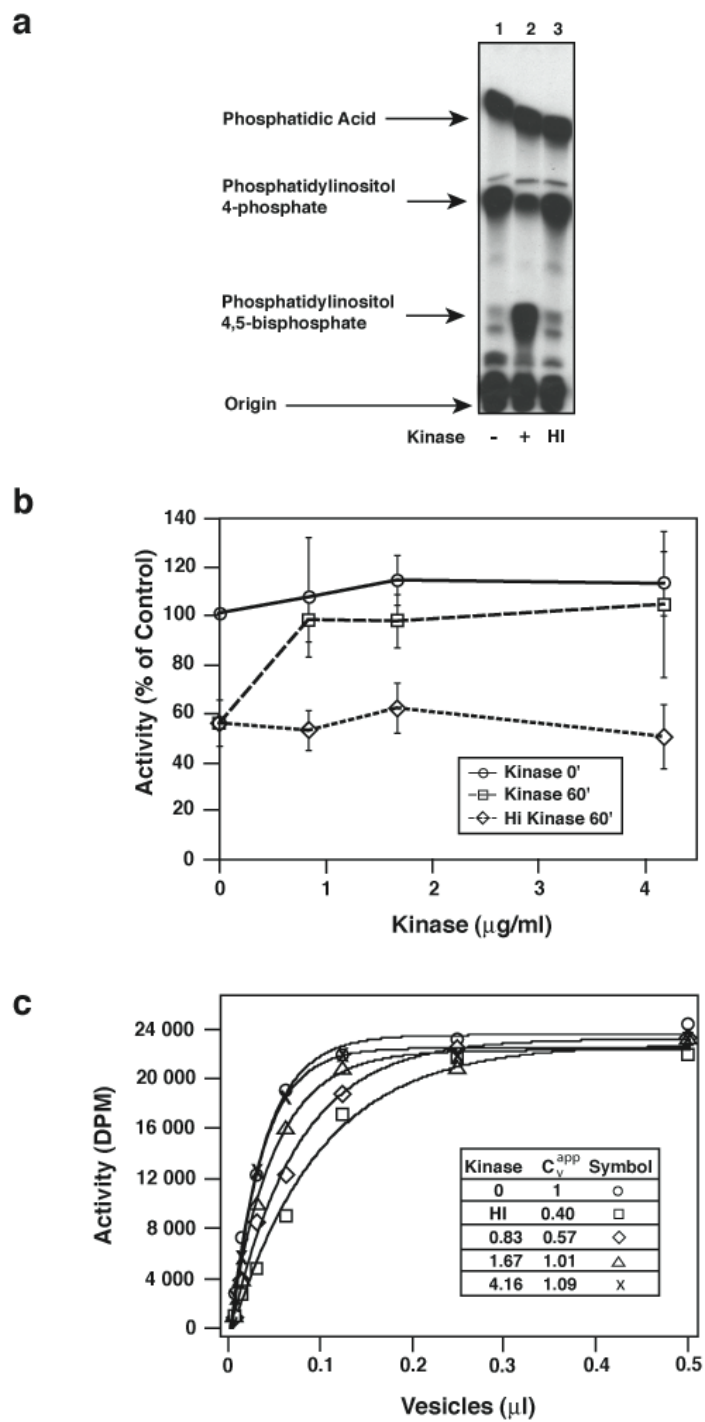


Figure 3, Laporte et al.

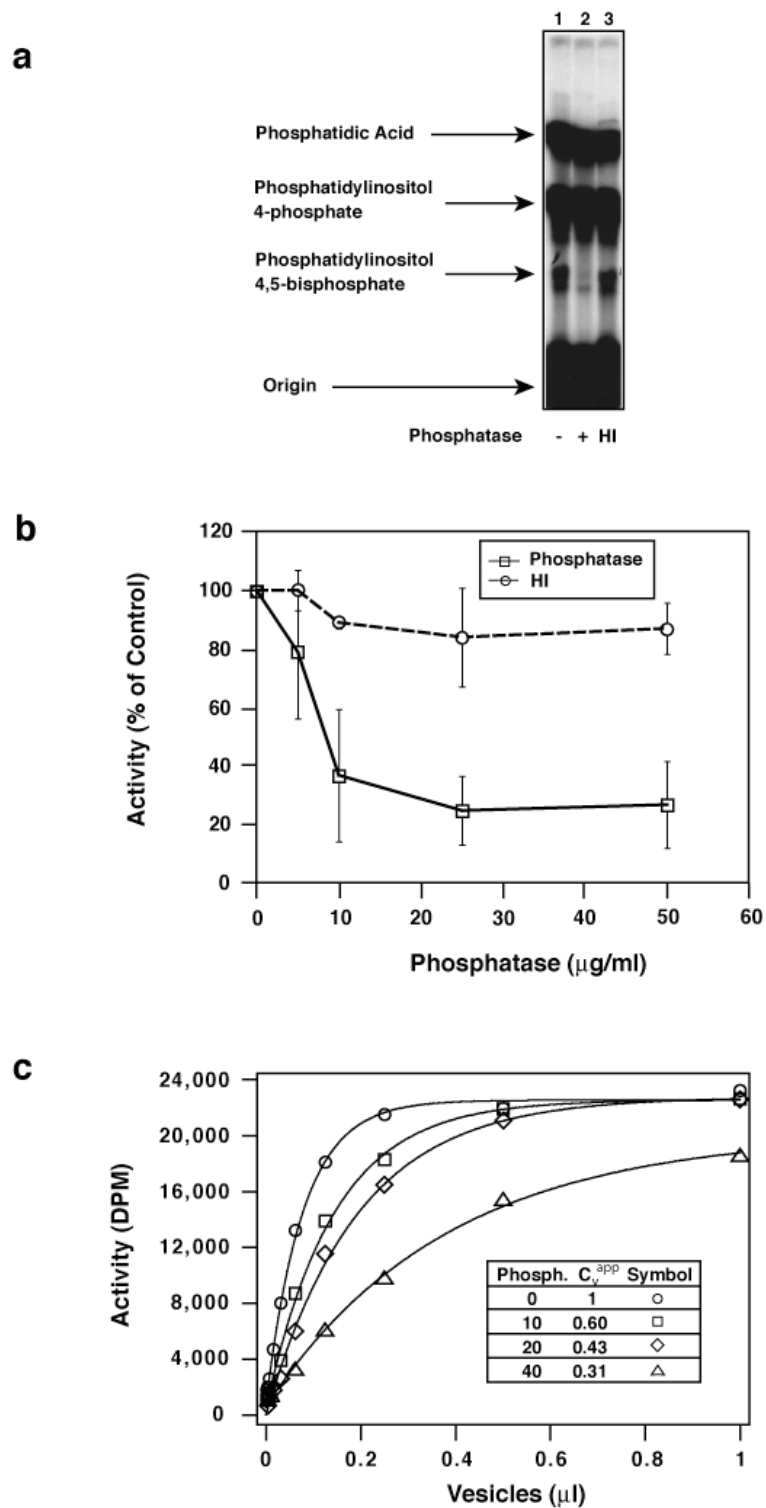
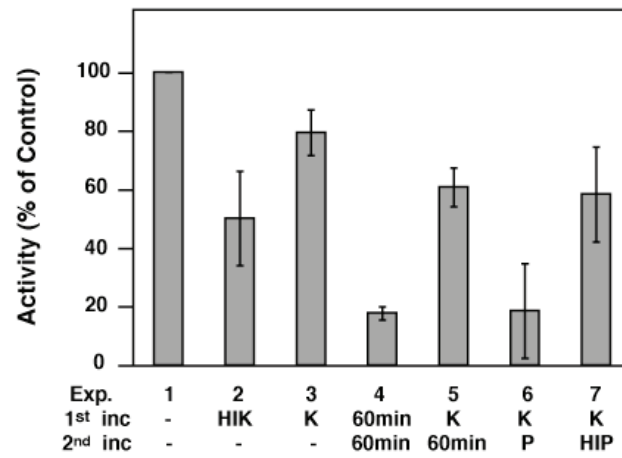
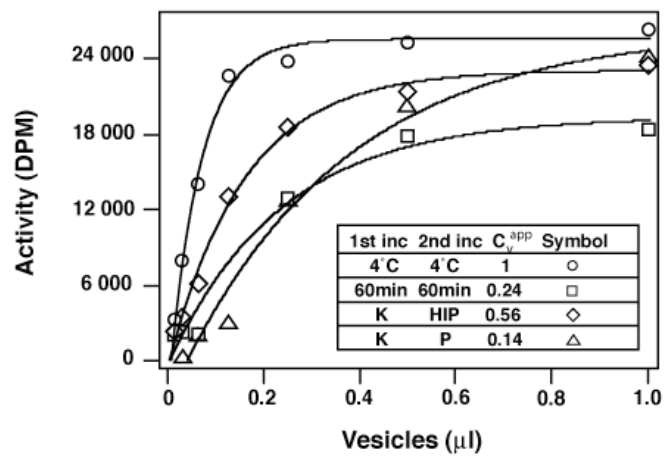


Figure 4, Laporte et al.

**a**



**b**



**Figure 5, Laporte et al.**

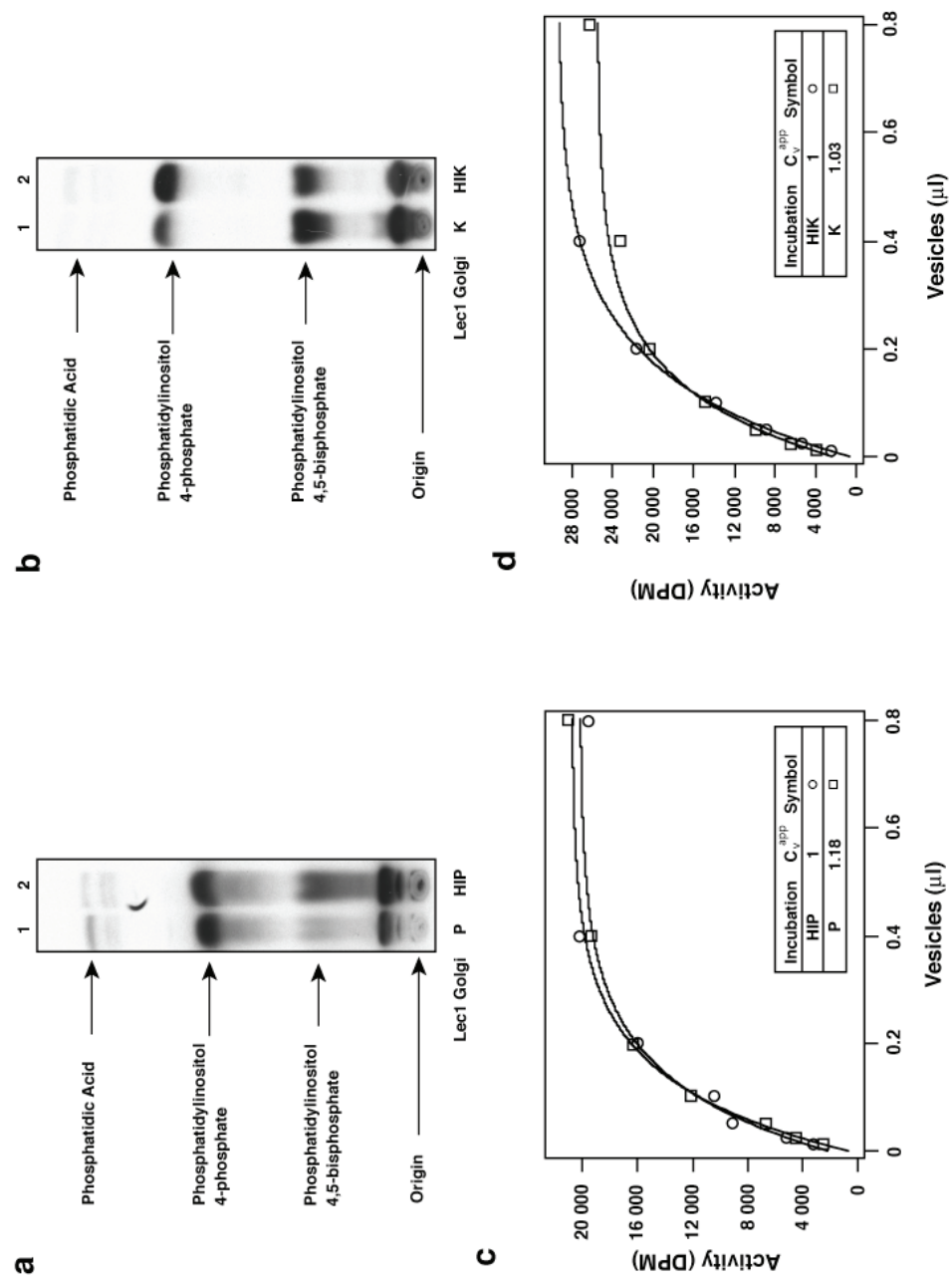


**Figure 6, Laporte et al.**

## Figure Legends

**Figure 1.** The modified transport assay and relevant parameters. **a**, Schematics of the transport assay showing two fates of vesicles, fusion or inactivation as described previously<sup>59</sup>. **b**, Purified COPI vesicles visualized by negative-stain and labeled with immuno-gold particles directed towards the cytoplasmic domain of p24 $\beta_1$ . **c**, The fusogenic ability of COPI vesicles described by the equation:  $a + c(1 - e^{(-bx)})$ , where "a" and "c" correspond to the minimal and maximum signal, respectively. The overall fusogenic ability, "b", is termed  $C_v^{app}$  and corresponds to the apparent concentration of vesicles<sup>59</sup> and "x" refers to the amount ( $\mu$ l) of vesicles added to the assay. Data are from a typical experiment with purified COPI vesicles and Lec1 Golgi membranes. **d**, COPI vesicles were formed in the presence of untreated control cytosol (C), cytosol depleted of coatomer using a mAb to  $\beta$ -COP ( $\Delta$ ) or cytosol incubated with an irrelevant antibody (M). Vesicle fractions were then probed for  $\beta$ -COP by immunoblotting. **e**,  $C_v^{app}$  determination using the vesicle fraction from experiments using control (O), mock-depleted ( $\square$ ) or coatomer-depleted ( $\diamond$ ) cytosol. The  $C_v^{app}$  values for the mock-depleted and coatomer depleted cytosol were  $0.44 \pm 0.28$  and  $0.04 \pm 0.01$ , respectively.

**Figure 2.** Inactivation and inhibition of COPI vesicle fusion. **a**, vesicles incubated for 0 or 60 min. at 37°C in the presence of buffer (25mM hepes pH 7.4, 150 mM KCl, 2.5mM MgCl<sub>2</sub>, 1mM EGTA, 0.25 mM ATP) prior to the cell-free assay. Vesicles incubated for 60 min. at 37°C ( $\square$ ) inactivated to the extent that their ability to fuse was only  $0.40 \pm 0.06$  times that of vesicles incubated for 0 min. (O). **b**, A non-saturating (see material and methods) amount of COPI vesicles was added to Lec1 membranes in the presence of increasing amounts of purified monoclonal IgG

antibodies directed towards PI(4,5)P<sub>2</sub> (□) or control (○). The control was composed of heat-inactivated antibodies (95°C for 15 min). These experiments as well as following experiments represent the mean of at least n=3 experiments ± SD.

**Figure 3.** PI4P 5-kinase type 1 inhibits inactivation of vesicles. **a**, Demonstration of the effect of the kinase by TLC. COPI vesicles (1.25 µg) in kinase buffer (see Materials and Methods) supplemented with P<sup>32</sup>-ATP were incubated for 60 min. at 37°C (lane 1) in the presence of 1.67 µg/ml kinase (lane 2) or heat inactivated (HI) kinase (lane 3). The migration of standards is indicated on the left. The film was exposed for two days. **b**, a non-saturating amount of vesicles was added to Lec1 target membranes in the presence of purified kinase at the onset of the incubation (○). To determine if the kinase could rescue vesicles from inactivation, vesicles were incubated in the presence of kinase (□) or heat inactivated (HI) Kinase (◇) for 60 min at 37°C before addition of Lec1 target membranes. This leads to an inactivation as seen in Figure 2 (compare (○) with (□) and (◇)). In the presence of functional kinase, the inactivation of COPI vesicles is restored (□). **c**, C<sub>v</sub><sup>app</sup> determination: Vesicles were incubated for 60 min at 37°C in the presence of 0 (□), 0.83 (◇), 1.67 (△) or 4.16 (X) µg/ml of kinase and compared to vesicles that had not been pre-incubated (○). Vesicles were inactivated to the extent of 0.40 ± 0.06 after the incubation using heat inactivated kinase compared to vesicles that had not been pre-incubated. In the presence of kinase, C<sub>v</sub><sup>app</sup> was restored to 0.57 ± 0.14 (0.83 µg/ml kinase), 1.01 ± 0.16 (1.67 µg/ml kinase) and 1.09 ± 0.30 (4.16 µg/ml kinase).

**Figure 4.** Removal of the 5-phosphate from PI(4,5)P<sub>2</sub> inhibits fusion. **a**, Demonstration of the effect of the phosphatase by thin layer chromatography (TLC). COPI vesicles (1.25 µg) in kinase buffer supplemented with P<sup>32</sup>-γ-ATP were incubated for 60 min at 37°C (lane 1) in the presence of 15µg/ml phosphatase (lane 2) or heat inactivated phosphatase (HI) (lane 3). The film was exposed for 4 days. **b**, non-saturating amount of vesicles was added to Lec1 membranes after pre-incubation for 60 min at 37°C with increasing amounts of phosphatase (□) or heat inactivated (HI) phosphatase (○). **c**, C<sub>v</sub><sup>app</sup> determination after vesicles were incubated with 0 (○), 10 (□), 20 (◇) or 40 (△) µg/ml of the purified phosphatase for 60 min at 37°C. Vesicles lost their activity to fuse to the extent of 0.60 ± 0.05 (10 µg/ml) 0.43 ± 0.05 (20 µg/ml) 0.31 ± 0.02 (40 µg/ml) as compared to control (no phosphatase).

**Figure 5.** Rescue of COPI vesicle fusion by kinase is reversed by phosphatase treatment. **a**, a non-saturating amount of vesicles was incubated at 37°C for 60 min in presence of 1.67 µg/ml of kinase type 1β (K, experiments 3,5,6,7) or heat inactivated kinase (HIK, experiment 2). Following the first incubation with kinase, vesicles were further incubated for a second round at 37°C for 60 min in the presence of 10 µg/ml of phosphatase (P, experiment 6), heat inactivated phosphatase (HIP, experiment 7) or without any further addition (60, experiment 5). The control consists of vesicles without pre-incubation (-, experiment 1), or vesicles incubated for 2 x 60min. (experiment 4). **b**, C<sub>v</sub><sup>app</sup> determination. Increasing amounts of vesicles were incubated at 37°C for 2 x 60 min (□, 0.24 ± 0.03), with 1.67 µg/ml of kinase the first 60 min. and 10 µg/ml phosphatase (△, 0.14 ± 0.04) or heat inactivated phosphatase (◇, 0.56 ± 0.16) for the second 60 min. Controls were kept on ice (○).

**Figure 6.** PI(4,5)P<sub>2</sub> synthesis does not affect the fusogenicity of target Golgi membranes. Lec1 Golgi (2.7 µg) in KB were incubated in the presence of 20 µg/ml of phosphatase (**a** and **c**) or 4.16 µg/ml of kinase (K) (**b** and **d**) for 60 min at 37°C. **a** and **b**, TLC separation of P<sup>32</sup>-labeled phospholipids formed in the presence of the phosphatase (P), heat-inactivated phosphatase (HIP), kinase (K) or heat-inactivated kinase (HIK). The film was exposed for 2 hours. **c**, Fusion assay determining the C<sub>v</sub><sup>app</sup> with Lec1 Golgi membranes pre-treated with phosphatase (□) or heat-inactivated phosphatase (○). C<sub>v</sub><sup>app</sup> after phosphatase treatment was 1.18 ± 0.30 compared to after incubation with heat-inactivated phosphatase, in **d**, Lec1 Golgi membranes pre-treated with kinase (□) or heat-inactivated kinase (○). C<sub>v</sub><sup>app</sup> after kinase treatment was 1.03 ± 0.18 compared to incubations with heat-inactivated kinase.



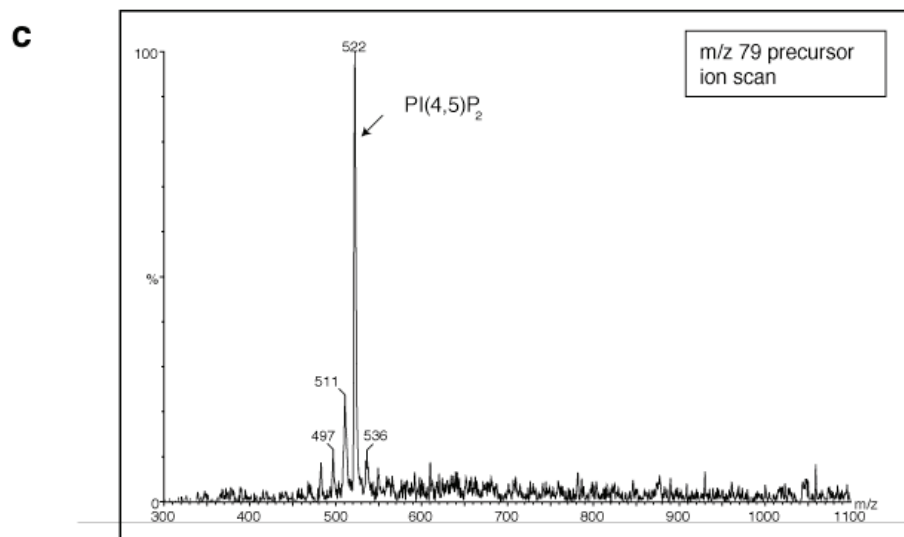
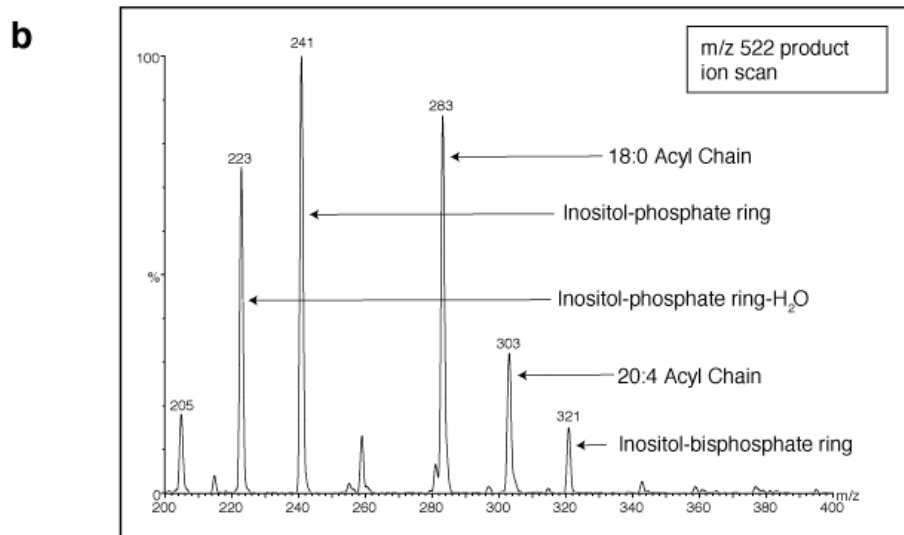
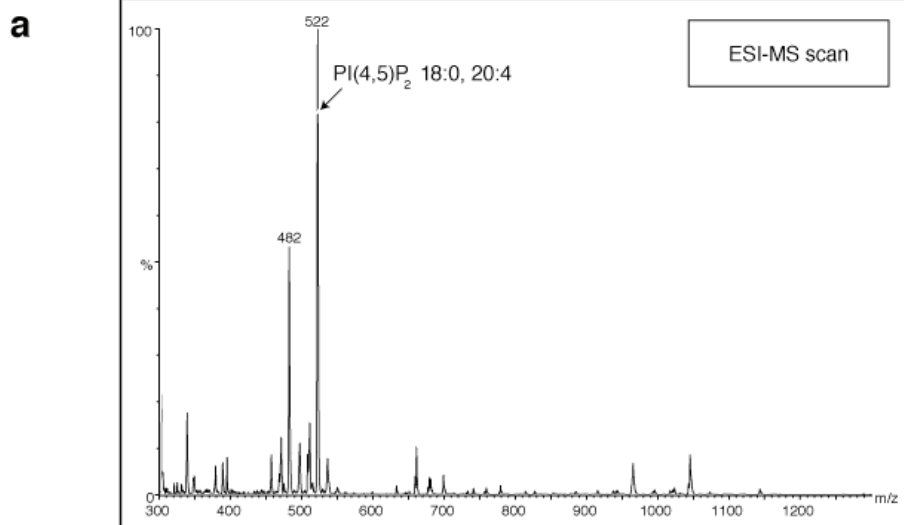
## Supplementary Material

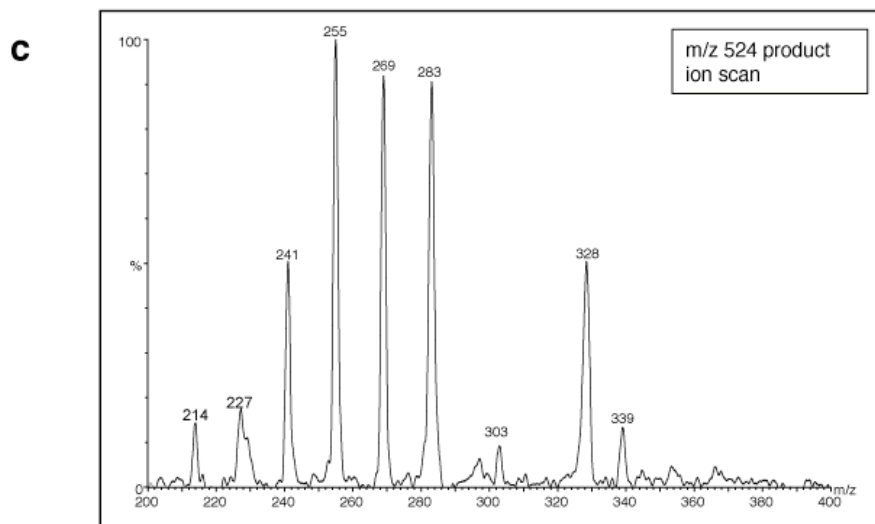
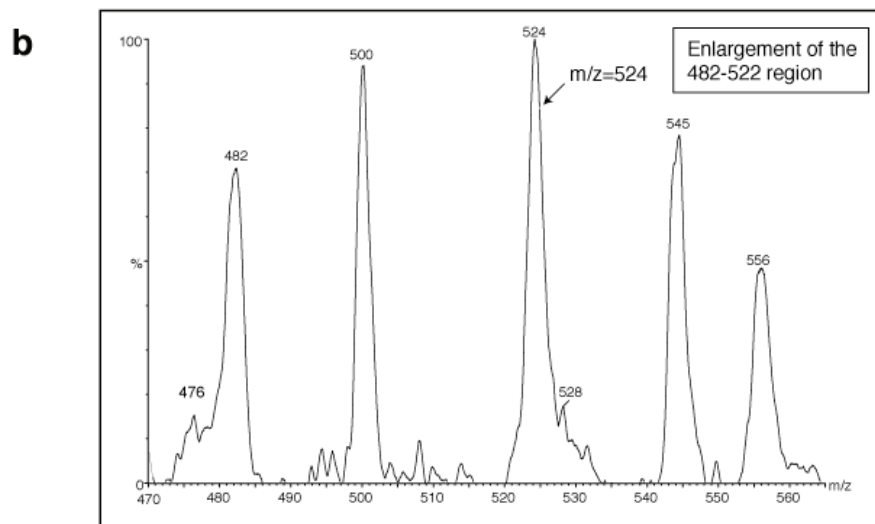
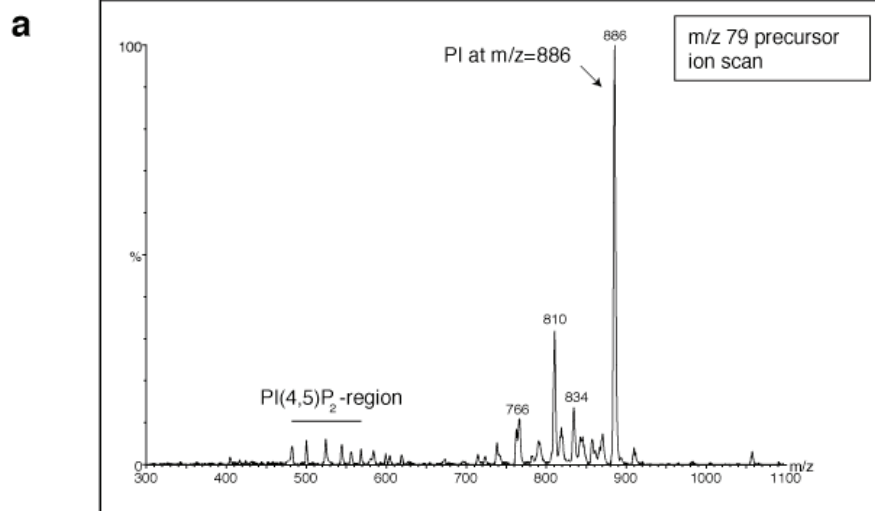
PI(4,5)P<sub>2</sub> has been identified in the Golgi apparatus, both *in vitro*<sup>48</sup> and *in vivo*<sup>49</sup>, however it is relatively unstable *in vitro*<sup>48</sup>. We have confirmed that there is little if any PI(4,5)P<sub>2</sub> in purified rat liver Golgi, and for this reason we have employed a protocol for the *in vitro* generation of PI(4,5)P<sub>2</sub> in our Golgi preparation<sup>48</sup>. PI(4,5)P<sub>2</sub> generated in this manner was then characterized by negative ion mode ESI-MS in order to authenticate its identity by comparison to PI(4,5)P<sub>2</sub> standards (Avanti, Alabaster AL).

ESI-MS analysis (Sup. 1a) of commercially available PI(4,5)P<sub>2</sub> (M.W. 1045, acyl chains 18:0 and 20:4) dissolved in 30 mM triethylamine (70% acetonitrile, 30% water) revealed the characteristic doubly charged negative ion at m/z 522 plus hydrolysis product PI(4)P at m/z 482 (which was diminished in intensity for fresh preparations (Sup. 1c)). Collision induced dissociation (CID) of either PI(4,5)P<sub>2</sub> (m/z 522) or PI(4)P (m/z 482) revealed the fragmentation pattern (Sup. 1b) of characteristic singly charged negative ions corresponding to the 18:0 and 20:4 acyl chains (m/z 283 and 303, respectively), the inositol phosphate and bisphosphate fragments (m/z, 241 and 321, respectively) and the dehydrated inositol phosphate (m/z 223)<sup>51, 52</sup>. Further characterization of the PI(4,5)P<sub>2</sub> standard by precursor ion (m/z 79) scans (Sup. 1c) confirmed the presence of phosphate on m/z 522 (PI(4,5)P<sub>2</sub>), 482 (PI(4)P) and probably other phosphoinositides with different acyl chains (m/z 497 and 511 corresponding to 34:1 and 36:1, respectively). Under these conditions, a detection limit of 10ng/ml was realized for PI(4,5)P<sub>2</sub>.

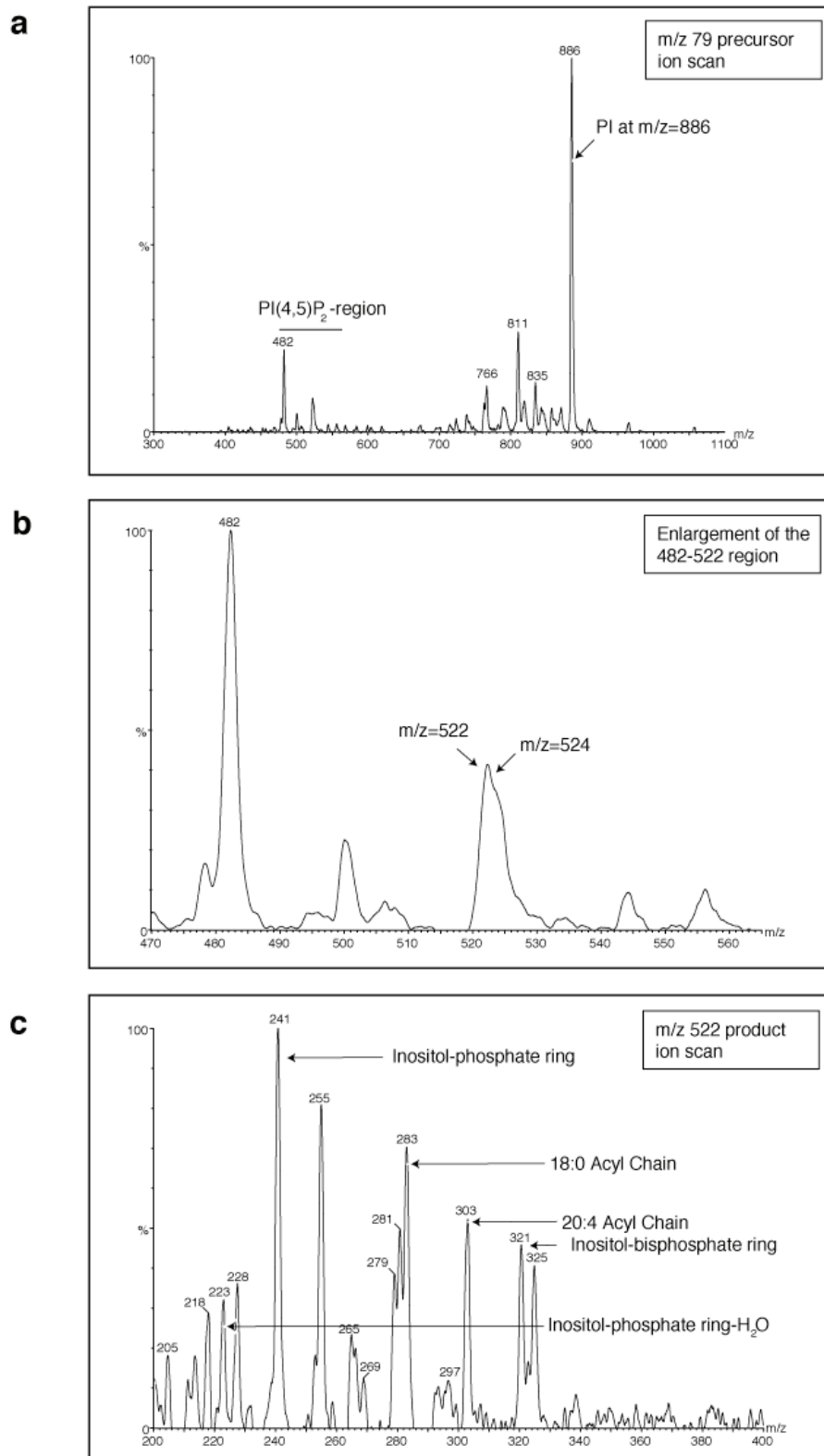
Employing the phospholipid extraction methodology of Siddhanta et al.<sup>48</sup>, we attempted to identify PI(4,5)P<sub>2</sub> in our Golgi preparations. Characterisation of chloroform/methanolic HCl extractions of purified rat liver Golgi by ESI-MS employing precursor ion scans of m/z 79 (Sup. 2a and b) failed to detect the characteristic m/z 522 of PI(4,5)P<sub>2</sub> (see Sup. 1c) but revealed an interfering phosphorylated ion of m/z 524. CID (Sup. 2c) of m/z 524 revealed a spectrum with fragment ions (m/z 255, 269, 328) unique to the 524 precursor ion and also fragment ions in common with those of PI(4,5)P<sub>2</sub> (namely m/z 241, 283 and 303). PI(4,5)P<sub>2</sub> fragmentation (Sup. 1c) however, generated ions (m/z 223, 321) that are unique and distinguishable from fragmentation product m/z 524 (compare Sup. 1b with 2c).

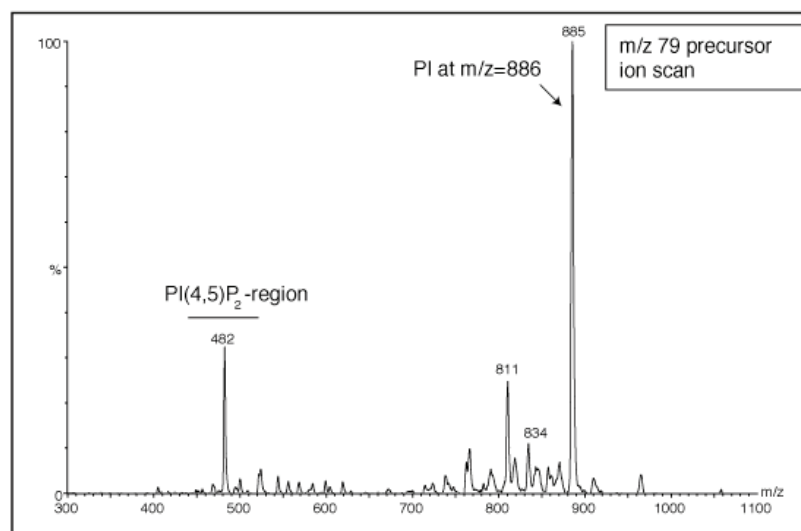
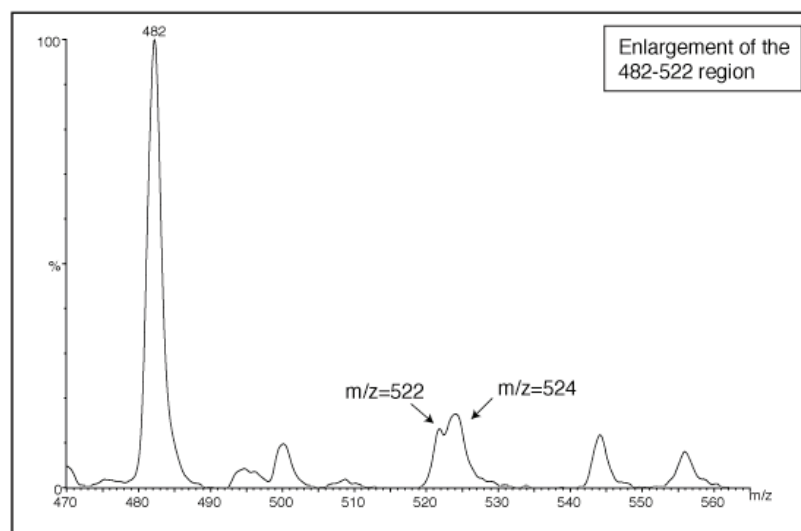
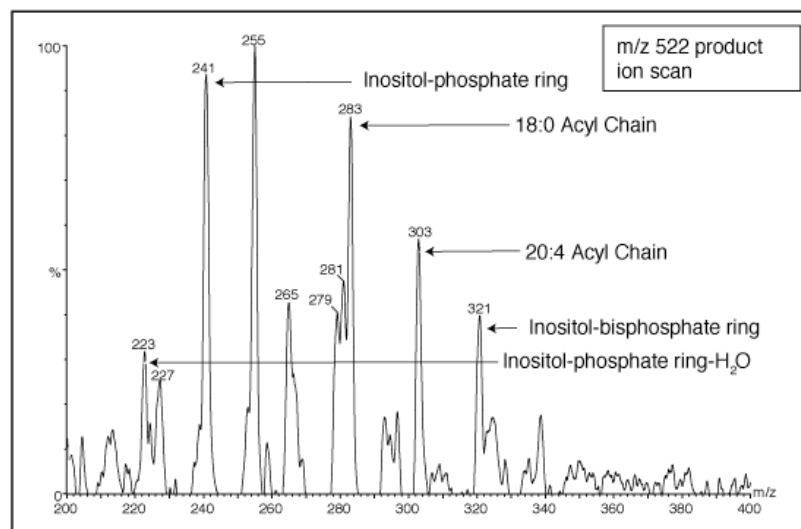
Treatment of purified rat liver Golgi with ATP and rat brain cytosol or purified mouse GST-PI(4)P5-kinase type 1 $\beta$  for 12 min. at 37°C, followed by phospholipid extraction and ESI-MS analysis resulted in the generation of PI(4,5)P<sub>2</sub> as indicated by detection of the 522 ion (compare Sup. 3a-b and Sup. 4a-b to Sup. 2b). Fragmentation of the *in vitro* generated m/z 522 revealed ions characteristic of PI(4,5)P<sub>2</sub> (m/z 223 and 321) and of the interfering 524 ions plus new ions probably related to ATP and cytosol (m/z 218, 228, 265, 281, 279, 297, 325) or purified kinase (m/z 227).





**Sup 2, Laporte et al.**



**a****b****c**

**Supplemental figure 1:** Characterization of PI(4,5)P<sub>2</sub>. **a**, Direct infusion (5µl/min) negative ion mode electrospray ionization mass spectrometry (ESI-MS) of commercial PI(4,5)P<sub>2</sub> dissolved in 30 mM triethylamine (70% acetonitrile, 30% water). **b**, CID (collision gas 2.0 x10<sup>-3</sup> mBar Argon) MS of PI(4,5)P<sub>2</sub> (m/z 522). **c**, Precursor ion scan (m/z 79) of freshly prepared PI(4,5)P<sub>2</sub> standard.

**Supplemental figure 2:** ESI-MS analysis of chloroform/methanolic HCl Golgi Extract. Purified rat liver Golgi (100µg) extract (see methods), dissolved in 30mM triethylamine (70% acetonitrile, 30% water) analyzed **a**) by precursor ion scan (m/z 79) with enlargement **b**) of the PI(4)P (m/z 482) and PI(4,5)P<sub>2</sub> (m/z 522) doubly charged ion region of the MS. **c**) CID MS of m/z 524 displaying the product ion profile.

**Supplemental Figure 3:** Generation of PI(4,5)P<sub>2</sub> by treatment of purified rat liver Golgi with rat brain cytosol plus ATP. As in Figure 2 but Golgi was pre-treated with rat brain cytosol (5mg/ml final) plus ATP (0.5mM) prior to phospholipid extraction. **a**, Precursor ion scan m/z 79 and **b**) enlargement of the PI(4)P (m/z 482) and PI(4,5)P<sub>2</sub> (m/z 522) doubly charged ion region of the MS. **c**, CID MS of the m/z 522/524 ion displaying the product ion profile.

**Supplemental Figure 4:** Generation of PI(4,5)P<sub>2</sub> by treatment of purified rat liver Golgi with kinase plus ATP. As in Figure 2 but Golgi was pre-treated with kinase (3.125 µg/ml) plus ATP (0.5mM) prior to phospholipid extraction. **a**, Precursor ion scan m/z 79 and **b**) enlargement of the PI(4)P (m/z 482) and PI(4,5)P<sub>2</sub> (m/z 522)

doubly charged ion region of the MS. **c**, CID MS of the  $m/z$  522/524 ion displaying the product ion profile.



## References

1. Watson, P., Forster, R., Palmer, K. J., Pepperkok, R. & Stephens, D. J. Coupling of ER exit to microtubules through direct interaction of COPII with dynactin. *Nat Cell Biol* 7, 48-55 (2005).
2. Presley, J. F. et al. ER-to-Golgi transport visualized in living cells. *Nature* 389, 81-5 (1997).
3. Scales, S. J., Pepperkok, R. & Kreis, T. E. Visualization of ER-to-Golgi transport in living cells reveals a sequential mode of action for COPII and COPI. *Cell* 90, 1137-48 (1997).
4. Kartberg, F., Elsner, M., Fröderberg, L., Asp, L. & Nilsson, T. Commuting between Golgi cisternae-mind the GAP! *Biochim Biophys Acta* in the press (2005).
5. Miller, E., Antonny, B., Hamamoto, S. & Schekman, R. Cargo selection into COPII vesicles is driven by the Sec24p subunit. *Embo J* 21, 6105-13 (2002).
6. Mossessova, E., Bickford, L. C. & Goldberg, J. SNARE selectivity of the COPII coat. *Cell* 114, 483-95 (2003).
7. Honda, A., Al-Awar, O. S., Hay, J. C. & Donaldson, J. G. Targeting of Arf-1 to the early Golgi by membrin, an ER-Golgi SNARE. *J Cell Biol* 168, 1039-51 (2005).
8. Lee, S. Y., Yang, J. S., Hong, W., Premont, R. T. & Hsu, V. W. ARFGAP1 plays a central role in coupling COPI cargo sorting with vesicle formation. *J Cell Biol* 168, 281-90 (2005).
9. Rein, U., Andag, U., Duden, R., Schmitt, H. D. & Spang, A. ARF-GAP-mediated interaction between the ER-Golgi v-SNAREs and the COPI coat. *J Cell Biol* 157, 395-404 (2002).
10. Rothman, J. E. & Warren, G. Implications of the SNARE hypothesis for intracellular membrane topology and dynamics. *Curr Biol* 4, 220-33 (1994).
11. Parlati, F. et al. Rapid and efficient fusion of phospholipid vesicles by the alpha-helical core of a SNARE complex in the absence of an N-terminal regulatory domain. *Proc Natl Acad Sci U S A* 96, 12565-70 (1999).
12. Fasshauer, D., Antonin, W., Margittai, M., Pabst, S. & Jahn, R. Mixed and non-cognate SNARE complexes. Characterization of assembly and biophysical properties. *J Biol Chem* 274, 15440-6 (1999).
13. Malsam, J., Gommel, D., Wieland, F. T. & Nickel, W. A role for ADP ribosylation factor in the control of cargo uptake during COPI-coated vesicle biogenesis. *FEBS Lett* 462, 267-72 (1999).
14. Lanoix, J. et al. GTP hydrolysis by arf-1 mediates sorting and concentration of Golgi resident enzymes into functional COP I vesicles. *Embo J* 18, 4935-48 (1999).
15. Pepperkok, R., Whitney, J. A., Gomez, M. & Kreis, T. E. COPI vesicles accumulating in the presence of a GTP restricted arf1 mutant are depleted of anterograde and retrograde cargo. *J Cell Sci* 113 (Pt 1), 135-44 (2000).
16. Stamnes, M., Schiavo, G., Stenbeck, G., Sollner, T. H. & Rothman, J. E. ADP-ribosylation factor and phosphatidic acid levels in Golgi membranes during budding of coatamer-coated vesicles. *Proc Natl Acad Sci U S A* 95, 13676-80 (1998).

17. Presley, J. F. et al. Dissection of COPI and Arf1 dynamics in vivo and role in Golgi membrane transport. *Nature* 417, 187-93 (2002).
18. Bigay, J., Gounon, P., Robineau, S. & Antonny, B. Lipid packing sensed by ArfGAP1 couples COPI coat disassembly to membrane bilayer curvature. *Nature* 426, 563-6 (2003).
19. Elsner, M. et al. Spatiotemporal dynamics of the COPI vesicle machinery. *EMBO Rep* 4, 1000-4 (2003).
20. Liu, W., Duden, R., Phair, R. D. & Lippincott-Schwartz, J. ArfGAP1 dynamics and its role in COPI coat assembly on Golgi membranes of living cells. *J Cell Biol* 168, 1053-63 (2005).
21. Brown, H. A., Gutowski, S., Moomaw, C. R., Slaughter, C. & Sternweis, P. C. ADP-ribosylation factor, a small GTP-dependent regulatory protein, stimulates phospholipase D activity. *Cell* 75, 1137-44 (1993).
22. Cockcroft, S. et al. Phospholipase D: a downstream effector of ARF in granulocytes. *Science* 263, 523-6 (1994).
23. Brown, H. A., Gutowski, S., Kahn, R. A. & Sternweis, P. C. Partial purification and characterization of Arf-sensitive phospholipase D from porcine brain. *J Biol Chem* 270, 14935-43 (1995).
24. Houle, M. G., Kahn, R. A., Naccache, P. H. & Bourgoïn, S. ADP-ribosylation factor translocation correlates with potentiation of GTP gamma S-stimulated phospholipase D activity in membrane fractions of HL-60 cells. *J Biol Chem* 270, 22795-800 (1995).
25. Ktistakis, N. T., Brown, H. A., Sternweis, P. C. & Roth, M. G. Phospholipase D is present on Golgi-enriched membranes and its activation by ADP ribosylation factor is sensitive to brefeldin A. *Proc Natl Acad Sci U S A* 92, 4952-6 (1995).
26. Ktistakis, N. T., Brown, H. A., Waters, M. G., Sternweis, P. C. & Roth, M. G. Evidence that phospholipase D mediates ADP ribosylation factor-dependent formation of Golgi coated vesicles. *J Cell Biol* 134, 295-306 (1996).
27. Chen, Y. G. et al. Phospholipase D stimulates release of nascent secretory vesicles from the trans-Golgi network. *J Cell Biol* 138, 495-504 (1997).
28. Siddhanta, A. & Shields, D. Secretory vesicle budding from the trans-Golgi network is mediated by phosphatidic acid levels. *J Biol Chem* 273, 17995-8 (1998).
29. Antonny, B., Huber, I., Paris, S., Chabre, M. & Cassel, D. Activation of ADP-ribosylation factor 1 GTPase-activating protein by phosphatidylcholine-derived diacylglycerols. *J Biol Chem* 272, 30848-51 (1997).
30. Bigay, J., Casella, J. F., Drin, G., Mesmin, B. & Antonny, B. ArfGAP1 responds to membrane curvature through the folding of a lipid packing sensor motif. *Embo J* (2005).
31. Yanagisawa, L. L. et al. Activity of specific lipid-regulated ADP ribosylation factor-GTPase-activating proteins is required for Sec14p-dependent Golgi secretory function in yeast. *Mol Biol Cell* 13, 2193-206 (2002).
32. Jenkins, G. H., Fiset, P. L. & Anderson, R. A. Type I phosphatidylinositol 4-phosphate 5-kinase isoforms are specifically stimulated by phosphatidic acid. *J Biol Chem* 269, 11547-54 (1994).
33. Oude Weernink, P. A., Schmidt, M. & Jakobs, K. H. Regulation and cellular roles of phosphoinositide 5-kinases. *Eur J Pharmacol* 500, 87-99 (2004).
34. Mayer, A. et al. Phosphatidylinositol 4,5-bisphosphate regulates two steps of homotypic vacuole fusion. *Mol Biol Cell* 11, 807-17 (2000).

35. Kanzaki, M., Furukawa, M., Raab, W. & Pessin, J. E. Phosphatidylinositol 4,5-bisphosphate regulates adipocyte actin dynamics and GLUT4 vesicle recycling. *J Biol Chem* 279, 30622-33 (2004).
36. Lee, E. & De Camilli, P. Dynamin at actin tails. *Proc Natl Acad Sci U S A* 99, 161-6 (2002).
37. Aikawa, Y. & Martin, T. F. ARF6 regulates a plasma membrane pool of phosphatidylinositol(4,5)bisphosphate required for regulated exocytosis. *J Cell Biol* 162, 647-59 (2003).
38. Gong, L. W. et al. Phosphatidylinositol phosphate kinase type I gamma regulates dynamics of large dense-core vesicle fusion. *Proc Natl Acad Sci U S A* 102, 5204-9 (2005).
39. Grishanin, R. N. et al. CAPS acts at a prefusion step in dense-core vesicle exocytosis as a PIP2 binding protein. *Neuron* 43, 551-62 (2004).
40. Sadakata, T. et al. The secretory granule-associated protein CAPS2 regulates neurotrophin release and cell survival. *J Neurosci* 24, 43-52 (2004).
41. Murthy, V. N. & De Camilli, P. Cell biology of the presynaptic terminal. *Annu Rev Neurosci* 26, 701-28 (2003).
42. Stojilkovic, S. S. Ca<sup>2+</sup>-regulated exocytosis and SNARE function. *Trends Endocrinol Metab* 16, 81-3 (2005).
43. Tucker, W. C. et al. Identification of synaptotagmin effectors via acute inhibition of secretion from cracked PC12 cells. *J Cell Biol* 162, 199-209 (2003).
44. Aoyagi, K. et al. The activation of exocytotic sites by the formation of phosphatidylinositol-4,5-bisphosphate microdomains at syntaxin clusters. *J Biol Chem* (2005).
45. Holz, R. W. et al. A pleckstrin homology domain specific for phosphatidylinositol 4, 5-bisphosphate (PtdIns-4,5-P<sub>2</sub>) and fused to green fluorescent protein identifies plasma membrane PtdIns-4,5-P<sub>2</sub> as being important in exocytosis. *J Biol Chem* 275, 17878-85 (2000).
46. Milosevic, I. et al. Plasmalemmal phosphatidylinositol-4,5-bisphosphate level regulates the releasable vesicle pool size in chromaffin cells. *J Neurosci* 25, 2557-65 (2005).
47. Sweeney, D. A., Siddhanta, A. & Shields, D. Fragmentation and re-assembly of the Golgi apparatus in vitro. A requirement for phosphatidic acid and phosphatidylinositol 4,5-bisphosphate synthesis. *J Biol Chem* 277, 3030-9 (2002).
48. Siddhanta, A., Radulescu, A., Stankewich, M. C., Morrow, J. S. & Shields, D. Fragmentation of the Golgi apparatus. A role for beta III spectrin and synthesis of phosphatidylinositol 4,5-bisphosphate. *J Biol Chem* 278, 1957-65 (2003).
49. Watt, S. A., Kular, G., Fleming, I. N., Downes, C. P. & Lucocq, J. M. Subcellular localization of phosphatidylinositol 4,5-bisphosphate using the pleckstrin homology domain of phospholipase C delta1. *Biochem J* 363, 657-66 (2002).
50. De Matteis, M., Godi, A. & Corda, D. Phosphoinositides and the golgi complex. *Curr Opin Cell Biol* 14, 434-47 (2002).
51. Wenk, M. R. et al. Phosphoinositide profiling in complex lipid mixtures using electrospray ionization mass spectrometry. *Nat Biotechnol* 21, 813-7 (2003).
52. Hsu, F. F. & Turk, J. Characterization of phosphatidylinositol, phosphatidylinositol-4-phosphate, and phosphatidylinositol-4,5-bisphosphate

- by electrospray ionization tandem mass spectrometry: a mechanistic study. *J Am Soc Mass Spectrom* 11, 986-99 (2000).
53. Godi, A. et al. ARF mediates recruitment of PtdIns-4-OH kinase-beta and stimulates synthesis of PtdIns(4,5)P<sub>2</sub> on the Golgi complex. *Nat Cell Biol* 1, 280-7 (1999).
  54. Jones, D. H. et al. Type I phosphatidylinositol 4-phosphate 5-kinase directly interacts with ADP-ribosylation factor 1 and is responsible for phosphatidylinositol 4,5-bisphosphate synthesis in the golgi compartment. *J Biol Chem* 275, 13962-6 (2000).
  55. Lin, C. C., Love, H. D., Gushue, J. N., Bergeron, J. J. & Ostermann, J. ER/Golgi intermediates acquire Golgi enzymes by brefeldin A-sensitive retrograde transport in vitro. *J Cell Biol* 147, 1457-72 (1999).
  56. Elazar, Z. et al. ADP-ribosylation factor and coatamer couple fusion to vesicle budding. *J Cell Biol* 124, 415-24 (1994).
  57. Balch, W. E., Dunphy, W. G., Braell, W. A. & Rothman, J. E. Reconstitution of the transport of protein between successive compartments of the Golgi measured by the coupled incorporation of N-acetylglucosamine. *Cell* 39, 405-16 (1984).
  58. Saraste, J. & Kuismänen, E. Pre- and post-Golgi vacuoles operate in the transport of Semliki Forest virus membrane glycoproteins to the cell surface. *Cell* 38, 535-49 (1984).
  59. Ostermann, J. Stoichiometry and kinetics of transport vesicle fusion with Golgi membranes. *EMBO Rep* 2, 324-9 (2001).
  60. Kartberg, F., Hiding, J. & Nilsson, T. Purification of COPI Vesicles (ed. Juilto E. Celis, N. C., Kai Simons) (Academic Pr, 2005).
  61. Lanoix, J. et al. Sorting of Golgi resident proteins into different subpopulations of COPI vesicles: a role for ArfGAP1. *J Cell Biol* 155, 1199-212 (2001).
  62. Guo, S., Stolz, L. E., Lemrow, S. M. & York, J. D. SAC1-like domains of yeast SAC1, INP52, and INP53 and of human synaptojanin encode polyphosphoinositide phosphatases. *J Biol Chem* 274, 12990-5 (1999).
  63. Wang, Y. J. et al. Phosphatidylinositol 4 phosphate regulates targeting of clathrin adaptor AP-1 complexes to the Golgi. *Cell* 114, 299-310 (2003).
  64. Yamazaki, M. et al. Phosphatidylinositol 4-phosphate 5-kinase is essential for ROCK-mediated neurite remodeling. *J Biol Chem* 277, 17226-30 (2002).
  65. Martin, B., Pallen, C. J., Wang, J. H. & Graves, D. J. Use of fluorinated tyrosine phosphates to probe the substrate specificity of the low molecular weight phosphatase activity of calcineurin. *J Biol Chem* 260, 14932-7 (1985).
  66. Stanley, P., Caillibot, V. & Siminovitch, L. Selection and characterization of eight phenotypically distinct lines of lectin-resistant Chinese hamster ovary cell. *Cell* 6, 121-8 (1975).
  67. Siddhanta, A., Backer, J. M. & Shields, D. Inhibition of phosphatidic acid synthesis alters the structure of the Golgi apparatus and inhibits secretion in endocrine cells. *J Biol Chem* 275, 12023-31 (2000).
  68. Stamnes, M. et al. An integral membrane component of coatamer-coated transport vesicles defines a family of proteins involved in budding. *Proc Natl Acad Sci U S A* 92, 8011-5 (1995).

## **Membrane binding and fusion ability of COPI vesicles upon protease treatment**

Frederic Laporte<sup>\*§</sup>, Joachim Ostermann<sup>\*§</sup>, Johan Hiding, Fredrik Kartberg, Joel Lanoix<sup>†</sup>, John JM Bergeron<sup>§</sup> and Tommy Nilsson

Department of Medical and Clinical Genetics, Institute of Biomedicine, Göteborg University, 405 30 Gothenburg, Sweden and <sup>§</sup> Department of Cell Biology and Anatomy, McGill University, Montreal, Quebec H3A 2B2, Canada

<sup>†</sup> Present addresss Caprion Pharmaceuticals Inc., 7150 Alexander Fleming Street, Montreal, Quebec, H4P 1P7, Canada.

\* The two first authors contributed equally to this work

**Correspondence to [Tommy.Nilsson@gu.se](mailto:Tommy.Nilsson@gu.se)**

## Summary

COPI vesicles are effective transport carriers of resident Golgi enzymes between cisternal Golgi membranes, *in vitro*. This was demonstrated using a modified version of the Rothman *in vitro* transport assay where donor membranes had been replaced with purified COPI vesicles. As predicted, COPI vesicles fused in an NSF and  $\alpha$ -SNAP dependent manner. One important aspect of the Rothman assay is that it enables kinetic evaluation of both budding, binding and final fusion of COPI vesicles. In this study, we use protease K to determine the effect on vesicle binding and fusion. Though we find that protease treatment decreases the rate of binding, we observe little or no effect on the actual fusion rate. In contrast, protease treatment of acceptor membranes effectively abolishes both binding and fusion. This suggests a heterotypic fusion event between COPI vesicles and Golgi cisternae supporting the notion that COPI transport carriers are both biochemically and functionally distinct from Golgi cisternae.

## Introduction

Transport of biosynthetic proteins through the secretory pathway requires two different types of carriers termed COPI and COPII vesicles. Whereas COPII vesicles are responsible for the controlled release of biosynthetic cargo from the ER, COPI vesicles form from multiple post-ER compartments such as the ER to Golgi intermediate compartment (ERGIC)/vesicular tubular carriers (VTCs) and Golgi cisternae. Though the precise role(s) of COPI vesicles in transport is still being elucidated, much data argues in favor for a role in both anterograde and retrograde transport (for recent reviews, see (Bethune et al., 2006; Kartberg et al., 2005)). The importance of COPI vesicles as transport intermediates has been underscored multiple times. Using an *in vitro*-based transport assay (Balch et al., 1984a) where the glycosylation status of vesicular stomatitis virus G (VSV-G) protein is monitored, Rothman and co-workers could identify, confirm or in other ways characterize most of the important intra Golgi transport components that we use today. This work was paralleled by Schekman and co-workers who used yeast genetics to identify and characterize much the same components. Together, Rothman and Schekman showed that COPI and COPII vesicles are vesicular transport carriers that can be defined by their coat and that both require a defined set of molecules for their formation, binding and fusion. The identification of NSF (N-ethylmaleimide-sensitive factor) and SNAP (soluble NSF attachment protein) as being required for fusion of vesicles led to the insight that the membrane constituents of synaptic vesicles, VAMP and syntaxin, were in fact receptors for NSF and SNAP (Sollner et al., 1993). Henceforth, these receptors were termed SNAREs (soluble NSF attachment receptors) and today, form a large family of receptors that consists of 36 members in humans (for a recent review, see (Jahn and Scheller, 2006)).

The exact mechanism whereby SNARE proteins contribute to fusion is still being



investigated. On a structural basis, they can be separated into R- and Q-SNAREs which form stable complexes in the membrane consisting of 3Q and 1R SNARE (Q and R refers to amino acids glutamine and arginine, respectively, and are found in the central position of the SNARE motif). The 3Q:1R ratio is important for SNARE function *in vivo* (Katz and Brennwald, 2000; Ossig et al., 2000).

The current view is that SNARE proteins on opposing membranes interact and form parallel bundles. This creates stable receptor complexes that persist after fusion and such *cis* SNARE complex then needs to be dissociated in order for SNARE proteins to be reused in further fusion cycles (Mayer et al., 1996). This dissociation is mediated by the NSF complex, which is recruited through the binding of  $\alpha$ -SNAP molecules to the SNARE complex (Hanson et al., 1997; Lenzen et al., 1998; Sollner et al., 1993; Yu et al., 1998). According to the SNARE-pin hypothesis for membrane fusion (Weber et al., 1998), the formation of a *trans* complex of SNAREs bridging both membranes is suggested to pull the membranes to within 4 nm of each other (Jahn and Sudhof, 1999). Indeed, Weber et al. (Weber et al., 1998) could fuse artificial liposomes containing SNAREs and this, together with the finding that such fusion depends on how the SNAREs are anchored to the membranes (McNew et al., 2000b), provide evidence for a SNARE-pin scenario which, albeit slowly, can drive fusion *in vitro*.

One of the postulates of the original SNARE hypothesis formulated by Rothman and coworkers in the early 90s was that SNARE proteins specifically target transport vesicles to the right membrane with which they are to fuse. In other words, each “cognate” SNARE proteins form stable complexes in only one particular trafficking step. This was later supported by findings showing that cognate SNAREs result in better fusion than non-cognate ones using artificial liposomes (McNew et al., 2000a). However, Scheller and coworkers



(Calakos et al., 1994) showed that synaptobrevin-2/VAMP-2 binds to different syntaxins. The yeast SNAREs Sed5p and Vti1p, also seem to function in more than one transport step suggesting extensive promiscuity among SNARE proteins (Tsui and Banfield, 2000). *In vitro*, complexes formed with four different SNAREs further shows that one of the Q-SNAREs has to belong to the syntaxin subfamily and the two others to subfamilies homologous to the first and the second SNARE motif of SNAP-25, respectively. Substitution of particular SNAREs within these defined subfamilies can occur without influencing complex formation (Fasshauer et al., 1999). Recent biochemical data suggest that the initial fusion pore of vacuoles is not lipidic (as it is in the case of viral fusion) but rather a proteinaceous channel formed by two opposing V0 hexamers of vacuolar H<sup>+</sup>-ATPases, binding head-to-head in a process that requires Ypt7GTP and calmodulin. Upon signaling by calcium-bound calmodulin, the V0 hexamers segregate whereby lipids are thought to invade the space to form an aqueous fusion pore (Peters et al., 2001). Fusion of vacuolar membranes requires the action of protein phosphatase 1 (PP1) which is complexed with calmodulin. This step is thought to be the final step triggering the actual fusion event and placed downstream of the action of SNARE proteins (Peters et al., 1999). Therefore, much data exist to suggest that the current model for how SNARE proteins drives fusion is too simplistic and that other steps and components are likely to be required.

When put into the context of intracellular transport, SNARE proteins are together with tethering factors and other accessory molecules thought to mediate the necessary specificity of fusion events so that correct membranes fuse. A requirement for high fidelity in fusion events is clear when considering the need to maintain the biochemical and functional differences between intracellular compartments of the cell at the same time as transporting

cargo between these compartments. This is perhaps why the cell uses distinct vesicle types; COPII vesicles to transport biosynthetic cargo out of ER towards the Golgi apparatus and COPI vesicles to return resident proteins such as SNAREs back to the ER. As the use of COPI vesicles is not restricted to the return of resident proteins to the ER but also includes multiple transport steps between adjacent cisternae of the Golgi apparatus, the makeup of COPI vesicles should differ between, for example, a vesicle that buds and fuses in the early part of the secretory pathway and one that buds and fuses in later parts. Indeed, we have others have demonstrated that sub-populations of COPI vesicles can be isolated and differentiated by their contents (Lanoix et al., 2001; Malsam et al., 2005). Such COPI vesicles were formed from highly purified rat liver Golgi membranes and when generated under conditions where GTP hydrolysis takes place, predominantly contain resident proteins of the secretory pathway (Gilchrist et al., 2006; Lanoix et al., 1999; Lanoix et al., 2001). Indeed, when used in a modified version of the Rothman transport assay where donor membranes were omitted, COPI vesicles effectively transferred the resident enzyme, N-acetylglucosaminyltransferase I (NAGTI), to acceptor membranes as judged by the resulting transfer of tritiated UDP-Nacetylglucoseamine onto the VSV-G protein. This transfer required NSF and  $\alpha$ -SNAP thus reflecting a functional transport event (Lanoix et al., 1999; Lanoix et al., 2001). Whether or not the transfer of NAGT-I activity by COPI vesicles reflected a homotypic or heterotypic fusion event was unclear.

In this study, we have investigated the relative sensitivity of SNARE proteins to protease treatment comparing vesicles and acceptor membranes. We find that whereas acceptor membranes are highly sensitive, vesicles remain fusigenic even after extensive protease treatment. Under these conditions, fusion remains cytosol, NSF and  $\alpha$ -SNAP dependent. This

is highly suggestive of a heterotypic fusion event where SNARE proteins on COPI vesicles have acquired a protease resistant conformation which is not present on the acceptor membrane.

## Material and Methods

### *In vitro* complementation assay and data analysis

Vesicles were isolated as described (Lanoix et al., 1999). Infection of lec1 Golgi membranes with VSV was performed essentially as described (Balch et al., 1984a) with the modifications described in (Colombo et al., 1991). Before homogenization and isolation of Golgi membranes, cells were incubated for 2 to 3 h at 15°C. *In vitro* complementation with [<sup>35</sup>S]-labeled VSV-G was done as described (Lin et al., 1999). Cytosol was prepared from lec1 cell homogenate and was desalted on PD10 columns. The cytosol concentration in the assay was 20% of the assay volume. The equations used to explain the assay signal in different experiments were derived from the experimental findings and models outlined in (Ostermann, 2001). Curve fitting of these equations to experimental data was done using MacCurveFit (Kevin Raner Software). Kinetic analysis of the complete reaction was done using Berkeley Madonna (Robert I. Macey and George F. Oster).

**Expression and purification of NSF, His<sub>6</sub>-tagged  $\alpha$ -SNAP<sup>wt</sup> and  $\alpha$ -SNAP<sup>dn</sup> mutant.** Recombinant His<sub>6</sub>-tagged NSF,  $\alpha$ -SNAP<sup>wt</sup> and  $\alpha$ -SNAP<sup>dn</sup> mutant were purified on Ni-NTA-agarose as described (Barnard et al., 1997). Recombinant proteins were desalted using a PD-10 column pre-equilibrated in 20 mM Hepes, pH 7.2, 150 mM NaCl, 1 mM MgCl<sub>2</sub>, 5% glycerol, 1 mM GSH and in the case of NSF, 5 mM ATP. Recombinant His<sub>6</sub>-tagged  $\alpha$ -SNAP<sup>dn</sup> mutant was aliquoted and snap-frozen.

## Results

**SNARE proteins are protease-sensitive components of transport vesicles.** We first determined whether transport vesicles formed *in vitro* (Lanoix et al., 1999) contained SNARE proteins, and whether these could be degraded by proteolysis. To digest peripherally exposed SNARE proteins and other cytoplasmically exposed proteins, we incubated vesicles with increasing amounts of proteinase K (PK) for 30 min on ice. PK was chosen as it is not selective. It can also be inactivated by covalent and irreversible modification with PMSF. The ability to inactivate PK after incubation with membranes is essential as it allows further studies of the protease-treated membranes in the absence of functional protease.

Of the known SNARE proteins of the Golgi, GS28 has been implicated in intra-Golgi vesicular trafficking as shown by addition of antibodies against GS28 (Nagahama et al., 1996) (see also (Subramaniam et al., 1996)). This is consistent with its observed steady state localization to the *medial* Golgi stack (42). GS28 has been shown to complex with the 34 kDa form of syntaxin 5 yielding a SNARE complex distinct from the 34/41 kDa forms of syntaxin 5 found in complex with membrin, rsec22b and rbet1, the three latter giving rise to a SNARE complex predominantly involved in ER to Golgi transport processes (Hay et al., 1998). As with all known SNARE proteins, GS28 is mostly cytoplasmically oriented and sensitive to proteolysis (Nagahama et al., 1996). This is also evident from Figure 1 where we monitored proteolytic removal of GS28 from COPI-derived vesicles formed *in vitro*. Approximately 50% of GS28 was degraded by 0.2

μg/ml PK. 2 μg/ml PK digested approximately 90% of GS28. The figure shows two exposures, one of which is overexposed to reveal small residual amounts of GS28 remaining

after proteolysis. We estimate that 90 to 99% of GS28 has been degraded when using between 2 and 20  $\mu\text{g/ml}$  PK. We also incubated Golgi membranes with PK and found that GS28 was equally sensitive as it is in vesicles, and no change in PK sensitivity was observed after prolonged incubation of Golgi membranes (data not shown). Other cytoplasmically exposed proteins with proposed roles in transport, such as GM130, had approximately equal sensitivities to protease digestion as GS28 (data not shown).

### **Target membranes are inactivated by proteolysis.**

The assay used to study Golgi transport measures the transfer of Golgi proteins between two different populations of Golgi membranes. One population is derived from vesicular stomatitis virus (VSV) infected *lec1* cells. Due to the molecular defect of *lec1* cells, the viral glycoprotein (VSV-G) is only partially glycosylated in the Golgi membranes of *lec1* cells. In this study, we incubated infected *lec1* Golgi membranes with transport vesicles formed *in vitro* through incubation of rat liver Golgi with cytosol followed by vesicle release and fractionation. The vesicles generated in this system contain high amounts of Golgi enzymes, which upon fusion with *lec1* membranes complete the glycosylation of VSV-G in these membranes (Lanoix et al., 1999; Ostermann, 2001). The glycosylation of VSV-G is detected as incorporation of radiolabeled N-acetylglucosamine (GlcNAc).

Before studying the effect of proteolysis on the properties of transport vesicles, we determined the amount of PK necessary to inactivate the *lec1* target membranes with which the vesicles fuse. We refer to these membranes as target membranes in order to avoid the previously used donor/acceptor nomenclature which is used to describe the hypothetical process of anterograde movement of secretory cargo originating from the *lec1* membranes to wild type (wt) Golgi membranes. Target membranes were incubated with increasing amounts

of PK for 30 min on ice, after which PMSF was added to inactivate PK. Treated membranes were then added to transport reactions containing vesicles, cytosol, an ATP-regenerating system and UDP-[<sup>3</sup>H]-GlcNAc. At all PK concentrations tested, we observed that the fusion of vesicles with these membranes was efficiently inhibited (Figure 2). Thus, the ability of target membranes to fuse with transport vesicles is highly sensitive to degradation of cytoplasmically oriented proteins on their surface.

### **Vesicle activity is partially resistant to proteolysis.**

If membrane fusion between transport vesicles and Golgi membranes is essentially symmetrical with both membranes contributing equally, vesicles should also be inactivated by proteolysis. Contrary to this, our initial experiments showed that vesicles fused with Golgi membranes even after vesicles had been treated with as much as 40 µg/ml PK. This finding prompted us to determine the kinetic parameters underlying the fusion event. Compared to target membranes, determining the fraction of vesicles that inactivates is less straightforward. As shown previously, the relationship between the amount of vesicles added and the assay signal is not linear (Ostermann, 2001). Rather, the dose-response curve is an inverse exponential curve and the relative initial increase (“slope”) of this curve is proportional to the concentration of functional vesicles in the assay. At saturating amounts of vesicles, the obtained assay signal is proportional to the concentration of target membranes that are capable of fusion with the added transport vesicles.

We added increasing amounts of vesicles to a transport mix with a fixed amount of Golgi membranes (Fig. 3A). Prior to addition to the assay, vesicles were either incubated for 30 min on ice with 2 µg/ml PK (squares) or left untreated (circles). 1 mM PMSF was then added to

inactivate PK before the vesicles were used in the transport assay. After addition of vesicles, the assay signal at the end of a 2 hour incubation at 37°C was determined. The maximum assay signal that could be obtained with the tested vesicle preparation and the slope of the measured dose-response curve were determined by curve fitting of the appropriate mathematical expression to the data (Ostermann, 2001). When vesicles were incubated with 2 µg/ml PK, which is enough to degrade at least 90% of GS28, the initial slope was reduced to  $62.4 \pm 7.8\%$  of the control value. In other words,  $62.4 \pm 7.8\%$  of vesicles remained active. Even at very high PK concentrations, such as 20 µg/ml, vesicles remained mostly active (Fig. 3B). At low PK concentrations, the assay signal at saturation was only slightly less ( $83.6 \pm 0.8\%$ ) than in the control incubation without PK. However, at high concentrations such as 20 µg/ml PK, the maximal assay signal was reduced by as much as 50%, even though there was no further decrease in the slope of the curve. As there was no further reduction in the slope of the curve, the addition of more PK did not decrease the activity of the vesicles. The reduction in the maximum assay signal can only be explained as an inactivation of the target membranes, in which the assay signal is generated. Most probably, at such high concentrations some PK had escaped inactivation with PMSF until the time the Golgi membranes were added. As Golgi membranes are highly sensitive to PK, even a small residual PK activity would reduce the assay signal. An inhibitory activity in the vesicle preparation that was treated with 20 µg/ml is evident in the data; when increasing amounts of vesicles are added the assay signal dropped rather than increased.

We decided to examine to what extent the partial inactivation of vesicles reflected a decrease in fusion and/or a preceding docking step. Given that proteins implicated in membrane docking are mostly cytoplasmically oriented, these are good targets for proteolysis.



Treatment of vesicles with PK would therefore be predicted to give rise to a decreased ability of COPI-derived vesicles to dock with target membranes. We showed previously that the ability of vesicles to fuse with target membranes is transient. The kinetics of inactivation was compared to the kinetics of binding revealing that a considerable fraction of all functional vesicles were inactivated over time in the cytosol before they had a chance to bind to Golgi membranes and fuse (Ostermann, 2001). For this reason, a reduction in the speed of binding is most easily detected by the reduction in the number of vesicles that fuse as more inactivate in the cytosol prior to binding. This inactivation-to-binding ratio can be measured by determining the sensitivity of a transport reaction to dilution. Dilution slows the binding step as it increases the distance between vesicles and Golgi membranes and reduces the number of collisions between them. If vesicles would not inactivate, dilution would have no effect on the number of vesicles that have fused at the end of the reaction. If inactivation were much faster than binding, than almost all vesicles would inactivate, and the assay signal would be generated by only a minor fraction of the vesicles that bound before inactivation. Thus, the fraction of vesicles that bind and fuse would be reduced by half if the reaction was diluted twofold.

Without proteolysis, we found that twofold dilution reduced the apparent vesicle concentration (or the slope of the dose-response curve) to  $73.6 \pm 1.0\%$  of the value measured before dilution (Fig. 4A). From this, we calculated that  $64.3 \pm 1.7\%$  of initially functional vesicles bind while the remainder inactivates. After incubation of vesicles with  $2 \mu\text{g/ml}$  PK, the apparent vesicle concentration dropped to  $63.4 \pm 1.5\%$  of the control value, or slightly less than what was determined (Fig. 4B). Therefore, after proteolysis only  $42.3 \pm 3.7\%$  of vesicles that were functional when added to the transport mix did actually bind and fuse

before they inactivated. When PK concentrations were added that degraded only a smaller fraction of cytoplasmically oriented vesicle proteins, then the reduction of the binding efficiency was less (Fig. 4C). The observed reduction in the binding to inactivation ratio can be explained as a reduction in the binding kinetics to about one third of the control value, or less if the rate of inactivation increases after proteolysis. The reduction of the fraction of vesicles that bind and fuse rather than inactivate, which is  $66.7 \pm 5.8\%$  when expressed as a fraction of the control without PK, is in good agreement with the observed reduction of the apparent vesicle concentration to

$62.4 \pm 7.8\%$ . This suggests that the reduction of the binding kinetics is the principal cause for the observed partial inactivation of a vesicle, not an inhibition of fusion. No other measurable effects in the overall reaction kinetics are caused by proteolysis.

So far, we have only looked at the kinetic end point of the vesicle/Golgi fusion reaction. To test whether protease-treated vesicles differ in other kinetic parameters from the untreated controls, the effect of protease pretreatment on the overall reaction kinetics was also determined. When comparing approximately an equal number of fusion events, more protease-treated vesicles had to be added to achieve the same apparent vesicle concentration as that of untreated vesicles.

The simplest description of the overall reaction kinetics is a sequence of two first order steps that occur at comparable speeds. One of these steps is vesicle binding or, more precisely, the kinetics of vesicle consumption, which is the sum of vesicle inactivation and binding. The second rate describes the fusion of docked vesicles. We found only small differences in the overall reaction kinetics (Fig. 5). Vesicles were in this experiment pre-incubated with or without PK on ice and then together with target membranes. At indicated times, fusion was

blocked by BAPTA. The measured data are in good agreement with the assumption that one of the two rate constants that determine the overall reaction kinetics remained unchanged, whereas the other one was reduced by approximately 20%. As we showed that the vesicle-binding rate is reduced after proteolysis, the overall vesicle consumption rate of which the binding rate is a part must be affected as well. As the vesicle consumption rate also includes the inactivation rate, the relative change in the consumption rate is smaller than the change in the binding rate. Therefore, the change in the binding rate alone is sufficient to explain the kinetic changes before and after proteolysis of vesicles. No additional effects, such as changes in the speed of membrane fusion are observed in the reaction kinetics after proteolysis of vesicles.

### **Proteolysis of vesicles changes the NSF response of the fusion reaction.**

It is formally possible that removal of SNARE proteins and other cytoplasmically exposed proteins from COPI-derived vesicles results in a new pathway for membrane fusion. If so, such fusion would be independent of the known cytosolic fusion proteins such as NSF/ $\alpha$ -SNAP. Though fusion using PK treated vesicles remained inhibited by BAPTA indicating that a new pathway for fusion had not been created, we also determined whether NSF function was still required upon PK treatment. Membrane-bound NSF was inactivated by NEM treatment (Block and Rothman, 1992) and cytosolic NSF was inactivated by incubating cytosol at 37°C in the absence of ATP. The efficiency of membrane fusion was tested at different concentrations of NSF (Fig. 6). Panel A shows the NSF response curve of vesicle fusion with Golgi membranes plotted against the NSF concentration on a linear scale and panel B shows the same data plotted logarithmically (circles). As can be seen, NSF is stimulatory at low concentrations but at high concentrations, it becomes slightly inhibitory.

The dose-response curve was parameterized by two exponential functions to separately express the stimulatory and inhibitory response to NSF. We then determined the NSF response curve of protease-treated vesicles (squares). This showed that the reaction remained strictly dependent on NSF even after proteolysis of vesicles. However, both the inhibitory and stimulatory activity of NSF differed when vesicles were PK treated. After proteolysis, the stimulatory activity of NSF was reduced to  $40.2 \pm 2.3\%$  of the control value (untreated vesicles). In other words, proteolysis of vesicles a little more than doubled the amount of NSF needed to stimulate membrane fusion. The inhibitory effect of high NSF concentrations was increased after proteolysis of vesicles by a factor of  $1.9 \pm 0.5$ , or approximately twofold. This change in the NSF response curve suggests a change in the way the fusing membranes interact with NSF. As SNARE proteins are known to mediate the recruitment of NSF to membranes, it seems likely that the protease treatment of vesicles had indeed destroyed functional SNARE proteins.

### **PK treatment abolishes the ability of vesicles to recruit an inhibitory $\alpha\text{-SNAP}^{\text{mut}}$ to the docking side.**

A mutant form of  $\alpha\text{-SNAP}$  ( $\alpha\text{-SNAP}^{\text{mut}}$ ) has been shown to inhibit fusion by failing to stimulate the ATPase activity of NSF (Barnard et al., 1997). Still, NSF is recruited to SNARE proteins with the same efficiency as when using wild type  $\alpha\text{-SNAP}$ . This mutant therefore allowed us to directly test whether vesicles and target membranes each contained functional SNARE proteins, and whether vesicles lost these after proteolysis. Both before and after proteolysis, addition of  $\alpha\text{-SNAP}^{\text{mut}}$  inhibited the assay signal (Fig. 7A). Inhibition was not complete though, and some vesicle fusion occurred even at the highest concentrations of  $\alpha\text{-SNAP}^{\text{mut}}$ . More  $\alpha\text{-SNAP}^{\text{mut}}$ -resistant fusion was observed using vesicles that had not been

incubated with PK. The failure of  $\alpha$ -SNAP<sup>mut</sup> to completely block fusion is likely due to the presence of wild type SNAP already bound to SNAREs on the membrane when  $\alpha$ -SNAP<sup>mut</sup> is added.

We explored this further by comparing how inhibition by the  $\alpha$ -SNAP<sup>mut</sup> changed when membranes had been preincubated separately with or without the mutant protein before vesicles and Golgi membranes were combined (Fig. 7B). Without preincubation,  $\alpha$ -SNAP<sup>mut</sup> inhibited approximately 80% of the assay signal such that  $\alpha$ -SNAP<sup>mut</sup>-resistant transport was 20% of the control. When both target membranes and vesicles were preincubated separately without  $\alpha$ -SNAP<sup>mut</sup> and then combined in the presence of  $\alpha$ -SNAP<sup>mut</sup>, the  $\alpha$ -SNAP<sup>mut</sup>-resistant transport increased to approximately 40% of control. When vesicles were preincubated with  $\alpha$ -SNAP<sup>mut</sup> but target membranes without, then the  $\alpha$ -SNAP<sup>mut</sup>-resistant transport was comparable to the situation without preincubation. Preincubation of target membranes with  $\alpha$ -SNAP<sup>mut</sup> and preincubation of vesicles without  $\alpha$ -SNAP<sup>mut</sup> resulted in a reduction of the  $\alpha$ -SNAP<sup>mut</sup>-resistant transport. Maximal inhibition was obtained when both vesicles and target membranes were preincubated with  $\alpha$ -SNAP<sup>mut</sup>. From this we conclude that preincubation of target membranes without  $\alpha$ -SNAP<sup>mut</sup> reduces inhibition whereas preincubation with  $\alpha$ -SNAP<sup>mut</sup> increases inhibition of membrane fusion by  $\alpha$ -SNAP<sup>mut</sup>. A similar but smaller effect was observed upon preincubation of vesicles. This suggests that  $\alpha$ -SNAP acts principally on the target membranes and, to a lesser extent also on the vesicles. Importantly, the smaller effect of  $\alpha$ -SNAP<sup>mut</sup> on vesicles was abolished when vesicles were preincubated with PK. The degree of  $\alpha$ -SNAP<sup>mut</sup> inhibition now depended solely on how the target membranes had been preincubated. From this we conclude that PK-treated vesicles no longer interact with  $\alpha$ -SNAP<sup>mut</sup>.

## **Discussion**

We have in this study examined *trans* pairing of SNARE proteins in membrane fusion between COPI vesicles and acceptor membranes. We find that whereas target membranes are highly sensitive to protease treatment, COPI-derived vesicles are not. Protease treatment of vesicles decreases their ability to dock with target membranes but not their ability to fuse. This is highly suggestive of a heterotypic fusion event where SNARE proteins on COPI vesicles have acquired a protease resistant conformation prior to fusion whereas acceptor membranes have not.

The *in vitro* assay deployed in this study should allow us to determine which factors actually drives the fusion event and to more precisely examine what roles are exerted by the different tethering factors that are thought to be involved in the docking of vesicles to Golgi membranes.

## **Acknowledgements**

We are indebted to Drs L. Tang and W. Hong (Institute of Molecular and Cell Biology, Singapore) for the kind gift of the mAb to GS28 and members of the Nilsson lab for critical comments to the manuscript.

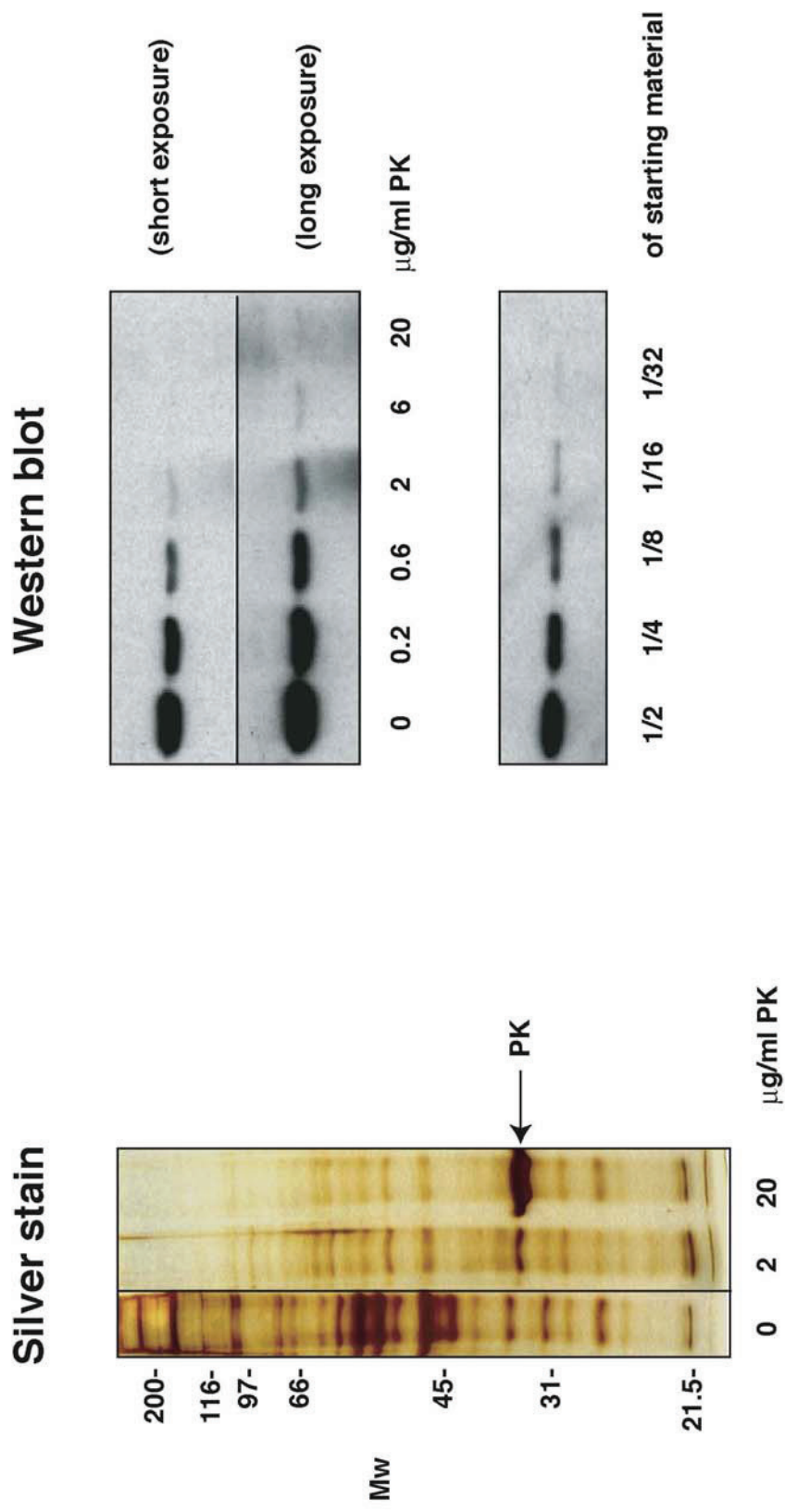
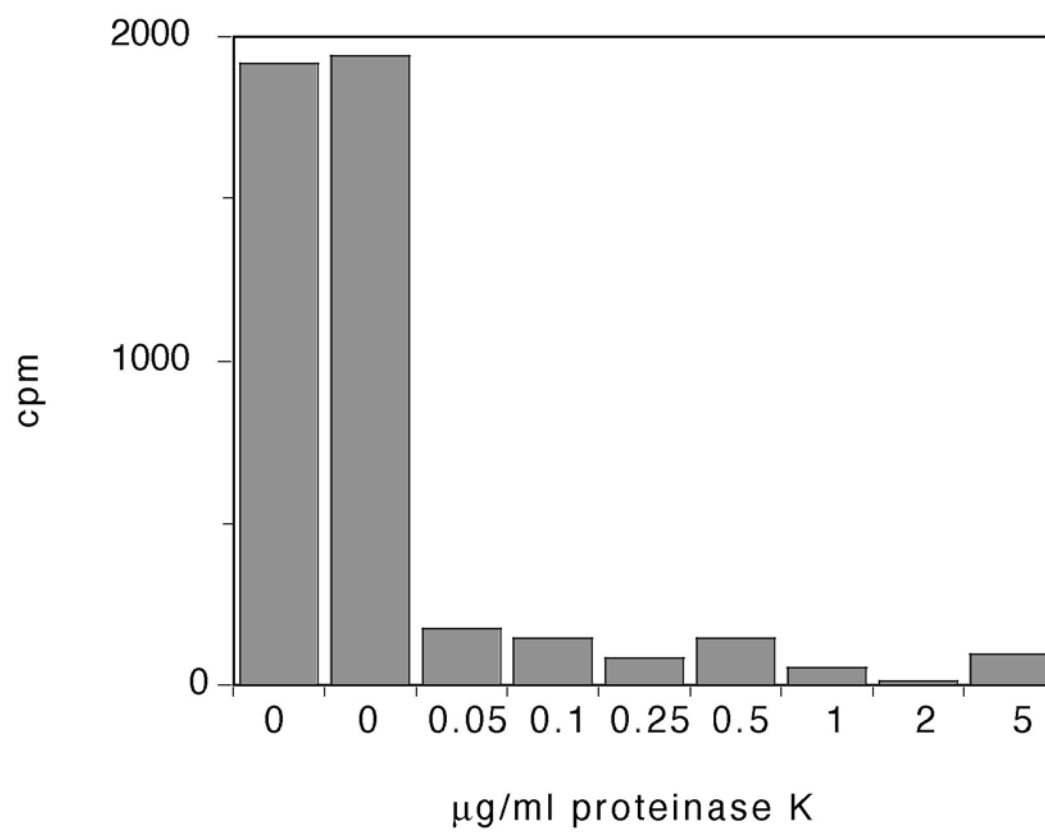


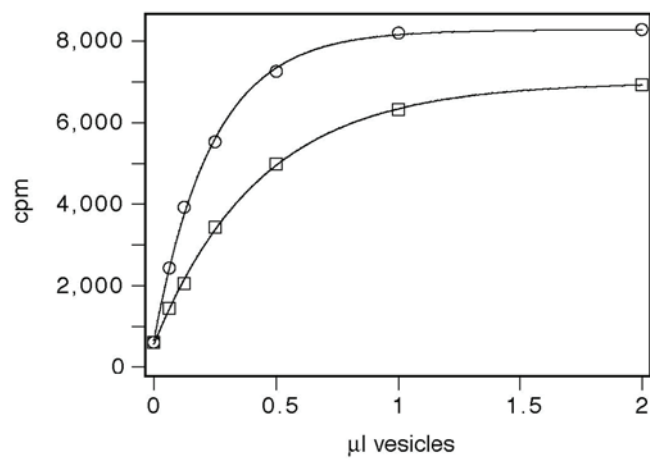
Figure 1 Laporte et al.



**Figure 2 Laporte et al.**



**A**



**B**

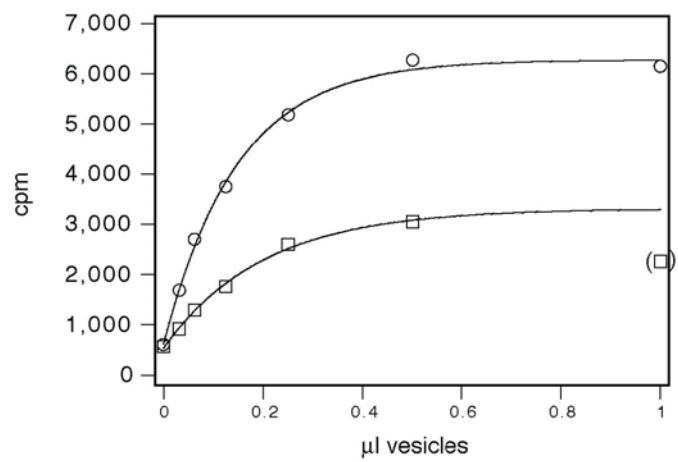


**Figure 3 Laporte et al.**

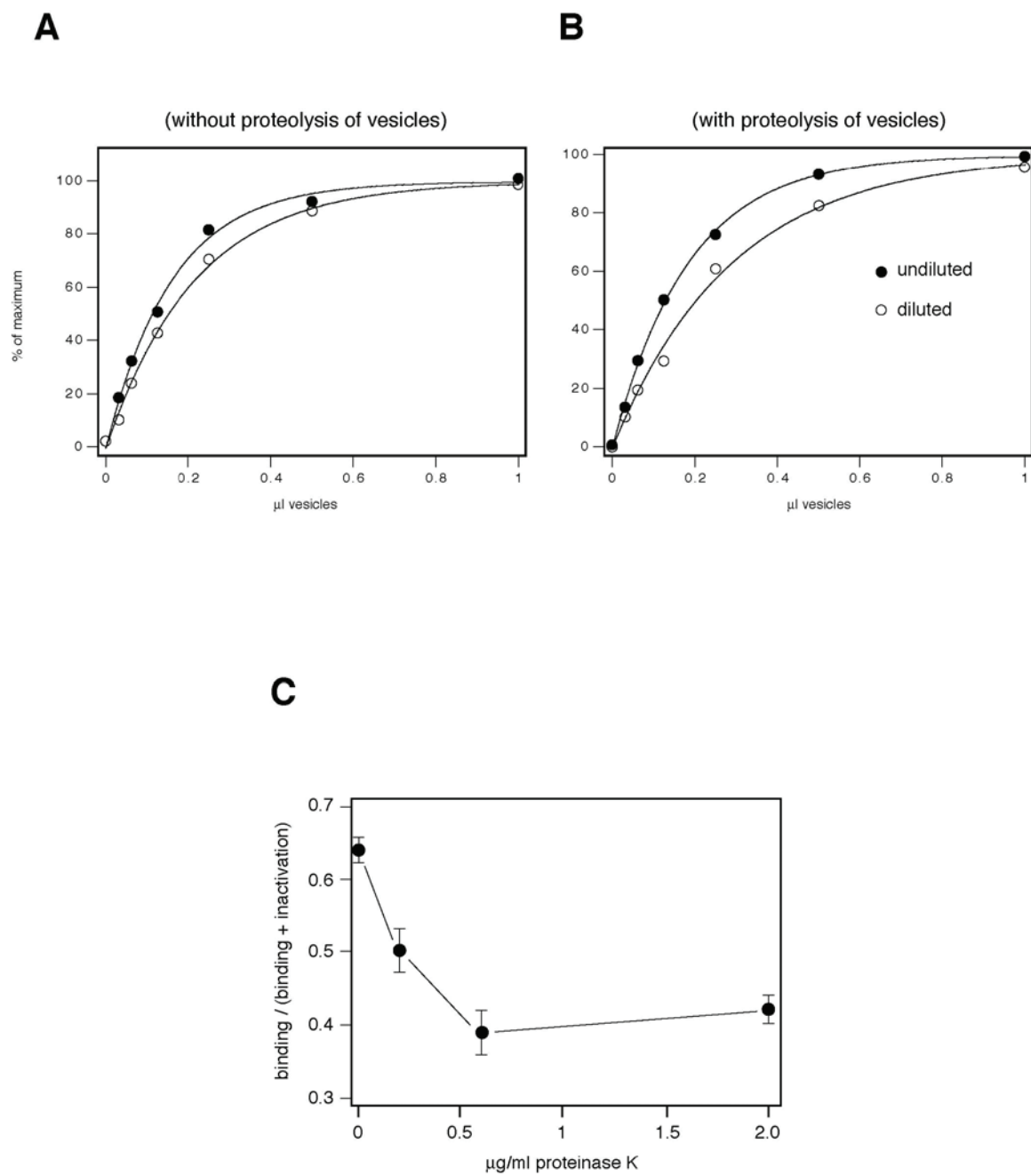


**Figure 4 Laporte et al.**

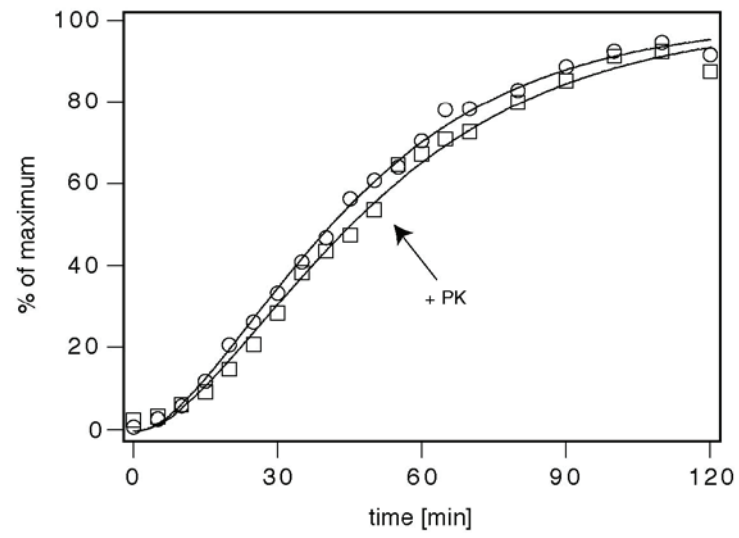
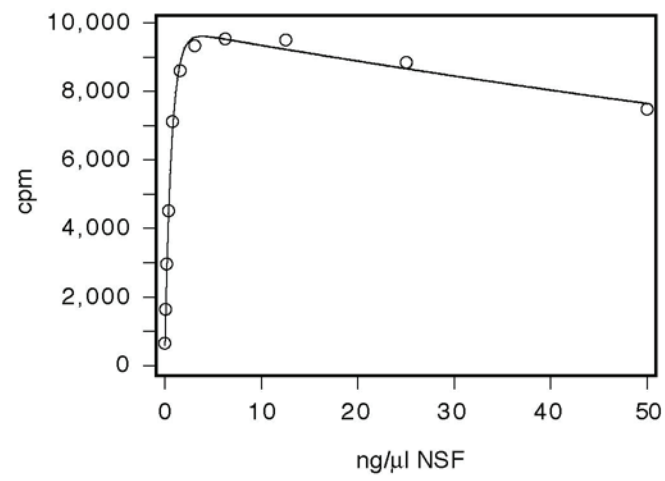
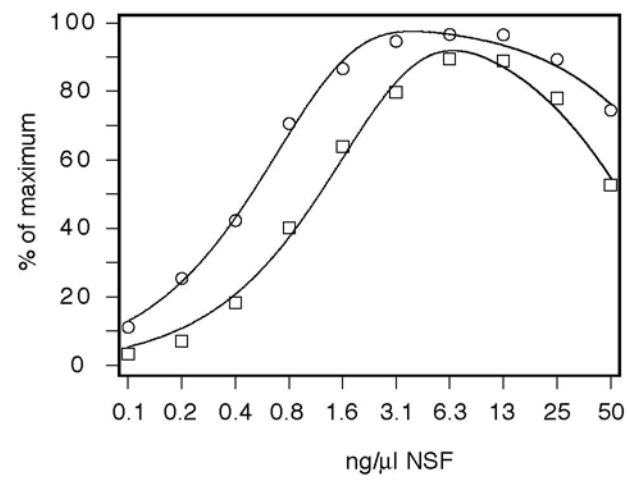


**Figure 5 Laporte et al.**

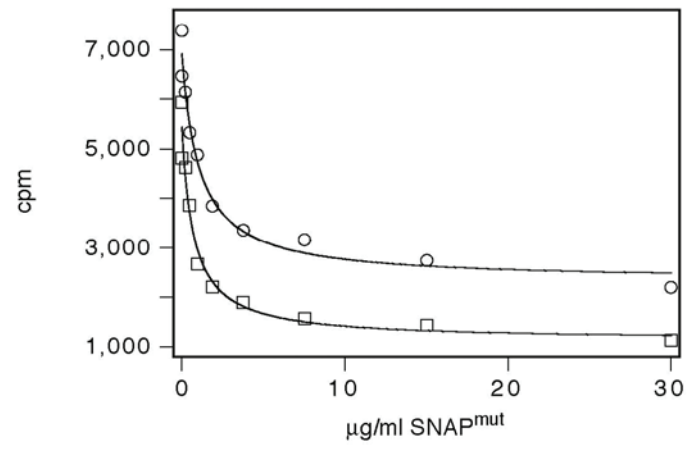
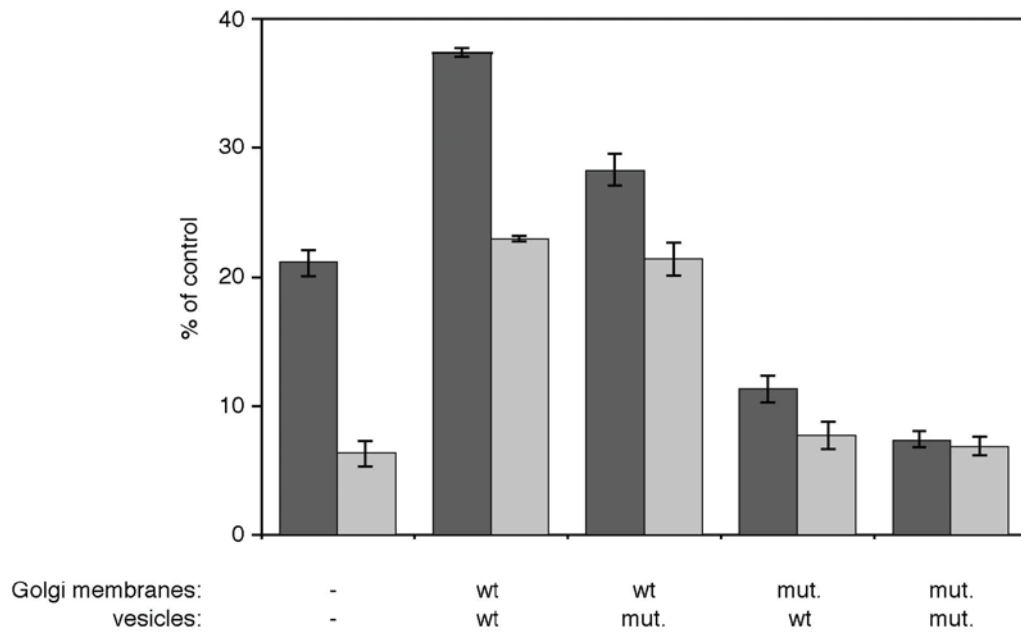
**A**



**B**



**Figure 6 Laporte et al.**

**A****B**

**Figure 7 Laporte et al.**

## Figure Legends

**Figure 1. Proteolysis of COPI derived vesicles.** Vesicles were isolated as described in Lanoix et al. (Lanoix et al., 1999) and incubated without or with the indicated concentrations of PK for 30 min on ice. At the end of the incubation, 1 mM PMSF was added to inactivate PK. Proteins were precipitated with 10% trichloroacetic acid, dissolved in electrophoresis sample buffer, and separated by denaturing gel electrophoresis. (A) Proteins were detected by silver staining. The band containing PK is indicated. (B) Proteins were transferred on PVDF and GS28 was detected by Western blotting. Two different exposures of the same filter are shown. A dilution series of the starting material is shown for comparison.

**Figure 2. Lec1 Golgi membranes are inactivated by proteolysis.** Lec1 Golgi membranes (“target membranes”) were incubated with the indicated concentrations of PK for 30 min on ice. After inactivation of PK with 1 mM PMSF, the Golgi membranes were incubated in a vesicle fusion assay with saturating amounts of vesicles and cytosol, and the assay signal was determined at the end of a 2 h incubation.

**Figure 3. Vesicles retain their activity after proteolysis.** Vesicles were incubated without (circles) or with (squares) PK for 30 min on ice. The PK concentration was 2  $\mu\text{g/ml}$  (A) or 20  $\mu\text{g/ml}$  (B). At the end of the incubation, PK was inactivated with 1 mM PMSF. The indicated amount of vesicles was added to each fusion assay. The dose response curve (the expression describing how the assay signal increases with increasing amounts of vesicles) is shown (Ostermann, 2001). The apparent vesicle concentration was measured by fitting of the dose response curve to the experimental data (the last data point in panel B was not used for curve

fitting as under these conditions, the inhibitory effect of PK on the target membranes becomes dominant).

**Figure 4. Inhibition of binding after proteolysis.** (A) Dose-response curve of vesicles with a fixed amount of target membranes before (closed circles) and after (open circles) twofold dilution. The relatively lower assay signal at low vesicle concentrations after dilution indicates a loss of active vesicles at the lower concentration of vesicles and target membranes. (B) Vesicles were incubated with 2  $\mu$ /ml PK for 30 min on ice, and the dose response curve was determined before and after twofold dilution. Note that after protease treatment, slightly vesicles inactivated after dilution. (C) The dose response curve is measured before and after dilution with vesicles that have been treated with the indicated concentrations of PK. The fraction of vesicles that binds rather than inactivates (the ratio of the binding rate constant to the sum of the binding and inactivation rate constants) is calculated from these measurements as described in (Ostermann, 2001). Note that the curve flattens at 0.6  $\mu$ g/ml PK, which is when most of GS28 is degraded by proteolysis (see Fig. 1).

**Figure 5. Kinetics before and after proteolysis.** Vesicles were incubated without (circles) or with (squares) 2  $\mu$ g/ml PK for 30 min on ice. Thereafter, vesicles and target membranes were incubated together (at a vesicle to Golgi membrane ration of approximately 1 to 1) with the other components of the vesicle fusion assay for 2 h at 37 degrees. At the indicated times during the incubation, any further fusion of vesicles after this time was blocked by the addition of BAPTA. The incubation was continued so that any partially glycosylated VSV-G could become fully glycosylated. At the end of the incubation, VSV-G was immunoprecipitated and the amount of incorporated 3H determined by scintillation counting.

Results are expressed as a percentage of the maximum amount of radioactivity that was incorporated into VSV-G.

**Figure 6. NSF dependence before and after proteolysis.** Membrane-bound and cytosolic NSF was inactivated, and the indicated amounts of recombinant NSF were added back. The curve connecting the data points describes the mathematical expression that was used to parameterize the experimental observation. (A) NSF concentration is on a linear scale, (B) NSF concentration is plotted on a logarithmic scale. Vesicles were either protease treated (squares) or left untreated (circles). Note that after proteolysis, the stimulation by low concentrations of NSF was reduced whereas the inactivation by high concentrations was more pronounced. For the experiment shown, the activation rate was 1480 before and 613  $\mu\text{g}/\text{nl}$  after proteolysis. The inactivation rate was 5.39 and 12.3  $\mu\text{g}/\text{nl}$  before and after proteolysis, respectively (the dimension of the rates is an inverse concentration; the product of the rate and the actual concentration is the exponent from which the activation or inactivation is calculated).

**Figure 7. Mutant SNAP inhibition of vesicle fusion.** (A) Vesicles were incubated without (circles) or with (squares) PK, and the indicated concentrations of mutant SNAP were added to the reaction. (B) Vesicles were incubated without (darker bars) or with (lighter bars) PK. Golgi membranes and vesicles were incubated separately for 15 min in cytosol (which contains wt SNAP) with mutant SNAP, when indicated. Both were combined and mutant SNAP was added to all to the same final concentration.

## References

Balch, W.E., Dunphy, W.G., Braell, W.A., and Rothman, J.E. (1984a). Reconstitution of the transport of protein between successive compartments of the Golgi measured by the coupled incorporation of N-acetylglucosamine. *Cell* 39, 405-416. Balch, W.E., Glick, B.S., and Rothman, J.E. (1984b). Sequential intermediates in the pathway of intercompartmental transport in a cell-free system. *Cell* 39, 525-536. Barnard, R.J., Morgan, A., and Burgoyne, R.D. (1997). Stimulation of NSF ATPase activity by alpha-SNAP is required for SNARE complex disassembly and exocytosis. *J Cell Biol* 139, 875-883. Bethune, J., Wieland, F., and



Moelleken, J. (2006). COPI-mediated transport. *The Journal of membrane biology* 211, 65-79.

Block, M.R., and Rothman, J.E. (1992). Purification of N-ethylmaleimide-sensitive fusion protein. *Methods Enzymol* 219, 300-309.

Brugger, B., Nickel, W., Weber, T., Parlati, F., McNew, J.A., Rothman, J.E., and Sollner, T. (2000). Putative fusogenic activity of NSF is restricted to a lipid mixture whose coalescence is also triggered by other factors. *Embo J* 19, 1272-1278.

Calakos, N., Bennett, M.K., Peterson, K.E., and Scheller, R.H. (1994). Protein-protein interactions contributing to the specificity of intracellular vesicular trafficking. *Science* 263, 1146-1149.

Colombo, M.I., Gonzalo, S., Weidman, P., and Stahl, P. (1991). Characterization of trypsin-sensitive factor(s) required for endosome- endosome fusion. *J Biol Chem* 266, 23438-23445.

Fasshauer, D., Antonin, W., Margittai, M., Pabst, S., and Jahn, R. (1999). Mixed and non-cognate SNARE complexes. Characterization of assembly and biophysical properties. *J Biol Chem* 274, 15440-15446.

Gilchrist, A., Au, C.E., Hiding, J., Bell, A.W., Fernandez-Rodriguez, J., Lesimple, S., Nagaya, H., Roy, L., Gosline, S.J., Hallett, M., *et al.* (2006). Quantitative proteomics analysis of the secretory pathway. *Cell* 127, 1265-1281.

Hanson, P.I., Roth, R., Morisaki, H., Jahn, R., and Heuser, J.E. (1997). Structure and conformational changes in NSF and its membrane receptor complexes visualized by quick-freeze/deep-etch electron microscopy. *Cell* 90, 523-535.

Hay, J.C., Klumperman, J., Oorschot, V., Steegmaier, M., Kuo, C.S., and Scheller, R.H. (1998). Localization, dynamics, and protein interactions reveal distinct roles for ER and Golgi SNAREs. *J Cell Biol* 141, 1489-1502.

Jahn, R., and Scheller, R.H. (2006). SNAREs--engines for membrane fusion. *Nat Rev Mol Cell Biol* 7, 631-643.

Jahn, R., and Sudhof, T.C. (1999). Membrane fusion and exocytosis. *Annu Rev Biochem* 68, 863-911.

Kartberg, F., Elsnér, M., Froderberg, L., Asp, L., and Nilsson, T. (2005). Commuting between Golgi cisternae--mind the GAP! *Biochimica et biophysica acta* 1744, 351-363.

Katz, L., and Brennwald, P. (2000). Testing the 3Q:1R "rule": mutational analysis of the ionic "zero" layer in the yeast exocytic SNARE complex reveals no requirement for arginine. *Mol Biol Cell* 11, 3849-3858.

Lanoix, J., Ouwendijk, J., Lin, C.C., Stark, A., Love, H.D., Ostermann, J., and Nilsson, T. (1999). GTP hydrolysis by arf-1 mediates sorting and concentration of Golgi resident enzymes into functional COP I vesicles. *Embo J* 18, 4935-4948.

Lanoix, J., Ouwendijk, J., Stark, A., Szafer, E., Cassel, D., Dejgaard, K., Weiss, M., and Nilsson, T. (2001). Sorting of Golgi resident proteins into different subpopulations of COPI vesicles: a role for ArfGAP1. *J Cell Biol* 155, 1199-1212.

Lenzen, C.U., Steinmann, D., Whiteheart, S.W., and Weis, W.I. (1998). Crystal structure of the hexamerization domain of N-ethylmaleimide- sensitive fusion protein. *Cell* 94, 525-536.

Lin, C.C., Love, H.D., Gushue, J.N., Bergeron, J.J., and Ostermann, J. (1999). ER/Golgi intermediates acquire golgi enzymes by brefeldin A-sensitive retrograde transport *In vitro* [In Process Citation]. *J Cell Biol* 147, 1457-1472.

Malsam, J., Satoh, A., Pelletier, L., and Warren, G. (2005). Golgin tethers define subpopulations of COPI vesicles. *Science* 307, 1095-1098.

Mayer, A., Wickner, W., and Haas, A. (1996). Sec18p (NSF)-driven release of Sec17p ( $\alpha$ -SNAP) can precede docking and fusion of yeast vacuoles. *Cell* 85, 83-94.

McNew, J.A., Parlati, F., Fukuda, R., Johnston, R.J., Paz, K., Paumet, F., Sollner, T.H., and Rothman, J.E. (2000a). Compartmental specificity of cellular membrane fusion encoded in SNARE proteins. *Nature* 407, 153-159.

McNew, J.A., Weber, T., Parlati, F., Johnston, R.J., Melia, T.J., Sollner, T.H., and Rothman, J.E. (2000b). Close is not enough: SNARE-dependent membrane fusion requires an active mechanism that transduces force to membrane anchors. *J Cell Biol*

150, 105-117.

- Moyer, B.D., Allan, B.B., and Balch, W.E. (2001). Rab1 interaction with a GM130 effector complex regulates COPII vesicle cis-Golgi tethering. *Traffic* 2, 268-276.
- Muller, J.M., Rabouille, C., Newman, R., Shorter, J., Freemont, P., Schiavo, G., Warren, G., and Shima, D.T. (1999). An NSF function distinct from ATPase-dependent SNARE disassembly is essential for Golgi membrane fusion. *Nat Cell Biol* 1, 335-340.
- Nagahama, M., Orci, L., Ravazzola, M., Amherdt, M., Lacomis, L., Tempst, P., Rothman, J.E., and Sollner, T.H. (1996). A v-SNARE implicated in intra-Golgi transport. *J Cell Biol* 133, 507-516.
- Ossig, R., Schmitt, H.D., de Groot, B., Riedel, D., Keranen, S., Ronne, H., Grubmuller, H., and Jahn, R. (2000). Exocytosis requires asymmetry in the central layer of the SNARE complex. *Embo J* 19, 6000-6010.
- Ostermann, J. (2001). Stoichiometry and kinetics of transport vesicle fusion with Golgi membranes. *EMBO Rep* 2, 324-329.
- Otter-Nilsson, M., Hendriks, R., Pecheur-Huet, E.I., Hoekstra, D., and Nilsson, T. (1999). Cytosolic ATPases, p97 and NSF, are sufficient to mediate rapid membrane fusion. *Embo J* 18, 2074-2083.
- Peters, C., Andrews, P.D., Stark, M.J., Cesaro-Tadic, S., Glatz, A., Podtelejnikov, A., Mann, M., and Mayer, A. (1999). Control of the terminal step of intracellular membrane fusion by protein phosphatase 1. *Science* 285, 1084-1087.
- Peters, C., Bayer, M.J., Buhler, S., Andersen, J.S., Mann, M., and Mayer, A. (2001). Trans-complex formation by proteolipid channels in the terminal phase of membrane fusion. *Nature* 409, 581-588.
- Sollner, T., Whiteheart, S.W., Brunner, M., Erdjument-Bromage, H., Geromanos, S., Tempst, P., and Rothman, J.E. (1993). SNAP receptors implicated in vesicle targeting and fusion. *Nature* 362, 318-324.
- Subramaniam, V.N., Peter, F., Philp, R., Wong, S.H., and Hong, W. (1996). GS28, a 28 kilodalton Golgi SNARE that participates in ER-Golgi transport. *Science* 272, 1161-1163.
- Tsui, M.M., and Banfield, D.K. (2000). Yeast Golgi SNARE interactions are promiscuous. *J Cell Sci* 113, 145-152.
- Ungermann, C., Sato, K., and Wickner, W. (1998). Defining the functions of trans-SNARE pairs. *Nature* 396, 543-548.
- Weber, T., Zemelman, B.V., McNew, J.A., Westermann, B., Gmachl, M., Parlati, F., Sollner, T.H., and Rothman, J.E. (1998). SNAREpins: minimal machinery for membrane fusion. *Cell* 92, 759-772.
- Yu, R.C., Hanson, P.I., Jahn, R., and Brunger, A.T. (1998). Structure of the ATP-dependent oligomerization domain of N-ethylmaleimide sensitive factor complexed with ATP. *Nat Struct Biol* 5, 803-811.
- Zerial, M., and McBride, H. (2001). Rab proteins as membrane organizers. *Nat Rev Mol Cell Biol* 2, 107-117.

Editorial Manager(tm) for Developmental Cell  
Manuscript Draft

Manuscript Number:

Title: Diacylglycerol is needed for peri-Golgi bud formation

Article Type: Research Article

Section/Category:

Keywords: Transport vesicle; Golgi, COPI, budformation, diacylglycerol, ARFGAP1

Corresponding Author: Professor Tommy Nilsson, Ph.D.

Corresponding Author's Institution: Institute of Biomedicine

First Author: Lennart Asp

Order of Authors: Lennart Asp; Fredrik Kartberg; Julia Fernandez-Rodriguez; Maria Smedh; Markus Elsner; Frederic Laporte; Montserrat Bárcena; Karen A Jansen; Jack A Valentijn; Abraham J Koster; John Bergeron; Tommy Nilsson, Ph.D.

Manuscript Region of Origin:

Abstract: We have investigated the role for diacylglycerol (DAG) in membrane bud-formation in the Golgi apparatus. Addition of propranolol to specifically inhibit phosphatidate phosphohydrolase (PAP), an enzyme responsible for converting phosphatidic acid into DAG, effectively prevents the formation of buds rendering cisternae devoid of vesicular and tubular profiles. The effect of PAP inhibition on Golgi membranes is rapid, occurring within minutes. Strikingly, removal of the PAP inhibitor results in a rapid burst of buds, vesicles and tubules that peaks within minutes. The inability to form buds and vesicles correlated with rapid loss of ARFGAP1 from Golgi membranes. Knockdown of ARFGAP1 by RNA interference, however, had little or no effect on actual bud-formation. Taken together, this suggests that DAG is required for bud formation and that subsequent steps such as fission are promoted by ARFGAP1.

Suggested Reviewers: Dennis Shields Professor

Department of Developmental and Molecular Biology, Albert Einstein College of Medicine of Yeshiva  
Universit

shields@aecom.yu.edu

expert in PC to PA/DAG lipid metabolism

William Brown Professor

Cornell, Itacha

wjb5@cornell.edu

expert in lipid metabolism and cell biology. Has elucidated the PA to LPA stage and its role for bud formation

Sean Munro

Division of Cell Biology, MRC Laboratory of Molecular Biology

sean@mrc-lmb.cam.ac.uk

expert in cell biology and Golgi transport. Knows the field of lipid metabolism and the role of this in transport.

Catherine Rabouille

Associate Professor of Cell Biology, Department of Cell Biology, University Medical Center Utrecht

C.Rabouille@umcutrecht.nl

expert in cell biology and electron microscopy/morphometry. Note that I have worked with her as a post doc in the lab of Graham Warren some 14 years ago but not since. Hers and Judith Klumpermans take on intra Golgi transport is highly appreciated and at the same time, very critical which is why I would prefer either to evaluate the microscopy and relevance to cell biology.

Benjamin Glick

Department of Molecular Genetics and Cell Biology, University of Chicago

bsglick@midway.uchicago.edu

expert in intra Golgi transport. A given leader in the transport field.

Opposed Reviewers:

Dear Editor(s)

This manuscript deals with bud formation in the Golgi apparatus, in vivo. By inhibiting the phosphatase responsible for converting phosphatidic acid into diacylglycerol, we show that bud formation is inhibited highlighting a previously unappreciated role for this lipid in both vesicle and tubule formation. All of our work is based on in vivo studies and we observe a very rapid response to modulating diacylglycerol synthesis such that the Golgi undergoes rapid changes in terms of bud and vesicle/tubule formation. Also, we were able to demonstrate that ARFGAP1 acts later in the process presumably at the level of pinching off formed vesicles or tubules.

We have suggested reviewers that we consider experts. This field is contentious at best and we hope that if you think this ms is appropriate for your journal, that you will manage to navigate through the different camps that exists to ensure this work gets a fair evaluation.

Best Regards

Tommy Nilsson

## **“Diacylglycerol is needed for peri-Golgi bud formation”**

Lennart Asp, Fredrik Kartberg, Julia Fernandez-Rodriguez<sup>1</sup>, Maria Smedh<sup>1</sup>, Markus Elsner, Frederic Laporte<sup>2</sup>, Montserrat Bárcena<sup>3</sup>, Karen A. Jansen<sup>3</sup>, Jack A. Valentijn<sup>3</sup>, Abraham, J. Koster<sup>3</sup>, John JM Bergeron<sup>2</sup>, Tommy Nilsson

Department of Medical and Clinical Genetics and <sup>1</sup>Centre for Cellular Imaging, the Sahlgrenska Academy at University of Gothenburg, 405 30 Gothenburg, Sweden, <sup>2</sup>Department of Anatomy and Cell Biology, McGill University, 3640 University Street, Montreal, Quebec, H3A 2B2 Canada, <sup>3</sup>Department of Molecular Cell Biology (MCB-EM), Leiden University Medical Center, 2333 ZC Einthovenweg 20, Leiden, The Netherlands.

Correspondence to: [tommy.nilsson@gu.se](mailto:tommy.nilsson@gu.se)

## **Summary**

**We have investigated the role for diacylglycerol (DAG) in membrane bud-formation in the Golgi apparatus. Addition of propranolol to specifically inhibit phosphatidate phosphohydrolase (PAP), an enzyme responsible for converting phosphatidic acid into DAG, effectively prevents the formation of buds rendering cisternae devoid of vesicular and tubular profiles. The effect of PAP inhibition on Golgi membranes is rapid, occurring within minutes. Strikingly, removal of the PAP inhibitor results in a rapid burst of buds, vesicles and tubules that peaks within minutes. The inability to form buds and vesicles correlated with rapid loss of ARFGAP1 from Golgi membranes. Knockdown of ARFGAP1 by RNA interference, however, had little or no effect on actual bud-formation. Taken together, this suggests that DAG is required for bud formation and that subsequent steps such as fission are promoted by ARFGAP1.**

## Introduction

Formation of buds to generate intracellular transport vesicles from membranes such as Golgi cisternae involves both coat-binding and local lipid conversion (for reviews and theoretical models, see (Bethune et al., 2006; Kirchhausen, 2000; Shemesh et al., 2003; Weiss and Nilsson, 2003)). For COPI vesicles, formation of buds is initiated by the small GTPase ADP-ribosylation factor 1 (ARF1) which, in its GTP-conferred conformation, drives coatomer recruitment from the cytosol to both Golgi and pre-Golgi membranes (Palmer et al., 1993). Indeed, ARF1 and coatomer are sufficient for both bud and vesicle formation as evidenced from *in vitro* experiments using liposomes from which coated vesicles formed in a controlled manner (Spang et al., 1998). Addition of an activating protein for ARF1, ARFGAP1, then yielded uncoated vesicles of the expected size of about 50-60 nm in diameter (Reinhard et al., 2003).

The situation in biological membranes is likely more refined involving additional as well as alternative components to promote or prevent vesicle formation such that Golgi function is maintained. Here, both ARF1 and ARFGAP1 have been implicated in vesicle formation through direct or indirect modulation of lipid synthesis such that bud formation and membrane fission is promoted. For example, ARF1 stimulates the production of phosphatidic acid (PA) from phosphatidylcholine (PC) (Brown et al., 1993; Cockcroft et al., 1994) through the activation of phospholipase D (PLD) in a nucleotide (GTP)-specific manner (Brown et al., 1995; Houle et al., 1995; Ktistakis et al., 1995). Such ARF1-mediated PLD stimulation results in an increased vesicle production (Chen et al., 1997; Ktistakis et al., 1996). This ability of ARF1 to stimulate lipid formation in the



Golgi apparatus offers a possibility to mechanistically link lipid conversion with coat recruitment. Theoretical models predict that formation of PA is required for the formation of vesicle buds such that this cone-shaped lipid enables the formation of negative curvature in the cytosolic leaflet of the lipid bilayer (for theoretical model, see (Shemesh et al., 2003) and references therein). Like-wise, conversion of PA into lyso-phosphatidic acid (LPA), an inverted cone-shaped lipid, is thought to allow for the formation of positive curvature needed for outward bending of the lipid-bilayer to form the bud. Indeed, addition of an inhibitor that prevents the formation of LPA from PA effectively inhibits retrograde transport between the Golgi apparatus and the ER, *in vivo* (de Figueiredo et al., 2000). The experimental evidence for a requirement for PA to form negative curvature is mostly based on work examining the metabolic activities of CtBP/Bars-50 which were shown to acylate LPA to form PA (Schmidt et al., 1999; Weigert et al., 1999). Here, the enzymatic activity of CtBP/Bars-50 was shown to be necessary to drive bud formation at the later stages through promotion of membrane fission, either to form vesicles or to pinch off tubules (Bonazzi et al., 2005). Indeed, mutation of CtBP/Bars-50 showed a marked decrease in its ability to promote vesicle formation, *in vitro* (Yang et al., 2005). It is likely, though, that the effect of CtBP/Bars-50 on promoting vesicle formation is not mediated by an enzymatic activity to acylate LPA as these proteins lack enzymatic activity. Rather, it is their ability to insert into PA-rich domains through their respective BAR-domain that mediate their stimulatory roles in vesicle formation (Gallop et al., 2005). As such, they would stabilize formed negative curvature such that vesicles and tubules can bud off. Indeed, many BAR-domain containing proteins have now been identified and implicated in membrane curvature

stabilization (Blood and Voth, 2006; Gallop et al., 2006). Furthermore, PA can be converted to diacylglycerol (DAG) through dephosphorylation of PA. This enzymatic step is mediated by phosphatidate phosphohydrolases (PAPs) and is effectively inhibited by the pharmaceutical agent, propranolol (proPr). Inhibition of PAP enzymes by proPr affects the ability of protein kinase D (PKD) to be recruited to Golgi membranes such that vesicle formation at the *trans*-side of the Golgi apparatus is impaired (Baron and Malhotra, 2002). This inhibition in vesicle formation was, at least in part, at the level of PA to DAG conversion and was recently extended to also include peri-Golgi vesicles (Fernandez-Ulibarri et al., 2007; Sonoda et al., 2007). Here, inhibition of PAP by proPr resulted in the inability to form vesicles. In the Fernandez-Ulibarri et al., study, this inability appeared at the stage of membrane fission and was explained by a concurrent and partial loss of ARFGAP1 from Golgi membranes. In this study, we show that the primary effect of DAG is at the level of bud formation whereas ARFGAP1 is needed at later stages such as fission.

## **Material and Methods**

### **Reagents**

Antipain aprotinin, apyrase benzamidine, GTP, leupeptin, pepstatin, PMSF, propranolol, N-ethylmaleimide polyvinylpyrrolidone (PVP-40T), soybean trypsin inhibitor, PBS-Tween (0,05%) and Kodak Biomax<sup>TM</sup> X-Omat XAR or MR films were from Sigma-Aldrich (Stockholm, Sweden). ATP, creatine phosphate, and creatine kinase were from Roche AB (Stockholm, Sweden). 1,4-dithiothreitol was from Biomol GmbH (Hamburg, Germany). ECL detection kit was from GE Healthcare Bio-Sciences AB (Uppsala, Sweden). 30% (wt/vol) acrylamide/0.8% (wt/vol) bis-acrylamide solution was from Bio-Rad (Sundbyberg, Sweden). Uranyl acetate, glutaraldehyde and glycerol were from E. Merck (Stockholm, Sweden). Osmiumtetroxide was from Agar Scientific (Essex, UK). Protran nitrocellulose membranes (0.45 µm) were from Schleicher and Schuell (Dassel, Germany). Minimum essential medium (MEM), foetal bovine serum (FBS), glutamine and Lipofectamine<sup>TM</sup> RNAiMAX was purchased from Invitrogen (Carlsbad CA).

### **Antibodies, western blotting, cytosol, membrane and vesicle preparation**

Rabbit polyclonal antibodies to ARFGAP1 have been described previously (Lanoix et al., 2001). Monoclonal antibodies to native coatamer, CM1A10 (Palmer et al., 1993) and βCOP, M3A5 (Allan and Kreis, 1986) were kind gifts from Drs Rothman and Kreis, respectively. HRP-labeled polyclonal antibodies to rabbit and mouse IgG were purchased from Dianova (Hamburg, Germany). Purified rat liver Golgi membranes and rat liver cytosol were prepared and treated as described (Lanoix et al., 1999). Typically, membranes were purified ≈100-fold over that of the homogenate.

### **Cell culture and transfection**

HeLa cells were grown in MEM supplemented with 10% FBS, Penicillin (100U/ml), streptomycin (100 µg/ml) and L-glutamine (2mM). Cells expressing ARFGAP1<sup>EGFP</sup> were grown in the presence of 200 µg/ml of geneticin (G-418). SiRNA constructs against ARFGAP1 and GFP (mock) were custom synthesized by Dharmacon using published sequences (Frigerio et al., 2007). Transfections were performed according to manufacture's instructions (Invitrogen, Carlsbad CA). The medium containing the transfection reagent was replaced by fresh medium 24h post-transfection. This did not affect the degree of RNA silencing but greatly improved the overall ultrastructural morphology of intracellular membranes as deduced by electron microscopy.

### **Light and electron microscopy**

Indirect immunofluorescence on fixed cells was performed as described (Dominguez et al., 1998). Imaging of living cells was performed as follows: HeLa cells stably expressing GalNAc-T2<sup>ECFP</sup> (Storrie et al., 1998) or ARFGAP1<sup>EGFP</sup> (Elsner et al., 2003) grown in MatTek dishes (MatTek Corporation) were imaged using an Axiovert 200/LSM 510 META system (Carl Zeiss) fitted with a water-corrected 40X Apochromat 1.2 NA objective, a humidified chamber with a constant temperature of 37°C and 5% CO<sub>2</sub> (CTI-Controller 3700 connected to Incubator S, Carl Zeiss). CFP was excited with a 405 nm Blue diode laser, and the emitted fluorescence was captured through a 475 long-pass filter. For GFP, a 488 nm Argon laser was used and the emitted fluorescence was captured through a 505 to -530 band-pass. Fluorescence level was coded with a gray

scale representing pixel intensity of 25–255. For semi-quantitation, background fluorescence was subtracted. Images were analyzed using the Volocity Quantitation 4.1 software (Improvision, Software for Scientific Imaging, UK).

For electron microscopy, cells were fixed using a double fixation protocol with osmium and tannic acid (Simionescu and Simionescu, 1976). Samples were dehydrated in graded ethanol series, and embedded in Epon 812 (Serva). After 48 h at 60°C, ultra-thin sections (60 nm) were cut and mounted on grids. Samples were examined on a LEO 912 OMEGA (Energy Filter Transmission Electron Microscope, Zeiss) at 120 kV accelerating voltage. Digital images were obtained through a side-mounted MegaView III TEM CCD camera. Stereology was performed essentially as described by Mistelli and Warren (Misteli and Warren, 1995). Briefly, Golgi areas were defined as a Golgi stack with associated vesicular and tubular profiles including intercisternal space but not inter-vesicular, cytoplasmic space. Stacked cisternae comprised two or more cisternal profiles separated by a gap of 15 nm or less and overlapping by more than half their cross-sectional length. Cisternae ranged from continuous to extensively fenestrated and were defined as membrane profiles with a length more than four times their width, the width being not more than 40 nm. Fenestrated cisternae were often wider and more translucent but could be distinguished from tubules by their fenestration. Tubules were defined as profiles with a length more than 1.5 times their width, the latter exceeding 40 nm. These were more undulating than cisternae and when branched, formed networks. Vesicular profiles had spherical or nearly spherical (length less than 1.5 times their width) profiles and were defined as being localized inside the Golgi zone of exclusion. In tangential thin sections,

the absence of a translucent lumen served as a criterion for the classification of 50 to 75 nm peri-Golgi round profiles as vesicles. Open profiles such as broken cisternae were not included in the quantitation. All membrane profiles on an image were counted except clearly identifiable contaminants such as mitochondria, plasma membrane or ER (which totaled less than 10% of all profiles). The length or width of each cisterna, tubule or vesicle profile was measured with the Volocity Classification 4.1 software (Improvision, UK).

Photoconversion was essentially performed as described previously (Grabenbauer et al., 2005). Briefly, cells were washed with pre-warmed calcium- and magnesium-free phosphate-buffered saline (PBS) pH 7.4 and fixed for 30 minutes with pre-warmed fixative containing 2% glutaraldehyde (25% stock solution, Merck, Darmstadt, Germany) and 2% sucrose (USB, Cleveland, Ohio) in PBS. After washing three times with PBS, samples were blocked with 100 mM glycine (Sigma) and 100 mM potassium cyanide (Merck) in PBS for 2 h followed by 40 minutes with 10 mg/ml sodium borohydride (Sigma) in PBS. For photoconversion, samples were washed twice in Tris/HCl buffer pH 7.4, followed by incubation in a freshly prepared and oxygen saturated solution of 1.5 mg/ml 3,3'-diaminobenzidine hexahydrate (DAB) (Polysciences, Eppelheim, Germany) in Tris/HCl buffer pH 7.4 at 10°C or below. To bleach, samples were illuminated with the appropriate filter settings for ECFP (excitation filter BP436/20) using a 100 W mercury lamp (FluoArc by Carl Zeiss, Oberkochen, Germany). After photoconversion, samples were washed with distilled water and postfixed for 30 minutes on ice in 1% osmium tetroxide reduced by 1.5% potassium ferrocyanide. Samples were dehydrated in graded

ethanol series, and embedded in Epon 812 (Serva). After 48h of polymerization, the glass bottom of the tissue culture dish was removed by hydrofluoric acid. Ultrathin sections (60 nm) of flat embedded cells were cut parallel to the surface on a Leica Ultracut S ultramicrotome (Leica, Bensheim) and mounted on Formvar coated grids.

For tomography, semi-thick sections (150 nm) of resin-embedded cells were prepared by microtomy and collected on copper grids covered with a carbon coated pioloform layer. The sections were post-stained in uranyl acetate and lead citrate as described in (Sato, 1967). As fiducial markers for tomography, 10 nm colloidal gold particles were applied on top of the sections. Several tilt series were collected for each condition in a 120 kV Tecnai electron microscope (FEI company, Eindhoven, The Netherlands), equipped with a 4k x 4k Eagle CCD camera (FEI company, Eindhoven, The Netherlands). The tilt series covered an angular range of 130-140° around two orthogonal axes (Penczek et al., 1995) sampled in 1° increments. The typical pixel size was 0.6 nm at the specimen level.

Processing of the tilt series was carried out with IMOD software package (Kremer et al., 1996). Mutual alignment of the images in the tilt series was performed using the fiducial gold markers on top of the sample. Independent local alignment of 5x5 overlapping patches showed a reduction of the residual error mean by a factor of ~2 and was therefore applied to the data. The tomograms were then computed from the aligned tilt series by weighted back projection. The two tomograms obtained for each field of view from orthogonal tilt series were finally combined into a single reconstruction in IMOD (Mastrorade, 1997).

## Results

### *PA-derived DAG is rapidly turned over in Golgi membranes*

Propranolol (proPr) has been used previously to highlight the importance of DAG in the recruitment of proteins that contain the DAG-binding domain, C1, to membranes (Carrasco and Merida, 2004, 2007). For example, PKD has been shown to rapidly dissociate from *trans*-Golgi membranes in the presence of 500  $\mu$ M proPr for 5 minutes (Baron and Malhotra, 2002). In that study, the conversion from PA into DAG was tested for using proPr and was compared to the conversion of PC and sphingomyelin into ceramide and DAG through ceramide synthase using fumonicin B1 at 25 $\mu$ g/ml for 24 hours. With both inhibitors, PKD dissociated from the *trans*-Golgi. Other proteins are also likely to show preference for DAG. Even though the ARF1 activating protein, ARFGAP1, lacks a defined C1 domain, its binding and activity on liposomes is enhanced upon inclusion of DAG (Antonny et al., 1997). The reason for such stimulation is not fully understood but is presumably due to a protein-lipid induced conformational change that is facilitated by DAG (Mesmin et al., 2007). Alternatively, membranes containing DAG have a higher propensity to form curved membranes thereby stimulating the activity of bound ARFGAP1 (Bigay et al., 2005). ARFGAP1 binding to Golgi membranes is also enhanced by DAG, *in vivo*, as evidenced by the addition of proPr to living cells. After 5 minutes, this resulted in a significant loss (approximately 50%) from the Golgi apparatus of an over-expressed ARFGAP1 protein fused to the enhanced green fluorescent protein (EGFP) (Fernandez-Ulibarri et al., 2007). This suggests that PA is continuously converted into DAG through the enzymatic activity of a phosphatidate



phosphohydrolase (PAP) and that this is required for efficient ARFGAP1 binding to Golgi membranes.

We first tested for which type of PAP was responsible for the PA to DAG conversion relevant to ARFGAP binding to Golgi membranes, *in vitro*. There are two types of PAPs, PAP1 which is cytosolic and PAP2 which is membrane bound (for review, see (Nanjundan and Possmayer, 2003)). To distinguish between PAP1 and PAP2, we monitored the effect of proPr on the binding of recombinant ARFGAP1 to purified Golgi in the presence or absence of cytosol. Figure 1A shows that the binding of recombinant and His-tagged ARFGAP1 to purified Golgi membranes is inhibited by proPr only in the presence of cytosol. In the absence of cytosol, there is a slight increase in ARFGAP1 binding with proPr. This is contrary to what would be expected if the relevant PAP activity correspond to PAP2 indicating that the relevant phosphatase targeted here by proPr likely corresponds to PAP1. With this, we also confirm that ARFGAP1 binding to Golgi membranes is affected by the inhibition of PA-DAG conversion as observed by Egea and colleagues using over-expressed ARFGAP1 fused to EGFP (Fernandez-Ulibarri et al., 2007). The use of 60 $\mu$ M proPr in the Egea study, however, is unlikely to inhibit PAP1 completely as this enzyme requires at least 250 $\mu$ M of proPr to be fully inhibited (as judged by the resulting increase of cellular PA levels) (Meier et al., 1998). To test if ARFGAP1 is affected differently at higher concentrations of proPr, *in vivo*, we monitored the effect of 60  $\mu$ M proPr on HeLa cells stably expressing ARFGAP1 fused to EGFP (ARFGAP1<sup>EGFP</sup>) (Elsner et al., 2003) and compared this to 300  $\mu$ M proPr. Figure 1 B-F shows that the effect of 60  $\mu$ M proPr on ARFGAP1<sup>EGFP</sup> is partial compared to 300  $\mu$ M. Even after 10 minutes, more than 25% of ARFGAP1<sup>EGFP</sup> (Fig. 1, B, C and D) remained

on the Golgi apparatus in the presence of 60  $\mu\text{M}$  whereas at 300  $\mu\text{M}$ , most if not all ARFGAP1<sup>EGFP</sup> had been lost already after 20 seconds (Fig. 1, B, E and F). At 20 seconds, we observed no detectable loss of ARFGAP1<sup>EGFP</sup> in the presence of 60  $\mu\text{M}$  proPr or at 4°C for 10 minutes in the presence of 300  $\mu\text{M}$  proPr (data not shown).

The rapid dissociation of ARFGAP1<sup>EGFP</sup> from Golgi membranes in the presence of 300  $\mu\text{M}$  proPr suggests that the half-life of PA-derived DAG is very short. To exclude that the rapid dissociation was not due to over-expression of an EGFP fusion protein, we confirmed the loss of endogenous ARFGAP1 from the juxta nuclear Golgi area in response to PAP inhibition by proPr. As can be seen in Supplementary Figure 1, most if not all Golgi-associated ARFGAP1 had redistributed to the cytosol after 3 minutes (compare Suppl. Fig. 1A with B). We also examined cells at shorter incubation times (down to 20 seconds) and found that most of the endogenous ARFGAP1 was lost from the Golgi area in less than a minute (data not shown). In the presence of proPr, endogenous COPI (revealed by antibodies to  $\beta\text{COP}$ ) remained largely unaffected (compare Suppl. Fig. 1D with E). After removal of the PAP inhibitor, ARFGAP1 was recruited back to the juxta nuclear Golgi area within 2 minutes (Suppl. Fig. 1C). In respect to the behavior of ARFGAP1, we observed no difference between the D-or the L-form of proPr (data not shown). This also ruled out the  $\beta$ -adrenergic receptor or signaling through this receptor as a cause for the observed effect. As proPr was dissolved in water and diluted more than 30 times before each experiment, additional vehicle experiments were deemed unnecessary.

*PA to DAG conversion is required for bud-formation*

The loss of ARFGAP1 but not coatomer suggests a partial impairment of COPI function. This is consistent with the observed inhibition of Golgi to ER recycling upon addition of proPr (Fernandez-Ulibarri et al., 2007). In that study, loss of Golgi to ER recycling was explained by the concurrent decrease of ARFGAP1 from the Golgi apparatus. As ARFGAP1 has been implicated in the formation of COPI transport intermediates at the stage of membrane fission, such a decrease should impair the late stage of the budding process, i.e. membrane fission. Indeed, addition of 60 $\mu$ M proPr for 30 minutes results in the accumulation of multiple membrane buds consistent with this interpretation (Fernandez-Ulibarri et al., 2007). To investigate how proPr affects the Golgi cisternae at the higher concentration of 300 $\mu$ M, we examined HeLa cells at the ultra structural level using ultra-thin plastic sections. Cells were incubated with 300  $\mu$ M proPr for 3 minutes, washed with medium and then incubated for a further 2 minutes. In untreated cells, Golgi stacks were typically aligned laterally as part of the Golgi ribbon (Fig. 2A). At higher magnification, a number of membrane buds and vesicular/tubular profiles (VTPs) could be seen in close proximity to the cisternal membranes of each Golgi stack (Fig. 2D). Addition of proPr for 3 minutes resulted in an increased frequency of curved stacks with smooth cisternal membranes seemingly devoid of both membrane buds as well as VTPs (Fig. 2B and E). Strikingly, removal of proPr to allow for DAG synthesis resulted in a dramatic increase of cisternal buds as well as VTPs already after 2 minutes. As can be seen in Figure 2C and F, this often resulted in Golgi areas with a reduced stack-like appearance. At 5-10 minutes after removal of proPr, the number of cisternae increased whereas associated membrane buds and VTPs decreased approaching levels to that

observed in control cells (see Fig. 2 G for quantitation and Suppl. Fig. 2 A and B for low magnification fields).

That membrane buds and associated VTPs were affected by proPr was confirmed by examining thick plastic sections followed by tomography. Representative tomograms constructed of Golgi areas from control cells (Fig. 3A, left field), cells incubated with proPr for 3 minutes (Fig. 3A, middle field) and cells incubated with proPr for 3 minutes followed by a 2 minutes incubation after proPr removal (Fig. 3A right field) revealed differences in the number of associated buds (yellow) as well as adjacent vesicles (red) and tubules (green) consistent with that observed and quantified using thin sections above. To perform tomography quantitatively would require an examination of a large number of tomograms and is outside the scope of this study. Round to oval structures were labeled as vesicles if they maintained their X-Y position while moving up and down (along the Z-axis) in the tomogram and had a clearly defined top and bottom, i.e. they should appear and then disappear when moving up and down along the Z-axis. Structures were labeled as tubules if having no defined top and bottom and if moving in the X-Y direction when moving up and down along the Z-axis. At higher magnification, a fuzzy coat consistent with that of COPI (Orci et al., 1986) was observed on buds and vesicles 2 minutes after removal of proPr (Fig. 3B). Some membrane buds also had an electron-dense region bridging the constricted neck-region (Fig. 3B-arrows) consistent with a protein/lipid-aided fission-machinery.

We next examined whether membrane buds and VTPs that form in response to proPr removal contain Golgi resident enzymes. To do this, we examined HeLa cells stably expressing N-acetylgalactosamine transferase-2 fused to the enhanced cyan fluorescent protein (GalNAcT2<sup>CFP</sup>). We previously showed that if illuminated post-fixation, GalNAcT2<sup>CFP</sup> yields sufficient amounts of free radicals to precipitate diaminobenzidine (DAB) both locally as well as quantitatively (Grabenbauer et al., 2005). As can be seen in Figure 4A, a gradient-like distribution of GalNAcT2<sup>CFP</sup> was observed across Golgi stacks under normal conditions. Some associated VTPs were filled with DAB products consistent with the notion that GalNAcT2<sup>CFP</sup> is capable of gaining access to these structures (Grabenbauer et al., 2005). Upon addition of proPr for 3 minutes, the DAB precipitate was seen exclusively in cisternae (Fig. 4B) whereas upon removal of proPr, DAB product was seen in both cisternal buds as well as VTPs (Fig. 4C and D). The diameter of observed VTPs were between 40-50nm which is consistent with the expected inner diameter of peri-Golgi vesicles such as COPI vesicles.

Taken together, evidence has been provided suggesting a direct requirement of PA-derived DAG in the formation of membrane buds and the resulting vesicles and tubules. Also, that the resident Golgi marker, GalNAcT2<sup>CFP</sup> gains access to at least a part of formed structures. The rapid shifts in observed morphologies further indicate that underlying PA to DAG conversion takes place at surprisingly high rate and that formed DAG has a relatively short half-life. This correlates well with the dissociation and re-binding of ARFGAP1 to Golgi membranes linking this ARFGAP to vesicle formation through DAG (Fernandez-Ulibarri et al., 2007). In that study, Fernandez-Ulibarri, Egea

and colleagues suggested that ARFGAP1 is required for the fission of membrane buds. Having observed that inhibition of DAG synthesis prevents the formation of membrane buds, we now tested for the role of ARFGAP1 in bud formation as well as fission of membrane buds. Cells were either transfected with control interference RNA (based on part of the green fluorescence protein, from here onwards referred to as RNAi<sup>Mock</sup>) or interference RNA specific for ARFGAP1 (RNAi<sup>ARFGAP1</sup>). As can be seen in Supplementary Figure 3, RNAi<sup>ARFGAP1</sup>-transfection of HeLa cells resulted in a marked decrease of endogenous ARFGAP1 as compared to RNAi<sup>Mock</sup>-transfected cells (shown are three independent experiments). In contrast, no significant changes were observed for endogenous  $\beta$ -COP in either RNAi<sup>Mock</sup>- or RNAi<sup>ARFGAP1</sup>-transfected cells. At the ultrastructural level, RNAi<sup>Mock</sup>-transfected cells revealed a somewhat higher incidence of associated VTPs and membrane buds to that observed in untransfected cells suggesting some unspecific influence of the transfection procedure on the experiment (compare Fig. 2A with Suppl. Fig. 4A). In cells transfected with RNAi<sup>ARFGAP1</sup>, there was a marked increase of membrane buds which was accompanied by a decreased number of associated VTPs as compared to RNAi<sup>Mock</sup>-transfected cells (Fig. 5A, D and Suppl. Fig. 4B) consistent with an impairment in vesicle fission as a consequence of lowering the endogenous ARFGAP1 protein level. As in untransfected cells (Fig. 2), addition of proPr resulted in a marked decrease in associated membrane buds and VTPs in both RNAi<sup>Mock</sup>- as well as RNAi<sup>ARFGAP1</sup>-transfected cells (Fig. 5B, D and Suppl. Fig. 4 C, D). At 2 minutes after removal of proPr, cells transfected with RNAi<sup>ARFGAP1</sup> revealed a dramatic increase in membrane buds compared to cells transfected with RNAi<sup>Mock</sup> over that of associated VTPs (Fig. 5C, D and Suppl. Fig. 4E, F). This shows that knockdown of

ARFGAP1 results in a lowered ability to complete the budding process (presumably at the level of membrane fission or scission) as in such cells, the number of stack-associated VTPs was significantly lower as compared to mock-transfected cells (Fig. 5D). At 5 minutes after proPr removal, RNAi<sup>ARFGAP1</sup>-transfected cells revealed similar ratios of VTPs and buds as compared to cells not treated with proPr (Ctrl).

## Discussion

We have presented evidence that show that synthesis of DAG from PA is required for bud-formation in the Golgi apparatus and that ARFGAP1 promotes vesicle and tubule formation, presumably at the level of scission. We distinguished between the role for ARFGAP1 in vesicle and tubule versus bud formation through the use of RNAi. Knockdown of endogenous ARFGAP1 resulted in a marked decrease in formed VTPs consistent with a role for ARFGAP1 at the level of membrane scission (Fernandez-Ulibarri et al., 2007; Yang et al., 2005). This also helped us to highlight a role for DAG at the level of bud-formation as removal of ARFGAP1 did not block this event. This was further supported by the observed increase in buds as suppose to VTPs at 2 minutes after removal of proPr in cells transfected with RNAi<sup>ARFGAP1</sup> (Fig. 5D, compare black bars between RNAi<sup>Mock</sup> and RNAi<sup>ARFGAP1</sup> in terms of VTPs and buds). The most simple explanation, therefore, is that DAG plays a role in bud formation and that ARFGAP1 is required for later events such as membrane scission through, for example, the BAR-domain containing protein Bars-50 or other factors, (Yang et al., 2005; Yang et al., 2006) and uncoating through the stimulation of GTP hydrolysis by ARF.

We also monitored the distribution of GalNAcT2<sup>CFP</sup> which, under normal conditions, resides in two cisternae of the Golgi stack and in adjacent VTPs, some which correspond to vesicles (Grabenbauer et al., 2005). Upon addition of proPr, such VTPs GalNAcT2<sup>CFP</sup>– filled VTPs were absent (Fig. 4B). In contrast, when removing proPr to restore DAG synthesis, the frequency of VTPs increased and often, such VTPs contained GalNAcT2<sup>CFP</sup> when examined using GFP excitation-induced DAB precipitation (Grabenbauer et al., 2005). After 5-10 minutes, the number of VTPs was comparable to those seen under normal conditions.

We specifically targeted the conversion of PA to DAG using the pharmacological drug, propranolol (proPr). This allowed us to monitor rapid events that took place within minutes upon the addition subsequent removal of proPr (see Fig. 6A). Other pharmacological agents such as BFA have proven indispensable in elucidating dynamic aspects of the Golgi apparatus (Sciaky et al., 1997) through its specific inhibition of COPI function through the ARF1 exchange factor GBF1 (Niu et al., 2005). For proPr, there are two types of PAPs to consider as known targets (for review, see (Nanjundan and Possmayer, 2003)). The first is cytosolic and is termed PAP1. This enzyme has not yet been identified but appears to be recruited to microsomal membranes, at least *in vitro* (Martin-Sanz et al., 1984). The second enzyme, PAP2, has been identified and extensively characterized and is incorporated into cellular membranes (mainly the plasma membrane) via multiple transmembrane domains. Both PAP1 and PAP2 are effectively inhibited by proPr. At present, we cannot make a formal distinction between PAP1 and PAP2 in terms of bud-formation in the Golgi apparatus though the *in vitro* binding study presented in Figure 1A supports a role for PAP1. Candidate enzymes for PAP1 are the



lipins (for review, see (Carman and Han, 2006)) and future testing should reveal the identity of which PAP is responsible for bud-formation in the Golgi apparatus once these enzymes have been characterized and reagents become available.

We find it unlikely that proPr affects ARFGAP1 directly since in the absence of cytosol, we observed an increased binding to Golgi membranes. Had proPr affected ARFGAP1 directly, such binding should not be expected. Furthermore, RNAi<sup>ARFGAP1</sup>-transfected cells were still capable of bud-formation and still responded to proPr. Hence, it is improbable that ARFGAP1 is a direct target for proPr. Similarly, we find it unlikely that coatomer is a target of proPr as its binding to Golgi membranes was not affected by proPr at any discernable rate (Supl. Fig. 1D-E). We also monitored ARF1 expressed as an EGFP-fusion protein and found that it was not lost from the Golgi apparatus upon proPr addition (data not shown). The presence or absence of coatomer on Golgi membranes is nevertheless not predicted to inhibit bud formation. Loss of coatomer from Golgi membranes upon BFA results in extensive tubule formation. The opposite, recruitment of coatomer under conditions where GTP hydrolysis by ARF1 is inhibited results in vesicle formation. In both cases, bud formation is a prerequisite making it unlikely that inhibition of COPI function could explain the observed decrease in bud formation. Rather, it is the lack of PA-derived DAG.

We were surprised by the rapid response of proPr in terms of bud and vesicle formation. At the concentration used (300  $\mu$ M), PAP1 is expected to be fully inhibited (Meier et al., 1998) consequently preventing conversion of PA into DAG (see Figure 6B). In the past,

much emphasis has been put on a role for PA in vesicle and tubule formation, in particular, the role of PA-binding proteins containing BAR domains such as Bars-50. These have been proposed to bind PA in order to stabilize negative curvature thereby promoting bud formation. As PA is cone-shaped, this lipid would promote negative curvature in the cytosolic leaflet ensuring that buds can proceed through the latter stages by the closing of the neck-region. Conversion of PA into DAG, also a cone-shaped lipid, would finally ensure that ARFGAP1 is recruited to complete the fission/scission event through BAR-containing proteins and other factors (Yang et al., 2005; Yang et al., 2006). Our finding that an inhibition of PA to DAG conversion results in a marked decrease in membrane buds is inconsistent with this model. Rather, an accumulation of PA seems less favorable for bud-formation suggesting that DAG rather than PA is required to form the bud (see (Shemesh et al., 2003) for theoretical modeling). We speculate that DAG promotes negative curvature in the luminal leaflet of the vesicle bud. This is possible since DAG flip-flop (Fig. 6B, FF) almost instantly (within seconds) (Bai and Pagano, 1997) once formed at the cytosolic leaflet. In contrast, PA and other phospholipids flip-flop at a much slower rate (within minutes or hours). We propose that bud formation and consequently, vesicle and tubule formation is the consequence of several events. First, local fluctuations in membranes that occur naturally enable bud structures to form transiently which are then stabilized by proteins such as coat proteins binding to the cytosolic surface of the membrane (see (Reynwar et al., 2007) and references therein). Such fluctuations are stimulated by the presence of membrane proteins (Kim et al., 1998) as well as DAG where the latter can flip-flop rapidly between the two leaflets. On the cytosolic leaflet, PA is also converted into lysophosphatidic acid which is an effective

promoter of positive curvature. The coated bud can now form and transformed into a vesicle or a tubule through elongation and constriction of the neck region. This is promoted by PA and DAG-binding proteins such as BAR-containing proteins and ARFGAP1 (Fig. 6B, PA-BP and DAG-BP).

### **Acknowledgements**

We would like to acknowledge Dr. David Mastronarde at the University of Colorado for his help and advise on tomographic reconstruction of 4K by 4K image stacks, Dr. Adrian C. Oprins (UMCU, Utrecht, The Netherlands) for graphics used in Figure 6A, Yvonne Josefsson and Dr. Bengt R. Johansson at the Inst. of Biomedicine, University of Gothenburg, Sweden for preparation of thin sections use of the transmission microscope, respectively.

## Figure Legends

**Figure 1. Inhibition of DAG formation through PAP1 results in a rapid loss of ARFGAP1 from Golgi membranes.** In A, inhibition of ARFGAP1 binding to Golgi membranes by proPr is cytosol-dependent. Recombinant His-tagged ARFGAP1 (0,1 µg) was incubated in a 200 µl reaction buffer (see Material and Methods) together with highly purified Golgi membranes (20 µg), rat liver cytosol (1 mg) or proPr (300 µM) for 15 minutes at 37°C. Incubation mixtures were terminated on ice and membranes pelleted at 13 000 rpm for 10 minutes. Solubilized proteins were then separated by SDS-PAGE and transferred to nitrocellulose for western blotting. His-ARFGAP1 was detected using a poly-His specific antibody followed by secondary HRP labelled rabbit anti-mouse antibody and an ECL detection system. In B-F, addition of 60 µM proPr for 600 seconds (C, D) or 300 µM proPr for 20 seconds (E, F) results in a partial or complete loss of the Golgi localized ARFGAP1<sup>EGFP</sup>, respectively. Scale bar 10 µm.

**Figure 2. DAG is required for bud-formation.** Thin plastic embedded sections (60 nm thick) were examined at the ultrastructural level. A-C shows representative low magnification fields (scale bar 1 µm) whereas D-G shows representative high magnification fields (scale bar 100 nm). In A and D, multiple Golgi stacks align laterally to form a part of the Golgi ribbon in untreated cells. Associated membrane buds (arrow) and VTPs (arrowhead) were seen in close proximity to cisternal membranes of the Golgi stack. In B and E, addition of 300 µM proPr for 3 minutes resulted in an increased frequency of curved stacks that consisted of smooth cisternal membranes seemingly devoid of both membrane buds as well as VTPs. Occasional VTPs and buds (arrowhead

in E) were observed but at a marked decreased frequency (see G for quantitation). In C and F, removal of proPr resulted in a dramatic increase of both membrane buds as well as VTPs already after 2 minutes. Arrow and arrowheads point to a bud and VTPs, respectively. In G, quantitation of cisternae, VTPs and membrane buds presented as the mean of total membranes and compared to untreated control (Ctrl) which was set at 100%.

**Figure 3. Electron tomography of Golgi stacks.** Dual axis tomography was performed to obtain good resolution of membrane delineations in all specimen planes. In A, a digital slice through the 3D volume of an electron tomographic reconstruction illustrates the appearance of the Golgi area seen before addition of proPr (left field), 3 minutes after addition of proPr (middle field) and 2 minutes after removal of proPr (right field). Each membrane-delineated structure present in this digital slice was analyzed throughout the 3D volume and color-coded. In blue, Golgi cisterna or structures continuous with a Golgi cisterna except membrane buds; In red, vesicles; In green, tubular structures; In yellow, membrane buds. Scale bar 100nm. In B, different close-up fields vesicles and membrane buds observed after removal of proPr. Arrows indicate necks of budding profiles that appear constricted by electron-dense material. Scale bar 40nm.

**Figure 4. Inhibition of DAG formation prevents GalNAcT2<sup>CFP</sup> from entering VTPs**

After photooxidation and epon embedding, DAB precipitate was examined by electron microscopy. In A, DAB precipitate is predominantly found in 2-3 cisternae reflecting a gradient-like distribution across the Golgi stack. Some associated VTPs are also positive

for the DAB precipitate consistent with that GalNAcT2<sup>CFP</sup> can gain access to these structures. In B, Upon addition of proPr (300  $\mu$ M) for 3 minutes, the DAB precipitate is seen exclusively in cisternal membranes but can not be detected in any associated buds or VTPs. In C, at 2 minutes after removal of proPr, the DAB product is seen in both cisternal membranes as well as VTPs. In D, magnified field corresponding to the box in C. Arrow points to a bud-like structure filled with DAB precipitate. Arrowheads point to VTPs with a diameter of 40-50 nm. Scale bar in A-C, 1 $\mu$ m, in D, 75nm.

**Figure 5. ARFGAP1 is required for membrane fission.** Thin plastic embedded sections (60 nm thick) of HeLa cells transfected with either RNAi<sup>Mock</sup> or RNAi<sup>ARFGAP1</sup> were examined at the ultrastructural level to discern structures associated with Golgi stacks. Observed structures were quantified (D) as in Figure 2. In A and D, RNAi<sup>ARFGAP1</sup>-transfected cells revealed an increased frequency of membrane buds accompanied by a decreased number of associated VTPs compared to RNAi<sup>Mock</sup>-transfected cells. In B and D, addition of proPr (300  $\mu$ M) for 3 minutes resulted in a marked decrease in associated membrane buds and VTPs in RNAi<sup>ARFGAP1</sup>-transfected cells. In C and D, removal of proPr, revealed a marked increase in membrane buds in cells transfected with RNAi<sup>ARFGAP1</sup> compared to cells transfected with RNAi<sup>Mock</sup> over that of associated VTPs. Scale bar 100 nm.

**Figure 6. Schematic overview and model.** In A, inhibition of DAG synthesis using proPr results in a rapid dissociation of ARFGAP1 and inhibition of bud formation in the Golgi. Removal of proPr and resumption of DAG synthesis results in a rapid rebinding of

ARFGAP1 and a dramatic increase in bud, vesicle and tube formation. SiRNA knockdown experiment suggests that ARFGAP1 is not involved in bud formation, but rather, that it promotes scission/fission of formed vesicles and tubules. After 5-10 minutes, stacks reform highlighting an underlying the dynamic behaviour of Golgi membranes in response to DAG synthesis. In B, a model illustrates the putative function of DAG in promoting bud formation. In this model, PA is converted to LPA (an inverted cone-shaped lipid) or to DAG (a cone-shaped lipid). LPA enriches in the tip of the membrane bud thereby promoting positive curvature. DAG on the other hand promotes negative curvature together with PA in the neck-region and importantly, also the negative curvature in the tip of the luminal leaflet of the vesicle bud. DAG flip-flop once formed in the cytosolic leaflet in order to enrich in the luminal leaflet,

**Supplementary Figure 1. Inhibition of DAG synthesis results in a rapid and reversible dissociation of endogenous ARFGAP1 from the juxta-nuclear Golgi area.**

In A-C, HeLa cells grown on coverslips were fixed (A) or incubated for 3 minutes in the presence of 300  $\mu$ M proPr and then either fixed (B) or washed with culture media and then incubated for an additional 2 minutes (C). Endogenous ARFGAP1 was detected using the polyclonal antibody described in Lanoix et al. (Lanoix et al., 2001). In D-E, cells shown in A-C were double-stained using the monoclonal antibody M3A5 directed towards  $\beta$ COP. Scale bar 10  $\mu$ m.

**Supplementary Figure 2. Restoration of Golgi stacks after 5 and 10 minutes after removal of proPr.** Thin plastic embedded sections (60 nm thick) were examined at the

ultrastructural level. In A and B, Golgi stacks became more definable and the number of associated membrane buds and VTPs decreased after 5 (A) and 10 (B) minutes following the initial burst seen after 2 minutes. For quantitation, see Figure 2 G. Scale bar 1  $\mu$ m.

**Supplementary Figure 3. Transfection of interference RNA to ARFGAP effectively decrease the level of endogenous ARFGAP1 in HeLa cells.** Shown are three independent experiments. HeLa cells were either mock transfected or transfected with interference RNA to ARFGAP1. After 48 hours, cells were scraped off and solubilized in 1% Triton in 25 mM Hepes pH 7.4. 100  $\mu$ g of each cell-lysate was then run on SDS-PAGE and separated proteins transferred to a nitrocellulose membrane.  $\beta$ COP was detected using the mAb M3A5 (Allan and Kreis, 1986) ( $\alpha$ -COP $^{\beta}$ ) and ARFGAP1 ( $\alpha$ -ARFGAP1) using a polyclonal antibody (Lanoix et al., 2001) followed by ECL. The difference in background for detected  $\beta$ COP as compared to ARFGAP1 is due to the use of an ultrasensitive film (Kodak Biomax<sup>tm</sup> MR film) in the case of the latter.

**Supplementary Figure 4. Electronmicroscopy of cells transfected with RNAi<sup>Mock</sup> and RNAi<sup>ARFGAP1</sup>.** Thin plastic embedded sections (60 nm thick) were examined at the ultrastructural level. In A and B, Golgi areas seen in RNAi<sup>Mock</sup>-transfected (A) and RNAi<sup>ARFGAP1</sup>-transfected (B) cells. In C and D, Golgi areas seen in RNAi<sup>Mock</sup>-transfected (C) and RNAi<sup>ARFGAP1</sup>-transfected (D) cells upon incubation with 300  $\mu$ M proPr for 3 minutes. In E and F, Golgi areas seen in RNAi<sup>Mock</sup>-transfected (E) and RNAi<sup>ARFGAP1</sup>-transfected (F) cells 2 minutes after removal of proPr. In G and H, Golgi areas seen in



RNAi<sup>Mock</sup>-transfected (G) and RNAi<sup>ARFGAP1</sup>-transfected (H) cells 5 minutes after removal of proPr. Scale bar 1  $\mu$ m.

## References

- Allan, V.J., and Kreis, T.E. (1986). A microtubule-binding protein associated with membranes of the Golgi apparatus. *J Cell Biol* 103, 2229-2239.
- Antonny, B., Huber, I., Paris, S., Chabre, M., and Cassel, D. (1997). Activation of ADP-ribosylation factor 1 GTPase-activating protein by phosphatidylcholine-derived diacylglycerols. *J Biol Chem* 272, 30848-30851.
- Bai, J., and Pagano, R.E. (1997). Measurement of spontaneous transfer and transbilayer movement of BODIPY-labeled lipids in lipid vesicles. *Biochemistry* 36, 8840-8848.
- Baron, C.L., and Malhotra, V. (2002). Role of diacylglycerol in PKD recruitment to the TGN and protein transport to the plasma membrane. *Science* 295, 325-328.
- Bethune, J., Wieland, F., and Moelleken, J. (2006). COPI-mediated transport. *The Journal of membrane biology* 211, 65-79.
- Bigay, J., Casella, J.F., Drin, G., Mesmin, B., and Antonny, B. (2005). ArfGAP1 responds to membrane curvature through the folding of a lipid packing sensor motif. *Embo J* 24, 2244-2253.
- Blood, P.D., and Voth, G.A. (2006). Direct observation of Bin/amphiphysin/Rvs (BAR) domain-induced membrane curvature by means of molecular dynamics simulations. *Proc Natl Acad Sci U S A* 103, 15068-15072.
- Bonazzi, M., Spano, S., Turacchio, G., Cericola, C., Valente, C., Colanzi, A., Kweon, H.S., Hsu, V.W., Polishchuck, E.V., Polishchuck, R.S., *et al.* (2005). CtBP3/BARS drives membrane fission in dynamin-independent transport pathways. *Nat Cell Biol* 7, 570-580.
- Brown, H.A., Gutowski, S., Kahn, R.A., and Sternweis, P.C. (1995). Partial purification and characterization of Arf-sensitive phospholipase D from porcine brain. *J Biol Chem* 270, 14935-14943.
- Brown, H.A., Gutowski, S., Moomaw, C.R., Slaughter, C., and Sternweis, P.C. (1993). ADP-ribosylation factor, a small GTP-dependent regulatory protein, stimulates phospholipase D activity. *Cell* 75, 1137-1144.
- Carman, G.M., and Han, G.S. (2006). Roles of phosphatidate phosphatase enzymes in lipid metabolism. *Trends in biochemical sciences* 31, 694-699.
- Carrasco, S., and Merida, I. (2004). Diacylglycerol-dependent binding recruits PKC $\theta$  and RasGRP1 C1 domains to specific subcellular localizations in living T lymphocytes. *Molecular biology of the cell* 15, 2932-2942.
- Carrasco, S., and Merida, I. (2007). Diacylglycerol, when simplicity becomes complex. *Trends in biochemical sciences* 32, 27-36.
- Chen, Y.G., Siddhanta, A., Austin, C.D., Hammond, S.M., Sung, T.C., Frohman, M.A., Morris, A.J., and Shields, D. (1997). Phospholipase D stimulates release of nascent secretory vesicles from the trans-Golgi network. *J Cell Biol* 138, 495-504.
- Cockcroft, S., Thomas, G.M., Fensome, A., Geny, B., Cunningham, E., Gout, I., Hiles, I., Totty, N.F., Truong, O., and Hsuan, J.J. (1994). Phospholipase D: a downstream effector of ARF in granulocytes. *Science* 263, 523-526.

de Figueiredo, P., Drecktrah, D., Polizotto, R.S., Cole, N.B., Lippincott-Schwartz, J., and Brown, W.J. (2000). Phospholipase A2 antagonists inhibit constitutive retrograde membrane traffic to the endoplasmic reticulum. *Traffic (Copenhagen, Denmark) 1*, 504-511.

Dominguez, M., Dejgaard, K., Fullekrug, J., Dahan, S., Fazel, A., Paccaud, J.P., Thomas, D.Y., Bergeron, J.J., and Nilsson, T. (1998). gp25L/emp24/p24 protein family members of the cis-Golgi network bind both COP I and II coatomer. *J Cell Biol 140*, 751-765.

Elsner, M., Hashimoto, H., Simpson, J.C., Cassel, D., Nilsson, T., and Weiss, M. (2003). Spatiotemporal dynamics of the COPI vesicle machinery. *EMBO Rep 4*, 1000-1004.

Fernandez-Ulibarri, I., Vilella, M., Lazaro-Dieguez, F., Sarri, E., Martinez, S.E., Jimenez, N., Claro, E., Merida, I., Burger, K.N., and Egea, G. (2007). Diacylglycerol is required for the formation of COPI vesicles in the Golgi-to-ER transport pathway. *Molecular biology of the cell 18*, 3250-3263.

Frigerio, G., Grimsey, N., Dale, M., Majoul, I., and Duden, R. (2007). Two Human ARFGAPs Associated with COP-I-Coated Vesicles. *Traffic (Copenhagen, Denmark) 8*, 1644-1655.

Gallop, J.L., Butler, P.J., and McMahon, H.T. (2005). Endophilin and CtBP/BARS are not acyl transferases in endocytosis or Golgi fission. *Nature 438*, 675-678.

Gallop, J.L., Jao, C.C., Kent, H.M., Butler, P.J., Evans, P.R., Langen, R., and McMahon, H.T. (2006). Mechanism of endophilin N-BAR domain-mediated membrane curvature. *Embo J 25*, 2898-2910.

Grabenbauer, M., Geerts, W.J., Fernandez-Rodriguez, J., Hoenger, A., Koster, A.J., and Nilsson, T. (2005). Correlative microscopy and electron tomography of GFP through photooxidation. *Nat Methods 2*, 857-862.

Houle, M.G., Kahn, R.A., Naccache, P.H., and Bourgoin, S. (1995). ADP-ribosylation factor translocation correlates with potentiation of GTP gamma S-stimulated phospholipase D activity in membrane fractions of HL-60 cells. *J Biol Chem 270*, 22795-22800.

Kim, K.S., Neu, J., and Oster, G. (1998). Curvature-mediated interactions between membrane proteins. *Biophysical journal 75*, 2274-2291.

Kirchhausen, T. (2000). Three ways to make a vesicle. *Nature reviews 1*, 187-198.

Kremer, J.R., Mastronarde, D.N., and McIntosh, J.R. (1996). Computer visualization of three-dimensional image data using IMOD. *Journal of structural biology 116*, 71-76.

Ktistakis, N.T., Brown, H.A., Sternweis, P.C., and Roth, M.G. (1995). Phospholipase D is present on Golgi-enriched membranes and its activation by ADP ribosylation factor is sensitive to brefeldin A. *Proc Natl Acad Sci U S A 92*, 4952-4956.

Ktistakis, N.T., Brown, H.A., Waters, M.G., Sternweis, P.C., and Roth, M.G. (1996). Evidence that phospholipase D mediates ADP ribosylation factor-dependent formation of Golgi coated vesicles. *J Cell Biol 134*, 295-306.

Lanoix, J., Ouwendijk, J., Lin, C.C., Stark, A., Love, H.D., Ostermann, J., and Nilsson, T. (1999). GTP hydrolysis by arf-1 mediates sorting and concentration of Golgi resident enzymes into functional COP I vesicles. *Embo J 18*, 4935-4948.

Lanoix, J., Ouwendijk, J., Stark, A., Szafer, E., Cassel, D., Dejgaard, K., Weiss, M., and Nilsson, T. (2001). Sorting of Golgi resident proteins into different subpopulations of COPI vesicles: a role for ArfGAP1. *J Cell Biol* 155, 1199-1212.

Martin-Sanz, P., Hopewell, R., and Brindley, D.N. (1984). Long-chain fatty acids and their acyl-CoA esters cause the translocation of phosphatidate phosphohydrolase from the cytosolic to the microsomal fraction of rat liver. *FEBS Lett* 175, 284-288.

Mastronarde, D.N. (1997). Dual-axis tomography: an approach with alignment methods that preserve resolution. *Journal of structural biology* 120, 343-352.

Meier, K.E., Gause, K.C., Wisheart-Johnson, A.E., Gore, A.C., Finley, E.L., Jones, L.G., Bradshaw, C.D., McNair, A.F., and Ella, K.M. (1998). Effects of propranolol on phosphatidate phosphohydrolase and mitogen-activated protein kinase activities in A7r5 vascular smooth muscle cells. *Cellular signalling* 10, 415-426.

Mesmin, B., Drin, G., Levi, S., Rawet, M., Cassel, D., Bigay, J., and Antonny, B. (2007). Two lipid-packing sensor motifs contribute to the sensitivity of ArfGAP1 to membrane curvature. *Biochemistry* 46, 1779-1790.

Misteli, T., and Warren, G. (1995). Mitotic disassembly of the Golgi apparatus in vivo. *J Cell Sci* 108 ( Pt 7), 2715-2727.

Nanjundan, M., and Possmayer, F. (2003). Pulmonary phosphatidic acid phosphatase and lipid phosphate phosphohydrolase. *American journal of physiology* 284, L1-23.

Niu, T.K., Pfeifer, A.C., Lippincott-Schwartz, J., and Jackson, C.L. (2005). Dynamics of GBF1, a Brefeldin A-sensitive Arf1 exchange factor at the Golgi. *Molecular biology of the cell* 16, 1213-1222.

Orci, L., Glick, B.S., and Rothman, J.E. (1986). A new type of coated vesicular carrier that appears not to contain clathrin: its possible role in protein transport within the Golgi stack. *Cell* 46, 171-184.

Palmer, D.J., Helms, J.B., Beckers, C.J., Orci, L., and Rothman, J.E. (1993). Binding of coatamer to Golgi membranes requires ADP-ribosylation factor. *J Biol Chem* 268, 12083-12089.

Penczek, P., Marko, M., Buttle, K., and Frank, J. (1995). Double-tilt electron tomography. *Ultramicroscopy* 60, 393-410.

Reinhard, C., Schweikert, M., Wieland, F.T., and Nickel, W. (2003). Functional reconstitution of COPI coat assembly and disassembly using chemically defined components. *Proc Natl Acad Sci U S A* 100, 8253-8257.

Reynwar, B.J., Illya, G., Harmandaris, V.A., Muller, M.M., Kremer, K., and Deserno, M. (2007). Aggregation and vesiculation of membrane proteins by curvature-mediated interactions. *Nature* 447, 461-464.

Schmidt, A., Wolde, M., Thiele, C., Fest, W., Kratzin, H., Podtelejnikov, A.V., Witke, W., Huttner, W.B., and Soling, H.D. (1999). Endophilin I mediates synaptic vesicle formation by transfer of arachidonate to lysophosphatidic acid. *Nature* 401, 133-141.

Sciaky, N., Presley, J., Smith, C., Zaal, K.J., Cole, N., Moreira, J.E., Terasaki, M., Siggia, E., and Lippincott-Schwartz, J. (1997). Golgi tubule traffic and the effects of brefeldin A visualized in living cells. *J Cell Biol* 139, 1137-1155.

Shemesh, T., Luini, A., Malhotra, V., Burger, K.N., and Kozlov, M.M. (2003). Prefission constriction of Golgi tubular carriers driven by local lipid metabolism: a theoretical model. *Biophysical journal* 85, 3813-3827.

Simionescu, N., and Simionescu, M. (1976). Galloylglucoses of low molecular weight as mordant in electron microscopy. I. Procedure, and evidence for mordanting effect. *J Cell Biol* 70, 608-621.

Sonoda, H., Okada, T., Jahangeer, S., and Nakamura, S. (2007). Requirement of phospholipase D for ilimaquinone-induced Golgi membrane fragmentation. *J Biol Chem* 282, 34085-34092.

Spang, A., Matsuoka, K., Hamamoto, S., Schekman, R., and Orci, L. (1998). Coatamer, Arf1p, and nucleotide are required to bud coat protein complex I-coated vesicles from large synthetic liposomes. *Proc Natl Acad Sci U S A* 95, 11199-11204.

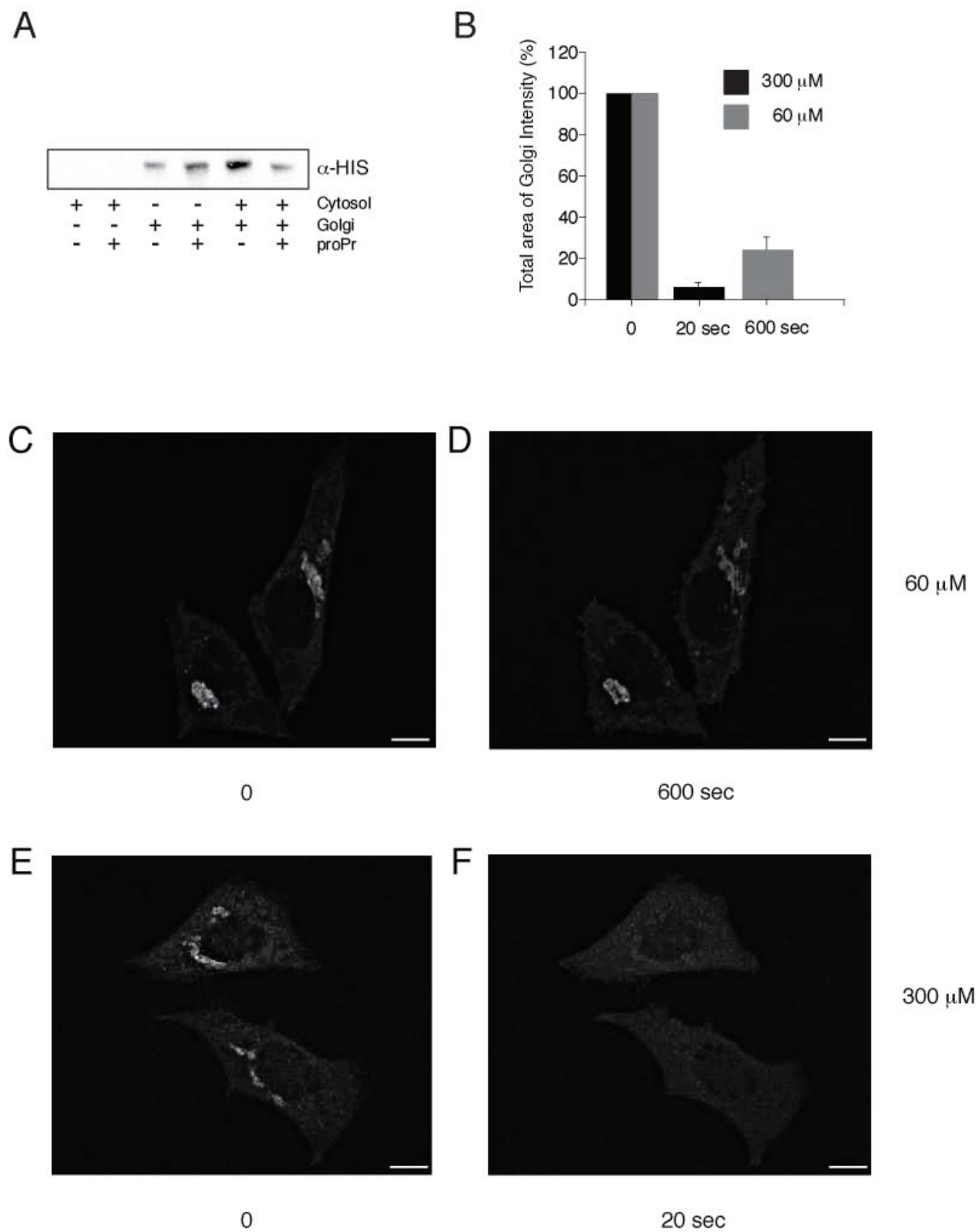
Storrie, B., White, J., Rottger, S., Stelzer, E.H., Suganuma, T., and Nilsson, T. (1998). Recycling of golgi-resident glycosyltransferases through the ER reveals a novel pathway and provides an explanation for nocodazole-induced Golgi scattering. *J Cell Biol* 143, 1505-1521.

Weigert, R., Silletta, M.G., Spano, S., Turacchio, G., Cericola, C., Colanzi, A., Senatore, S., Mancini, R., Polishchuk, E.V., Salmona, M., *et al.* (1999). CtBP/BARS induces fission of Golgi membranes by acylating lysophosphatidic acid. *Nature* 402, 429-433.

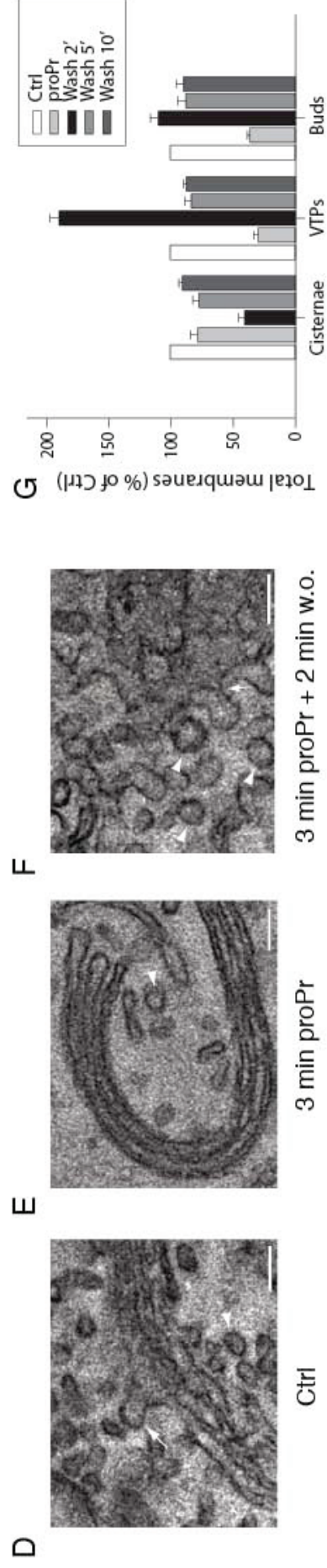
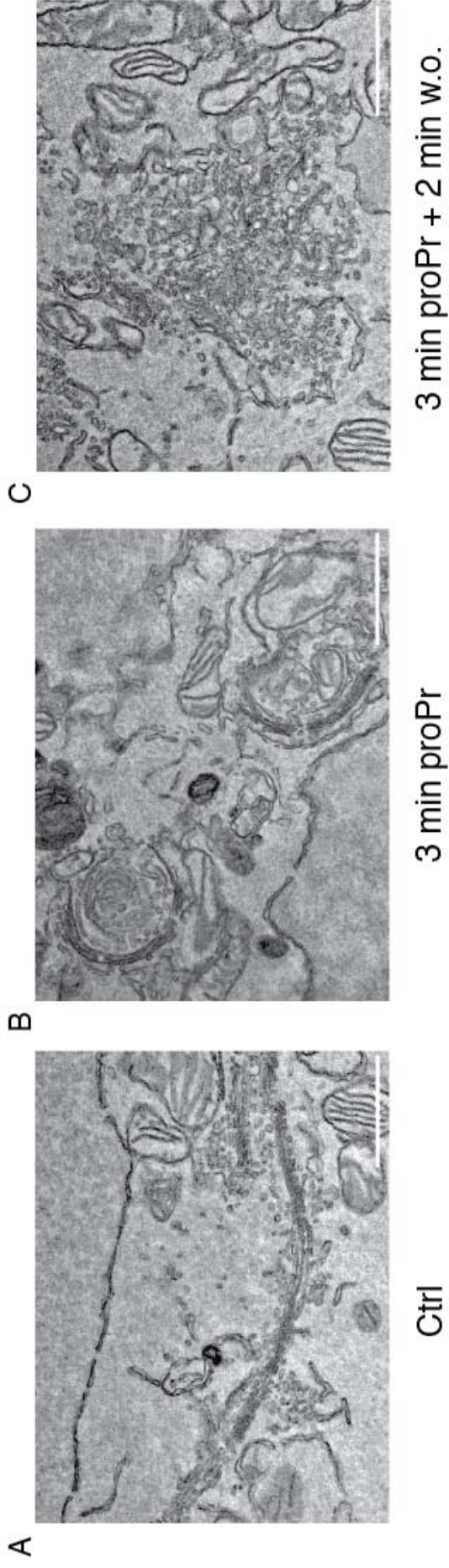
Weiss, M., and Nilsson, T. (2003). A kinetic proof-reading mechanism for protein sorting. *Traffic (Copenhagen, Denmark)* 4, 65-73.

Yang, J.S., Lee, S.Y., Spano, S., Gad, H., Zhang, L., Nie, Z., Bonazzi, M., Corda, D., Luini, A., and Hsu, V.W. (2005). A role for BARS at the fission step of COPI vesicle formation from Golgi membrane. *Embo J* 24, 4133-4143.

Yang, J.S., Zhang, L., Lee, S.Y., Gad, H., Luini, A., and Hsu, V.W. (2006). Key components of the fission machinery are interchangeable. *Nat Cell Biol.*

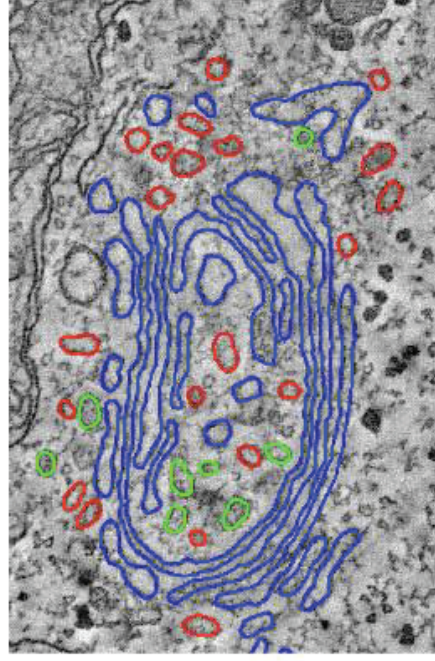




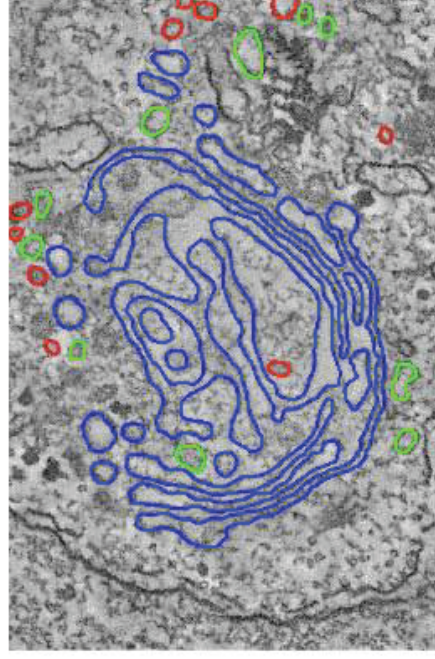




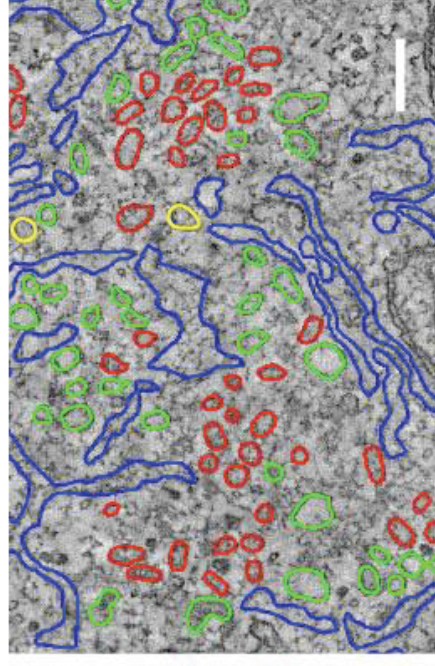
A



Ctrl

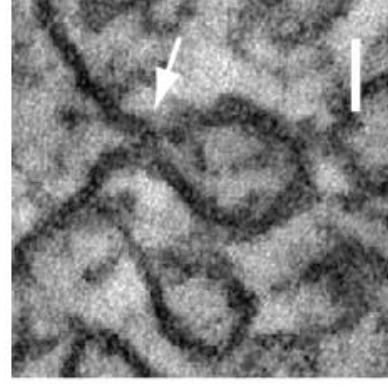
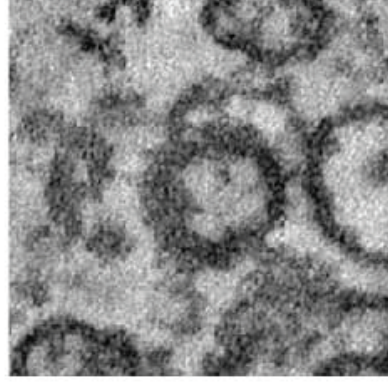
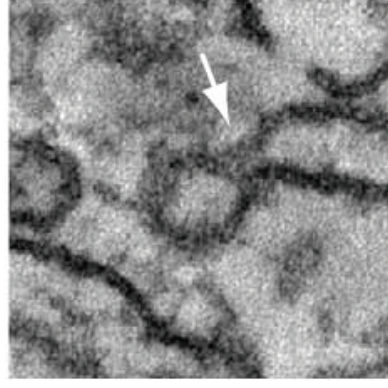
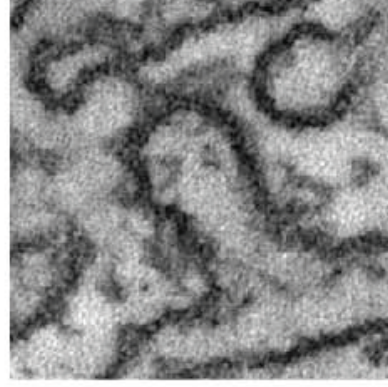
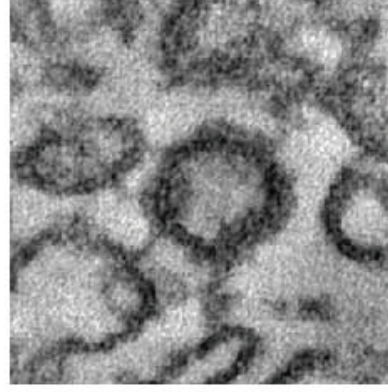


3 min proPr



3 min proPr + 2 min w.o.

B



← 3 min proPr + 2 min w.o. →



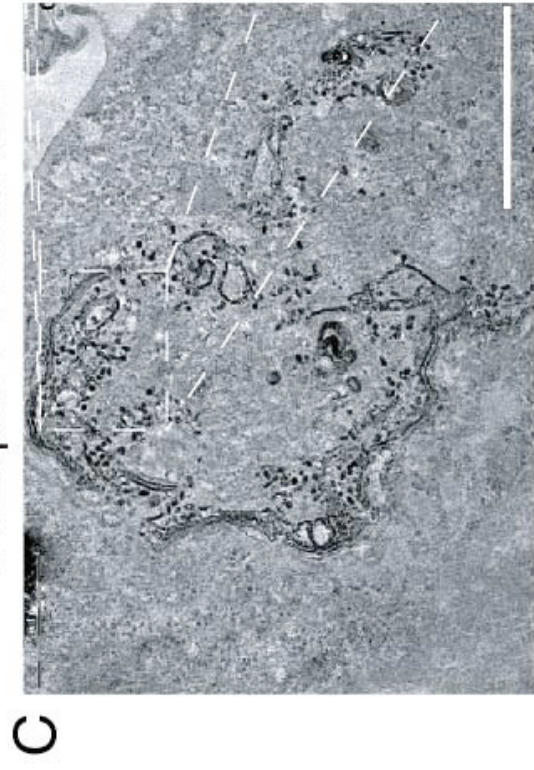
Ctrl



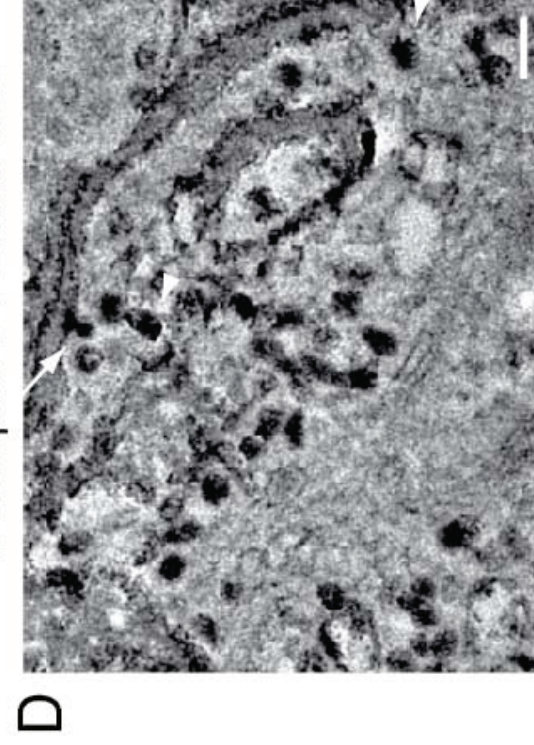
3 min proPr



3 min proPr + 2 min w.o.

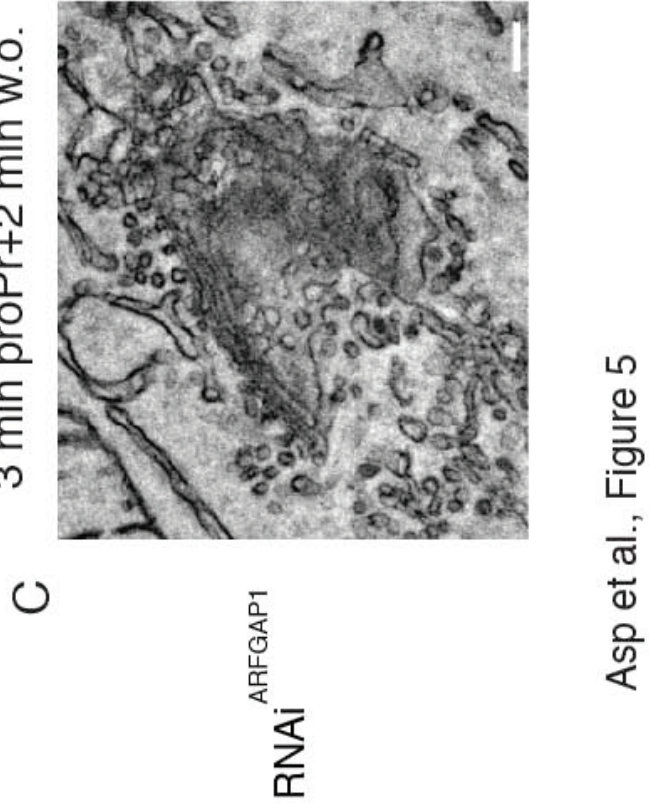
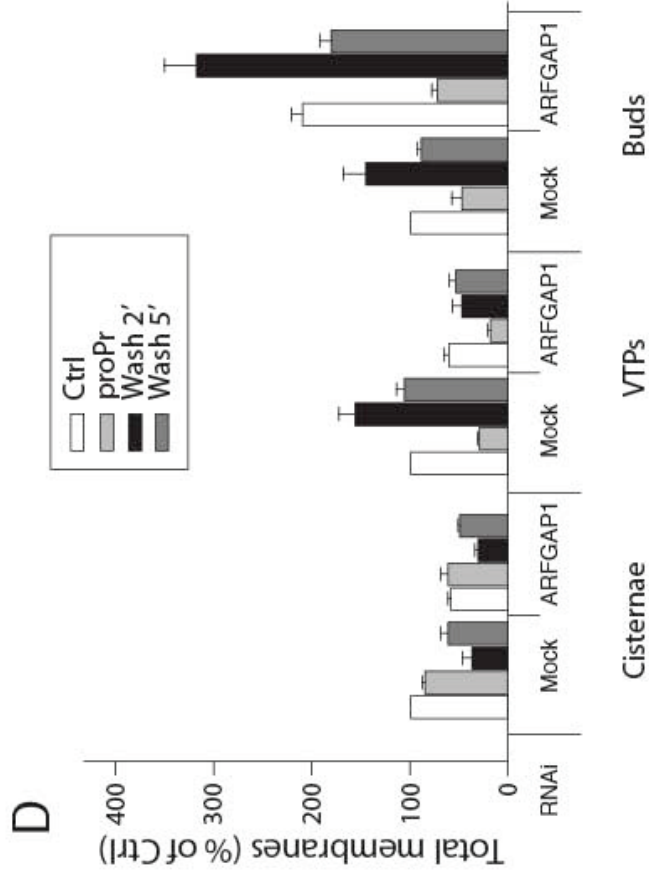
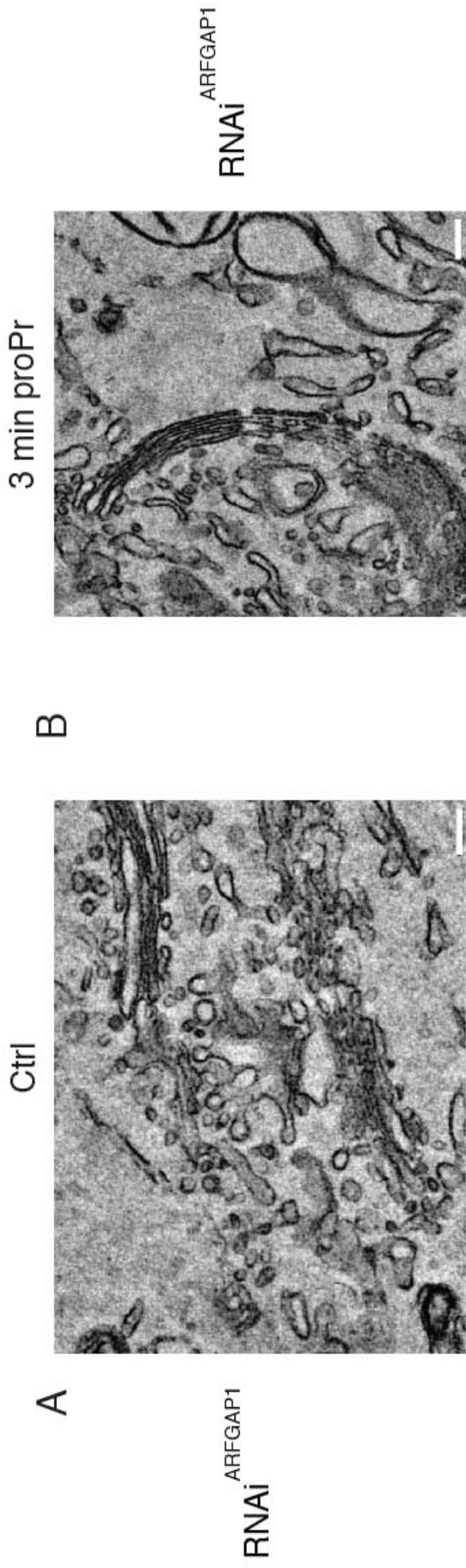


3 min proPr + 2 min w.o.



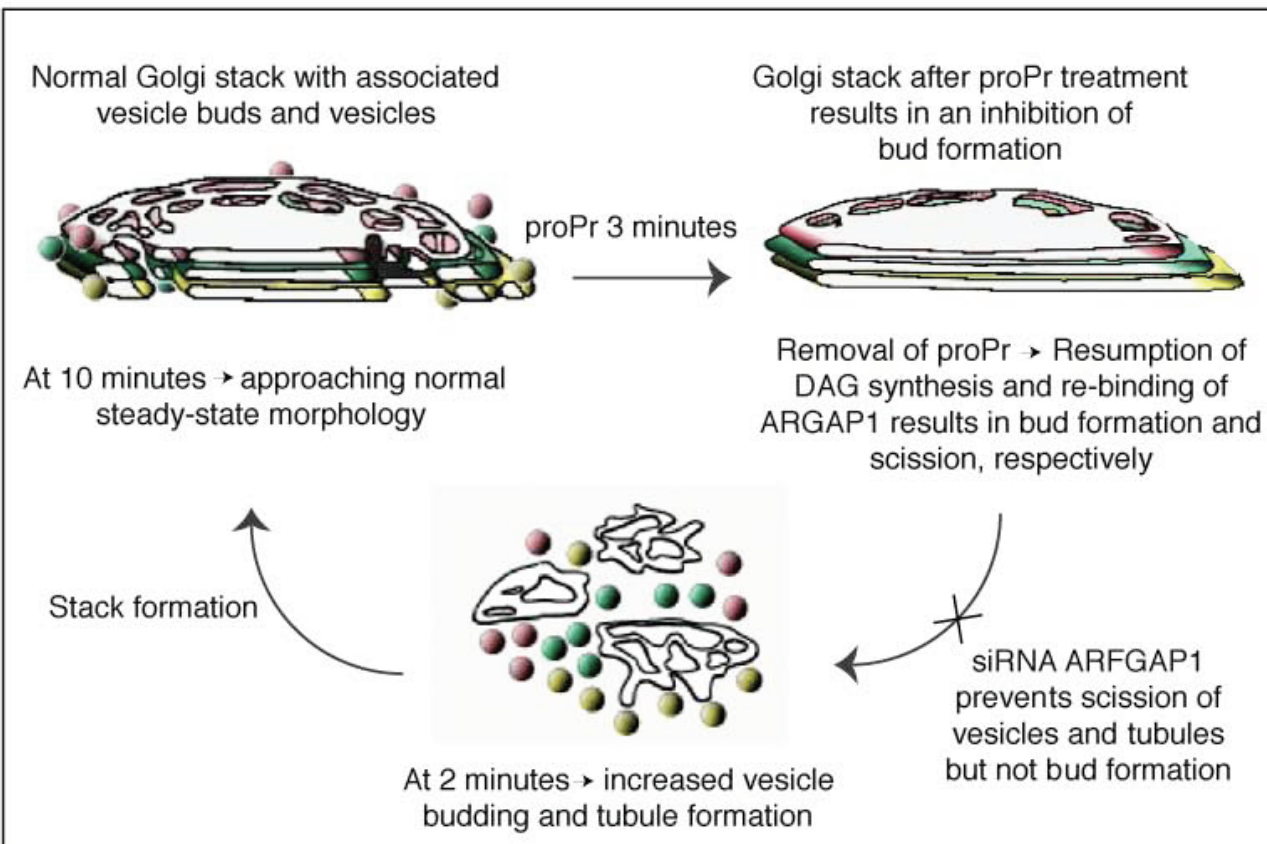
Asp et al., Figure 4



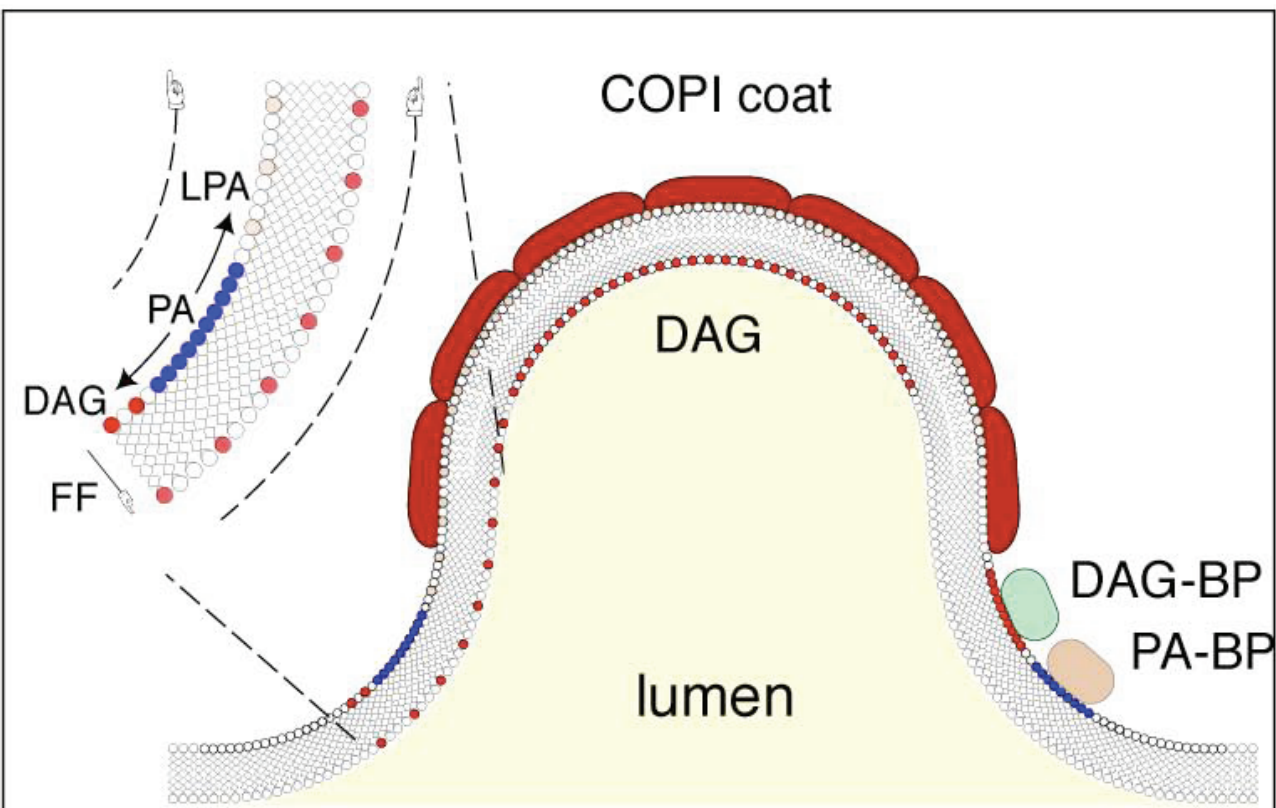


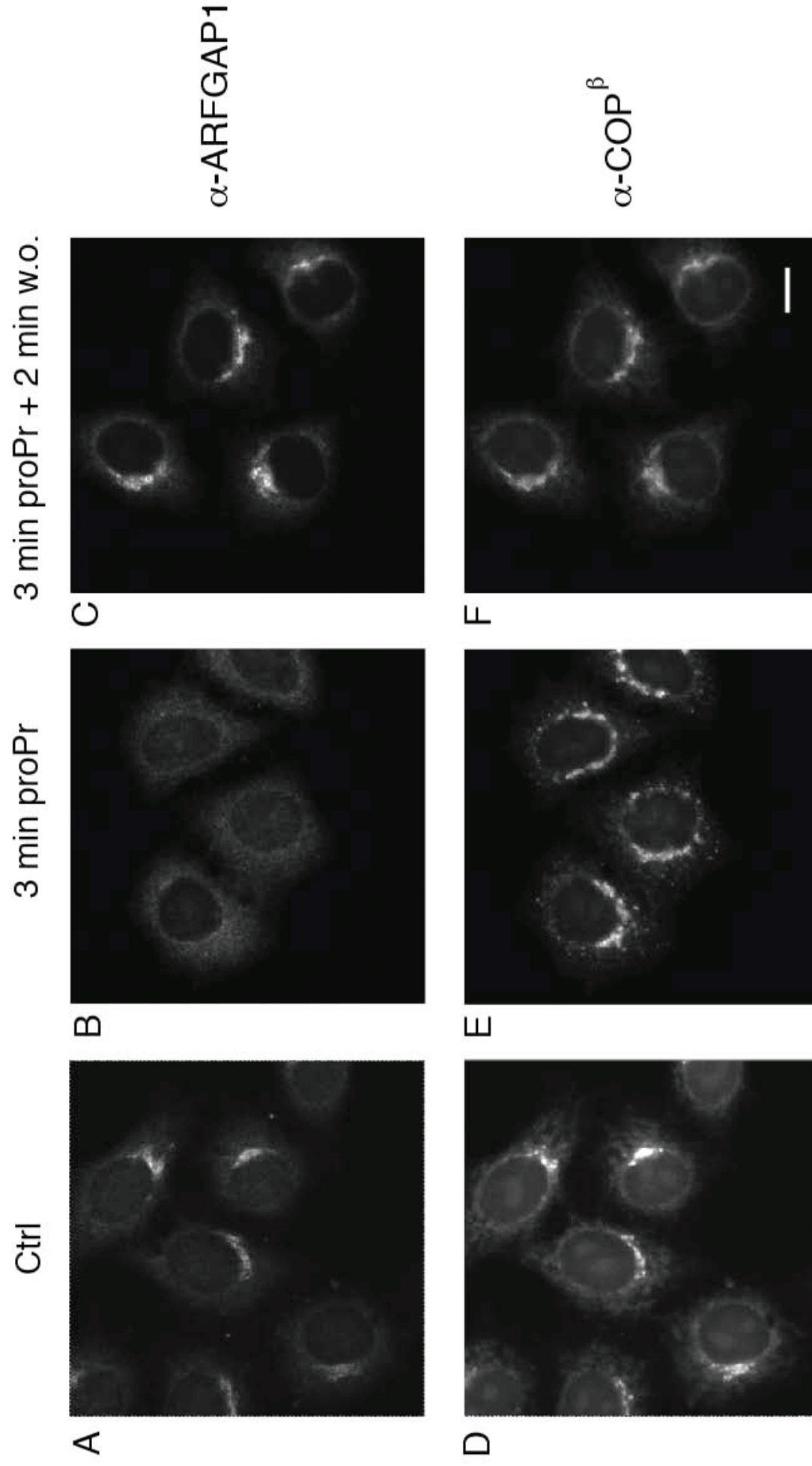
Asp et al., Figure 5

A



B

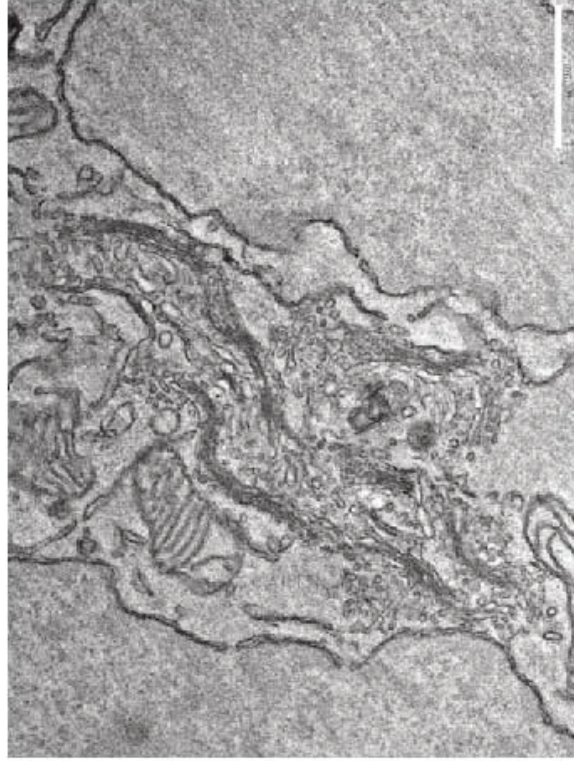




Asp et al., Supplementary Figure 1

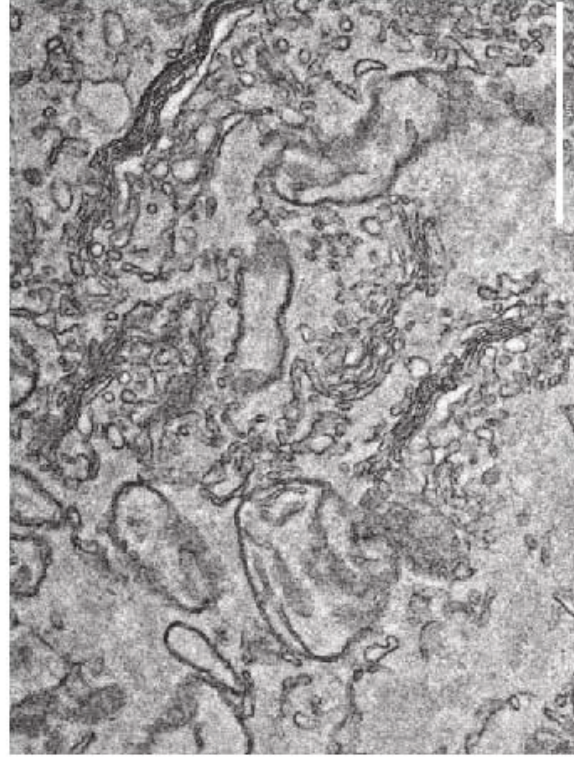


A

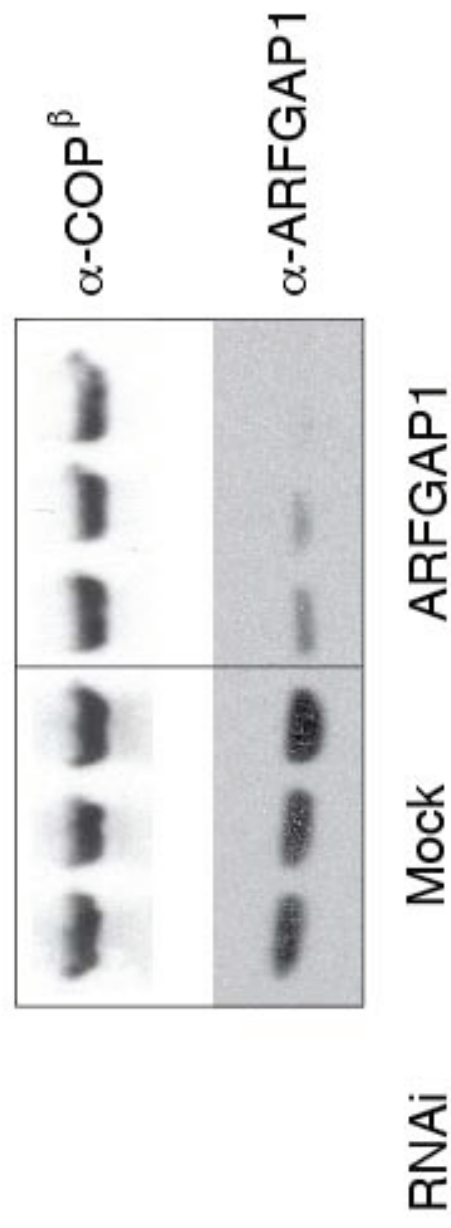


3 min proPr + 5 min w.o.

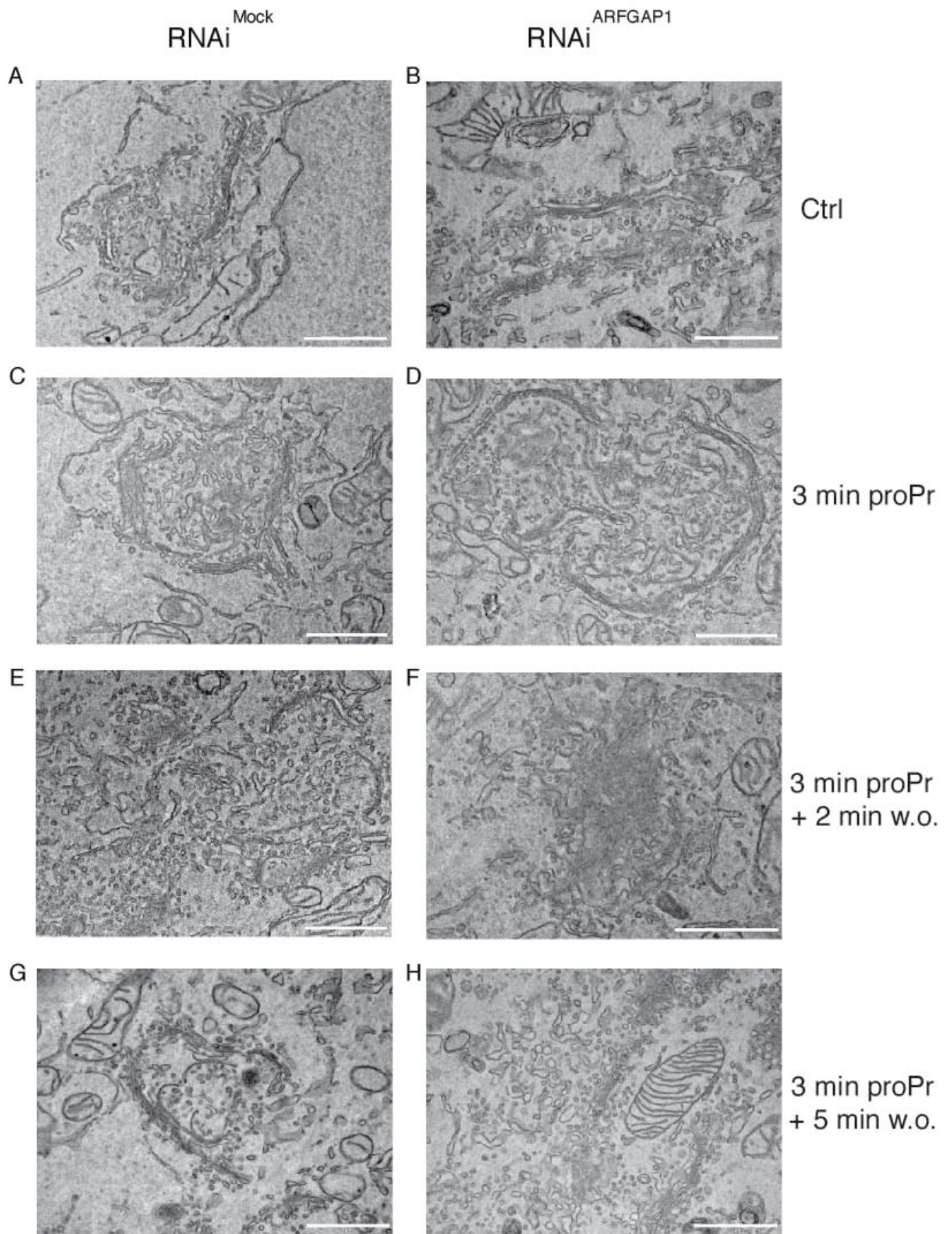
B



3 min proPr + 10 min w.o.







Asp et al., Supplementary Figure 4

# Carboxyl-Terminal Disulfide Bond of Acid Sphingomyelinase Is Critical for Its Secretion and Enzymatic Function<sup>†</sup>

Ching Yin Lee,<sup>‡</sup> Taku Tamura,<sup>§</sup> Nadia Rabah,<sup>||</sup> Dong-Young Donna Lee,<sup>‡</sup> Isabelle Ruel,<sup>‡</sup> Anouar Hafiane,<sup>‡</sup> Iulia Iatan,<sup>‡</sup> Dana Nyholt,<sup>‡</sup> Frédéric Laporte,<sup>⊥</sup> Claude Lazure,<sup>||</sup> Ikuo Wada,<sup>§</sup> Larbi Krimbou,<sup>‡</sup> and Jacques Genest<sup>\*,‡</sup>

Cardiovascular Genetics Laboratory, Cardiology Division, McGill University Health Center/Royal Victoria Hospital, Montréal, Québec H3A 1A1, Canada, Department of Cell Science, Institute of Biomedical Sciences, Fukushima Medical University School of Medicine, Fukushima, Japan, Laboratory of Structure and Metabolism of Neuropeptides, Institut de recherches cliniques de Montréal, Montréal, Canada, and Cell Map Laboratory, McGill University, Montréal, Canada

Received April 30, 2007; Revised Manuscript Received October 26, 2007

**ABSTRACT:** The human acid sphingomyelinase (ASM, EC 3.1.4.12), a lysosomal and secretory protein coded by the sphingomyelin phosphodiesterase 1 (SMPD-1) gene, catalyzes the degradation of sphingomyelin (SM) to ceramide and phosphorylcholine. We examined the structural–functional properties of its carboxyl-terminus (amino acids 462–629), which harbors  $\sim 1/3$  of all mutations discovered in the SMPD-1 gene. We created four naturally occurring mutants ( $\Delta$ R608, R496L, G577A, and Y537H) and five serial carboxyl-terminal deletion mutants (N620, N590, N570, N510, and N490). Transient transfection of the His/V5-tagged wild-type and mutant recombinant ASM in Chinese hamster ovary cells showed that all the mutants were normally expressed. Nonetheless, none of them, except the smallest deletion mutant N620 that preserved all post-translational modifications, were found capable of secretion to the medium. Furthermore, only the N620 conserved functional integrity (100% activity of the wild type); all other mutants completely lost the ability to catalyze SM hydrolysis. Importantly, cell surface biotinylation revealed that mutant  $\Delta$ R608 transfected CHO cells and fibroblasts from a compound heterozygous Niemann–Pick disease type B (NPD-B) patient ( $\Delta$ R608 and R441X) have defective translocation to the plasma membrane. Furthermore, we demonstrated that the  $\Delta$ R608 and N590 were trapped in the endoplasmic reticulum (ER) quality control checkpoint in contrast to the wild-type lysosomal localization. Interestingly, while the steady-state levels of ubiquitination were minimal for the wild-type ASM, a significant amount of Lys63-linked polyubiquitinated  $\Delta$ R608 and N590 could be purified by S5a-affinity chromatography, indicating an important misfolding in the carboxyl-terminal mutants. Altogether, we provide evidence that the carboxyl-terminus of the ASM is crucial for its protein structure, which in turns dictates the enzymatic function and secretion.

Sphingomyelinase (sphingomyelin phosphodiesterase) hydrolyzes sphingomyelin (SM)<sup>1</sup> to form phosphocholine and ceramide (1). Several enzymes catalyzing this reaction have been described (2). The acidic form of sphingomyelinase, ASM (EC 3.4.12), is a product of the sphingomyelin phosphodiesterase 1 (SMPD-1) gene. It works at optimal pH

of 5.0 and is ubiquitously distributed in all mammalian tissues (3). Schissel et al. (4) have shown that the same gene gives rise to two different products, lysosomal ASM and secretory ASM, presumably by differential posttranslational modification.

Deficiency of the ASM enzyme due to mutations in SMPD-1 leads to the inherited sphingolipidosis Niemann–Pick disease types A and B (5). In the study of this metabolic defect, ASM has been shown to be implicated in many important physiological and pathological processes involving SM hydrolysis. For example, ASM plays an important role in the regulation of the metabolism of biologically active sphingolipids, including ceramide and sphingosine 1-phosphate, which in turn are key players in cancer pathogenesis (6, 7), cellular differentiation, and various immune and inflammatory responses (8, 9). Our laboratory and others have also demonstrated that ASM is involved in the regulation of intracellular cholesterol trafficking and metabolism (10). Because SM and cholesterol are membrane lipids with important structural roles in the regulation of the fluidity and subdomain structure of the lipid bilayers (11), it is conceivable that any elevation of SM and secondary

<sup>†</sup> This research was supported in part by Grants CIHR MOP 15042 and CIHR MOP 62834 from the Canadian Institutes of Health Research.

<sup>\*</sup> To whom correspondence should be addressed at the Division of Cardiology, McGill University Health Center/Royal Victoria Hospital, H7-17, 687 Pine Ave. West, Montreal, QC, Canada H3A 1A1. Phone (514) 842-1231, ext 34642; fax (514) 843-2813; e-mail jacques.genest@mhcc.mcgill.ca.

<sup>‡</sup> Royal Victoria Hospital and McGill University Health Centre.

<sup>§</sup> Fukushima Medical University School of Medicine.

<sup>||</sup> Institut de recherches cliniques de Montréal.

<sup>⊥</sup> Cell Map Laboratory, McGill University.

<sup>1</sup> Abbreviations: ASM, acid sphingomyelinase; EDTA, ethylenediaminetetraacetic acid; ER, endoplasmic reticulum; HA, hemagglutinin; HEPES, N-(2-hydroxyethyl)piperazine-N'-ethanesulfonic acid; IBMX, isobutyl methylxanthine; NPD-A/B, Niemann–Pick disease, type A/B; PBS, phosphate-buffered saline; PMA, phorbol myristate acetate; PMSF, phenylmethanesulfonyl fluoride; PVDF, poly(vinylidene difluoride); SDS–PA(G)GE, sodium dodecyl sulfate–polyacrylamide (gradient) gel electrophoresis; SM, sphingomyelin; SMPD-1, sphingomyelin phosphodiesterase 1; YFP, yellow fluorescent protein.



increase in cholesterol due to defects in ASM could lead to impairment of many other normal cellular functions. Furthermore, it has been recently shown by Tabas and co-workers (12) and by our group (13) that ASM is possibly an important key player in plasma lipoprotein metabolism and thus modulates the susceptibility to atherogenesis.

The emerging functions for the biologically active sphingolipids have therefore underscored the importance of a better understanding of the ASM protein. It will help elucidate the mechanism of ASM functions and unveil the complex pathways of sphingolipid metabolism, as well as increase the understanding of the nature of the phenotypic variations in sphingolipid storage disorders or in cancers. Human ASM was first described in the late 1960s (14, 15) and subsequently purified from a variety of sources (16, 17). However, its full-length cDNA and genomic sequences were isolated and characterized only in 1992 by Schuchman et al. (18). Although the SMPD-1 gene was cloned, there was very little molecular and structural information of the protein available. ASM is formed by 629 amino acids with a predicted molecular mass of ~70 kDa. On the basis of structure and motif prediction analyses (19–21), ASM belongs to the metallophosphoesterase family that includes a diverse range of phosphoesterases, including protein phosphoserine phosphatases, nucleotidases, and 2',3'-cAMP phosphodiesterases. Its predicted catalytic domain spans from amino acid 199 to 461, as illustrated in Figure 1. The ASM protein also contains a signal peptide at the N-terminal region and a saposin B domain (amino acid 87–165), which appears to serve as activator in the lipid degradation (22). The peptide sequence is also spanned by six *N*-glycosylation sites, 10 putative phosphorylation sites, and six disulfide bonds (23). Site-directed mutagenesis has revealed that five of these sites were used (24) and mass spectrometry has confirmed the presence of the disulfide bonding (25). A detailed crystal structure of ASM is not yet available, but its prediction has been recently attempted on the basis of its similarity to purple acid phosphatase (lute) by using comparative modeling (26). However, this prediction model shares a sequence identity of only <15% of the template, and the C-terminal region of ASM was excluded.

Analyses of SMPD-1 sequence in families with NPD have led to the identification of over 100 NPD-A (severe phenotype) and NPD-B (milder phenotype) mutations (27–30). These mutations span all across the protein peptide sequence. Surprisingly, the C-terminal region harbored the second highest number of mutations after the catalytic domain. It also includes  $\Delta R608$ , which represents one of the most prevalent NPD mutations (31). Although this C-terminal region from amino acids 490–620 does not hold a recognizable functional domain or motif, it contains some important posttranslational modification sites (Figure 1). Substitution or deletion of these C-terminal residues might substantially alter the structure as well as affect the catalytic ability or efficiency of SM hydrolysis. Therefore, the C-terminal region of ASM seems to be important despite the lack of any known functions. Nonetheless, full information on the structure and function of ASM is still lacking in the literature. The essential features governing its catalytic activity remain unknown.

Herein, we dissected the structure and functions of the C-terminal region (N490–N629) of ASM and demonstrated

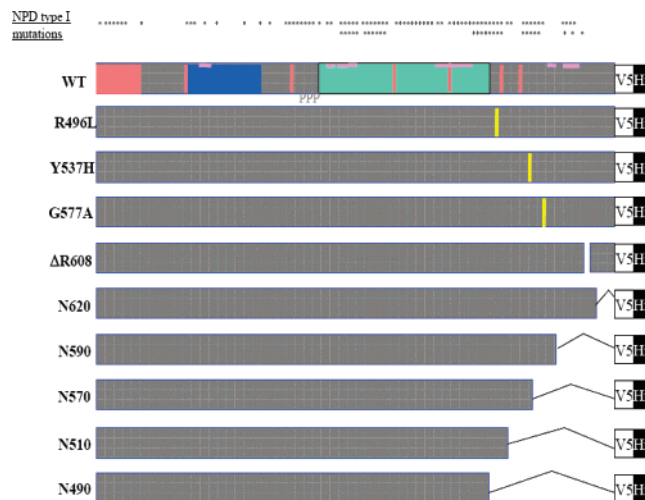


FIGURE 1: ASM sequence and mutagenesis. ASM is a relatively small protein (629 amino acids with a theoretical molecular mass of 70 kDa) consisting of a signal peptide (amino acids 1–46) in the N-terminal region (in red), a small transmembrane domain (amino acids 25–47) (in yellow), a saposin B region (amino acids 87–165) (in blue) that serves as an activator of various lysosomal lipid-degrading enzymes, a proline-rich region (amino acids 179–197) (as black P), followed by the metallophosphoesterase catalytic domain (amino acids 199–461) (in green). In addition, the ASM contains six glycosylation sites [five of which are used according to Ferlinz et al. (26)], six disulfide bonds, and multiple highly putative phosphorylation sites. NPD type A or B mutations [summarized by Sikora et al. and Simonaro et al. (29, 30)] were discovered throughout the entire protein. Interestingly, the C-terminal region of the ASM harbors the second highest number of mutations (29 in total), many of which lead to severe enzymatic defects. The  $\Delta R608$  within this region is one of the most prevalent NPD mutations (33) and is also the mutation that we have discovered in the kindred under our investigation (34). Glycosylation sites are indicated as orange vertical lines; disulfide bonds are drawn as pink horizontal lines. Five serial deletion mutants are designed such that the entire C-terminal region (amino acids 462–629) is spanned: N620 has the smallest deletion and retains all posttranslational modification sites in the C-terminus. N590 conserves all posttranslational modification sites except the sixth disulfide bonding sites (C594–C607). N570 lacks both the fifth (C584–C588) and sixth (C594–C607) disulfide bonding sites. N510 excludes the sixth glycosylation site (N520) in addition to the loss of the two disulfide bonds. N490 retains only the 28 amino acids adjacent to the catalytic domains, missing all posttranslational modification sites in the C-terminus. Point mutants (indicated as vertical yellow lines) R496L, Y537H, and G577A are naturally occurring NPD-A mutants that are known to have severely defective enzymatic function.  $\Delta R608$  is a naturally occurring NPD-B mutant.

that this region, narrowed down to the minimal 30 amino acids (N590–N620) containing the sixth disulfide bond, significantly contributed to the overall conformational integrity dictating its enzymatic functions and secretion. The information in this report should prove useful for future studies that explore the enzymology, regulation, and functions of ASM as well as the pathophysiology related to different SMPD-1 gene defects.

## MATERIALS AND METHODS

**Materials.** All tissue culture media and transfection reagents were from Invitrogen (Carlsbad, CA). Chinese hamster ovarian (CHO) cells and *Spodoptera frugiperda* sf9 cells as well as their culture medium and transfection reagents were from Invitrogen (Carlsbad, CA); *Cercopithecus aethiops*

(COS-7) cells were from the American Type Culture Collection (Manassas, VA). Primary skin fibroblasts were prepared from a compound heterozygous Niemann–Pick disease type B (NPD-B) patient ( $\Delta R608$  and  $R441X$ ) as we have previously described (32). Precast 10% Tris–glycine gels were from Mirador DNA Design (Montreal, QC).  $\beta$ -Galactosidase assay kits were from Promega (Madison, WI). Quikchange II site-directed mutagenesis kits and cloning reagents were from Stratagene (La Jolla, CA). Mouse anti-V5 antibodies were from Invitrogen (Carlsbad, CA), rat anti-HA monoclonal antibodies were from Roche Applied Sciences (Indianapolis, IN), and rabbit anti-YFP polyclonal and mouse anti-KDEL monoclonal antibodies were a generous gift from Dr. Wada, Fukushima Medical University, Japan. Horseradish peroxidase-conjugated rabbit anti-mouse antibodies and PVDF were from GE Healthcare Bio-Sciences (Piscataway, NJ). Mouse anti-mono/polyubiquitinated proteins (clone FK2), S5a agarose, and ubiquitin aldehyde were from Biomol International (Plymouth Meeting, PA). Magnetic beads for small-scale His-tagged protein purification by immobilized metal affinity chromatography were from Dynal Biotech (Brown Deer, WI). Protein A beads for immunoprecipitation were from either Miltenyi Biotec (Auburn, CA) or GE Healthcare Bio-Sciences (Piscataway, NJ).  $\beta$ -Endo-*N*-acetylglucosaminidase H (endoH) and peptide-*N*-glycanase F (PNGase F) were from New England Biolabs (Ipswich, MA). [ $^3H$ ]Sphingomyelinase scintillation proximity assay kits were from GE Healthcare Bio-Sciences (Piscataway, NJ). Sphingomyelin, phosphatidylcholine, and other lipids were from AvantiLipids (Alabaster, AL). All other chemicals were from Sigma (St. Louis, MO).

**Construction of Mammalian Expression Plasmids and Cell Culture.** Mammalian cell culture was maintained in DMEM containing 5–10% fetal bovine serum, 0.1 mM nonessential amino acids, with or without penicillin/streptomycin. CHO or COS cells were transiently transfected with wild-type or mutant ASM cDNAs with lipofectamine 2000 (Invitrogen, Carlsbad, CA) according to the manufacturer's instructions. In some cases,  $\beta$ -galactosidase cDNA (pCMV $\beta$ ) was cotransfected to control transfection efficiency. Mutagenesis of the pcDNA3.1/GS wild-type ASM (Invitrogen, Carlsbad, CA) was performed with Quikchange II Mutagenesis kit (Stratagene, La Jolla, CA). The authenticity of all mutants was confirmed by nucleotide sequencing.

**Immunoblot, Immunoprecipitation, and Protein Purification.** For expression study, cell lysates were harvested 24 h after transfection and prepared with 1% Triton X-100 lysis buffer (150 mM NaCl, 1% Triton X-100, 50 mM Tris-HCl, pH 8.0, with EDTA-free protease inhibitor cocktails, Roche Applied Sciences, Indianapolis, IN). The cellular homogenates were then assayed for  $\beta$ -galactosidase activity for transfection efficiency control. Conditioned medium was collected, spun at 800 g for 15 min to pellet any contaminating cells, and concentrated down to  $\leq 1$  mL by use of a Centrprep 30 concentrator (Amicon, Beverly, MA). Cell lysates or concentrated medium were mixed with bromophenol blue-containing loading buffer, boiled, and directly loaded on 10% Tris–glycine SDS–PAGE after normalization with the transfection efficiency. Gels were then electrottransferred to PVDF for immunoblotting. Blots were incubated with 5% dry milk and various primary and horseradish peroxidase-conjugated secondary antibodies. Finally, the blots were

soaked in chemiluminescence reagent (Pierce, Rockford, IL) and exposed to Omat-Blue X-ray films.

For other experiments, the His/V5-tagged ASM was first purified by metal affinity chromatography or, alternatively, immunoprecipitated with protein A–Sephareose and different antibodies. In ubiquitination studies, lysis buffer containing *N*-ethylmaleimide (NEM) and ubiquitin aldehyde (50 mM HEPES, pH 7.5, 5 mM EDTA, 150 mM NaCl, 1% Triton X-100, EDTA-free protease inhibitors cocktail, 10 mM NEM, and 100 nM ubiquitin aldehyde) was used to lyse the cells treated with epoxomicin (25 mM, Calbiochem, San Diego, CA). Polyubiquitinated proteins were purified by S5a-affinity chromatography as previously described (Biomol International, Plymouth Meeting, PA) (33). After electrophoresis and transfer, membranes were preincubated in denaturing buffer (6 M guanidine hydrochloride, 20 mM Tris-HCl, pH 7.5, 5 mM  $\beta$ -mercaptoethanol, and 1 mM PMSF) for 1 h at 4 °C followed by extensive PBS washing before anti-FK2 antibody incubation. Immunoblots were performed as described above.

**Cell Surface Biotinylation.** Surface proteins were biotinylated with 500  $\mu$ g/mL sulfo succinimido 2-(biotinamido)-ethyl-1,3-dithiopropionate (Pierce) for 30 min at 4 °C. The biotinylation reaction was quenched for 10 min at 4 °C by addition of 1 M Tris-HCl (pH 7.5) to the reaction mixture to a final concentration of 20 mM. Cells were washed twice with ice-cold PBS, lysed, and homogenized. Protein (200  $\mu$ g) was added to 30  $\mu$ L of streptavidin–Sephareose beads, and the mixture was incubated overnight on a platform mixer at 4 °C. The pellet (plasma membrane; PM) was separated on SDS–PAGE (4–22.5%) and ASM associated with the PM was detected with the appropriate antibody.

**Sphingomyelinase Assay.** ASM activity was assessed by the scintillation proximity assay. The standard 100  $\mu$ L assay mixture consisted of up to 40  $\mu$ L of sample (cell lysates, conditioned medium, or immunoprecipitates) and 0.1 M sodium acetate assay buffer, pH 5.0, with or without 0.1 M  $Zn^{2+}$ , and 0.625 pmol of [ $^3H$ ]biotinylated SM substrate. The assay mixtures were incubated at 37 °C for 1 h and the reactions were stopped by the addition of streptavidin–scintillation beads. Only nonhydrolyzed [ $^3H$ ]SM could be precipitated by the beads and detected by  $\beta$ -counter, thus the radioactivity was inversely related to the amount of SM hydrolyzed.

**Immunofluorescence Localization Study.** The sorting fate of the wild-type and mutant ASM was monitored by confocal microscopy. After 16-h transient transfection in the absence or presence of anti-protease inhibitors (leupeptin and pepstatin) or cyclohexamide, cells were washed, fixed, and permeabilized with methanol. They were then immunostained with mouse anti-V5 primary antibodies (Invitrogen, Carlsbad, CA) and Alexa Fluor 546 rabbit anti-mouse secondary antibody (absorbance 556 nm, emission 573 nm; Invitrogen, Carlsbad, CA). In colocalization studies, cells were treated with LysoTracker for 30 min before cell harvest (Molecular Probes, Eugene, OR) or co-immunostained with various organelle markers labeled with Oregon Green 488 goat anti-rabbit secondary antibody (absorbance 496 nm, emission 524 nm; Invitrogen, Carlsbad, CA). In all experimental conditions, cells on each coverslip were photographed in multiple fields and appropriate negative controls were used. In separate experiments, wild-type ASM as well as  $\Delta R608$  and

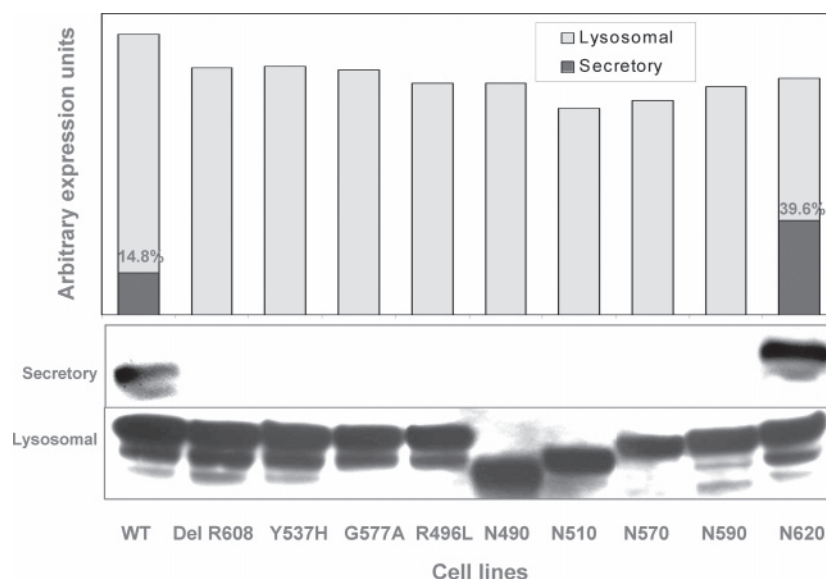


FIGURE 2: Protein expression of wild-type and mutant ASM in cell and in medium. After 24 h, cotransfection of pcDNA3.0/GS-SMPD-1 and pCMVb  $\beta$ -gal in subconfluent CHO cells grown in 10-cm dishes, 1 mL of total cell lysates was harvested and 20  $\mu$ L of this latter was used in the immunoblot analyses to study the expression of wild-type and mutant lysosomal ASM. The total medium (15 mL) was also harvested and concentrated with Amicon Ultra 15 (MW cutoff 30 000) down to 1 mL in volume. An aliquot (20  $\mu$ L) of this latter was used in the immunoblot analyses to study the expression of wild-type and mutant secretory ASM. The immunoblots for both lysosomal and secretory expression were handled in parallel with identical experimental conditions as following: anti-V5 primary antibodies were used against the recombinant ASM, while streptavidin-conjugated monoclonal rabbit anti-mouse secondary antibodies were used for subsequent detection. The bands in the blots exposed for 1 min were quantified by use of AlphaMager, normalized by the transfection efficiency assessed by  $\beta$ -galactosidase assay, and plotted for the calculation of the ratio between secretory (upper lane) and lysosomal (lower lane) expression levels.

N590 mutants were subcloned into N-terminally YFP- or HA-tagged vectors, and their localization was examined by use of polyclonal anti-YFP and monoclonal anti-HA antibodies, respectively (34).

**Statistics.** All experiments were independently repeated 3–5 times. When applicable, results were given as means  $\pm$  SD ( $n = 3$ ).

## RESULTS

**Normal Expression yet Defective Secretion in ASM Mutants.** In order to study the role of the C-terminal region of ASM protein, four naturally occurring mutations and five serial deletions were created as illustrated in Figure 1. The protein expression of all nine mutants was assessed. We found that all of them, including N490 with a deletion of 139 amino acids, were properly expressed in the cells (Figure 2). The SDS-PAGE analysis revealed that the His/V5-tagged wild-type ASM migrated as a single band with an apparent molecular mass of  $\sim$ 72 kDa, similar to the previously reported FLAG-ASM (35). Occasionally, a minor faster-migrating band appeared, representing the protease-induced degradation products (36). Like many lysosomal proteins, the same SMPD-1 gene gives rise to both lysosomal and secretory ASM (37). The secreted wild-type ASM characterized in this paper had a molecular mass of  $\sim$ 75 kDa (Figure 2) and represent less than 15% of total cell ASM, consistent with a previous study (4). The more rapid migration of the lysosomal ASM on SDS-PAGE compared to the secretory ASM was due both to proteolytic processing and to differences in oligosaccharide structure (Supporting Information). Surprisingly, while the cellular expression of the mutants was comparable to that of the wild-type ASM, we observed a quasi-absence of mutant ASM in medium,

except for N620, the mutant that has the smallest deletion and that preserves all post-translational modification sites. The secretion defects in mutant ASM were also confirmed in *Sf21* insect models (Supporting Information), for which we have generated wild-type and mutant ASM baculovirus transfer vectors using the Gateway BaculoDirect baculovirus expression system (Invitrogen, Carlsbad, CA) as detailed in Rabah et al. (38) and Bartelsen et al. (39). Since the protein expression was normal, the lack of secreted mutant ASM appeared to be caused by hindrance either in the transit through the ER after the protein synthesis or during the trafficking through the Golgi secretory pathway.

**Enzymatic Activity of Mutant ASM Was Severely Abolished.** Although all ASM mutants have normal cellular expression, we speculated that their enzymatic function may not be preserved, at least for the largest deletion mutants and the four naturally occurring mutants known to be inactive in patients with Niemann–Pick disease types A and B. As expected, the truncations in the four deletion mutants and the mutations in the four naturally occurring mutants led to total inactivation of ASM (Figure 3). Importantly, instead of observing a gradual decrease in activity as increasing numbers of residues were deleted from the C-terminus, we revealed that the only mutant that conserves intact ASM activity was N620, the smallest deletion mutant that has only 9 amino acids deleted from its C-terminal end (Figure 1). Interestingly, this pattern of loss of function in the lysosomal mutant ASM is closely related to impaired secretion (Figure 2). Thus, it is clear that the C-terminus of ASM plays an important role in structure–function yet to be characterized. In effect, we could narrow down to the minimal region from amino acids 590 to 620 that appear to be essential to safeguard the enzymatic function and protein secretion.



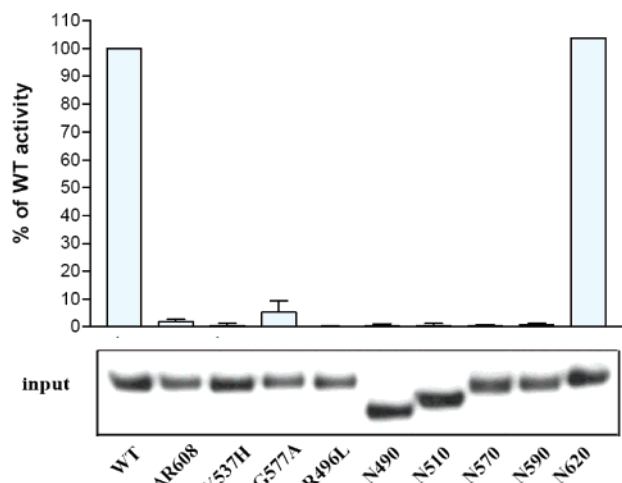


FIGURE 3: ASM mutant enzymatic activity. Recombinant ASM proteins were pulled down by magnetic immobilized metal affinity chromatography. The purified enzymes were incubated with [ $^3$ H] biotinylated SM for 1 h at 37 °C. The enzymatic reaction was stopped with streptavidin-coated yttrium silicate beads and counted. The enzymatic activity was inversely proportional to the counted cpm. The uniformity of the input in the enzymatic activity assay was assessed by monoclonal anti-V5 primary antibodies and monoclonal rabbit anti-mouse secondary antibodies.

Accordingly, only the  $\Delta$ R608 and N590 mutants were used for all subsequent experiments.

The ASM activity was also examined in conditioned medium, and an identical abolished activity pattern was found in the same mutants (data not shown). Although their functional inactivation was highly plausible, this lack of SM hydrolysis by the secreted mutant ASM was likely to be caused by their barely detectable levels in the medium (Figure 2). In order to exclude the possibility of an “enzyme secretion–recapture” mechanism that some believed to play a role in enzyme processing and activation (40), excess receptor-specific ligands mannose 6-phosphate (10 mM) (41) were loaded onto CHO cells transfected with wild-type ASM cDNA in order to compete for the receptor binding and to inhibit protein reuptake. Our data indicated that the blockade of the cell-surface mannose phosphate receptors by free mannose inhibiting the reinternalization of the secreted ASM did not affect the cellular wild-type ASM function (data not shown). Therefore, this mechanism could not be a plausible explanation for the functional inactivation in ASM mutants. This result was consistent with the finding in the report by von Figura and Weber (42), who provided evidence that secretion–recapture plays a minor role in the targeting and maturation of newly synthesized lysosomal enzymes. Furthermore, recent studies confirmed that ASM, like many other lysosomal proteins, also uses mannose 6-phosphate-independent targeting system to reach the lysosomal compartments (43).

**ER Entrapment of Mutant ASM.** Defects in secretion and functions indicated that the ASM mutants were most likely trapped in the ER quality control machinery. We examined by confocal microscopy the intracellular localization of the C-terminally V5-tagged wild-type and mutant recombinant ASM subsequent to a 16-h transient transfection in COS cells. While we found that  $\Delta$ R608 and N590 were trapped in the ER as predicted, we also observed ER-localized fluorescence for the wild-type ASM (data not shown). ASM

is known to be located in the lysosomal compartments, and this observation could be explained by two possibilities: (1) The C-terminus of the ASM may be cleaved after reaching the lysosomal compartment, as seen with other lysosomal proteins. Thus, the V5 tag may be cleaved in mature ASM such that the anti-V5 antibodies could only detect the unprocessed wild-type ASM that remains in the ER compartments. (2) Alternatively, the overexpression system overloaded the protein biosynthesis machinery such that many of the overexpressed ASM proteins remained unprocessed and entrapped in the ER after protein translation.

To validate our aforementioned observations and premises, we have separately subcloned the wild-type and mutant ASM into N-terminally YFP- and HA-tagged vectors. We also suppressed protein overproduction by treating the cells with cycloheximide. As shown in Figure 4, we consistently found that the  $\Delta$ R608 and N590 mutants were localized in the ER; the presence or absence of protease inhibitors did not alter this distribution (44). The strong fluorescence signals also supported an expression (Figure 2) and half-life (Supporting Information) comparable to that of wild type. In contrast, under these new experimental conditions, we could clearly observe the lysosomal fluorescence in wild-type ASM-transfected cells that were colocalized with lysosomal but not ER markers (Figure 4). This is consistent with our finding that mutant  $\Delta$ R608-transfected CHO cells and fibroblasts from a compound heterozygous Niemann–Pick disease type B (NPD-B) patient ( $\Delta$ R608 and R441X) (32) have defective translocation of the enzyme to the plasma membrane (PM) (Figure 5). Our confocal and cell surface biotinylation data, together with the results from the secretion and enzymatic assays, strongly suggested that the C-terminal mutations led to aberrant structural folding and important functional defects that prevent the mutant proteins from trafficking through the ER quality control checkpoint and their translocation to the PM.

**Ubiquitinated Mutant ASM Was Found in the Cells.** Proteins that fail to pass the ER are eventually eliminated by ubiquitination and proteosomal degradation. In order to further examine the impact of mutations in the ASM C-terminus, we studied the ubiquitination of the N590 and  $\Delta$ R608 mutants by pull-down with S5a-agarose from total cell lysates prepared with epocimycin and ubiquitin aldehyde. S5a is a subunit of the 19S regulator of the 26S proteasome that has been shown to bind multiubiquitinated proteins containing chains of at least four ubiquitin moieties (45). As predicted from their ER localization, we revealed that while there was little steady-state ubiquitinated wild-type ASM in the cells, there was a substantial amount of high-molecular weight polyubiquitinated mutant ASM (Figure 6). The ubiquitination of the mutants was concomitantly confirmed by immunoprecipitation with anti-V5 followed by immunoblotting with anti-mono/polyubiquitinated protein antibodies. Interestingly, we also observed an ubiquitinated form of ASM with an apparent molecular mass of  $\sim$ 50 kDa. This band has previously been characterized in the initial molecular cloning and characterization of ASM (24), even though its role and functionality remained elusive. Our observation that this molecular form was highly ubiquitinated and was barely detectable indicated that it was likely an alternately processed isoform (reported to constitute  $\leq$ 10%

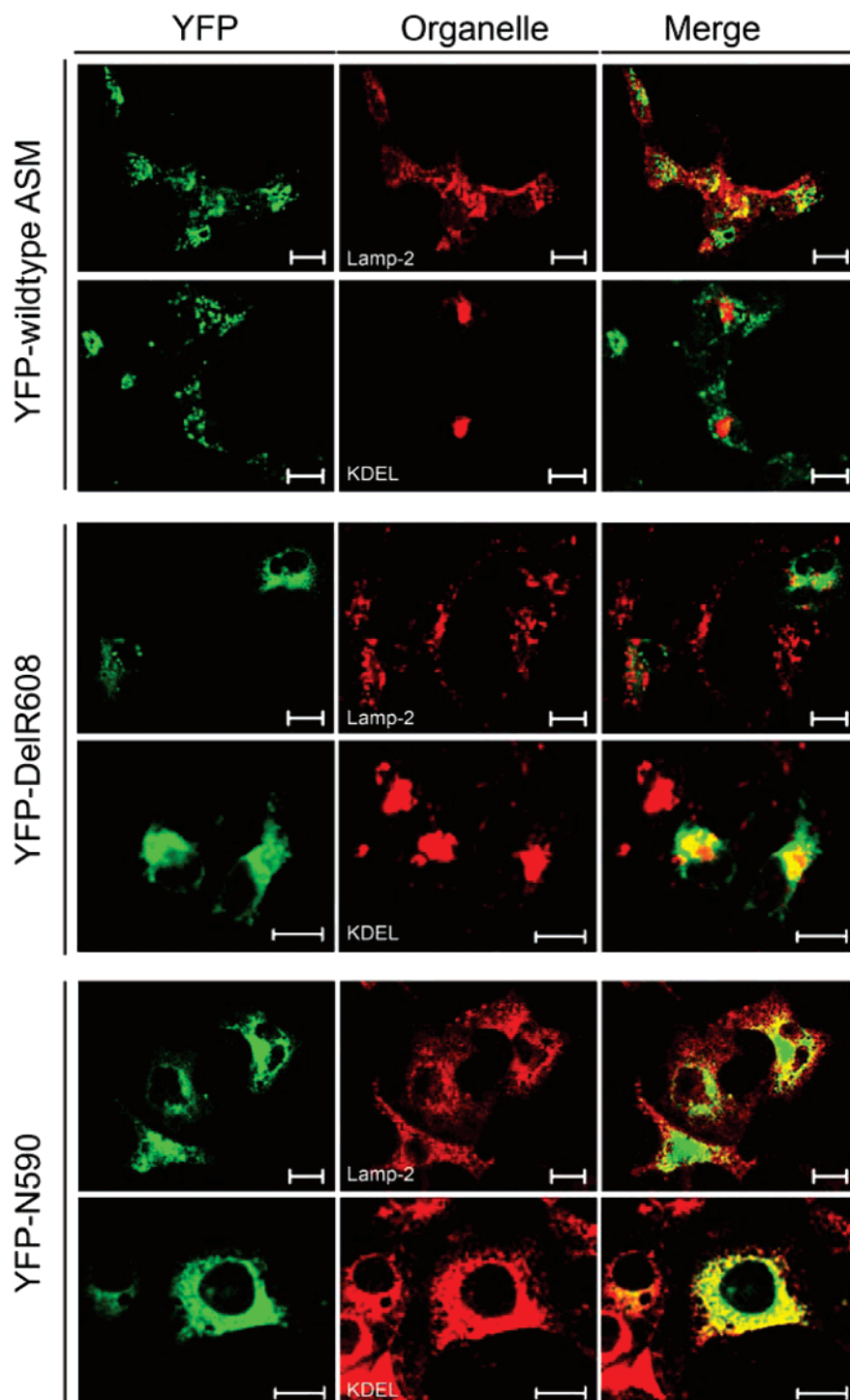


FIGURE 4: ASM mutant entrapment in the ER. COS cells grown on coverslips were transiently transfected with N-terminally YFP-tagged wild type and  $\Delta R608$  and N590 mutant ASM for 10 h in the presence of leupeptin ( $10 \mu\text{g/mL}$ ) and pepstatin ( $10 \mu\text{g/mL}$ ), followed by an incubation with cycloheximide for an additional 6 h. Cells were fixed with methanol for 10 min at  $-20^\circ\text{C}$  and washed with immunostaining blocking buffer for 20 min. After being labeled with rabbit anti-YFP polyclonal antibodies (1:400) and mouse anti-lamp2 (lysosomal markers, 1:100) or anti-KDEL (ER markers, 1:100) monoclonal antibodies for 20 min, the cells were washed and further labeled with Oregon Green 488 goat anti-rabbit and Alexa Fluor 546 anti-mouse secondary antibodies. Scale bar =  $20 \mu\text{m}$ .

of ASM product) (46) that was catalytically inactive and was usually degraded rapidly.

## DISCUSSION

The role of the C-terminus in the secretion has been described in other lysosomal proteins. For example, Chauhan et al. (47) and Claveau et al. (48) have independently demonstrated the involvement of the C-terminal amino acids

in the secretion of human lysosomal protease cathepsin L. Our data are consistent with the concept that the functional integrity of a protein is governed by its tertiary and quaternary structures and not solely by an intact catalytic domain. In ASM, the predicted catalytic site lies in the amino acids 199–461. The activity of all truncation mutants illustrated that the removal of a 30-minimal amino acid region in the C-terminus (amino acids 590–620) was

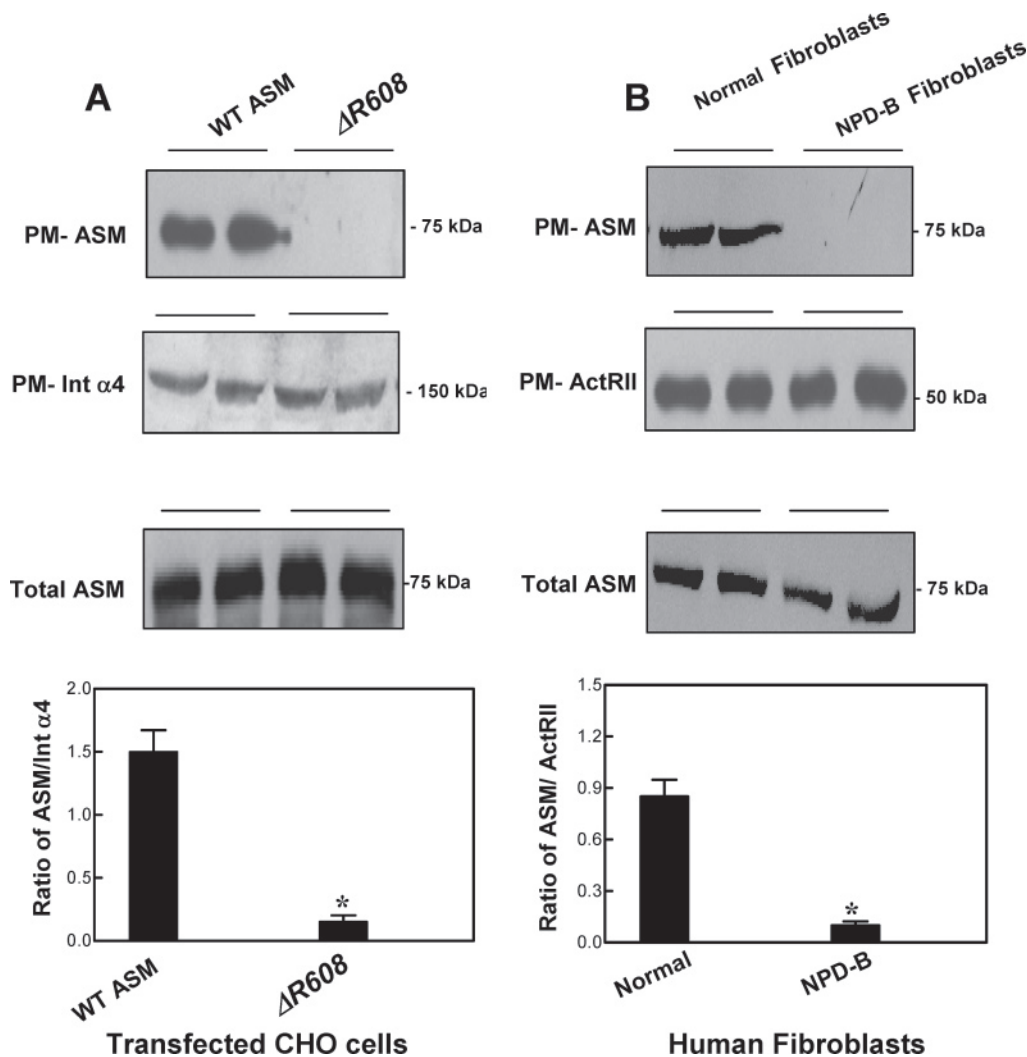


**FIGURE 5:** ASM mutation  $\Delta R608$  impairs the translocation of the enzyme to the plasma membrane in transfected CHO cells and NPD-B fibroblasts. Transfected CHO cells (A) and fibroblasts from NPD-B subjects (B) were subjected to cell surface biotinylation as described under Materials and Methods. Cells were washed twice with ice-cold PBS, lysed, and homogenized, and 200  $\mu$ g of protein was added to 45  $\mu$ L of streptavidin–Sepharose beads and incubated overnight on a platform mixer at 4  $^{\circ}$ C. The PM samples or total cell lysates were separated by SDS–PAGE. Transfected ASM in CHO cells was revealed by anti-V5 primary antibodies as described above. ASM associated with the PM or total cell ASM in NPD-B fibroblasts was detected by polyclonal human anti-ASM antibody (Santa Cruz). Integrin  $\alpha 4$  (Int  $\alpha 4$ ) and activin receptor type (ActRII) associated with the PM samples were detected with appropriate antibodies and were used as controls for protein loading. The ratios of PM-ASM to Int  $\alpha 4$  and of PM-ASM to ActRII were quantitated by densitometric scanning. Results shown are representative of two independent experiments. \* $p < 0.001$  by Student's  $t$  test.

sufficient to inactivate the enzyme, implying the crucial role of this C-terminal region even though it apparently does not harbor recognizable domains or motifs.

The misfolding of  $\Delta R608$  and N590 C-terminal ASM mutants was not unpredictable on the basis of the location of their deletion/truncation (Figure 7): the former has one arginine deletion at position amino acid 608, immediately adjacent to the cysteine residue at position 607 that has been shown to form one of the six disulfide bonds in ASM (25). Similarly, the only difference between the inactive N590 mutant and active N620 mutant (which conserves 100% of the ASM activity) was the deletion of this same disulfide bond. Disulfide bonds play crucial roles in the tertiary conformation of a protein (49). The peculiarity of the cysteine residues in the ASM C-terminus was once reported by Qiu et al. (50), who activated the ASM by deleting the terminal free thiol (cysteine<sup>629</sup>). They explained the observation by a “cysteine switch mechanism”, which is coordinated by the free cysteine along with other cysteine residues structurally

paired in disulfide bonds. The precise coordination and association of both free and bonded cysteines, especially when they are in close proximity, appear critical, as any disarrangement could lead not only to activation but also to inactivation (as shown in Figure 3), as well as disulfide shuffling causing intermolecular cross-links and ER retention (51). Although the precise mechanism by which the C-terminal mutations impact the function and structure of ASM has not been defined in this paper, we believe that this was a consequence of a significant alteration in the tertiary conformation brought about by the absence of an important disulfide bond. Importantly, our finding that C-terminal mutations impaired the trafficking of mutant enzymes as described in the present heterologous overexpression system was strongly supported by our observation that a naturally occurring mutation ( $\Delta R608$ ) associated with NPD-B (Figure 5) had defective translocation to the plasma membrane.

Posttranslational modifications such as glycosylation and phosphorylation are commonly affected when a protein is



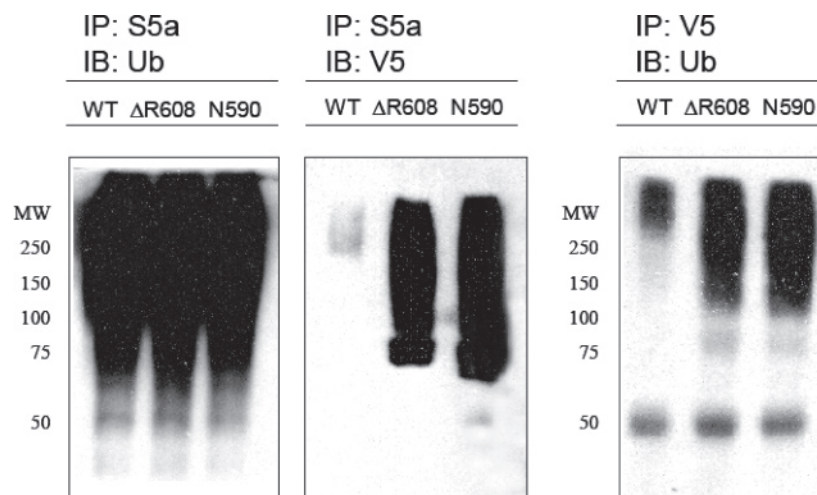


FIGURE 6: ASM mutant ubiquitination. Wild-type and mutant ASM proteins were pulled down by either S5a-agarose (left panels) or by anti-V5 antibodies (right panels). The precipitated samples were then revealed by anti-ubiquitin or anti-V5 antibodies. The blot on the left (IP: S5a/ IB: Ub) was a control for the pull down of ubiquitinated proteins by S5a-agarose. The blots in the middle (IP: S5a/ IB: V5) and on the right (IP: V5/ IB: Ub) concomitantly demonstrated the presence of increased levels of mutant ASM in ubiquitinated forms.

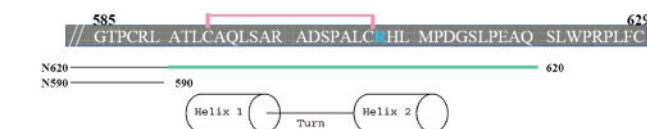


FIGURE 7: Amino acid sequence alignment of human ASM C-terminus with ASM homologues from different species. Within the C-terminal 30-amino acid region of ASM (amino acids 590–620), there is a disulfide bond involving a cysteine residue at position 607 and a 20-amino acid long helix–loop–helix pattern that contains 12 nonpolar and four charged residues. The human ASM shared 81% homology with the murine counterpart. Although it is only 30% homologous to the *Caenorhabditis elegans* ASM-1 and ASM-2, its cysteine residues within this region are well conserved, hinting the importance of the disulfide bond for the structural conformation.

misfolded. The wild-type ASM has 10 putative phosphorylation sites in the C-terminal region, but its phosphorylation status has never been demonstrated. Our preliminary data showed that the wild-type ASM was not phosphorylated even when stimulated with PMA (52), forskolin (53), or IBMX (54) and that its phosphorylation was solely derived from its mannose 6-phosphate moieties (Supporting Information). Surprisingly, we found that the  $\Delta R608$  and N590 mutant ASM were phosphorylated even under basal conditions (Supporting Information). We speculate that the structural alterations made those phosphorylation sites in mutants ASM accessible for kinases. In addition, we have found a significant amount of mutant aggregates revealed under nonreducing conditions (Supporting Information). It is commonly believed that aggregates were caused by aberrant interchain disulfide bonds and that they are often abnormally phosphorylated (55). Intriguingly, Zeidan and Hannun (56) have recently published their findings on ASM phosphorylation. While different experimental systems and conditions could explain the discrepancies, more in-depth investigation as well as characterization by methods such as circular dichroism and X-ray crystallography will be necessary in the future to better elucidate the ASM structure.

Our structure–function study in ASM significantly contributed to the mechanistic elucidation of how specific mutations could affect its biological function, whether it involves the catalytic ability, affinity to cofactor, secretion, or substrate binding. We have demonstrated here that the C-terminus of ASM contains a 30-amino acid sequence essential for at least one of these functions. Current research has shown that defects in ASM could lead to Niemann–Pick diseases and disturbance in lipid/lipoprotein metabolism as well as deregulation in many signaling cascades regulating apoptosis (57, 58). Therefore, a better understanding of its structure will enable us to more efficiently and accurately predict the severity of a SMPD-1 mutation under these pathophysiological conditions and to find potential therapeutic strategies.

## SUPPORTING INFORMATION AVAILABLE

ASM wild-type and mutant glycosylation (Figure 1S), ASM mutant secretory defects in Sf21 insect models (Figure 2S), ASM wild-type and mutant half-life (Figure 3S), and ASM mutant aberrant phosphorylation and aggregation (Figure 4S). This material is available free of charge via the Internet at <http://pubs.acs.org>.

## REFERENCES

- Merrill, A. H., Jr., and Jones, D. D. (1990) An update of the enzymology and regulation of sphingomyelin metabolism, *Biochim. Biophys. Acta* 1044, 1–12.
- Scriver, C. R., Beaudet, A. L., Sly, W. S., Valle, D., Childs, B., Kinzler, K. W., and Vogelstein, B., Eds. (2001) *The Metabolic & Molecular Bases of Inherited Disease*, Vol. III, 8th ed., pp 3371–3894, McGraw-Hill, New York.
- Schuchman, E. H., Levran, O., Pereira, L. V., and Desnick, R. J. (1992) Structural organization and complete nucleotide sequence of the gene encoding human acid sphingomyelinase (SMPD1), *Genomics* 12, 197–205.
- Schissel, S. L., Schuchman, E. H., Williams, K. J., and Tabas, I. (1996) Zn<sup>2+</sup>-stimulated sphingomyelinase is secreted by many cell types and is a product of the acid sphingomyelinase gene, *J. Biol. Chem.* 271, 18431–18436.
- Brady, R. O., Kanfer, J. N., Mock, M. B., and Fredrickson, D. S. (1966) The metabolism of sphingomyelin. II. Evidence of an enzymatic deficiency in Niemann–Pick disease, *Proc. Natl. Acad. Sci. U.S.A.* 55, 366–369.

6. Ion, G., Fajka-Boja, R., Kovacs, F., Szebeni, G., Gombos, I., Czibula, A., Matko, J., and Monostori, E. (2006) Acid sphingomyelinase mediated release of ceramide is essential to trigger the mitochondrial pathway of apoptosis by galectin-1, *Cell. Signalling* 18, 1887–1896.
7. Kolesnick, R., and Fuks, Z. (2003) Radiation and ceramide-induced apoptosis, *Oncogene* 22, 5897–5906.
8. Pozo, D., Vales-Gomez, M., Mavaddat, N., Williamson, S. C., Chisholm, S. E., and Reyburn, H. (2006) CD161 (human NKR-P1A) signaling in NK cells involves the activation of acid sphingomyelinase, *J. Immunol.* 176, 2397–2406.
9. Wong, M. L., Xie, B., Beatini, N., Phu, P., Marathe, S., Johns, A., Gold, P. W., Hirsch, E., Williams, K. J., Licinio, J., and Tabas, I. (2002) Acute systemic inflammation up-regulates secretory sphingomyelinase in vivo: a possible link between inflammatory cytokines and atherogenesis, *Proc. Natl. Acad. Sci. U.S.A.* 97, 8681–8686.
10. Leventhal, A. R., Chen, W., Tall, A. R., and Tabas, I. (2001) Acid sphingomyelinase-deficient macrophages have defective cholesterol trafficking and efflux, *J. Biol. Chem.* 276, 44976–44983.
11. Ridgway, N. D., Byers, D. M., Cook, H. W., and Storey, M. K. (1999) Integration of phospholipid and sterol metabolism in mammalian cells, *Prog. Lipid Res.* 38, 337–360.
12. Marathe, S., Kuriakose, G., Williams, K. J., and Tabas, I. (1999) Sphingomyelinase, an enzyme implicated in atherogenesis, is present in atherosclerotic lesions and binds to specific components of the subendothelial extracellular matrix, *Arterioscler. Thromb. Vasc. Biol.* 19, 2648–2658.
13. Lee, C. Y., Lesimple, A., Denis, M., Vincent, J., Larsen, A., Mamer, O., Krimbou, L., Genest, J., and Marcil, M. (2006) Increased sphingomyelin content impairs HDL biogenesis and maturation in human Niemann-Pick disease type B, *J. Lipid Res.* 47, 622–632.
14. Schneider, P. B., and Kennedy, E. P. (1967) Sphingomyelinase in normal human spleens and in spleens from subjects with Niemann-Pick disease, *J. Lipid Res.* 8, 202–209.
15. Kanfer, J. N., Young, O. M., Shapiro, D., and Brady, R. O. (1966) The metabolism of sphingomyelin. I. Purification and properties of a sphingomyelin-cleaving enzyme from rat liver tissue, *J. Biol. Chem.* 241, 1081–1084.
16. Quintern, L. E., Weitz, G., Nehrkorn, H., Tager, J. M., Schram, A. W., and Sandhoff, K. (1987) Acid sphingomyelinase from human urine: purification and characterization, *Biochim. Biophys. Acta* 922, 323–336.
17. Lansmann, S., Ferlinz, K., Hurwitz, R., Bartelsen, O., Glombitza, G., and Sandhoff, K. (1996) Purification of acid sphingomyelinase from human placenta: characterization and N-terminal sequence, *FEBS Lett.* 399, 227–231.
18. Schuchman, E. H., Suchi, M., Takahashi, T., Sandhoff, K., and Desnick, R. J. (1991) Human acid sphingomyelinase. Isolation, nucleotide sequence and expression of the full-length and alternatively spliced cDNAs, *J. Biol. Chem.* 266, 8531–8539.
19. Gattiker, A., Gasteiger, E., and Bairoch, A. (2002) ScanProsite: a reference implementation of a PROSITE scanning tool, *Appl. Bioinf.* 1, 107–108.
20. Bateman, A., Coin, L., Durbin, R., Finn, R. D., Hollich, V., Griffiths-Jones, S., Khanna, A., Marshall, M., Moxon, S., Sonhammer, E. L. L., Studholme, D. J., Yeats, C., and Eddy, S. R. (2004) The Pfam Protein Families Database, *Nucleic Acids Res. Database* 32, 138–141.
21. Gorodkin, J., Heyer, L. J., and Stormo, G. D. (1997) Finding the most significant common sequences and structure motifs in a set of RNA sequences, *Nucleic Acids Res.* 25, 3724–3732.
22. Kolzer, M., Ferlinz, K., Bartelsen, O., Hoops, S. L., Lang, F., and Sandhoff, K. (2004) Functional characterization of the postulated intramolecular sphingolipid activator protein domain of human acid sphingomyelinase, *Biol. Chem.* 385, 1193–1195.
23. CBS Prediction Servers: <http://www.cbs.dtu.dk/services/>.
24. Ferlinz, K., Hurwitz, R., Mocall, H., Lansmann, S., Schuchman, E. H., and Sandhoff, K. (1997) Functional characterization of the N-glycosylation sites of human acid sphingomyelinase by site-directed mutagenesis, *Eur. J. Biochem.* 243, 511–517.
25. Lansmann, S., Schuette, C. G., Bartelsen, O., Hoernschmeyer, J., Linke, T., Weisgerber, J., and Sandhoff, K. (2003) Human acid sphingomyelinase, *Eur. J. Biochem.* 270, 1076–1088.
26. Seto, M., Whitlow, M., McCarrick, M. A., Srinivasan, S., Zhu, Y., Pagila, R., Mintzer, R., Light, D., Johns, A., and Meurer-Ogden, J. A. (2004) A model of the acid sphingomyelinase phosphoesterase domain based on its remote structural homolog purple acid phosphatase, *Protein Sci.* 13, 3172–3186.
27. Sikora, J., Pavlu-Pereira, H., Elleder, M., Roelofs, H., and Wevers, R. A. (2003) Seven novel acid sphingomyelinase gene mutations in Niemann-Pick type A and B patients, *Ann. Hum. Genet.* 67, 63–70.
28. Simonaro, C. M., Desnick, R. J., McGovern, M. M., Wasserstein, M. P., and Schuchman, E. H. (2002) The demographics and distribution of type B Niemann-Pick disease: novel mutations lead to new genotype/phenotype correlations, *Am. J. Hum. Genet.* 71, 1413–1419.
29. Wasserstein, M. P., Desnick, R. J., Schuchman, E. H., Hossain, S., Wallenstein, S., Lamm, C., and McGovern, M. M. (2004) The natural history of type B Niemann-Pick disease: results from a 10-year longitudinal study, *Pediatrics* 114, 672–677.
30. Dardis, A., Zampieri, S., Filocamo, M., Burlina, A., Bembi, B., and Pittis, M. G. (2005) Functional in vitro characterization of 14 SMPD1 mutations identified in Italian patients affected by Niemann Pick Type B disease, *Hum. Mutat.* 26, 164.
31. Vanier, M. T., Ferlinz, K., Rousson, R., Duthel, S., Louisot, P., Sandhoff, K., and Suzuki, K. (1993) Deletion of arginine (608) in acid sphingomyelinase is the prevalent mutation among Niemann-Pick disease type B patients from northern Africa, *Hum. Genet.* 92, 325–330.
32. Lee, C. Y., Krimbou, L., Vincent, J., Bernard, C., Larramee, P., Genest, J., Jr., and Marcil, M. (2003) Compound heterozygosity at the sphingomyelin phosphodiesterase-1 (SMPD1) gene is associated with low HDL cholesterol, *Hum. Genet.* 112, 552–562.
33. Walters, K. J., Kleijnen, M. F., Goh, A. M., Wagner, G., and Howley, P. M. (2002) Structural studies of the interaction between ubiquitin family proteins and proteasome subunit S5a, *Biochemistry* 41, 1767–1777.
34. Kamada, A., Nagaya, H., Tamura, T., Kinjo, M., Jin, H. Y., Yamashita, T., Jimbow, K., Kanoh, H., and Wada, I. (2004) Regulation of immature protein dynamics in the endoplasmic reticulum, *J. Biol. Chem.* 279, 21533–21542.
35. He, X., Miranda, S. R., Xiong, X., Dagan, A., Gatt, S., and Schuchman, E. H. (1999) Characterization of human acid sphingomyelinase purified from the media of overexpressing Chinese hamster ovary cells, *Biochim. Biophys. Acta* 1432, 251–264.
36. Ferlinz, K., Hurwitz, R., Vielhaber, G., Suzuki, K., and Sandhoff, K. (1994) Occurrence of two molecular forms of human acid sphingomyelinase, *Biochem. J.* 301, 855–862.
37. Schissel, S. L., Keesler, G. A., Schuchman, E. H., Williams, K. J., and Tabas, I. (1998) The cellular trafficking and zinc dependence of secretory and lysosomal sphingomyelinase, two products of the acid sphingomyelinase gene, *J. Biol. Chem.* 273, 18250–18259.
38. Rabah, N., Gauthier, D. J., Gauthier, D., and Lazure, C. (2004) Improved PC1/3 production through recombinant expression in insect cells and larvae, *Protein Expression Purif.* 37, 377–384.
39. Bartelsen, O., Lansmann, S., Nettersheim, M., Lemm, T., Ferlinz, K., and Sandhoff, K. (1998) Expression of recombinant human acid sphingomyelinase in insect Sf21 cells: purification, processing and enzymatic characterization, *J. Biotechnol.* 63, 29–40.
40. Hickman, S., and Neufeld, E. F. (1972) A hypothesis for I-cell disease: defective hydrolases that do not enter lysosomes, *Biochem. Biophys. Res. Commun.* 49, 992–999.
41. Faust, P. L., Wall, D. A., Perara, E., Lingappa, V. R., and Kornfeld, S. (1987) Expression of human cathepsin D in *Xenopus* oocytes: phosphorylation and intracellular targeting, *J. Cell Biol.* 105, 1937–1945.
42. von Figura, K., and Weber, E. (1978) An alternative hypothesis of cellular transport of lysosomal enzymes in fibroblasts. Effect of inhibitors of lysosomal enzyme endocytosis on intra- and extra-cellular lysosomal enzyme activities, *Biochem. J.* 176, 943–950.
43. Ni, X., and Morales, C. R. (2006) The lysosomal trafficking of acid sphingomyelinase is mediated by sortilin and mannose 6-phosphate receptor, *Traffic* 7, 889–902.
44. Montenez, J. P., Delaisse, J. M., Tulkens, P. M., and Kishore, B. K. (1994) Increased activities of cathepsin B and other lysosomal hydrolases in fibroblasts and bone tissue cultured in the presence of cysteine proteinase inhibitors, *Life Sci.* 55, 1199–1208.
45. Layfield, R., Tooth, D., Landon, M., Dawson, S., Mayer, J., and Alban, A. (2001) Purification of poly-ubiquitinated proteins by S5a-affinity chromatography, *Proteomics* 1, 773–777.
46. Quintern, L. E., Schuchman, E. H., Levrin, O., Suchi, M., Ferlinz, K., Reinke, H., Sandhoff, K., and Desnick, R. J. (1989) Isolation



- of cDNA clones encoding human acid sphingomyelinase: occurrence of alternatively processed transcripts, *EMBO J.* 8, 2469–2473.
47. Chauhan, S. S., Ray, D., Kane, S. E., Willingham, M. C., and Gottesman, M. M. (1998) Involvement of carboxy-terminal amino acids in secretion of human lysosomal protease cathepsin L, *Biochemistry* 37, 8584–8594.
48. Claveau, D., and Riendeau, D. (2001) Mutations of the C-terminal end of cathepsin K affect proenzyme secretion and intracellular maturation, *Biochem. Biophys. Res. Commun.* 281, 551–557.
49. Wedemeyer, W. J., Welker, E., Narayan, M., and Scheraga, H. A. (2000) Disulfide bonds and protein folding, *Biochemistry* 39, 4207–4216.
50. Qiu, H., Edmunds, T., Baker-Malcolm, J., Karey, K. P., Estes, S., Schwarz, C., Hughes, H., and Van Patten, S. M. (2003) Activation of human acid sphingomyelinase through modification or deletion of C-terminal cysteine, *J. Biol. Chem.* 278, 32744–32752.
51. Wilbourn, B., Nesbeth, D. N., Wainwright, L. J., and Field, M. C. (1998) Proteasome and thiol involvement in quality control of glycosylphosphatidylinositol anchor addition, *Biochem. J.* 332, 111–118.
52. Liu, W. S., and Heckman, C. A. (1998) The sevenfold way of PKC regulation, *Cell. Signalling* 10, 529–542.
53. Insel, P. A., and Ostrom, R. S. (2003) Forskolin as a tool for examining adenylyl cyclase expression, regulation, and G protein signaling, *Cell. Mol. Neurobiol.* 23, 305–314.
54. Tesmer, J. J., and Sprang, S. R. (1998) The structure, catalytic mechanism and regulation of adenylyl cyclase, *Curr. Opin. Struct. Biol.* 8, 713–719.
55. Seibenhener, M. L., Babu, J. R., Geetha, T., Wong, H. C., Krishna, N. R., and Wooten, M. W. (2004) Sequestosome 1/p62 is a polyubiquitin chain binding protein involved in ubiquitin proteasome degradation, *Mol. Cell. Biol.* 24, 8055–8068.
56. Zeidan, Y. H., and Hannun, Y. A. (2007) Activation of acid sphingomyelinase by protein kinase C $\delta$ -mediated phosphorylation, *J. Biol. Chem.* 282, 11549–11561.
57. Santana, P., Pena, L. A., Haimovitz-Friedman, A., Martin, S., Green, D., McLoughlin, M., Cordon-Cardo, C., Schuchman, E. H., Fuks, Z., and Kolesnick, R. (1996) Acid sphingomyelinase-deficient human lymphoblasts and mice are defective in radiation-induced apoptosis, *Cell* 86, 189–199.
58. Ogretmen, B., and Hannun, Y. A. (2004) Biologically active sphingolipids in cancer pathogenesis and treatment, *Nat. Rev. Cancer* 4, 604–616.

BI700817G



COPYRIGHT CLEARANCE CENTER

**Confirmation Number: 1885326**  
**Order Date: 08/22/2008**

**Customer Information**


**Customer:** Frederic Laporte  
**Account Number:** 3000146208  
**Organization:** McGill University  
**Email:** frederic.laporte@mail.mcgill.ca  
**Phone:** 1-514-769-8388  
**Payment Method:** Credit Card ending in 7012

**Special Order Invoices billed to:**  
McGill University

**Order Details**

**JOURNAL OF BIOLOGICAL CHEMISTRY**  
**Order detail ID: 22720148**

**ISBN/ISSN:** 00219258  
**Publication Year:** 2009  
**Publisher:** AMERICAN SOCIETY FOR  
BIOCHEMISTRY AND MOLECULAR BIOLOGY  
**Rightsholder:** American Soc for  
Biochemistry & Molecular Biology  
**Author/Editor:** Bascom et al

**Permission Status:**  **Granted**  
**Permission type:** Republish into a book, journal,  
newsletter...  
**Requested use:** Dissertation  
**Republishing organization:** MCGILL UNIVERSITY  
PRESS  
**Organization status:** Not for profit  
**Republication date:** 01/01/2009  
**Circulation/Distribution:** 1  
**Type of content:** Figure, diagram, or table  
**Description of requested content:** Figure about the  
pk treatment  
**Page range(s):** 2354  
**Requested content's publication date:** 01/01/2009  
**Your reference:** FREDERIC THESIS CHAPTER 8

Billing Status:  
**Charged to  
Credit Card**

**\$3.00****Order Total: \$3.00**

[About Us](#) | [Contact Us](#) | [Careers](#) | [Privacy Policy](#) | [Terms & Conditions](#)  
[Site Index](#) | [Copyright Labs](#)

Copyright 2008 Copyright Clearance Center



COPYRIGHT CLEARANCE CENTER



## Creative Commons License Deed

---

Attribution-Noncommercial-Share Alike 3.0 Unported

### You are free:

- **to Share** — to copy, distribute and transmit the work
- **to Remix** — to adapt the work

### Under the following conditions:

• **Attribution.** You must attribute the work in the manner specified by the author or licensor (but not in any way that suggests that they endorse you or your use of the work).

• **Noncommercial.** You may not use this work for commercial purposes.

•

• **Share Alike.** If you alter, transform, or build upon this work, you may distribute the resulting work only under the same or similar license to this one.

- For any reuse or distribution, you must make clear to others the license terms of this work. The best way to do this is with a link to this web page.
- Any of the above conditions can be waived if you get permission from the copyright holder.
- Nothing in this license impairs or restricts the author's moral rights.

**Your fair dealing and other rights are in no way affected by the above.**

This is a human-readable summary of the [Legal Code](#) (the full license).

## American Chemical Society's Policy on Theses and Dissertations

**If your university requires a signed copy of this letter see contact information below.**

Thank you for your request for permission to include **your** paper(s) or portions of text from **your** paper(s) in your thesis. Permission is now automatically granted; please pay special attention to the implications paragraph below. The Copyright Subcommittee of the Joint Board/Council Committees on Publications approved the following:

### Copyright permission for published and submitted material from theses and dissertations

ACS extends blanket permission to students to include in their theses and dissertations their own articles, or portions thereof, that have been published in ACS journals or submitted to ACS journals for publication, provided that the ACS copyright credit line is noted on the appropriate page(s).

### Publishing implications of electronic publication of theses and dissertation material

Students and their mentors should be aware that posting of theses and dissertation material on the Web prior to submission of material from that thesis or dissertation to an ACS journal may affect publication in that journal. Whether Web posting is considered prior publication may be evaluated on a case-by-case basis by the journal's editor. If an ACS journal editor considers Web posting to be "prior publication", the paper will not be accepted for publication in that journal. If you intend to submit your unpublished paper to ACS for publication, check with the appropriate editor prior to posting your manuscript electronically.

If your paper has **not** yet been published by ACS, we have no objection to your including the text or portions of the text in your thesis/dissertation in **print and microfilm formats**; please note, however, that electronic distribution or Web posting of the unpublished paper as part of your thesis in electronic formats might jeopardize publication of your paper by ACS. Please print the following credit line on the first page of your article: "Reproduced (or 'Reproduced in part') with permission from [JOURNAL NAME], in press (or 'submitted for publication'). Unpublished work copyright [CURRENT YEAR] American Chemical Society." Include appropriate information.

If your paper has already been published by ACS and you want to include the text or portions of the text in your thesis/dissertation in **print or microfilm formats**, please print the ACS copyright credit line on the first page of your article: "Reproduced (or 'Reproduced in part') with permission from [FULL REFERENCE CITATION.] Copyright [YEAR] American Chemical Society." Include appropriate information.

**Submission to a Dissertation Distributor:** If you plan to submit your thesis to UMI or to another dissertation distributor, you should not include the unpublished ACS paper in your thesis if the thesis will be disseminated electronically, until ACS has published your paper. After publication of the paper by ACS, you may release the entire thesis (**not the individual ACS article by itself**) for electronic dissemination through the distributor; ACS's copyright credit line should be printed on the first page of the ACS paper.

**Use on an Intranet:** The inclusion of your ACS unpublished or published manuscript is permitted in your thesis in print and microfilm formats. If ACS has published your paper you may include the manuscript in your thesis on an intranet that is not publicly available. Your ACS article cannot be posted electronically on a publicly available medium (i.e. one that is not password protected), such as but not limited to, electronic archives, Internet, library server, etc. The only material from your paper that can be posted on a public electronic medium is the article abstract, figures, and tables, and you may link to the article's DOI or post the article's author-directed URL link provided by ACS. This paragraph does not pertain to the dissertation distributor paragraph above.

**ELSEVIER LICENSE  
TERMS AND CONDITIONS**

Aug 20, 2008

This is a License Agreement between Frederic Laporte ("You") and Elsevier ("Elsevier"). The license consists of your order details, the terms and conditions provided by Elsevier, and the payment terms and conditions.

Supplier	Elsevier Limited The Boulevard, Langford Lane Kidlington, Oxford, OX5 1GB, UK
Registered Company Number	1982084
Customer name	Frederic Laporte
Customer address	201 Chemin Club Marin, #1009 Montreal, QC H3E1T4
License Number	2013360275238
License date	Aug 20, 2008
Licensed content publisher	Elsevier
Licensed content publication	Biochimica et Biophysica Acta (BBA) - Molecular Cell Research
Licensed content title	Commuting between Golgi cisternae—Mind the GAP!
Licensed content author	Fredrik Kartberg, Markus Elsner, Linda Fröderberg, Lennart Asp and Tommy Nilsson
Licensed content date	10 July 2005
Volume number	1744
Issue number	3
Pages	13
Type of Use	Thesis / Dissertation
Portion	Figures/table/illustration/abstracts
Portion Quantity	1
Format	Electronic
You are an author of the Elsevier article	No
Are you translating?	No
Purchase order number	
Expected publication date	Jan 2008
Elsevier VAT number	GB 494 6272 12
Permissions price	0.00 USD
Value added tax 0.0%	0.00 USD
Total	0.00 USD

[Terms and Conditions](#)

## INTRODUCTION

1. The publisher for this copyrighted material is Elsevier. By clicking "accept" in connection with completing this licensing transaction, you agree that the following terms and conditions apply to this transaction (along with the Billing and Payment terms and conditions established by Copyright Clearance Center, Inc. ("CCC"), at the time that you opened your Rightslink account and that are available at any time at [<http://myaccount.copyright.com>](http://myaccount.copyright.com)).

## GENERAL TERMS

2. Elsevier hereby grants you permission to reproduce the aforementioned material subject to the terms and conditions indicated.

3. Acknowledgement: If any part of the material to be used (for example, figures) has appeared in our publication with credit or acknowledgement to another source, permission must also be sought from that source. If such permission is not obtained then that material may not be included in your publication/copies. Suitable acknowledgement to the source must be made, either as a footnote or in a reference list at the end of your publication, as follows:

“Reprinted from Publication title, Vol /edition number, Author(s), Title of article / title of chapter, Pages No., Copyright (Year), with permission from Elsevier [OR APPLICABLE SOCIETY COPYRIGHT OWNER].” Also Lancet special credit - “Reprinted from The Lancet, Vol. number, Author(s), Title of article, Pages No., Copyright (Year), with permission from Elsevier.”

4. Reproduction of this material is confined to the purpose and/or media for which permission is hereby given.

5. Altering/Modifying Material: Not Permitted. However figures and illustrations may be altered/adapted minimally to serve your work. Any other abbreviations, additions, deletions and/or any other alterations shall be made only with prior written authorization of Elsevier Ltd. (Please contact Elsevier at [permissions@elsevier.com](mailto:permissions@elsevier.com))

6. If the permission fee for the requested use of our material is waived in this instance, please be advised that your future requests for Elsevier materials may attract a fee.

7. Reservation of Rights: Publisher reserves all rights not specifically granted in the combination of (i) the license details provided by you and accepted in the course of this licensing transaction, (ii) these terms and conditions and (iii) CCC's Billing and Payment terms and conditions.

8. License Contingent Upon Payment: While you may exercise the rights licensed immediately upon issuance of the license at the end of the licensing process for the transaction, provided that you have disclosed complete and accurate details of your proposed use, no license is finally effective unless and until full payment is received from you (either by publisher or by CCC) as provided in CCC's Billing and Payment terms and conditions. If full payment is not received on a timely basis, then any license preliminarily granted shall be deemed automatically revoked and shall be void as if never granted. Further, in the event

that you breach any of these terms and conditions or any of CCC's Billing and Payment terms and conditions, the license is automatically revoked and shall be void as if never granted. Use of materials as described in a revoked license, as well as any use of the materials beyond the scope of an unrevoked license, may constitute copyright infringement and publisher reserves the right to take any and all action to protect its copyright in the materials.

9. **Warranties:** Publisher makes no representations or warranties with respect to the licensed material.

10. **Indemnity:** You hereby indemnify and agree to hold harmless publisher and CCC, and their respective officers, directors, employees and agents, from and against any and all claims arising out of your use of the licensed material other than as specifically authorized pursuant to this license.

11. **No Transfer of License:** This license is personal to you and may not be sublicensed, assigned, or transferred by you to any other person without publisher's written permission.

12. **No Amendment Except in Writing:** This license may not be amended except in a writing signed by both parties (or, in the case of publisher, by CCC on publisher's behalf).

13. **Objection to Contrary Terms:** Publisher hereby objects to any terms contained in any purchase order, acknowledgment, check endorsement or other writing prepared by you, which terms are inconsistent with these terms and conditions or CCC's Billing and Payment terms and conditions. These terms and conditions, together with CCC's Billing and Payment terms and conditions (which are incorporated herein), comprise the entire agreement between you and publisher (and CCC) concerning this licensing transaction. In the event of any conflict between your obligations established by these terms and conditions and those established by CCC's Billing and Payment terms and conditions, these terms and conditions shall control.

14. **Revocation:** Elsevier or Copyright Clearance Center may deny the permissions described in this License at their sole discretion, for any reason or no reason, with a full refund payable to you. Notice of such denial will be made using the contact information provided by you. Failure to receive such notice will not alter or invalidate the denial. In no event will Elsevier or Copyright Clearance Center be responsible or liable for any costs, expenses or damage incurred by you as a result of a denial of your permission request, other than a refund of the amount(s) paid by you to Elsevier and/or Copyright Clearance Center for denied permissions.

### LIMITED LICENSE

The following terms and conditions apply to specific license types:

15. **Translation:** This permission is granted for non-exclusive world **English** rights only unless your license was granted for translation rights. If you licensed translation rights you may only translate this content into the languages you requested. A professional translator must perform all translations and reproduce the content word for word preserving the integrity of the article. If this license is to re-use 1 or 2 figures then permission is granted for non-exclusive world rights in all languages.

16. **Website:** The following terms and conditions apply to electronic reserve and author



websites:

**Electronic reserve:** If licensed material is to be posted to website, the web site is to be password-protected and made available only to bona fide students registered on a relevant course if:

This license was made in connection with a course,

This permission is granted for 1 year only. You may obtain a license for future website posting,

All content posted to the web site must maintain the copyright information line on the bottom of each image,

A hyper-text must be included to the Homepage of the journal from which you are licensing at <http://www.sciencedirect.com/science/journal/xxxxx> or the Elsevier homepage for books at <http://www.elsevier.com> , and

Central Storage: This license does not include permission for a scanned version of the material to be stored in a central repository such as that provided by Heron/XanEdu.

17. **Author website** for journals with the following additional clauses:

This permission is granted for 1 year only. You may obtain a license for future website posting,

All content posted to the web site must maintain the copyright information line on the bottom of each image, and

The permission granted is limited to the personal version of your paper. You are not allowed to download and post the published electronic version of your article (whether PDF or HTML, proof or final version), nor may you scan the printed edition to create an electronic version,

A hyper-text must be included to the Homepage of the journal from which you are licensing at <http://www.sciencedirect.com/science/journal/xxxxx> , or the Elsevier homepage for books at <http://www.elsevier.com> and

Central Storage: This license does not include permission for a scanned version of the material to be stored in a central repository such as that provided by Heron/XanEdu.

18. **Author website** for books with the following additional clauses:

Authors are permitted to place a brief summary of their work online only.

A hyper-text must be included to the Elsevier homepage at <http://www.elsevier.com>

This permission is granted for 1 year only. You may obtain a license for future website posting,

All content posted to the web site must maintain the copyright information line on the bottom of each image, and

The permission granted is limited to the personal version of your paper. You are not allowed to download and post the published electronic version of your article (whether PDF or HTML, proof or final version), nor may you scan the printed edition to create an electronic version,

A hyper-text must be included to the Homepage of the journal from which you are licensing at <http://www.sciencedirect.com/science/journal/xxxxx> , or the Elsevier homepage for books at <http://www.elsevier.com> and

Central Storage: This license does not include permission for a scanned version of the material to be stored in a central repository such as that provided by Heron/XanEdu.

19. **Website** (regular and for author): “A hyper-text must be included to the Homepage of the journal from which you are licensing at

<http://www.sciencedirect.com/science/journal/xxxxx>.”

20. **Thesis/Dissertation:** If your license is for use in a thesis/dissertation your thesis may be submitted to your institution in either print or electronic form. Should your thesis be published commercially, please reapply for permission. These requirements include permission for the Library and Archives of Canada to supply single copies, on demand, of the complete thesis and include permission for UMI to supply single copies, on demand, of the complete thesis. Should your thesis be published commercially, please reapply for permission.

v1.2

21. **Other conditions:**

None

---

---

## NATURE PUBLISHING GROUP LICENSE TERMS AND CONDITIONS

Aug 20, 2008

This is a License Agreement between Frederic Laporte ("You") and Nature Publishing Group ("Nature Publishing Group"). The license consists of your order details, the terms and conditions provided by Nature Publishing Group, and the payment terms and conditions.

License Number	2013370256135
License date	Aug 20, 2008
Licensed content publisher	Nature Publishing Group
Licensed content publication	The EMBO Journal
Licensed content title	GTP hydrolysis by arf-1 mediates sorting and concentration of Golgi resident enzymes into functional COP I vesicles
Licensed content author	Joel Lanoix, Joke Ouwendijk, Chung-Chih Lin, Annika Stark, Harold D Love et al.
Volume number	
Issue number	
Pages	
Year of publication	1999
Portion used	Figures / tables
Requestor type	Student
Type of Use	Thesis / Dissertation
Total	0.00 USD
Terms and Conditions	

### Terms and Conditions for Permissions

Nature Publishing Group hereby grants you a non-exclusive license to reproduce this material for this purpose, and for no other use, subject to the conditions below:

1. NPG warrants that it has, to the best of its knowledge, the rights to license reuse of this material. However, you should ensure that the material you are requesting is original to Nature Publishing Group and does not carry the copyright of another entity (as credited in the published version). If the credit line on any part of the material you have requested indicates that it was reprinted or adapted by NPG with permission from another source, then you should also seek permission from that source to reuse the material.
2. Permission granted free of charge for material in print is also usually granted for any electronic version of that work, provided that the material is incidental to the work as a whole and that the electronic version is essentially equivalent to, or substitutes for, the print version. Where print permission has been granted for a fee, separate permission must be obtained for any additional, electronic re-use (unless, as in the case of a full paper, this has already been accounted for during your initial request in

the calculation of a print run). NB: In all cases, web-based use of full-text articles must be authorized separately through the 'Use on a Web Site' option when requesting permission.

3. Permission granted for a first edition does not apply to second and subsequent editions and for editions in other languages (except for signatories to the STM Permissions Guidelines, or where the first edition permission was granted for free).
4. Nature Publishing Group's permission must be acknowledged next to the figure, table or abstract in print. In electronic form, this acknowledgement must be visible at the same time as the figure/table/abstract, and must be hyperlinked to the journal's homepage.
5. The credit line should read:

Reprinted by permission from Macmillan Publishers Ltd: [JOURNAL NAME]  
(reference citation), copyright (year of publication)

For AOP papers, the credit line should read:

Reprinted by permission from Macmillan Publishers Ltd: [JOURNAL NAME],  
advance online publication, day month year (doi: 10.1038/sj.[JOURNAL  
ACRONYM].XXXXX)

6. Adaptations of single figures do not require NPG approval. However, the adaptation should be credited as follows:

Adapted by permission from Macmillan Publishers Ltd: [JOURNAL NAME]  
(reference citation), copyright (year of publication)

7. Translations of 401 words up to a whole article require NPG approval. Please visit <http://www.macmillanmedicalcommunications.com> for more information. Translations of up to a 400 words do not require NPG approval. The translation should be credited as follows:

Translated by permission from Macmillan Publishers Ltd: [JOURNAL NAME]  
(reference citation), copyright (year of publication).

We are certain that all parties will benefit from this agreement and wish you the best in the use of this material. Thank you.

v1.1

---

---

**ELSEVIER LICENSE  
TERMS AND CONDITIONS**

Aug 20, 2008

This is a License Agreement between Frederic Laporte ("You") and Elsevier ("Elsevier"). The license consists of your order details, the terms and conditions provided by Elsevier, and the payment terms and conditions.

Supplier	Elsevier Limited The Boulevard, Langford Lane Kidlington, Oxford, OX5 1GB, UK
Registered Company Number	1982084
Customer name	Frederic Laporte
Customer address	201 Chemin Club Marin, #1009 Montreal, QC H3E1T4
License Number	2013370765131
License date	Aug 20, 2008
Licensed content publisher	Elsevier
Licensed content publication	Cell
Licensed content title	The Debate about Transport in the Golgi—Two Sides of the Same Coin?
Licensed content author	Hugh R. B. Pelham and James E. Rothman
Licensed content date	15 September 2000
Volume number	102
Issue number	6
Pages	7
Type of Use	Thesis / Dissertation
Portion	Figures/table/illustration/abstracts
Portion Quantity	1
Format	Electronic
You are an author of the Elsevier article	No
Are you translating?	No
Purchase order number	
Expected publication date	Jan 2009
Elsevier VAT number	GB 494 6272 12
Permissions price	0.00 USD
Value added tax 0.0%	0.00 USD
Total	0.00 USD
Terms and Conditions	

## INTRODUCTION

1. The publisher for this copyrighted material is Elsevier. By clicking "accept" in connection with completing this licensing transaction, you agree that the following terms and conditions apply to this transaction (along with the Billing and Payment terms and conditions established by Copyright Clearance Center, Inc. ("CCC"), at the time that you opened your Rightslink account and that are available at any time at [<http://myaccount.copyright.com>](http://myaccount.copyright.com)).

## GENERAL TERMS

2. Elsevier hereby grants you permission to reproduce the aforementioned material subject to the terms and conditions indicated.

3. Acknowledgement: If any part of the material to be used (for example, figures) has appeared in our publication with credit or acknowledgement to another source, permission must also be sought from that source. If such permission is not obtained then that material may not be included in your publication/copies. Suitable acknowledgement to the source must be made, either as a footnote or in a reference list at the end of your publication, as follows:

“Reprinted from Publication title, Vol /edition number, Author(s), Title of article / title of chapter, Pages No., Copyright (Year), with permission from Elsevier [OR APPLICABLE SOCIETY COPYRIGHT OWNER].” Also Lancet special credit - “Reprinted from The Lancet, Vol. number, Author(s), Title of article, Pages No., Copyright (Year), with permission from Elsevier.”

4. Reproduction of this material is confined to the purpose and/or media for which permission is hereby given.

5. Altering/Modifying Material: Not Permitted. However figures and illustrations may be altered/adapted minimally to serve your work. Any other abbreviations, additions, deletions and/or any other alterations shall be made only with prior written authorization of Elsevier Ltd. (Please contact Elsevier at [permissions@elsevier.com](mailto:permissions@elsevier.com))

6. If the permission fee for the requested use of our material is waived in this instance, please be advised that your future requests for Elsevier materials may attract a fee.

7. Reservation of Rights: Publisher reserves all rights not specifically granted in the combination of (i) the license details provided by you and accepted in the course of this licensing transaction, (ii) these terms and conditions and (iii) CCC's Billing and Payment terms and conditions.

8. License Contingent Upon Payment: While you may exercise the rights licensed immediately upon issuance of the license at the end of the licensing process for the transaction, provided that you have disclosed complete and accurate details of your proposed use, no license is finally effective unless and until full payment is received from you (either by publisher or by CCC) as provided in CCC's Billing and Payment terms and conditions. If full payment is not received on a timely basis, then any license preliminarily granted shall be deemed automatically revoked and shall be void as if never granted. Further, in the event that you breach any of these terms and conditions or any of CCC's Billing and Payment

terms and conditions, the license is automatically revoked and shall be void as if never granted. Use of materials as described in a revoked license, as well as any use of the materials beyond the scope of an unrevoked license, may constitute copyright infringement and publisher reserves the right to take any and all action to protect its copyright in the materials.

9. **Warranties:** Publisher makes no representations or warranties with respect to the licensed material.

10. **Indemnity:** You hereby indemnify and agree to hold harmless publisher and CCC, and their respective officers, directors, employees and agents, from and against any and all claims arising out of your use of the licensed material other than as specifically authorized pursuant to this license.

11. **No Transfer of License:** This license is personal to you and may not be sublicensed, assigned, or transferred by you to any other person without publisher's written permission.

12. **No Amendment Except in Writing:** This license may not be amended except in a writing signed by both parties (or, in the case of publisher, by CCC on publisher's behalf).

13. **Objection to Contrary Terms:** Publisher hereby objects to any terms contained in any purchase order, acknowledgment, check endorsement or other writing prepared by you, which terms are inconsistent with these terms and conditions or CCC's Billing and Payment terms and conditions. These terms and conditions, together with CCC's Billing and Payment terms and conditions (which are incorporated herein), comprise the entire agreement between you and publisher (and CCC) concerning this licensing transaction. In the event of any conflict between your obligations established by these terms and conditions and those established by CCC's Billing and Payment terms and conditions, these terms and conditions shall control.

14. **Revocation:** Elsevier or Copyright Clearance Center may deny the permissions described in this License at their sole discretion, for any reason or no reason, with a full refund payable to you. Notice of such denial will be made using the contact information provided by you. Failure to receive such notice will not alter or invalidate the denial. In no event will Elsevier or Copyright Clearance Center be responsible or liable for any costs, expenses or damage incurred by you as a result of a denial of your permission request, other than a refund of the amount(s) paid by you to Elsevier and/or Copyright Clearance Center for denied permissions.

### LIMITED LICENSE

The following terms and conditions apply to specific license types:

15. **Translation:** This permission is granted for non-exclusive world **English** rights only unless your license was granted for translation rights. If you licensed translation rights you may only translate this content into the languages you requested. A professional translator must perform all translations and reproduce the content word for word preserving the integrity of the article. If this license is to re-use 1 or 2 figures then permission is granted for non-exclusive world rights in all languages.

16. **Website:** The following terms and conditions apply to electronic reserve and author websites:



**Electronic reserve:** If licensed material is to be posted to website, the web site is to be password-protected and made available only to bona fide students registered on a relevant course if:

This license was made in connection with a course,

This permission is granted for 1 year only. You may obtain a license for future website posting,

All content posted to the web site must maintain the copyright information line on the bottom of each image,

A hyper-text must be included to the Homepage of the journal from which you are licensing at <http://www.sciencedirect.com/science/journal/xxxxx> or the Elsevier homepage for books at <http://www.elsevier.com> , and

Central Storage: This license does not include permission for a scanned version of the material to be stored in a central repository such as that provided by Heron/XanEdu.

17. **Author website** for journals with the following additional clauses:

This permission is granted for 1 year only. You may obtain a license for future website posting,

All content posted to the web site must maintain the copyright information line on the bottom of each image, and

The permission granted is limited to the personal version of your paper. You are not allowed to download and post the published electronic version of your article (whether PDF or HTML, proof or final version), nor may you scan the printed edition to create an electronic version,

A hyper-text must be included to the Homepage of the journal from which you are licensing at <http://www.sciencedirect.com/science/journal/xxxxx> , or the Elsevier homepage for books at <http://www.elsevier.com> and

Central Storage: This license does not include permission for a scanned version of the material to be stored in a central repository such as that provided by Heron/XanEdu.

18. **Author website** for books with the following additional clauses:

Authors are permitted to place a brief summary of their work online only.

A hyper-text must be included to the Elsevier homepage at <http://www.elsevier.com>

This permission is granted for 1 year only. You may obtain a license for future website posting,

All content posted to the web site must maintain the copyright information line on the bottom of each image, and

The permission granted is limited to the personal version of your paper. You are not allowed to download and post the published electronic version of your article (whether PDF or HTML, proof or final version), nor may you scan the printed edition to create an electronic version,

A hyper-text must be included to the Homepage of the journal from which you are licensing at <http://www.sciencedirect.com/science/journal/xxxxx> , or the Elsevier homepage for books at <http://www.elsevier.com> and

Central Storage: This license does not include permission for a scanned version of the material to be stored in a central repository such as that provided by Heron/XanEdu.

19. **Website** (regular and for author): “A hyper-text must be included to the Homepage of the journal from which you are licensing at <http://www.sciencedirect.com/science/journal/xxxxx>.”

**20. Thesis/Dissertation:** If your license is for use in a thesis/dissertation your thesis may be submitted to your institution in either print or electronic form. Should your thesis be published commercially, please reapply for permission. These requirements include permission for the Library and Archives of Canada to supply single copies, on demand, of the complete thesis and include permission for UMI to supply single copies, on demand, of the complete thesis. Should your thesis be published commercially, please reapply for permission.

v1.2

**21. Other conditions:**

None

---

---

**ELSEVIER LICENSE  
TERMS AND CONDITIONS**

Aug 20, 2008

This is a License Agreement between Frederic Laporte ("You") and Elsevier ("Elsevier"). The license consists of your order details, the terms and conditions provided by Elsevier, and the payment terms and conditions.

Supplier	Elsevier Limited The Boulevard, Langford Lane Kidlington, Oxford, OX5 1GB, UK
Registered Company Number	1982084
Customer name	Frederic Laporte
Customer address	201 Chemin Club Marin, #1009 Montreal, QC H3E1T4
License Number	2013390624832
License date	Aug 20, 2008
Licensed content publisher	Elsevier
Licensed content publication	Cell
Licensed content title	Transport through the Golgi Apparatus by Rapid Partitioning within a Two-Phase Membrane System
Licensed content author	George H. Patterson, Koret Hirschberg, Roman S. Polishchuk, Daniel Gerlich, Robert D. Phair and Jennifer Lippincott-Schwartz
Licensed content date	13 June 2008
Volume number	133
Issue number	6
Pages	13
Type of Use	Thesis / Dissertation
Portion	Figures/table/illustration/abstracts
Portion Quantity	3
Format	Electronic
You are an author of the Elsevier article	No
Are you translating?	No
Purchase order number	
Expected publication date	Jan 2009
Elsevier VAT number	GB 494 6272 12
Permissions price	0.00 USD
Value added tax 0.0%	0.00 USD

Total

0.00 USD

[Terms and Conditions](#)

## INTRODUCTION

1. The publisher for this copyrighted material is Elsevier. By clicking "accept" in connection with completing this licensing transaction, you agree that the following terms and conditions apply to this transaction (along with the Billing and Payment terms and conditions established by Copyright Clearance Center, Inc. ("CCC"), at the time that you opened your Rightslink account and that are available at any time at [<http://myaccount.copyright.com>](http://myaccount.copyright.com)).

## GENERAL TERMS

2. Elsevier hereby grants you permission to reproduce the aforementioned material subject to the terms and conditions indicated.

3. Acknowledgement: If any part of the material to be used (for example, figures) has appeared in our publication with credit or acknowledgement to another source, permission must also be sought from that source. If such permission is not obtained then that material may not be included in your publication/copies. Suitable acknowledgement to the source must be made, either as a footnote or in a reference list at the end of your publication, as follows:

“Reprinted from Publication title, Vol /edition number, Author(s), Title of article / title of chapter, Pages No., Copyright (Year), with permission from Elsevier [OR APPLICABLE SOCIETY COPYRIGHT OWNER].” Also Lancet special credit - “Reprinted from The Lancet, Vol. number, Author(s), Title of article, Pages No., Copyright (Year), with permission from Elsevier.”

4. Reproduction of this material is confined to the purpose and/or media for which permission is hereby given.

5. Altering/Modifying Material: Not Permitted. However figures and illustrations may be altered/adapted minimally to serve your work. Any other abbreviations, additions, deletions and/or any other alterations shall be made only with prior written authorization of Elsevier Ltd. (Please contact Elsevier at [permissions@elsevier.com](mailto:permissions@elsevier.com))

6. If the permission fee for the requested use of our material is waived in this instance, please be advised that your future requests for Elsevier materials may attract a fee.

7. Reservation of Rights: Publisher reserves all rights not specifically granted in the combination of (i) the license details provided by you and accepted in the course of this licensing transaction, (ii) these terms and conditions and (iii) CCC's Billing and Payment terms and conditions.

8. License Contingent Upon Payment: While you may exercise the rights licensed immediately upon issuance of the license at the end of the licensing process for the transaction, provided that you have disclosed complete and accurate details of your proposed use, no license is finally effective unless and until full payment is received from you (either by publisher or by CCC) as provided in CCC's Billing and Payment terms and conditions. If

full payment is not received on a timely basis, then any license preliminarily granted shall be deemed automatically revoked and shall be void as if never granted. Further, in the event that you breach any of these terms and conditions or any of CCC's Billing and Payment terms and conditions, the license is automatically revoked and shall be void as if never granted. Use of materials as described in a revoked license, as well as any use of the materials beyond the scope of an unrevoked license, may constitute copyright infringement and publisher reserves the right to take any and all action to protect its copyright in the materials.

9. Warranties: Publisher makes no representations or warranties with respect to the licensed material.

10. Indemnity: You hereby indemnify and agree to hold harmless publisher and CCC, and their respective officers, directors, employees and agents, from and against any and all claims arising out of your use of the licensed material other than as specifically authorized pursuant to this license.

11. No Transfer of License: This license is personal to you and may not be sublicensed, assigned, or transferred by you to any other person without publisher's written permission.

12. No Amendment Except in Writing: This license may not be amended except in a writing signed by both parties (or, in the case of publisher, by CCC on publisher's behalf).

13. Objection to Contrary Terms: Publisher hereby objects to any terms contained in any purchase order, acknowledgment, check endorsement or other writing prepared by you, which terms are inconsistent with these terms and conditions or CCC's Billing and Payment terms and conditions. These terms and conditions, together with CCC's Billing and Payment terms and conditions (which are incorporated herein), comprise the entire agreement between you and publisher (and CCC) concerning this licensing transaction. In the event of any conflict between your obligations established by these terms and conditions and those established by CCC's Billing and Payment terms and conditions, these terms and conditions shall control.

14. Revocation: Elsevier or Copyright Clearance Center may deny the permissions described in this License at their sole discretion, for any reason or no reason, with a full refund payable to you. Notice of such denial will be made using the contact information provided by you. Failure to receive such notice will not alter or invalidate the denial. In no event will Elsevier or Copyright Clearance Center be responsible or liable for any costs, expenses or damage incurred by you as a result of a denial of your permission request, other than a refund of the amount(s) paid by you to Elsevier and/or Copyright Clearance Center for denied permissions.

#### LIMITED LICENSE

The following terms and conditions apply to specific license types:

15. **Translation:** This permission is granted for non-exclusive world **English** rights only unless your license was granted for translation rights. If you licensed translation rights you may only translate this content into the languages you requested. A professional translator must perform all translations and reproduce the content word for word preserving the integrity of the article. If this license is to re-use 1 or 2 figures then permission is granted for non-exclusive world rights in all languages.

16. **Website:** The following terms and conditions apply to electronic reserve and author websites:

**Electronic reserve:** If licensed material is to be posted to website, the web site is to be password-protected and made available only to bona fide students registered on a relevant course if:

This license was made in connection with a course,

This permission is granted for 1 year only. You may obtain a license for future website posting,

All content posted to the web site must maintain the copyright information line on the bottom of each image,

A hyper-text must be included to the Homepage of the journal from which you are licensing at <http://www.sciencedirect.com/science/journal/xxxxxx> or the Elsevier homepage for books at <http://www.elsevier.com> , and

Central Storage: This license does not include permission for a scanned version of the material to be stored in a central repository such as that provided by Heron/XanEdu.

17. **Author website** for journals with the following additional clauses:

This permission is granted for 1 year only. You may obtain a license for future website posting,

All content posted to the web site must maintain the copyright information line on the bottom of each image, and

The permission granted is limited to the personal version of your paper. You are not allowed to download and post the published electronic version of your article (whether PDF or HTML, proof or final version), nor may you scan the printed edition to create an electronic version,

A hyper-text must be included to the Homepage of the journal from which you are licensing at <http://www.sciencedirect.com/science/journal/xxxxxx> , or the Elsevier homepage for books at <http://www.elsevier.com> and

Central Storage: This license does not include permission for a scanned version of the material to be stored in a central repository such as that provided by Heron/XanEdu.

18. **Author website** for books with the following additional clauses:

Authors are permitted to place a brief summary of their work online only.

A hyper-text must be included to the Elsevier homepage at <http://www.elsevier.com>

This permission is granted for 1 year only. You may obtain a license for future website posting,

All content posted to the web site must maintain the copyright information line on the bottom of each image, and

The permission granted is limited to the personal version of your paper. You are not allowed to download and post the published electronic version of your article (whether PDF or HTML, proof or final version), nor may you scan the printed edition to create an electronic version,

A hyper-text must be included to the Homepage of the journal from which you are licensing at <http://www.sciencedirect.com/science/journal/xxxxxx> , or the Elsevier homepage for books at <http://www.elsevier.com> and

Central Storage: This license does not include permission for a scanned version of the material to be stored in a central repository such as that provided by Heron/XanEdu.

19. **Website** (regular and for author): “A hyper-text must be included to the Homepage of the journal from which you are licensing at <http://www.sciencedirect.com/science/journal/xxxxx>.”

20. **Thesis/Dissertation**: If your license is for use in a thesis/dissertation your thesis may be submitted to your institution in either print or electronic form. Should your thesis be published commercially, please reapply for permission. These requirements include permission for the Library and Archives of Canada to supply single copies, on demand, of the complete thesis and include permission for UMI to supply single copies, on demand, of the complete thesis. Should your thesis be published commercially, please reapply for permission.

v1.2

21. **Other conditions:**

None

---

---



**ELSEVIER LICENSE  
TERMS AND CONDITIONS**

Aug 24, 2008

This is a License Agreement between Frederic Laporte ("You") and Elsevier ("Elsevier"). The license consists of your order details, the terms and conditions provided by Elsevier, and the payment terms and conditions.

Supplier	Elsevier Limited The Boulevard, Langford Lane Kidlington, Oxford, OX5 1GB, UK
Registered Company Number	1982084
Customer name	Frederic Laporte
Customer address	201 Chemin Club Marin, #1009 Montreal, QC H3E1T4
License Number	2015350299671
License date	Aug 24, 2008
Licensed content publisher	Elsevier
Licensed content publication	Biochimica et Biophysica Acta (BBA) - Molecular Cell Research
Licensed content title	The role of the phosphoinositides at the Golgi complex
Licensed content author	Maria Antonietta De Matteis, Antonella Di Campli and Anna Godi
Licensed content date	10 July 2005
Volume number	1744
Issue number	3
Pages	10
Type of Use	Thesis / Dissertation
Portion	Figures/table/illustration/abstracts
Portion Quantity	1
Format	Print
You are an author of the Elsevier article	No
Are you translating?	No
Purchase order number	
Expected publication date	Jan 2009
Elsevier VAT number	GB 494 6272 12
Permissions price	0.00 USD
Value added tax 0.0%	0.00 USD
Total	0.00 USD
Terms and Conditions	

## INTRODUCTION

1. The publisher for this copyrighted material is Elsevier. By clicking "accept" in connection with completing this licensing transaction, you agree that the following terms and conditions apply to this transaction (along with the Billing and Payment terms and conditions established by Copyright Clearance Center, Inc. ("CCC"), at the time that you opened your Rightslink account and that are available at any time at [<http://myaccount.copyright.com>](http://myaccount.copyright.com)).

## GENERAL TERMS

2. Elsevier hereby grants you permission to reproduce the aforementioned material subject to the terms and conditions indicated.

3. Acknowledgement: If any part of the material to be used (for example, figures) has appeared in our publication with credit or acknowledgement to another source, permission must also be sought from that source. If such permission is not obtained then that material may not be included in your publication/copies. Suitable acknowledgement to the source must be made, either as a footnote or in a reference list at the end of your publication, as follows:

“Reprinted from Publication title, Vol /edition number, Author(s), Title of article / title of chapter, Pages No., Copyright (Year), with permission from Elsevier [OR APPLICABLE SOCIETY COPYRIGHT OWNER].” Also Lancet special credit - “Reprinted from The Lancet, Vol. number, Author(s), Title of article, Pages No., Copyright (Year), with permission from Elsevier.”

4. Reproduction of this material is confined to the purpose and/or media for which permission is hereby given.

5. Altering/Modifying Material: Not Permitted. However figures and illustrations may be altered/adapted minimally to serve your work. Any other abbreviations, additions, deletions and/or any other alterations shall be made only with prior written authorization of Elsevier Ltd. (Please contact Elsevier at [permissions@elsevier.com](mailto:permissions@elsevier.com))

6. If the permission fee for the requested use of our material is waived in this instance, please be advised that your future requests for Elsevier materials may attract a fee.

7. Reservation of Rights: Publisher reserves all rights not specifically granted in the combination of (i) the license details provided by you and accepted in the course of this licensing transaction, (ii) these terms and conditions and (iii) CCC's Billing and Payment terms and conditions.

8. License Contingent Upon Payment: While you may exercise the rights licensed immediately upon issuance of the license at the end of the licensing process for the transaction, provided that you have disclosed complete and accurate details of your proposed use, no license is finally effective unless and until full payment is received from you (either by publisher or by CCC) as provided in CCC's Billing and Payment terms and conditions. If full payment is not received on a timely basis, then any license preliminarily granted shall be deemed automatically revoked and shall be void as if never granted. Further, in the event that you breach any of these terms and conditions or any of CCC's Billing and Payment

terms and conditions, the license is automatically revoked and shall be void as if never granted. Use of materials as described in a revoked license, as well as any use of the materials beyond the scope of an unrevoked license, may constitute copyright infringement and publisher reserves the right to take any and all action to protect its copyright in the materials.

9. **Warranties:** Publisher makes no representations or warranties with respect to the licensed material.

10. **Indemnity:** You hereby indemnify and agree to hold harmless publisher and CCC, and their respective officers, directors, employees and agents, from and against any and all claims arising out of your use of the licensed material other than as specifically authorized pursuant to this license.

11. **No Transfer of License:** This license is personal to you and may not be sublicensed, assigned, or transferred by you to any other person without publisher's written permission.

12. **No Amendment Except in Writing:** This license may not be amended except in a writing signed by both parties (or, in the case of publisher, by CCC on publisher's behalf).

13. **Objection to Contrary Terms:** Publisher hereby objects to any terms contained in any purchase order, acknowledgment, check endorsement or other writing prepared by you, which terms are inconsistent with these terms and conditions or CCC's Billing and Payment terms and conditions. These terms and conditions, together with CCC's Billing and Payment terms and conditions (which are incorporated herein), comprise the entire agreement between you and publisher (and CCC) concerning this licensing transaction. In the event of any conflict between your obligations established by these terms and conditions and those established by CCC's Billing and Payment terms and conditions, these terms and conditions shall control.

14. **Revocation:** Elsevier or Copyright Clearance Center may deny the permissions described in this License at their sole discretion, for any reason or no reason, with a full refund payable to you. Notice of such denial will be made using the contact information provided by you. Failure to receive such notice will not alter or invalidate the denial. In no event will Elsevier or Copyright Clearance Center be responsible or liable for any costs, expenses or damage incurred by you as a result of a denial of your permission request, other than a refund of the amount(s) paid by you to Elsevier and/or Copyright Clearance Center for denied permissions.

#### LIMITED LICENSE

The following terms and conditions apply to specific license types:

15. **Translation:** This permission is granted for non-exclusive world **English** rights only unless your license was granted for translation rights. If you licensed translation rights you may only translate this content into the languages you requested. A professional translator must perform all translations and reproduce the content word for word preserving the integrity of the article. If this license is to re-use 1 or 2 figures then permission is granted for non-exclusive world rights in all languages.

16. **Website:** The following terms and conditions apply to electronic reserve and author websites:

**Electronic reserve:** If licensed material is to be posted to website, the web site is to be password-protected and made available only to bona fide students registered on a relevant course if:

This license was made in connection with a course,

This permission is granted for 1 year only. You may obtain a license for future website posting,

All content posted to the web site must maintain the copyright information line on the bottom of each image,

A hyper-text must be included to the Homepage of the journal from which you are licensing at <http://www.sciencedirect.com/science/journal/xxxxx> or the Elsevier homepage for books at <http://www.elsevier.com> , and

Central Storage: This license does not include permission for a scanned version of the material to be stored in a central repository such as that provided by Heron/XanEdu.

17. **Author website** for journals with the following additional clauses:

This permission is granted for 1 year only. You may obtain a license for future website posting,

All content posted to the web site must maintain the copyright information line on the bottom of each image, and

The permission granted is limited to the personal version of your paper. You are not allowed to download and post the published electronic version of your article (whether PDF or HTML, proof or final version), nor may you scan the printed edition to create an electronic version,

A hyper-text must be included to the Homepage of the journal from which you are licensing at <http://www.sciencedirect.com/science/journal/xxxxx> , or the Elsevier homepage for books at <http://www.elsevier.com> and

Central Storage: This license does not include permission for a scanned version of the material to be stored in a central repository such as that provided by Heron/XanEdu.

18. **Author website** for books with the following additional clauses:

Authors are permitted to place a brief summary of their work online only.

A hyper-text must be included to the Elsevier homepage at <http://www.elsevier.com>

This permission is granted for 1 year only. You may obtain a license for future website posting,

All content posted to the web site must maintain the copyright information line on the bottom of each image, and

The permission granted is limited to the personal version of your paper. You are not allowed to download and post the published electronic version of your article (whether PDF or HTML, proof or final version), nor may you scan the printed edition to create an electronic version,

A hyper-text must be included to the Homepage of the journal from which you are licensing at <http://www.sciencedirect.com/science/journal/xxxxx> , or the Elsevier homepage for books at <http://www.elsevier.com> and

Central Storage: This license does not include permission for a scanned version of the material to be stored in a central repository such as that provided by Heron/XanEdu.

19. **Website** (regular and for author): “A hyper-text must be included to the Homepage of the journal from which you are licensing at <http://www.sciencedirect.com/science/journal/xxxxx>.”

20. **Thesis/Dissertation:** If your license is for use in a thesis/dissertation your thesis may be submitted to your institution in either print or electronic form. Should your thesis be published commercially, please reapply for permission. These requirements include permission for the Library and Archives of Canada to supply single copies, on demand, of the complete thesis and include permission for UMI to supply single copies, on demand, of the complete thesis. Should your thesis be published commercially, please reapply for permission.

v1.2

21. **Other conditions:**

None

---

---

**ELSEVIER LICENSE  
TERMS AND CONDITIONS**

Aug 20, 2008

This is a License Agreement between Frederic Laporte ("You") and Elsevier ("Elsevier"). The license consists of your order details, the terms and conditions provided by Elsevier, and the payment terms and conditions.

Supplier	Elsevier Limited The Boulevard, Langford Lane Kidlington, Oxford, OX5 1GB, UK
Registered Company Number	1982084
Customer name	Frederic Laporte
Customer address	201 Chemin Club Marin, #1009 Montreal, QC H3E1T4
License Number	2013360626126
License date	Aug 20, 2008
Licensed content publisher	Elsevier
Licensed content publication	Cell
Licensed content title	Quantitative Proteomics Analysis of the Secretory Pathway
Licensed content author	Annalyn Gilchrist, Catherine E. Au, Johan Hiding, Alexander W. Bell, Julia Fernandez-Rodriguez, Souad Lesimple, Hisao Nagaya, Line Roy, Sara J.C. Gosline, Michael Hallett, Jacques Paiement, Robert E. Kearney, Tommy Nilsson and John J.M. Bergeron
Licensed content date	15 December 2006
Volume number	127
Issue number	6
Pages	17
Type of Use	Thesis / Dissertation
Portion	Figures/table/illustration/abstracts
Portion Quantity	1
Format	Both print and electronic
You are an author of the Elsevier article	No
Are you translating?	No
Purchase order number	
Expected publication date	Jan 2009
Elsevier VAT number	GB 494 6272 12
Permissions price	0.00 USD
Value added tax 0.0%	0.00 USD

Total

0.00 USD

[Terms and Conditions](#)

## INTRODUCTION

1. The publisher for this copyrighted material is Elsevier. By clicking "accept" in connection with completing this licensing transaction, you agree that the following terms and conditions apply to this transaction (along with the Billing and Payment terms and conditions established by Copyright Clearance Center, Inc. ("CCC"), at the time that you opened your Rightslink account and that are available at any time at [<http://myaccount.copyright.com>](http://myaccount.copyright.com)).

## GENERAL TERMS

2. Elsevier hereby grants you permission to reproduce the aforementioned material subject to the terms and conditions indicated.

3. Acknowledgement: If any part of the material to be used (for example, figures) has appeared in our publication with credit or acknowledgement to another source, permission must also be sought from that source. If such permission is not obtained then that material may not be included in your publication/copies. Suitable acknowledgement to the source must be made, either as a footnote or in a reference list at the end of your publication, as follows:

“Reprinted from Publication title, Vol /edition number, Author(s), Title of article / title of chapter, Pages No., Copyright (Year), with permission from Elsevier [OR APPLICABLE SOCIETY COPYRIGHT OWNER].” Also Lancet special credit - “Reprinted from The Lancet, Vol. number, Author(s), Title of article, Pages No., Copyright (Year), with permission from Elsevier.”

4. Reproduction of this material is confined to the purpose and/or media for which permission is hereby given.

5. Altering/Modifying Material: Not Permitted. However figures and illustrations may be altered/adapted minimally to serve your work. Any other abbreviations, additions, deletions and/or any other alterations shall be made only with prior written authorization of Elsevier Ltd. (Please contact Elsevier at [permissions@elsevier.com](mailto:permissions@elsevier.com))

6. If the permission fee for the requested use of our material is waived in this instance, please be advised that your future requests for Elsevier materials may attract a fee.

7. Reservation of Rights: Publisher reserves all rights not specifically granted in the combination of (i) the license details provided by you and accepted in the course of this licensing transaction, (ii) these terms and conditions and (iii) CCC's Billing and Payment terms and conditions.

8. License Contingent Upon Payment: While you may exercise the rights licensed immediately upon issuance of the license at the end of the licensing process for the transaction, provided that you have disclosed complete and accurate details of your proposed use, no license is finally effective unless and until full payment is received from you (either



by publisher or by CCC) as provided in CCC's Billing and Payment terms and conditions. If full payment is not received on a timely basis, then any license preliminarily granted shall be deemed automatically revoked and shall be void as if never granted. Further, in the event that you breach any of these terms and conditions or any of CCC's Billing and Payment terms and conditions, the license is automatically revoked and shall be void as if never granted. Use of materials as described in a revoked license, as well as any use of the materials beyond the scope of an unrevoked license, may constitute copyright infringement and publisher reserves the right to take any and all action to protect its copyright in the materials.

9. Warranties: Publisher makes no representations or warranties with respect to the licensed material.

10. Indemnity: You hereby indemnify and agree to hold harmless publisher and CCC, and their respective officers, directors, employees and agents, from and against any and all claims arising out of your use of the licensed material other than as specifically authorized pursuant to this license.

11. No Transfer of License: This license is personal to you and may not be sublicensed, assigned, or transferred by you to any other person without publisher's written permission.

12. No Amendment Except in Writing: This license may not be amended except in a writing signed by both parties (or, in the case of publisher, by CCC on publisher's behalf).

13. Objection to Contrary Terms: Publisher hereby objects to any terms contained in any purchase order, acknowledgment, check endorsement or other writing prepared by you, which terms are inconsistent with these terms and conditions or CCC's Billing and Payment terms and conditions. These terms and conditions, together with CCC's Billing and Payment terms and conditions (which are incorporated herein), comprise the entire agreement between you and publisher (and CCC) concerning this licensing transaction. In the event of any conflict between your obligations established by these terms and conditions and those established by CCC's Billing and Payment terms and conditions, these terms and conditions shall control.

14. Revocation: Elsevier or Copyright Clearance Center may deny the permissions described in this License at their sole discretion, for any reason or no reason, with a full refund payable to you. Notice of such denial will be made using the contact information provided by you. Failure to receive such notice will not alter or invalidate the denial. In no event will Elsevier or Copyright Clearance Center be responsible or liable for any costs, expenses or damage incurred by you as a result of a denial of your permission request, other than a refund of the amount(s) paid by you to Elsevier and/or Copyright Clearance Center for denied permissions.

#### LIMITED LICENSE

The following terms and conditions apply to specific license types:

15. **Translation:** This permission is granted for non-exclusive world **English** rights only unless your license was granted for translation rights. If you licensed translation rights you may only translate this content into the languages you requested. A professional translator must perform all translations and reproduce the content word for word preserving the integrity of the article. If this license is to re-use 1 or 2 figures then permission is granted for

non-exclusive world rights in all languages.

**16. Website:** The following terms and conditions apply to electronic reserve and author websites:

**Electronic reserve:** If licensed material is to be posted to website, the web site is to be password-protected and made available only to bona fide students registered on a relevant course if:

This license was made in connection with a course,

This permission is granted for 1 year only. You may obtain a license for future website posting,

All content posted to the web site must maintain the copyright information line on the bottom of each image,

A hyper-text must be included to the Homepage of the journal from which you are licensing at <http://www.sciencedirect.com/science/journal/xxxxx> or the Elsevier homepage for books at <http://www.elsevier.com> , and

Central Storage: This license does not include permission for a scanned version of the material to be stored in a central repository such as that provided by Heron/XanEdu.

**17. Author website** for journals with the following additional clauses:

This permission is granted for 1 year only. You may obtain a license for future website posting,

All content posted to the web site must maintain the copyright information line on the bottom of each image, and

The permission granted is limited to the personal version of your paper. You are not allowed to download and post the published electronic version of your article (whether PDF or HTML, proof or final version), nor may you scan the printed edition to create an electronic version,

A hyper-text must be included to the Homepage of the journal from which you are licensing at <http://www.sciencedirect.com/science/journal/xxxxx> , or the Elsevier homepage for books at <http://www.elsevier.com> and

Central Storage: This license does not include permission for a scanned version of the material to be stored in a central repository such as that provided by Heron/XanEdu.

**18. Author website** for books with the following additional clauses:

Authors are permitted to place a brief summary of their work online only.

A hyper-text must be included to the Elsevier homepage at <http://www.elsevier.com>

This permission is granted for 1 year only. You may obtain a license for future website posting,

All content posted to the web site must maintain the copyright information line on the bottom of each image, and

The permission granted is limited to the personal version of your paper. You are not allowed to download and post the published electronic version of your article (whether PDF or HTML, proof or final version), nor may you scan the printed edition to create an electronic version,

A hyper-text must be included to the Homepage of the journal from which you are licensing at <http://www.sciencedirect.com/science/journal/xxxxx> , or the Elsevier homepage for books at <http://www.elsevier.com> and

Central Storage: This license does not include permission for a scanned version of the material to be stored in a central repository such as that provided by Heron/XanEdu.

19. **Website** (regular and for author): “A hyper-text must be included to the Homepage of the journal from which you are licensing at <http://www.sciencedirect.com/science/journal/xxxxx>.”

20. **Thesis/Dissertation**: If your license is for use in a thesis/dissertation your thesis may be submitted to your institution in either print or electronic form. Should your thesis be published commercially, please reapply for permission. These requirements include permission for the Library and Archives of Canada to supply single copies, on demand, of the complete thesis and include permission for UMI to supply single copies, on demand, of the complete thesis. Should your thesis be published commercially, please reapply for permission.

v1.2

21. **Other conditions:**

None

---

---